APPENDIX A

MODELING TECHNICAL SUPPORT DOCUMENT (TSD)

Dallas-Fort Worth Moderate Area Attainment Demonstration
State Implementation Plan Revision for the 2015 Eight-Hour
Ozone National Ambient Air Quality Standard

Project Number 2022-021-SIP-NR
SFR 112/2022-021-SIP-NR

This page intentionally left blank

TABLE OF CONTENTS

LIST OF ACRONYMS

AD	Attainment Demonstration
AEO	annual energy outlook
AFS	AIRS Facility Subsystem
AGL	above ground level
AIS	Automatic Identification System
APEI	Air Pollutant Emission Inventory
BEIS	Biogenic Emission Inventory System
BOEM	Bureau of Ocean Energy Management
CAMPD	Clean Air Markets Program Data
CAMS	Continuous Air Monitoring Stations
CAMx	Comprehensive Air Quality Model with Extensions
CEDS	Community Emissions Data System
CEMS	Continuous Emissions Monitoring System
CFR	Code of Federal Regulations
CMAQ	Community Multiscale Air Quality Modeling
CMAS	Community Modeling and Analysis System
CMV	Commercial Marine Vessels
CO	Carbon Monoxide
CONUS	continental United States
CSAPR	Cross-State Air Pollution Rule
DERC	Discrete Emission Reduction Credit program
DFW	Dallas-Fort Worth
DVB	base case design value
DVF	future case design value
EBT	Emissions Banking and Trading
ECCC	Environment and Climate Change Canada
ECMWF	European Centre for Medium-Range Forecast
EE	Emission Events
EGU	electric generating units
EPA	United States Environmental Protection Agency
EPS3	Emissions Processing System version 3
ERA-Interim	European Re-Analysis Interim

ERC	Emission Reduction Credit
ERCOT	Electric Reliability Council of Texas
ERG	Eastern Research Group
ERTAC	Eastern Regional Technical Advisory Committee
FAA	Federal Aviation Agency
FCAA	Federal Clean Air Act
GRIB	Gridded Binary
GSE	ground support equipment
GWEI	Gulfwide Emission Inventory
HECT	Highly Reactive Volatile Organic Compounds Emissions Cap and Trade
HGB	Houston-Brazoria-Galveston
hPa	hectopascal
HRVOC	Highly Reactive Volatile Organic Compounds
IC/BC	initial and boundary conditions
K_v	vertical diffusivity
LCC	Lambert conformal conic
LULC	Land Use/Land Cover
MAERT	Maximum Allowable Emission Rate Table
MCIP	Meteorology-Chemistry Interface Processor
MDERC	Mobile Discrete Emission Reduction Credit Program
MECT	Mass Emissions Cap and Trade
MOVES3	Motor Vehicle Emissions Simulator
MPE	Model Performance Evaluation
MSS	maintenance, startup, shutdown
NAAQS	National Ambient Air Quality Standard
NAAQS	National Ambient Air Quality Standards
NCTCOG	North Central Texas Council of Governments
NEEDS	National Electric Energy Data System
NEI	National Emissions Inventory
NH_3	Ammonia
non-IPM	non-Integrated Planning Model
NO_X	nitrogen oxides
OSD	Ozone Season Daily

PBL	Planetary Boundary Layer
ppb	parts per billion
ppm	parts per million
psia	pounds per square inch absolute
RMR	Reliability Must Run
RMSE	Root Mean Square Error
RRC	Railroad Commission of Texas
RRTM	Rapid Radiative Transfer Model
SCC	Source Classification Code
SIC	Standard Industrial Classification
SIP	State Implementation Plan
SMOKE	Sparse Matrix Operation Kernel Emissions
SMSS	scheduled maintenance startup and shutdown
STARS	State of Texas Air Reporting System
TAC	Texas Administrative Code
TAC	Texas Administrative Code
TACB	Texas Air Control Board
TASP	Texas Airport System Plan
TCAA	Texas Clean Air Act
TCEQ	Texas Commission on Environmental Quality (commission)
TDM	Travel Demand Model
TNRCC	Texas Natural Resource Conservation Commission
tpd	tons per day
TTI	Texas Transportation Institute
TxLED	Texas Low Emission Diesel
VOC	volatile organic compounds
WPS	WRF Preprocessing System
WRF	Weather Research and Forecasting
WRFSFDDA	WRF Surface Four-Dimensional Data Assimilation

LIST OF TABLES

LIST OF FIGURES

1. PHOTOCHEMICAL MODELING

1.1 INTRODUCTION

This appendix provides details of the modeling platform that was used to conduct photochemical modeling by the Texas Commission on Environmental Quality (TCEQ) in support of the attainment demonstration (AD) state implementation plan (SIP) revisions for the Bexar County, Dallas-Fort Worth (DFW), and Houston-Brazoria-Galveston (HGB) 2015 eight-hour ozone National Ambient Air Quality Standard (NAAQS) nonattainment areas. As part of these AD SIP revisions, the TCEQ conducted photochemical modeling in accordance with the United States Environmental Protection Agency's (EPA) "*Modeling Guidance for Demonstrating Air Quality Goals for Ozone, PM2.5, and Regional Haze*" (EPA, 2018; hereafter referred to as the EPA modeling guidance).

AD modeling for the three SIP revisions included two photochemical modeling runs, the 2019 base case and the 2023 future case, the results of which were used to estimate the 2023 attainment year design value. The TCEQ's choice of Comprehensive Air Quality Model with Extension (CAMx) is in line with the criteria specified in the EPA modeling guidance for model selection. This appendix provides details of the different components of AD modeling, such as episode selection, modeling domain, development of necessary model inputs such as meteorological parameters, emission inputs, and initial and boundary conditions and model performance evaluation.

1.2 MODELING EPISODE SELECTION

The TCEQ 2019 modeling platform has a modeling episode of April 1 through October 31, 2019. This episode was selected by the TCEQ following the recommendations provided in the EPA modeling guidance to develop an ozone modeling platform that would be appropriate for use for ozone AD SIP revisions and other ozone modeling applications for the State of Texas. The EPA's recommendations are intended to ensure that the selected episode is representative of conditions that lead to exceedances of the eight-hour ozone NAAQS. The EPA modeling guidance recommends that the modeling episode:

- has a sufficient number of exceedance days;
- has ozone exceedances following historically observed temporal patterns;
- includes a variety of meteorological conditions that frequently correspond to high ozone;
- has at least five days in the episode for each regulatory monitor in each nonattainment area with a monitored maximum daily eight-hour average (MDA8) ozone greater than or equal to 60 parts per billion (ppb); and
- is in the recent past, preferably close to a National Emissions Inventory (NEI) year.

The calendar year that a modeling episode is from is called the base year. The base years that the TCEQ considered for the modeling platform were 2016, 2017, 2018, and 2019. 2019 was the most recent year available with complete data when development of the TCEQ modeling platform began. Figure 1-1: *Number of Exceedances by Year in Texas Areas* show the total number of observed MDA8 ozone exceedances of the 2015 ozone NAAQS of 70 ppb at all monitors in five Texas areas: HGB, DFW, Bexar County

(represented as BEX in the figure), El Paso (ELP), and Beaumont-Port Arthur (BPA). Of the four years evaluated, 2018 had the highest number of exceedances for all areas, followed by 2019 for four of the five areas. Based on observed exceedances, the potential modeling episode base years were narrowed to 2018 and 2019.

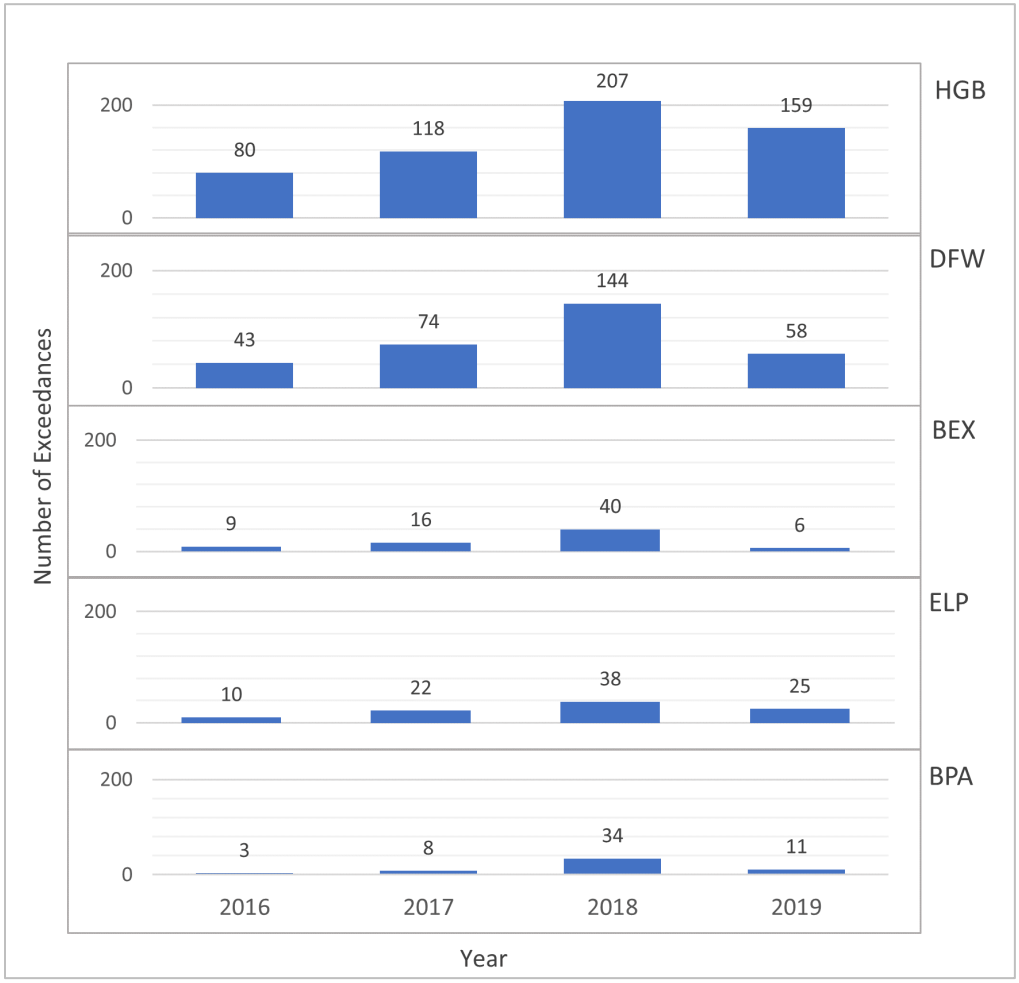

Figure 1-1: Number of Exceedances by Year in Texas Areas

While 2018 had a higher number of exceedances than 2019, the temporal profile of the exceedances throughout the ozone season in HGB and DFW was more typical in 2019. Figure 1-2: *Temporal Profile of Exceedance Days in HGB and DFW* shows the total number of MDA8 ozone exceedances of the 70 ppb standard observed at monitors in DFW and HGB in 2018 and 2019 compared to the 10-year average of 2010 through 2019. The temporal profile of exceedances over the 10-year average shows a bimodal trend with a peak in May, a low in July, and another peak in August and September. While 2019 did not have a high number of ozone exceedances observed in August, the bimodal pattern was observed, with a peak in May, a low in July, and a second peak in September. The temporal profile of exceedances in 2018 also had a bimodal pattern, but the timing of the peaks and troughs did not align with previous years, with a low in June, high in July, and low in September. Based on this assessment, 2019 appears to be the more typical year for ozone formation compared to 2018.

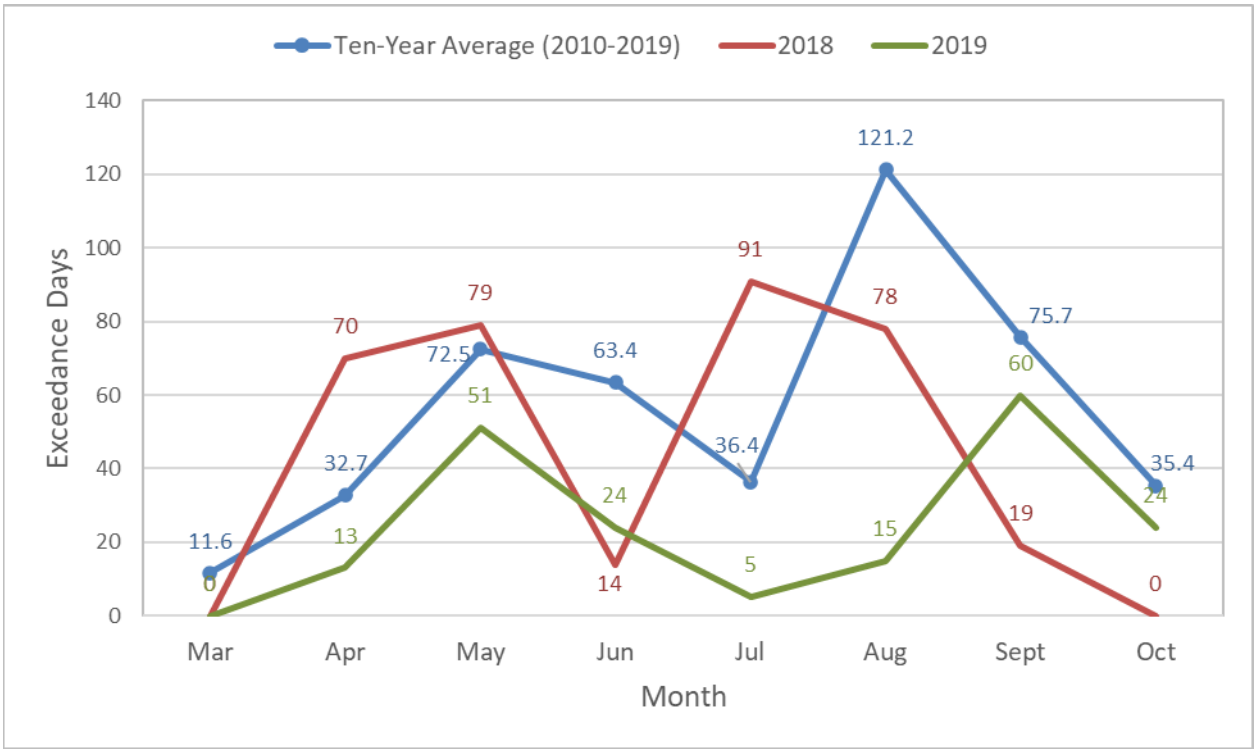

Figure 1-2: Temporal Profile of Exceedance Days in HGB and DFW

The TCEQ conducted a meteorological analysis focused on 2018 and 2019 to determine whether Texas meteorology was typical for ozone formation during these two potential base years. Multiple variables associated with ozone formation were compared to climatological averages, including temperature, stagnation, relative humidity, and precipitation. A comparative analysis of wind speed and direction was done at several monitors across the state. As an example, Figure 1-3: *Wind Roses from 2000 through 2019 for the Houston Aldine and Eagle Mountain Lake Monitors* shows the wind direction and wind speed for regulatory monitors in HGB and DFW, respectively. At both monitors, and at other monitors that were assessed, the dominant wind directions in 2018 and 2019 aligned with the previous years.

Monthly temperatures for 2018 and 2019 were compared to climatological averages to determine if either of the years exhibited anomalies. As another example, Figure 1-4: *Divisional Maximum Temperature Ranks from 1895 through 2019 for May and August in 2018 and 2019* shows the divisional maximum temperature rank from the 1895 through 2019 average, categorized from record coldest to record warmest. Looking at the month of May, May 2018 had much above average to record warmest temperatures in Texas, whereas May of 2019 was close to average or below average in Texas. The pattern was reversed for the month of August, where August 2018 had close to average temperatures in Texas while August 2019 had much above average temperatures.

Across many of the meteorological variables considered, certain time periods out of the episode were more typical in one year than the other. Ultimately, no meteorological variables stood out as significantly unusual for either year, and the analysis concluded

that both 2018 and 2019 were reasonable for ozone modeling based on meteorology alone.

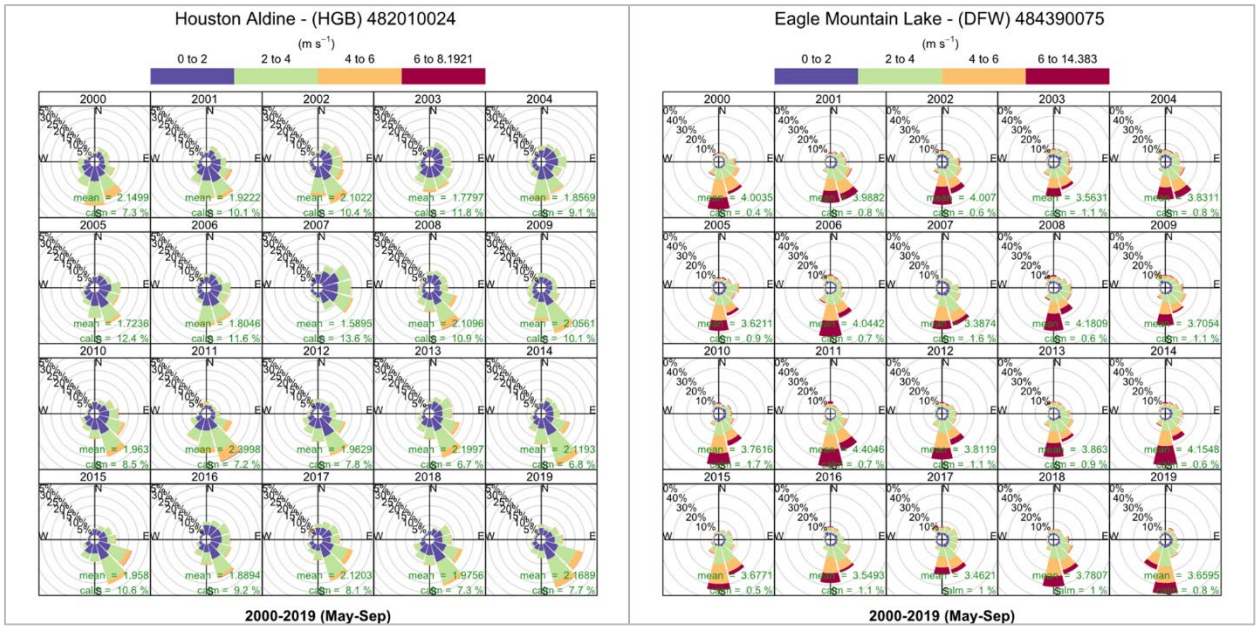

Figure 1-3: Wind Roses from 2000 through 2019 for the Houston Aldine and Eagle Mountain Lake Monitors

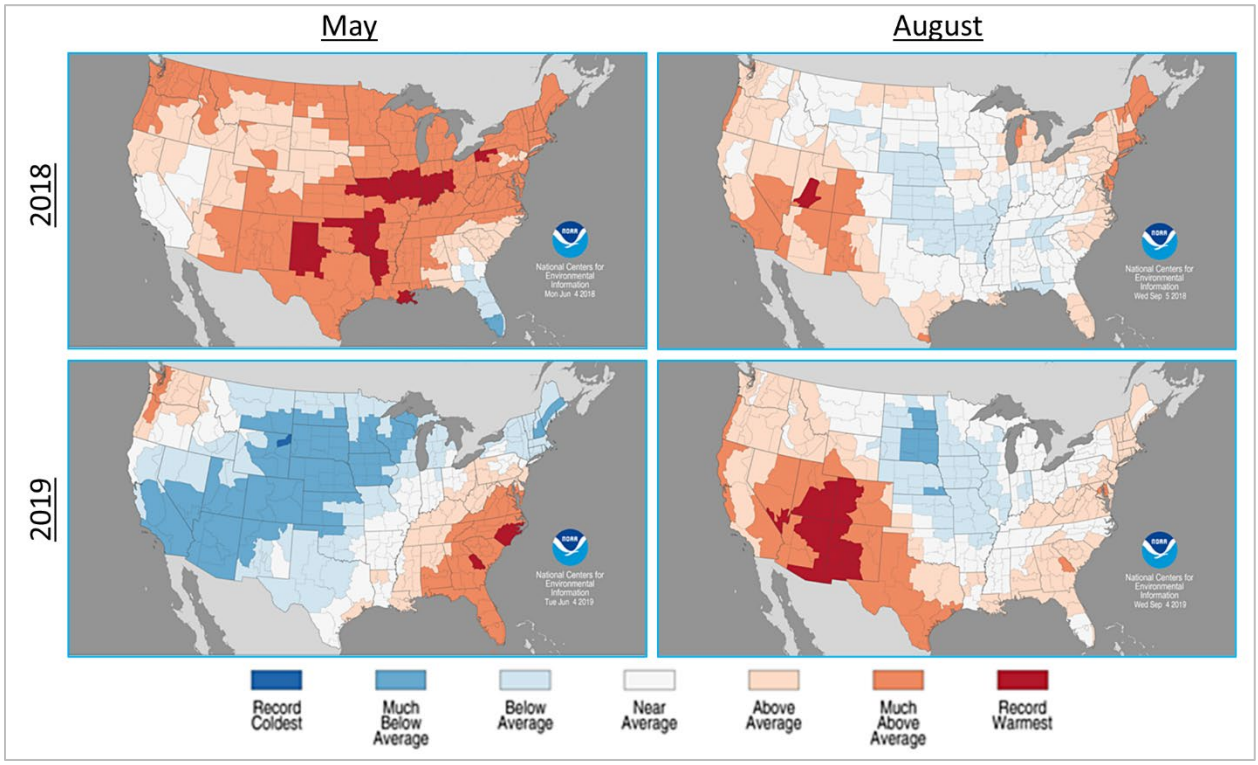

Figure 1-4: Divisional Maximum Temperature Ranks from 1895 through 2019 for May and August in 2018 and 2019

From the TCEQ's assessment of the ozone exceedances and meteorological patterns, the April through October 2019 episode was the best available episode for the TCEQ modeling platform. This seven-month episode has sufficient exceedance days for both the 2015 and 2008 eight-hour ozone NAAQS (223 and 82 days, respectively). Exceedances in HGB and DFW nonattainment areas follow the expected temporal pattern, and 2019 meteorology is representative of typical ozone-forming conditions. All but one monitor in DFW have at least five days with a monitored MDA8 value greater than 60 ppb. 2019 was the latest year with complete data, and the modeling platform will remain representative in terms of emissions and fleet characteristics for longer.

1.3 MODEL SELECTION

The TCEQ used the CAMx version 7.20 for this AD modeling.

1.4 CAMX MODELING DOMAINS

CAMx was configured with three nested domains: a 36-kilometer (km) grid resolution domain (named na_36km) covering most of North America, a 12 km grid resolution domain (named us_12km) covering continental United States, and a four km grid resolution domain (named txs_4km) covering central and east Texas. Dimensions of the CAMx domains are shown in Table 1-1: *CAMx Horizontal Domain Parameters*. The geographical extent of each domain is shown in Figure 1-5: *CAMx Modeling Domains*. Bexar County, DFW, and HGB are contained within tx_4km, the finest resolution domain. Each CAMx domain has 30 vertical layers that reach up to over 18 km, the resolution of layers decreases with increasing distance from the surface layer, details of which are presented Section 2: *Meteorological Modeling* of this appendix.

Table 1-1: CAMx Horizontal Domain Parameters

Domain Name	Range West to East (km)	Range South to North (km)	Number of Cells West to East	Number of Cells South to North	Cell Size (km)
na_36km	-2,952 to 3,240	-2,772 to 2,556	172	148	36
us_12km	-2,412 to 2,340	-1,620 to 1,332	396	246	12
txs_4km	-324 to 432	-1,584 to -648	189	234	4

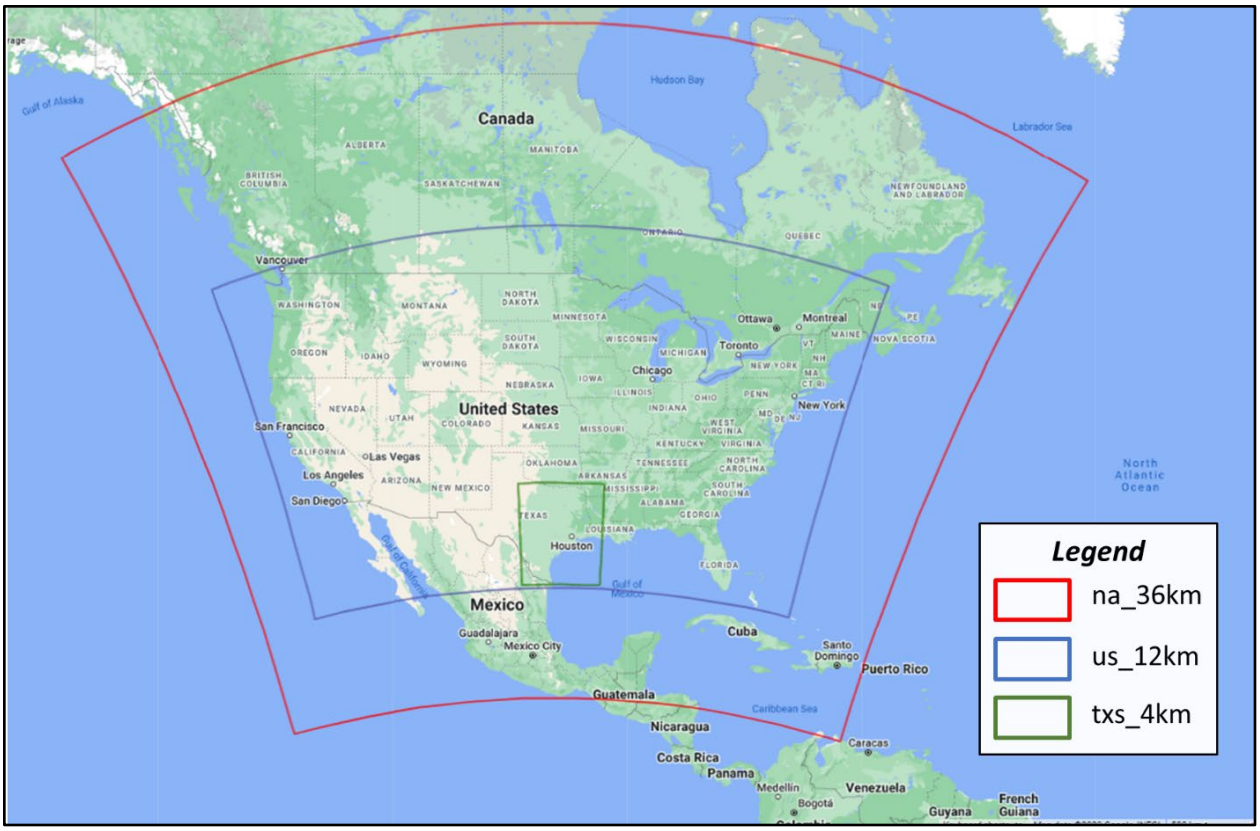

Figure 1-5: CAMx Modeling Domains

1.5 CAMX OPTIONS

The TCEQ used the CAMx options summarized in Table 1-2: *CAMx Configuration Options*.

Table 1-2: CAMx Configuration Options

CAMx Option	Option Selected
Time Zone	Coordinated Universal Time
Chemistry Mechanism	Carbon Bond version 6 revision 5 gas-phase mechanism (CB6r5)
Photolysis Mechanism	Tropospheric Ultraviolet and Visible radiative transfer model, version 4.8, with Total Ozone Mapping Spectrometer ozone column data
Chemistry Solver	Euler-Backward Iterative
Dry Deposition Scheme	Zhang03
Vertical Diffusion	K-theory
Iodine Emissions	Oceanic iodine emission computed from saltwater masks

The TCEQ chose the above options after evaluating model performance for different configurations as discussed in Section 5.1.4: *Evaluation of CAMx Configuration Options* of this appendix.

2. METEOROLOGICAL MODELING

Meteorological parameters during the modeling episode in the 2019 are one of the key inputs to the photochemical model. The TCEQ used version 4.1.5 of the Weather Research and Forecasting (WRF) model to generate the meteorological inputs for the photochemical modeling supporting these SIP revisions. The WRF run for the 2019 modeling platform was done for March 15, 2019 through November 1, 2019.

WRF was configured with a single 12 kilometer (km) horizontal grid resolution that covered most of north America, named nca_12km. A second 4 km fine grid domain, named txe_4km, covering the eastern half of Texas was also utilized. This 4 km fine grid domain focused on metropolitan areas classified as nonattainment under one or more of the eight-hour ozone NAAQS. Figure 2-1: *WRF Modeling Domain,* shows the geographic expanse of the two WRF domains and their nested configuration. Each WRF grid embeds a corresponding photochemical grid of the same horizontal resolution.

Figure 2-1: WRF Modeling Domain

The easting and northing ranges and number of grid points for each grid in the Lambert conformal conic (LCC) projection are defined in Table 2-1: *WRF Modeling Domain Definitions* with range in units of km.

Table 2-1: WRF Modeling Domain Definitions

Domain Name	Grid Resolution (km)	West to East Range (km)	South to North Range (km)	East/West Grid Points
nca_12km	12	(-3492, 3492)	(-3024, 3024)	583
txe_4km	4	(-420, 552)	(-1644, -492)	244

Table 2-2: *Vertical Layer Structure for the txe_4km Domain*, provides details regarding the heights and thickness of the vertical layers in WRF, with distance in meters above ground level (AGL), for the 4km domain that covers all of central and east Texas.

Table 2-2: Vertical Layer Structure for the txe_4km Domain

WRF Layer	Sigma Level	Top (m AGL)	Center (m AGL)	Thickness (m)
44	0.000	20,508	19,978	1,060
43	0.010	19,448	18,803	1,290
42	0.025	18,158	17,478	1,359
41	0.045	16,799	16,248	1,102
40	0.065	15,697	15,120	1,154
39	0.090	14,543	14,050	986
38	0.115	13,557	13,043	1,028
37	0.145	12,529	12,076	905
36	0.175	11,624	11,152	943
35	0.210	10,681	10,200	962
34	0.250	9,719	9,286	866
33	0.290	8,853	8,459	788
32	0.330	8,064	7,702	725
31	0.370	7,340	7,045	590
30	0.405	6,750	6,472	554
29	0.440	6,195	5,934	523
28	0.475	5,672	5,425	495
27	0.510	5,177	4,975	405
26	0.540	4,772	4,578	388
25	0.570	4,384	4,197	374
24	0.600	4,010	3,830	360
23	0.630	3,650	3,476	348
22	0.660	3,302	3,134	336
21	0.690	2,966	2,803	326
20	0.720	2,640	2,483	316
19	0.750	2,325	2,197	256
18	0.775	2,069	1,944	250
17	0.800	1,819	1,697	244
16	0.825	1,575	1,455	239
15	0.850	1,336	1,265	141
14	0.865	1,195	1,126	139
13	0.880	1,056	987	137
12	0.895	919	851	136

WRF Layer	Sigma Level	Top (m AGL)	Center (m AGL)	Thickness (m)
11	0.910	783	738	90
10	0.920	693	649	89
9	0.930	604	560	88
8	0.940	516	472	88
7	0.950	429	385	87
6	0.960	342	298	86
5	0.970	255	212	86
4	0.980	170	127	85
3	0.990	84	59	51
2	0.996	34	25	17
1	0.998	17	8	17
0	1.000	0	0	0

The WRF vertical layer structure is intended to provide high resolution in the lowest part of the atmosphere where pollutant mixing is critical, as shown in Figure 2-2: *WRF Vertical Layer Structure for the txe_4km Domain* with distance in meters AGL. Of the total 44 layers, 22 are less than 3500 AGL. A similar but slightly different WRF vertical layer structure is used for the 12km domain. The difference occurs because the center points in the two domains are at different ground-level air pressure and the top of the domains are at the same air pressure. Splitting both domains into the same number of layers results in different height boundaries between vertical layers. Though the WRF domains have 42 vertical layers extending to over 20 km from the Earth's surface, CAMx has 30 vertical layers reaching 18 km above surface. The lowest CAMx layer corresponds to the first two WRF layers. CAMx layers 2 through 21 align with the WRF domain. Layers 22 through 30 of the CAMx domain encompass multiple WRF layers as displayed in Figure 2-2: *WRF and CAMx Vertical Layers for the respective 4km Domains*.

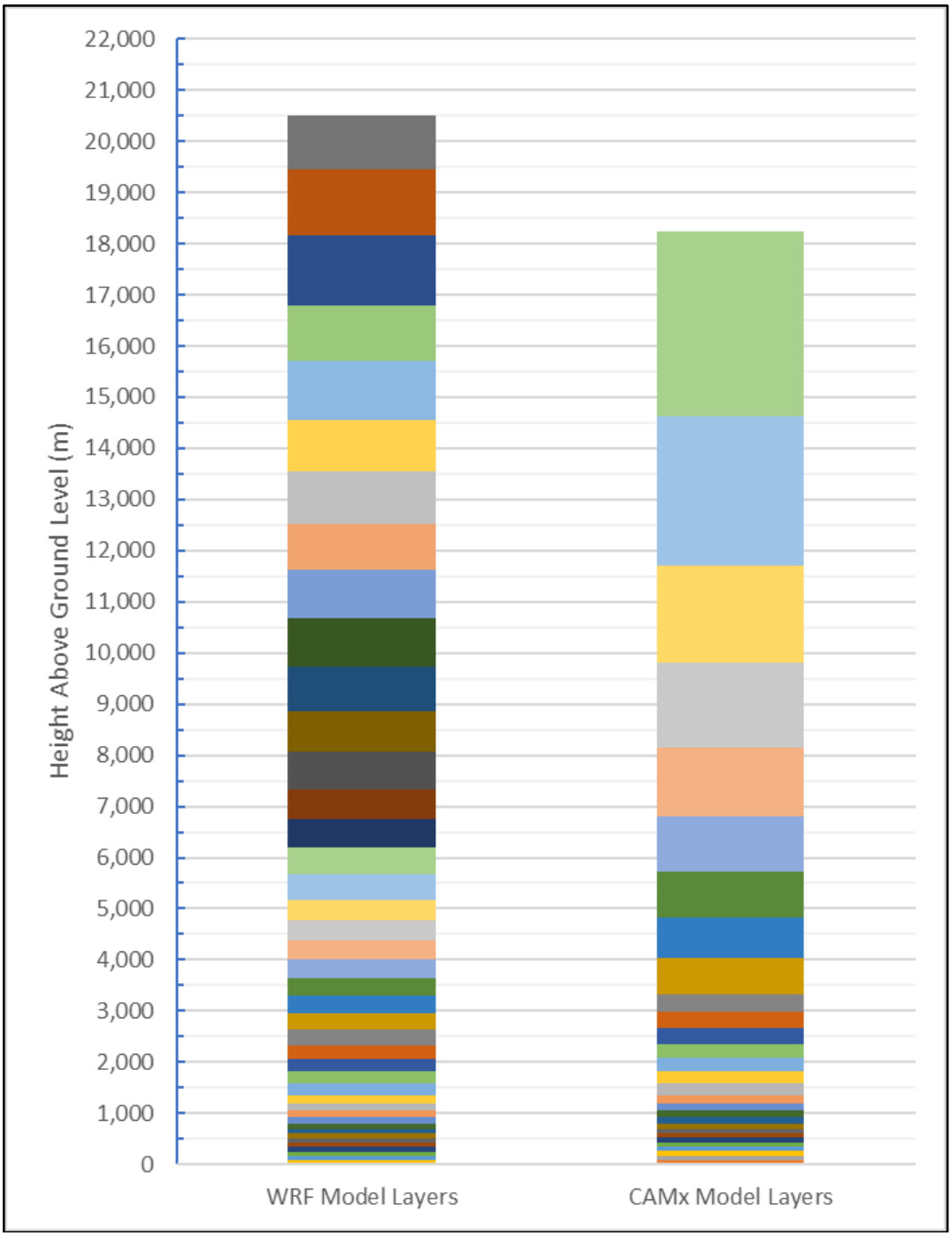

Figure 2-2: WRF and CAMx Vertical Layers for the respective 4km Domains

2.1 WRF PREPROCESSING SYSTEM (WPS)

The preparation of WRF input files involves the execution of different modules within the WPS as described below.

GEOGRID defines the WRF grids on a LCC Projection and allocates the Land Use/Land Cover (LULC) data that was included in the WRF v3.7.1 release.

European Re-Analysis Interim (ERA-Interim) archived by the European Centre for Medium-Range Weather Forecast (ECMWF) has the highest temporal resolution (three-hour as well as six-hour) and extends to 50 millibars (mb) and is used for processing into initial and boundary conditions for the months of March through August 2019. The ERA-Interim reanalysis data stopped being produced on 31 August 2019. The ERA5 data replaced the ERA-Interim reanalysis data and was used to create initial and boundary conditions to model the months after August 2019.

UNGRIB unpacks the Gridded Binary (GRIB) files with surface- and upper-level meteorological data to standard pressure levels native to ERA-Interim and ERA-5.

METGRID re-gridded the unpacked data onto the WRF grids defined in GEOGRID into a Network Common Data Form (NetCDF) format.

An optional program, OBSGRID, was used to develop the WRF Surface Four-Dimensional Data Assimilation (WRFSFDDA) for the 4 km inner grid. In addition to generating the surface nudging files, new gridded data files consistent with the surface analysis replace the gridded met data for the 4 km grid generated by the METGRID program. Furthermore, running the WRF model with the Pleim-Xiu (PX) land surface model with soil nudging requires the WRFSFDDA file.

The Real program defined the WRF sigma level vertical structure (Table 2-2) and mapped the archived data retrieved on pressure levels to the sigma levels defined by the WRF user, consistent with surface land use data and definitions of the upper atmosphere. Base state variables were set to Texas summer values: 1013 hPa sea-level pressure, a reference temperature lapse rate of 45 (K/ln p), and a 304 degrees K sea-level temperature. The Real program produced the WRF initial condition files, boundary condition files, and WRF Four-Dimensional Data Assimilation (WRFFDDA) nudging files, where the four dimensions are three spatial dimensions plus time.

2.2 WRF MODEL CONFIGURATION

The selection of the final meteorological modeling configuration for the April through October 2019 episode resulted from numerous sensitivity tests and WRF model performance evaluation. The final WRF parameterization schemes and options selected are shown in Table 2-3: *WRF Configuration*.

Table 2-3: WRF Configuration

Domain	Nudging Type	PBL	Cumulus	Radiation	Land-Surface	Microphysics
nca_12km	3-D Analysis	YSU	Kain-Fritsch	RRTMG/Dudhia	Noah	WSM6
txe_4km	3-D, Surface Analysis	YSU	Kain-Fritsch	RRTMG/Dudhia	Noah	WSM6

Note: RRTM = Rapid Radiative Transfer Model

WRF output was post-processed using the WRFCAMx version 5.1 utility to convert the WRF meteorological fields for input to CAMx. The WRFCAMx generates several alternative vertical diffusivity (K_v) files based upon multiple methodologies for

estimating mixing given the same WRF meteorological fields. The WRF K_v option based upon the Community Multiscale Air Quality Modeling PBL profile was selected.

2.3 WRF MODEL PERFORMANCE EVALUATION (MPE)

To evaluate the performance of WRF, comparisons to observed data are made. For surface data, observed data from the TCEQ Continuous Air Monitoring Stations (CAMS) are used for comparison with WRF modeled output. During the 2019 modeling period, there were 42 CAMS sites are in the HGB, 20 CAMS sites in DFW and 16 in the greater San Antonio metropolitan area that includes Bexar County. This appendix focuses on WRF model performance during those periods within the 2019 modeling episode months that had overlapping exceedance days for the Bexar County, DFW, and HGB nonattainment areas.

For each nonattainment area, the monthly average statistics for wind speed, wind direction, temperature and humidity are displayed using “soccer plot” displays. Each soccer plot displays the bias in the x axis and the error in the y axis. For the wind speed, the root mean square error (RMSE) is used instead of the error. Each soccer plot also displays the threshold for acceptable performance for simple conditions in blue and complex (terrain) conditions in red. Statistical symbols within the benchmark goals indicate acceptable performance. In each soccer plot for each area, wind speed is depicted in the top left, wind direction is depicted in the top right, temperature is depicted in the bottom left, and humidity is depicted in the bottom right.

This section of the appendix provides details of the WRF MPE conducted for each nonattainment area and the conclusions drawn.

2.3.1 HGB

The distribution of monitors with meteorological observations in HGB are shown in Figure 2-3: *HGB CAMS Sites*.

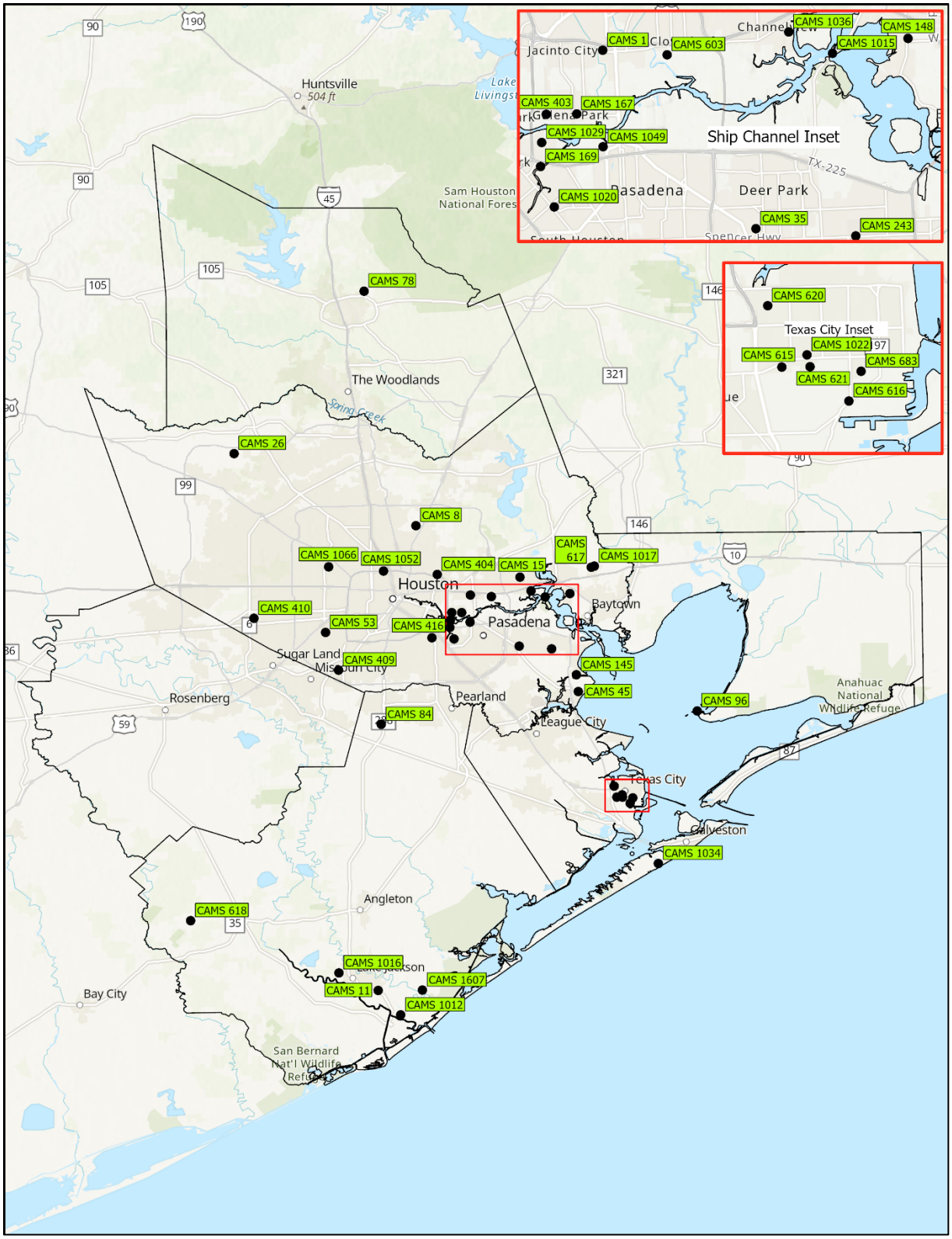

Figure 2-3: HGB CAMS Sites

Soccer plots comparing monthly bias and error for temperature, wind direction, and humidity, and a soccer plot comparing monthly bias and RMSE for wind speed for HGB

are shown in Figure 2-4: *Soccer Plot for HGB Area Average for Wind Speed, Wind Direction, Temperature, and Humidity.*

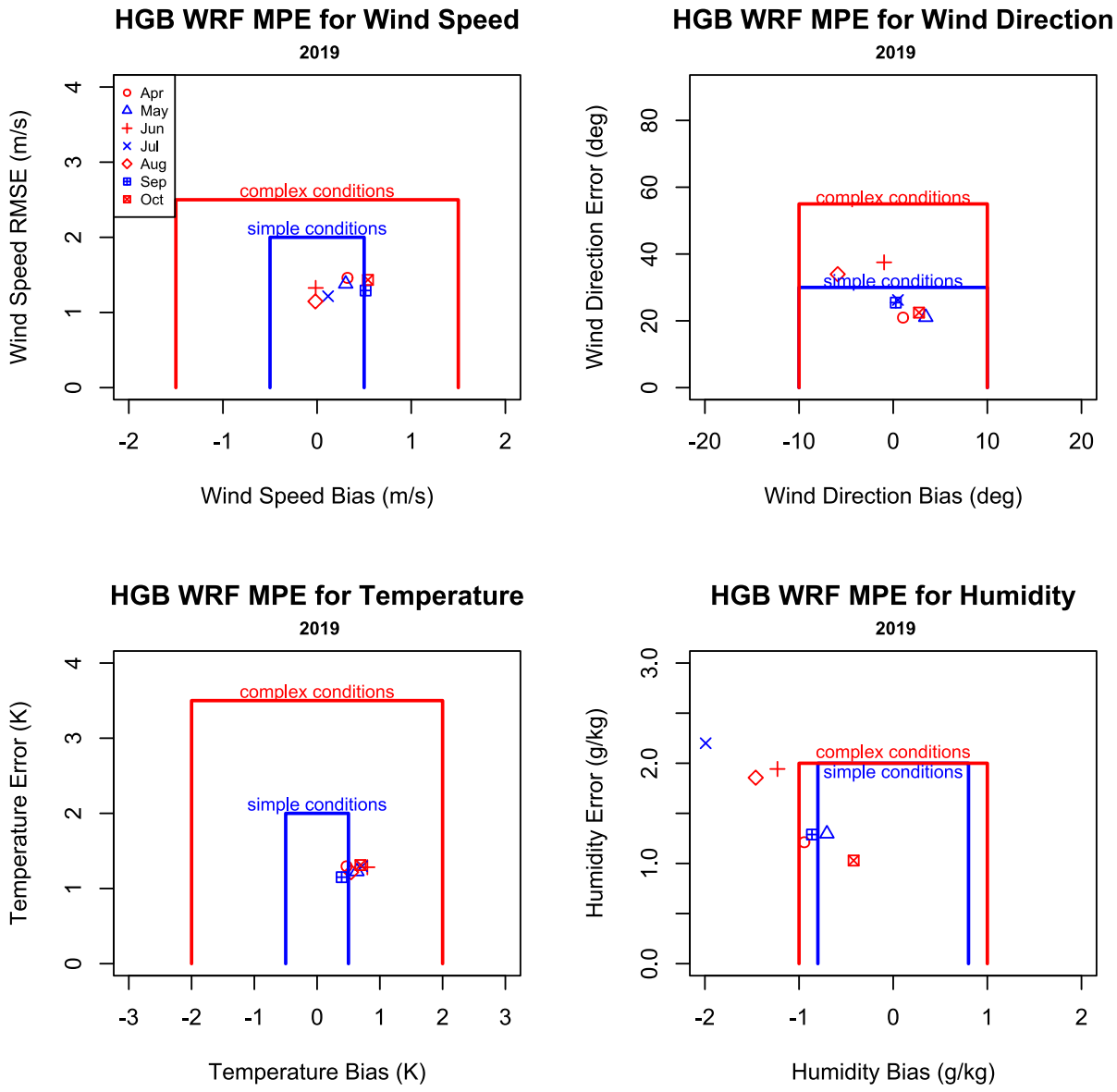

Figure 2-4: Soccer Plot for HGB Area Average for Wind Speed, Wind Direction, Temperature, and Humidity

The monthly performance for the wind speed (top left of Figure 2-4) shows a bias less than 0.5 m/s and meets the simple benchmark (≤±0.5 m/s) for all episode months. The RMSE for all months are between 1 and 2 m/s which is within the simple benchmark (2.0 m/s). For wind direction (top right of Figure 2-4), the soccer plots show that the wind direction errors for all months are within the 30 degrees simple benchmark. In case of temperatures (bottom left of Figure 2-4), the plot shows that April and September with a bias within the simple benchmark (≤±0.5 K). The remaining months have biases less than 1K. The error for all seven months is within the simple

benchmark (2 K). For Humidity, the plot shows that except for June, July, and August all monthly humidity biases are within the complex benchmark for bias (≤±2.0 g/kg). Except for July, all monthly humidity errors are within the simple/complex benchmark (< 2.0 g/kg).

Monthly statistics for HGB is summarized in Table 2-4: *HGB Meteorological Modeling Percent Accuracy for Wind* and Table 2-5*: HBG Meteorological Modeling Percent Accuracy for Temperature and Humidity*. The first performance benchmark for each parameter has been consistently used to characterize desirable performance (Emery, 2001). The tighter bounds for wind direction, wind speed, and temperature are also included. Given the general complex meteorology along the Texas coast, these statistics are considered reasonably robust. The lower percent accuracy performance for the humidity for June and July 2019 is because of the limited number of CAMS sites in HGB that measure humidity. June, July, and August are the same three months that had the largest errors with July not meeting the benchmark for the simple/complex error for humidity as displayed in the lower right Figure 2-4.

Table 2-4: HGB Meteorological Modeling Percent Accuracy for Wind

Month	Wind Direction Error ≤ 30 deg (%)	Wind Direction Error ≤ 20 deg (%)	Wind Direction Error ≤ 10 deg (%)	Wind Speed Error ≤ 2 m/s (%)	Wind Speed Error ≤ 1 m/s (%)	Wind Speed Error ≤ 0.5 m/s (%)
Apr	81.50	68.20	41.70	83.80	52.70	28.70
May	81.60	68.40	42.50	86.40	55.00	29.30
Jun	61.30	48.60	28.10	88.30	60.20	33.40
Jul	73.30	58.30	33.60	90.10	62.20	35.00
Aug	64.00	49.60	27.80	92.30	64.20	35.80
Sep	74.00	59.10	34.80	89.00	59.60	33.10
Oct	78.40	65.20	39.50	85.60	57.80	32.60

Table 2-5: HBG Meteorological Modeling Percent Accuracy for Temperature and Humidity

Month	Temperature Error ≤ 2 K (%)	Temperature Error ≤ 1 K (%)	Temperature Error ≤ 0.5 K (%)	Humidity Error ≤ 2 g/kg (%)	Humidity Error ≤ 1 g/kg (%)	Humidity Error ≤ 0.5 g/kg (%)
Apr	78.60	47.00	25.40	83.40	49.60	24.60
May	80.80	50.90	29.40	78.00	46.90	24.40
Jun	80.20	49.10	26.70	59.80	31.90	16.10
Jul	80.80	49.50	26.60	57.40	33.00	15.90
Aug	82.50	53.40	29.10	62.30	39.40	21.60
Sep	83.70	52.40	28.60	80.10	49.00	25.50
Oct	81.50	49.00	25.70	87.60	59.40	33.90

2.3.2 DFW

The distribution of monitors with meteorological observations in DFW are shown in Figure 2-5: *DFW CAMS Sites*.

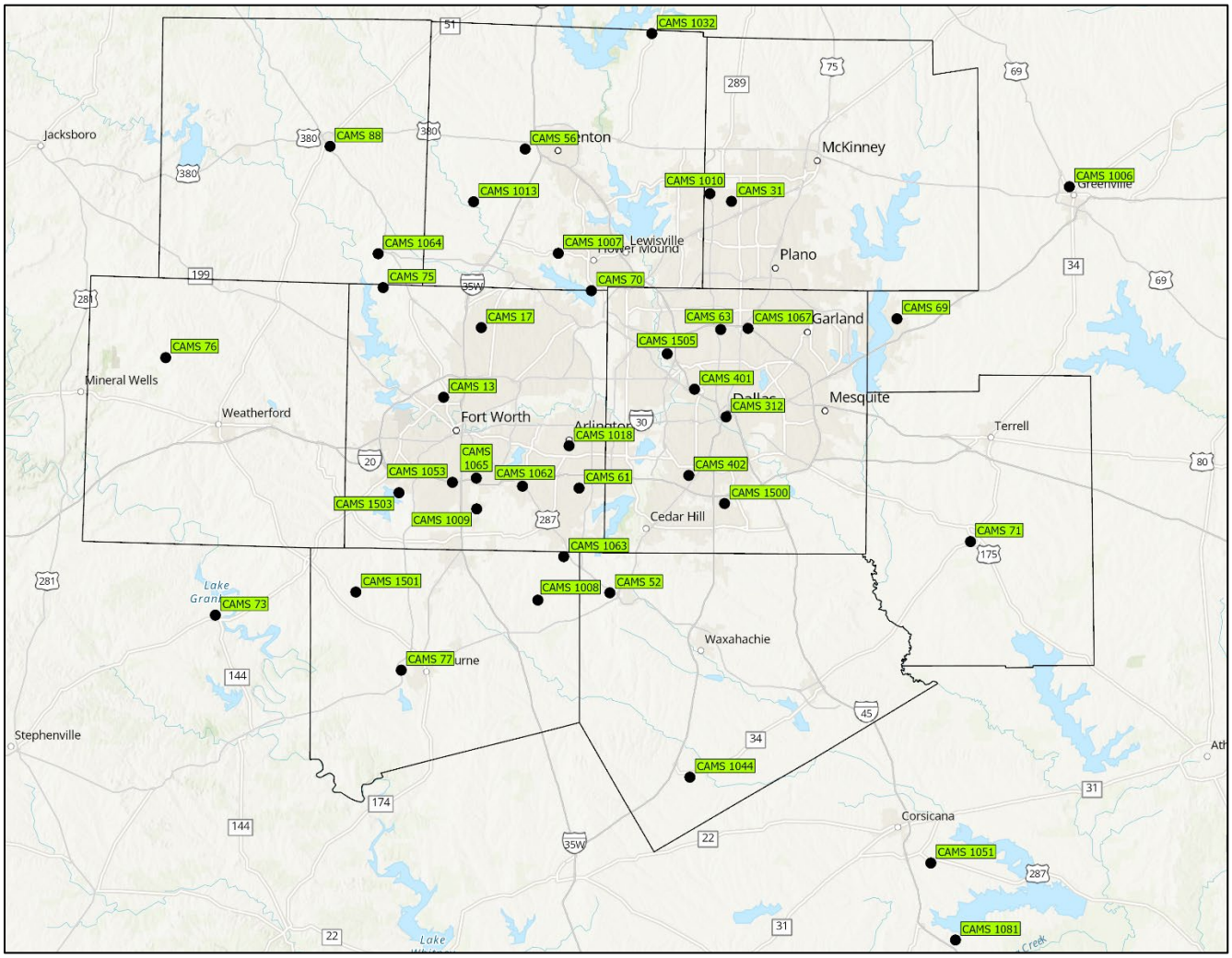

Figure 2-5: DFW CAMS Sites

Soccer plots comparing monthly bias and error for temperature, wind direction, and humidity, and a soccer plot comparing monthly bias and RMSE for wind speed for DFW are shown in Figure 2-6: *Soccer Plot for DFW Domain Area for Wind Speed, Wind Direction, Temperature, and Humidity*.

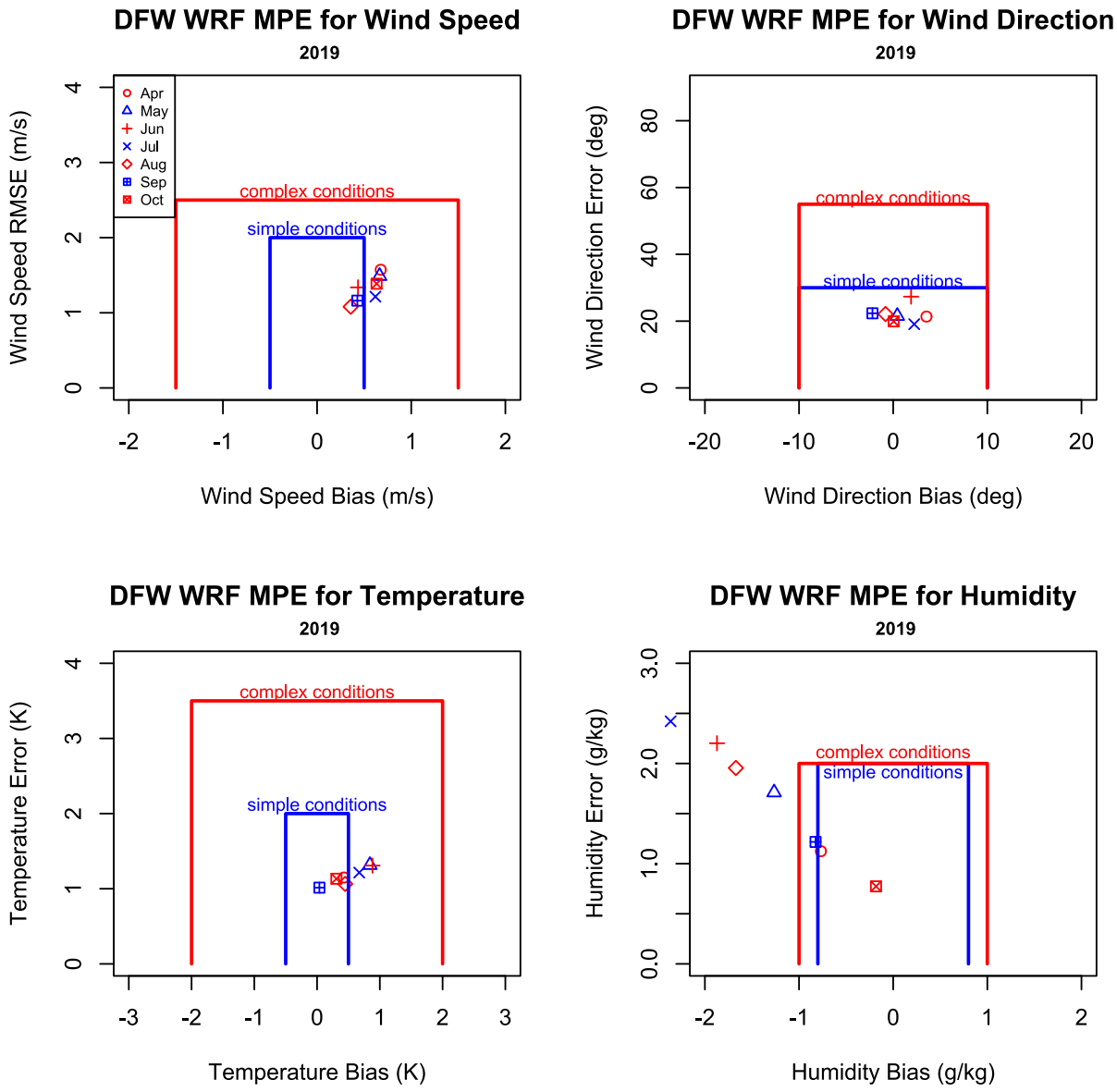

Figure 2-6: Soccer Plot for DFW Area for Wind Speed, Wind Direction, Temperature, and Humidity

The monthly performance for the wind speed has a bias between 0.4 and 0.7 m/s with three months meeting the simple benchmark and four meeting the complex benchmark. The RMSE for all months are between 1 and 2 m/s and are within the simple benchmark (2.0 m/s). For wind direction performance (upper right), the soccer plot shows a bias between -2.2 to 3.5 degrees that is within the simple/complex benchmark (≤±10 degrees) goal. The seven months had errors within the 30 degrees simple benchmark and ranging between 19.1 to 27.3 degrees. The plot also displays monthly temperature performance (lower left) where April, August, September, and October 2019 show a bias between 0.0 and 0.5 K, which is within the simple benchmark (≤±0.5 K). May, June, and July of 2019 showed biases between 0.5 and 1.0 K, which is between the simple and complex benchmarks. The error for all seven months is between 1.0 and 1.3 K, which is within the simple benchmark (2 K). For the

monthly humidity performance (lower right), April, September, and October had biases between -0.2 and -0.8 g/kg (within the complex benchmark). The remaining four months had values that were outside the complex benchmark. April, May, August, September, and October had errors within the simple/complex benchmark (< 2.0 g/kg). June and July had errors greater than 2.0 g/kg. The limited number of CAMS sites in DFW (1 or 2) that record the humidity on any given day may have contributed to some of the larger errors.

Monthly statistics for DFW is summarized in Table 2-6: *DFW Meteorological Modeling Percent Accuracy for Wind* and Table 2-7: *DFW Meteorological Modeling Percent Accuracy for Temperature and Humidity.* Like the HGB performance, the DFW performance statistics are also considered reasonably robust. The DFW area has a limited number of CAMS sites that record humidity. This is reflected in the lower percent accuracy performance for humidity for May, June, and July 2019. Note that these are the same three months that did not meet the benchmark for the simple/complex error for humidity for DFW as displayed in the lower right of Figure 2-6.

Table 2-6: DFW Meteorological Modeling Percent Accuracy for Wind

Month	Wind Direction Error ≤ 30 deg (%)	Wind Direction Error ≤ 20 deg (%)	Wind Direction Error ≤ 10 deg (%)	Wind Speed Error ≤ 2 m/s (%)	Wind Speed Error ≤ 1 m/s (%)	Wind Speed Error ≤ 0.5 m/s (%)
Apr	80.80	69.30	44.70	82.20	50.60	26.60
May	80.90	68.80	44.40	82.80	52.40	28.50
Jun	72.00	58.30	36.20	87.20	58.50	32.50
Jul	84.00	71.30	44.50	90.00	59.40	33.00
Aug	78.40	64.70	39.50	94.00	67.20	37.90
Sep	78.80	66.80	42.40	91.30	62.70	35.30
Oct	82.10	69.90	45.60	86.00	56.30	31.00

Table 2-7: DFW Meteorological Modeling Percent Accuracy for Temperature and Humidity

Month	Temperature Error ≤ 2 K (%)	Temperature Error ≤ 1 K (%)	Temperature Error ≤ 0.5 K (%)	Humidity Error ≤ 2 g/kg (%)	Humidity Error ≤ 1 g/kg (%)	Humidity Error ≤ 0.5 g/kg (%)
Apr	85.30	52.80	28.00	85.40	53.20	24.00
May	82.00	52.00	26.90	66.30	37.30	19.60
Jun	82.00	49.90	26.40	51.30	27.80	13.90
Jul	84.30	53.30	28.20	45.90	22.30	10.80
Aug	89.10	59.00	31.40	57.20	32.00	17.80
Sep	89.00	60.30	33.10	79.70	52.30	28.80
Oct	85.70	55.50	29.40	92.60	74.40	48.60

2.3.3 Bexar County

The distribution of monitors in Bexar and adjacent counties that make up the San Antonio metropolitan area (SAN) that were used to evaluate WRF performance in and near Bexar County are shown in Figure 2-7: *Bexar and Adjacent Counties CAMS Sites.*

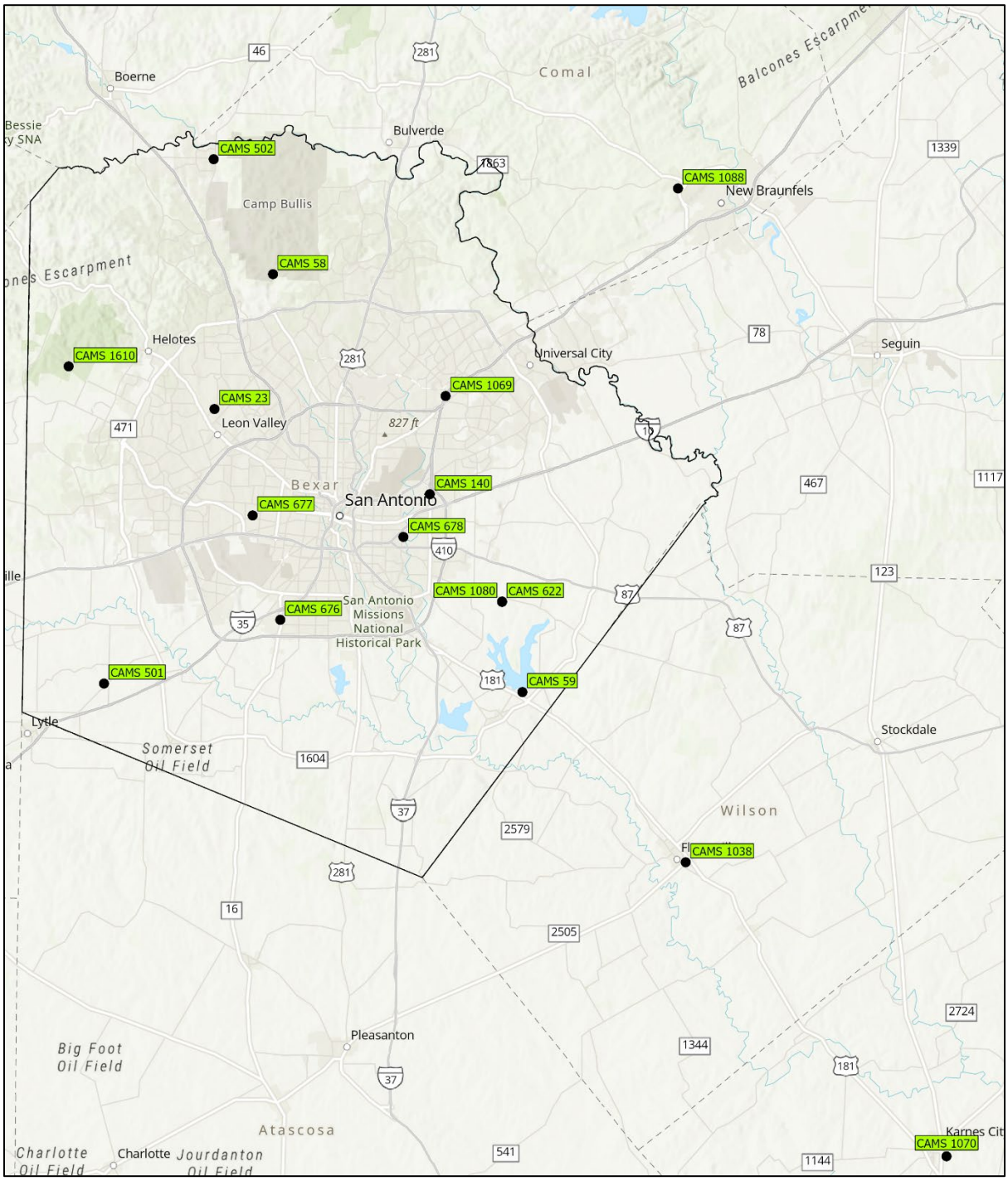

Figure 2-7: Bexar and Adjacent Counties CAMS Sites

Soccer plots comparing monthly bias and error for temperature, wind direction, and humidity, and a soccer plot comparing monthly bias and RMSE for wind speed for Bexar and adjacent counties are shown in Figure 2-8: *Soccer Plot for Bexar and Adjacent Counties Average for Wind Speed, Wind Direction, Temperature, and Humidity.*

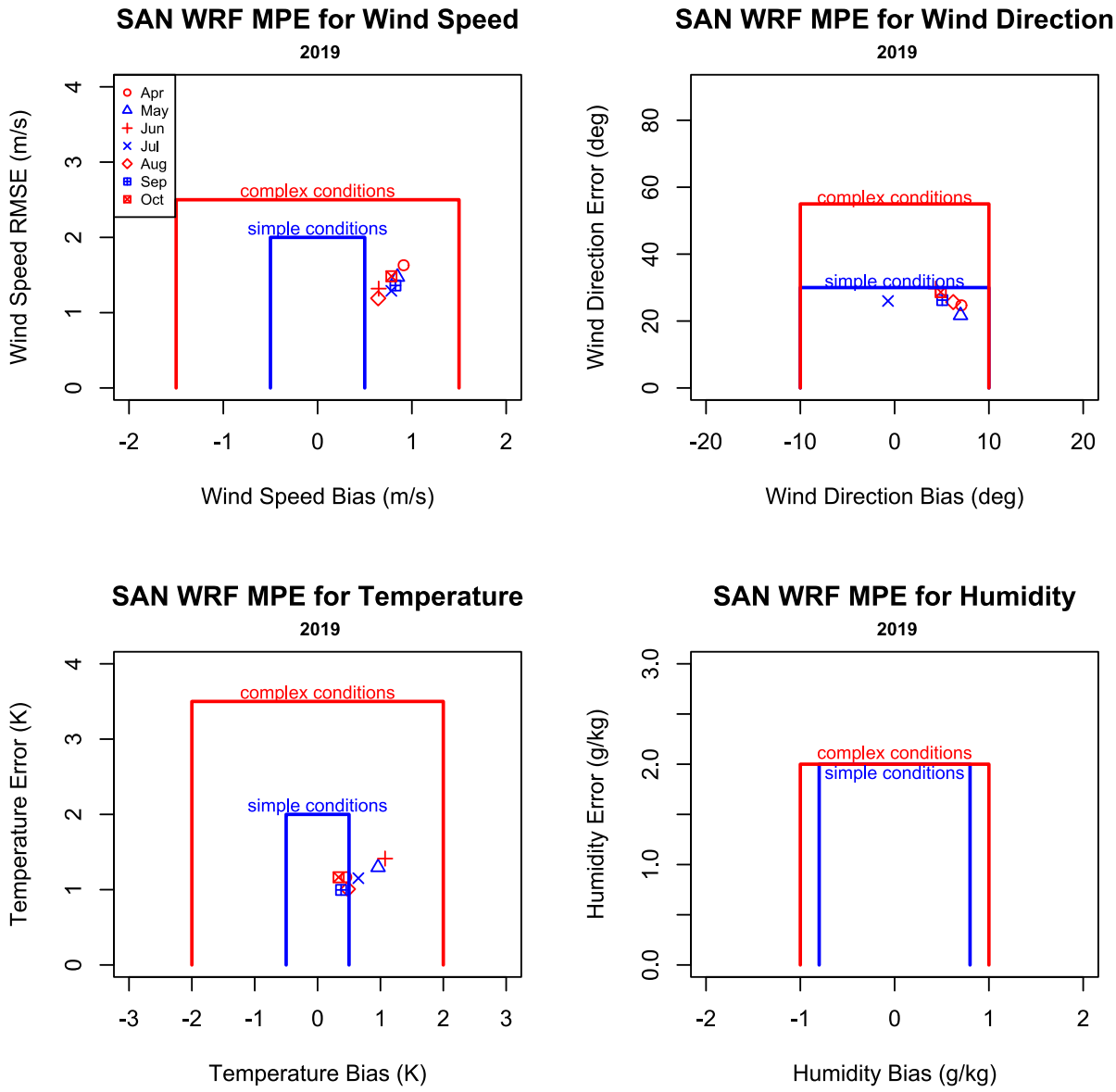

Figure 2-8: Soccer Plot for Bexar and Adjacent Counties Average for Wind Speed, Wind Direction, Temperature, and Humidity

The performance for the average wind speed has a bias of 0.8 m/s which is slightly higher than the 0.5 m/s simple benchmark but less than the complex benchmark. The average RMSE for July is 1.3 m/s and is within the simple benchmark (2.0 m/s). For wind direction performance (upper right), there is a bias of -0.7 deg. and an error of 26.0 deg. which are within the simple/complex benchmark goal. For temperature

performance (lower left), there is a bias of 0.6 K, which is slightly greater than the simple benchmark (≤±0.5 K), but less than the complex benchmark (≤±1.0 K). The error is 1.2 K which is less than simple benchmarks of 2.0 K. For humidity performance (lower right), the bias and the error are not calculated as there are not CAMS sites reporting humidity in Bexar for July.

Table 2-8: Bexar and Adjacent Counties Meteorological Modeling Percent Accuracy for Wind

Month	Wind Direction Error ≤ 30 deg (%)	Wind Direction Error ≤ 20 deg (%)	Wind Direction Error ≤ 10 deg (%)	Wind Speed Error ≤ 2 m/s (%)	Wind Speed Error ≤ 1 m/s (%)	Wind Speed Error ≤ 0.5 m/s (%)
Apr	77.00	64.70	40.30	81.00	49.00	25.90
May	80.60	69.10	43.60	83.50	52.00	27.60
June	69.20	56.10	34.10	88.10	58.00	31.70
July	77.20	65.00	40.40	88.30	55.90	29.80
Aug	74.80	63.20	39.70	91.10	61.10	33.20
Sep	74.90	61.90	37.60	87.10	56.00	31.20
Oct	72.20	59.60	36.40	85.10	57.50	32.10

Monthly statistics for Bexar and adjacent counties are summarized in Table 2-8: *Bexar and Adjacent Counties Meteorological Modeling Percent Accuracy for Wind* and Table 2-9: *Bexar and Adjacent Counties Meteorological Modeling Percent Accuracy for Temperature*. These statistics are considered reasonably robust.

Table 2-9: Bexar and Adjacent Counties Meteorological Modeling Percent Accuracy for Temperature

Month	Temperature Error ≤2 K (%)	Temperature Error ≤1 K (%)	Temperature Error ≤0.5 K (%)
Apr	83.20	52.40	28.20
May	79.30	46.20	23.10
Jun	78.70	46.00	24.00
Jul	86.30	48.70	25.00
Aug	90.30	57.40	30.30
Sep	90.20	59.40	31.60
Oct	84.30	57.00	30.60

WRF modeling of the 2019 modeling episode consistently provided good area-wide performance across several metrics. This meteorology was considered suitable for input into photochemical modeling.

3. EMISSIONS MODELING

3.1 BIOGENIC EMISSIONS

Biogenic sources are trees, shrubs, grasses, and soils that emit nitrogen oxides (NO_X), volatile organic compounds (VOC), and/or aerosols.

The TCEQ used version 3.7 of the Biogenic Emission Inventory System (BEIS) within Sparse Matrix Operation Kernel Emissions (SMOKE) System version 4.8 with stand-alone meteorology data to estimate the modeling emissions from vegetation. The CB6 VOC speciation profiles are included within SMOKE. Other BEIS inputs were downloaded from the Community Modeling and Analysis System (CMAS) Data Warehouse[1] and the Biogenic Emission Landuse Database version 5 (BELD5). The "aggwndw" utility program within SMOKE was used to create the grid-specific land-use input files. The na_12km emission output files from SMOKE were post-processed to derive the na_36km and us_12km CAMx-ready files. The WRF outputs were processed with the Meteorology-Chemistry Interface Processor (MCIP) version V5.1 FROZEN 11/21/2019 to generate the 2-D cross-point surface meteorology data, 3-D dot-point layered meteorology data, and 2-D grid parameters needed by BEIS.

The BEIS model was run for each day of the 2019 modeling episode, including ramp up days. Since biogenic emissions are dependent upon the meteorological conditions on a given day, the same episode specific emissions for the 2019 base case were used in the 2023 future case modeling. Figure 3-1: *Daily Total Isoprene Biogenic Emissions for June 12, 2019*, Figure 3-2: *Daily Total VOC Biogenic Emissions for June 12, 2019*, Figure 3-3: *Daily Total NO_X Biogenic Emissions for June 12, 2019* displays the spatial distribution of daily isoprene, total VOC, and total NO_X emission totals for the us_12km domain on June 12, 2019.

[1] https://drive.google.com/drive/folders/1v3i0iH3lqW36oyN9aytfkczkX5hl-zF0

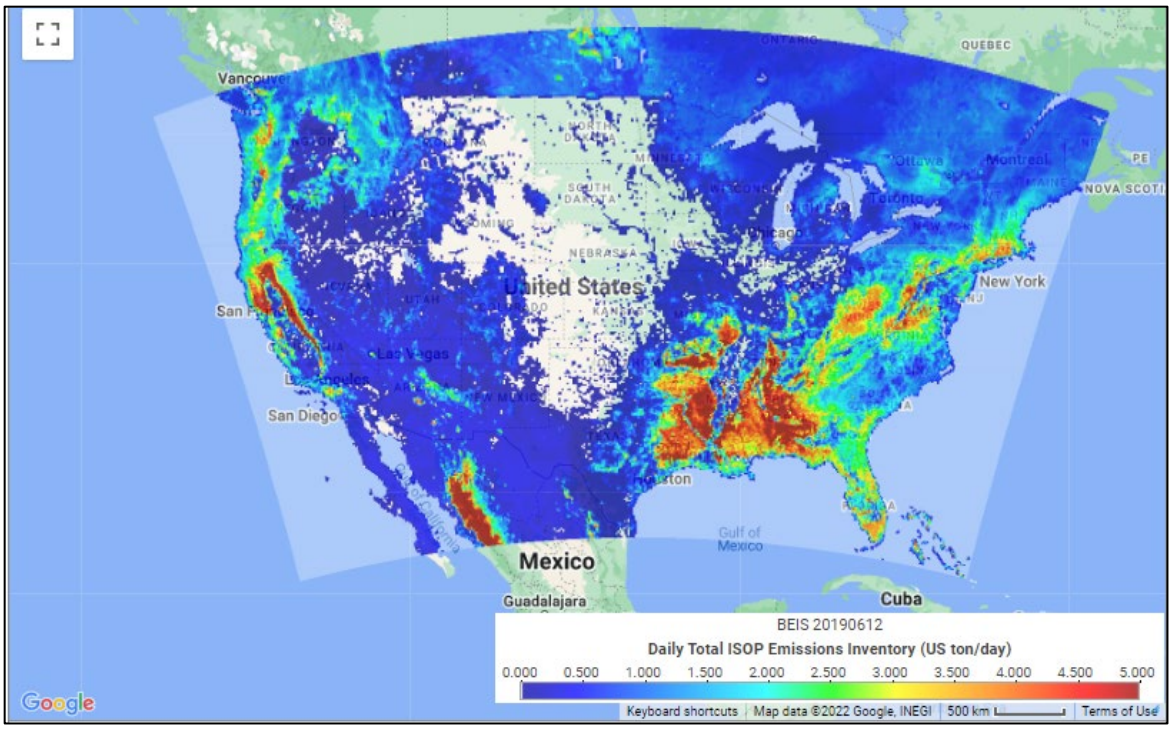

Figure 3-1: Daily Total Isoprene Biogenic Emissions for June 12, 2019

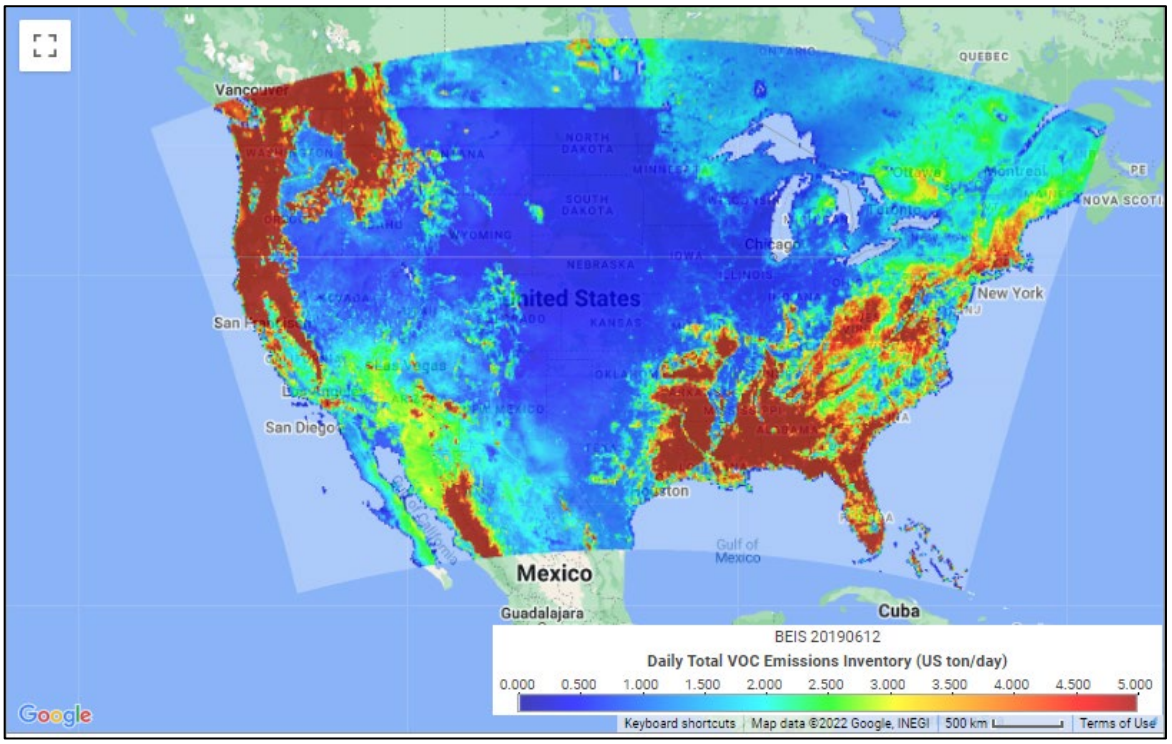

Figure 3-2: Daily Total VOC Biogenic Emissions for June 12, 2019

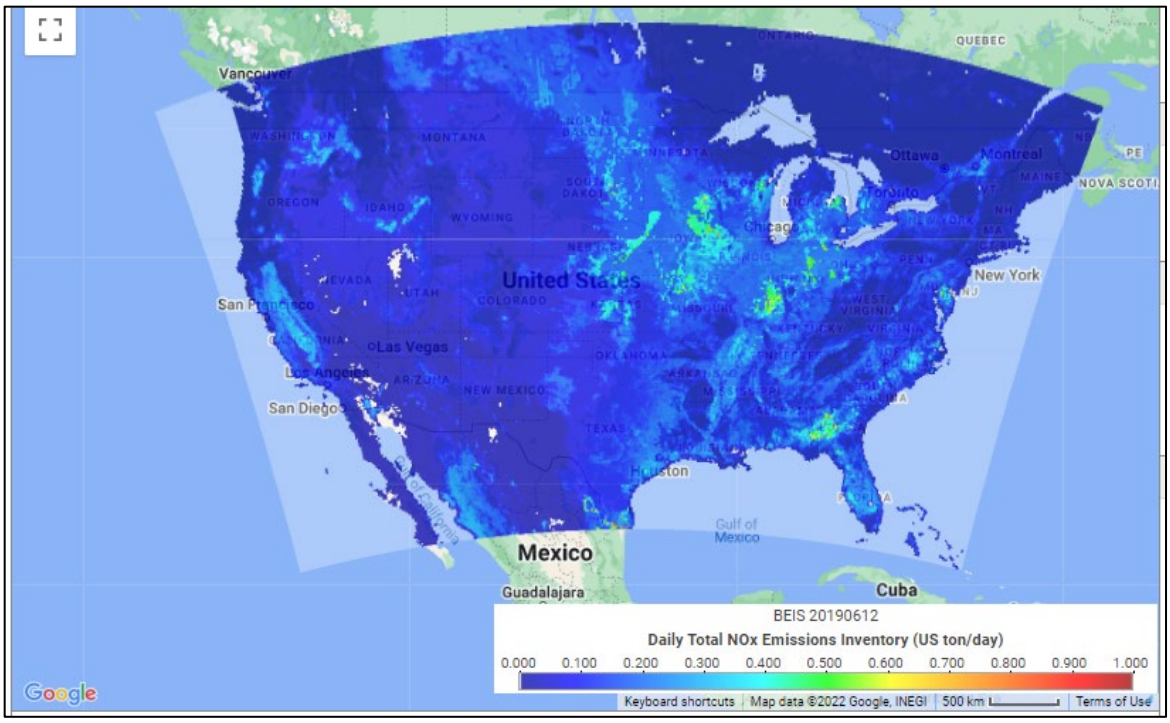

Figure 3-3: Daily Total NO_x Biogenic Emissions for June 12, 2019

3.2 FIRE EMISSIONS

The TCEQ used the Fire Inventory from NCAR version 2.2 (FINNv2.2; Weidinmyer et al., 2022; Kimura et al., 2019) modeling system to obtain CAMx ready fire emissions for the TCEQ 2019 modeling platform.

FINNv2.2 fire emissions data were downloaded from the data portal on the National Center for Atmospheric Research's website[2] by selecting fire count type 'MODIS + VIIRS', year '2019', and speciation type 'MOZART'. These selections provided fire emissions data for 2019 based on active fire satellite detections from both the Moderate Resolution Imaging Spectroradiometer (MODIS) and Visible Infrared Imaging Radiometer Suite (VIIRS) satellite instruments, with chemical speciation from Model for Ozone and Related chemical Tracers (MOZART-T1).

The downloaded FINN fire estimates were then processed through two programs to extract emissions from the desired na_36km domain, re-project the fire locations to the Lambert Conformal Conic projection, remap chemical species from MOZART-T1 to Carbon Bond version 6 revision 4 (CB6r4), and group fires that were within 5 km. Each fire was then treated as a point source and processed using the Emissions Processing System version 3 (EPS3). The fire emissions were temporally allocated using a diurnal profile developed by Randerson et al. (2012), and vertically distributed based on the Western Regional Air Partnership Fire Emissions Joint Forum (WRAP-FEJF).

The FINNv2.2 model was run for each day of the 2019 episode, including ramp up days. Since fire emissions are dependent upon a given day, the same episode specific

[2] https://www.acom.ucar.edu/Data/fire/

fire emissions for the 2019 base case were used in the 2023 future case modeling. Below, Figure 3-4: *Daily Total VOC Fire Emissions for June 12, 2019* and Figure 3-5: *Daily Total NO_X Fire Emissions for June 12, 2019* are the daily totals of NO_x and VOC emissions from fires for June 12, 2019.

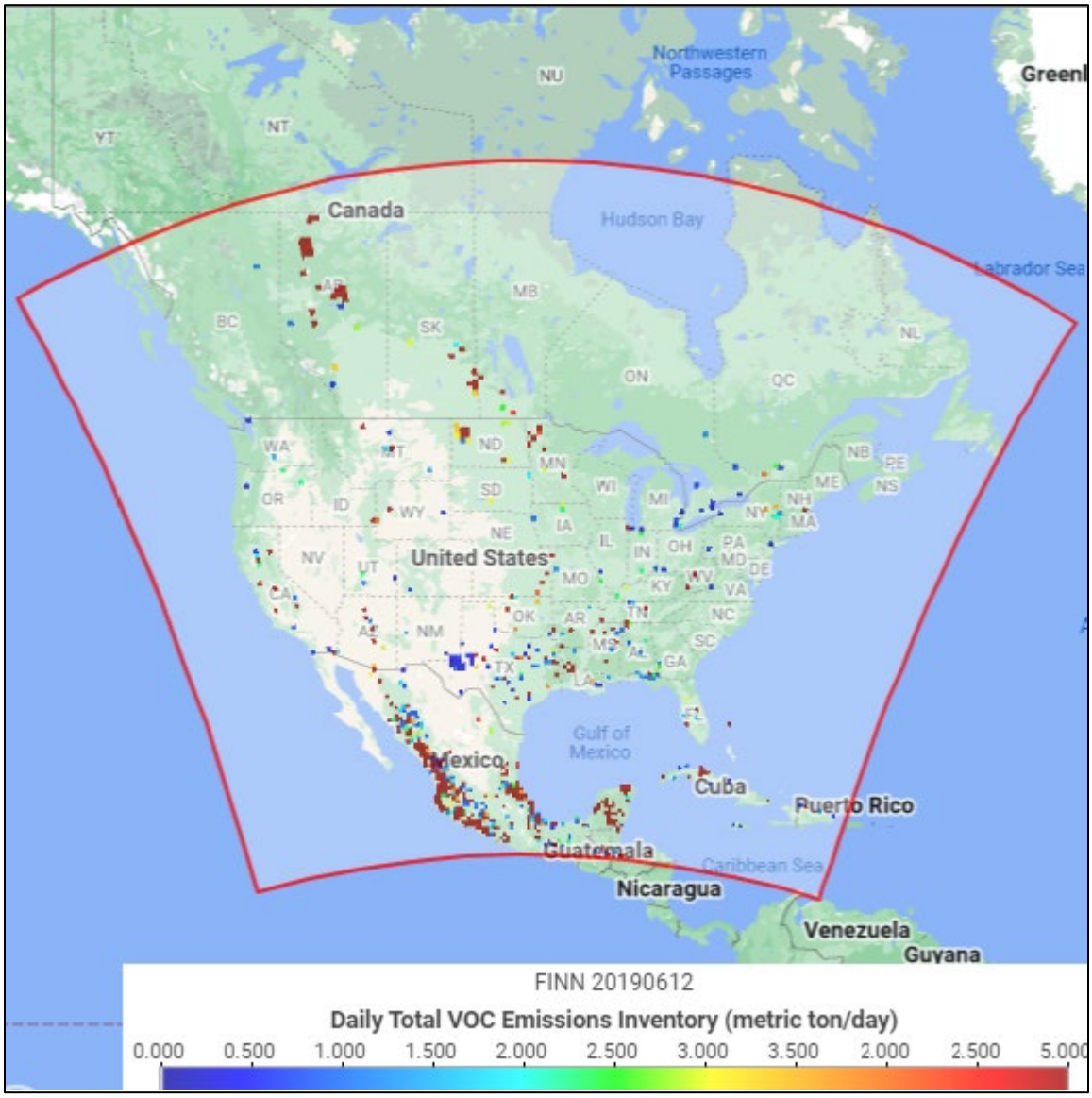

Figure 3-4: Daily Total VOC Fire Emissions for June 12, 2019

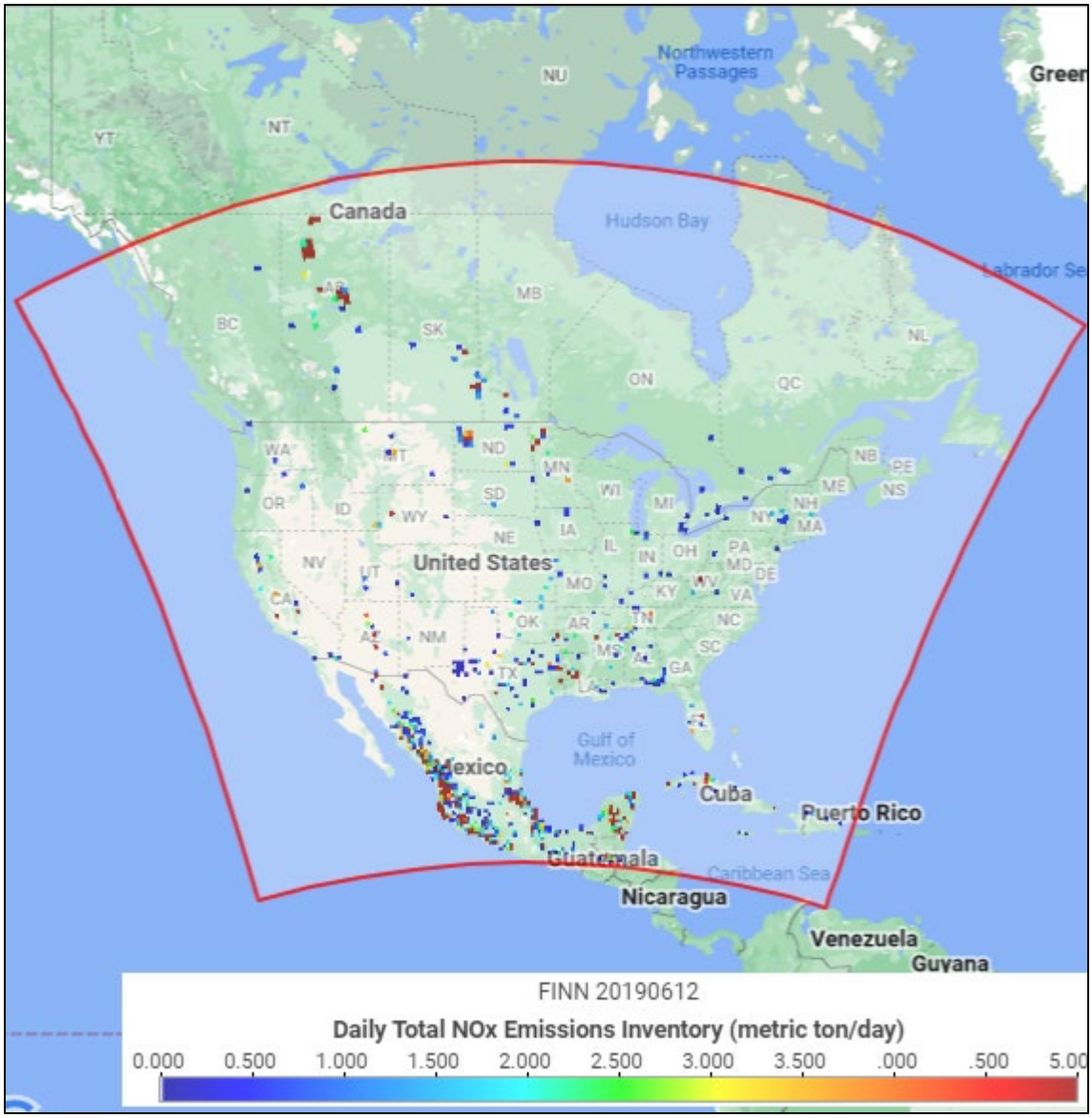

Figure 3-5: Daily Total NO_x Fire Emissions for June 12, 2019

3.3 POINT SOURCES

The point source category includes large stationary sources of emissions, such as electric generating units (EGU), smelters, industrial boilers, petroleum refineries, and manufacturing facilities. Point source emissions were developed for the April 1 through October 31, 2019, ozone modeling episode. The data sources for development of the point source modeling emissions are summarized in Table 3-1: *Sources of Point Source Emissions Data.* The data were compiled and formatted to generate modeling datasets for the 2019 base case and 2023 future case model runs as detailed in subsequent sections.

Table 3-1: Sources of Point Source Emissions Data

Sources of Data	Calendar Year(s) Used
TCEQ State of Texas Air Reporting System (STARS)	2019 Reported Emissions
TCEQ Mass Emissions Cap and Trade (MECT)	2023 Program Cap and Available Allocation
TCEQ Highly Reactive Volatile Organic Compounds (HRVOC) Emissions Cap and Trade (HECT)	2023 Program Cap and Available Allocation
Environmental Protection Agency (EPA) - Clean Air Markets Program Data (CAMPD) for all states	2019 Hourly Reported Emissions for EGU
EPA Cross-State Air Pollution Rule (CSAPR) allocations for applicable states	2023 State Budgets
Electric Reliability Council of Texas (ERCOT) Capacity, Demand, and Reserve report	2022
TCEQ Air Permits for proposed EGUs	2022
U.S. Department of the Interior Emissions Inventory (EI) of offshore platforms	2017 EI data
EPA's 2016 Modeling Platform Version 1 (2016v1 platform)	2016 and projected 2023 EI data for non-Texas including Canada and Mexico

The TCEQ used EPS3 to process the emissions in the AIRS Facility Subsystem (AFS) file into a format ready for CAMx input. EPS3 processing of point source emissions is divided into low-level and elevated streams. A plume cutoff height of 30 meters was chosen to divide the point sources into low-level and elevated categories to correspond to the 34-meter height of the first CAMx model layer. This division allows for merging of low-level files, and for a better distribution of elevated emissions prior to mixing and reacting with surface emissions within CAMx. For all EGUs and Non-EGUs in nonattainment areas, a plume cutoff of 0.1 meter was used to "force" all emissions as elevated to facilitate emissions tracking.

This subsection provides details of emissions inventory development for point sources in the continental United States, Gulf of Mexico, and Mexico and Canada. Details of emissions for point sources in other countries within the CAMx modeling domain are detailed in section 3.9: *Other Countries.*

3.3.1 Continental United States (CONUS)

3.3.1.1 EGU Point Sources

In the TCEQ's modeling, point sources located in the CONUS with emissions reported the EPA's CAMPD website form the EGU sector. Under the Clean Air Act's several cap-and-trade programs, EGUs are required to report their emissions of sulfur dioxide (SO_2), NO_X, and carbon dioxide (CO_2), along with other parameters such as heat input collected using continuous emissions monitoring systems (CEMS). The EPA's CAMPD quality assures the reported raw hourly data and provides datasets and a query wizard

on the CAMPD website[3] for downloading the data. Missing or invalid hourly data that arise from CEMS equipment problems are handled by the EPA using specific substitution criteria. To develop base case modeling emissions for EGU in the U.S., hourly records from CAMPD were used. The TCEQ downloaded hourly data from the EPA's CAMPD website for the contiguous lower 48 states for April through October 2019 which served as the basis for EGU emissions inventory development for both the base and future case as described below.

Within Texas

Base Case

For base case emissions of Texas units, the TCEQ used the 2019 CAMPD reported hourly emissions for NO_X and SO_2. Pollutant to heat input ratios were computed from the year 2019 STARS inventory annual emissions, and annual heat input from 2019 CAMPD for each unit for the following pollutants: volatile organic compound (VOC), ammonia (NH3), and carbon monoxide (CO). The ratios were multiplied by the hourly heat input from 2019 CAMPD to calculate the hourly pollutant emissions. The hourly EGU emissions records were collated into an AFS file format that can be processed with the modules of EPS3. Non-emissions parameters, such as stack parameters, were obtained from the TCEQ's STARS database. The TCEQ maintains a STARS-to-CAMPD cross reference file to assist with matching units between the two databases. CAMPD Texas units that match STARS were removed from the STARS dataset to avoid double counting of emissions.

[3] https://campd.epa.gov/data/custom-data-download

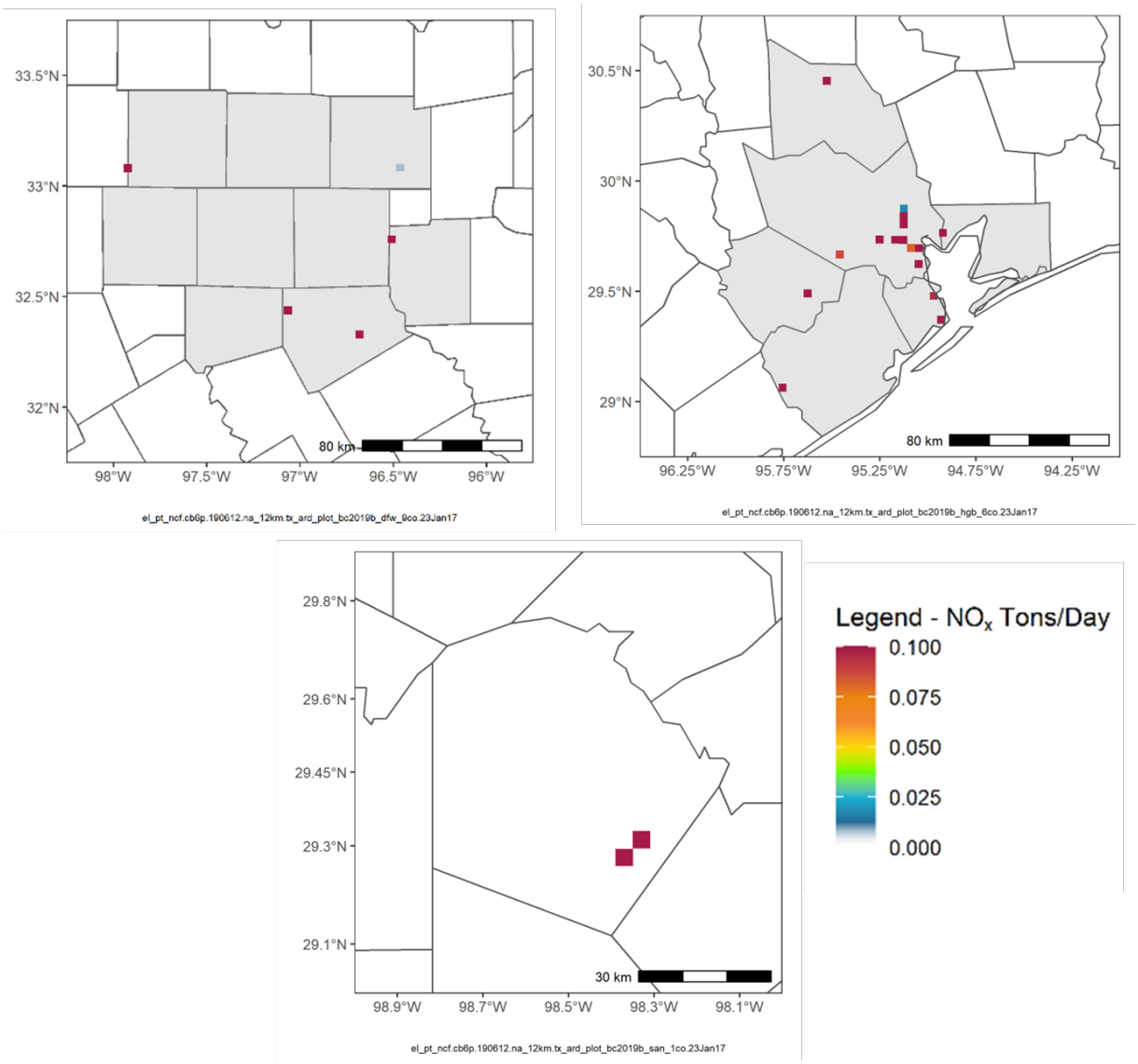

Figure 3-6: 2019 Base Case EGU NO_X Emissions in DFW (Top Left), HGB (Top Right), and Bexar County (Bottom Center) for June 12 Episode Day

Figure 3-6: *2019 Base Case EGU NO_X Emissions in DFW (Top Left), HGB (Top Right), and Bexar County (Bottom Center) for June 12 Episode Day* shows the spatial distribution of 2019 base case EGU NO_X emissions in tons per day as tile plots for the DFW, HGB, and Bexar County 2015 moderate eight-hour ozone nonattainment areas for the modeled episode day of June 12.

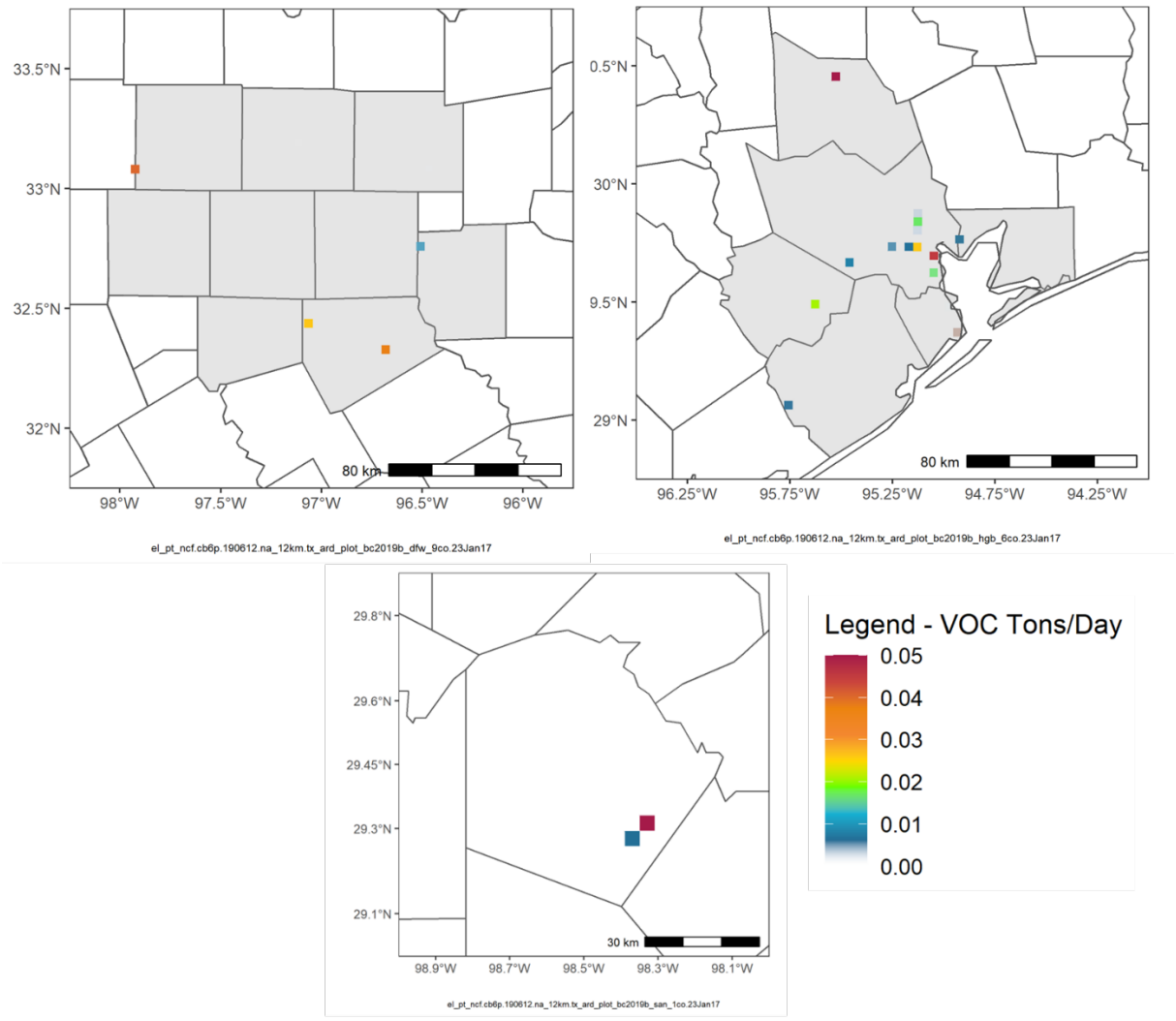

Figure 3-7: 2019 Base Case EGU VOC Emissions in DFW (Top Left), HGB (Top Right), and Bexar County (Bottom Center) for June 12 Episode Day

Figure 3-7: *2019 Base Case EGU VOC Emissions in DFW (Top Left), HGB (Top Right), and Bexar County (Bottom Center) for June 12 Episode Day* shows the spatial distribution of the 2019 base case EGU VOC emissions in tons per day as tile plots for the DFW, HGB, and Bexar County 2015 moderate eight-hour ozone nonattainment areas for the modeled episode day of June 12.

Future Case

Texas EGU emissions for 2023 were developed using the 2019 hourly base case as the projection base. Growth, retirements, and consideration of Cross-State Air Pollution Rule (CSAPR) requirements were included in the hourly 2023 emissions. The TCEQ assumes growth in EGU in Texas is accomplished with the addition of newly permitted EGU since 2019. EGU with planned retirement are also considered, and in combination with the new units, net growth was established.

Newly Permitted EGU

New EGU were identified by researching and compiling data from sources such as the Electric Reliability Council of Texas (ERCOT), TCEQ air permitting projects with combustion turbines, TCEQ New Source Review permits, and the U.S. Energy Information Administration (EIA). Newly permitted EGU emission rates were calculated based on the permit Maximum Allowable Emission Rates Table (MAERT). Emission rates for NO_X, VOC, CO, $PM_{2.5}$ and SO_2, stack parameters and location coordinates were obtained from permits. If available, maintenance, startup, and shutdown (MSS) emission limits were included in the rates. The temporal distributions of the newly permitted EGU emissions are based on those of existing units of similar equipment type or source classification codes (SCC).

Retirement of EGU

The TCEQ assumed that units with planned retirement dates prior to January 1, 2023, on EIA Form 860 (2020) or ERCOT's Capacity, Demand, and Reserves report (May 2021) would be retired.[4] EGU'scheduled to be mothballed or placed on Reliability Must Run (RMR) status were not removed.

CSAPR Update

EGU in Texas must meet the requirements of the CSAPR Update.[5] The CSAPR Update specified the ozone season NO_X emission for EGU in CSAPR Update states. The TCEQ scaled the applicable Texas 2019 CAMPD EGU ozone season NO_X emissions to the CSAPR Update ozone season state allocation cap, such that the CSAPR Update emission limit was modeled. Hourly 2019 CAMPD EGU emissions were used with no scaling for the months of April and October.

[4] https://www.ercot.com/files/docs/2022/05/16/CapacityDemandandReservesReport_May2022.pdf
[5] https://www.epa.gov/csapr/final-cross-state-air-pollution-rule-update

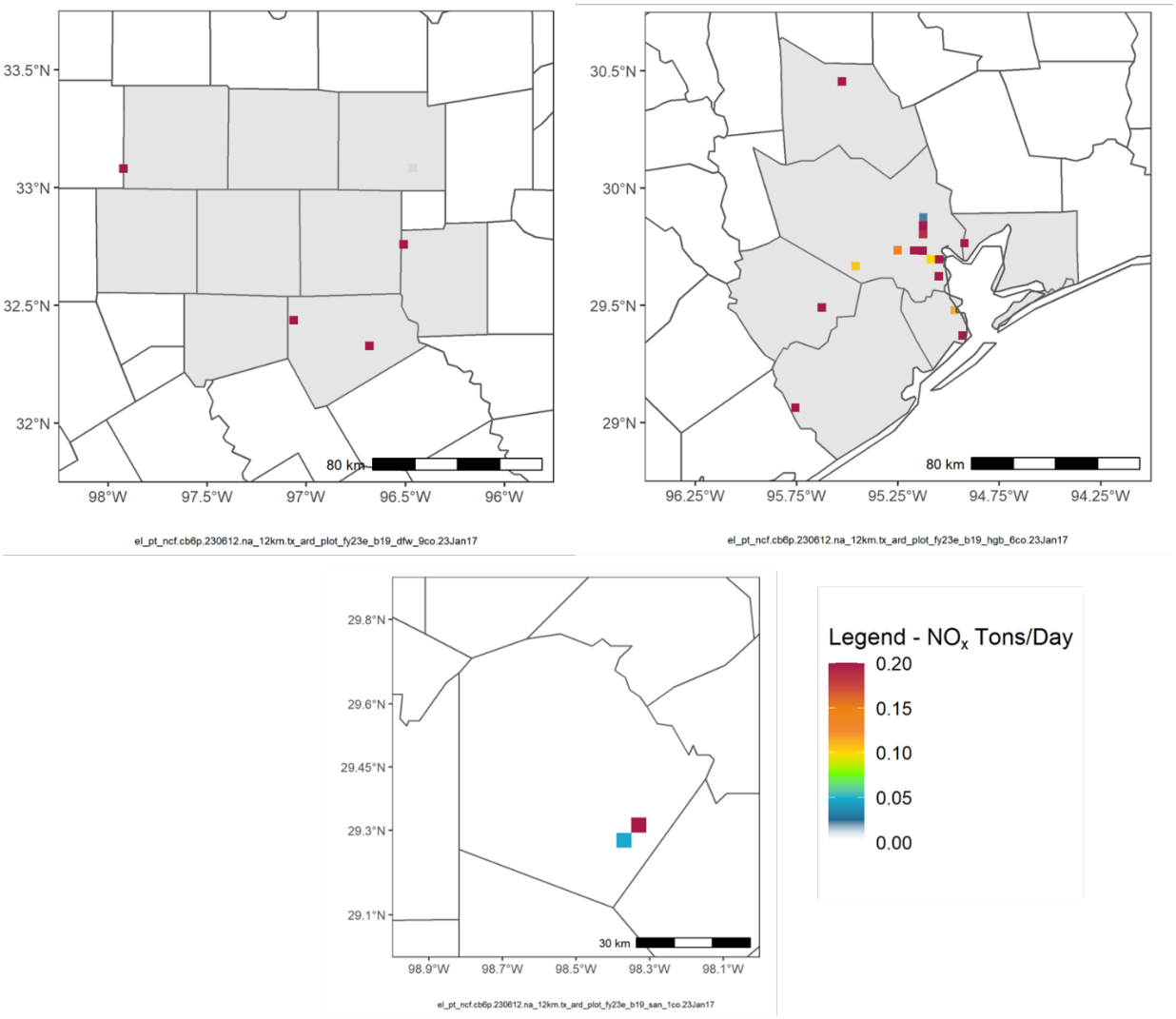

Figure 3-8: 2023 Future Case EGU NO_X Emissions in DFW (Top Left), HGB (Top Right), and Bexar County (Bottom Center) for June 12 Episode Day

Figure 3-8: *2023 Future Case EGU NO_X Emissions in DFW (Top Left), HGB (Top Right), and Bexar County (Bottom Center) for June 12 Episode Day* shows the spatial distribution of 2023 future case EGU NO_X emissions in tons per day as tile plots for the DFW, HGB, and Bexar County 2015 moderate eight-hour ozone nonattainment areas for the modeled episode day of June 12.

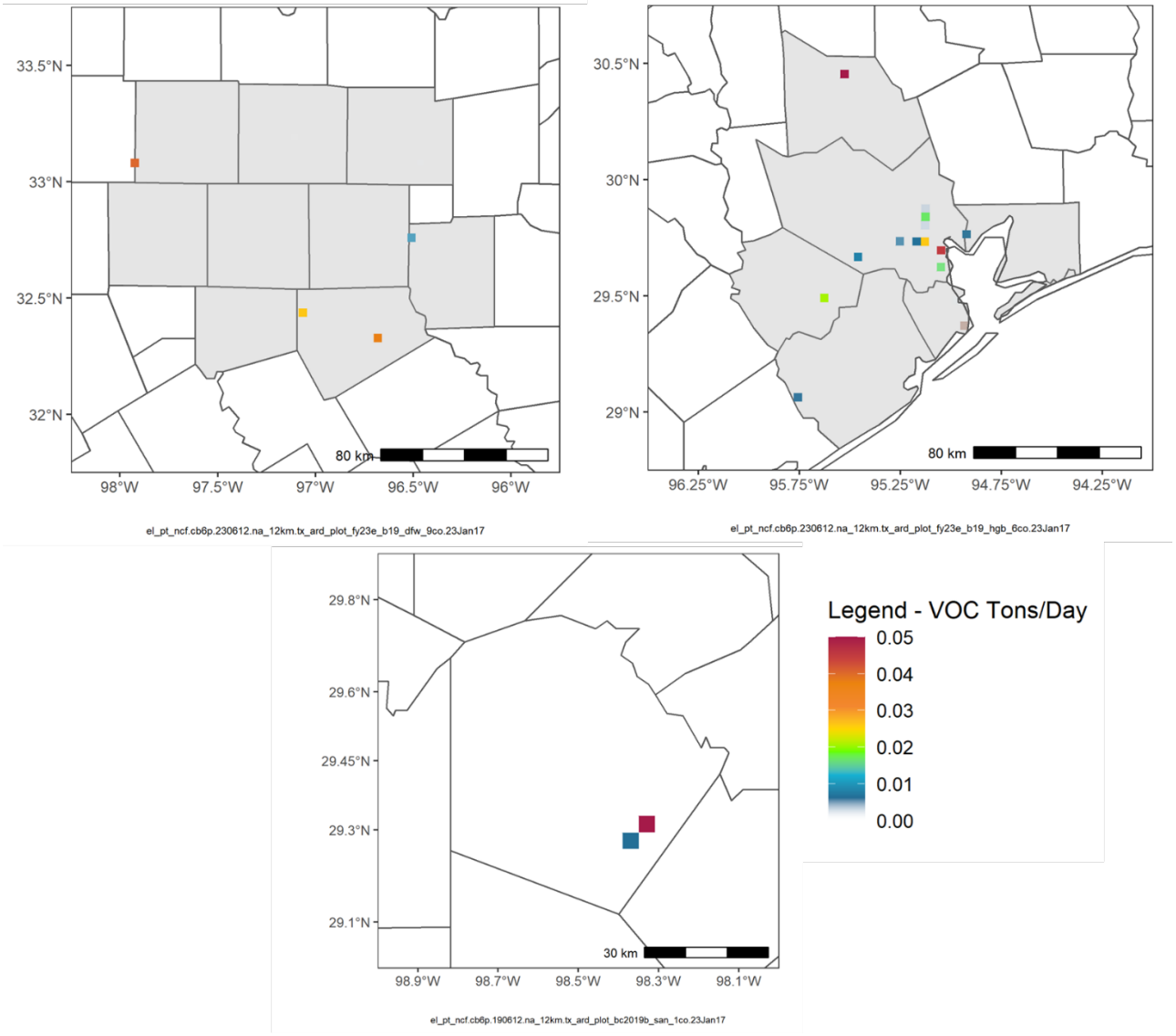

Figure 3-9: 2023 Future Case EGU VOC Emissions in DFW (Top Left), HGB (Top Right), and Bexar County (Bottom Center) for June 12 Episode Day

Figure 3-9: *2023 Future Case EGU VOC Emissions in DFW (Top Left), HGB (Top Right), and Bexar County (Bottom Center) for June 12 Episode Day* shows the spatial distribution of 2023 future case EGU NO_X emissions in tons per day as tile plots for the DFW, HGB, and Bexar County 2015 moderate eight-hour ozone nonattainment areas for the modeled episode day of June 12. Additional tile plots that shown the difference between the 2019 base case and 2023 future case are included in Attachment 1.

3.3.1.2 Outside Texas

Base Case

Similar to Texas EGU, the TCEQ used the 2019 AMPD hourly data to develop base case emissions for EGU from the non-Texas states in CONUS. The TCEQ used the 2019 CAMPD reported hourly emissions for NO_X and SO_2. Pollutant to heat input ratios

computed from reported emissions and heat input values were used to generate hourly emissions for each unit for the following pollutants: VOC, NH_3, and CO.

For units outside of Texas, the pollutant to heat input ratios were computed from the year 2017 NEI annual emissions, and annual heat input from 2017 CAMPD. The ratios were multiplied to the hourly heat input from 2019 CAMPD to calculate the hourly pollutant emissions. Non-emissions parameters, such as stack parameters, were obtained from the 2017 NEI for non-Texas CONUS units. The TCEQ maintains NEI-to-CAMPD cross reference file to assist with matching units. CAMPD units that match NEI were removed from the NEI dataset to avoid double counting of emissions. The hourly EGU emissions records were compiled into an AFS file format that can be processed with the modules of EPS3.

Future Case

States outside of Texas must meet the requirements of either the CSAPR Update or the Revised CSAPR Update or are exempt from CSAPR requirements.[6] The TCEQ scaled each state's 2019 CAMPD EGU ozone season NO_X emissions to their corresponding CSAPR ozone season state allocation cap where applicable, such that all CSAPR emission limits were modeled. 2019 CAMPD EGU ozone season NO_X emissions were used for states exempt from CSAPR requirements. The TCEQ assumed that units with consistent planned retirement dates prior to January 1, 2023, on EIA Form 860 (2020), in National Electric Energy Data System[7] (NEEDS) v6 data, and in the Eastern Regional Technical Advisory Committee[8] (ERTAC) data would be retired and removed them from model files. Hourly 2019 CAMPD EGU emissions were used with no scaling for the months of April and October for all states.

3.3.1.3 Non-EGU Point Sources

Within Texas

Base Case

Emissions modeling data for the 2019 base case Texas non-EGU were extracted from the TCEQ's STARS database on August 20, 2021. The TCEQ's STARS database has emissions data for all criteria pollutants from Texas point sources that meet the reporting threshold specified in 30 Texas Administrative Code (TAC) §101.10. The STARS modeling extract report is a snapshot of 2019 emissions from Texas point sources on August 20, 2021, since regulated entities are allowed to update their information, when warranted, at any time.[9]

The STARS extract was parsed and formatted into the necessary AFS file using the SAS program that also performed various logical checks and comparisons, assigned defaults for missing data, removed EGU that have CAMPD data. Each record of the AFS

[6] https://www.epa.gov/csapr/revised-cross-state-air-pollution-rule-update
[7] https://www.epa.gov/power-sector-modeling/national-electric-energy-data-system-needs-v6
[8] https://www.epa.gov/air-emissions-inventories/eastern-regional-technical-advisory-committee-ertac-electricity
[9] On April 9, 2021, the TCEQ requested regulated entities submit revisions to the 2019 point source EI by July 9, 2021.

file contains references for the TCEQ account (RN), equipment (FIN), and exhaust point (EPN), making up a unique emissions path.

The STARS extract contains four types of emission rates: annual, Ozone Season Daily (OSD), which spans from May to September, annual Emission Events (EE), and annual scheduled maintenance startup and shutdown (SMSS). When supplied, the OSD emissions in tpd are modeled for ozone attainment demonstrations, plus any EE/SMSS for the source (after conversion to tpd). If OSD is not provided by the source, an OSD is computed from the reported summer use percentage (which describes months June, July, and August), operational parameters, and any EE/SMSS reported. If summer use percentage is not provided, a default of 25% is used.

Speciation of Texas Non-EGU Point

VOC emissions in STARS can be reported as individual compounds, mixtures, classes of compounds, total VOC, and unclassified VOC. The majority of TCEQ Emissions Inventory Questionnaire (EIQ) responses include constituent VOC emission rates, which are used to develop point-specific speciation profiles. When the composition of the VOC reported for a specific source is unknown or not fully-speciated, the default speciation profile from EPA's SPECIATE database software program (EPA, 2014b) is applied based on the SCC.

Ethane and acetone, which are not VOC by the EPA's definition, are also extracted from STARS and used to develop point-specific speciation. Ethane and acetone are included in VOC totals in tables and tile plots in subsections below, because the CAMx uses these compounds as lumped species categories of their own, along with all the other VOC species in its Carbon Bond chemical mechanism. The modeled and tabulated VOC from EPS3 will always be greater when acetone or ethane are reported in STARS.

Future Case

To develop future case 2023 emissions, 2019 STARS data was used as the projection base for non-EGU projections in Texas. The 2019 projection base year become the SIP EI year used in the analysis for future potential emission reduction credit generation. Projection base year emissions were grown to the 2023 attainment year and controls that will be in place prior to the future year were applied. Texas non-EGU sources were further separated into sources in attainment counties, sources subject to cap-and-trade-programs, and sources in nonattainment areas. In addition, NO_X emissions from cement kilns in the DFW nonattainment area are subject to site (account) level caps and agreed orders, which were considered when estimating future year emissions.

Sources in Attainment Counties

For the Texas non-EGU point sources located in attainment counties, the TCEQ estimated the 2023 future year emissions by starting with the 2019 projection base STARS extract and projecting it to 2023 using growth factors developed by ERG in 2016 under contract to the TCEQ.[10] The TCEQ applied growth factors to all 2019 STARS emissions paths. The ERG data provided growth factors for most of the STARS paths (county code, plant, stack and point). In situations where there was not a county

[10] Factors and documentation are presented on the TCEQ's webpage at ftp://amdaftp.tceq.texas.gov/pub/EI/2012_episodes/hgb_sip/future_2020/point/

specific Standard Industrial Classification (SIC) growth factor, the emissions path was assigned a growth factor equal to the SIC average for the state. If there was no SIC match, the next default applied was the county average growth, and then the statewide average. All pollutants for a path were assigned the same growth factor, since the growth factors are percentages by which the projection base emissions are grown (or reduced), on a county/SIC basis.

Sources Subject to Cap-and-Trade

Two cap-and-trade programs administered by the TCEQ affect future year non-EGU emissions: (1) the Mass Emissions Cap and Trade program (MECT) for NO_x emissions in the HGB nonattainment area, and (2) the Highly Reactive Volatile Organic Compound Emissions Cap and Trade Program (HECT) for HRVOC emissions in Harris County. The TCEQ estimates future year emissions taking into consideration the future year program cap for the MECT and HECT programs. The program caps used to model future year NO_x and HRVOC emissions in the eight-county 2008 HGB ozone nonattainment area and Harris County are summarized in Table 3-2: *2023 Program Caps for MECT and HECT Programs in Texas.*

Table 3-2: 2023 Program Caps for MECT and HECT Programs in Texas

Program	Pollutant Affected	Geographical Scope of Program	2023 Program Cap for Texas Sources (tpy)
MECT	NO_x	2008 HGB nonattainment area	39,071.20
HECT	HRVOC	Harris County	2,570.70

For the MECT Program to account for the possible use of discrete emission reduction credits (DERCs) and mobile DERCs (MDERCs) to be used for MECT compliance, an additional 1,230.4 tpy, or 3.4 tpd, of emissions was added to the MECT cap, listed in Table 1-4, for a total of 40,301.6 tpy modeled MECT program cap. The spatial representation of future year emissions of the sources subject to cap-and- trade programs is made uncertain due to the trading provisions of these programs. The information currently available to estimate future emissions from sources subject to cap-and-trade programs includes the 2023 future year program caps, future year allocations for subject sources (specific amount of NO_x allowances to each applicable point source (i.e., piece of equipment) at a site (account) for each compliance year), and historical compliance trends for previous compliance periods. While the total future emissions from the sources subject to each program is limited to the 2023 program cap, the TCEQ spatially distributed the 2023 cap to sources expected to be operational in the future using historical trend analysis for the MECT and HECT programs. Details of the methodology used to spatially distribute MECT and HECT program emissions are provided in previous SIP revision documentation.[11] Details of the MECT and HECT

[11] HGB Serious AD 2008 Eight-Hour Ozone NAAQS SIP Appendix B (archive-it.org) can be found at https://wayback.archive-it.org/414/20210529163328/https:/www.tceq.texas.gov/assets/public/implementation/air/sip/hgb/hgb_serious_AD_2019/HGB_AD_SIP_19077SIP_AppendixB_adoption.pdf.

program rules and subject sources are provided in 30 TAC 101, Subchapter H, Divisions 3 and 6, respectively.

Sources in Nonattainment Areas

Sources in nonattainment areas are typically required to offset growth in emissions using offsets. Sources subject to cap-and-trade programs are allowed to use allowances to offset their emissions growth for the subject pollutant. Sources that are not subject to cap-and-trade programs are required to offset their emissions growth either by purchasing certified credits through programs such as the Emission Reduction Credit program (ERC), Discrete Emission Reduction Credit program (DERC), and Mobile Discrete Emission Reduction Credit program (MDERC) available in the TCEQ's Emission Credit and Discrete Emission Credit Registries (EBT Credit Registry) or by making contemporaneous period (internal) reductions. Hence, the total certified credits available in the TCEQ's EBT Credit Registry could limit the projected emissions growth estimated using the economic growth factors developed by Eastern Research Group, Inc., (ERG) for the TCEQ.

To estimate the 2023 emissions of non-EGU in nonattainment areas that are not subject to cap-and-trade programs or site-level caps, the TCEQ used the more restrictive of the projected economic growth or the certified credits available in the TCEQ's Emissions Banking and Trading (EBT) Credit Registry. If sufficient certified credits were available in the TCEQ's EBT Credit Registry, the 2023 emissions were limited based on economic growth projected using ERG growth factors. Otherwise, the 2023 emissions were limited to the total certified credits available in the TCEQ's EBT Credit Registry. Table 3-3: *Comparison of the 2023 Modelable Bank and Predicted Growth* depicts the resulting Modelable Bank emissions for 2023 and the predicted growth values for 2023.

Table 3-3: Comparison of the 2023 Modelable Bank and Predicted Growth

Area	Pollutant	Total STARS 2019 Reported Emissions (tpd)	Modelable Bank (tpd)	Total FY2023 Emissions Projected with Only the Bank (tpd)	Total FY2023 Emissions Projected with Only Growth (tpd)	FY2023 Modeling Emissions (tpd)	Future Year Projection
DFW	NO_x	15.13	17.00	32.13	11.34	11.34	Growth
DFW	VOC	26.85	0.10	26.95	22.48	22.48	Growth
HGB	NO_x	18.11	51.3	69.41	19.24	19.24	Growth
HGB	VOC	80.28	4.40	84.68	85.93	84.68	Bank

Emission Reduction Credit Modeling Sensitivity

A sensitivity modeling run was performed to determine the impact of certified and potential (reductions that have already occurred but have not yet been certified) Emissions Reduction Credits (ERCs) on the future design value. The sensitivity was performed to ensure that the emissions associated with ERCs remain surplus, as

required by 30 TAC Chapter 101, Subchapter H, Division 1. In the sensitivity model run, emissions from all ERCs (certified and potential) were included in 2023 future case emissions on non-EGU sources not subject to cap-and-trade programs or site caps. Based on the amount of certified and potential credits provided by EBT on March 18, 2022, emissions from ERCs were modeled for non-EGU point sources in both DFW and HGB non-attainment areas. The ERCs were processed to account for the offset ratio and converted to tpd prior to being applied to the applicable point sources. The resulting modelable emissions for 2023 used in the sensitivity are depicted in Table 3-4: *Comparison of the 2023 Modelable Bank and Predicted Growth for Emission Reduction Credit Modeling Sensitivity.*

Table 3-4: Comparison of the 2023 Modelable Bank and Predicted Growth for Emission Reduction Credit Modeling Sensitivity

Area	Pollutant	Total STARS 2019 Reported Emissions (tpd)	Total FY2023 Emissions Projected without Sensitivity (tpd)	Modelable Sensitivity ERCs (tpd)	FY2023 Modeling Emissions with ERCs Sensitivity (tpd)	Future Year Emissions Basis in ERC Sensitivity
DFW	NO_X	15.13	11.34	0.10	15.23	ERC
DFW	VOC	26.85	22.48	0.03	26.88	ERC
HGB	NO_X	18.11	19.24	1.80	19.91	ERC
HGB	VOC	80.28	85.93	0.80	85.93	Bank

DFW Cement Kilns

Holcim's cement kilns were modeled at the account-specific NO_X cap specified in 30 TAC §117.3123. Modeled emissions for TXI and Ash Grove's kilns were based on NO_X per ton clinker limits specified in agreed orders and permitted production limits. The future year emissions for all other pollutants from the kilns were determined using growth factors, as described above.

Tile plots that show the spatial distribution of non-EGU emissions in 2019 base case and 2023 future case in each nonattainment area are provided in Attachment 1: *Emission and Model Performance Evaluation (MPE) Figures* to this appendix.

Outside Texas

Base Case

The 2019 EI for states outside Texas was derived from the non-Integrated Planning Model (non-IPM, referred to as non-EGU) files from the 2016v1 platform.[12] The 2016v1 platform was used because it was the closest in year to the base case and includes model years of 2016 and 2023. Emissions were interpolated between 2016 and 2023 to create 2019 base case emissions. Small EGU that do not report hourly varying emissions to CAMPD are included in this category. The temporal allocation file for the SMOKE modeling system associated with the EPA's 2016v1 platform was used to create the daily-varying temporal distribution of emissions, based on SCC and county, for

[12] https://www.epa.gov/air-emissions-modeling/2016v1-platform

each day of the episode. For non-Texas, non-EGU point sources, the TCEQ chose a weekday during ozone season to represent a typical episode day, therefore emissions for each modeled day are identical.

Future Case
The 2016v1 platform was used for future case non-EGU emissions for states outside of Texas; the platform includes a 2023 model year projection which was used for point sources outside of Texas.

3.3.2 Gulf of Mexico

The Gulfwide Emission Inventory (GWEI), developed by ERG under contract to the Bureau of Ocean Energy Management (BOEM), Department of the Interior, is typically updated every three years.[13] The 2017 GWEI was used because it is the closest in year to the base case. The 2017 emissions were used as is without being projected to 2019. The TCEQ used the 2017 GWEI for the 2023 Gulf of Mexico offshore EI, the same as was used in the base case.

The report and data are divided into two parts, oil and gas exploration and production platform (point) sources, and non-platform (area) sources. Emissions are provided on a monthly basis for each of the twelve months. Diurnal curves to temporalize the emissions to hourly are not available for the 2017 GWEI, so curves developed for 2008 GWEI were used, as advised in ERG's 2017 documentation. A summary of the modeled tpd GWEI platform emissions by month can be found in Table 3-5: *2019 Platform Elevated Emissions by Month.* The base case offshore NO_X and VOC emissions are shown in Figure 3-10: *2019 Base Case and 2023 Future Case Elevated Platform Sources NO_X Emissions for June* and Figure 3-11: *2019 Base Case and 2023 Future Case Elevated* Platform Sources VOC Emissions for June 2019, respectively.

Table 3-5: 2019 Platform Elevated Emissions by Month

Month	NO_X (tpd)	VOC (tpd)	CO (tpd)
January	132.40	31.60	137.50
February	133.30	39.00	136.20
March	133.80	32.20	139.90
April	131.60	32.90	137.40
May	125.00	31.10	126.20
June	132.70	33.60	138.40
July	129.30	30.00	131.80
August	125.80	30.30	126.10
September	131.80	29.90	132.00
October	116.60	27.10	119.40
November	129.90	30.50	134.00

[13] The Year 2017 Emissions Inventory Study is available at https://espis.boem.gov/final%20reports/BOEM_2019-072.pdf.

Month	NO_x (tpd)	VOC (tpd)	CO (tpd)
December	124.70	29.30	127.00
Average	128.90	31.50	132.20

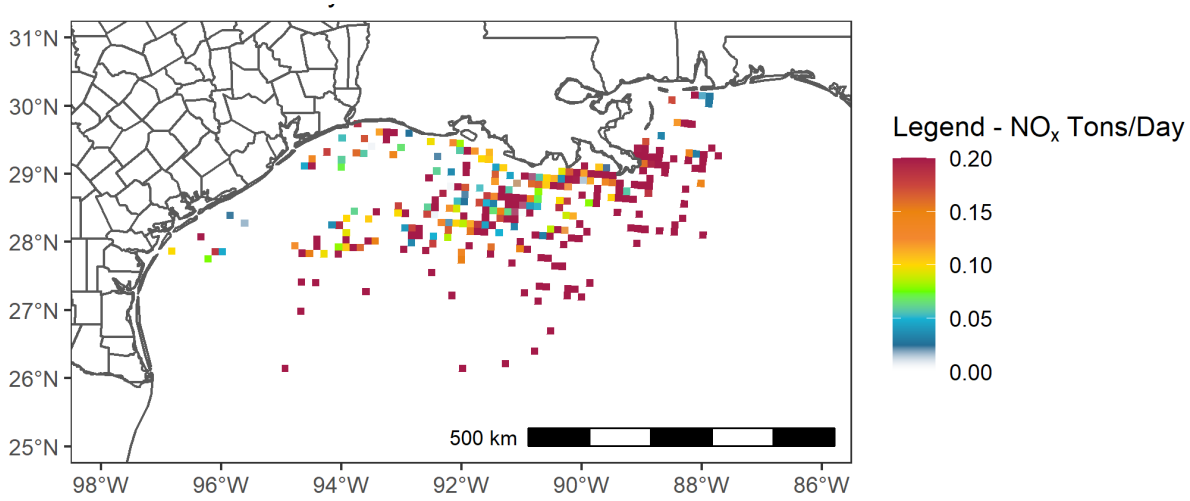

Figure 3-10: 2019 Base Case and 2023 Future Case Elevated Platform Sources NO_x Emissions for June Episode Day

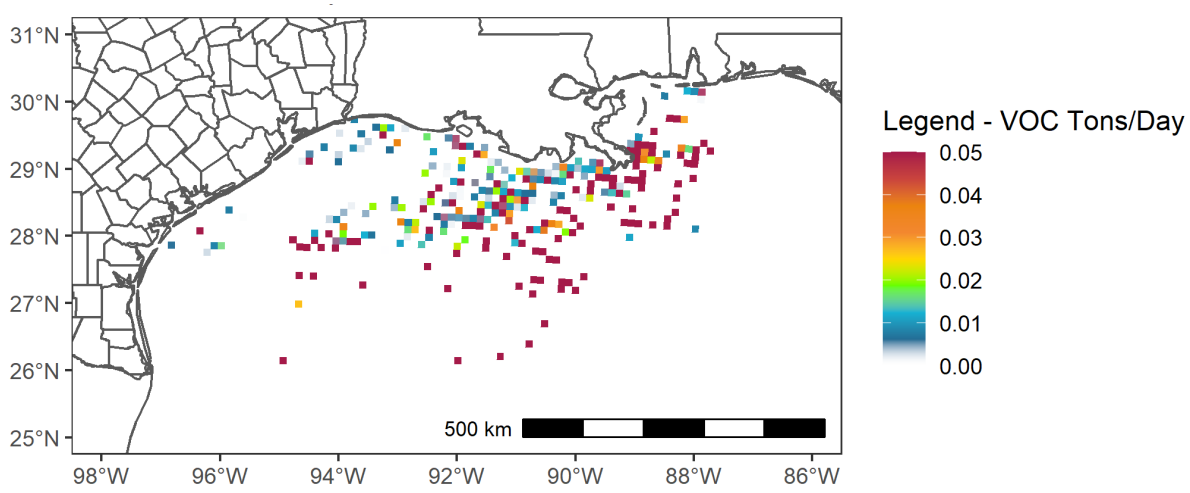

Figure 3-11: 2019 Base Case and 2023 Future Case Elevated Platform Sources VOC Emissions for June Episode Day

3.3.3 Mexico and Canada

For both Mexican and Canadian point source emissions, the TCEQ used data from the 2016v1 platform, which were the latest data available at the time the modeling emissions were compiled. The 2016v1 platform Canadian point sources were derived from the Environment and Climate Change Canada (ECCC) 2015 emission inventory and the Mexico inventory was based on Mexico's 2008 Inventario Nacional de Emisiones de Mexico. The 2016v1 platform includes model years of 2016 and 2023,

and emissions were interpolated to create 2019 base case emissions. The NO_X emissions for Mexico and Canada modeled on the June 12 episode day are represented in Figure 3-12: *2019 Base Case NO_X Emissions for June 12 Episode Day in Mexico* and Figure 3-13: *2019 Base Case NO_X Emissions for June 12 Episode Day in Canada.*

For both Mexican and Canadian 2023 future year point source emissions, the TCEQ used the 2016v1 platform which includes the 2023 model year. The 2016v1 platform future case Canadian point source emissions were provided by ECCC or projected from 2015 with data provided by ECCC. The 2016v1 platform Mexico emissions inventory is based on ERG projections of a 2008 inventory.

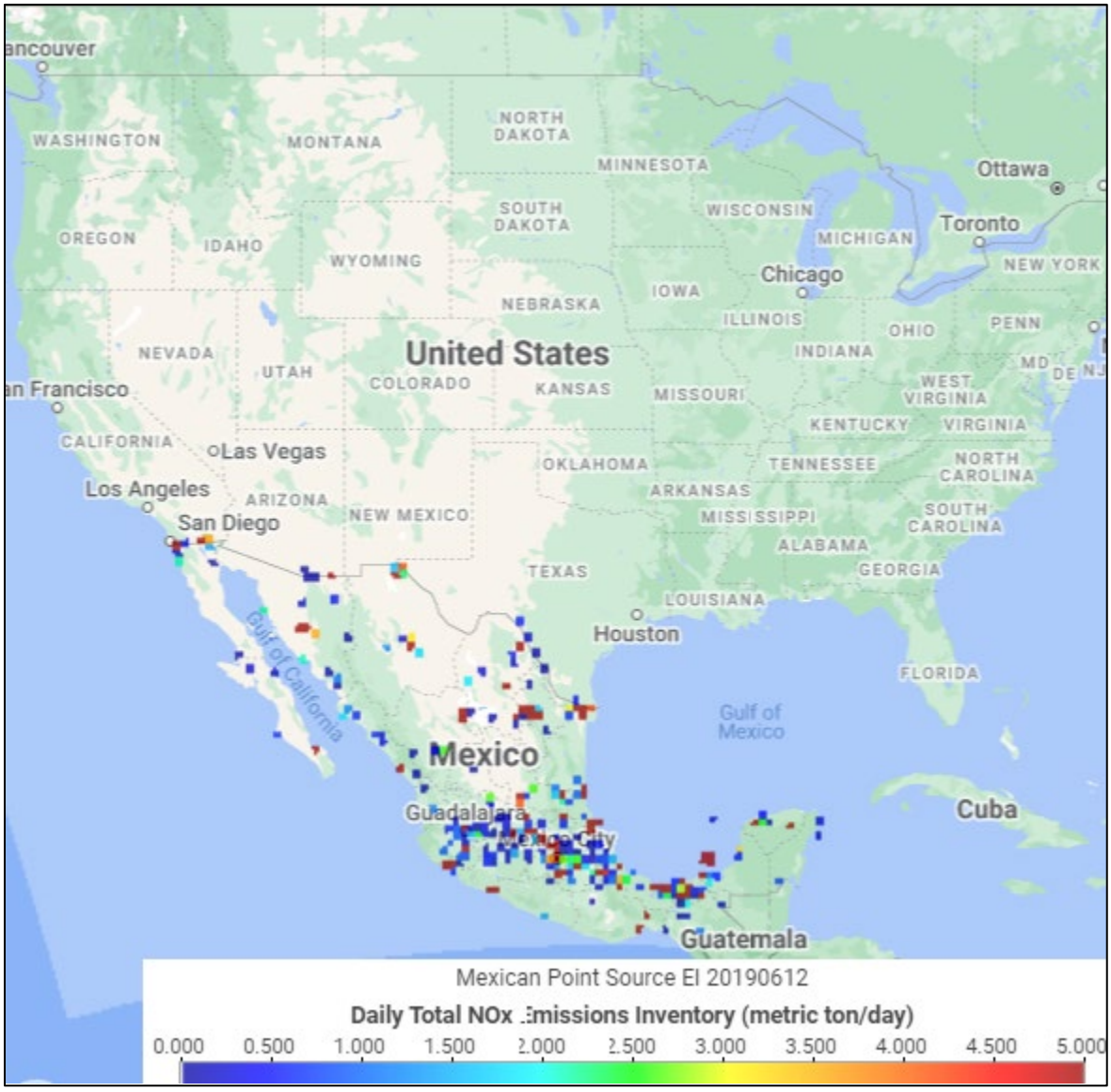

Figure 3-12: 2019 Base Case NO_x Emissions for June 12 Episode Day in Mexico

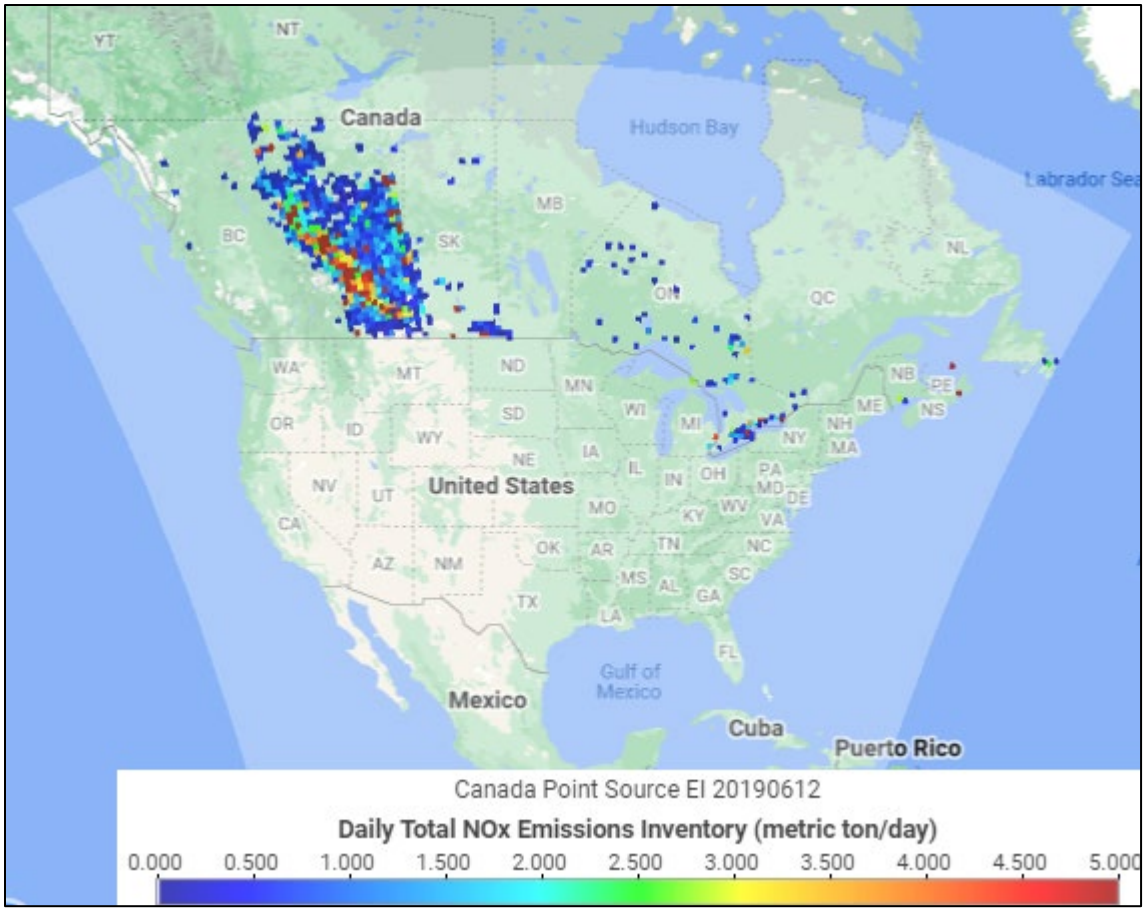

Figure 3-13: 2019 Base Case NO_x Emissions for June 12 Episode Day in Canada

The summary of Mexico and Canada 2019 base case emissions for any day is presented in Table 3-6: *2019 Base Case Emissions for the June 12 Episode Day in Mexico and Canada.*

Table 3-6: 2019 Base Case Emissions for the June 12 Episode Day in Mexico and Canada

Emission Source	NO_x (tpd)	VOC (tpd)
Mexico	2000.00	1031.54
Canada	1138.70	966.26

3.4 ON-ROAD MOBILE SOURCES

On-road mobile emissions sources consist of automobiles, trucks, motorcycles, and other motor vehicles traveling on public roadways. On-road mobile source ozone precursor emissions are usually categorized as combustion-related emissions or evaporative hydrocarbon emissions. Combustion-related emissions are estimated for vehicle engine exhaust. Evaporative hydrocarbon emissions are estimated for the fuel tank and other evaporative leak sources on the vehicle. To calculate emissions, both the rate of emissions per unit of activity (emissions factors) and the number of units of activity must be determined.

Emission factors for these AD SIP revisions were developed using the EPA's mobile emissions factor model, version 3 of the Motor Vehicle Emission Simulator (MOVES3) model.[14] The MOVES3 model may be run using national default information, or the default information may be modified to simulate data specific to an area, such as the control programs in place, driving behavior, meteorological conditions, and vehicle characteristics. Because modifications to the national default values influence the emission factors calculated by MOVES3, to the extent that local values are available, parameters that reflect local conditions are used. The localized inputs used for the on-road mobile EI development include vehicle speeds for each roadway link, vehicle populations, vehicle hours idling, temperature, humidity, vehicle age distributions for each vehicle type, percentage of miles traveled for each vehicle type, type of inspection and maintenance program, fuel control programs, and gasoline vapor pressure controls.

3.4.1 Within Texas

The TCEQ contracted with Texas Transportation Institute (TTI) and the North Central Texas Council of Governments (NCTCOG) to develop the Texas on-road emission inventories. TTI provided emission inventories for Bexar County and the HGB nonattainment area, and NCTCOG provided the DFW nonattainment area inventories. Both TTI and NCTCOG used the MOVES3 model to generate emission rates for 33 different pollutants that were included in the emission inventories.

Vehicle traffic count data from 2011 to 2019 was used to estimate emissions for the base case of 2019. For the future year of 2023, projections were based on the 2023 Travel Demand Model (TDM) and all emissions were adjusted for day type (weekday, Friday, Saturday, and Sunday) and for time of year (school vs Summer). For 2019 base case and 2023 future case, the on-road emissions estimates from MOVES3 for each episode day were prepared for photochemical model input using EPS3.

Table 3-7: *2019 Base Case On-Road Emissions for June 12 Episode Day in DFW* and Table 3-8: *2023 Future Case On-Road Emissions for June 12 Episode Day in DFW* show modeled NO_X, VOC, and CO emissions for the June 12 episode day for the 2019 base and 2023 future case in the DFW, respectively. Between base and future case emissions in all counties showed a decrease for all three pollutants.

Table 3-7: 2019 Base Case On-Road Emissions for June 12 Episode Day in DFW

County Name	NO_X (tpd)	VOC (tpd)	CO (tpd)
Colin	9.70	5.91	112.36
Dallas	35.76	18.30	375.28
Denton	8.89	4.95	86.62
Ellis	4.90	1.51	32.29
Johnson	3.62	1.28	22.10
Kaufman	4.37	1.19	27.07

[14] Latest Version of Motor Vehicle Emission Simulator (MOVES) can be found at https://www.epa.gov/moves/latest-version-motor-vehicle-emission-simulator-moves.

County Name	NO_x (tpd)	VOC (tpd)	CO (tpd)
Parker	4.10	1.20	21.99
Tarrant	26.58	13.08	235.12
Wise	2.89	0.80	16.94
DFW Nine-County Total	100.81	48.22	929.77

Table 3-8: 2023 Future Case On-Road Emissions for June 12 Episode Day in DFW

County Name	NO_x (tpd)	VOC (tpd)	CO (tpd)
Colin	6.75	4.75	97.40
Dallas	24.41	14.36	319.42
Denton	6.31	4.00	75.66
Ellis	3.55	1.19	28.56
Johnson	2.71	1.02	19.14
Kaufman	3.22	0.93	24.18
Parker	3.06	0.93	18.60
Tarrant	19.19	10.41	202.29
Wise	2.15	0.62	14.68
DFW Nine-County Total	71.34	38.21	799.93

Table 3-9: *2019 Base Case On-Road Emissions in for June 12 Episode Day in HGB* and Table 3-10: *2023 Future Case On-Road Emissions for June 12 Episode Day in HGB* show modeled NO_x, VOC, and CO emissions for the June 12 episode day for the 2019 base and 2023 future case in the HGB, respectively. Overall emissions in HGB decreased between base and future case.

Table 3-9: 2019 Base Case On-Road Emissions in for June 12 Episode Day in HGB

County Name	NO_x (tpd)	VOC (tpd)	CO (tpd)
Brazoria	4.24	2.18	40.09
Chambers	3.05	0.50	14.18
Fort Bend	6.01	3.70	61.10
Galveston	2.99	1.89	33.72
Harris	54.20	27.22	560.53
Montgomery	7.14	2.56	64.57
HGB Six-County Total	77.64	39.06	774.19

Table 3-10: 2023 Future Case On-Road Emissions for June 12 Episode Day in HGB

County Name	NO_x (tpd)	VOC (tpd)	CO (tpd)
Brazoria	2.82	1.85	34.20
Chambers	2.25	0.37	12.92

County Name	NO_X (tpd)	VOC (tpd)	CO (tpd)
Fort Bend	4.91	3.18	59.13
Galveston	1.90	1.17	26.77
Harris	37.71	21.55	484.26
Montgomery	5.28	2.98	57.50
HGB Six-County Total	54.87	31.09	674.78

Similar to DFW and HGB, Bexar County saw a decrease in emissions of NO_X, VOC, and CO between the 2019 base case and 2023 future case as shown in Table 3-11: *2019 Base Case On-Road Emissions for June 12 Episode Day in Bexar County* and Table 3-12: *2023 Future Case On-Road Emissions for June 12 Episode Day Bexar County*, respectively.

Table 3-11: 2019 Base Case On-Road Emissions for June 12 Episode Day in Bexar County

County Name	NO_X (tpd)	VOC (tpd)	CO (tpd)
Bexar	28.27	14.95	281.22

Table 3-12: 2023 Future Case On-Road Emissions for June 12 Episode Day Bexar County

County Name	NO_X (tpd)	VOC (tpd)	CO (tpd)
Bexar	20.26	12.37	257.76

Figure 3-14: *2019 Base Case On-Road Mobile Source NO_X Emissions in the txs_4km CAMx Domain for June 12 Episode Day* and Figure 3-15: *2019 Base Case On-Road Mobile Source VOC Emissions in the txs_4km CAMx Domain for June 12 Episode Day* show the spatial distribution of 2019 base case NO_X and VOC emissions modeled in the txs_4km CAMx domain for the June 12 episode day.

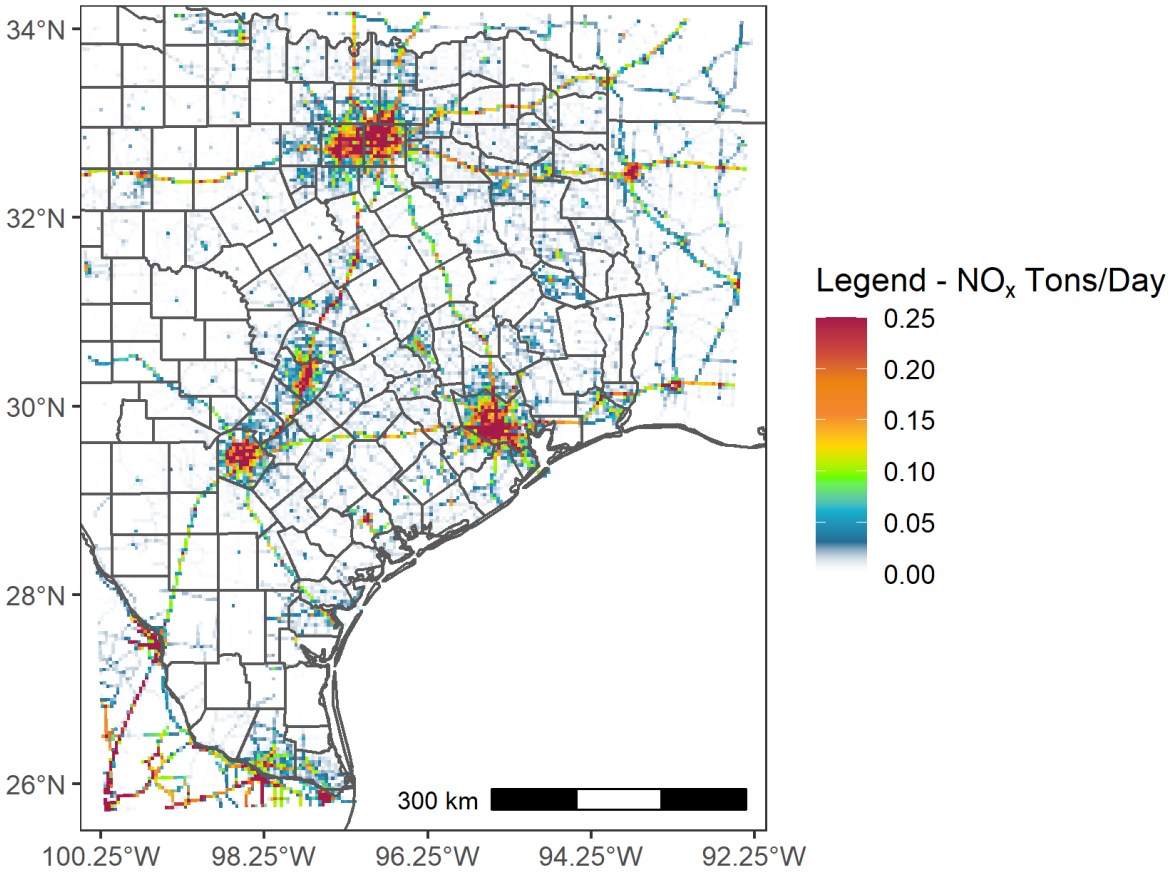

Figure 3-14: 2019 Base Case On-Road Mobile Source NO_x Emissions in the txs_4km CAMx Domain for June 12 Episode Day

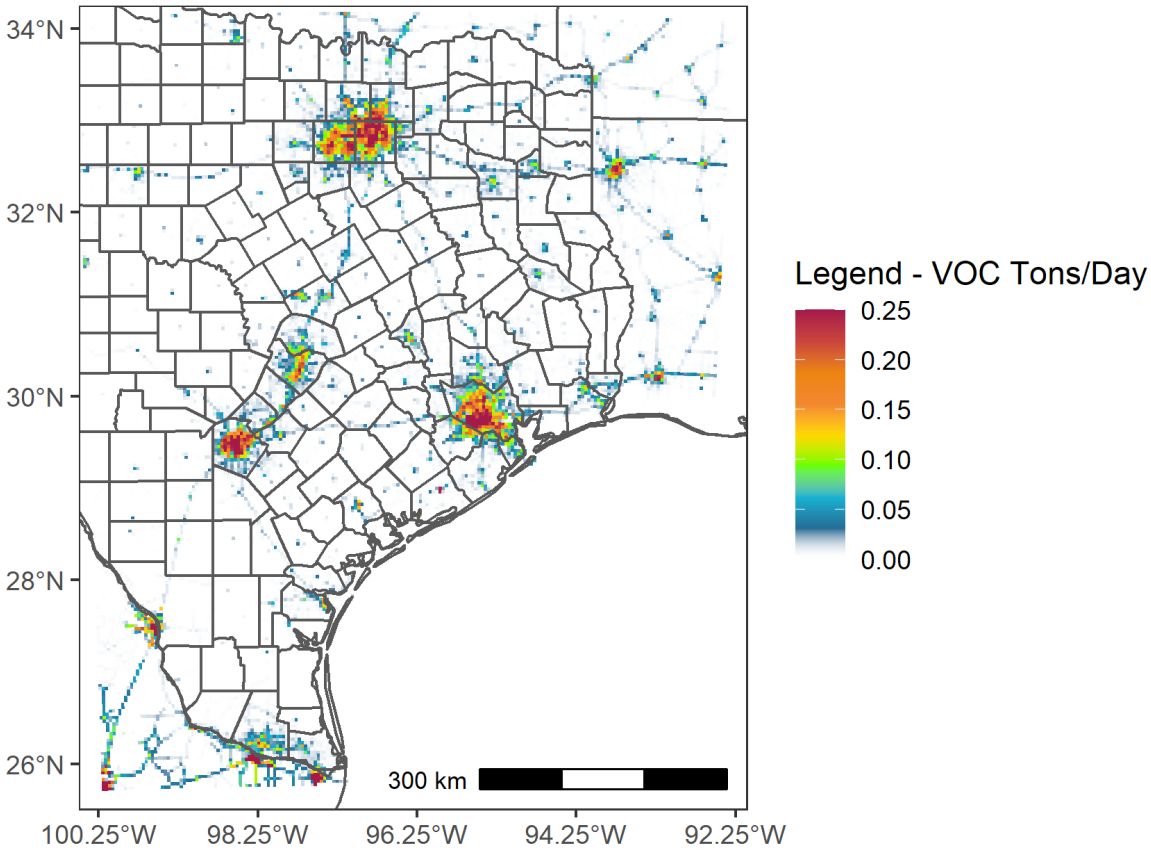

Figure 3-15: 2019 Base Case On-Road Mobile Source VOC Emissions in the txs_4km CAMx Domain for June 12 Episode Day

Figure 3-16: *2023 Future Case On-Road Mobile Source NO_x Emissions in the txs_4km CAMx Domain for June 12 Episode Day* and Figure 3-17: *2023 Future Case On-Road Mobile Source VOC Emissions in the txs_4km CAMx Domain for June 12 Episode Day* show the spatial distribution of 2023 base case NO_x and VOC emissions modeled in the txs_4km CAMx domain for the June 12 episode day.

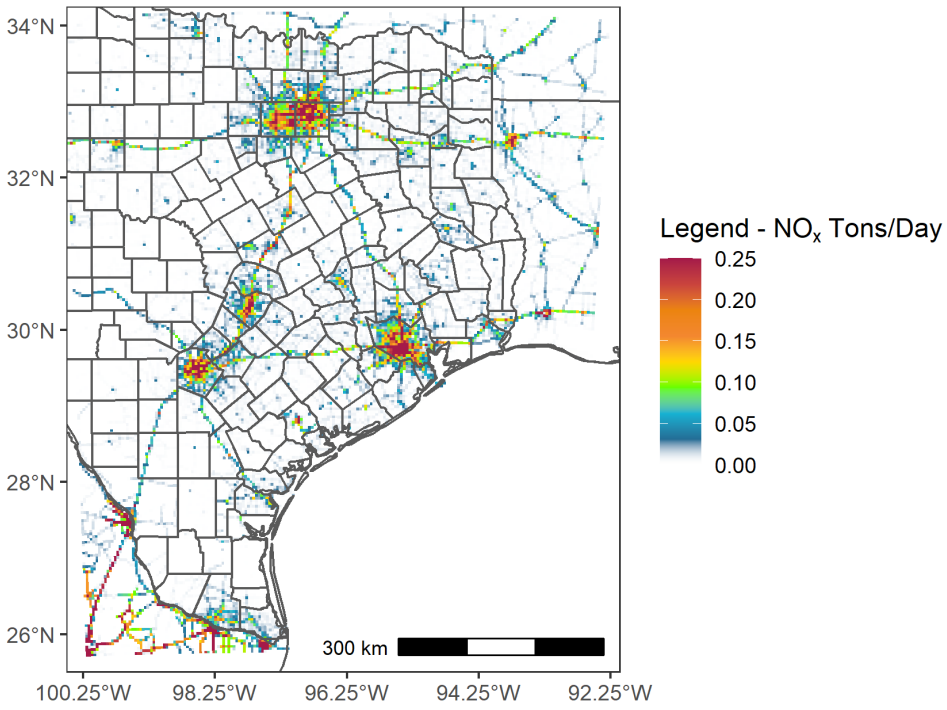

Figure 3-16: 2023 Future Case On-Road Mobile Source NO_x Emissions in the txs_4km CAMx Domain for June 12 Episode Day

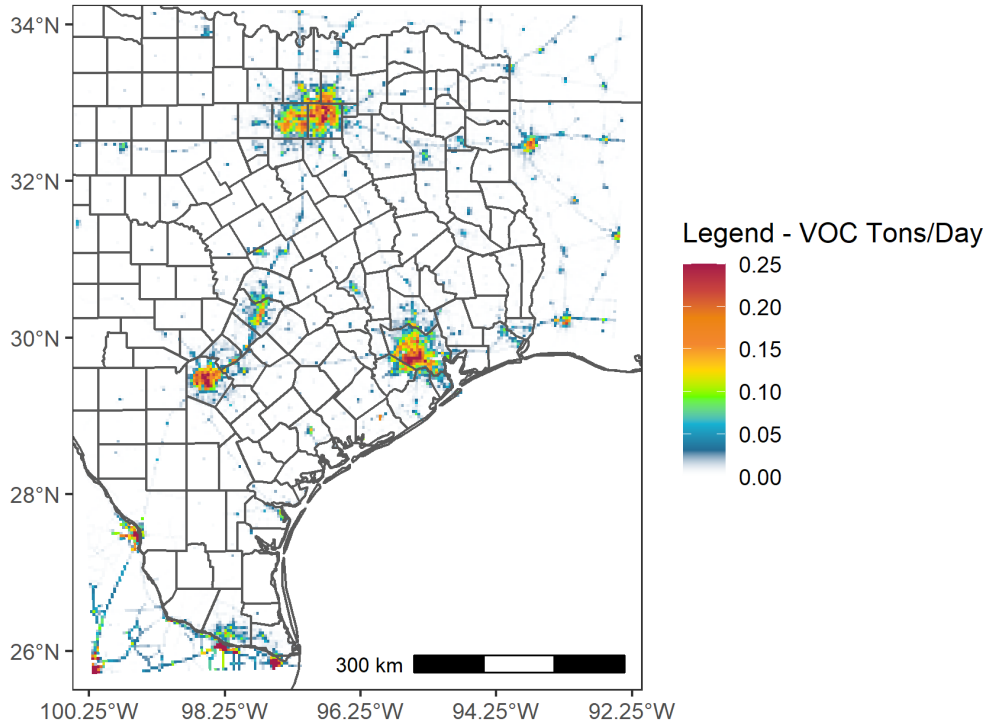

Figure 3-17: 2023 Future Case On-Road Mobile Source VOC Emissions in the txs_4km CAMx Domain for June 12 Episode Day

The above figures (Figure 3-14, Figure 3-15, Figure 3-16, and Figure 3-17) show emissions concentrated in around major metropolitan areas and along major roadways for both 2019 base case and 2023 future case. Additional figures focused on the DFW, HGB, and Bexar County nonattainment areas are provided in Attachment 1 of this appendix.

3.4.2 Outside Texas

Emission estimates outside of Texas were developed using MOVES3 with county-based defaults. No local inputs were used with these, and 2023 projections are based on national historical data. For 2019 base case and 2023 future case, the on-road emissions estimates from MOVES3 for each modeled day were prepared for photochemical model input using EPS3.

3.5 NON-ROAD MOBILE SOURCES

Non-road sources include equipment used for agricultural, commercial, construction, industrial, lawn/garden, and recreational purposes. Construction, industrial, and agricultural equipment powered primarily by diesel engines tend to be the largest contributors of non-road NO_x emissions. Lawn/garden, commercial, and recreational equipment powered primarily by gasoline engines tend to be the largest contributors of non-road VOC emissions. Below are details on emissions estimate methodologies used for the non-road mobile source sector.

3.5.1 Within Texas

Non-road emissions for 2019 and 2023 for nine-county DFW, six-county HGB, and the remaining Texas counties were estimated with version 2.2 of the Texas NONROAD (TexN2.2) model. TexN2.2 is a customized tool that interfaces with the non-road emissions calculations performed MOVES3. For each Texas county, TexN2.2 performs up to 25 separate runs of MOVES3 to account for Texas-specific equipment population estimates for multiple diesel equipment subcategories. TexN2.2 runs were performed to obtain average weekday emissions for the four seasons of Spring, Summer, Fall, and Winter for all 254 Texas counties. TexN2.2 outputs emissions estimates for up to 198 SCCs associated with specific non-road equipment. For each calendar year and season, the average weekday non-road emissions estimates by county and SCC were prepared for photochemical model input with EPS3.

Table 3-13: *2019 Base Case Non-Road Emissions for June 12 Episode Day in DFW* and Table 3-14: *2023 Future Case Non-Road Emissions for June 12 Episode Day in DFW* show modeled NO_X, VOC, and CO emissions from the non-road sector for the June 12 episode day for the 2019 base and 2023 future case in each county of DFW, respectively.

Table 3-13: 2019 Base Case Non-Road Emissions for June 12 Episode Day in DFW

County Name	NO_X (tpd)	VOC (tpd)	CO (tpd)
Colin	4.83	6.42	123.76
Dallas	15.85	18.12	388.00
Denton	3.49	3.82	68.94
Ellis	1.87	0.83	13.65

County Name	NO_X (tpd)	VOC (tpd)	CO (tpd)
Johnson	0.94	0.59	11.38
Kaufman	1.08	0.55	8.36
Parker	0.78	0.57	9.10
Tarrant	8.72	9.50	196.46
Wise	0.59	0.33	3.95
DFW Nine-County Total	38.15	40.73	823.59

Table 3-14: 2023 Future Case Non-Road Emissions for June 12 Episode Day in DFW

County Name	NO_x (tpd)	VOC (tpd)	CO (tpd)
Colin	4.54	6.69	133.68
Dallas	14.05	18.86	418.41
Denton	2.94	3.84	73.80
Ellis	1.68	0.80	14.05
Johnson	0.79	0.59	12.07
Kaufman	0.89	0.51	8.73
Parker	0.61	0.56	9.69
Tarrant	7.91	9.84	211.07
Wise	0.42	0.29	4.11
DFW Nine-County Total	33.83	41.98	885.61

Table 3-15: *2019 Base Case Non-Road Emissions in for June 12 Episode Day in HGB* and Table 3-16: *2023 Future Case On-Road Emissions in for June 12 Episode Day in HGB* show modeled NO_X, VOC, and CO emissions from the non-road sector for the June 12 episode day for the 2019 base and 2023 future case in each county of HGB, respectively.

Table 3-15: 2019 Base Case Non-Road Emissions in for June 12 Episode Day in HGB

County Name	NO_x (tpd)	VOC (tpd)	CO (tpd)
Brazoria	2.07	1.96	28.35
Chambers	0.44	0.49	4.46
Fort Bend	2.48	2.54	51.28
Galveston	1.70	2.09	29.71
Harris	26.71	26.75	567.29
Montgomery	2.74	2.82	48.64
HGB Six-County Total	36.13	36.65	729.72

Table 3-16: 2023 Future Case On-Road Emissions in for June 12 Episode Day in HGB

County Name	NO_x (tpd)	VOC (tpd)	CO (tpd)
Brazoria	1.83	1.79	29.88
Chambers	0.39	0.40	4.42

County Name	NO_X (tpd)	VOC (tpd)	CO (tpd)
Fort Bend	2.14	2.59	55.12
Galveston	1.49	1.92	31.47
Harris	22.18	27.27	608.25
Montgomery	2.22	2.80	52.12
HGB Six-County Total	30.26	36.78	781.25

Table 3-17: *2019 Base Case Non-Road Emissions in for June 12 Episode Day in Bexar County* and Table 3-18: *2023 Future Case Non-Road Emissions in for June 12 Episode Day in Bexar County* show modeled NO_X, VOC, and CO emissions from the non-road sector for the June 12 episode day for the 2019 base and 2023 future case in Bexar County, respectively.

Table 3-17: 2019 Base Case Non-Road Emissions in for June 12 Episode Day in Bexar County

County Name	NO_X (tpd)	VOC (tpd)	CO (tpd)
Bexar	7.82	11.36	222.94

Table 3-18: 2023 Future Case Non-Road Emissions in for June 12 Episode Day in Bexar County

County Name	NO_X (tpd)	VOC (tpd)	CO (tpd)
Bexar	6.99	11.92	241.36

Figure 3-18: *2019 Base Case Non-Road Mobile Source NO_X Emissions in the txs_4km CAMx Domain for June 12 Episode Day* and Figure 3-19: *2019 Base Case Non-Road Mobile Source VOC Emissions in the txs_4km CAMx Domain for June 12 Episode Day* show the distribution of non-road 2019 base case NO_X and VOC emissions, respectively, in the txs_4km CAMx domain for the June 12 episode day. Similarly, Figure 3-20: *2023 Future Case Non-Road Mobile Source NO_X Emissions in the txs_4km CAMx Domain for June 12 Episode Day* and Figure 3-21: *2023 Future Case Non-Road Mobile Source VOC Emissions in the txs_4km CAMx Domain for June 12 Episode Day* show the distribution of non-road 2023 future case NO_X and VOC emissions, respectively, in the txs_4km CAMx domain for the same June 12 episode day. The figures show that non-road emissions are concentrated around major metropolitan areas and that emissions mostly decrease between 2019 base case and 2023 future

case. Additional figures focused on the DFW, HGB, and Bexar County nonattainment areas are provided in Attachment 1 of this appendix.

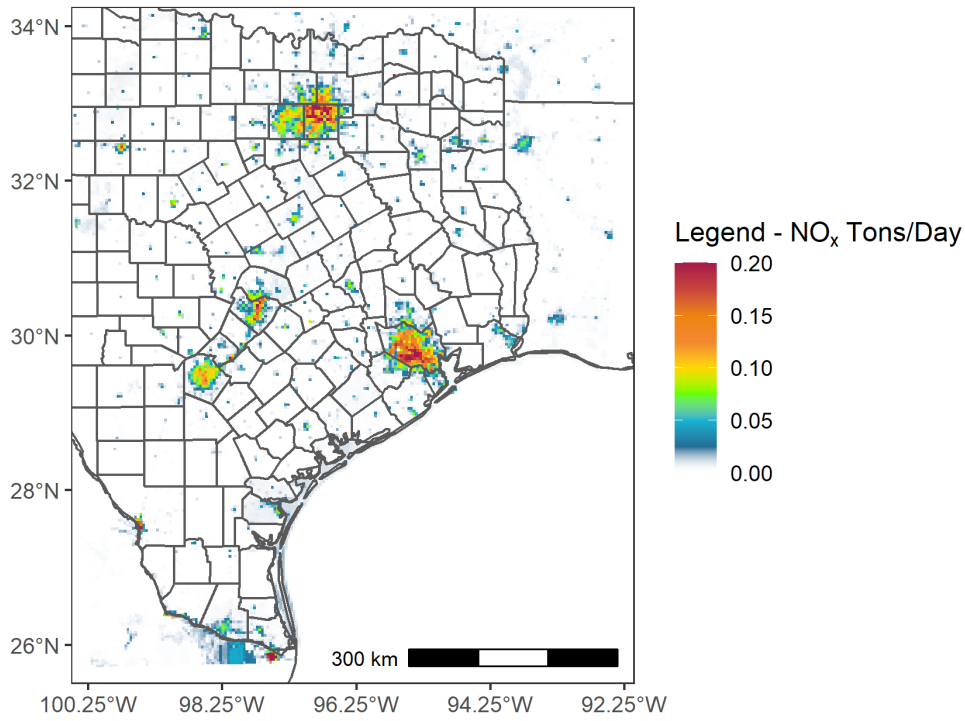

Figure 3-18: 2019 Base Case Non-Road Mobile Source NO_x Emissions in the txs_4km CAMx Domain for June 12 Episode Day

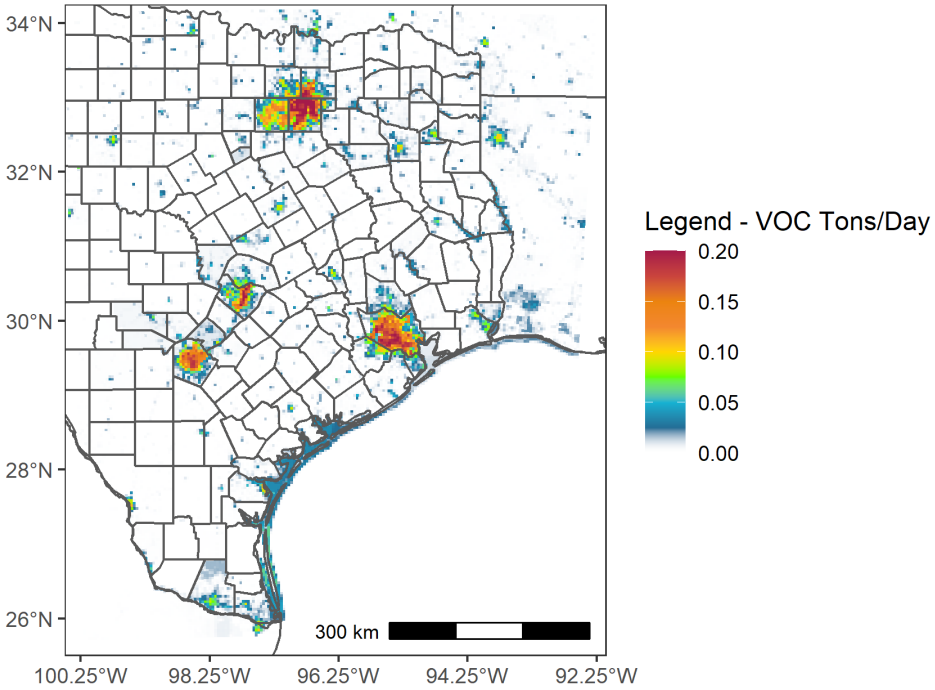

Figure 3-19: 2019 Base Case Non-Road Mobile Source VOC Emissions in the txs_4km CAMx Domain for June 12 Episode Day

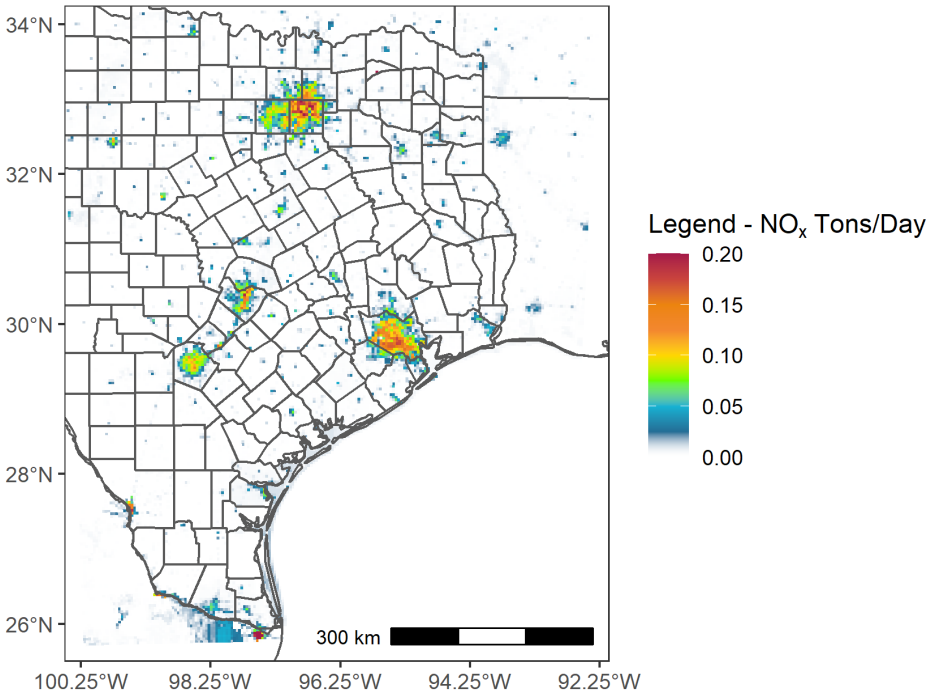

Figure 3-20: 2023 Future Case Non-Road Mobile Source NO_x Emissions in the txs_4km CAMx Domain for June 12 Episode Day

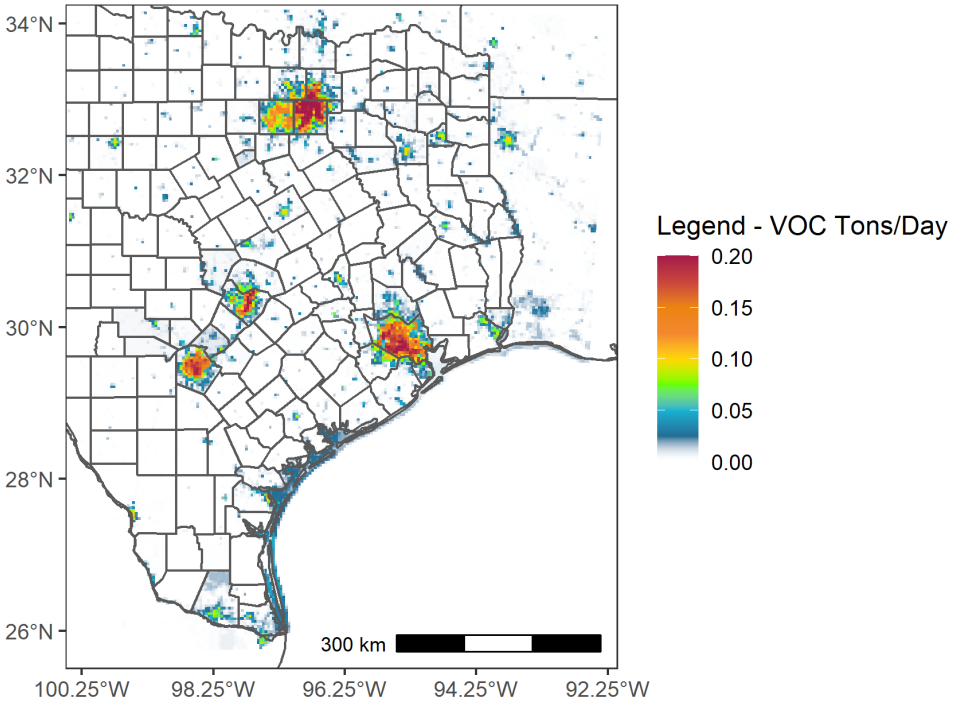

Figure 3-21: 2023 Future Case Non-Road Mobile Source VOC Emissions in the txs_4km CAMx Domain for June 12 Episode Day

3.5.2 Outside Texas

Non-road emissions for 2019 and 2023 for all non-Texas U.S. counties were estimated with MOVES3. For each non-Texas U.S. county, MOVES3 runs were performed to obtain

average weekday non-road emissions for the four seasons of Spring, Summer, Fall, and Winter. MOVES3 outputs emissions estimates for up to 206 SCCs associated with specific non-road equipment. For each calendar year and season, the average weekday non-road emissions estimates by county and SCC were prepared for photochemical model input with EPS3.

Non-road emissions for Canada and Mexico were obtained from the EPA's 2016v1 platform. For Canada, non-road emissions for 11 provinces and 205 SCCs were available for the 2015 and 2023 calendar years. With these data sets, 2023 estimates were used directly while 2019 emissions were linearly interpolated by province and SCC between 2015 and 2023. For Mexico, non-road emissions for 2,194 municipalities and two aggregate SCCs were available for the 2016 and 2023 calendar years. With these data sets, 2023 estimates were used directly while 2019 emissions were linearly interpolated by municipality and SCC between 2016 and 2023. For each calendar year and season, the average weekday non-road emissions estimates by county and SCC were prepared for photochemical model input with EPS3.

3.6 OFF-ROAD MOBILE SOURCES

3.6.1 Commercial Marine Vessels (CMV)

3.6.1.1 Within Texas

Commercial marine emission estimates were developed within Texas from publicly available Automatic Identification System (AIS) ship-tracking data.[15] The 2019 base case emissions inventory was constructed from these data using the MARINER Python tool developed by Ramboll US Consulting, Inc. (Ramboll), for the TCEQ. The tool was designed to follow the 2020 EPA guidance *Ports Emissions Inventory Guidance: Methodologies for Estimating Port-Related and Goods Movement Mobile Source Emissions.*[16] The emission estimates were projected to 2023 based on expected changes in shipping activity and reductions in emission rates from engine turnover as detailed in Ramboll's report *2020 Texas CMV Emissions Inventory and 2011 through 2050 Trend Inventories.*[17] The 2019 base and 2023 future case emissions were prepared for photochemical model input with EPS3 were seasonal and day-of-week temporal profiles were applied.

Table 3-19: *2019 Base Case CMV Emissions for June 12 Episode Day in HGB* and Table 3-20: *2023 Future Case CMW Emissions for June 12 Episode Day in HGB* show modeled NO_x, VOC, and CO emissions on the June 12 episode day for each county of HGB in the 2019 base case and 2023 future case, respectively. Table 3-19 and Table 3-20 indicate that counties that make up the Houston Ship Channel have the most emissions in both the base and future case and that emissions decreased between 2019 and 2023. Tile plots that show the spatial distribution of CMV emissions are provided in Attachment 1 of this appendix.

[15] https://marinecadastre.gov/ais/
[16] https://nepis.epa.gov/Exe/ZyPDF.cgi?Dockey=P1014J1S.pdf
[17] https://www.tceq.texas.gov/downloads/air-quality/research/reports/emissions-inventory/582211 1294fy2021-20210730-ramboll-2020-cmv-ei-trends.pdf

Table 3-19: 2019 Base Case CMV Emissions for June 12 Episode Day in HGB

County	NO_x (tpd)	VOC (tpd)	CO (tpd)
Brazoria	5.69	0.25	0.95
Chambers	2.81	0.16	0.41
Fort Bend	0.00	0.00	0.00
Galveston	25.9	1.45	4.0
Harris	29.00	1.75	4.46
Montgomery	3.09E-05	1.46E-06	4.91E-06
Six-County HGB Total	63.40	3.62	9.82

Table 3-20: 2023 Future Case CMW Emissions for June 12 Episode Day in HGB

County	NO_x (tpd)	VOC (tpd)	CO (tpd)
Brazoria	4.92	0.24	0.99
Chambers	2.45	0.17	0.43
Fort Bend	0.00	0.00	0.00
Galveston	22.48	1.44	4.20
Harris	25.25	1.77	4.70
Montgomery	2.66E-05	1.18E-06	5.09E-06
Six-County HGB Total	55.10	3.62	10.33

3.6.1.2 Outside Texas

Outside of the Texas 4km modeling domain, the EPA's 2016v1 platform was used for the 2019 and 2023 emissions inputs. This 2016 data was used as is for the 2019 base case. The 2016v1 platform has projected 2023 emissions, which was used as the input for the 2023 future case emissions input for non-Texas CMV source emissions. The 2019 base and 2023 future case emissions were prepared for photochemical model input with EPS3.

3.6.2 Airport Emissions Inventory

3.6.2.1 Within Texas

Airport emissions within Texas were developed using the data from trend inventories developed by TTI as 2019 and 2023 emission inputs. TTI used the Federal Aviation Agency (FAA) TAF 2019 dataset as well TxDOT Texas Airport System Plan (TASP), and the EPA's National Emission Inventory (NEI) database to develop activity rates. The activity rates were used in conjuncture with the fuel consumption data from the EIA's annual energy outlook (AEO) to estimate emissions. Projections are based on ratios of base year operations to each projected years operations using EIA's AEO and the TAF dataset projections. Details of TTI's methodology are detailed in the report *2020 Texas Statewide Airport Emissions Inventory and 2011 through 2050 Trend Inventories.*[18]

[18] https://www.tceq.texas.gov/downloads/air-quality/research/reports/emissions-inventory/5822111196-20211015-tti-texas-airport-2020-aerr-trend-ei.pdf

Table 3-21: *2019 Base Case Airport Emissions for June 12 Episode Day in DFW* and Table 3-22: *2023 Future Case Airport Emissions for June 12 Episode Day in DFW* provide a summary of NO_x, VOC, and CO emissions from airports in DFW for the June 12 episode day in the 2019 base and 2023 future case, respectively.

Table 3-21: 2019 Base Case Airport Emissions for June 12 Episode Day in DFW

Name	Airport Code	NO_x (tpd)	VOC (tpd)	CO (tpd)
DALLAS-FORT WORTH INTL	DFW	11.31	1.31	11.37
DALLAS LOVE FLD	DAL	2.01	0.43	2.48
FORT WORTH ALLIANCE	AFW	1.40	0.36	2.03
MCKINNEY NTL	TKI	0.70	0.22	1.99
FORT WORTH MEACHAM INTL	FTW	0.63	0.46	1.91
ADDISON	ADS	0.28	0.24	1.67
DENTON ENTERPRISE	DTO	0.18	0.22	1.73
ARLINGTON MUNI	GKY	0.14	0.14	1.09
MID-WAY RGNL	JWY	0.07	0.08	0.69
FORT WORTH SPINKS	FWS	0.07	0.13	1.09
Remaining 313 DFW Airports	313 Other	0.33	0.71	16.89
DFW Nine-County Airports Total		17.12	4.30	42.94

Table 3-22: 2023 Future Case Airport Emissions for June 12 Episode Day in DFW

Name	Airport Code	NO_x (tpd)	VOC (tpd)	CO (tpd)
DALLAS-FORT WORTH INTL.	DFW	9.97	1.16	10.03
DALLAS LOVE FLD	DAL	1.86	0.39	2.29
FORT WORTH ALLIANCE	AFW	1.40	0.36	2.02
MCKINNEY NTL	TKI	0.70	0.22	2.00
FORT WORTH MEACHAM INTL	FTW	0.61	0.45	1.87
ADDISON	ADS	0.31	0.26	1.81
DENTON ENTERPRISE	DTO	0.18	0.22	1.75
ARLINGTON MUNI	GKY	0.16	0.15	1.24
MID-WAY RGNL	JWY	0.07	0.08	0.69
FORT WORTH SPINKS	FWS	0.07	0.13	1.12
Remaining 313 DFW Airports	313 Other	0.37	0.79	17.57
DFW Nine-County Airport Total		15.69	4.23	42.38

Table 3-23: *2019 Base Case Airport Emissions for June 12 Episode Day in HGB* and Table 3-24: *2023 Future Case Airport Emissions for June 12 Episode Day in HGB* provides a summary of NO_x, VOC, and CO emissions from airports in HGB for the June 12 episode day in the 2019 base and 2023 future case, respectively.

Table 3-23: 2019 Base Case Airport Emissions for June 12 Episode Day in HGB

Name	Airport Code	NO_x (tpd)	VOC (tpd)	CO (tpd)
GEORGE BUSH INTCNTL/HOUSTON	IAH	6.40	0.93	7.69
WILLIAM P HOBBY	HOU	1.76	0.49	2.54
SUGAR LAND RGNL	SGR	0.28	0.19	0.98
DAVID WAYNE HOOKS MEML	DWH	0.22	0.18	1.43
CONROE-NORTH HOUSTON RGNL	CXO	0.21	0.13	1.14
ELLINGTON	EFD	0.07	0.28	1.55
TEXAS GULF COAST RGNL	LBX	0.07	0.16	1.18
WEST HOUSTON	IWS	0.05	0.10	1.80
HOUSTON-SOUTHWEST	AXH	0.04	0.05	0.63
SCHOLES INTL AT GALVESTON	GLS	0.04	0.05	0.52
Remaining 225 HGB Airports	225 Other	0.05	0.20	3.57
HGB Six-County Airport Total		9.20	2.77	23.04

Table 3-24: 2023 Future Case Airport Emissions for June 12 Episode Day in HGB

Name	Airport Code	NO_x (tpd)	VOC (tpd)	CO (tpd)
GEORGE BUSH INTCNTL/HOUSTON	IAH	5.00	0.72	6.01
WILLIAM P HOBBY	HOU	1.34	0.39	1.60
SUGAR LAND RGNL	SGR	0.28	0.19	0.98
DAVID WAYNE HOOKS MEML	DWH	0.25	0.20	1.58
CONROE-NORTH HOUSTON RGNL	CXO	0.23	0.15	1.26
ELLINGTON	EFD	0.07	0.28	1.55
TEXAS GULF COAST RGNL	LBX	0.07	0.18	1.28
WEST HOUSTON	IWS	0.05	0.11	1.91
HOUSTON-SOUTHWEST	AXH	0.05	0.06	0.70
SCHOLES INTL AT GALVESTON	GLS	0.04	0.06	0.57
Remaining 225 HGB Airports	225 Other	0.05	0.21	3.72
HGB Six-County Airport Total		7.44	2.54	21.16

Table 3-25: *2019 Base Case Airport Emissions for June 12 Episode Day in Bexar County*
Table 3-26: *2023 Future Case Airport Emissions for June 12 Episode Day in Bexar County* provide a summary of NO_x, VOC, and CO provides a summary of NO_x, VOC, and CO emissions from airports in Bexar County for the June 12 episode day in the 2019 base and 2023 future case, respectively.

Table 3-25: 2019 Base Case Airport Emissions for June 12 Episode Day in Bexar County

Name	Airport Code	NO_x (tpd)	VOC (tpd)	CO (tpd)
SAN ANTONIO INTL	SAT	1.77	0.32	2.01
STINTON MUNI	SSF	0.04	0.09	1.78
RANDOLPH AFB	RND	0.02	0.12	0.67
BOERNE STAGE FLD	5C1	0.01	0.03	0.71
CAMP BULLIS	9R7	0.01	0.00	0.02
Remaining 32 Bexar County Airports	32 Other	0.03	0.06	0.44
Bexar County Airport Total		1.89	0.62	5.63

Table 3-26: 2023 Future Case Airport Emissions for June 12 Episode Day in Bexar County

Name	Airport Code	NO_x (tpd)	VOC (tpd)	CO (tpd)
SAN ANTONIO INTL	SAT	1.60	0.29	1.82
STINTON MUNI	SSF	0.04	0.08	1.69
RANDOLPH AFB	RND	0.02	0.13	0.07
BOERNE STAGE FLD	5C1	0.01	0.03	0.07
CAMP BULLIS	9R7	0.01	0.00	0.02
Remaining 32 Bexar County Airports	32 Other	0.03	0.06	0.46
Bexar County Airport Total		1.72	0.59	5.38

Table 3-23 to Table 3-26 above show that there are a number of airports in each nonattainment area, emissions from the major airports with significant flight activity make up majority of the airport emissions inventory. Figures that show the spatial distribution of emissions in DFW, HGB, and Bexar County in the base and future case as well as the difference in emissions between 2019 and 2023 are provided in Attachment 1 of this appendix.

3.6.2.2 Outside Texas

For non-Texas US, Canadian, and Mexican areas, the EPA's 2016v1 platform was used for 2019 and 2023 emission inputs. The 2016 emissions were used as is for the 2019 base case while the projected 2023 emissions available in the EPA's 2016v1 platform was used for 2023 future case. Both the 2019 base case and 2023 future case emissions were processed with EPS3 for CAMx input.

3.6.3 Locomotives

3.6.3.1 Within Texas

Locomotive sources include railroad equipment, line-haul locomotives, class I/II/III operations, passenger trains, commuter lines, yard locomotives mobile sources, and internal combustion engine yard locomotives. Emission estimates were calculated by multiplying activity rate by emission rate based on engine types and fuel usage. 2019 base and 2023 future case locomotive emissions were estimated based on trend

inventories developed by TTI for the TCEQ. Projection factors for the trend inventories that were the basis for the 2019 and 2023 emissions were based on 2020 and 2021 AEO projections using an analysis of the United States energy supply, demand, and prices. Details of TTI's methodology are detailed in the final report *2020 Texas Statewide Locomotive and Rail Yard Emissions Inventory and 2011 through 2050 Trend Inventories.*[19] Both the 2019 base case and 2023 future case emissions were processed with EPS3 for CAMx input.

Table 3-27: *2019 Base Case Locomotive Emissions for June 12 Episode Day in DFW* and Table 3-28: *2023 Future Case Locomotive Emissions for June 12 Episode Day in DFW* provide a summary of NO_X, VOC, and CO emissions from locomotives and rail yards in DFW for the June 12 episode day in the 2019 base and 2023 future case, respectively.

Table 3-27: 2019 Base Case Locomotive Emissions for June 12 Episode Day in DFW

County Name	NO_X (tpd)	VOC (tpd)	CO (tpd)
Colin	0.43	0.02	0.10
Dallas	1.55	0.08	0.35
Denton	1.61	0.07	0.41
Ellis	0.79	0.04	0.20
Johnson	0.91	0.04	0.24
Kaufman	0.33	0.01	0.09
Parker	0.52	0.02	0.14
Tarrant	3.59	0.17	0.86
Wise	0.77	0.03	0.20
DFW Nine-County Total	10.50	0.49	2.60

Table 3-28: 2023 Future Case Locomotive Emissions for June 12 Episode Day in DFW

County Name	NO_X (tpd)	VOC (tpd)	CO (tpd)
Colin	0.33	0.02	0.09
Dallas	1.18	0.06	0.31
Denton	1.20	0.05	0.37
Ellis	0.59	0.03	0.18
Johnson	0.67	0.03	0.22
Kaufman	0.24	0.01	0.08
Parker	0.38	0.02	0.13
Tarrant	2.70	0.12	0.78
Wise	0.57	0.02	0.18
DFW Nine-County Total	7.87	0.35	2.35

Table 3-29: *2019 Base Case Locomotive Emissions for June 12 Episode Day in HGB* and Table 3-30: *2023 Future Case Locomotive Emissions for June 12 Episode Day in HGB*

[19] https://www.tceq.texas.gov/downloads/air-quality/research/reports/emissions-inventory/5822111027-20211015-tti-texas-locomotive-railyard-2020-aerr-trend-ei.pdf

provide a summary of NO_x, VOC, and CO emissions from locomotives and rail yards in HGB for the June 12 episode day in the 2019 base and 2023 future case, respectively.

Table 3-29: 2019 Base Case Locomotive Emissions for June 12 Episode Day in HGB

County Name	NO_x (tpd)	VOC (tpd)	CO (tpd)
Brazoria	1.18	0.06	0.28
Chambers	0.07	0.00	0.01
Fort Bend	1.46	0.06	0.40
Galveston	0.47	0.02	0.11
Harris	6.51	0.36	1.31
Montgomery	0.80	0.03	0.22
HGB Six-County Total	10.48	0.54	2.33

Table 3-30: 2023 Future Case Locomotive Emissions for June 12 Episode Day in HGB

County Name	NO_x (tpd)	VOC (tpd)	CO (tpd)
Brazoria	0.88	0.04	0.26
Chambers	0.05	0.00	0.01
Fort Bend	1.07	0.04	0.36
Galveston	0.36	0.02	0.10
Harris	4.97	0.26	1.18
Montgomery	0.59	0.02	0.20
HGB Six-County Total	7.93	0.39	2.11

Table 3-31: *2019 Base Case Locomotive Emissions for June 12 Episode Day in Bexar County* and Table 3-32: *2023 Future Case Locomotive Emissions for June 12 Episode Day in Bexar County* provide a summary of NO_x, VOC, and CO emissions from locomotives and rail yards in Bexar County for the June 12 episode day in the 2019 base and 2023 future case, respectively.

Table 3-31: 2019 Base Case Locomotive Emissions for June 12 Episode Day in Bexar County

County Name	NO_x (tpd)	VOC (tpd)	CO (tpd)
Bexar	1.98	0.09	0.5

Table 3-32: 2023 Future Case Locomotive Emissions for June 12 Episode Day in Bexar County

County Name	NO_x (tpd)	VOC (tpd)	CO (tpd)
Bexar	1.48	0.07	0.45

Figure 3-22: *2019 Base Case Locomotive NO_x Emissions in the txs_4km CAMx Domain for June 12 Episode Day* and Figure 3-23: *2019 Base Case Locomotive VOC Emissions in the txs_4km CAMx Domain for June 12 Episode Day* show the distribution of locomotive 2019 base case NO_x and VOC emissions, respectively, in the txs_4km CAMx domain for

the June 12 episode day. Similarly, Figure 3-24: *2023 Future Case Locomotive NO_X Emissions in the txs_4km CAMx Domain for June 12 Episode Day* and Figure 3-25: *2023 Future Case Locomotive VOC Emissions in the txs_4km CAMx Domain for June 12 Episode Day* show the distribution of locomotive 2023 future case NO_x and VOC emissions, respectively, in the txs_4km CAMx domain for the same June 12 episode day. The figures show that locomotive emissions are concentrated along rail lines and that emissions mostly decrease between 2019 base case and 2023 future case. Additional figures focused on the DFW, HGB, and Bexar County nonattainment areas are provided in Attachment 1 of this appendix.

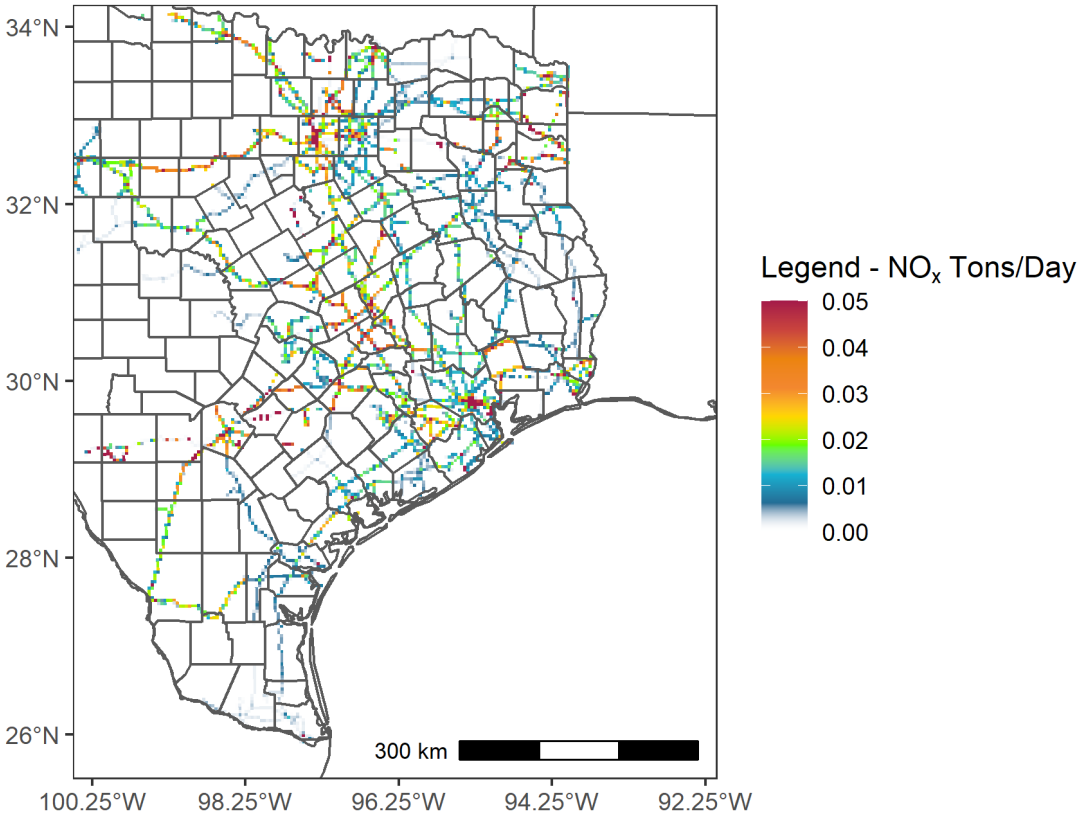

Figure 3-22: 2019 Base Case Locomotive NO_x Emissions in the txs_4km CAMx Domain for June 12 Episode Day

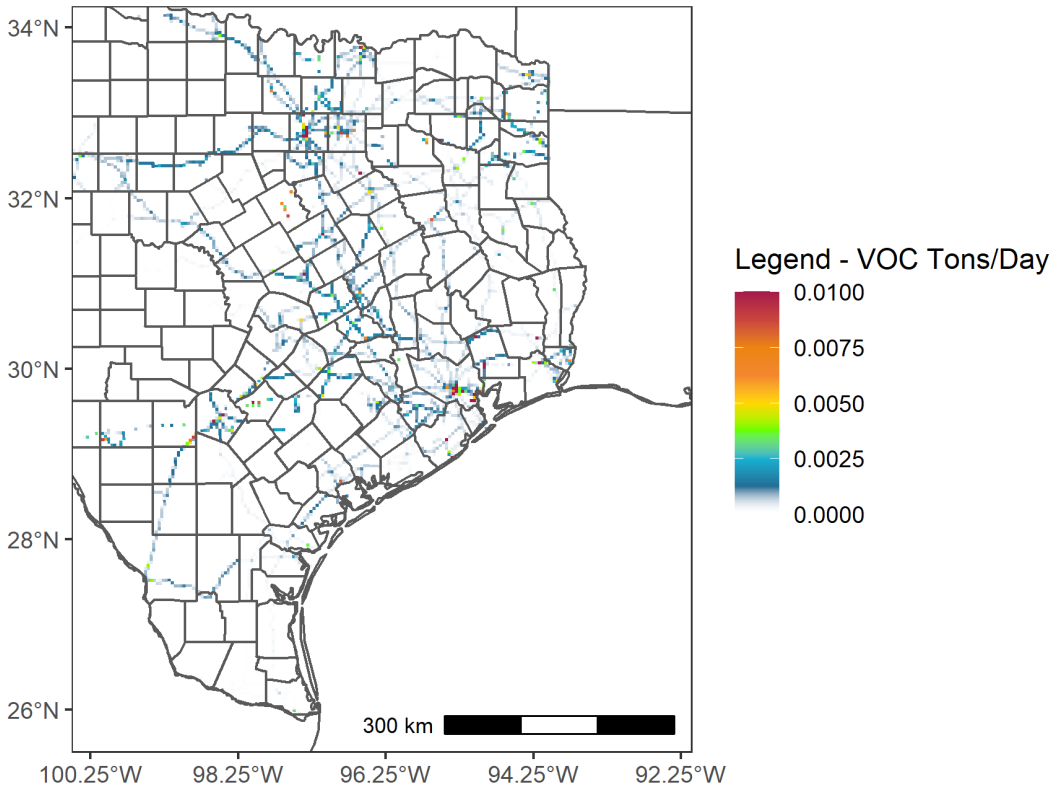

Figure 3-23: 2019 Base Case Locomotive VOC Emissions in the txs_4km CAMx Domain for June 12 Episode Day

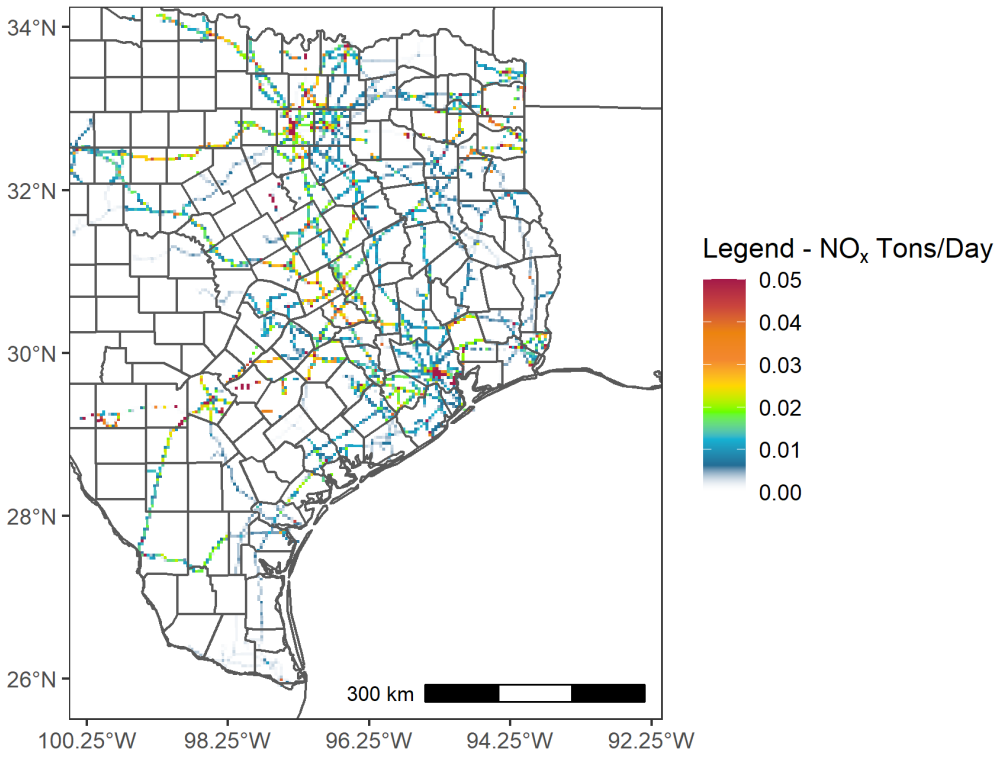

Figure 3-24: 2023 Future Case Locomotive NO_x Emissions in the txs_4km CAMx Domain for June 12 Episode Day

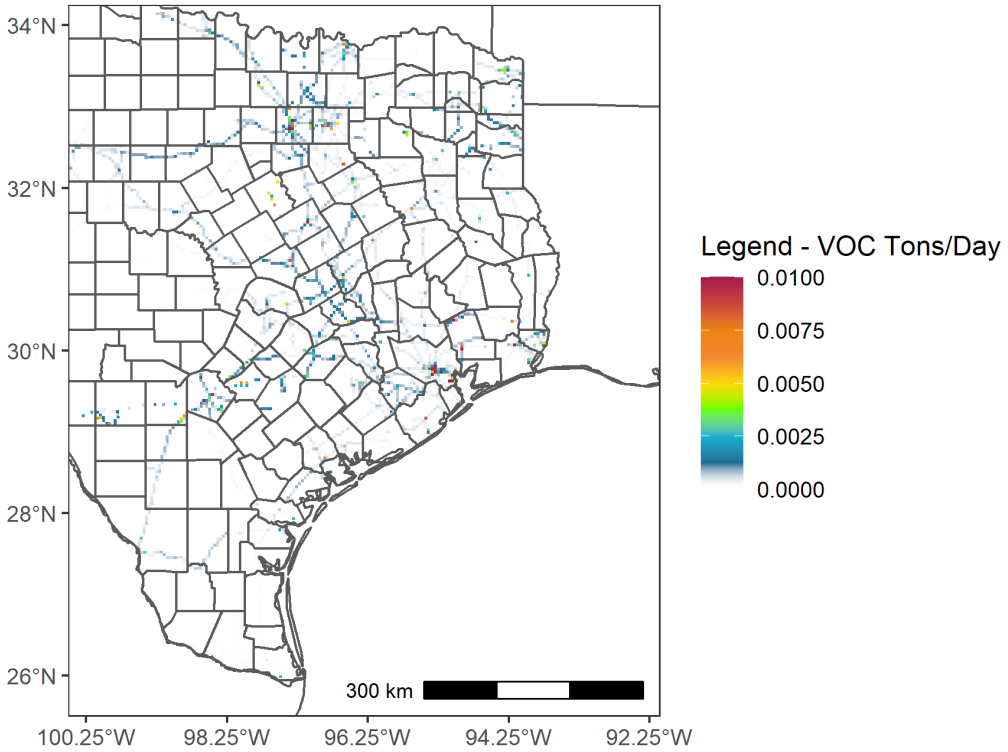

Figure 3-25: 2023 Future Case Locomotive VOC Emissions in the txs_4km CAMx Domain for June 12 Episode Day

3.6.3.2 Outside Texas

For non-Texas data CONUS, Canada and Mexico, the EPA's 2016v1 platform was used as inputs for 2019 base and 2023 future case. The 2016 emissions from 2016v1 were used as is for the 2019 base case scenario. For the 2023 future case, emissions were adjusted using the United State EIA fuel combustion data for all states outside of Texas. Both the 2019 base case and 2023 future case emissions were processed with EPS3 for CAMx input.

3.7 AREA SOURCE EMISSIONS INVENTORY DEVELOPMENT

3.7.1 Within Texas

Emissions sources referred to as area sources include commercial, small-scale industrial, and residential activities that use materials or conduct processes that can generate emissions. This includes dry-cleaners, gas stations, residential heating, and numerous other "miscellaneous" source categories. With some exceptions, area source emission estimates are obtained by multiplying an established emission factor by the appropriate activity or activity surrogate (e.g. human population) responsible for generating the emissions.

Base case 2019 area source emissions estimates were developed from a TexAER 2020 version 4 periodic inventory that was back-casted to 2019 using projection factors from an ERG study entitled Growth Factors for Area and Point Sources (https://www.tceq.texas.gov/assets/public/implementation/air/am/contracts/reports/ei/582166257608FY1608-20160630-erg-growth_factors_area_point.pdf). Projection factors from the same study were also used to project the 2020 inventory for the 2023 future case.

Seasonal adjustments were made by applying factors based on U.S. EIA seasonal fuel combustion data. Both the 2019 base case and 2023 future case emissions were processed with EPS3 for CAMx input.

Summaries of the 2019 base case and 2023 future case emissions by county for the DFW, HGB, and Bexar County 2015 eight-hour ozone nonattainment areas are provided below in Table 3-33: *2019 Base Case Area Source Emissions for June 12* Episode *Day in DFW*, Table 3-34: *2023 Future Case Area Source Emissions for June 12 Episode Day in DFW*, Table 3-35: *2019 Base Case Area Source Emissions for June 12 Episode Day in HGB*, Table 3-36: *2023 Future Case Area Source Emissions for June 12 Episode Day in HGB*, and Table 3-37: *2019 Base Case and 2023 Future Case Area Source Emissions for June 12 Episode Day in Bexar County*.

Table 3-33: 2019 Base Case Area Source Emissions for June 12 Episode Day in DFW

County	NO_x (tpd)	VOC (tpd)	CO (tpd)
Collin	4.54	28.59	6.46
Dallas	12.75	93.01	18.00
Denton	2.98	25.26	4.22
Ellis	1.38	7.10	3.39
Johnson	0.78	7.36	3.00
Kaufman	0.61	5.18	2.68
Parker	0.52	5.86	1.21
Tarrant	9.11	71.00	13.90
Wise	0.27	4.12	0.83
Nine-County DFW Total	32.93	247.47	53.69

Table 3-34: 2023 Future Case Area Source Emissions for June 12 Episode Day in DFW

County	NO_x (tpd)	VOC (tpd)	CO (tpd)
Collin	4.56	30.97	6.77
Dallas	13.30	96.11	18.67
Denton	3.03	27.23	4.49
Ellis	1.45	7.57	3.62
Johnson	0.82	7.79	3.18
Kaufman	0.64	5.56	2.91
Parker	0.53	6.34	1.30
Tarrant	9.58	74.40	14.56
Wise	0.28	4.33	0.86
Nine-County DFW Total	34.18	260.32	56.36
Difference between 2023 and 2019	1.25	12.85	2.67

Table 3-35: 2019 Base Case Area Source Emissions for June 12 Episode Day in HGB

County	NO_X (tpd)	VOC (tpd)	CO (tpd)
Brazoria	8.81	20.96	19.48
Chambers	0.46	2.49	1.24
Fort Bend	2.29	20.50	3.79

County	NO_X (tpd)	VOC (tpd)	CO (tpd)
Galveston	1.34	12.15	1.77
Harris	19.27	180.45	25.78
Montgomery	2.97	19.32	34.42
Six-County HGB Total	35.16	255.86	86.47

Table 3-36: 2023 Future Case Area Source Emissions for June 12 Episode Day in HGB

County	NO_x (tpd)	VOC (tpd)	CO (tpd)
Brazoria	8.86	22.02	20.97
Chambers	0.48	2.82	1.34
Fort Bend	2.34	22.49	4.06
Galveston	1.38	12.62	1.84
Harris	20.08	188.92	27.03
Montgomery	3.12	21.19	38.34
Six-County HGB Total	36.27	270.06	93.57
Difference between 2023 and 2019	1.11	14.20	7.10

Table 3-37: 2019 Base Case and 2023 Future Case Area Source Emissions for June 12 Episode Day in Bexar County

Year	NO_X (tpd)	VOC (tpd)	CO (tpd)
2019	5.34	77.40	9.66
2023	5.53	81.14	10.10
Difference between 2023 and 2019	0.19	3.74	0.44

Area source emissions are typically tied to activity from sources based on human population (i.e., agricultural production, residential processes, industrial sources). Therefore, more densely populated areas, such as Texas metropolitan areas, experience more emissions from these sources as seen in Figure 3-26: *2019 Base Case (left) and 2023 Future Case (right) Area Source NO_X Emissions in the txs_4km Domain for June 12 Episode Day* and Figure 3-29: *2019 Base Case (left) and 2023 Future Case (right) Area Source VOC Emissions in the txs_4km Domain for June 12 Episode Day*. Figure 3-26 and Figure 3-29 show the spatial distribution of NO_X and VOC emissions within the txs_4km domain for the June 12 modeled episode day in the 2019 base and 2023 future case.

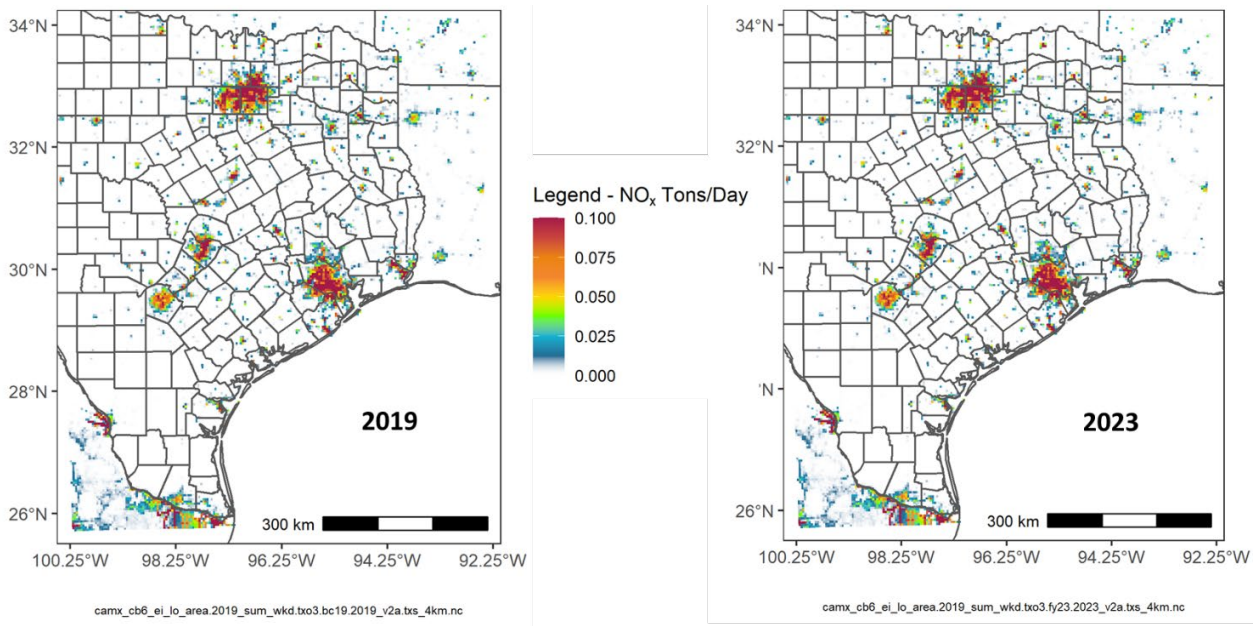

Figure 3-26: 2019 Base Case (left) and 2023 Future Case (right) Area Source NO_x Emissions in the txs_4km Domain for June 12 Episode Day

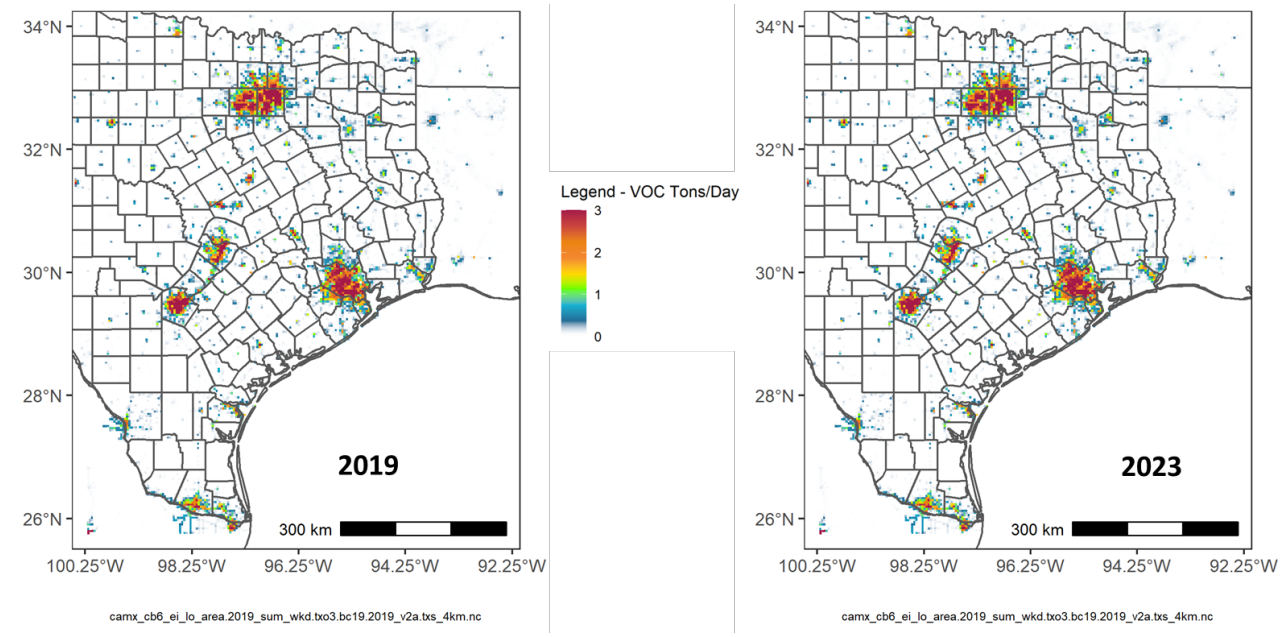

Figure 3-27: 2019 Base Case (left) and 2023 Future Case (right) Area Source VOC Emissions in the txs_4km Domain for June 12 Episode Day

As population in Texas metropolitan areas is expected to increase, emissions from area sources also tend to increase as can be seen from the difference in precursor emissions shown in Table 3-34, Table 3-36, and Table 3-37. The spatial distribution of these differences in precursor emissions between 2023 and 2019 for the June 12 episode day in the DFW, HGB, and Bexar County nonattainment areas are shown in Figure 3-28: *Difference Between 2023 and 2019 for the June 12 Episode Day in Area Source NO_x Emissions in the DFW (top left), HGB (top right), and Bexar County (bottom*

center) Nonattainment Areas and Figure 3-29: *Difference Between 2023 and 2019 for the June 12 Episode Day in Area Source VOC Emissions in the DFW (top left), HGB (top right), and Bexar County (bottom center) Nonattainment Areas.* Figures showing the spatial distribution of area source emissions are available in Attachment 1.

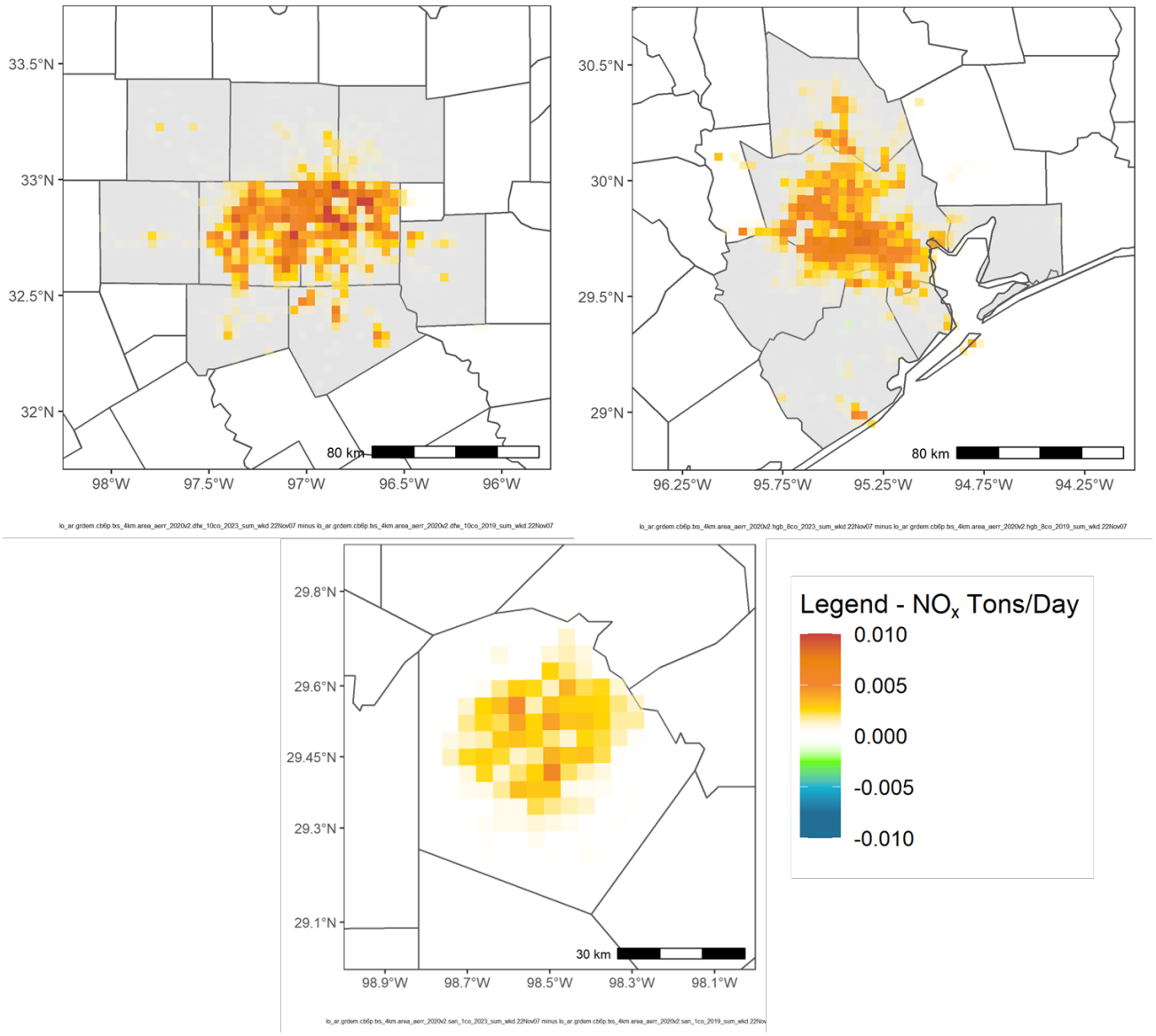

Figure 3-28: Difference Between 2023 and 2019 for the June 12 Episode Day in Area Source NO_x Emissions in the DFW (top left), HGB (top right), and Bexar County (bottom center) Nonattainment Areas

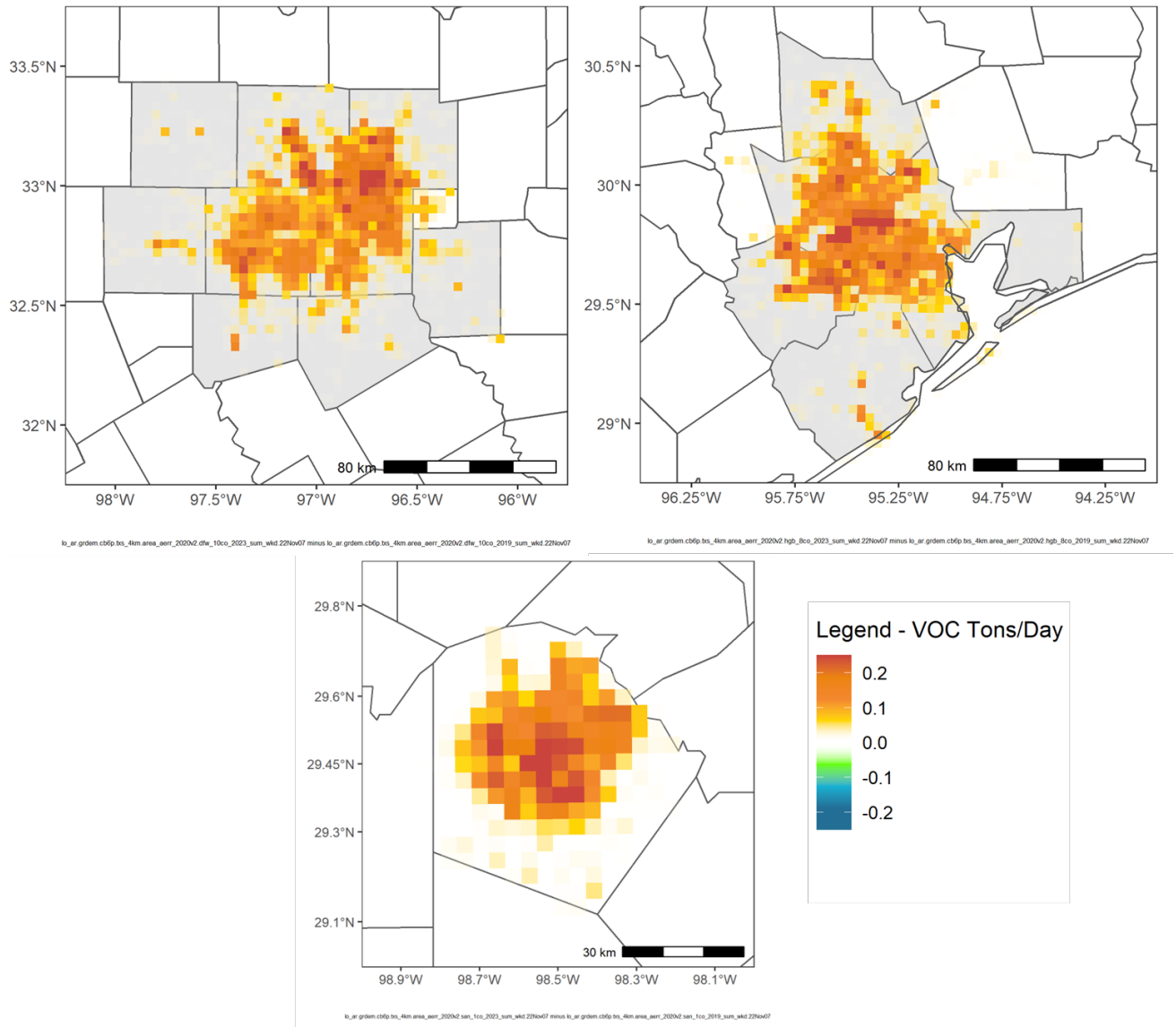

Figure 3-29: Difference Between 2023 and 2019 for the June 12 Episode Day in Area Source VOC Emissions in the DFW (top left), HGB (top right), and Bexar County (bottom center) Nonattainment Areas

3.7.2 Outside Texas

For non-Texas U.S. areas, the EPA's 2016v1 platform was used for the 2019 and 2023 emissions inputs. This 2016 data was used without any projections as 2019 base case emissions. The 2016v1 platform has projected 2023 future year emissions, which was used as the input for the 2023 non-Texas area source emissions. These emissions were also adjusted by season using U.S. EIA fuel combustion data by state for all states outside of Texas. Both the 2019 base case and 2023 future case emissions were processed with EPS3 for CAMx input.

3.8 OIL AND GAS AND GWEI

3.8.1 Oil and Gas Production and Drilling Emissions

3.8.1.1 Within Texas

Production Emissions

Base case 2019 oil and gas production emission estimates were developed based on 2019 activity data obtained from the Railroad Commission of Texas (RRC) multiplied by emission factors for specific operations and types of equipment.[20] Sources included for these emissions include onshore oil and gas production, onshore oil and gas exploration, and natural gas and crude oil production.

Oil and gas production emissions estimates for the 2023 future case were developed using shale based 2019-to-2023 projection factors from an ERG study entitled *Growth Factors for Area and Point Sources.*[21] The ERG study provided projection factors for counties in the different shales - the Barnett Shale, Eagle Ford Shale, Haynesville Shale, and Permian Basin (see Figure 3-30: *Texas Oil and Gas Shale Formation by County*).

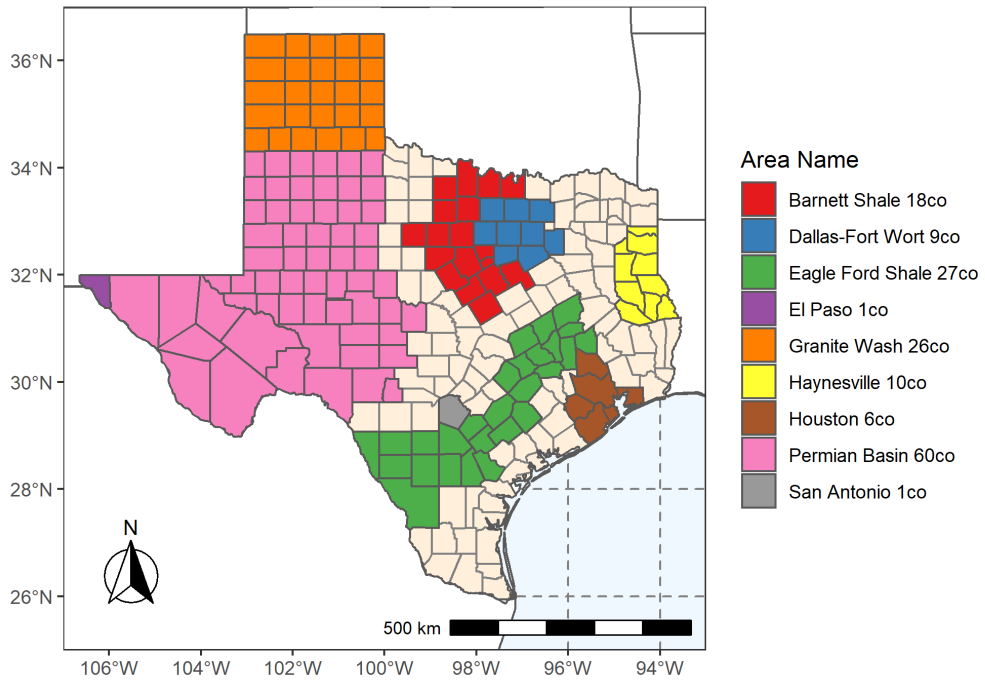

Figure 3-30: Texas Oil and Gas Shale Formation by County

In addition to projected 2023 activity where available, current regulations that are expected to reduce emissions in 2023 were also considered when developing the 2023 future case emissions. Rules in Texas Administrative Code Chapter 115, Subchapter B,

[20] https://www.rrc.texas.gov/resource-center/research/data-sets-available-for-download/#oil-and-gas-regulatory-data-table

[21] https://www.tceq.texas.gov/assets/public/implementation/air/am/contracts/reports/ei/582166257608FY1608-20160630-erg-growth_factors_area_point.pdf

Division 7 include requirements with a compliance date of January 1, 2023, that will reduce oil and gas production fugitive VOC emissions in DFW and HGB.

Since the DFW area is fully contained in the Barnett Shale, the Barnett Shale projection factors from the ERG study were applied to DFW. The emissions reductions from the Chapter 115 rule for production fugitive emissions were applied on top of the 2023 oil and gas production projections for DFW to obtain the 2023 future case estimates for DFW. Table 3-39: *2019 Base Case Production Emissions for June 12 Episode Day in DFW* and Table 3-40: *2023 Future Case Production Emissions for June 12 Episode Day* in *DFW* provide the ozone precursor emissions by county for the June 12 modeled episode day in DFW for the 2019 base case and 2023 future case, respectively. Table 3-40 also includes the difference in emission between the 2023 future case and 2019 base case which shows that NO_x, VOC, and CO emissions reduced with a significant decrease in VOC emissions.

Table 3-38: 2019 Base Case Production Emissions for June 12 Episode Day in DFW

County	NO_x (tpd)	VOC (tpd)	CO (tpd)
Collin	0.00	0.00	0.00
Dallas	0.04	0.14	0.09
Denton	0.49	8.93	0.84
Ellis	0.02	0.17	0.03
Johnson	0.51	8.59	0.73
Kaufman	0.01	0.25	0.03
Parker	0.18	4.62	0.28
Tarrant	1.41	12.04	2.11
Wise	7.73	15.59	3.55
Nine-County DFW Total	10.39	50.33	7.66

Table 3-39: 2023 Future Case Production Emissions for June 12 Episode Day in DFW

County	NO_x (tpd)	VOC (tpd)	CO (tpd)
Collin	0.00	0.00	0.00
Dallas	0.01	0.04	0.03
Denton	0.17	2.74	0.28
Ellis	0.01	0.06	0.02
Johnson	0.17	2.75	0.23
Kaufman	0.01	0.18	0.03
Parker	0.06	1.46	0.09
Tarrant	0.45	3.72	0.66
Wise	2.55	5.60	1.31
Nine-County DFW Total	3.42	16.56	2.65
Total Difference between 2023 and 2019	-6.97	-33.77	-5.01

Figure 3-31: *2019 Base Case NO_X (top left) and VOC (bottom left) and 2023 Future Case NO_X (top right) and VOC (bottom right) Production Emissions in DFW for June 12 Episode Day* shows the spatial distribution of NO_X and VOC emissions in DFW 2015 eight-hour ozone nonattainment area (shaded lighly grey) for the June 12 modeled episode day for the 2019 base case and 2023 future case. Figure 3-31 shows in line with Table 3-39 and Table 3-40, that in DFW VOC production emissions are greater than NO_X emissions in both the 2019 base and 2023 future case.

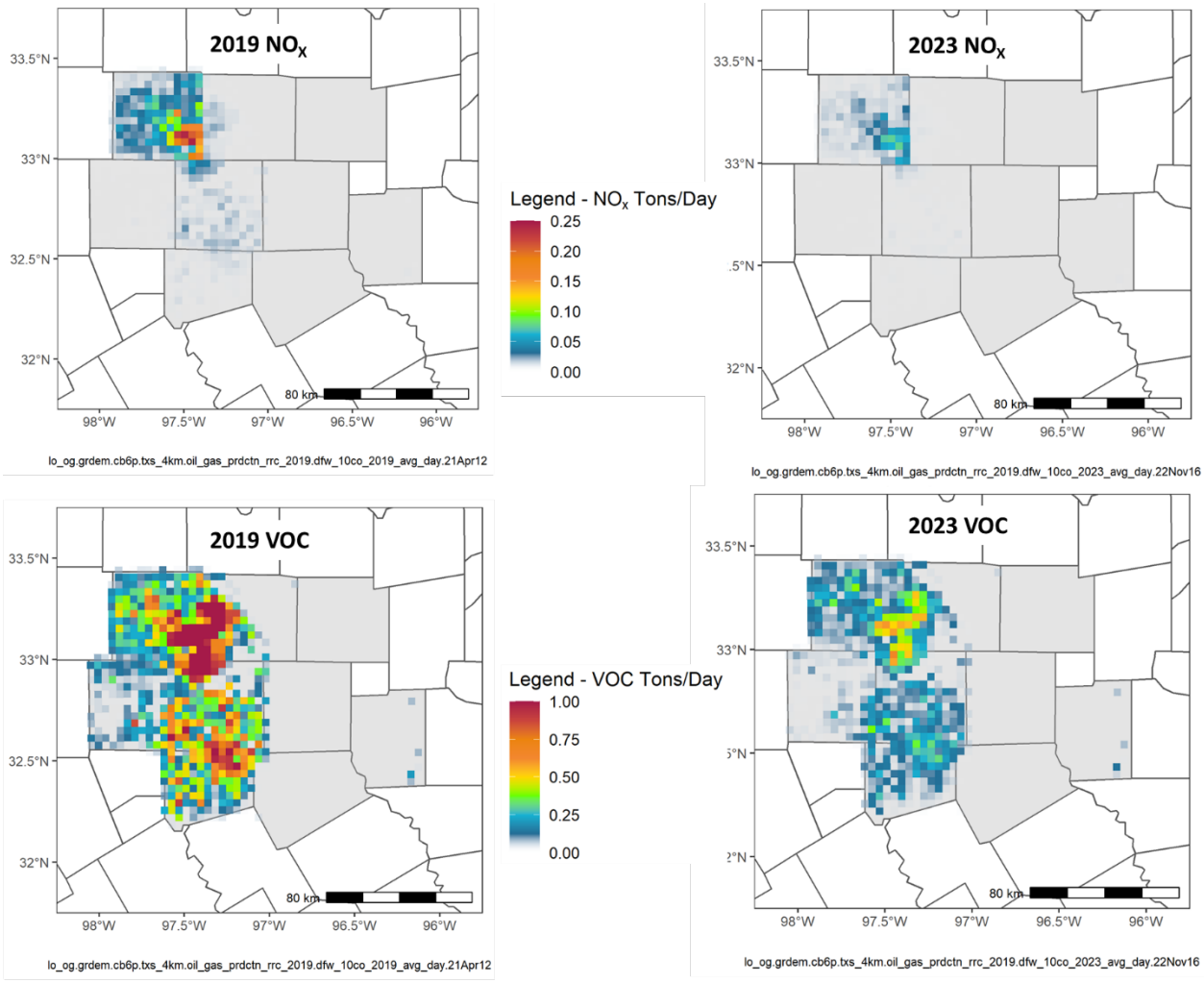

Figure 3-31: 2019 Base Case NO_X (top left) and VOC (bottom left) and 2023 Future Case NO_X (top right) and VOC (bottom right) Production Emissions in DFW for June 12 Episode Day

Figure 3-32: *Difference Between 2023 and 2019 for June 12 Episode Day in Production NO_X (left) and VOC (right) Emissions in DFW* shows the spatial distribution of the reductions in oil and gas production emissions in DFW.

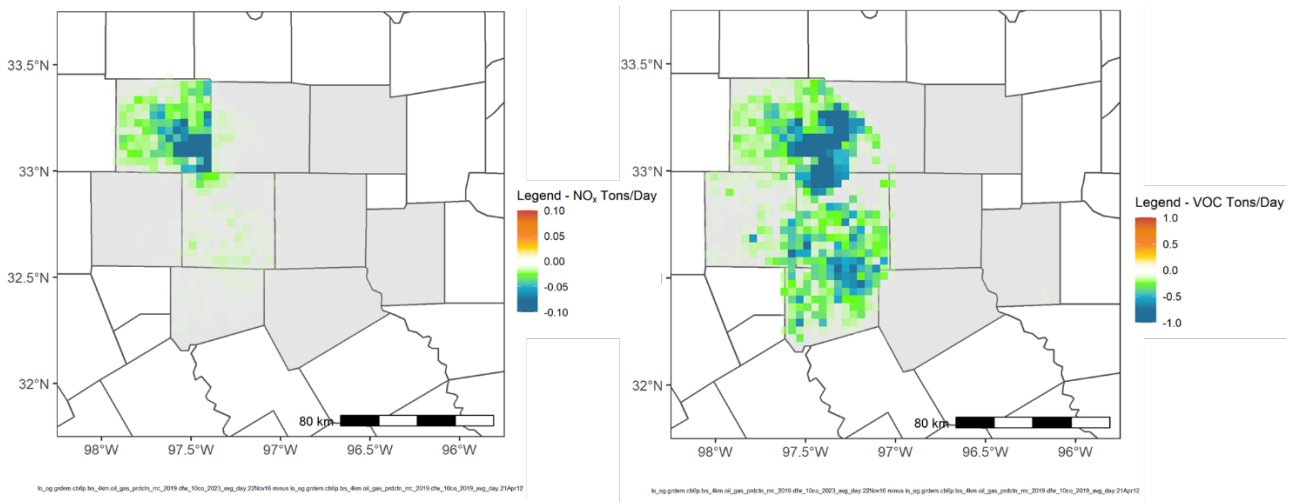

Figure 3-32: Difference Between 2023 and 2019 for June 12 Episode Day in Production NO_x (left) and VOC (right) Emissions in DFW

Since HGB is not contained within one of Texas shales, 2023 projected oil and gas production activity is not available so except for VOC emissions, the 2019 base case emissions were used as 2023 future case. For the 2023 future case VOC emission estimates, the emissions reductions from the Chapter 115 rule for production fugitive emissions were applied on top of the HGB 2019 VOC emissions estimates.

Table 3-40: 2019 Base Case Production Emissions by County for June 12 Episode Day in HGB

County	NO_x (tpd)	VOC (tpd)	CO (tpd)
Brazoria	0.28	14.88	0.39
Chambers	0.14	6.83	0.19
Fort Bend	0.23	4.21	0.33
Galveston	0.05	1.06	0.07
Harris	0.21	4.11	0.34
Montgomery	0.11	4.16	0.16
Six-County HGB Total	1.01	35.25	1.48

Table 3-41: 2023 Future Case Production Emissions by County for June 12 Episode Day in HGB

County	NO_x (tpd)	VOC (tpd)	CO (tpd)
Brazoria	0.28	5.89	0.39
Chambers	0.14	3.35	0.19
Fort Bend	0.23	2.17	0.33
Galveston	0.05	0.55	0.07
Harris	0.21	2.32	0.34
Montgomery	0.11	2.70	0.16
Six-County HGB Total	1.01	16.98	1.48
Difference between 2023 and 2019	0.00	-18.27	0.00

Since Bexar County is not contained within one of these shales projected oil and gas production activity for 2023 were not available and the 2019 base case emissions were used as is for 2023 future case. Table 3-43: *2019 Base Case and 2023 Future Case Production Emissions for June 12 Episode Day in Bexar County Day* provides NO_x, VOC, and CO emissions modeled for the June 12 episode day for both the 2019 base and 2023 future case.

Table 3-42: 2019 Base Case and 2023 Future Case Production Emissions for June 12 Episode Day in Bexar County Day

County	NO_x (tpd)	VOC (tpd)	CO (tpd)
Bexar	1.71	6.38	2.59

A small portion of the total oil and gas production emissions for Texas include offshore oil and gas production and exploration in 5 counties. This data comes from a TexAER 2020 version 4 periodic inventory done for area source emissions. These 2020 offshore oil and gas emissions estimates were kept as is for 2019 and 2023. Table 3-44: *2019 Base Case and 2023 Future Case Offshore Oil and Gas Production Emissions for June 12 Episode Day* shows emissions from offshore oil and gas production for 2019 base and 2023 future case modeled for the June 12 episode day.

Table 3-43: 2019 Base Case and 2023 Future Case Offshore Oil and Gas Production Emissions for June 12 Episode Day

County	NO_x (tpd)	VOC (tpd)	CO (tpd)
Galveston	0.06	0.01	0.06
Jefferson	0.01	0.00	0.01
Kleberg	0.01	0.00	0.01
Calhoun	0.04	0.00	0.04
Nueces	0.01	0.00	0.02
Five-County Offshore Total	0.12	0.01	0.15

Drilling Rig Emissions

2019 oil and gas drilling emission estimates were based on the ERG study, *2014 Statewide Drilling Rig Emissions Inventory with Updated Trends Inventories*[22] and RRC activity data. 2019 emissions estimates were developed by applying fleet turnover activity projections from the ERG study to the 2019 RRC activity data. Emissions sources for these estimates include vertical drilling less than 7,000 feet, vertical drilling greater than 7,000 feet, and horizontal/directional drilling. San Antonio had no oil & gas drilling rig activity in 2019.

Oil and gas drilling rig emissions estimates were projected to the 2023 future year by applying the 2023 fleet turnover activity projections to the 2019 estimates, where activity is held constant but the emissions rate changes. Table 3-45: *2019 Base Case*

[22] https://wayback.archive-it.org/414/20210527185246/https://www.tceq.texas.gov/assets/public/implementation/air/am/contracts/reports/ei/5821552832FY1505-20150731-erg-drilling_rig_2014_inventory.pdf

and 2023 Future Case Drilling Rig Emissions for June 12 Episode Day in DFW and Table 3-46: *2019 Base Case and 2023 Future Case Drilling Rig Emissions for June 12 Episode Day in HGB* shown below provide the drilling rig emissions for NO_x, VOC, and CO in tpd for both the 2019 base case and 2023 future case.

Table 3-44: 2019 Base Case and 2023 Future Case Drilling Rig Emissions for June 12 Episode Day in DFW

Model Case	NO_x (tpd)	VOC (tpd)	CO (tpd)
2019 Base Case	0.20	0.01	0.01
2023 Future Case	0.19	0.01	0.01

Table 3-45: 2019 Base Case and 2023 Future Case Drilling Rig Emissions for June 12 Episode Day in HGB

Model Case	NO_x (tpd)	VOC (tpd)	CO (tpd)
2019 Base Case	0.29	0.03	0.06
2023 Future Case	0.25	0.02	0.03

Figure 3-33: *2019 Base Case Oil & Gas NO_x Emissions in the txs_4km CAMx Domain for June 12 Episode Day* and Figure 3-34: *2019 Base Case Oil & Gas VOC Emissions in the txs_4km CAMx Domain for June 12 Episode Day* show the spatial distribution of 2019 base case emissions NO_x and VOC emissions within the txs_4km domain for June 12 modeled episode.

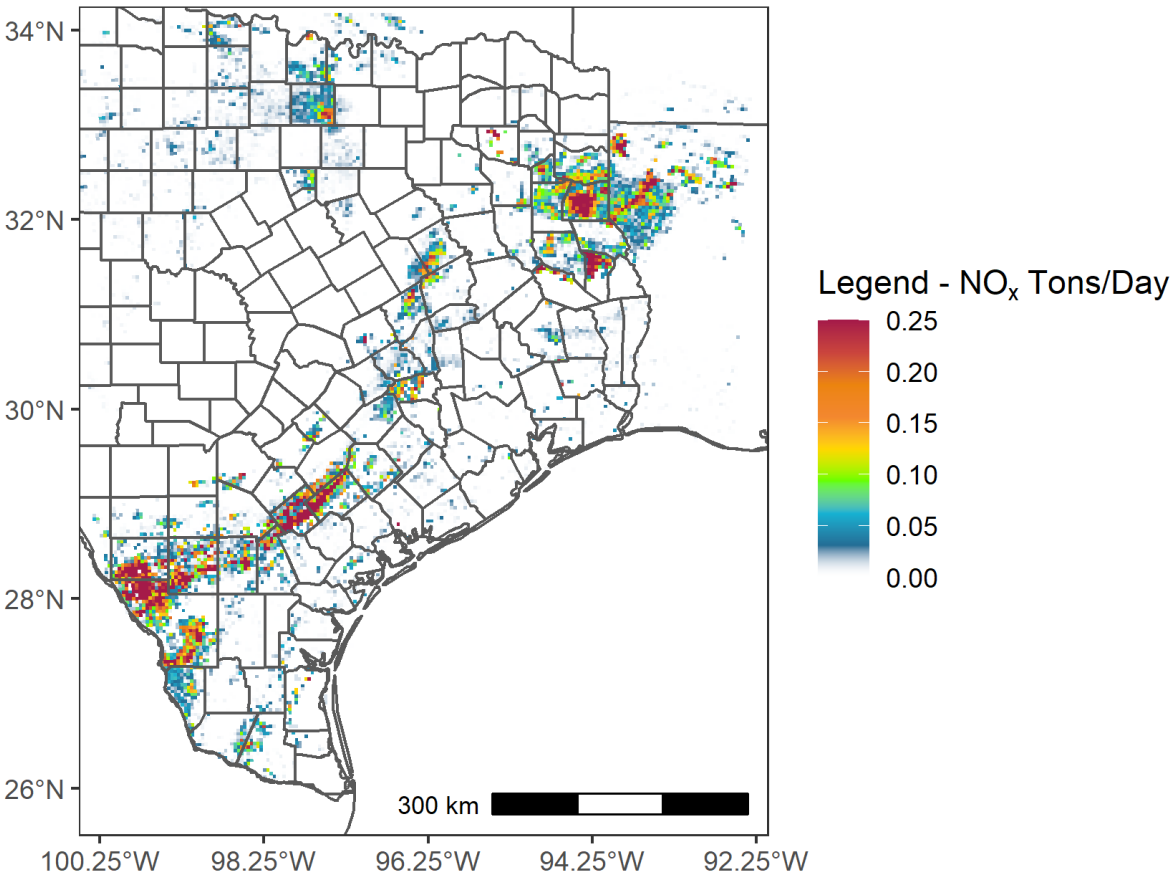

Figure 3-33: 2019 Base Case Oil & Gas NO_x Emissions in the txs_4km CAMx Domain for June 12 Episode Day

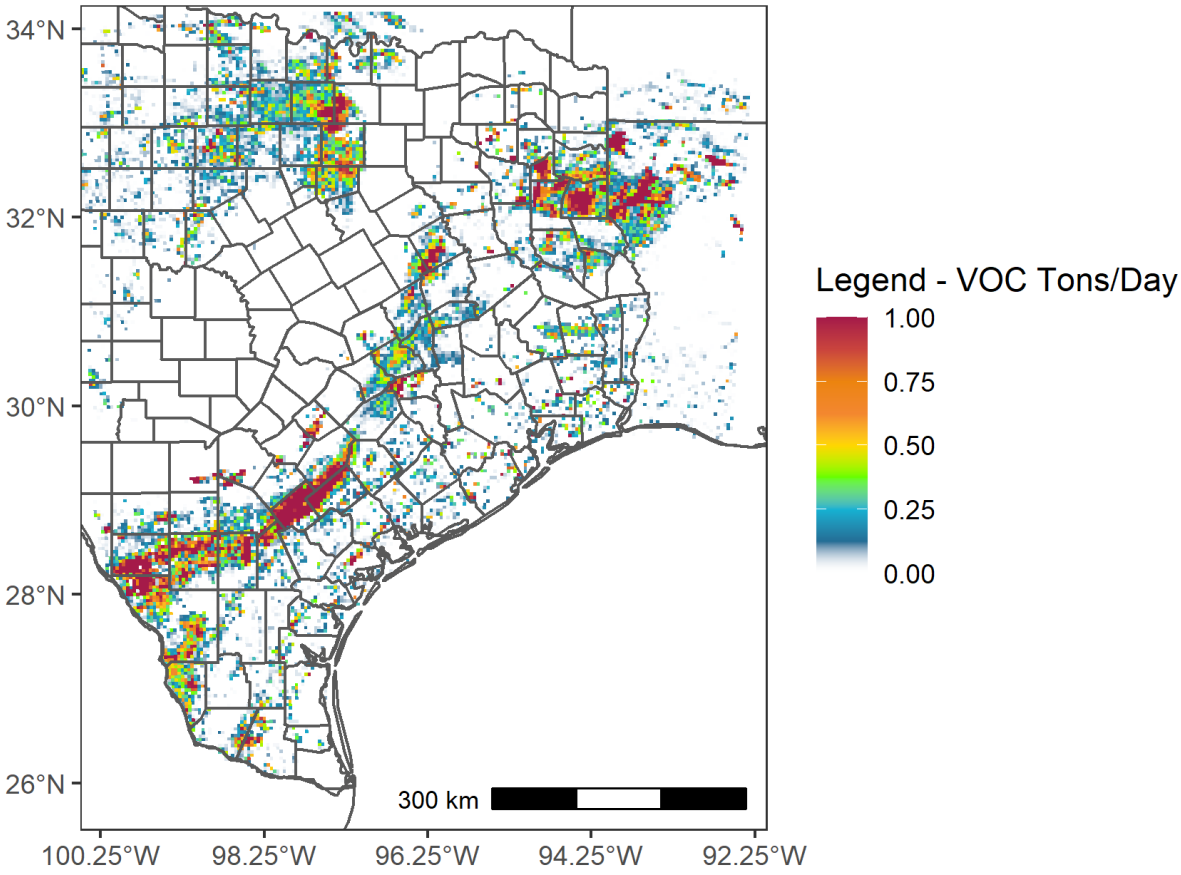

Figure 3-34: 2019 Base Case Oil & Gas VOC Emissions in the txs_4km CAMx Domain for June 12 Episode Day

In both Figure 3-33 and Figure 3-34, it can be seen how the spatial distribution of the emissions correspond to the different shales depicted in Figure 3-30.

Figure 3-35: *2023 Future Case Oil & Gas NO_x Emissions in the txs_4km CAMx Domain for June 12 Episode Day* and Figure 3-36: *2023 Future Case Oil & Gas VOC Emissions in the txs_4km CAMx Domain for June 12 Episode Day* show the spatial distribution of 2023 future case emissions NO_x and VOC emissions within the txs_4km domain for June 12 modeled episode. Additional figures showing the spatial distribution of emissions in the three nonattainment areas are available in Attachment 1.

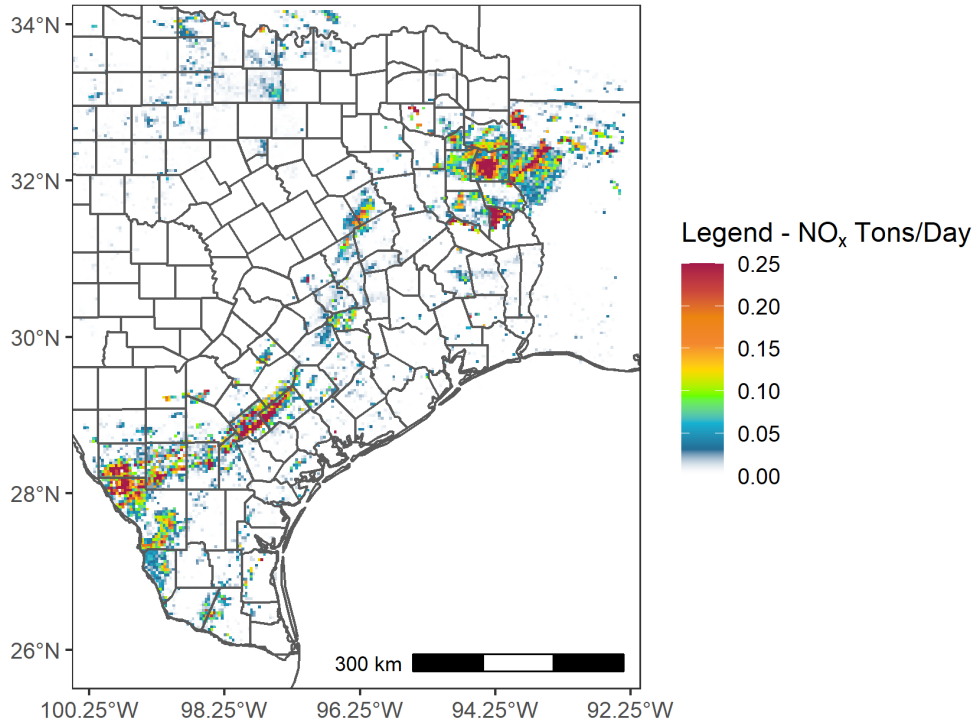

Figure 3-35: 2023 Future Case Oil & Gas NO_x Emissions in the txs_4km CAMx Domain for June 12 Episode Day

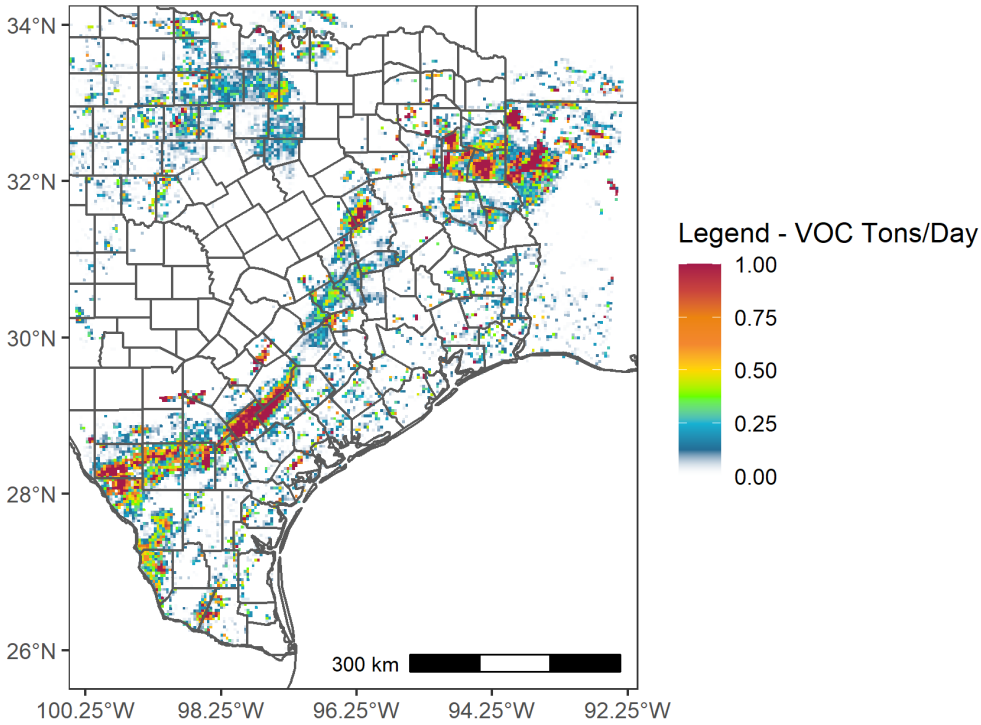

Figure 3-36: 2023 Future Case Oil & Gas VOC Emissions in the txs_4km CAMx Domain for June 12 Episode Day

3.8.1.2 Outside Texas

Non-Texas oil and gas emissions from the rest of the United States excluding Texas were obtained from SMOKE inputs from the 2017gb version of the EPA 2017 modeling platform.[23] These emissions were projected from 2017 to the 2019 base year by applying U.S. EIA historical oil and gas production levels. Non-Texas 2023 future case oil and gas emissions were developed from SMOKE input files from EPA's 2016v1 platform which included a projected 2023 future year emissions.

3.8.2 Off-Shore (Gulf of Mexico) Non-Platform

Emissions estimates for the Offshore – Gulf of Mexico sector for non-platform sources were obtained from the 2017 GWEI, developed by ERG under contract BOEM. 2017 is the most recent available inventory for these emissions. The report[24] and data are divided into two parts: oil and gas exploration and production platform (point) sources, and non-platform (area) sources. Non-platform related emissions are provided by month and are based on activity data from the relevant sources. The platform emissions estimates data provided by BOEM also include low-level emissions, which can be seen in Table 3-47: *Gulf Low-Level Emissions for June 12 Episode Day*. The elevated platform point source emissions are described in Section 3.3 *Point Sources*.

The non-platform emissions include several SCCs that are accounted for with better resolution in the CMV emissions inventory. This includes most ocean-going vessels, both recreational and commercial. Therefore, these SCCs were excluded from the non-platform emissions processing so as not to double count with the emissions accounted for by the same SCCs in the CMV sector, leaving five source categories associated with the non-platform emissions: helicopters, floating production storage and offloading, recreational fishing, crude oil lightering activity, and biogenic/geogenic sources. Table 3-48: *Gulf Non-Platform Emissions by Source Category for June 12 Episode Day* shows non-platform emissions by SCC. Diurnal curves to temporalize the emissions to hourly are not available for the 2017 GWEI, so curves developed for the 2008 GWEI were used to process emissions. These emissions were not projected to 2019 or any future year since projection factors or activity estimates are not available.

Table 3-46: Gulf Low-Level Emissions for June 12 Episode Day

Emissions Type	NO_X (tpd)	VOC (tpd)	CO (tpd)
Platform	7.52	74.89	9.54
Non-Platform	16.72	39.26	3.49
Total	24.24	114.15	13.03

[23] The EPA 2017gb modeling platform is available at: https://gaftp.epa.gov/Air/emismod/2017/2017emissions/.
[24] The BOEM 2019 Gulf-wide Emissions Inventory report is available at: https://espis.boem.gov/final%20reports/BOEM_2019-072.pdf.

Table 3-47: Gulf Non-Platform Emissions by Source Category for June 12 Episode Day

SCC	SCC Description	NO_x (tpd)	VOC (tpd)	CO (tpd)
2275050012	General Aviation - Turbine - Assigned Here for Helicopters	0.41	0.22	0.23
22800021FP (custom)	Custom - Commercial Marine - Floating Production Storage and Offloading	3.12	0.04	0.58
22800021RF (custom)	Custom - Commercial Marine - Recreational Fishing	10.60	0.56	2.10
22800022LP (custom)	Custom - Louisiana Offshore Oil Port - Crude Oil Lightering Activity	2.60	0.78	0.58
2701200000	Biogenic - Vegetation - Assigned Here for Crude Oil Seepage and Mud Volcanoes	0.00	37.67	0.00
	Total	16.72	39.26	3.49

Figure 3-37: *2019 Base and 2023 Future Case Offshore Non-Platform NO_X Emissions for June 12 Episode Day in Gulf of Mexico* and Figure 3-38: *2019 Base and 2023 Future Case Offshore Non-Platform VOC Emissions for June 12 Episode Day in Gulf of Mexico* show the NO_x and VOC emissions from pffshore non-platform sources modeled for the June episode day.

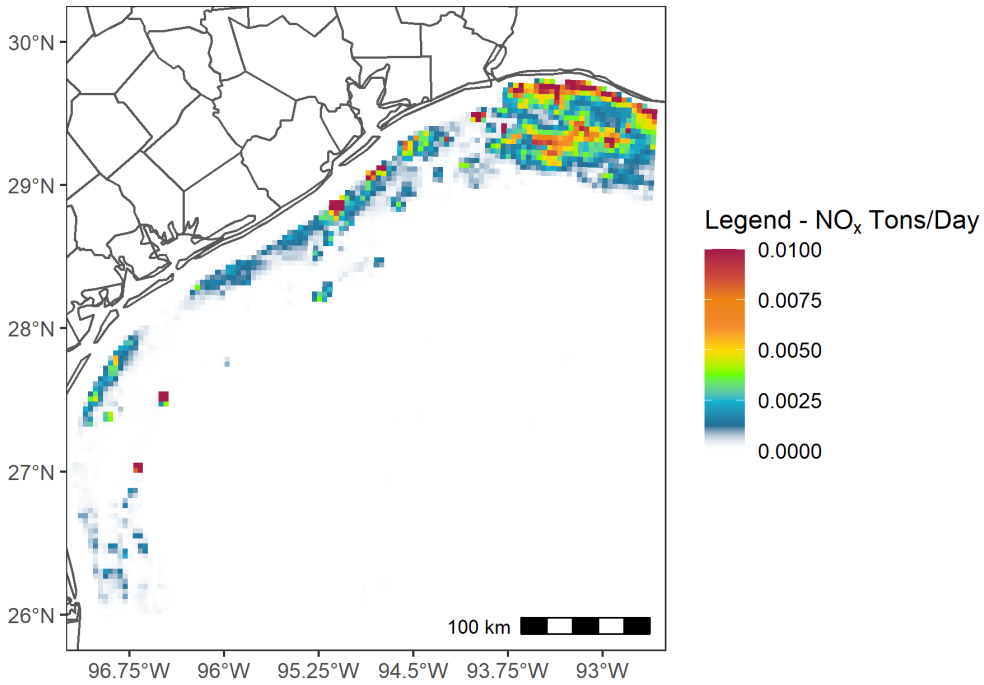

Figure 3-37: 2019 Base and 2023 Future Case Offshore Non-Platform NO_x Emissions for June 12 Episode Day in Gulf of Mexico

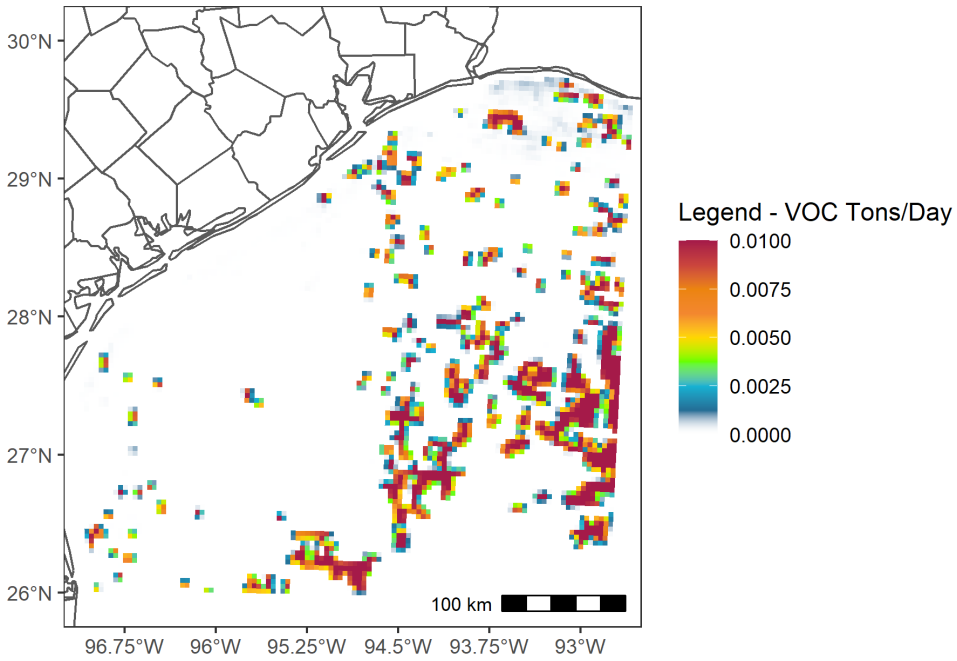

Figure 3-38: 2019 Base and 2023 Future Case Offshore Non-Platform VOC Emissions for June 12 Episode Day in Gulf of Mexico

3.9 OTHER COUNTRIES (NON-US, NON-CANADA, AND NON-MEXICO)

The TCEQ 36km and 12km domains include countries or portions of countries other than US, Canada, and Mexico. The Emissions from these other counties were estimated using a platform consisting of the Hemispheric Transport of Air Pollutants Version 2 (HTAPv2) emission inventory, the SMOKE modeling system version 4.7, the Community Emissions Data System (CEDS), and custom post-processing scripts; this system is referred to as the CEDS Platform[25]. The 2010 HTAPv2 gridded inventory was projected to 2019 using scale factors by sector, pollutant, and country from the CEDS emission totals of 2019 and 2010. To avoid potential double counting emissions, data from the HTAPv2 shipping and aircraft sectors were excluded. The 2019 base case emissions from the CEDS Platform were used as is for the 2023 future case for emission from countries other than US, Canada, or Mexico that lie within the 36km and 12km domain. Figure 3-39: CEDS Elevated NO_X Emissions for June 12 Episode Day is a plot of the elevated NO_x emissions from the CEDS platform for the na_36-km domain on June 12, 2019. The elevated emissions are from the aircraft cruising, aircraft climbing/descending, and energy sectors. Figure 3-40: *CEDS Low-Level NO_X Emissions for June 12 Episode Day* is a plot of the low-level NO_x emissions from the CEDS platform for the na_36-km domain on June 12, 2019. The low-level emissions are from the agricultural, industrial, residential, and transportation.

[25] The CEDS Platform and methodology are detailed in the "Processing Global Anthropogenic Emissions from CEDS" report that is available at https://wayback.archive-it.org/414/20210529064327/https://www.tceq.texas.gov/assets/public/implementation/air/am/contracts/reports/pm/5822010973010-20200629-ramboll-ProcessingGlobalAnthropogenicEmissionsfromCEDS.pdf

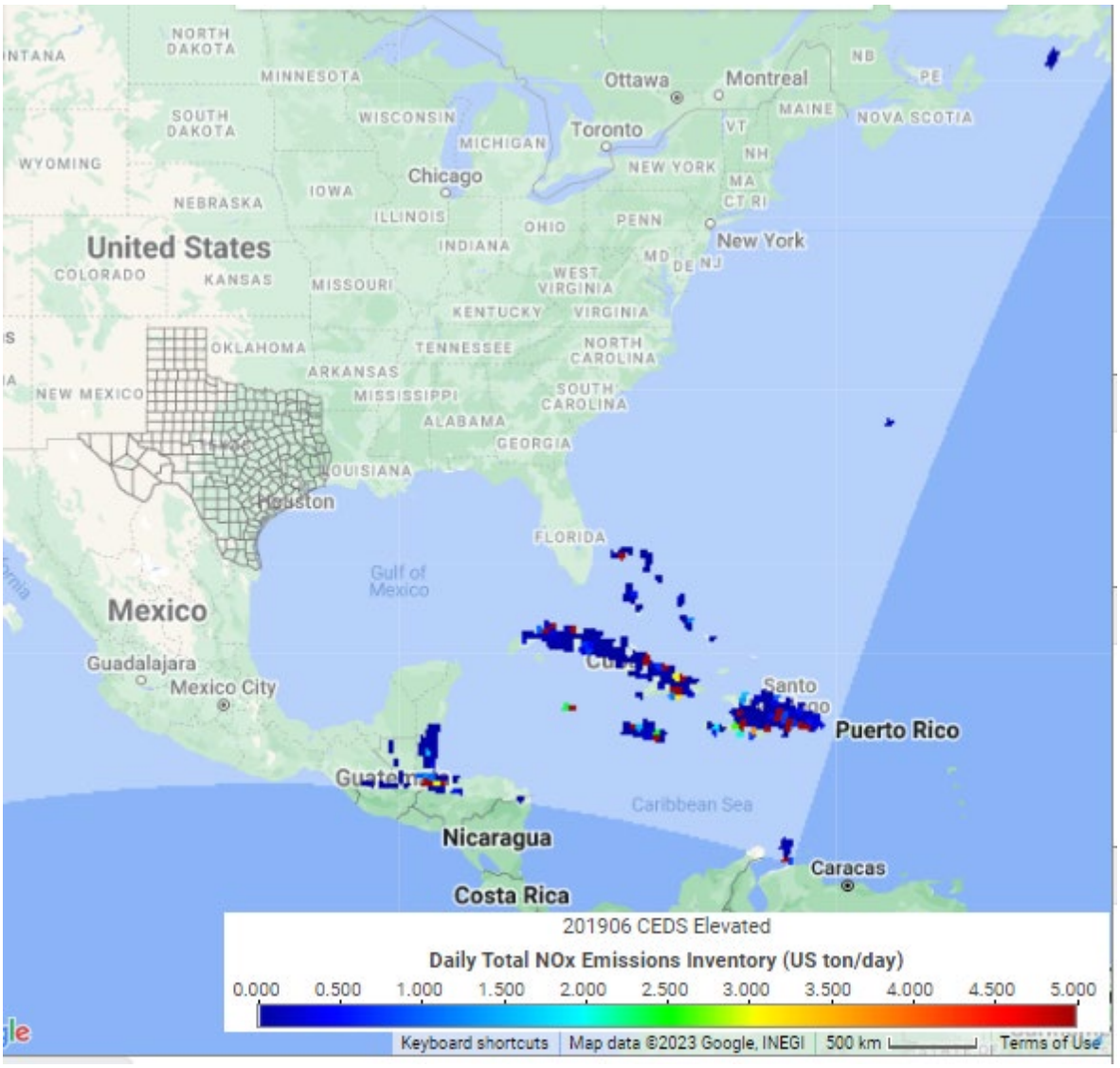

Figure 3-39: CEDS Elevated NO_x Emissions for June 12 Episode Day

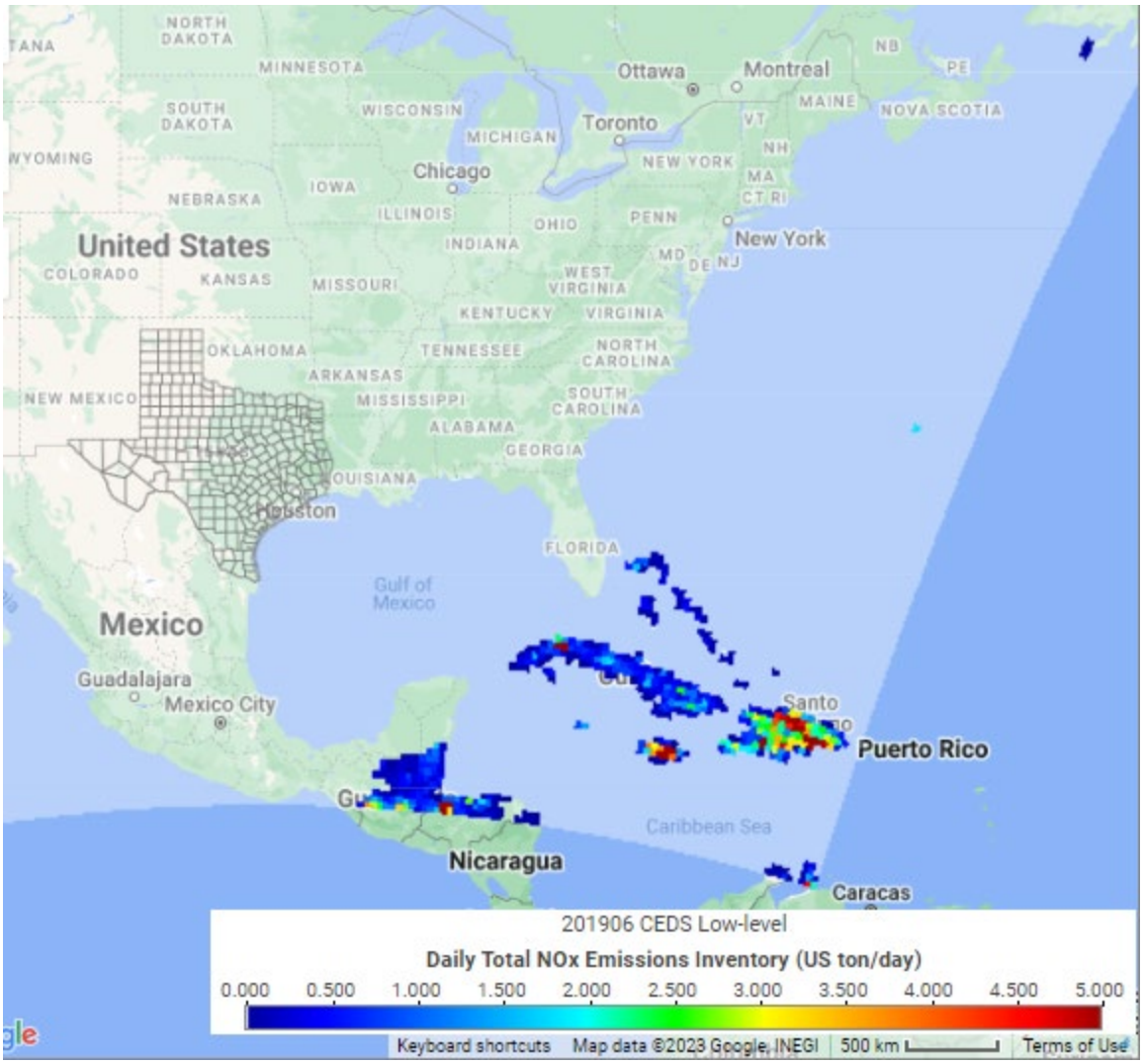

Figure 3-40: CEDS Low-Level NO_x Emissions for June 12 Episode Day

4. INITIAL AND BOUNDARY CONDITIONS

Initial and boundary conditions (IC/BC) for 2019 and 2023 were derived from global model simulations using the Goddard Earth Observing Station global atmospheric model with Chemistry (GEOS-Chem) model. The TCEQ contracted with the University of Houston (UofH) to complete the GEOS-Chem model runs necessary for IC/BC development. The GEOS-Chem simulations were run from March to October with a two-month spin-up time. For both modeled years, GEOS-Chem version 12.7.1 was run at 2° × 2.5° horizontal resolution using tropospheric chemistry with simplified secondary organic aerosols (Tropchem+simpleSOA), which was the recommended GEOS-Chem configuration. Both modeled years used 2019 meteorology from the Modern-Era Retrospective analysis for Research and Applications, Version 2 (MERRA-2).

For emissions inputs, the simulations performed for IC/BC development used the Community Emission Data System (CEDS) global inventory superimposed by the National Emission Inventory (NEI) for the continental US, Air Pollutant Emission Inventory (APEI) for Canada, and MIX inventory for Asia. For the 2019 anthropogenic EI, UofH used the 2011 NEI scaled to year-2013 emission level, 2014 APEI, and 2010 MIX. These emissions were the latest available inventories in GEOS-Chem for the respective regions. The 2023 future anthropogenic EI were interpolated according to a moderate emission scenario from Representative Concentration Pathways (RCP4.5), with regional scaling factors for the US, Canada, Mexico, and Asia. UofH generated county-level scaling factors for the US and Mexico and provincial-level scaling factors for Canada based the 2023 and 2025 emissions inventories from the EPA 2016v1 modeling platform. For Asia, grided scaling factors based on the latest version (v6b) of Evaluating the Climate and Air Quality Impact of Short-Lived Pollutants (ECLIPSE) inventory from the International Institute for Applied Systems Analysis (IIASA) were used.

From the GEOS-Chem model results, lateral boundary conditions were extracted for each grid cell along all four lateral boundaries of the outer 36 km modeling domain. The ozone boundary conditions on all four lateral boundaries are plotted for June 12, 2019, in Figure 4-1: *Lateral Boundary Conditions for Ozone on June 12, 2019.* Top boundary conditions were also developed to represent pollutant concentrations from atmospheric layers above the highest CAMx vertical layer. The top boundary condition for June 12 in the base and future years is mapped in Figure 4-2: *Top Boundary Condition for Ozone on June 12 in 2019 and 2023.* As shown, the future year has an increased amount of ozone present in the boundary conditions.

The GEOS-Chem model results were also used to develop initial conditions, which are used to initiate the CAMx model runs. Only one initial condition file is needed for each month, taken from hour 00:00 on the fifteenth day of each month in the ozone season. Ozone concentrations from the June initial condition file for 2019 and 2023 are mapped in Figure 4-3: *June Initial Condition for Ozone in 2019 and 2023.*

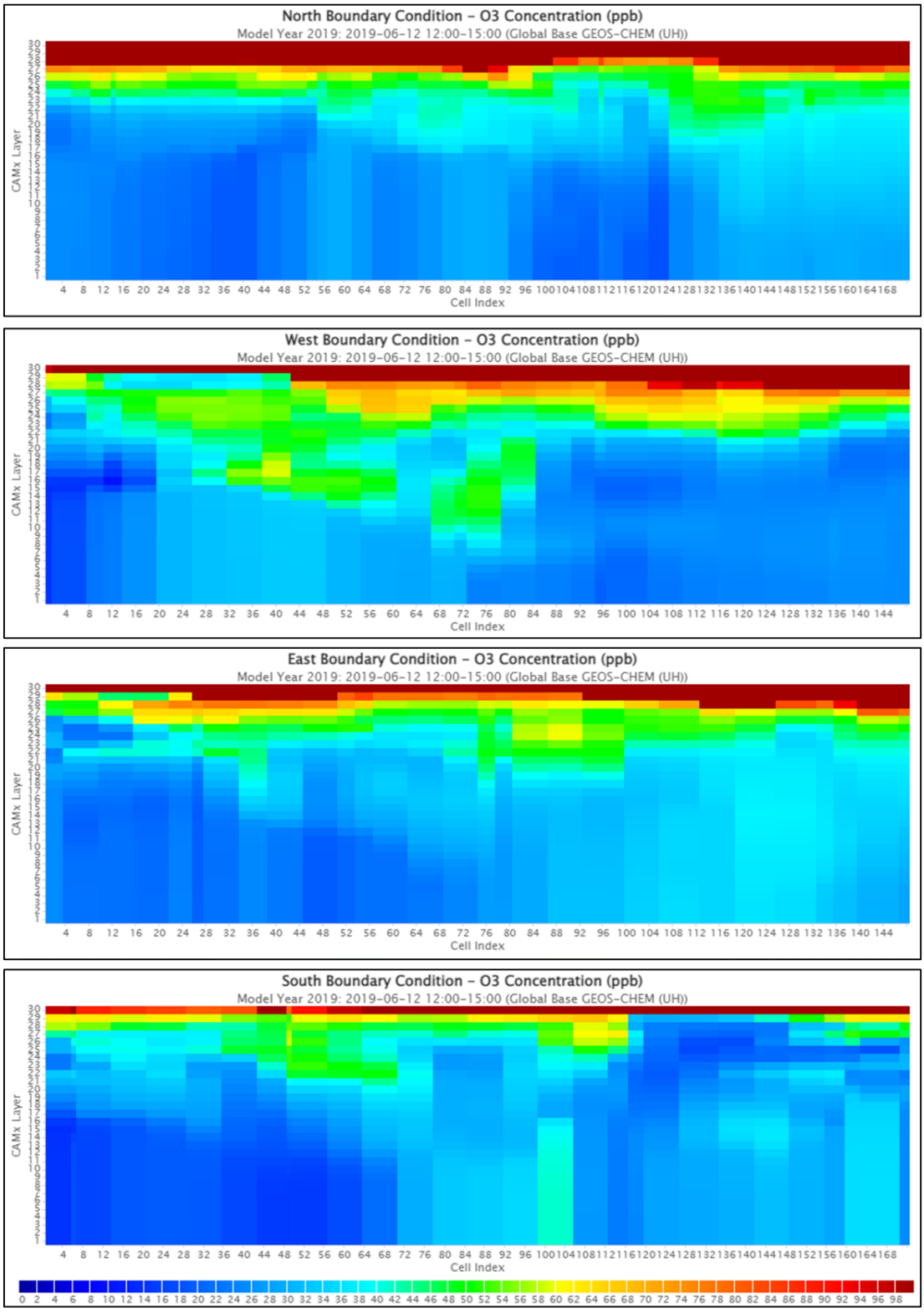

Figure 4-1: Lateral Boundary Conditions for Ozone on June 12, 2019

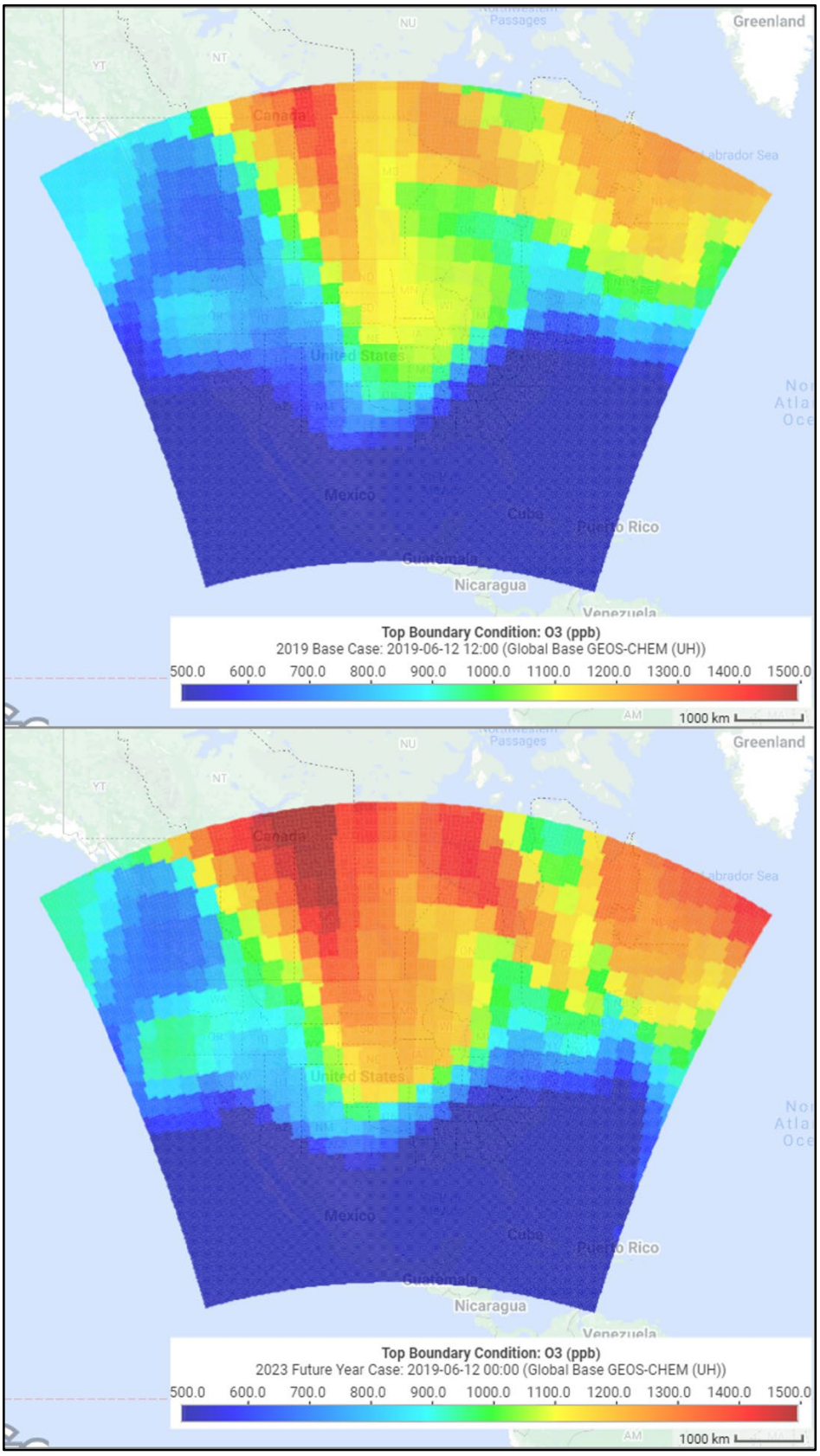

Figure 4-2: Top Boundary Condition for Ozone on June 12 in 2019 and 2023

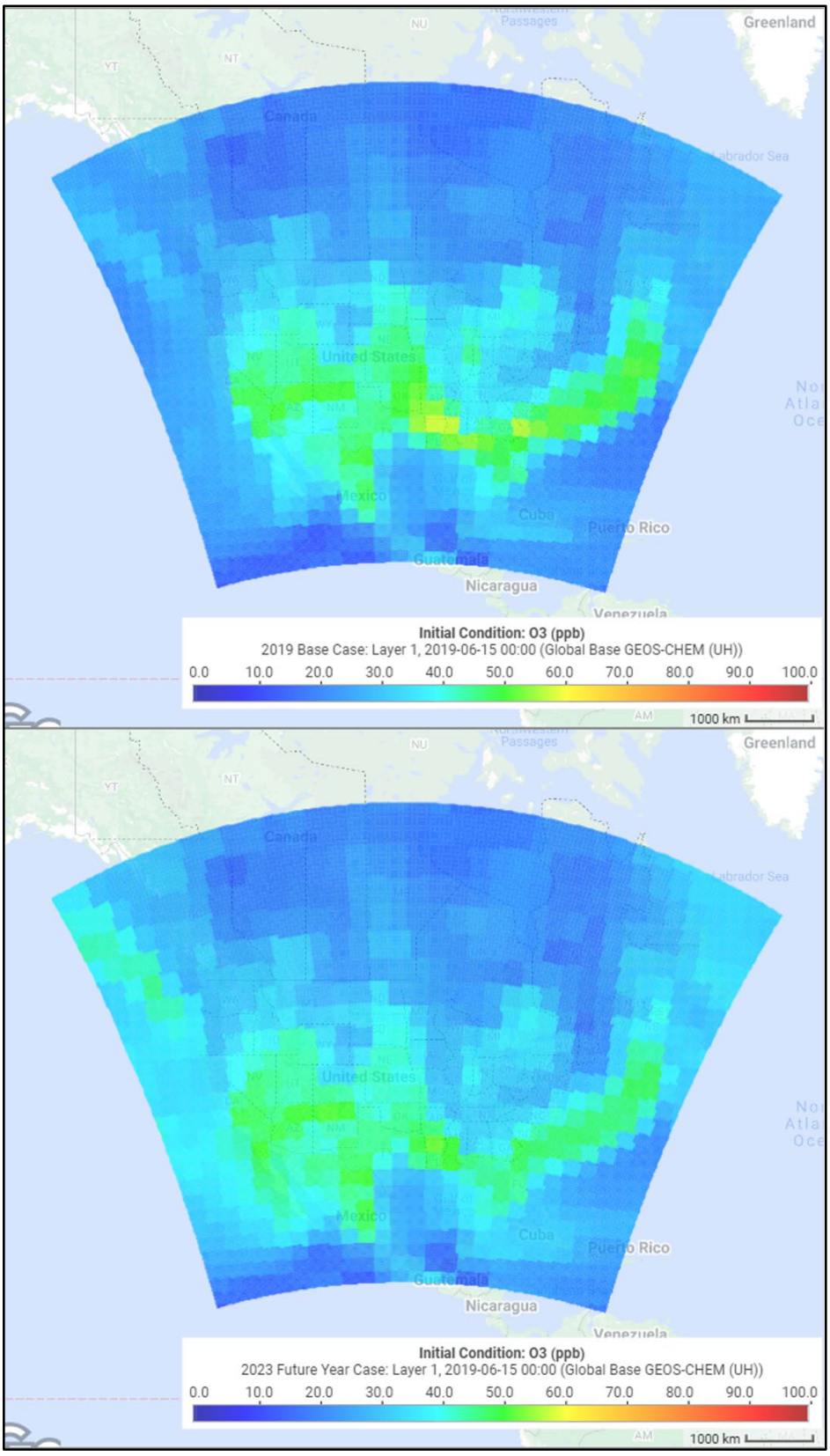

Figure 4-3: June Initial Condition for Ozone in 2019 and 2023

5. PHOTOCHEMICAL MODEL PERFORMANCE EVALUATION

The purpose of model performance evaluation (MPE) is to determine how well the model reproduces measured concentrations of pollutants. The EPA modeling guidance recommends performing operational model evaluation consisting of calculating multiple statistical parameters and graphical analyses. In addition, the EPA modeling guidance recommends comparing the MPE results against other similar model applications such as those compiled by Emery et al. (2017). The Emery et al. (2017) review paper provides benchmarks based on the performance of many photochemical modeling applications in the United States. The statistical benchmarks for one-hour and MDA8 ozone are listed in Table 5-1: *Statistical Benchmarks for Photochemical Model Evaluation* and can be used to assess model performance. The goal benchmarks indicate performance demonstrated by the top third of model runs evaluated. The criteria benchmark indicates performance achieved by the top two-thirds of model runs evaluated.

Table 5-1: Statistical Benchmarks for Photochemical Model Evaluation

Benchmark	Normalized Mean Bias (NMB; %)	Normalized Mean Error (NME; %)	Correlation Coefficient (R; unitless)
Goal	Less than ± 5	Less than 15	Bigger than 0.75
Criteria	Less than ± 15	Less than 25	Bigger than 0.50

This section contains an operational MPE for each of the three 2015 eight-hour ozone NAAQS nonattainment areas: HGB, DFW, and Bexar County. As recommended in the EPA modeling guidance, the TCEQ evaluations include eight-hour and one-hour performance measures calculated by comparing measured and four-cell bi-linearly interpolated modeled ozone concentrations for all episode days.

5.1 HGB MODEL PERFORMANCE EVALUATION

For HGB, evaluations were performed at all ozone monitors in the six-county nonattainment area, including regulatory and non-regulatory monitors shown on map in Figure 5-1: *Monitors in the HGB Area*. The monitors along with ozone related parameters are also listed in Table 5-2: *Regulatory Monitor-Specific Ozone Conditions During April through October 2019 Episode* and Table 5-3: *Non-Regulatory Monitor-Specific Ozone Conditions During April through October 2019 Episode*. Three non-regulatory monitors, Sheldon (C551), Mercer Arboretum (C557), and Bunker Hill (C562) did not have ozone data for month April through July and therefore ozone parameters presented in Table 5-3 for those monitors are based on August through October data. Also, the statistical model evaluations for these monitors are calculated for August through October data.

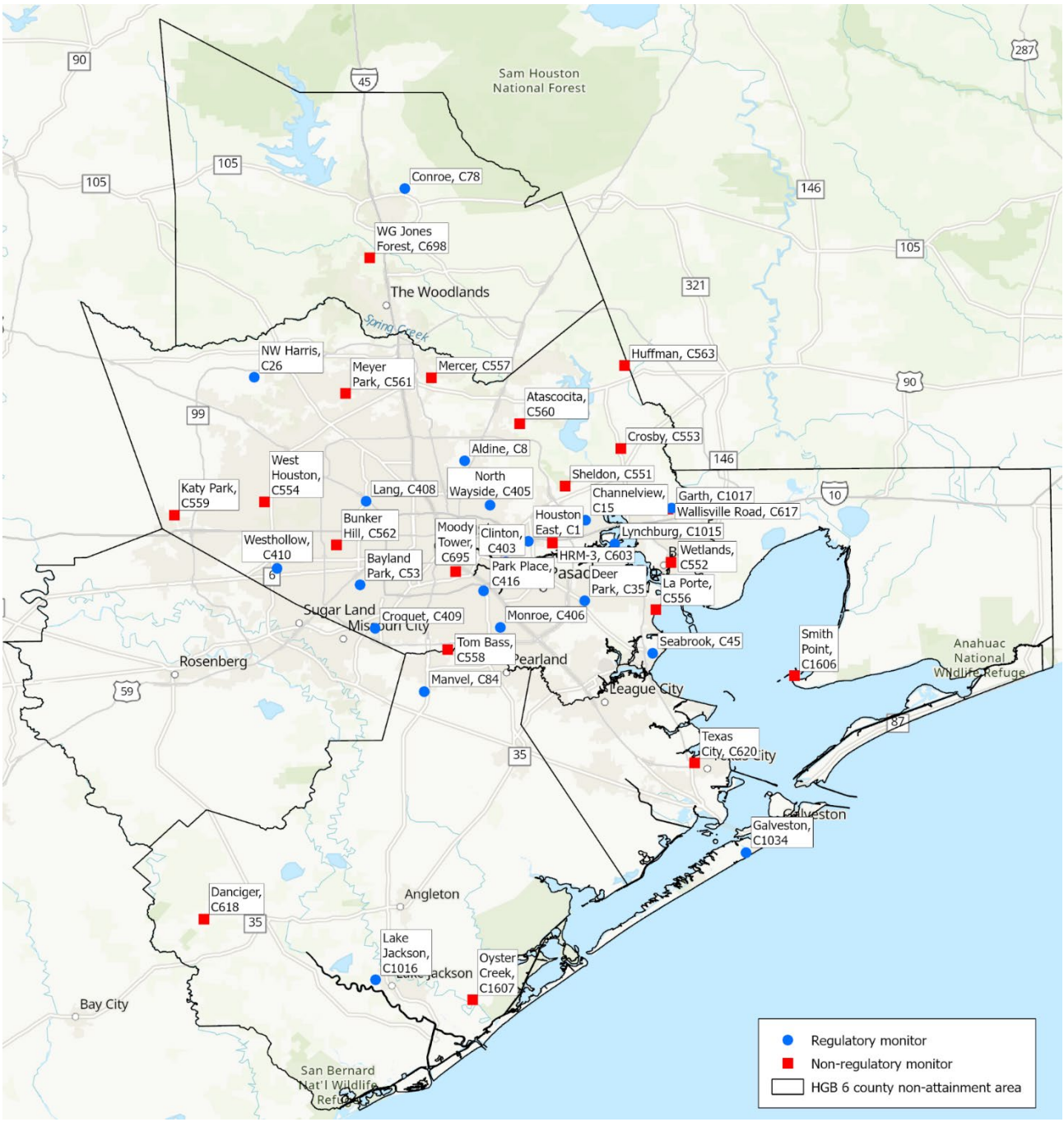

Figure 5-1: Monitors in the HGB Area

Table 5-2: Regulatory Monitor-Specific Ozone Conditions During April through October 2019 Episode

Monitor Short Name	Monitor Name	CAMS Number	Episode Maximum Eight-Hour Ozone (ppb)	Number of Days Above 70 ppb	2019 Regulatory Ozone Design Value (ppb)
Aldine	Houston Aldine	8	93	8	81
Bayland Park	Houston Bayland Park	53	91	16	77
Channelview	Channelview	15	76	3	70
Clinton	Clinton	403	92	3	72
Conroe	Conroe Relocated	78	83	4	76
Croquet	Houston Croquet	409	84	5	70
Deer Park	Houston Deer Park #2	35	107	5	75
Galveston	Galveston 99th St.	1034	81	6	76
Garth	Baytown Garth	1017	76	2	74
Houston East	Houston East	1	88	3	74
Lake Jackson	Lake Jackson	1016	68	0	65
Lang	Lang	408	88	6	73
Lynchburg	Lynchburg Ferry	1015	77	1	N/A
Manvel	Manvel Croix Park	84	90	6	75
Monroe	Houston Monroe	406	82	4	66
North Wayside	Houston North Wayside	405	74	3	67
NW Harris	Northwest Harris Co.	26	86	4	74
Park Place	Park Place	4016	88	5	73
Seabrook	Seabrook Friendship Park	45	90	2	71
Westhollow	Houston Westhollow	410	77	6	71

Table 5-3: Non-Regulatory Monitor-Specific Ozone Conditions During April through October 2019 Episode

Monitor Short Name	Monitor Name	CAMS Number	Episode Maximum Eight-Hour Ozone (ppb)	Number of Days Above 70 ppb
Atascocita	Atascocita	560	59	0
Bunker Hill	Bunker Hill Village	562	68	0
Crosby	Crosby Library	553	74	1
Danciger	Danciger	618	73	1
HRM-3	HRM-3 Haden Road	603	86	3

Monitor Short Name	Monitor Name	CAMS Number	Episode Maximum Eight-Hour Ozone (ppb)	Number of Days Above 70 ppb
Huffman	Huffman Wolf Road	563	77	1
Katy Park	Katy Park	559	81	4
La Porte	La Porte Sylvan Beach	556	72	1
Mercer	Mercer Arboretum	557	72	1
Meyer Park	Meyer Park	561	90	2
Moody Tower	UH Moody Tower	695	93	10
Oyster Creek	Oyster Creek	1607	71	1
Sheldon	Sheldon	551	65	0
Smith Point	UH Smith Point	1606	70	0
Texas City	Texas City 34th St.	620	83	7
Tom Bass	Tom Bass	558	91	8
Wallisville Road	Wallisville Road	617	76	2
West Houston	West Houston	554	78	2
Wetlands	Baytown Wetlands Center	552	67	0
WG Jones Forest	UH WG Jones Forest	698	83	6

5.1.1 Area-Wide Statistics

An evaluation of modeled eight-hour ozone concentrations in the HGB area for each month and for the episode is presented in Table 5-4: *Performance Statistics for Observed MDA8 >= 60 ppb At All Monitors.* The values represent monthly and seven-month averages from the HGB area monitors shown in Figure 5-1. When evaluated for all observations over 60 ppb, the mean bias ranges between -7.60 ppb and 2.67 ppb, the mean error ranges between 4.93 ppb and 10.33 ppb. The normalized mean bias for MDA8 ozone is within the criteria range of 15% and the normalized mean error is within criteria range of 25% for all months.

Table 5-4: Performance Statistics for Observed MDA8 ≥ 60 ppb At All Monitors

Month	Count of Valid Data	Mean Observed Ozone (ppb)	Mean Modeled Ozone (ppb)	Mean Bias (ppb)	Mean Error (ppb)	NMB (%)	NME (%)	R^2
Apr	97	65.85	58.25	-7.60	8.06	-11.54	12.24	0.29
May	41	65.43	64.55	-0.87	6.23	-1.34	9.52	0.11
Jun	150	70.52	67.55	-2.97	10.33	-4.21	14.65	0.16
Jul	39	66.86	65.86	-1.00	5.15	-1.49	7.70	0.21
Aug	62	68.21	70.88	2.67	9.41	3.92	13.79	0.04
Sep	102	67.69	69.73	2.04	4.93	3.02	7.29	0.42

Month	Count of Valid Data	Mean Observed Ozone (ppb)	Mean Modeled Ozone (ppb)	Mean Bias (ppb)	Mean Error (ppb)	NMB (%)	NME (%)	R^2
Oct	41	67.23	64.77	-2.46	8.26	-3.66	12.28	0.36
Apr - Oct	532	67.94	66.09	-1.85	7.92	-2.72	11.66	0.186

The NMB and NME for high ozone days with maximum observed daily eight-hour ozone concentrations at or above 60 ppb for monitoring sites in the HGB area is presented in Figure 5-2: *NMB of MDA8 Ozone at or Above 60 ppb for HGB Monitors* and Figure 5-3: *NME of MDA8 Ozone at or Above 60 ppb for HGB Monitors*. The Atascocita site is not shown as it did not have MDA8 ozone values above 60 ppb. All monitors in the HGB area have NMB within the criteria range except the Lynchburg monitor. Many monitors have NMB values within the goal range. This indicates acceptable model performance. All monitors in the HGB area have NME within the criteria range and most monitors fall within goal range indicating acceptable model performance.

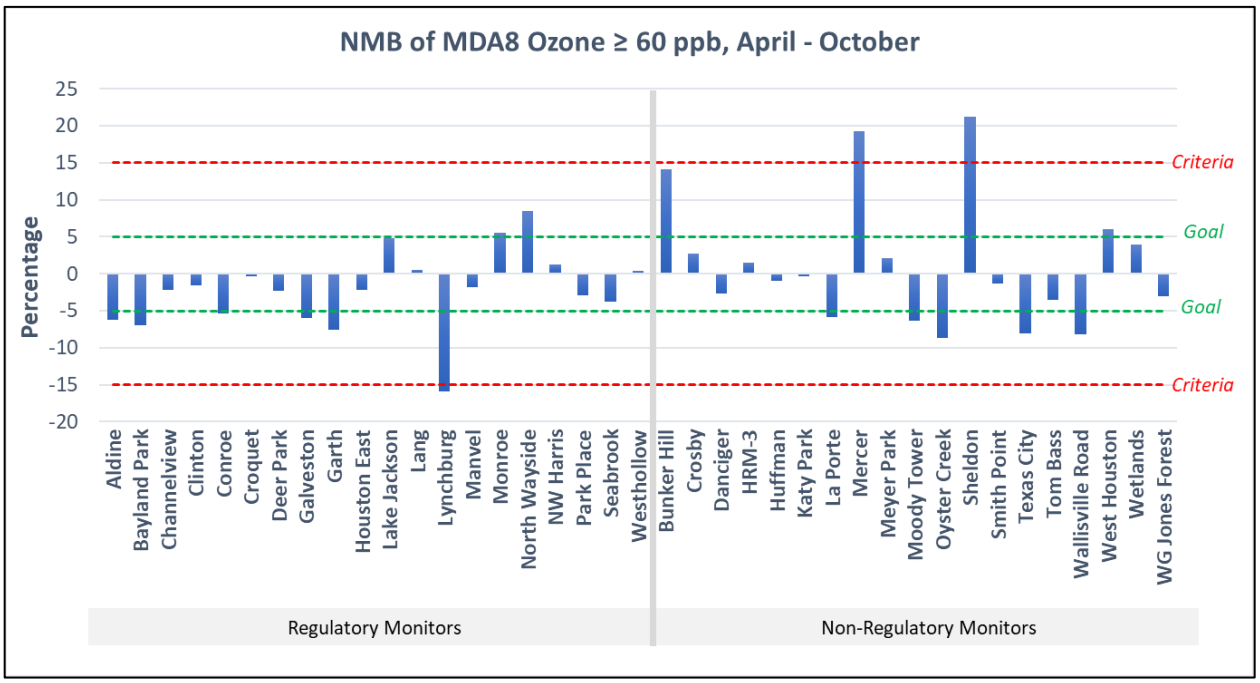

Figure 5-2: NMB of MDA8 Ozone at or Above 60 ppb for HGB Monitors

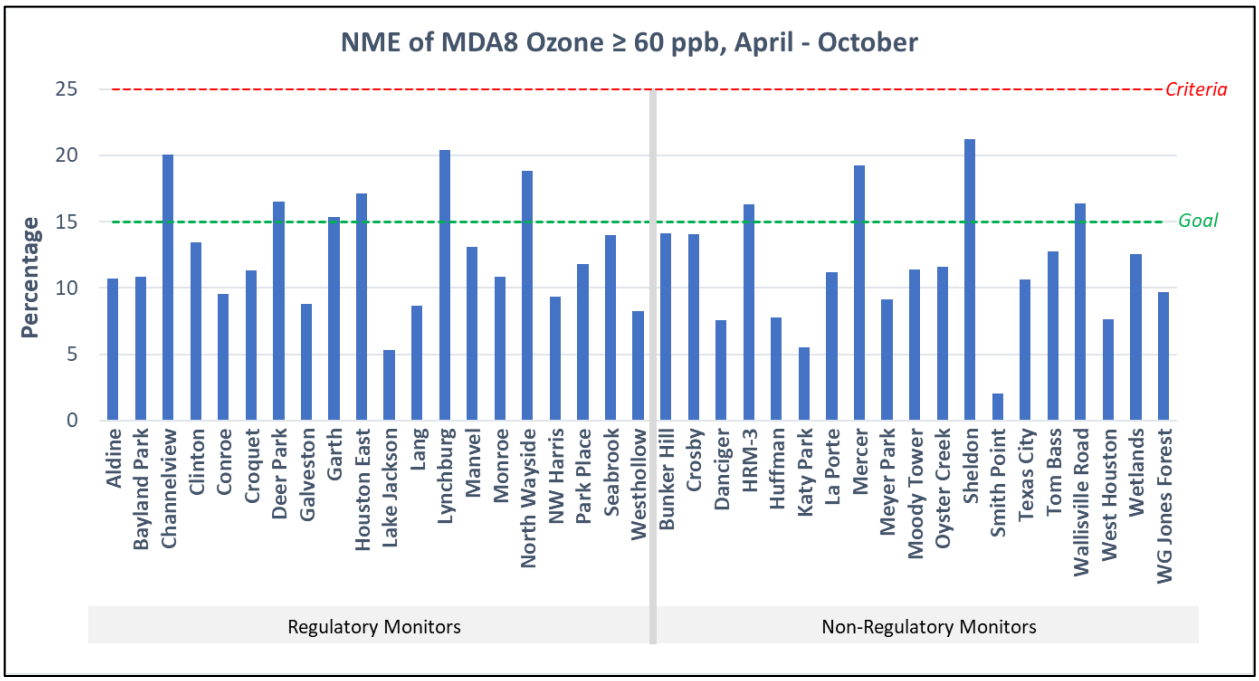

Figure 5-3: NME of MDA8 Ozone at or Above 60 ppb for HGB Monitors

5.1.2 Monitor-Specific Statistics

Soccer plots showing normalized mean error and normalized mean bias per month and for the entire episode are shown in Figure 5-4: *Soccer plots showing NME and NMB of MDA8 Ozone*. Data for four monitors having highest 2019 DV values are presented, which are Aldine, Bayland Park, Conroe, and Galveston monitors. The inner rectangle marks the Emery et al. (2017) criteria benchmarks and symbols within those rectangles indicate acceptable performance.

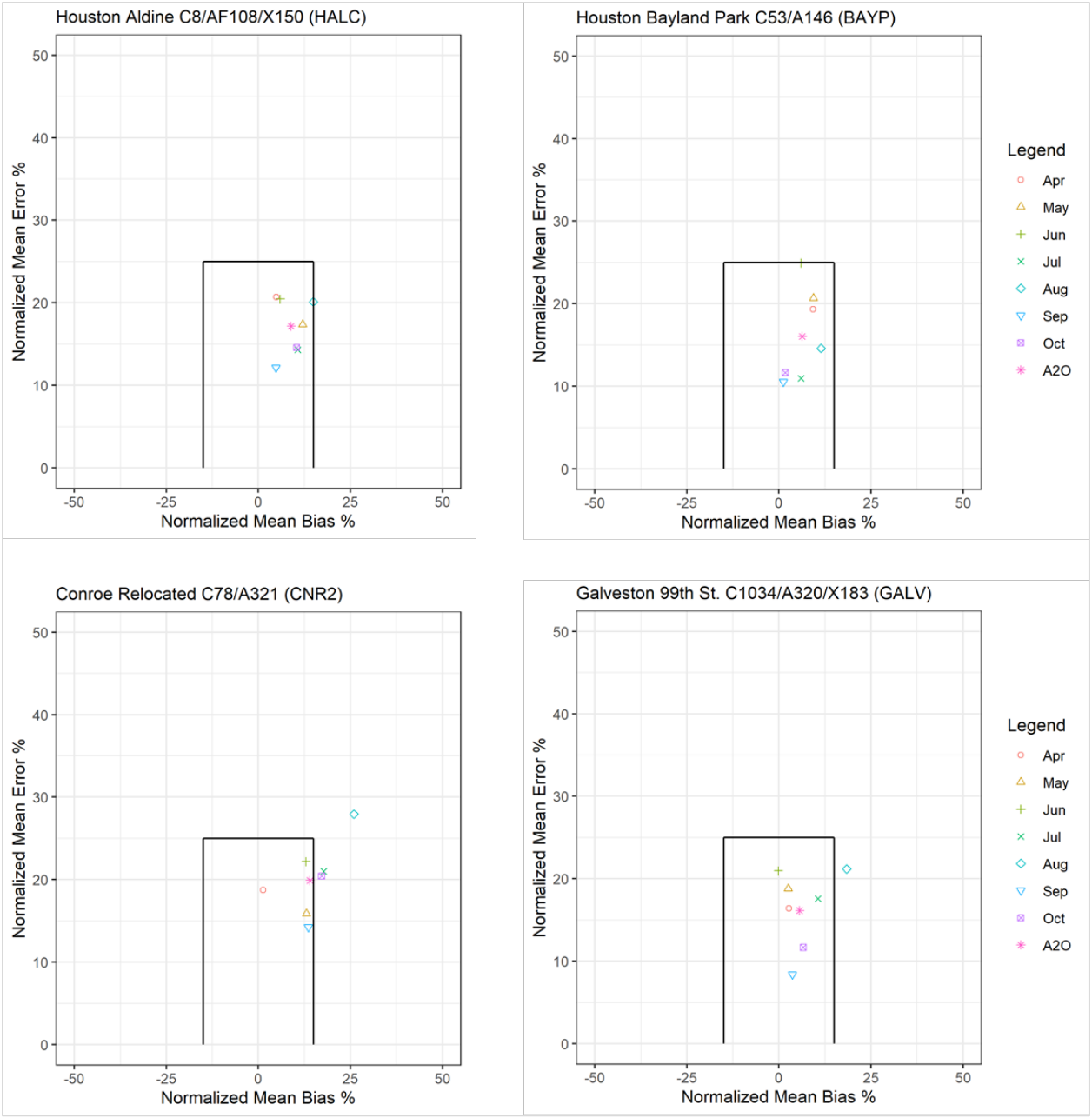

Figure 5-4: Soccer plots showing NME and NMB of MDA8 Ozone

5.2 DFW MODEL PERFORMANCE EVALUATION

Model performance is evaluated for the DFW 2015 ozone NAAQS nonattainment area at the 16 monitors shown in Figure 5-5: *Monitors in the DFW Area*. All of the monitors that measure ozone within the nine-county DFW area are regulatory monitors, so all of the monitors were considered for the attainment test for the DFW 2015 Ozone NAAQS Moderate AD SIP Revision. Information about the ozone conditions at each monitor during the April through October 2019 episode are presented in Table 5-5: *DFW Monitor-Specific Ozone Conditions During April through October 2019 Episode*. In 2019, 11 of the 16 monitors had a 2019 DV exceeding the 2015 ozone NAAQS of 70 ppb. The highest MDA8 ozone value recorded in the April through October 2019 episode was 88

ppb at the Frisco monitor, which is also the monitor with the highest base case DV (DVB).

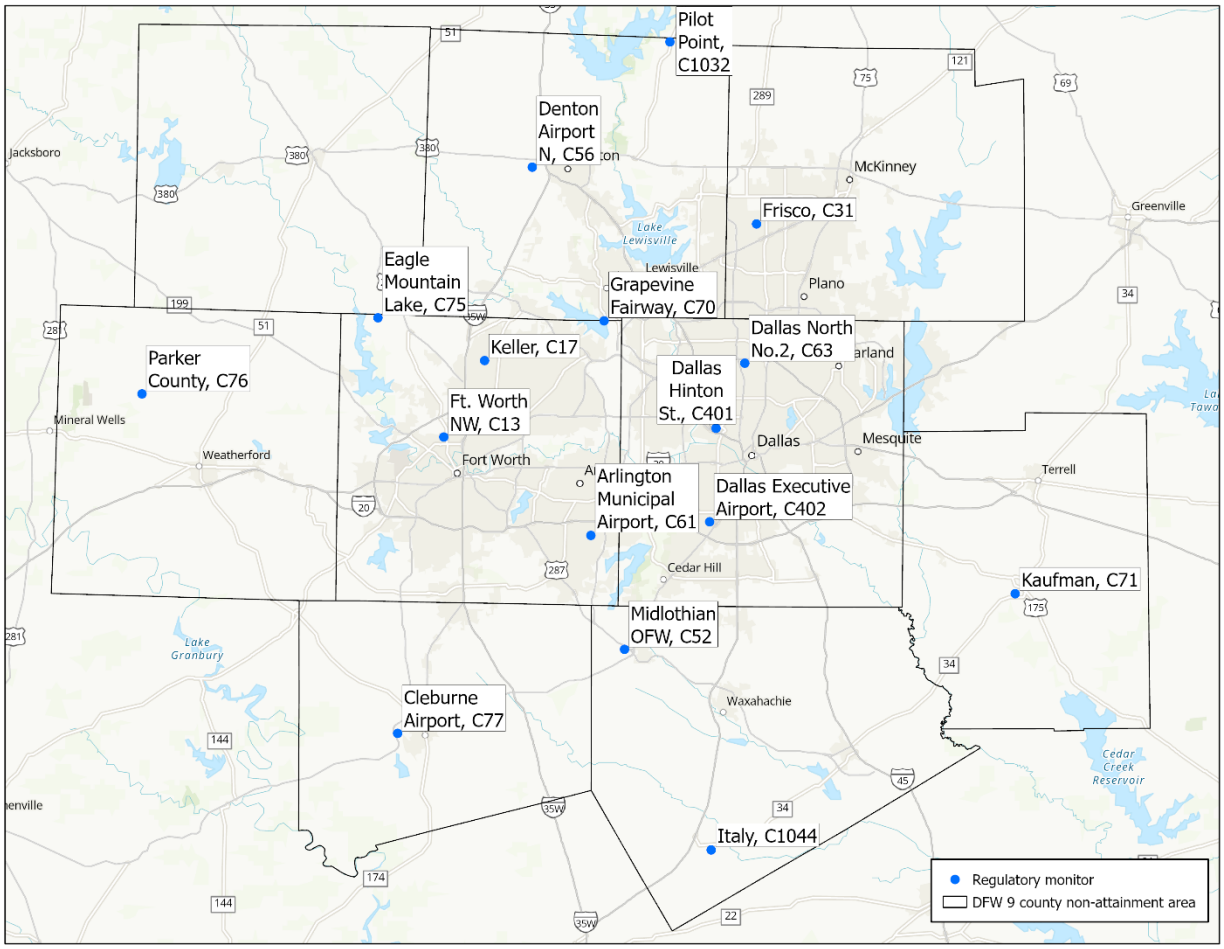

Figure 5-5: Monitors in the DFW Area

Table 5-5: DFW Monitor-Specific Ozone Conditions During April through October 2019 Episode

DFW Monitor	CAMS number	Number of Observed Days Above 70 ppb	Episode Highest MDA8 Ozone (ppb)	2019 Regulatory Eight-Hour Ozone DV (ppb)	2019 DVB (ppb)
Arlington Municipal Airport	61	2	76	70	70.00
Cleburne Airport	77	7	83	76	73.33
Dallas Executive Airport	402	1	74	68	68.33
Dallas Hinton Street	401	0	70	73	69.67
Dallas North No.2	63	5	83	77	74.00
Denton Airport North	56	5	79	73	73.00
Eagle Mountain Lake	75	10	82	73	74.33
Fort Worth Northwest	13	2	75	72	72.00
Frisco	31	8	88	76	75.33
Grapevine Fairway	70	4	81	75	75.00

DFW Monitor	CAMS number	Number of Observed Days Above 70 ppb	Episode Highest MDA8 Ozone (ppb)	2019 Regulatory Eight-Hour Ozone DV (ppb)	2019 DVB (ppb)
Italy	1044	0	62	65	63.00
Kaufman	71	0	68	63	63.67
Keller	17	4	84	74	73.00
Midlothian OFW	52	0	69	66	64.00
Parker County	76	0	70	69	68.67
Pilot Point	1032	7	80	71	73.00

5.2.1 Area-Wide Statistics

An evaluation of modeled eight-hour ozone concentrations in the DFW area for each month and for the whole April through October episode is presented in Table 5-6: *Performance Statistics for Observed MDA8 ≥ 60 ppb at All DFW Monitors.* The values represent monthly and seven-month averages from the DFW area monitors shown in Figure 5-5: *Monitors in the DFW Area*. When evaluated for all MDA8 ozone observations over 60 ppb, the mean bias ranges between -8.26 ppb and 1.04 ppb, the mean error ranges between 4.27 ppb and 9.75 ppb. The NMB for MDA8 ozone is within the criteria range of ±15% for all months and the NME is within the goal range of < 15% for all months.

Table 5-6: Performance Statistics for Observed MDA8 ≥ 60 ppb at All DFW Monitors

Month	Count of Valid Data	Mean Observed Ozone (ppb)	Mean Modeled Ozone (ppb)	Mean Bias (ppb)	Mean Error (ppb)	NMB (%)	NME (%)	R^2
Apr	38	63.35	59.40	-3.95	5.84	-6.24	9.22	0.19
May	47	65.79	61.95	-3.84	4.99	-5.83	7.58	0.05
Jun	59	65.79	57.53	-8.26	9.75	-12.56	14.81	0.02
Jul	46	65.82	63.08	-2.73	6.87	-4.15	10.45	0.24
Aug	63	67.89	64.78	-3.11	5.11	-4.58	7.52	0.31
Sep	70	67.95	68.98	1.04	4.27	1.52	6.29	0.47
Oct	16	63.05	59.74	-3.30	5.04	-5.24	8.00	0.08
Apr - Oct	339	66.23	62.92	-3.30	6.05	-4.99	9.13	0.23

The NMB and NME for high ozone days in the April through October episode with (MDA8 ozone concentrations at or above 60 ppb) for each monitor in the DFW area is presented in Figure 5-6: *NMB of MDA8 Ozone ≥ 60 ppb for DFW Monitors* and Figure 5-7: *NME of MDA8 Ozone ≥ 60 ppb for DFW Monitors*. Modeled MDA8 ozone on days with observed MDA8 greater than or equal to 60 ppb is biased low at all monitors except for Forth Worth NW and Grapevine Fairway, which have a slight positive bias. All monitors in the DFW area have NMB within the criteria range (< ±15%), with seven monitors have NMB within the goal range (< ±5%). This indicates acceptable to good

model performance at all monitors. All monitors in the DFW area have NME within the goal range, which indicates good performance.

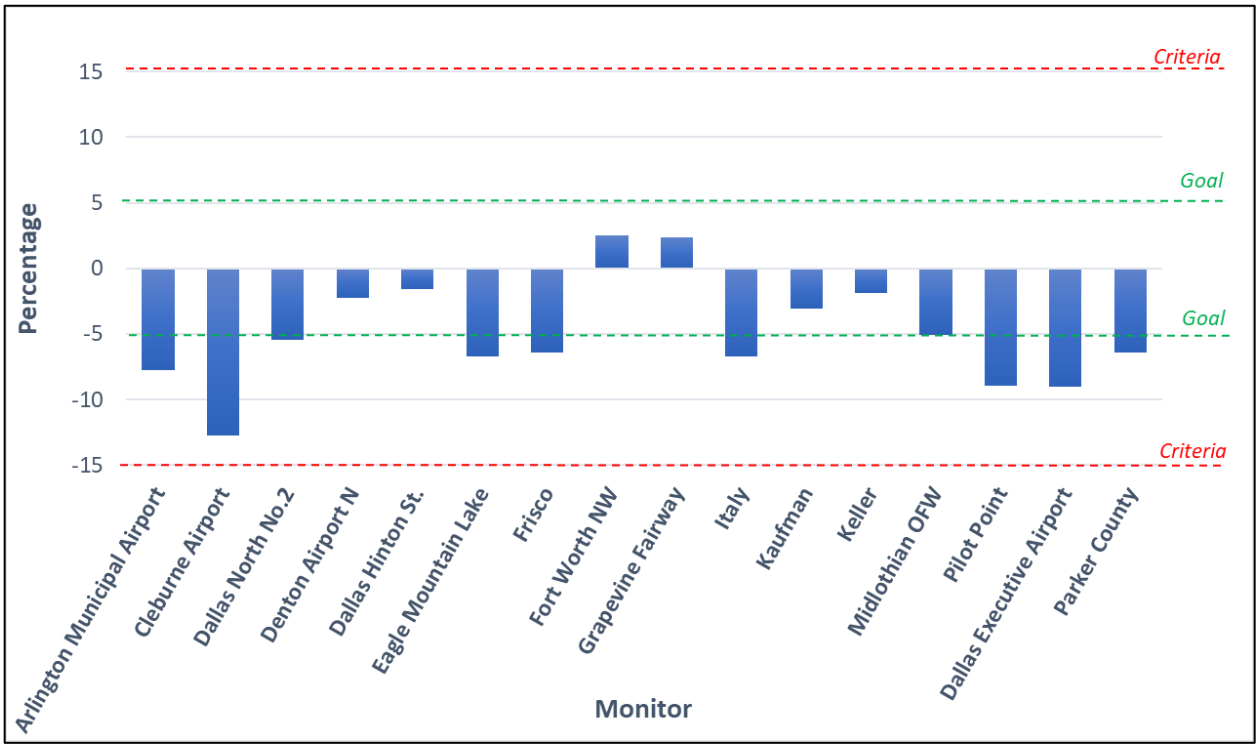

Figure 5-6: NMB of MDA8 Ozone ≥ 60 ppb for DFW Monitors

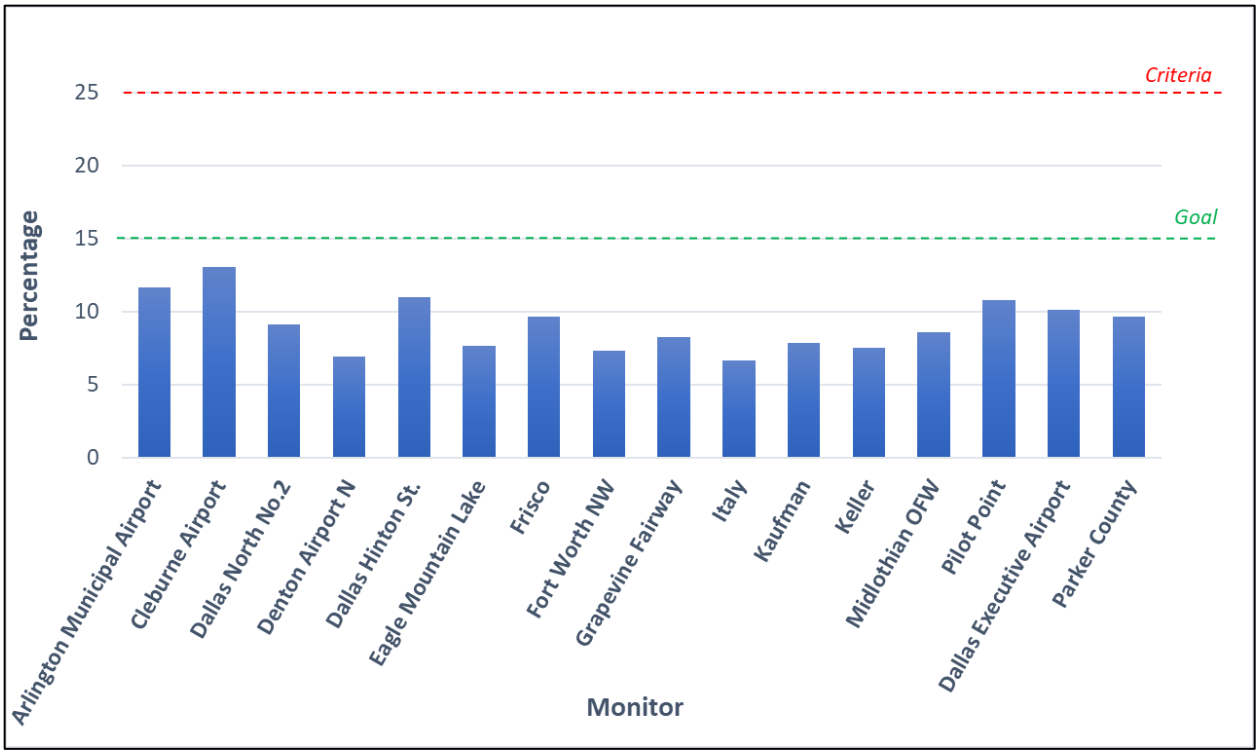

Figure 5-7: NME of MDA8 Ozone ≥ 60 ppb for DFW Monitors

5.2.2 Monitor-Specific Statistics

Soccer plots showing NME and NMB of all MDA8 ozone values per month and for the entire episode at four monitors are shown in Figure 5-8: *Soccer Plots of NMB and NME of MDA8 Ozone at DFW Monitors*. The four monitors shown had the top four highest 2019 regulatory DVs: Dallas North No.2 (C63) with 77 ppb, Cleburne Airport (C77) with 76 ppb, Frisco (C31) with 76 ppb, and Grapevine Fairway (C70) with 75 ppb. The inner rectangle marks the Emery et al. (2017) criteria benchmarks and symbols within those rectangles indicate acceptable performance. Every month at each of the monitors falls within the inner rectangle, except for May at the Grapevine Fairway monitor which has a higher NMB than the criteria range.

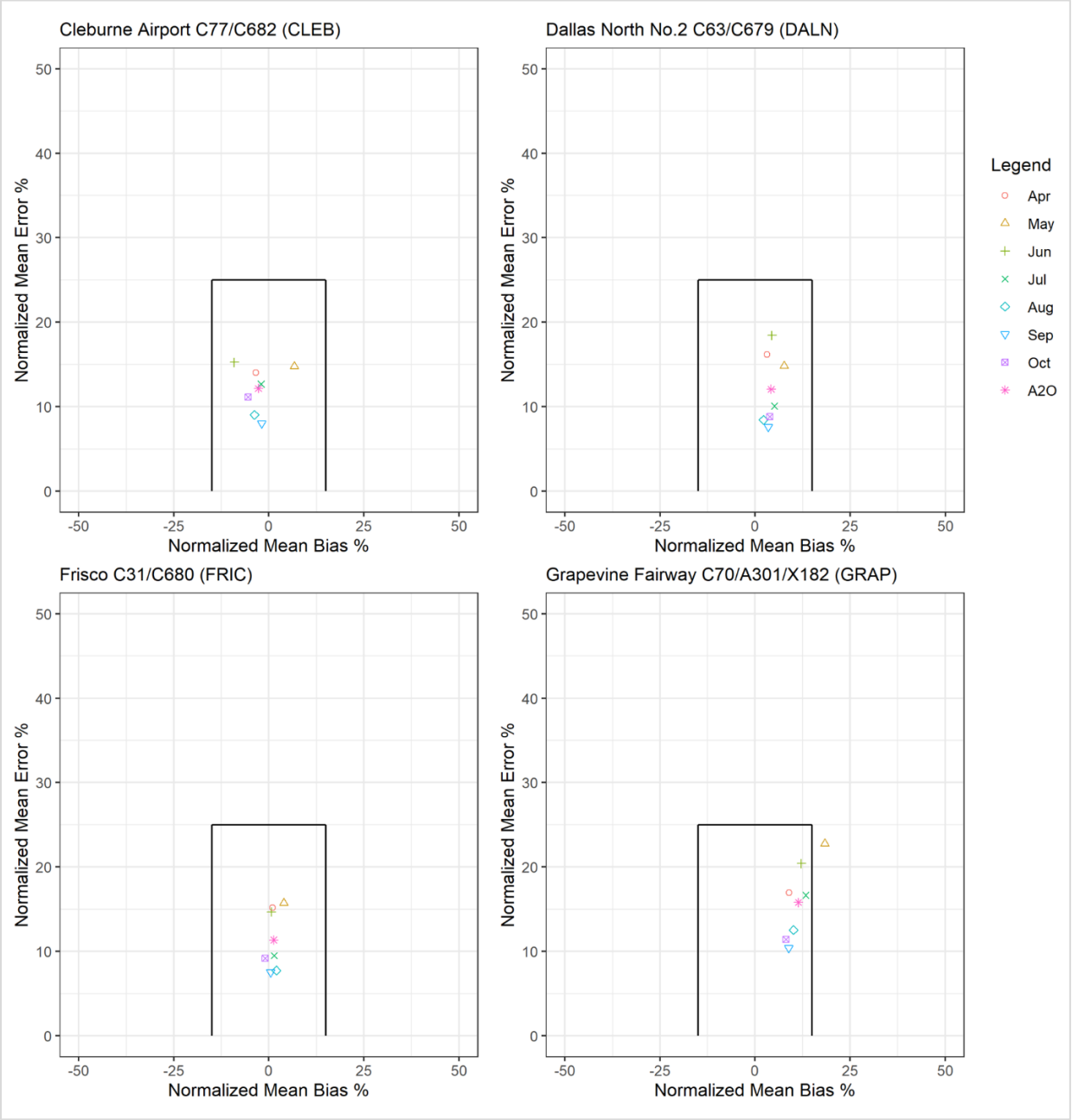

Figure 5-8: Soccer Plots of NMB and NME of MDA8 Ozone at DFW Monitors

5.3 BEXAR COUNTY MODEL PERFORMANCE EVALUATION

Model performance is evaluated for the Bexar County area at the monitors shown in Figure 5-9: *Ozone Monitors in Bexar and Adjacent Counties*. Four additional nonregulatory ozone monitors in counties adjacent to Bexar County are added to the eight ozone monitors in Bexar County to provide an analysis over a broader area and to increase the number of monitors in the statistics.

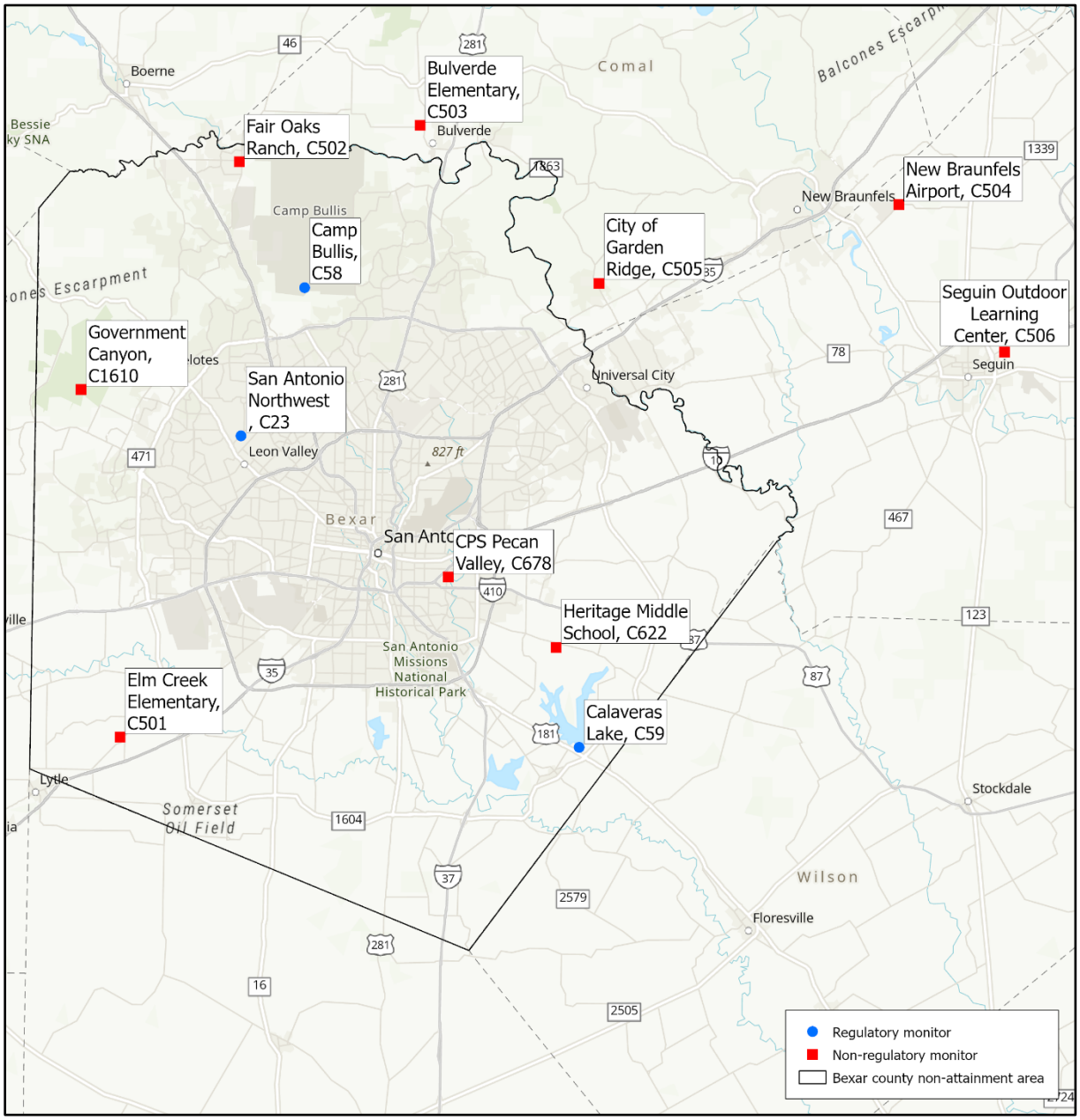

Figure 5-9: Ozone Monitors in Bexar and Adjacent Counties

The 2019 episode in Bexar County had eight-hour ozone values over 70 ppb at two regulatory monitors, Camp Bullis and San Antonio Northwest, and at one non-regulatory monitor, Government Canyon. Additional data about the monitors and ozone values are presented in Table 5-7: *Ozone Conditions at Bexar and Adjacent*

County Monitors During April through October 2019 Episode, including a short name for the Seguin Outdoor Learning Center monitor that will be used in subsequent figures. The highest observed eight-hour ozone value, 78, was recorded at the San Antonio Northwest monitor. The Camp Bullis and San Antonio monitors share the same high 2019 regulatory design value, 72. Nonregulatory monitors, noted as type NR, do not have a regulatory design value.

Table 5-7: Ozone Conditions at Bexar and Adjacent County Monitors During April through October 2019 Episode

Monitor Name	CAMS ID	Type	Episode Max Eight-hour Observed Ozone (ppb)	Number of Observed Days Above 70 ppb	2019 Regulatory Eight-Hour Ozone DV (ppb)	2019 DVB (ppb)
Camp Bullis	58	R	76	1	72	70.45
Calaveras Lake	59	R	64	0	65	67.74
San Antonio Northwest	23	R	78	4	72	73.06
Bulverde Elementary	503	NR	67	0	N/A	N/A
City of Garden Ridge	505	NR	66	0	N/A	N/A
Elm Creek Elementary	501	NR	70	0	N/A	N/A
Fair Oaks Ranch	502	NR	67	0	N/A	N/A
Government Canyon	1610	NR	72	3	N/A	N/A
Heritage Middle School	622	NR	60	0	N/A	N/A
New Braunfels Airport	504	NR	63	0	N/A	N/A
CPS Pecan Valley	678	NR	68	0	N/A	N/A
Seguin Outdoor Learning Center (Seguin)	506	NR	59	0	N/A	N/A

5.3.1 Area-Wide Statistics

Model performance statistics for the monitors shown in Figure 5-9 are provided in Table 5-8: *Model Performance Statistics for Eight-hour Ozone, Bexar and Adjacent County Monitors, MDA8 ≥ 60 ppb*.

There were no days in May with observed eight-hour ozone averages over 60 ppb at a monitor in Bexar or adjacent counties. Due to the small sample size of monitors, the number of monthly valid data pairs are smaller than the desired number for optimally rigorous statistics analyses. However, expanding the area of analysis to include sufficient data for more rigorous analysis would require analyzing data from the Austin area, which is a metropolitan area outside the nonattainment area.

The study area as a whole exhibits acceptable model performance for each month individually and for the episode average. Good error performance is shown in all months, with NME values less than 15%. Good bias performance is shown in all months except April, May, and August with NMB values between ±5 percent.

Table 5-8: Model Performance Statistics for Eight-hour Ozone, Bexar and Adjacent County Monitors, MDA8 ≥ 60 ppb

Month	Count of Valid Data	Observed Mean (ppb)	Modeled Mean (ppb)	Mean Bias (ppb)	Mean Error (ppb)	NMB (%)	NME (%)	R^2
Apr	21	63	59.53	-3.47	3.81	-5.51	6.04	0.44
May	0	N/A	N/A	N/A	N/A	N/A	N/A	N/A
Jun	17	67.72	64.45	-3.27	5.83	-4.83	8.61	0.27
Jul	19	66.85	69.48	2.64	4.85	3.95	7.25	0.35
Aug	3	62.48	58.58	-3.9	6.11	-6.24	9.77	0.18
Sep	6	60.9	59.14	-1.76	3.96	-2.9	6.5	0
Oct	6	63.47	63.65	0.18	3.23	0.29	5.09	0.02
Apr - Oct	72	64.97	63.59	-1.38	4.62	-2.13	7.11	0.37

As seen in Figure 5-10: *NMB by Monitor, MDA8 Ozone with Observations over 60 ppb, April through October*, all monitors are within the NMB criteria values indicating acceptable model performance and all regulatory monitors except San Antonio Northwest are within the goal values indicating good model performance across the episode.

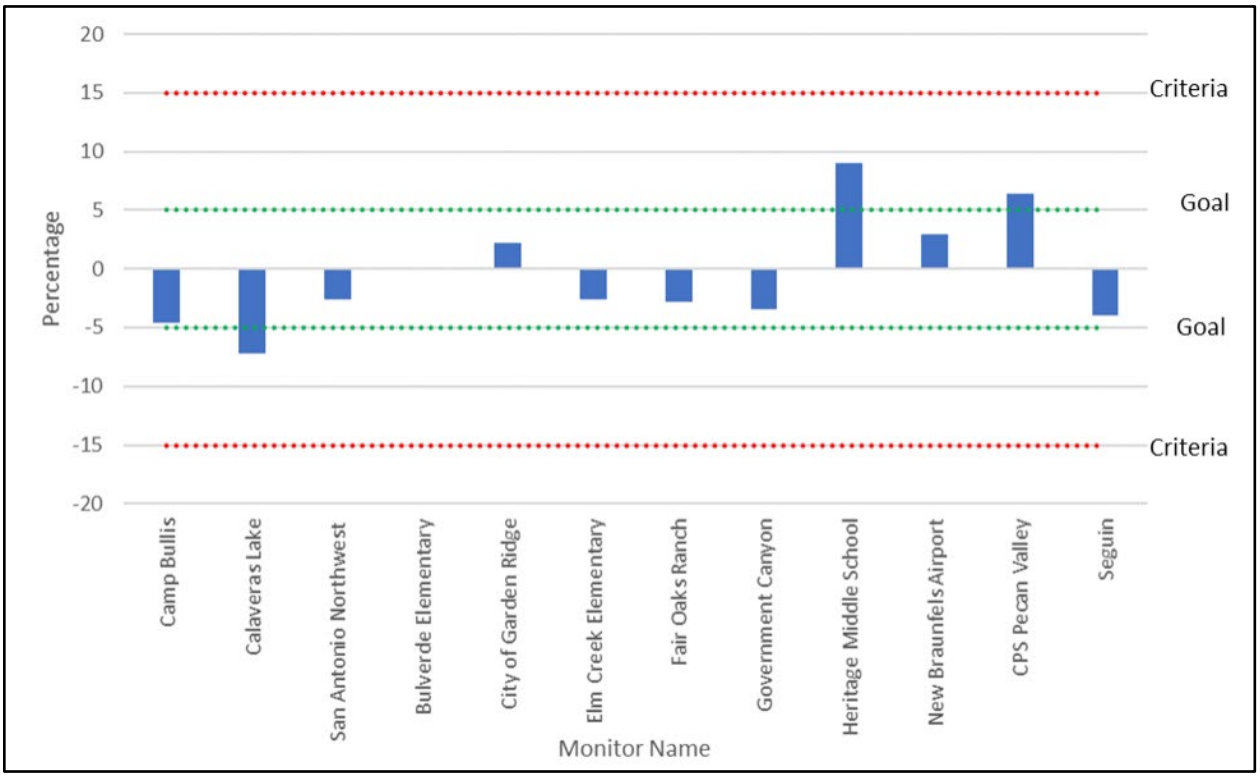

Figure 5-10: NMB by Monitor, MDA8 Ozone with Observations over 60 ppb, April through October

As seen in Figure 5-11: *NME by Monitor, MDA8 Ozone with Observations over 60 ppb, April through October*, all monitors are well within the NME goal range indicating good performance across the episode.

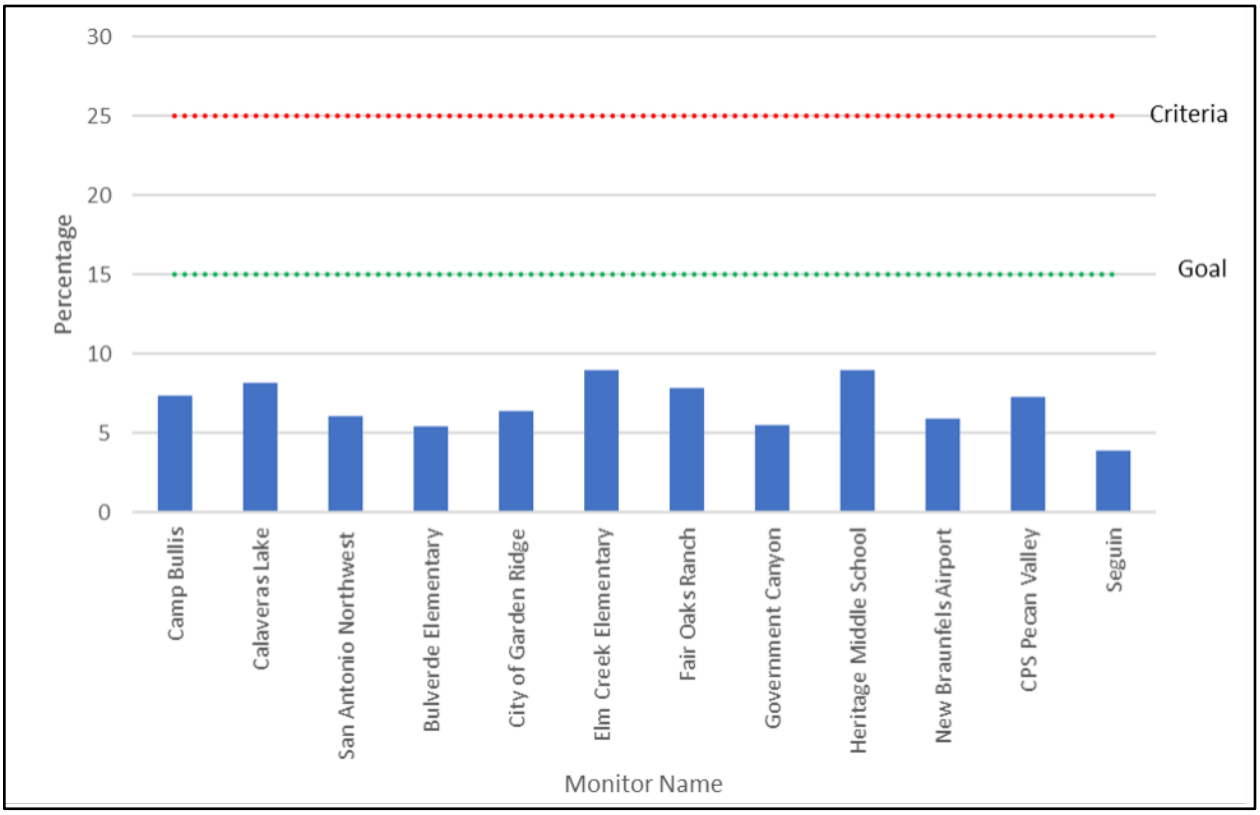

Figure 5-11: NME by Monitor, MDA8 Ozone with Observations over 60 ppb, April through October

5.3.2 Monitor-Specific Statistics

A soccer plot for each of the three monitors noted in Table 5-7 to have an exceedance of the 2015 70 ppb NAAQS are shown in Figure 5-12: *Soccer Plot for MDA8 Ozone for San Antonio Northwest (top left), Camp Bullis (top right), and Government Canyon (bottom) Monitors, April through October*. Since the statistic shown is MDA8 without the 60 ppb minimum, each monitor has statistics for May. The values for May exhibit the highest bias and error of any month. This may be due to the high bias associated with fire influence, as described in the (Section 5.3.1: *Fire Influence* of the Bexar County 2015 Eight-Hour Ozone NAAQS AD SIP revision). All other months at San Antonio Northwest and Camp Bullis show acceptable model performance. The Government Canyon monitor shows NMB over 15 percent in four months, the fire-influenced months of April and May, along with June and July.

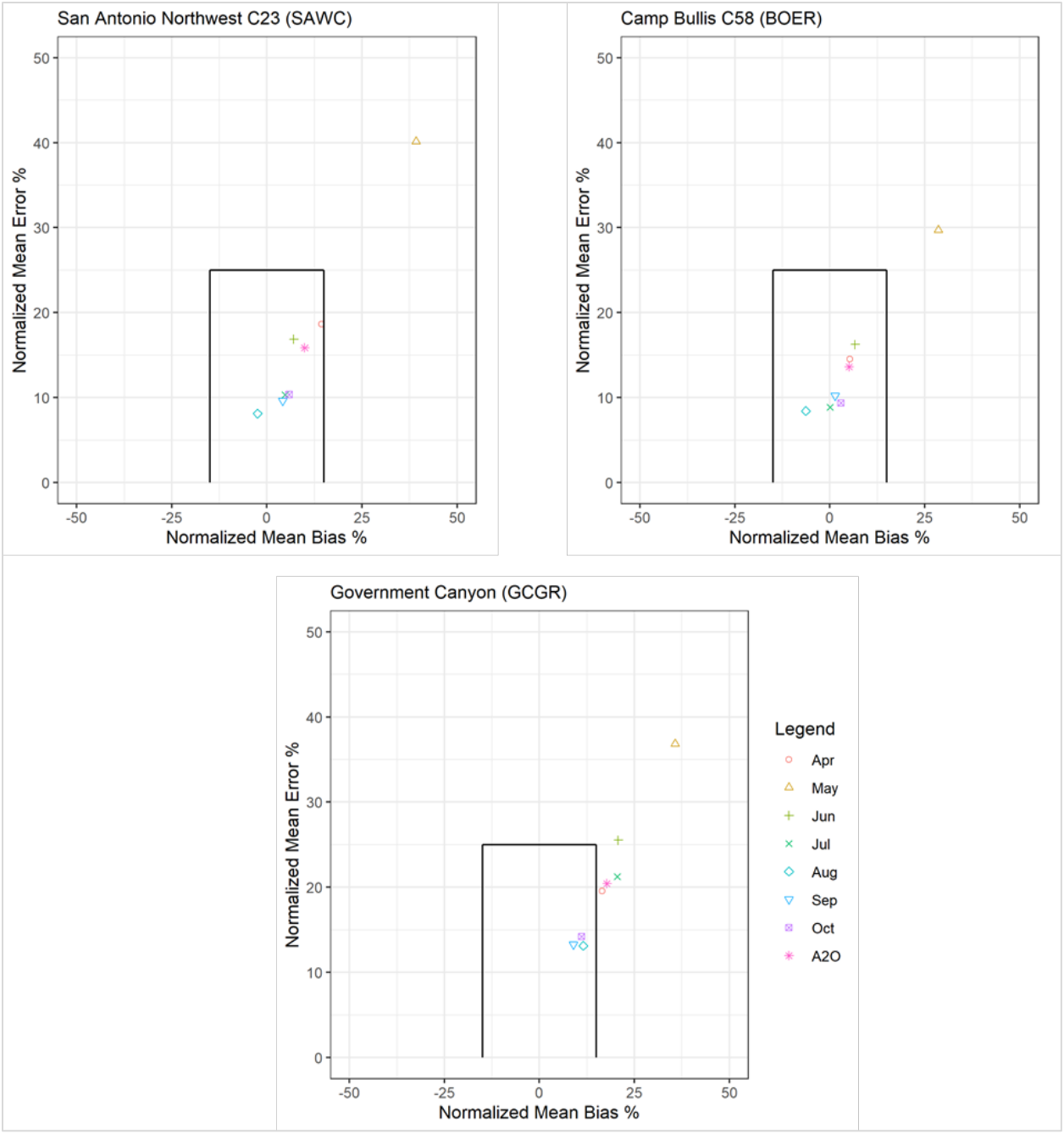

Figure 5-12: Soccer Plot for MDA8 Ozone for San Antonio Northwest (top left), Camp Bullis (top right), and Government Canyon (bottom) Monitors, April through October

5.4 EVALUATION OF CAMX CONFIGURATION OPTIONS

The TCEQ evaluated the model performance for two dry-deposition schemes and two vertical diffusion schemes in CAMx. The dry-deposition schemes tested were Wesely89 (Wesely and Lesht, 1989), which is the CAMx default, and Zhang03 (Zhang et. al, 2003). The vertical diffusion schemes tested were K-Theory (the CAMx default) and the Asymmetric Convective Model, version 2 (ACM2).

Four CAMx runs were conducted to test each combination of configuration schemes (Wesely89/K-Theory; Wesely89/ACM2; Zhang03/K-Theory; and Zhang03/ACM2) for three test months (June, August, and September) for a total of 12 model runs.

This section summarizes the MPE conducted to determine which configuration to use for the TCEQ's 2019 Modeling Platform. Based on this evaluation and other factors, the Zhang03 dry-deposition scheme and K-Theory vertical diffusion scheme were selected.

The CAMx runs were conducted using the TCEQ's preliminary 2019 modeling platform and various updates to EIs and other aspects have been added to the modeling platform since the time of testing. Therefore, the modeling results and MPE statistics of the tested configurations are slightly different than the final CAMx results used in the DFW/Bexar County/HGB 2015 Eight-Hour Ozone Nonattainment Area AD SIP revisions.

5.4.1 HGB CAMx Configuration Assessment

Statistics for MDA8 and hourly ozone NMB and NME at all HGB area monitors are shown for each test month in *Table 5-12: CAMx Configuration Test Performance Statistics, HGB, June*, *Table 5-13: CAMx Configuration Test Performance Statistics, HGB, August*, and *Table 5-14: CAMx Configuration Test Performance Statistics, HGB, September*. When all data are considered, Wesely89 outperforms Zhang03 dry-deposition scheme. However, when ozone concentrations at or above 60 ppb are considered, the Zhang03 shows improved performance over the Wesely89 scheme. The ACM2 vertical diffusion scheme slightly improved performance in most cases, but to much less effect than the Zhang03 dry-deposition scheme.

Table 5-9: CAMx Configuration Test Performance Statistics, HGB, June

Configuration	MDA8 All Obs. NMB (%)	MDA8 All Obs. NME (%)	MDA8 ≥ 60 ppb NMB (%)	MDA8 ≥ 60 ppb NME (%)	One-Hour Ozone ≥ 60 ppb NMB (%)	One-Hour Ozone ≥ 60 ppb NME (%)
Wesely89/K-Theory	13.22	27.32	-8.80	15.33	-12.53	17.75
Zhang03/K-Theory	17.40	28.81	-4.29	14.83	-8.06	16.16
Wesely89/ACM2	14.18	27.52	-7.09	15.23	-11.17	17.34
Zhang03/ACM2	18.49	29.31	-2.42	15.30	-6.54	16.06

Table 5-10: CAMx Configuration Test Performance Statistics, HGB, August

Configuration	MDA8 All Obs. NMB (%)	MDA8 All Obs. NME (%)	MDA8 ≥ 60 ppb NMB (%)	MDA8 ≥ 60 ppb NME (%)	One-Hour Ozone ≥ 60 ppb NMB (%)	One-Hour Ozone ≥ 60 ppb NME (%)
Wesely89/K-Theory	23.89	26.98	0.78	12.74	-5.70	14.64
Zhang03/K-Theory	25.56	29.02	4.51	13.31	-2.60	14.43
Wesely89/ACM2	24.30	27.27	1.99	13.10	-4.44	14.46
Zhang03/ACM2	27.10	29.42	5.90	13.96	-1.17	14.45

Table 5-11: CAMx Configuration Test Performance Statistics, HGB, September

Configuration	MDA8 All Obs. NMB (%)	MDA8 All Obs. NME (%)	MDA8 ≥ 60 ppb NMB (%)	MDA8 ≥ 60 ppb NME (%)	One-Hour Ozone ≥ 60 ppb NMB (%)	One-Hour Ozone ≥ 60 ppb NME (%)
Wesely89/K-Theory	12.90	17.45	-0.27	6.95	-5.27	10.33
Zhang03/K-Theory	15.62	19.34	2.85	7.39	-2.55	9.88
Wesely89/ACM2	13.25	17.66	-0.2	6.85	-5.26	10.58
Zhang03/ACM2	16.07	19.64	3.01	7.38	-2.46	10.17

Time series of hourly modeled and observed ozone for each configuration in each test month are presented in Figure 5-18: *Observed Hourly Ozone in June at the Houston Aldine monitor and Values Modeled with Different CAMx Configurations*, Figure 5-19: *Observed Hourly Ozone in August at the Houston Aldine Monitor and Values Modeled with Different CAMx Configurations*, and Figure 5-20: *Observed Hourly Ozone in September at the Houston Aldine Monitor and Values Modeled with Different CAMx Configurations*. In many cases the Zhang03 scheme resulted in higher hourly modeled ozone than the Wesely89 scheme, meeting the higher observed hourly ozone more often. On occasions, the Zhang06 scheme showed overprediction of hourly ozone concentrations. The ACM2 vertical diffusion scheme did not result in any noticable differences in modeled hourly ozone compared to the K-Theory scheme.

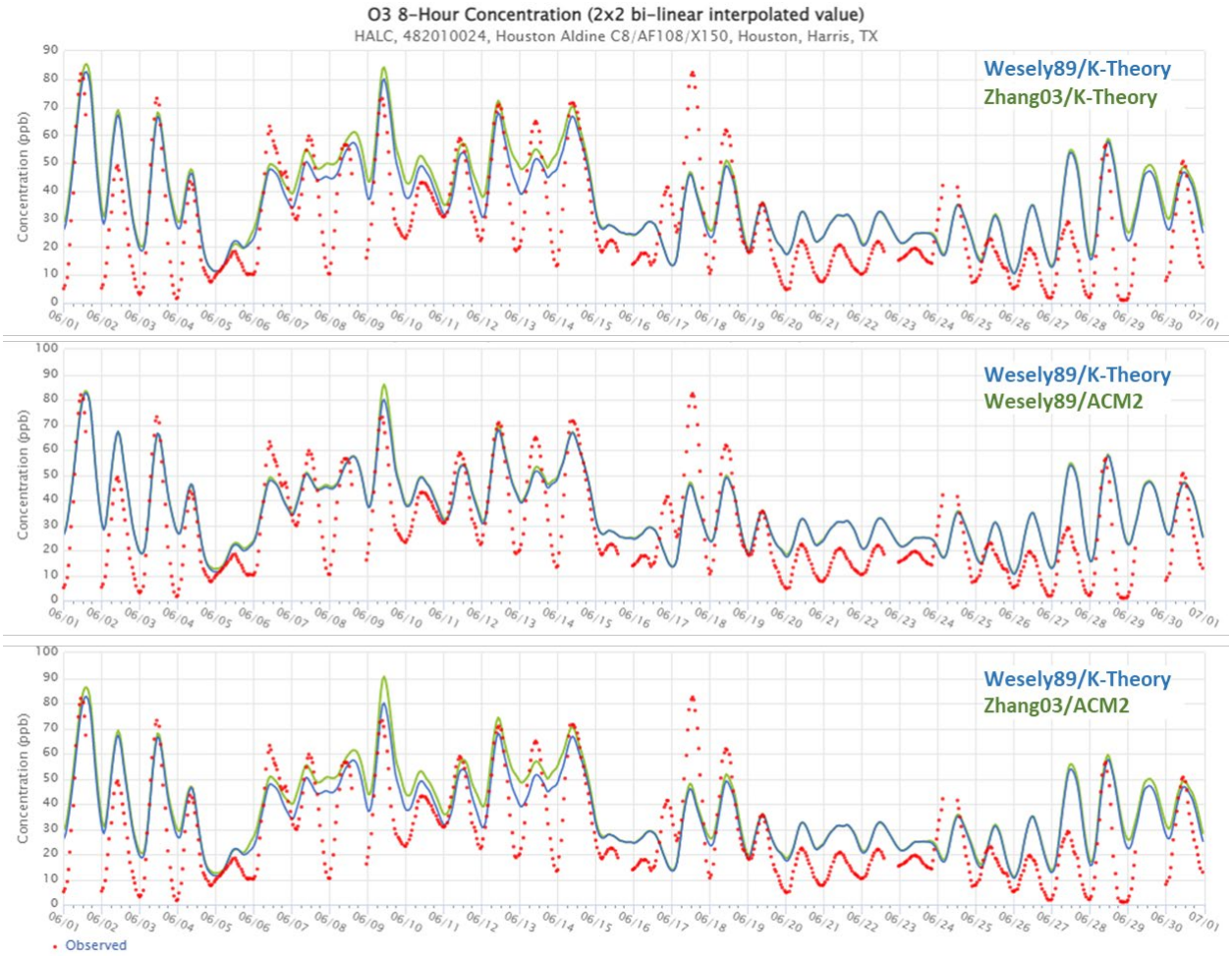

Figure 5-13: June Eight-Hour Average Ozone Comparing Wesely89/K-Theory to Zhang03/K-Theory (top), to Wesely89/ACM2 (middle), and to Zhang03/ACM2 (bottom) at the Houston Aldine Monitor

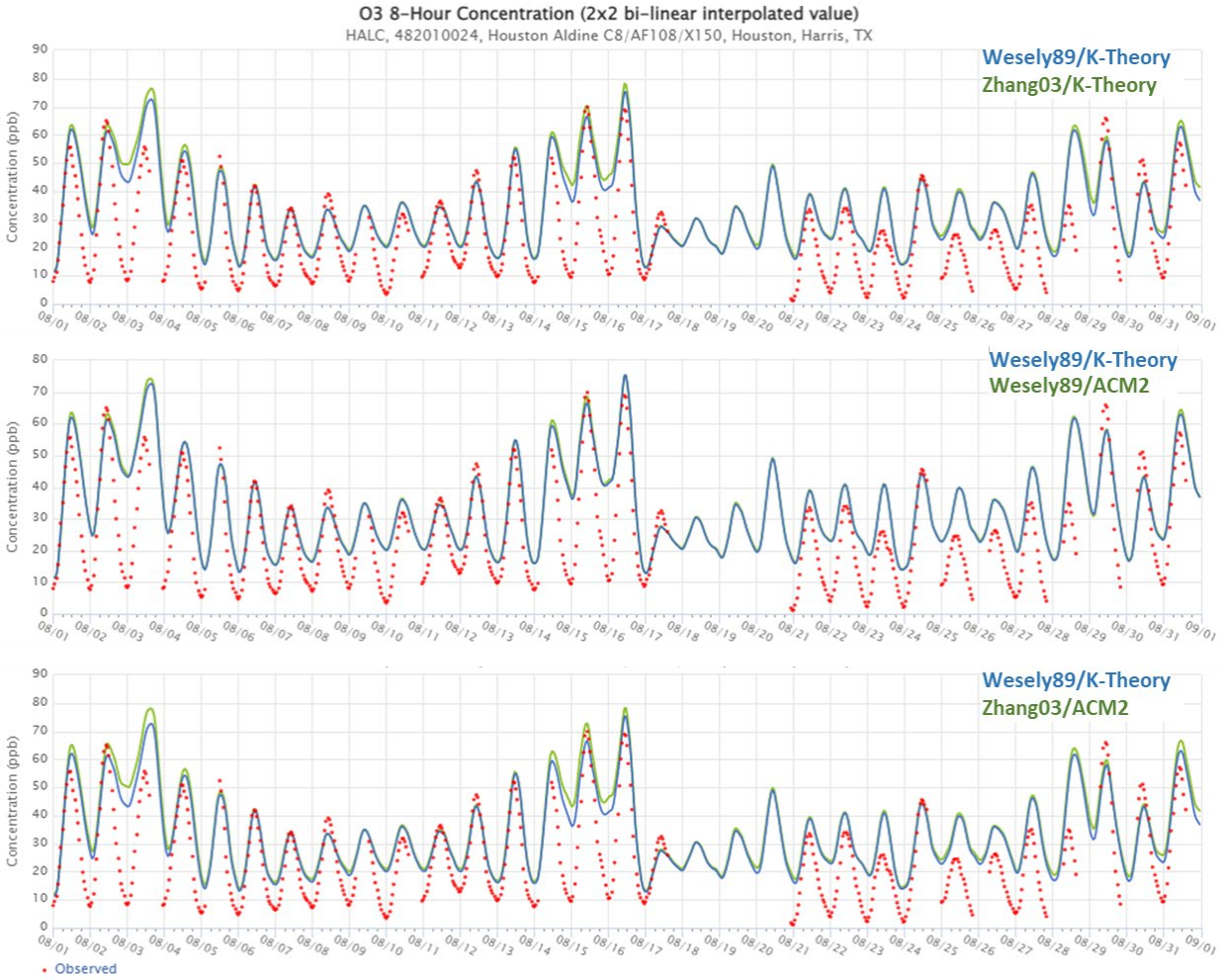

Figure 5-14: August Eight-Hour Average Ozone Comparing Wesely89/K-Theory to Zhang03/K-Theory (top), to Wesely89/ACM2 (middle), and to Zhang03/ACM2 (bottom) at the Houston Aldine Monitor

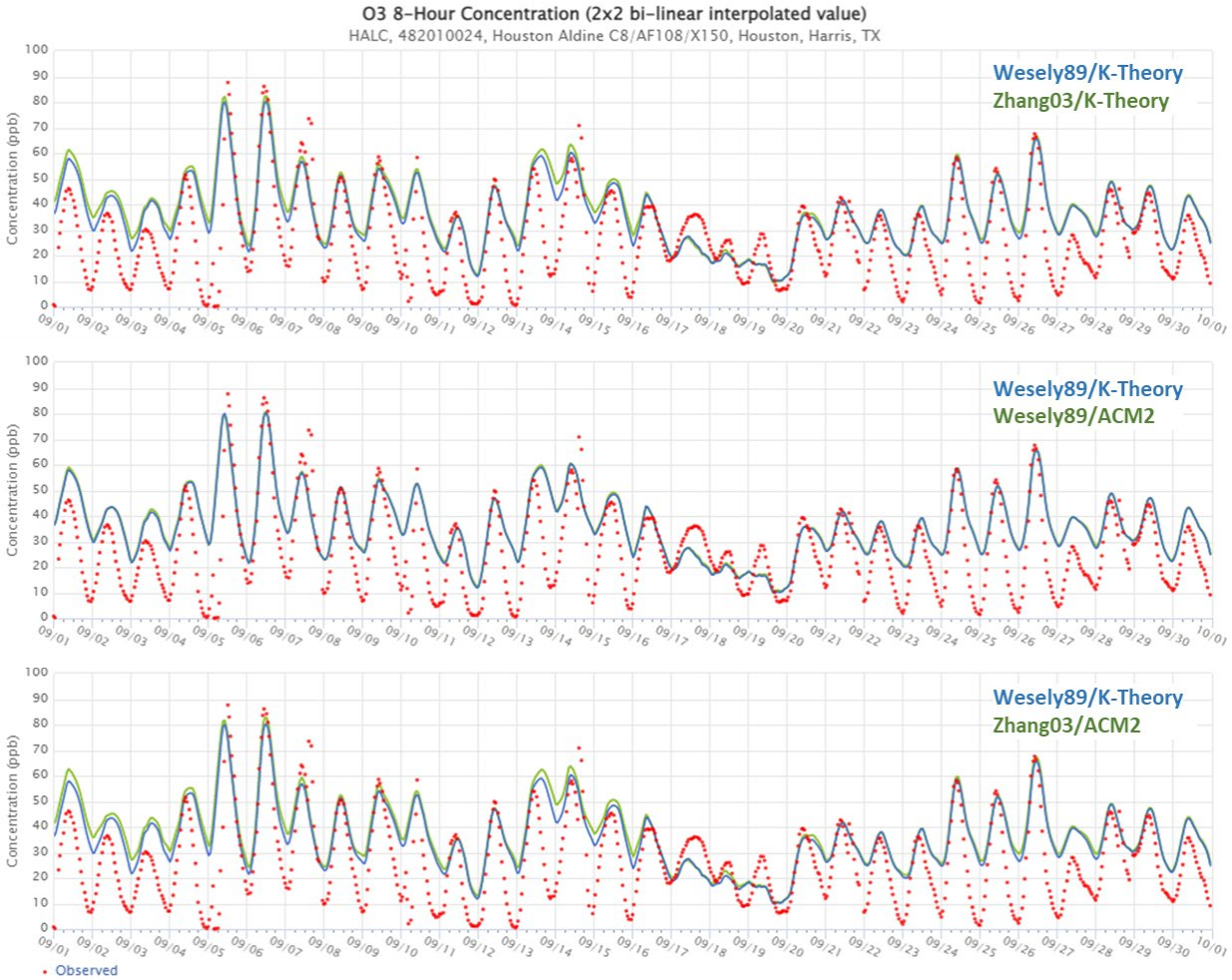

Figure 5-15: September Eight-Hour Average Ozone Comparing Wesely89/K-Theory to Zhang03/K-Theory (top), to Wesely89/ACM2 (middle), and to Zhang03/ACM2 (bottom) at the Houston Aldine Monitor

Modeled MDA8 ozone concentration maps of the HGB area for two high days (June 1 and September 6) are plotted for the Zhang03/K-Theory and the Wesely89/K-Theory in Figure 5-21: *June 1 MDA8 Ozone Comparison: Wesely89/K-Theory (left) versus Zhang03/K-Theory (right)* and *Figure 5-22: September 6 MDA8 Ozone Comparison: Wesely89/K-Theory (left) versus Zhang03/K-Theory (right).* Observed MDA8 ozone values are shown in round circles.

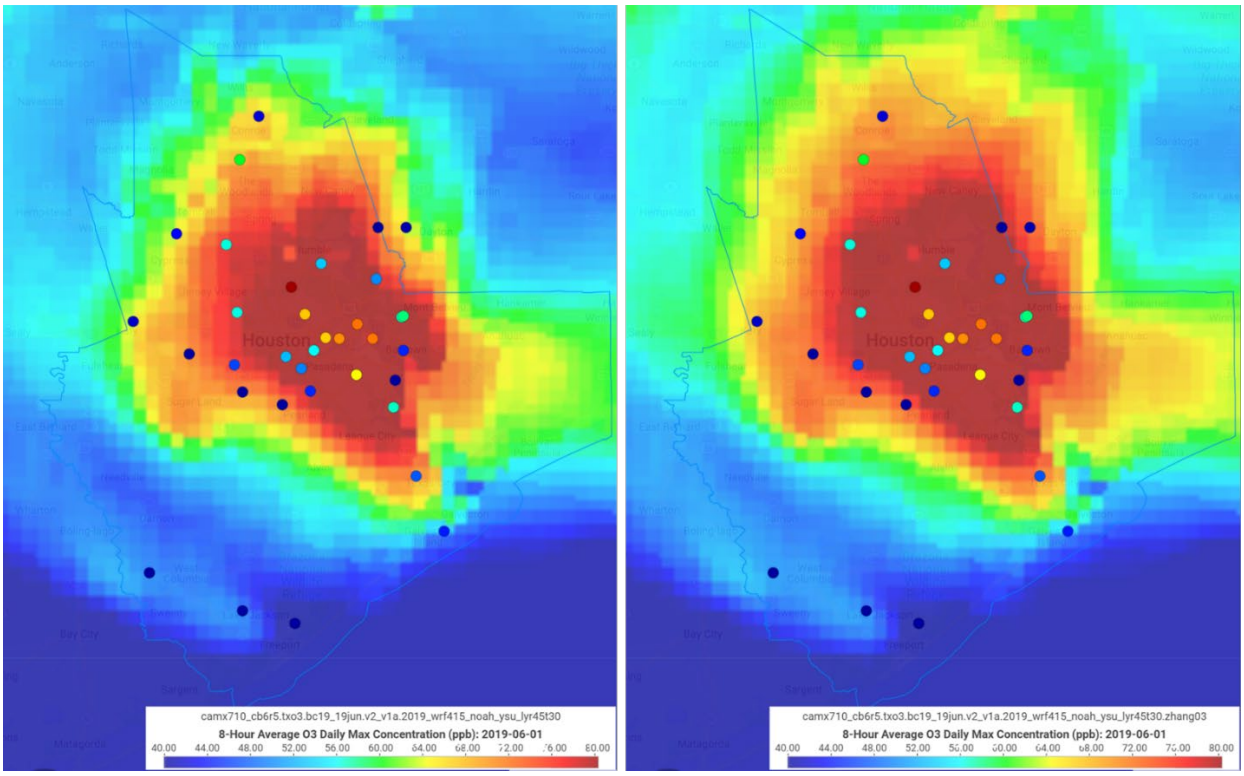

Figure 5-16: June 1 MDA8 Ozone Comparison in HGB: Wesely89/K-Theory (left) versus Zhang03/K-Theory (right)

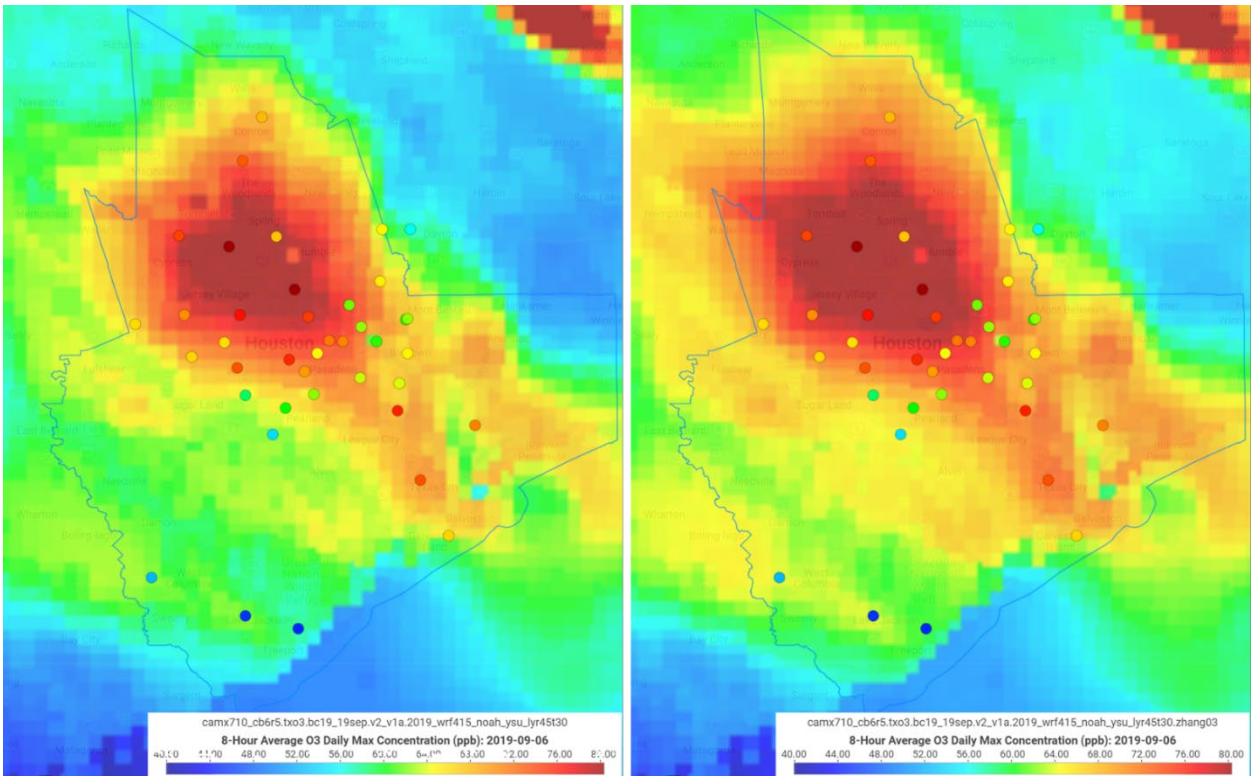

Figure 5-17: September 6 MDA8 Ozone Comparison in HGB: Wesely89/K-Theory (left) versus Zhang03/K-Theory (right)

5.4.2 DFW CAMx Configuration Assessment

Statistics for MDA8 and hourly ozone NMB and NME at all DFW area monitors are shown for each test month in Table 5-9: *CAMx Configuration Test Performance Statistics, DFW, June*, Table 5-10: *CAMx Configuration Test Performance Statistics, DFW, August*, and Table 5-11: *CAMx Configuration Test Performance Statistics, DFW, September*. In nearly all categories across all months, the inclusion of the Zhang03 dry-deposition scheme improved performance over the Wesely89 scheme. The ACM2 vertical diffusion scheme also improved performance slightly in most cases, but to much less effect than the Zhang03 dry-deposition scheme.

Table 5-12: CAMx Configuration Test Performance Statistics, DFW, June

Configuration	MDA8 All Obs. NMB (%)	MDA8 All Obs. NME (%)	MDA8 ≥ 60 ppb NMB (%)	MDA8 ≥ 60 ppb NME (%)	One-Hour Ozone ≥ 60 ppb NMB (%)	One-Hour Ozone ≥ 60 ppb NME (%)
Wesely89/K-Theory	-1.95	17.47	-17.74	18.95	-19.37	20.74
Zhang03/K-Theory	3.53	17.28	-12.84	15.01	-14.56	17.00
Wesely89/ACM2	-1.46	17.43	-16.80	18.25	-18.56	20.15
Zhang03/ACM2	4.18	17.35	-11.76	14.28	-13.64	16.57

Table 5-13: CAMx Configuration Test Performance Statistics, DFW, August

Configuration	MDA8 All Obs. NMB (%)	MDA8 All Obs. NME (%)	MDA8 ≥ 60 ppb NMB (%)	MDA8 ≥ 60 ppb NME (%)	One-Hour Ozone ≥ 60 ppb NMB (%)	One-Hour Ozone ≥ 60 ppb NME (%)
Wesely89/K-Theory	-0.39	10.79	-8.82	9.99	-11.37	12.66
Zhang03/K-Theory	3.69	10.82	-4.56	7.63	-7.40	10.22
Wesely89/ACM2	-0.08	10.73	-8.10	9.60	-10.72	12.28
Zhang03/ACM2	4.11	10.85	-3.70	7.34	-6.60	10.00

Table 5-14: CAMx Configuration Test Performance Statistics, DFW, September

Configuration	MDA8 All Obs. NMB (%)	MDA8 All Obs. NME (%)	MDA8 ≥ 60 ppb NMB (%)	MDA8 ≥ 60 ppb NME (%)	One-Hour Ozone ≥ 60 ppb NMB (%)	One-Hour Ozone ≥ 60 ppb NME (%)
Wesely89/K-Theory	-0.56	8.53	-4.13	6.67	-6.34	8.86
Zhang03/K-Theory	3.73	9.06	1.57	6.44	-1.13	7.46
Wesely89/ACM2	0.07	8.56	-2.91	6.54	-5.21	8.60
Zhang03/ACM2	4.50	9.39	2.93	6.88	0.15	7.66

Time series of hourly modeled and observed ozone for each configuration in each test month are presented in Figure 5-13: *Hourly Ozone Comparing Wesely89/K-Theory to Zhang03/K-Theory (top), Wesely89/ACM2 (middle), and Zhang03/ACM2 (bottom) at*

Cleburne Airport in June, Figure 5-14: *Hourly Ozone Comparing Wesely89/K-Theory to Zhang03/K-Theory (top), to Wesely89/ACM2 (middle), and to Zhang03/ACM2 (bottom) at Keller in August*, and Figure 5-15: *Hourly Ozone Comparing Default (Wesely89/K-Theory) to Zhang03/K-Theory (top), to Wesely89/ACM2 (middle), and to Zhang03/ACM2 (bottom) at Frisco in September*. In many cases the Zhang03 dry-deposition scheme resulted in higher hourly modeled ozone than the Wesely89 scheme, meeting the higher observed hourly ozone more often. The ACM2 vertical diffusion scheme did not result in any noticable differences in modeled hourly ozone compared to the K-Theory scheme.

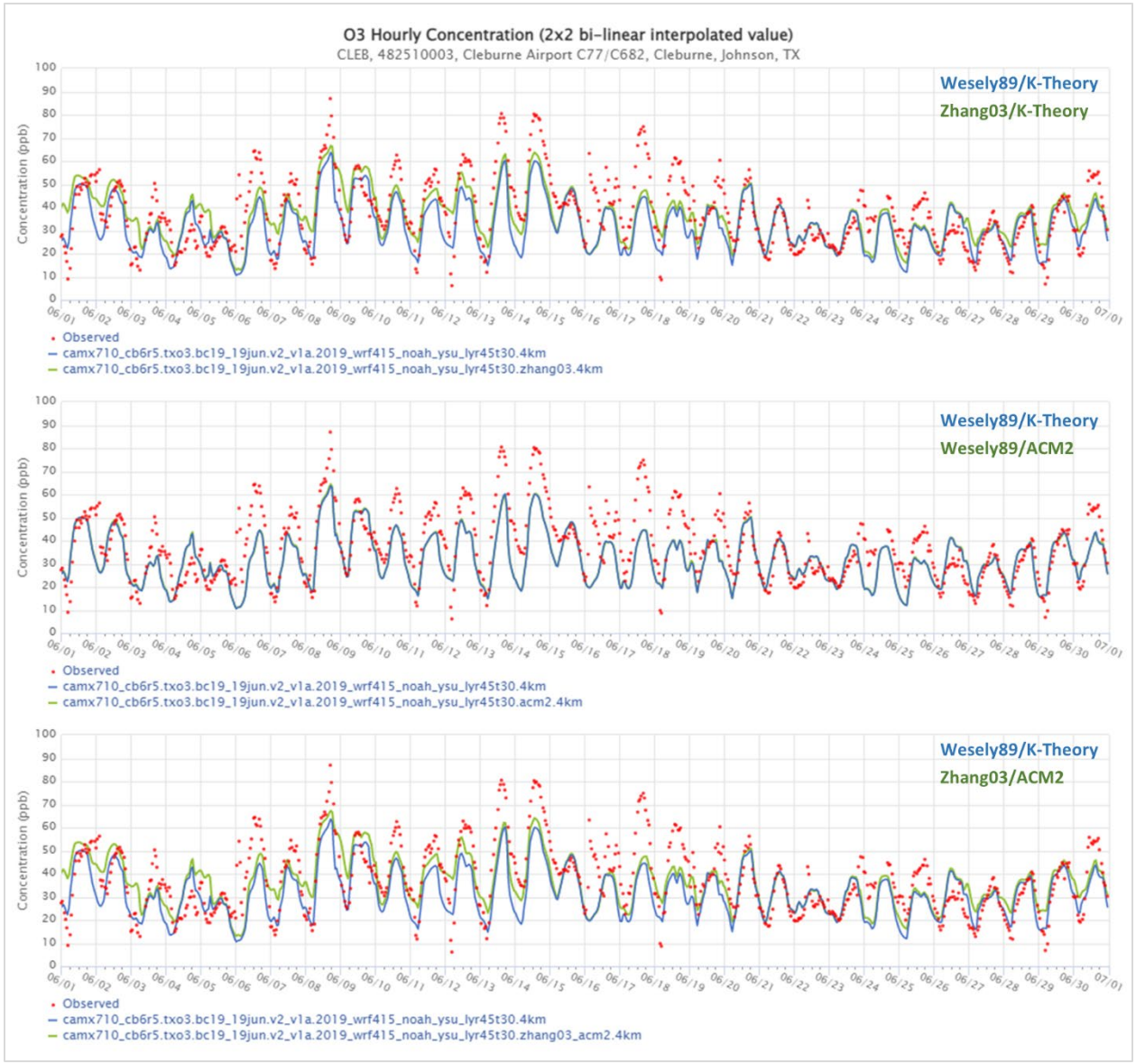

Figure 5-18: June Hourly Ozone Comparing Wesely89/K-Theory to Zhang03/K-Theory (top), to Wesely89/ACM2 (middle), and to Zhang03/ACM2 (bottom) at the Cleburne Airport Monitor

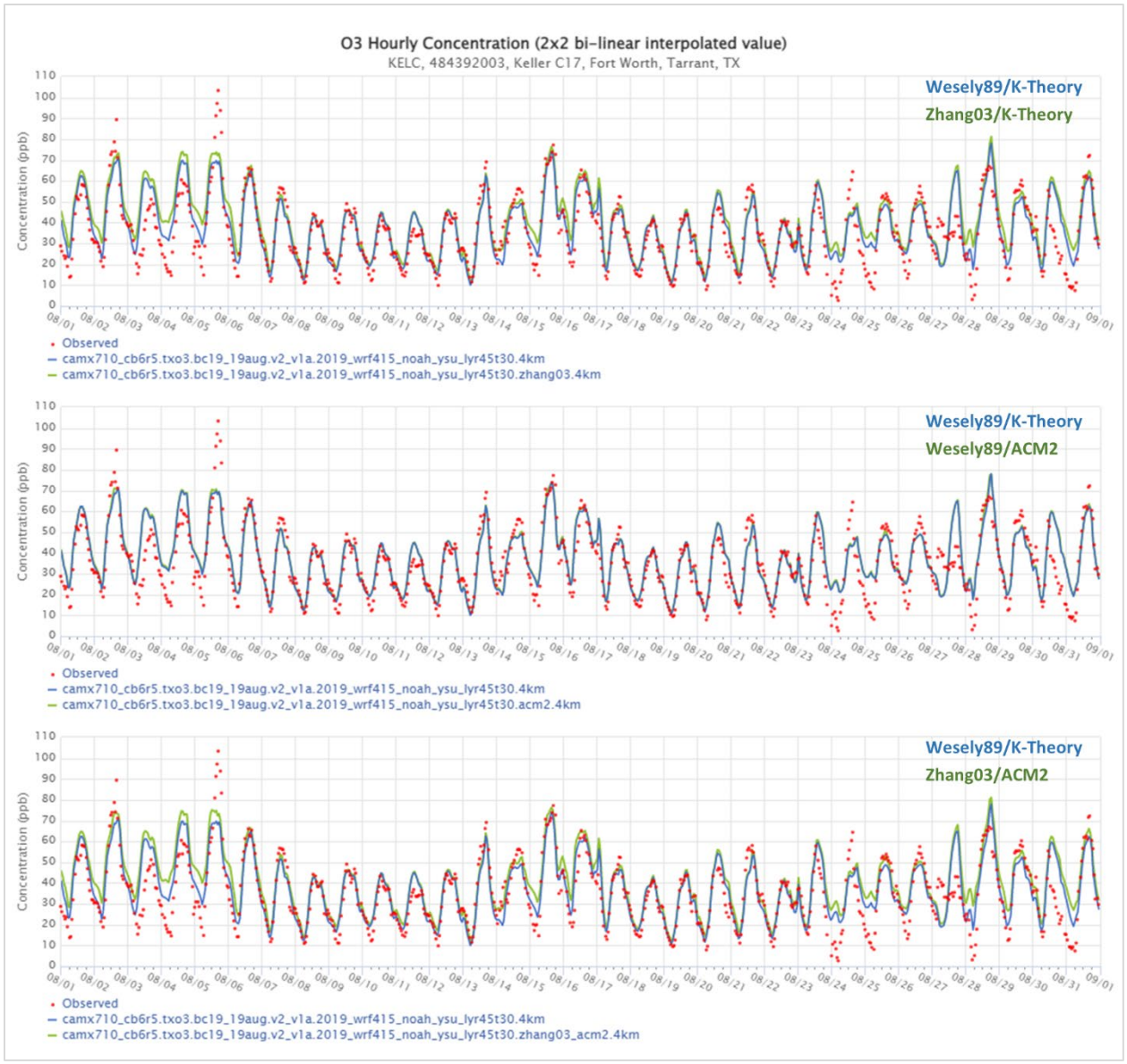

Figure 5-19: August Hourly Ozone Comparing Wesely89/K-Theory to Zhang03/K-Theory (top), to Wesely89/ACM2 (middle), and to Zhang03/ACM2 (bottom) at the Keller Monitor

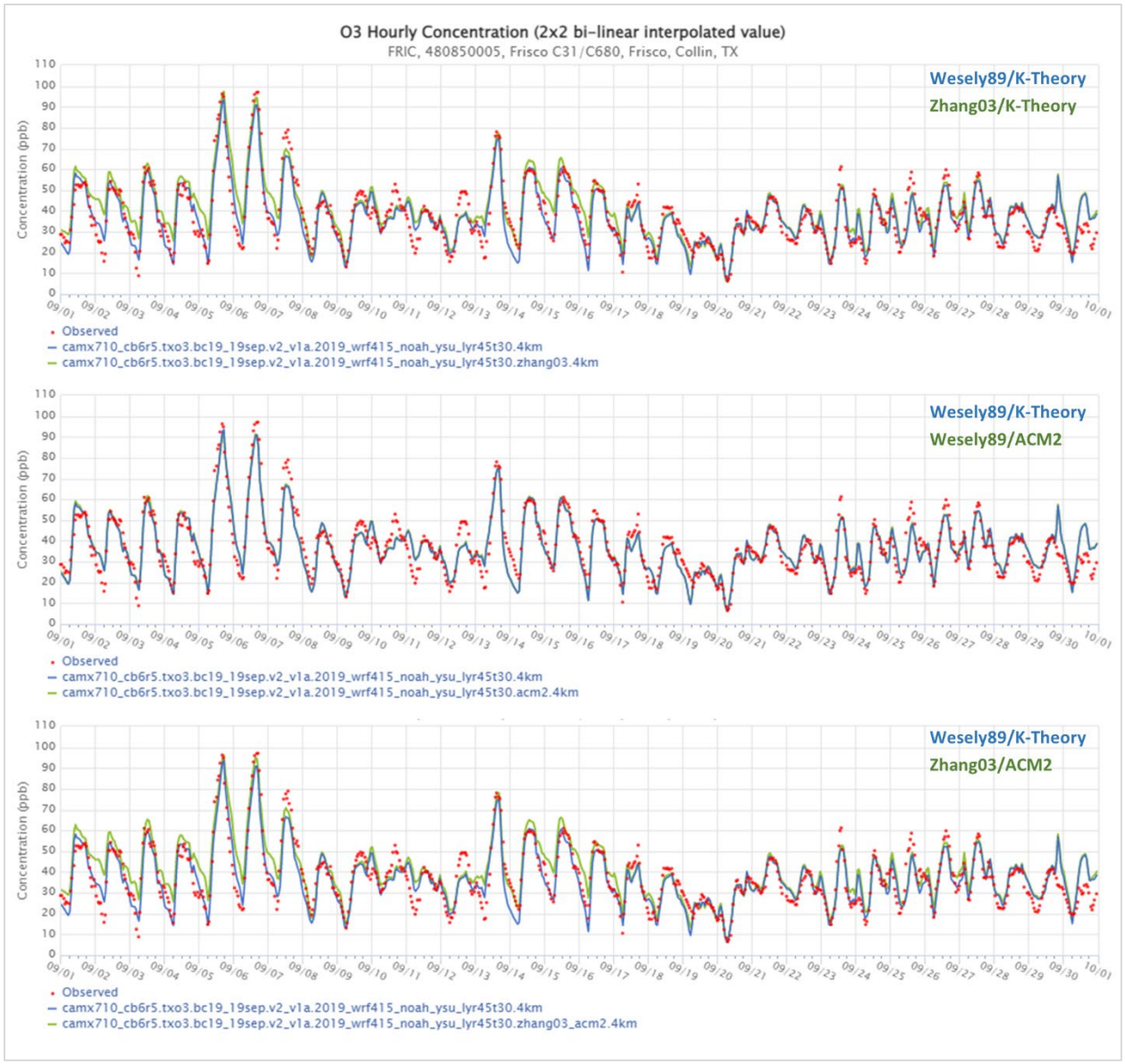

Figure 5-20: September Hourly Ozone Comparing Wesely89/K-Theory to Zhang03/K-Theory (top), to Wesely89/ACM2 (middle), and to Zhang03/ACM2 (bottom) at the Frisco Monitor

MDA8 ozone concentration maps of the DFW area for two high days (June 18 and August 6) are plotted for the Zhang03/K-Theory and the Wesely89/K-Theory in Figure 5-16: *June 18 MDA8 Ozone Comparison: Wesely89/K-Theory (left) versus Zhang03/K-Theory (right)* and Figure 5-17: *August 6 MDA8 Ozone Comparison: Wesely89/K-Theory (left) versus Zhang03/K-Theory (right)*. Observed MDA8 at DFW monitors is mapped on Figure 5-16 and Figure 5-17 as round markers colored with their corresponding MDA8 ozone concentration. The Zhang03/K-Theory configuration results in less underprediction across the DFW area on June 18 and August 6.

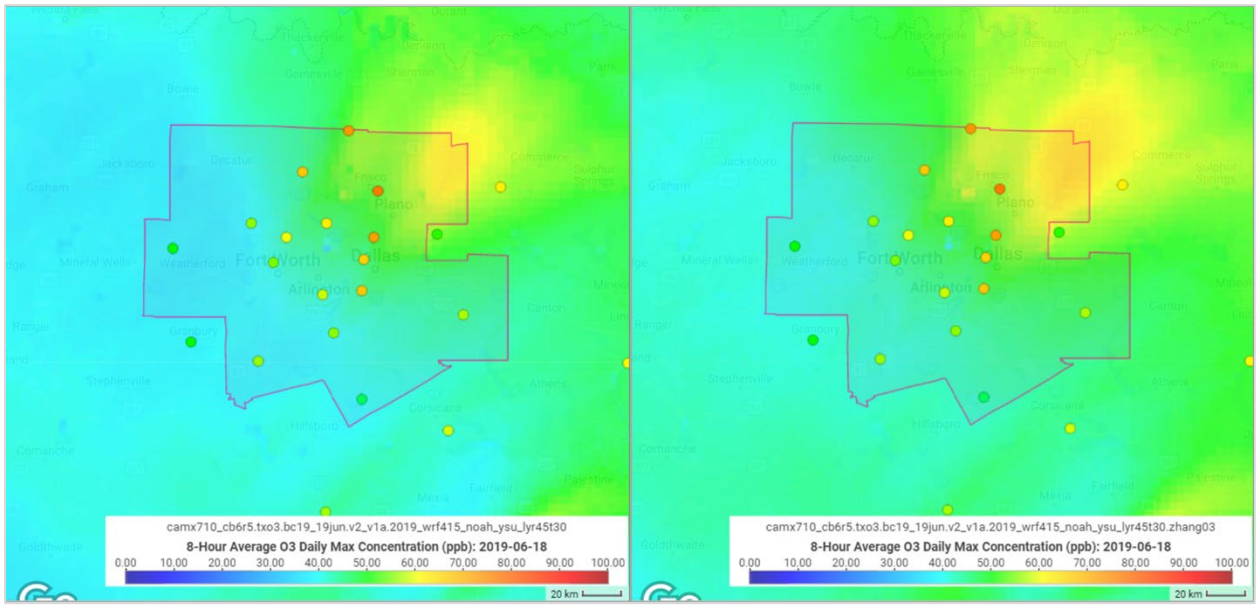

Figure 5-21: June 18 MDA8 Ozone Comparison in DFW: Wesely89/K-Theory (left) versus Zhang03/K-Theory (right)

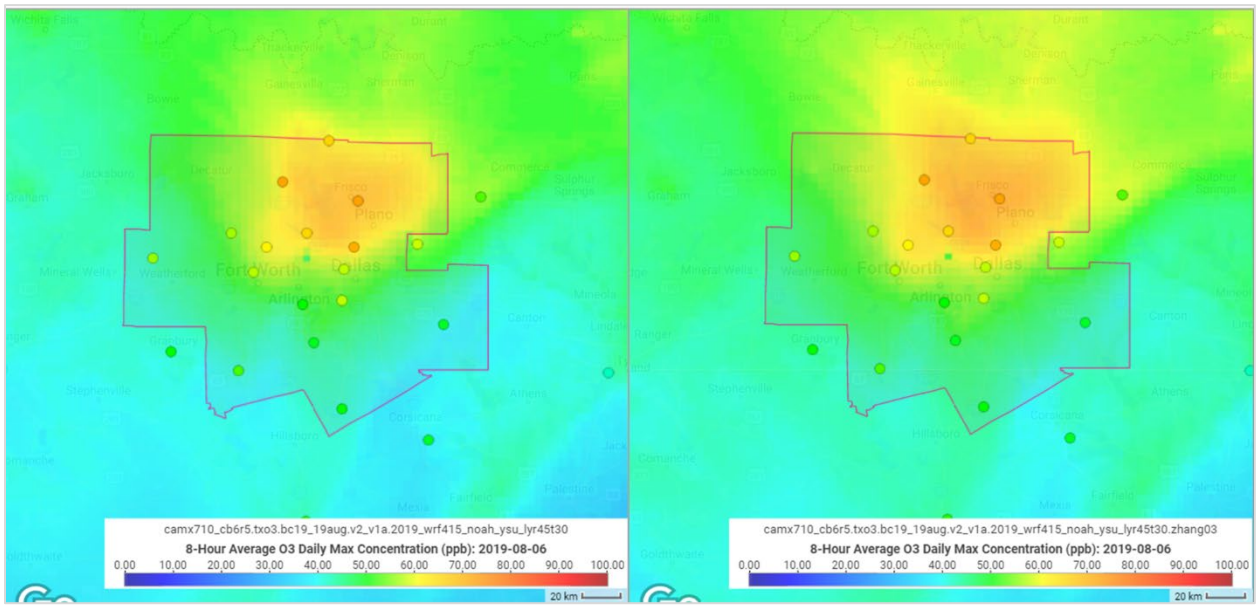

Figure 5-22: August 6 MDA8 Ozone Comparison in DFW: Wesely89/K-Theory (left) versus Zhang03/K-Theory (right)

5.4.3 Bexar County CAMx Configuration Assessment

Statistics for MDA8 and hourly ozone NMB and NME for observations over 60 ppb are shown in Table 5-15: *CAMx Configuration Test Performance Statistics, Bexar County, June,* Table 5-16: *CAMx Configuration Test Performance Statistics, Bexar County, August*, and Table 5-17: *CAMx Configuration Test Performance Statistics, Bexar County, September*. The combination of Zhang03 and ACM2 is the best overall, exhibiting the NMB values closest to zero for MDA8 for June and September and hourly ozone values over 60 ppb in all three months. However, CAMx is currently unable to run source

apportionment with ACM2, so the next best performing combination, Zhang03/K-Theory was chosen.

Table 5-15: CAMx Configuration Test Performance Statistics, Bexar County, June

Configuration	MDA8 All Obs. NMB (%)	MDA8 All Obs. NME (%)	MDA8 ≥ 60 ppb NMB (%)	MDA8 ≥ 60 ppb NME (%)	One-Hour Ozone ≥ 60 ppb NMB (%)	One-Hour Ozone ≥ 60 ppb NME (%)
Wesely89/K-Theory (default)	9.27	20.1	-12.92	13.12	-16.05	16.99
Zhang03/K-Theory	14.01	21.05	-5.96	9.00	-9.89	12.40
Wesely89/ACM2	9.57	19.98	-11.84	12.23	-15.11	16.12
Zhang03/ ACM2	14.4	21.08	-4.8	8.44	-8.83	11.55

Table 5-16: CAMx Configuration Test Performance Statistics, Bexar County, August

Configuration	MDA8 All Obs. NMB (%)	MDA8 All Obs. NME (%)	MDA8 ≥ 60 ppb NMB (%)	MDA8 ≥ 60 ppb NME (%)	One-Hour Ozone ≥ 60 ppb NMB (%)	One-Hour Ozone ≥ 60 ppb NME (%)
Wesely89/K-Theory (default)	4.63	10.73	-8.71	10.26	-12.8	13.58
Zhang03/K-Theory	7.42	11.68	-5.74	9.44	-10.00	11.90
Wesely89/ACM2	4.76	10.75	-9.37	11.2	-12.29	13.47
Zhang03/ACM2	7.65	11.73	-6.30	10.36	-9.38	11.88

Table 5-17: CAMx Configuration Test Performance Statistics, Bexar County, September

Configuration	MDA8 All Obs. NMB (%)	MDA8 All Obs. NME (%)	MDA8 ≥ 60 ppb NMB (%)	MDA8 ≥ 60 ppb NME (%)	One-Hour Ozone ≥ 60 ppb NMB (%)	One-Hour Ozone ≥ 60 ppb NME (%)
Wesely89/K-Theory (default)	6.51	12.03	-6.65	7.02	-10.90	11.10
Zhang03/K-Theory	9.50	13.73	-3.55	5.73	-8.08	8.80
Wesely89/ACM2	6.88	12.15	-6.08	6.67	-10.11	10.46
Zhang03/ACM2	10.00	14.01	-2.90	5.53	-7.21	8.42

As seen in Figure 5-21: *Time Series: Eight-Hour Ozone Comparing Default (Wesely89/K-Theory) versus Zhang03/K-Theory (top), Default versus Wesely89/ACM2 (middle), and Default versus Zhang03/ACM2 (bottom) at San Antonio Northwest*, Zhang03 dry deposition leads to higher June peak eight-hour ozone values than Wesely89, while the effect of ACM2 vertical diffusion is virtually indistinguishable from K-Theory.

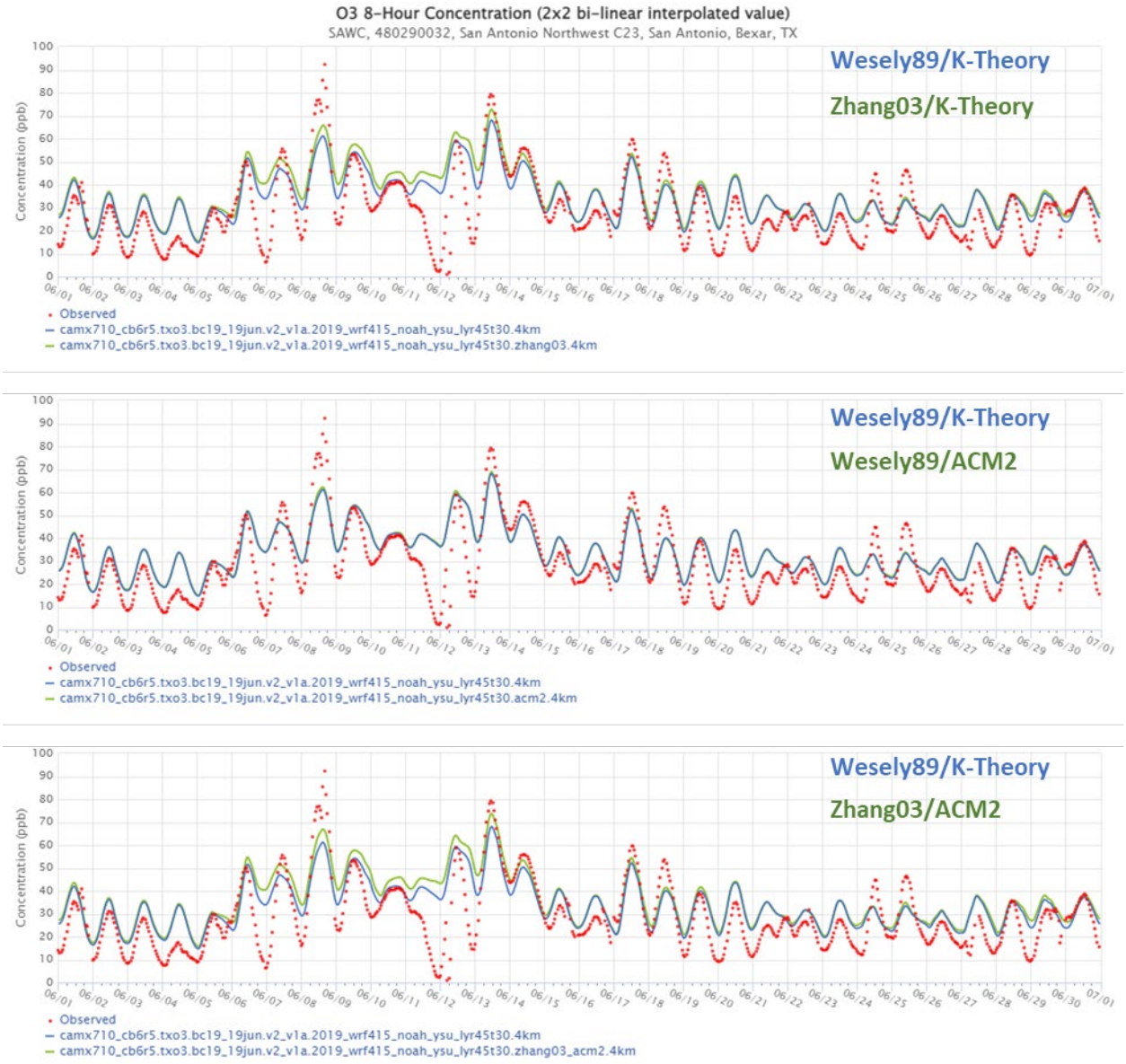

Figure 5-23: June Eight-Hour Ozone Comparing Wesely89/K-Theory to Zhang03/K-Theory (top), to Wesely89/ACM2 (middle), and to Zhang03/ACM2 (bottom) at the San Antonio Northwest Monitor

Results for the Camp Bullis Monitor in August shown in Figure 5-22: *Time Series: Eight-Hour Ozone Comparing Default (Wesely89/K-Theory) versus Zhang03/K-Theory (top), Default versus Wesely89/ACM2 (middle), and Default versus Zhang03/ACM2 (bottom) and Camp Bullis in August* show less improvement on peak eight-hour ozone than seen in June, potentially because peak values are lower in August.

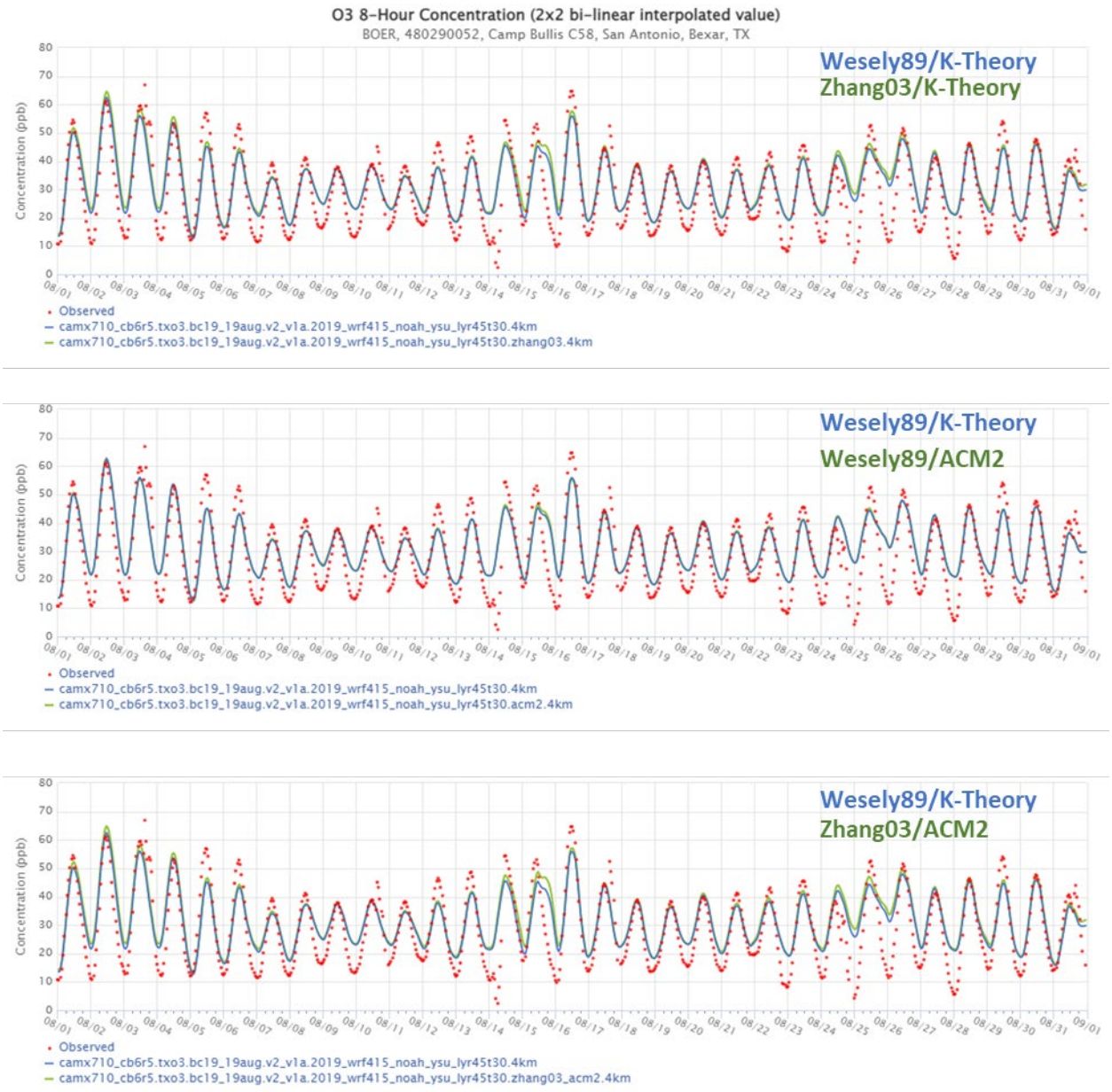

Figure 5-24: August Eight-Hour Ozone Comparing Wesely89/K-Theory to Zhang03/K-Theory (top), to Wesely89/ACM2 (middle), and to Zhang03/ACM2 (bottom) at the Camp Bullis Monitor

Results at San Antonio Northwest in September shown in Figure 5-23: *Time Series: Eight-Hour Ozone Comparing Default (Wesely89/K-Theory) versus Zhang03/K-Theory (top), Default versus Wesely89/ACM2 (middle), and Default versus Zhang03/ACM2 (bottom) at San Antonio Northwest in September* are between the June and August results with the high nighttime ozone values of September 1-3 and 14-15 exhibiting higher peaks with Zhang03.

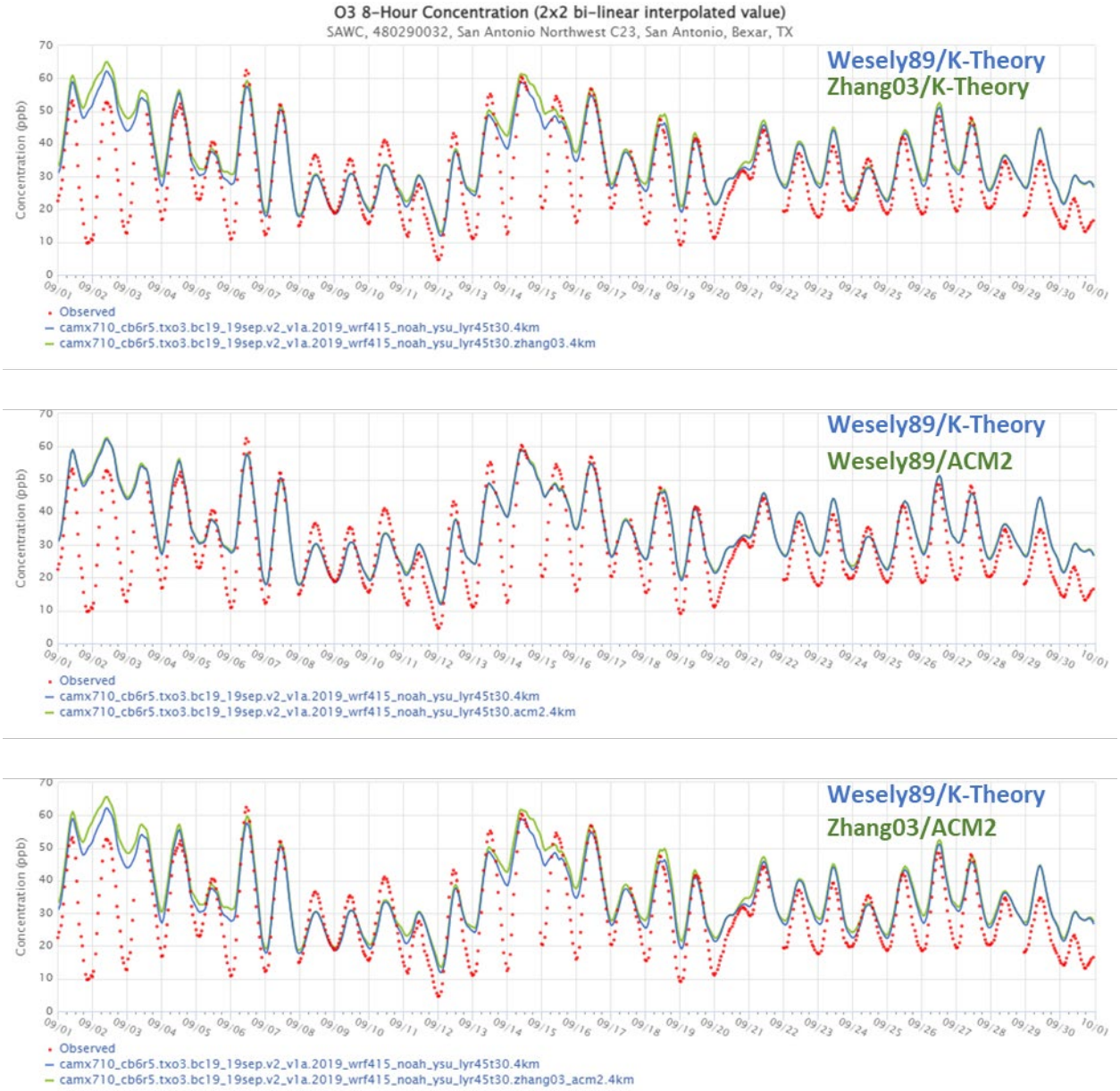

Figure 5-25: September Eight-Hour Ozone Comparing Wesely89/K-Theory to Zhang03/K-Theory (top), to Wesely89/ACM2 (middle), and to Zhang03/ACM2 (bottom) at the San Antonio Northwest Monitor

The improvement of the Zhang03/K-Theory parameterizations over Wesely89/K-Theory is seen in Figure 5-24: *MDA8 Ozone Comparison: Wesely89/K-Theory (left) versus Zhang03/K-Theory (right)* where the observation dot colors match the modeled MDA8 values much better with Zhang03 dry deposition.

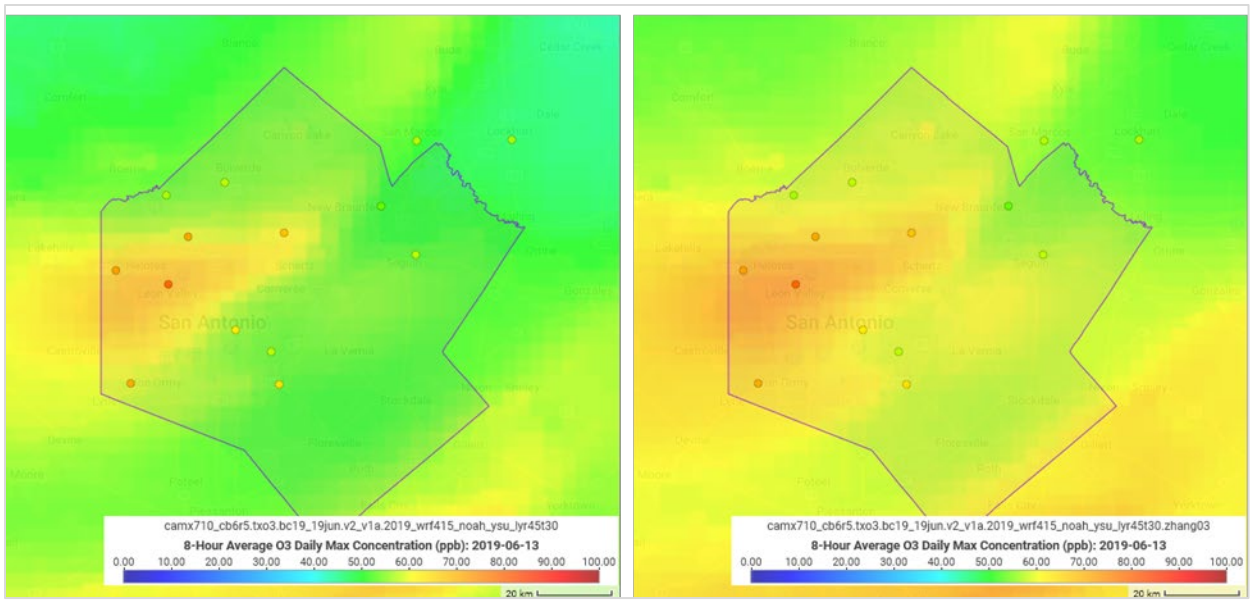

Figure 5-26: June 13 MDA8 Ozone Comparison in Bexar County: Wesely89/K-Theory (left) versus Zhang03/K-Theory (right)

6. MODELING DATA ARCHIVE

The TCEQ has archived all modeling input, output, and processing files used or generated as part of this attainment demonstration SIP revision modeling analysis. Interested parties can contact the TCEQ for information regarding data access or documentation.

CAMx modeling files may be accessed from the TCEQ Air Modeling FTP site using an FTP client software and the following information:

- FTP address: amdaftp.tceq.texas.gov
- FTP directory: /TXO3/camx

Emissions Files may be access from TCEQ Air Modeling FTP site using an FTP client software and the following information:

- FTP address: amdaftp.tceq.texas.gov
- FTP directory: /EI/2019_episodes

FTP client software, such as FileZilla, is recommended to efficiently retrieve the modeling and emissions files from the above directories. To access the files use the following login information:

- User ID: anonymous
- Password: user's email address

For meteorological files used in these SIP revisions, please email us at amda@tceq.texas.gov with "2019 WRF Modeling Files" in the subject line.

7. REFERENCES

Emery, C., Liu, Z., Russell, A.G., Odman, M.T., Yarwood, G. and Kumar, N., 2017. Recommendations on statistics and benchmarks to assess photochemical model performance. *Journal of the Air & Waste Management Association*, 67(5), pp.582-598. DOI: 10.1080/10962247.2016.1265027.

Kimura, Y., McDonald-Buller, E., Wiedinmyer, C., Pavlovic, N., McClure, C., Brown, S., and Lurmann, F., 2019. AQRP Project 18-022 Final Report: Development and Evaluation of the FINNv.2.2 Global Model Application and Fire Emissions Estimates for the Expanded Texas Air Quality Modeling Domain. https://aqrp.ceer.utexas.edu/projectinfoFY18_19/18-022/18-022%20Final%20Report.pdf, last accessed on January 27, 2023

Ramboll. 2022. User's Guide, Comprehensive Air Quality Model with Extensions, Version 7.20. https://camx-wp.azurewebsites.net/Files/CAMxUsersGuide_v7.20.pdf, last accessed on Jan. 20, 2023.

Stohl, A., Aamaas, B., Amann, M., Baker, L.H., Bellouin, N., Berntsen, T.K., Boucher, O., Cherian, R., Collins, W., Daskalakis, N. and Dusinska, M., 2015. Evaluating the climate and air quality impacts of short-lived pollutants. *Atmospheric Chemistry and Physics*, 15(18), pp.10529-10566. DOI: 10.5194/acp-15-10529-2015

U.S. Environmental Protection Agency. 2018. Modeling Guidance for Demonstrating Air Quality Goals for Ozone, PM*2.5* and Regional Haze. https://www.epa.gov/sites/default/files/2020-10/documents/o3-pm-rh-modeling_guidance-2018.pdf, last accessed on Jan. 20, 2023.

Wiedinmyer, C., Kimura, Y., McDonald-Buller, E., Seto, K., Emmons, L., Tang, W., Buccholz, R., Orlando, J. The Fire INventory from NCAR version 2 (FINNv2): updates to a high resolution global fire emissions model. In preparation for submission to the Journal of Advances in Modeling Earth Systems. https://www.acom.ucar.edu/Data/fire/, download date May 5, 2021

Wesely, M. L., and Lesht, B. M.. 1989. Comparison of RADM dry deposition algorithms with a site-specific method for inferring dry deposition. Water, Air, and Soil Pollution, 44, 273-293. DOI: 10.1007/BF00279259

Zhang, L., Brook, J.R. and Vet, R.. 2003. A revised parameterization for gaseous dry deposition in air-quality models. Atmospheric Chemistry and Physics, 3(6), pp.2067-2082. DOI: 10.5194/acp-3-2067-2003

ATTACHMENT 1

Emission and Model Performance Evaluation (MPE) Figures

LIST OF FIGURES

1. EMISSION PLOTS

This section of Attachment 1 presents detailed emissions plots of major ozone precursors, nitrogen oxides (NO_X) and volatile organic emissions (VOC), for the different anthropogenic sectors discussed in Section 3: Emissions Modeling of this appendix. Emissions plots are provided for the Bexar County, Dallas-Fort Worth (DFW), and Houston-Brazoria-Galveston (HGB) 2015 Eight-Hour Ozone National Ambient Air Quality Standard (NAAQS) nonattainment areas. Emissions plots shown are of two types:

- Tile plots that shown the spatial distribution for the 2019 base case and the 2023 future case gridded emissions.
- Difference tile plots that show the spatial distribution of the change in the emissions between the 2023 future case and 2019 base case gridded emissions.

While photochemical modeling uses emissions inputs in hourly resolution, based on the availability of datasets, emissions for most sectors with the exception of the electric generating units (EGU) are the same for most hours of the modeled episode. Therefore, emissions are shown for the modeled episode day of June 12 for all sectors. Emissions plots for the EGU sector is not included since it varies for each hour of every modeled episode day.

Unless otherwise noted, the resolution of the gridded emissions is the finest resolution of 4 kilometer.

1.1 NON EGU POINT SOURCES

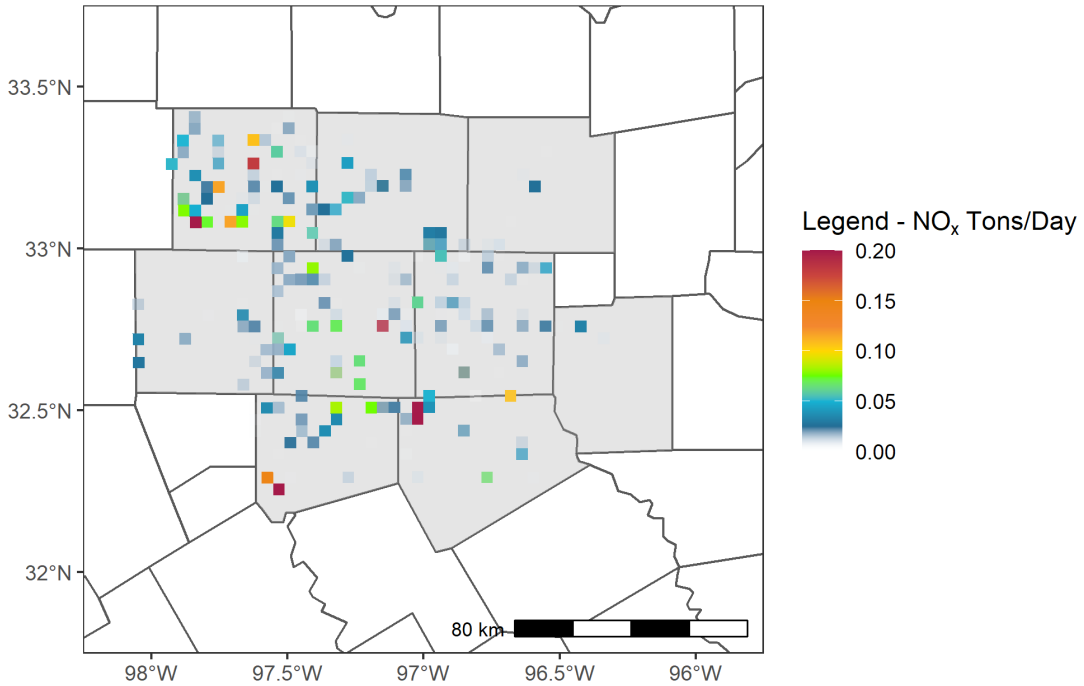

Figure 1-1: 2019 Base Case Non-EGU NO_x Emissions for June 12 Episode Day in DFW

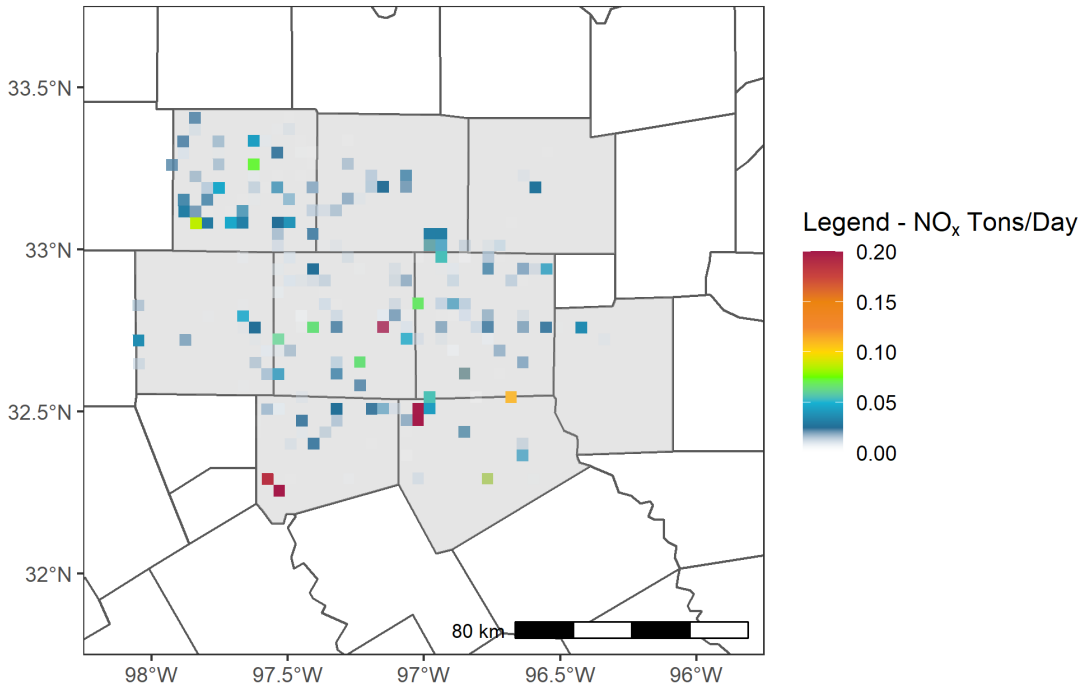

Figure 1-2: 2023 Future Case Non-EGU NO_x Emissions for June 12 Episode Day in DFW

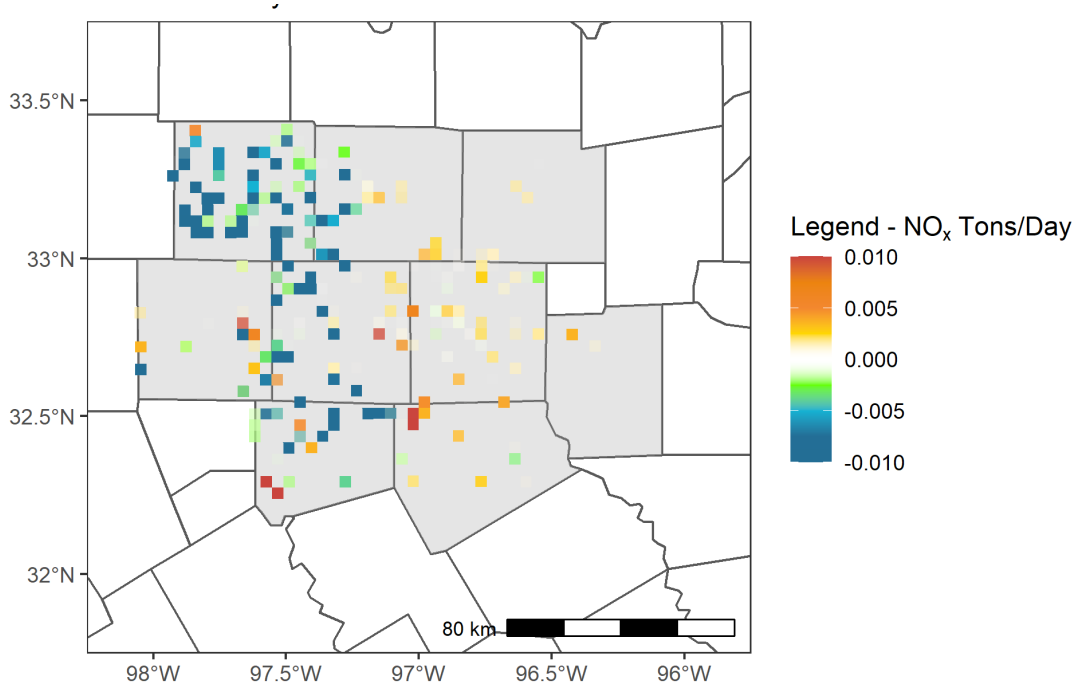

Figure 1-3: Difference in Non-EGU NO_x Emissions for the June 12 Episode Day Between 2023 and 2019 in DFW

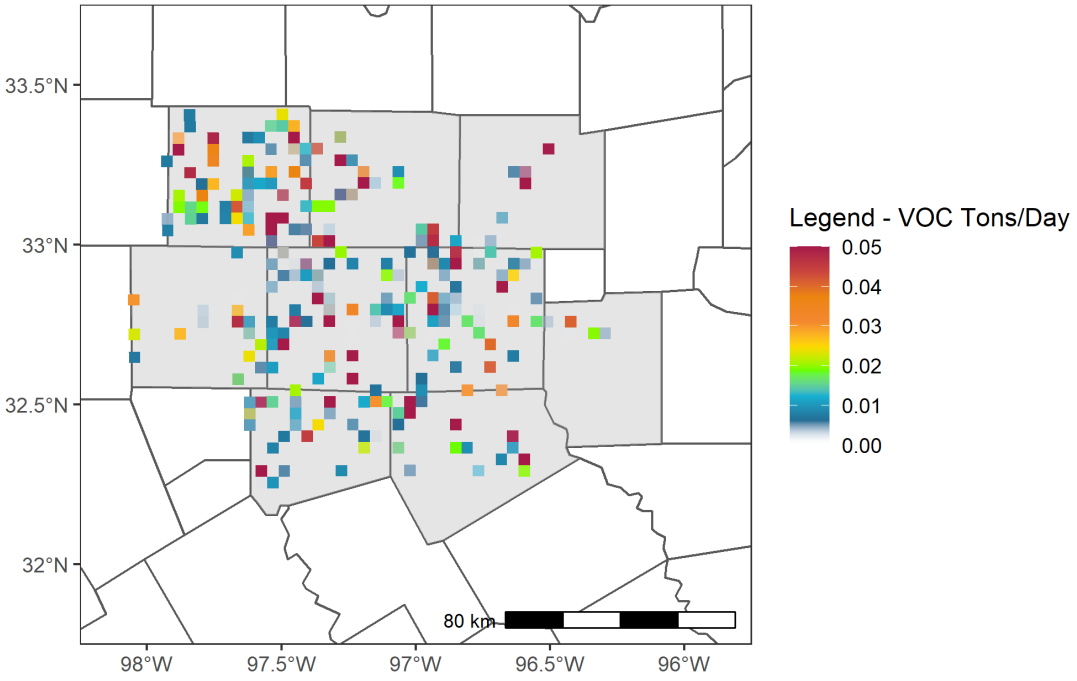

Figure 1-4: 2019 Base Case Non-EGU VOC Emissions for June 12 Episode Day in DFW

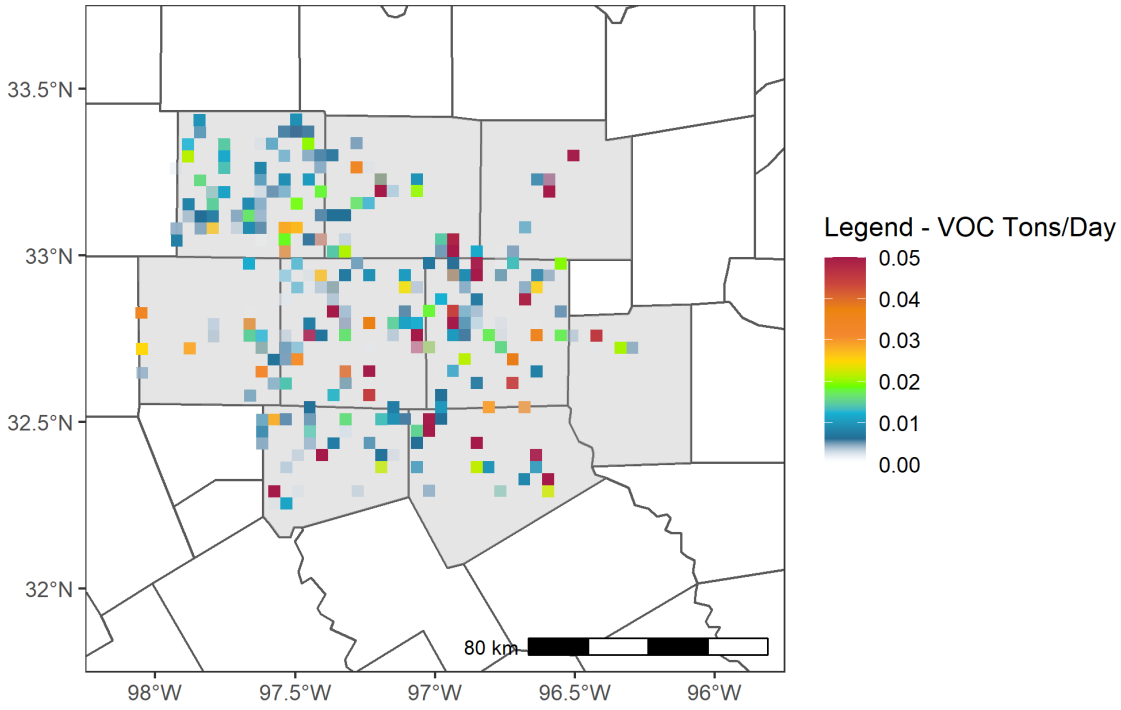

Figure 1-5: 2023 Future Case Non-EGU VOC Emissions for June 12 Episode Day in DFW

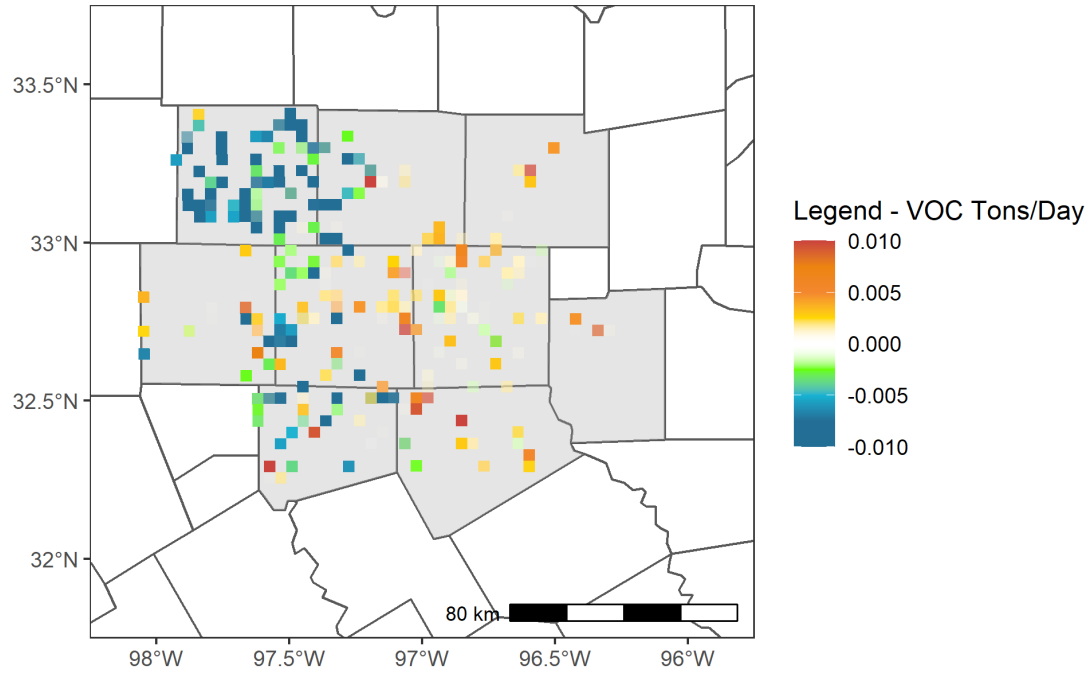

Figure 1-6: Difference in VOC Emissions for the June 12 Episode Day Between 2023 and 2019 in DFW

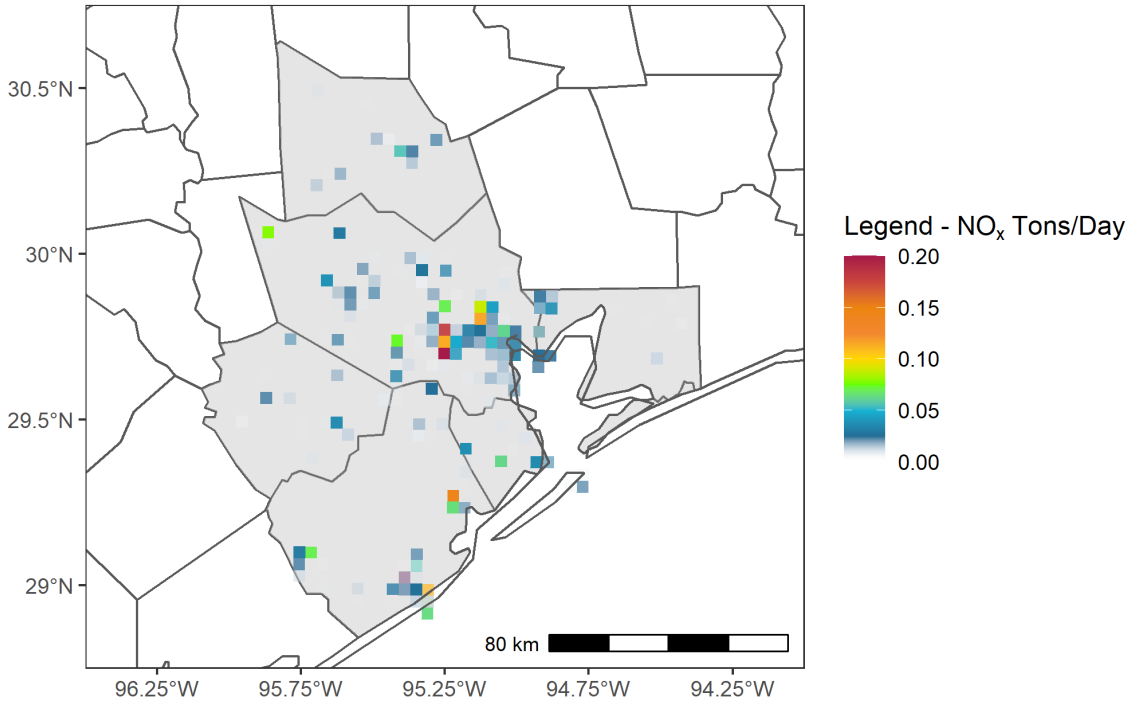

Figure 1-7: 2019 Base Case Non-EGU NO_x Emissions for June 12 Episode Day in HGB

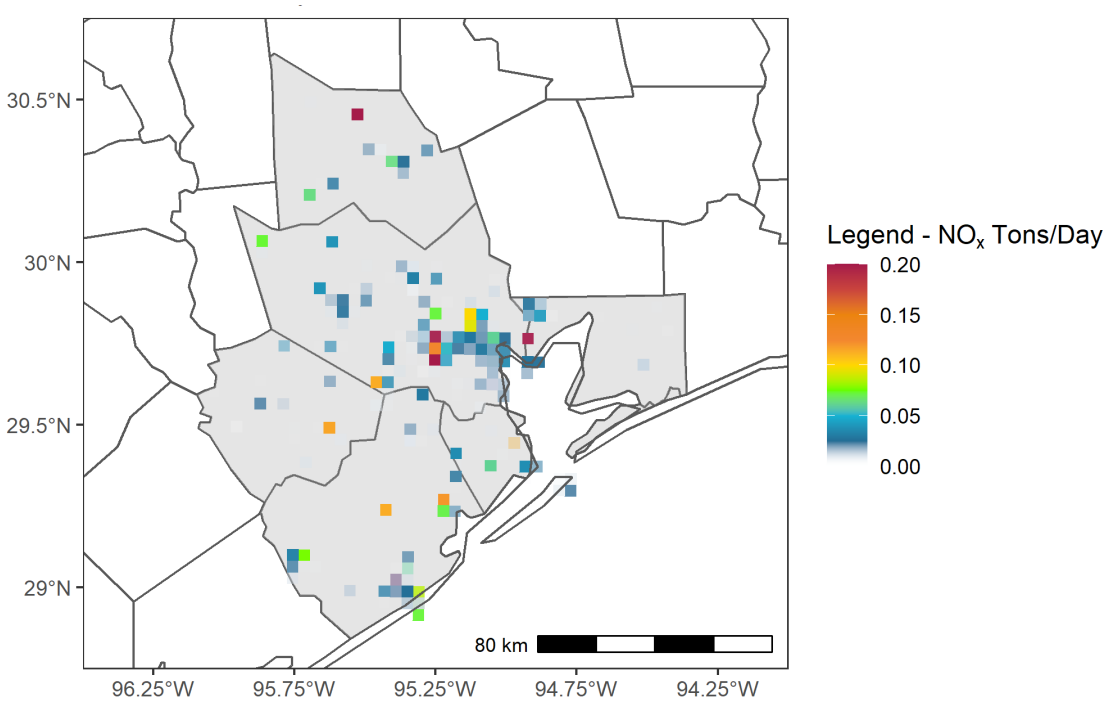

Figure 1-8: 2023 Future Case Non-EGU NO_x Emissions for June 12 Episode Day in HGB

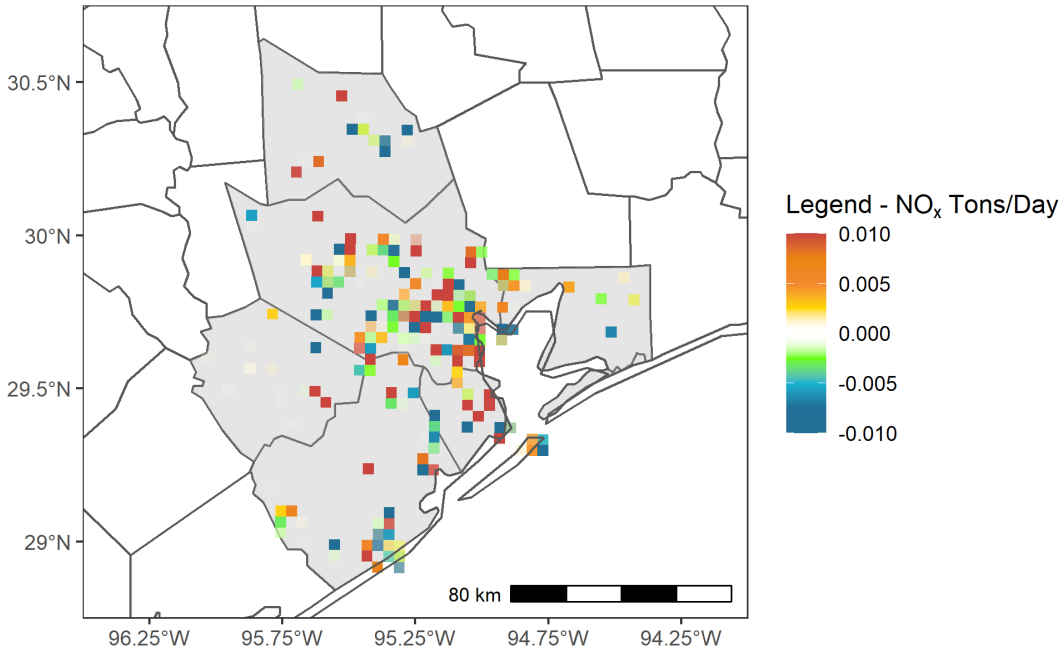

Figure 1-9: Difference in Non-EGU NO_x Emissions for the June 12 Episode Day Between 2023 and 2019 in HGB

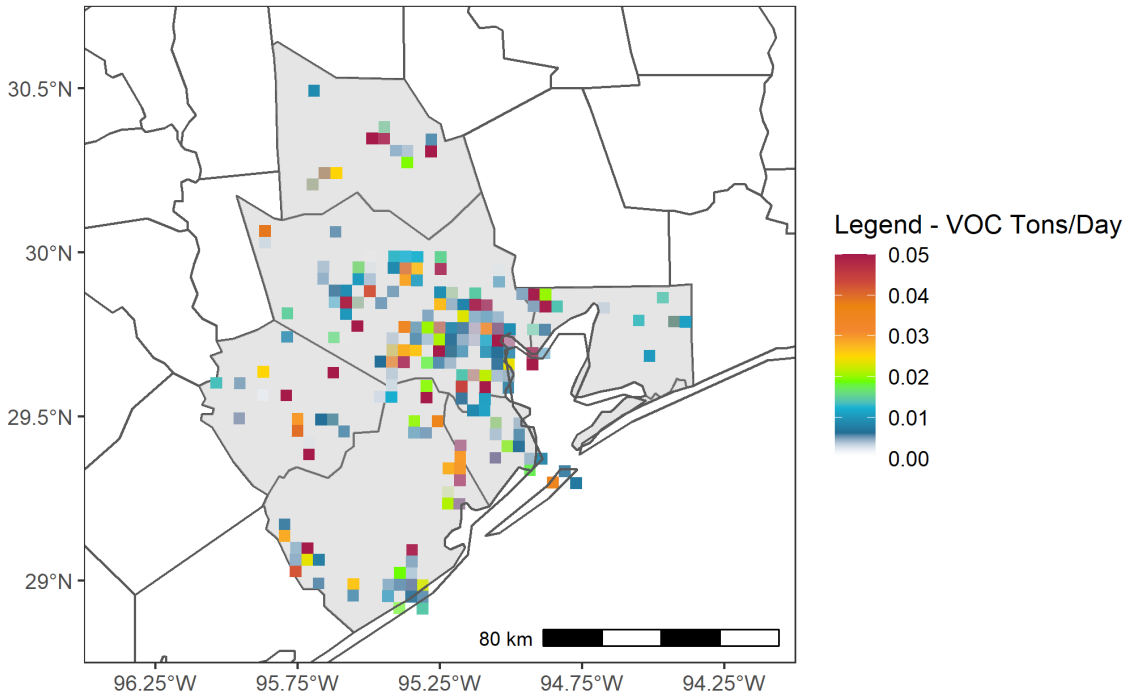

Figure 1-10: 2019 Base Case Non-EGU VOC Emissions for June 12 Episode Day in HGB

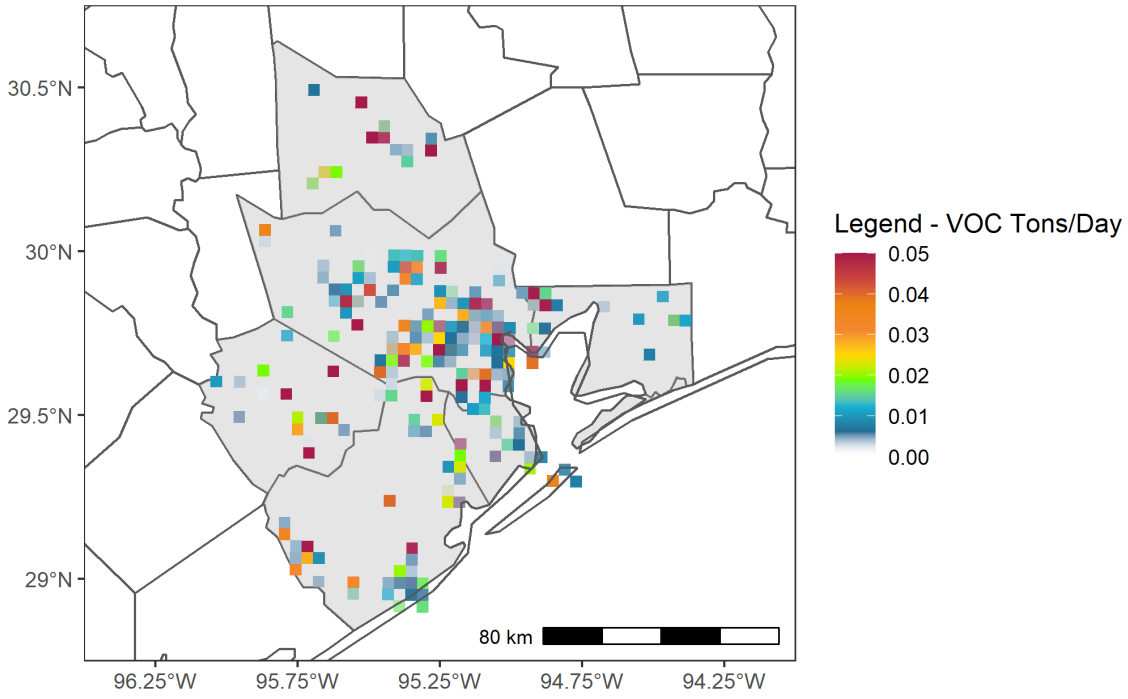

Figure 1-11: 2023 Future Case Non-EGU VOC Emissions for June 12 Episode Day in HGB

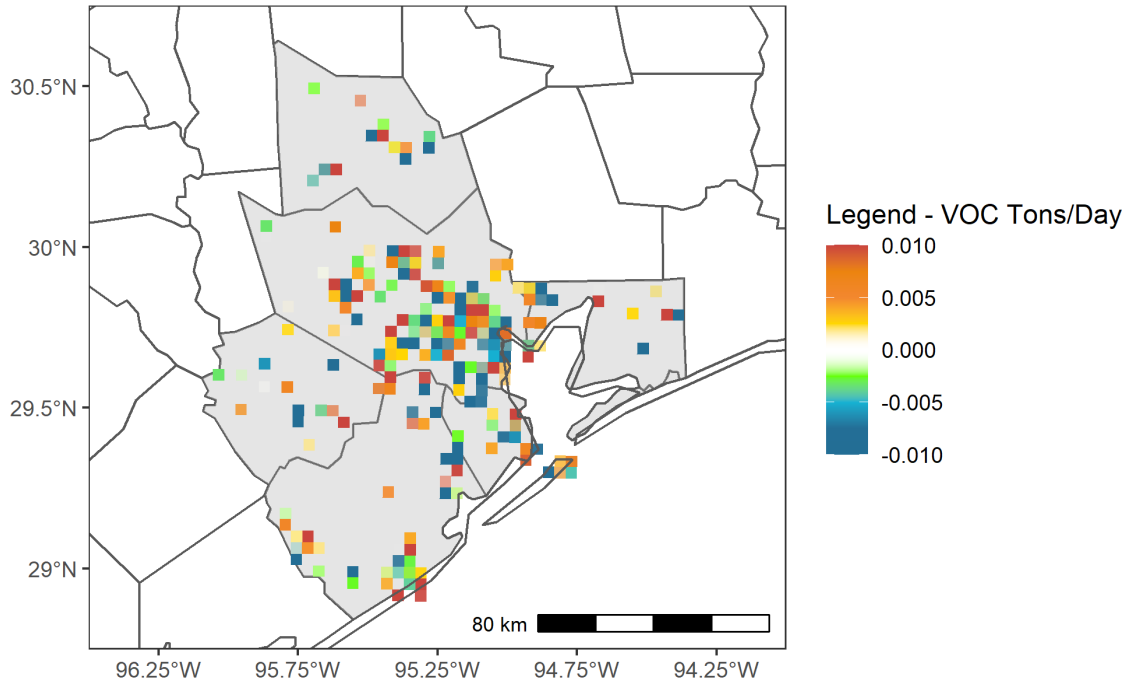

Figure 1-12: Difference in Non-EGU VOC Emissions for the June 12 Episode Day Between 2023 and 2019 in HGB

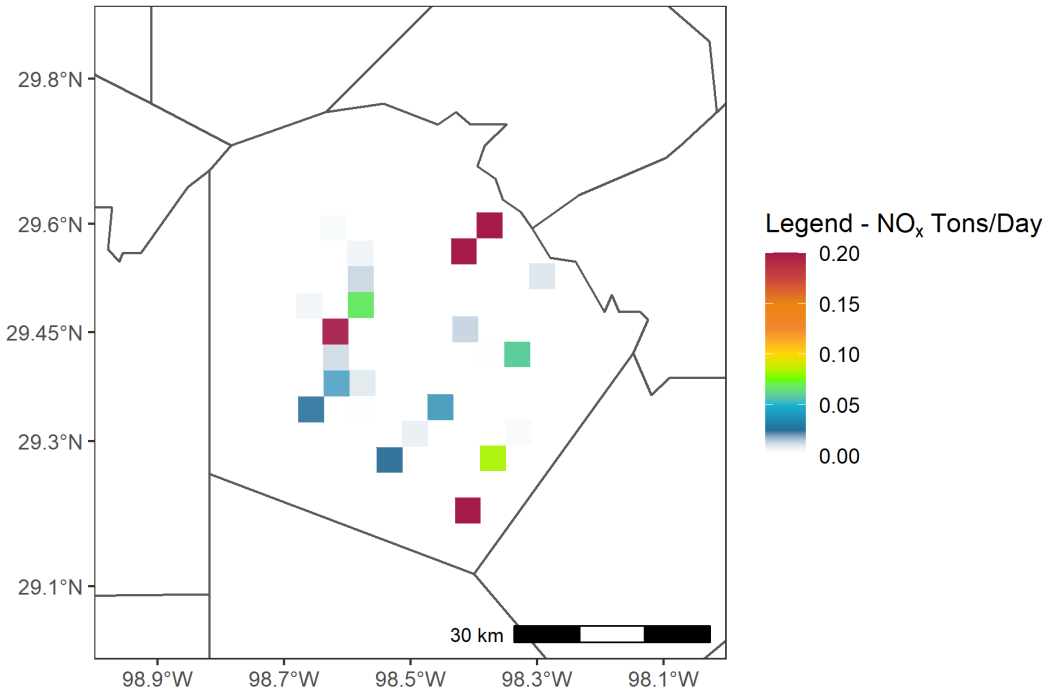

Figure 1-13: 2019 Base Case Non-EGU NO_x Emissions for June 12 Episode Day in Bexar County

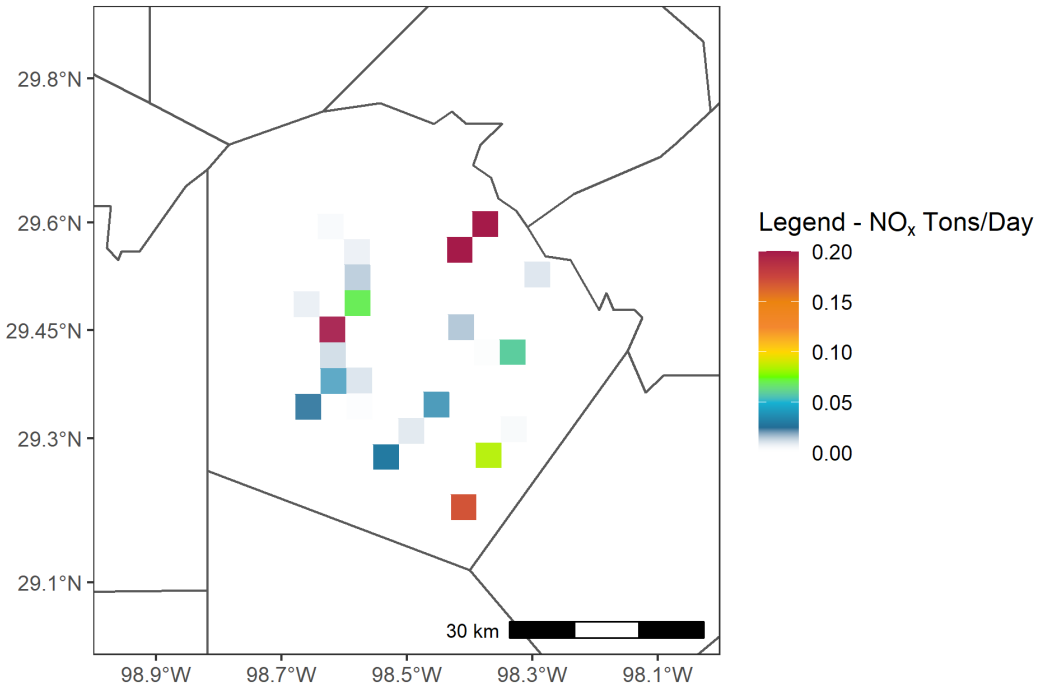

Figure 1-14: 2023 Future Case Non-EGU NO_x Emissions for June 12 Episode Day in Bexar County

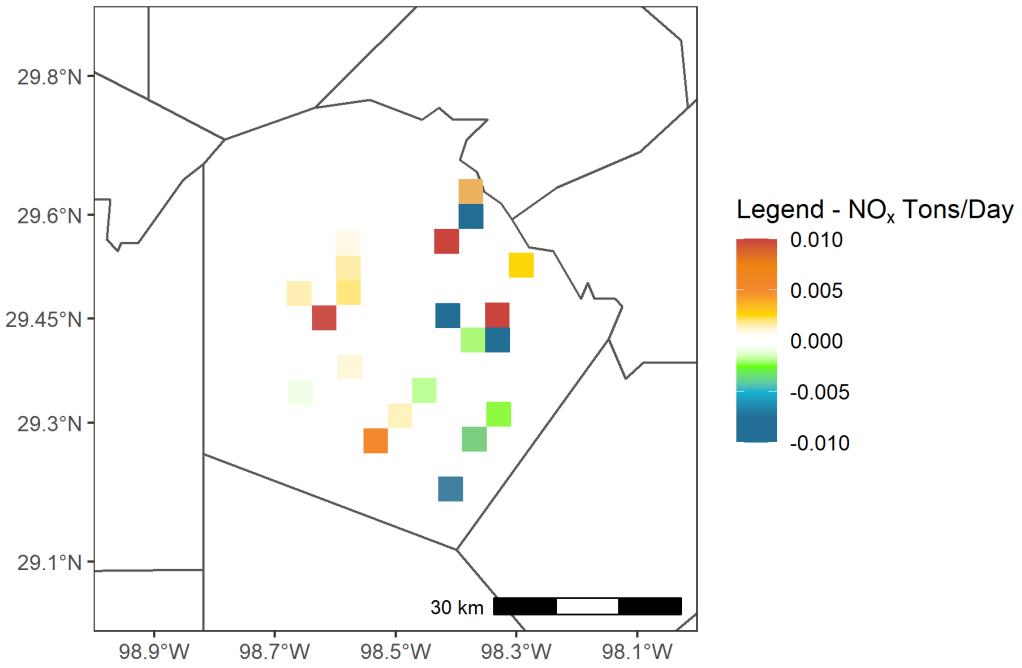

Figure 1-15: Difference in Non-EGU NO_x Emissions for the June 12 Episode Day Between 2023 and 2019 in Bexar County

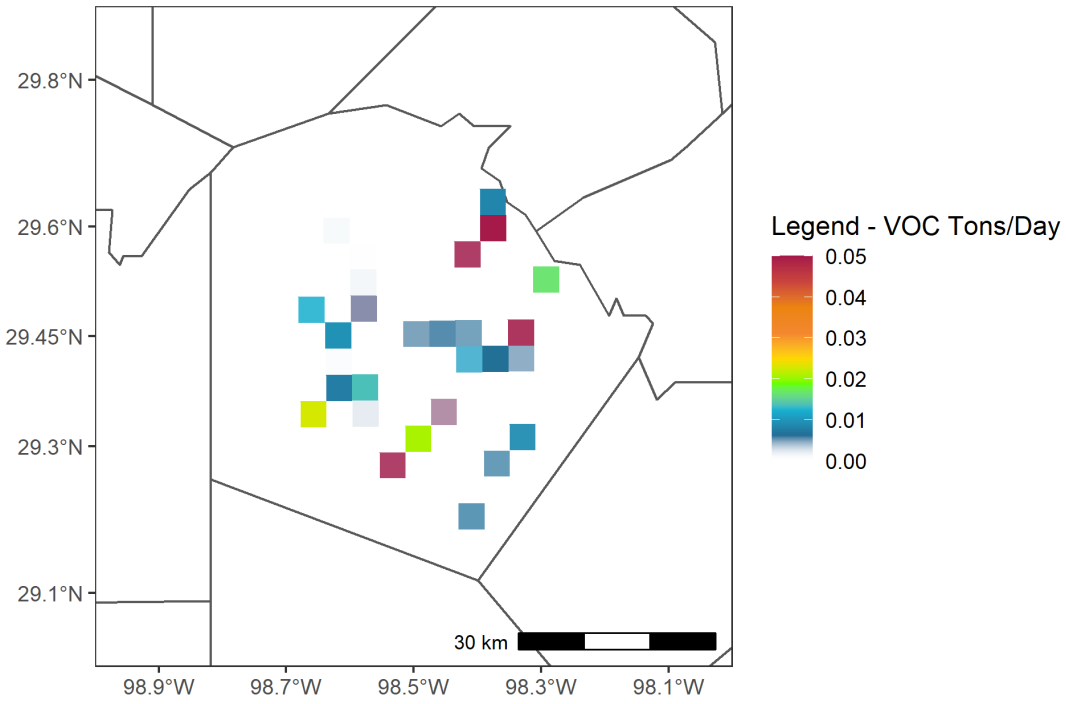

Figure 1-16: 2019 Base Case Non-EGU VOC Emissions for June 12 Episode Day in Bexar County

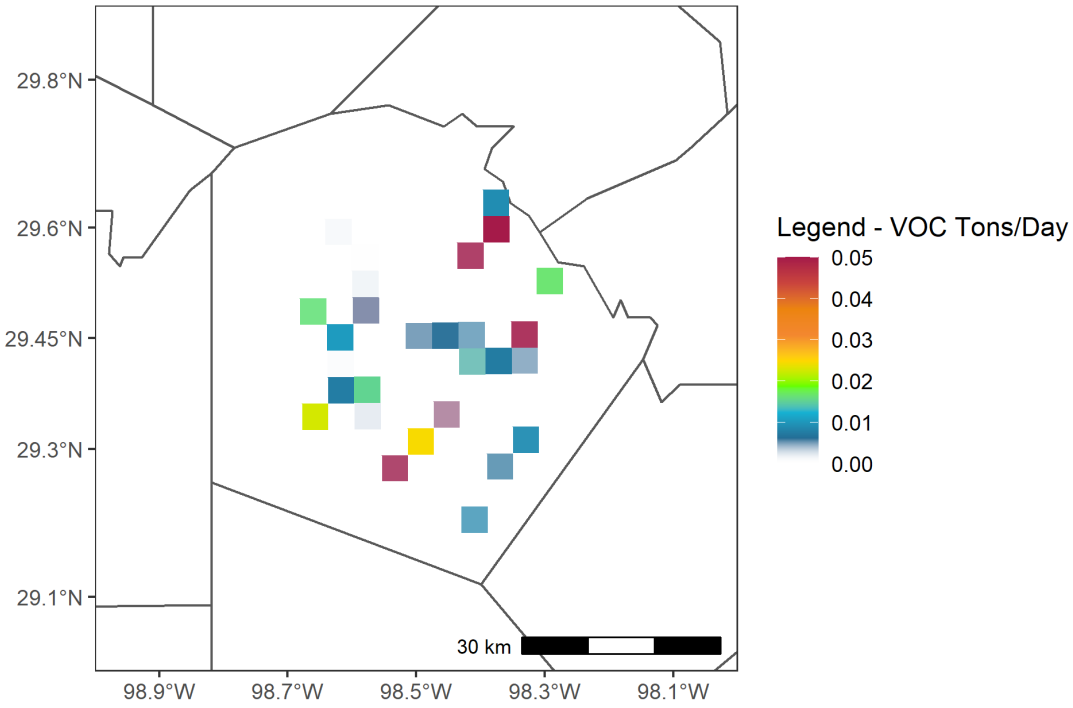

Figure 1-17: 2023 Future Case Non-EGU VOC Emissions for June 12 Episode Day in Bexar County

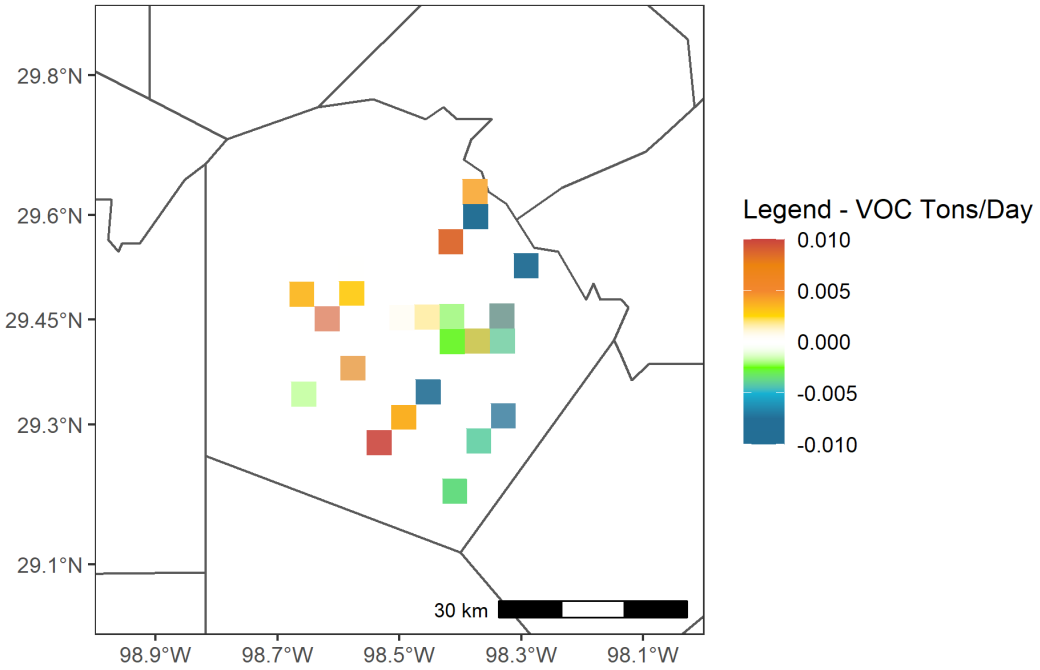

Figure 1-18: Difference in Non-EGU VOC Emissions for the June 12 Episode Day Between 2023 and 2019 in Bexar County

1.2 ON-ROAD MOBILE SOURCES

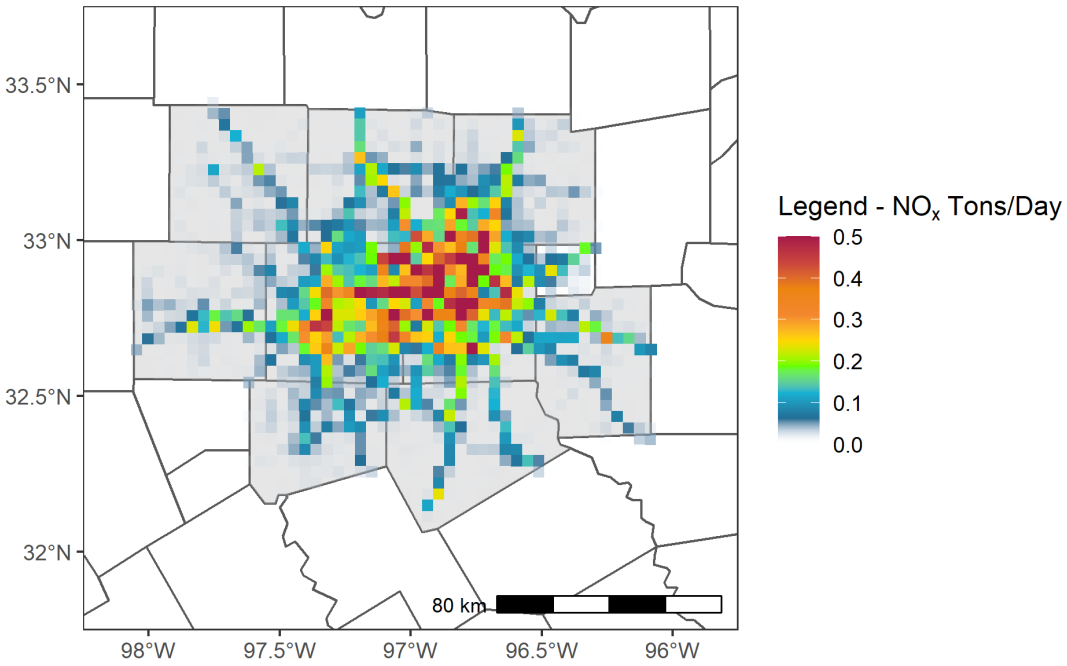

Figure 1-19: 2019 Base Case On-Road NO_x Emissions for June 12 Episode Day in DFW

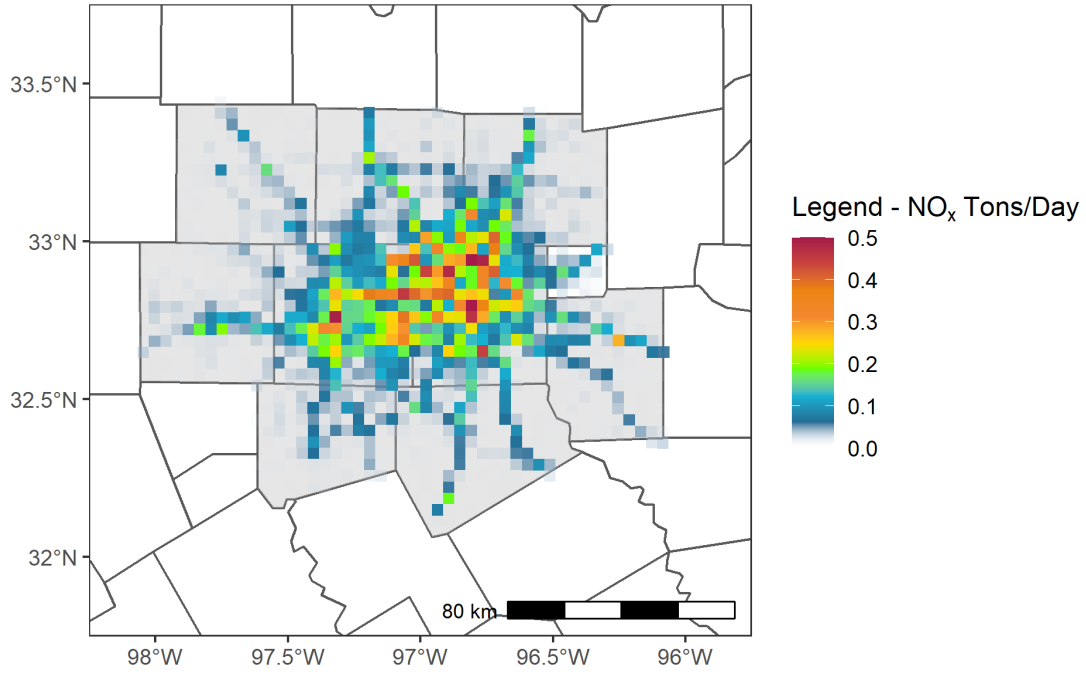

Figure 1-20: 2023 Future Case On-Road NO_x Emissions for June 12 Episode Day in DFW

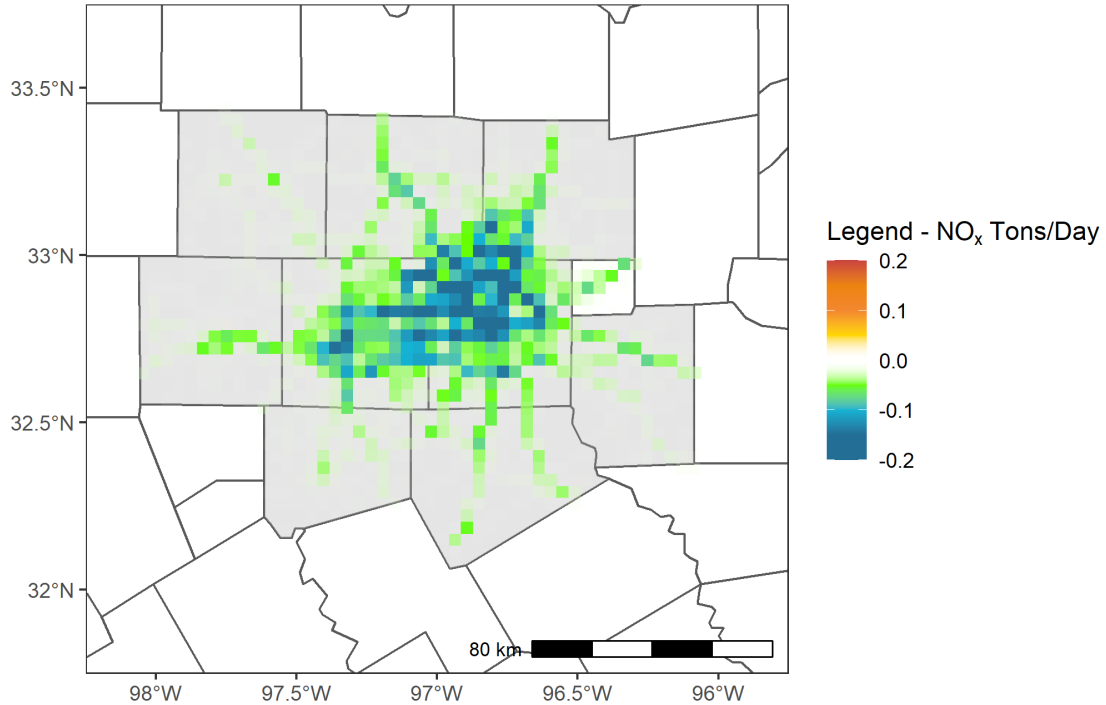

Figure 1-21: Difference in On-Road NO_x Emissions for the June 12 Episode Day Between 2023 and 2019 in DFW

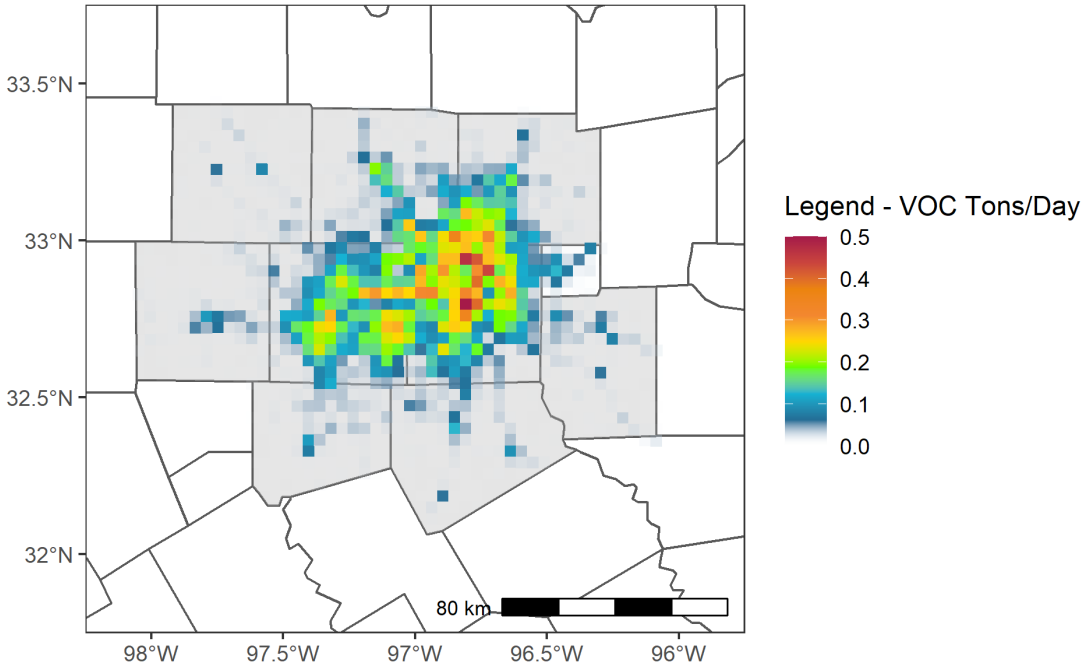

Figure 1-22: 2019 Base Case On-Road VOC Emissions for June 12 Episode Day in DFW

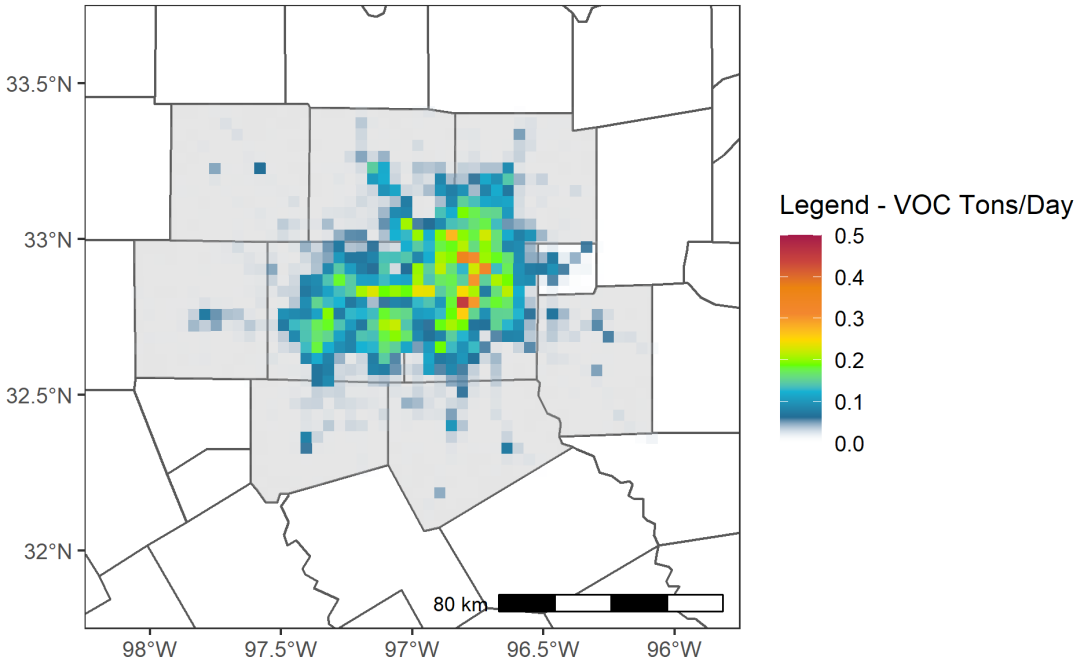

Figure 1-23: 2023 Future Case On-Road VOC Emissions for June 12 Episode Day in DFW

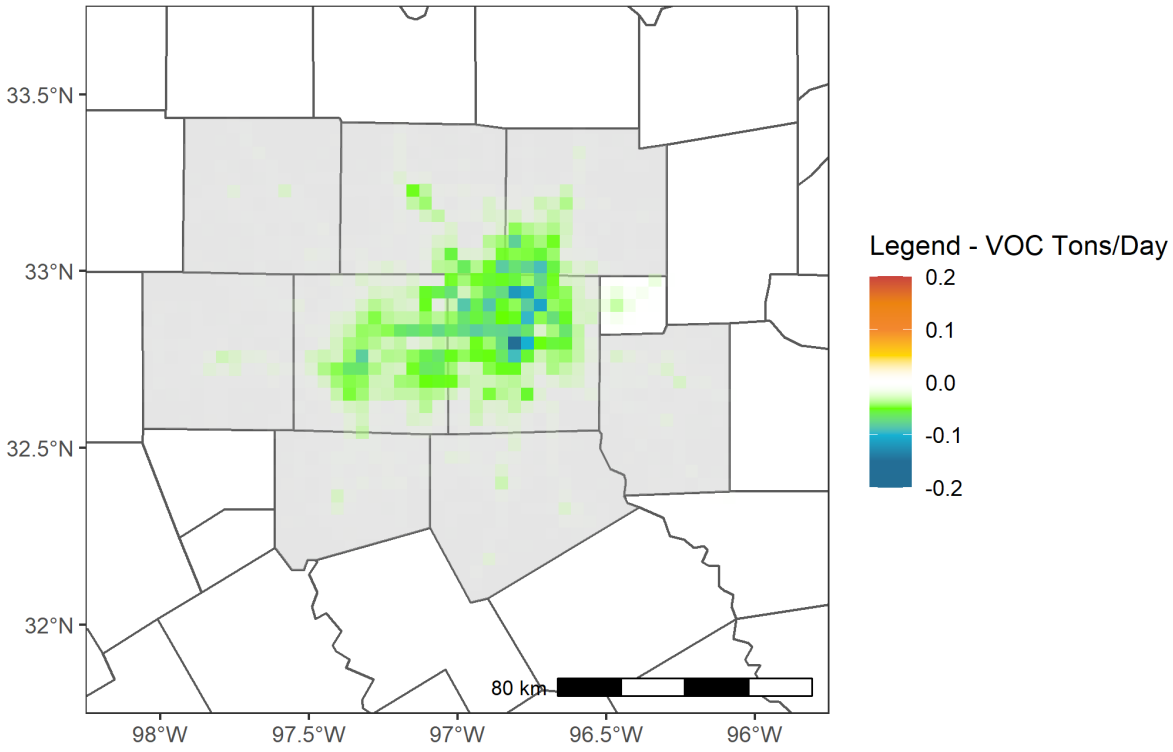

Figure 1-24: Difference in On-Road VOC Emissions for the June 12 Episode Day Between 2023 and 2019 in DFW

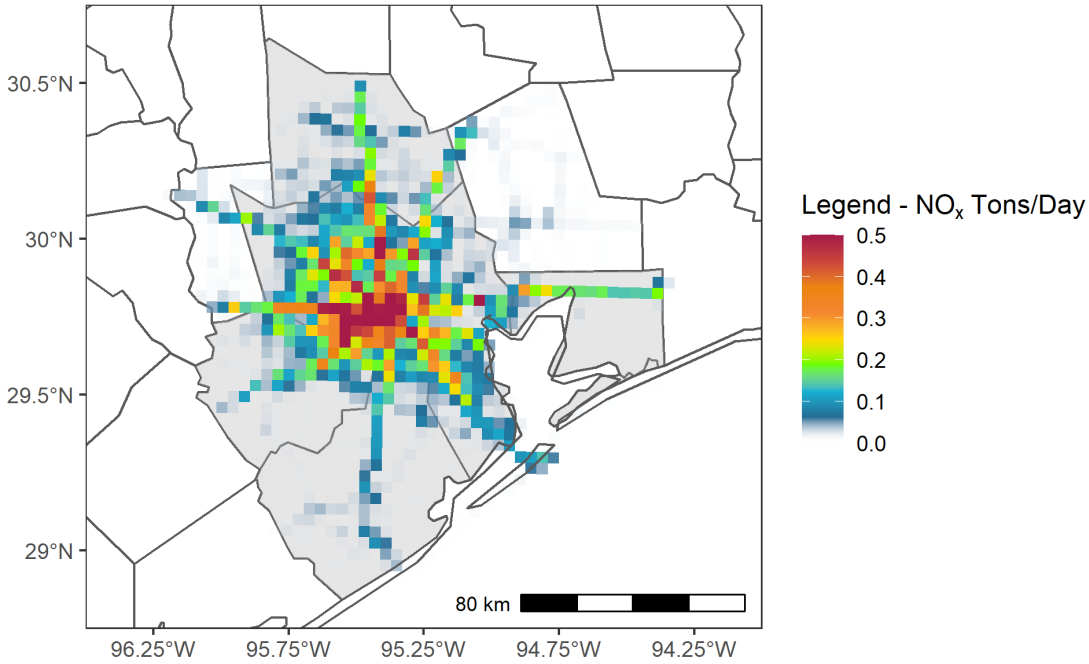

Figure 1-25: 2019 Base Case On-Road NO_x Emissions for June 12 Episode Day in HGB

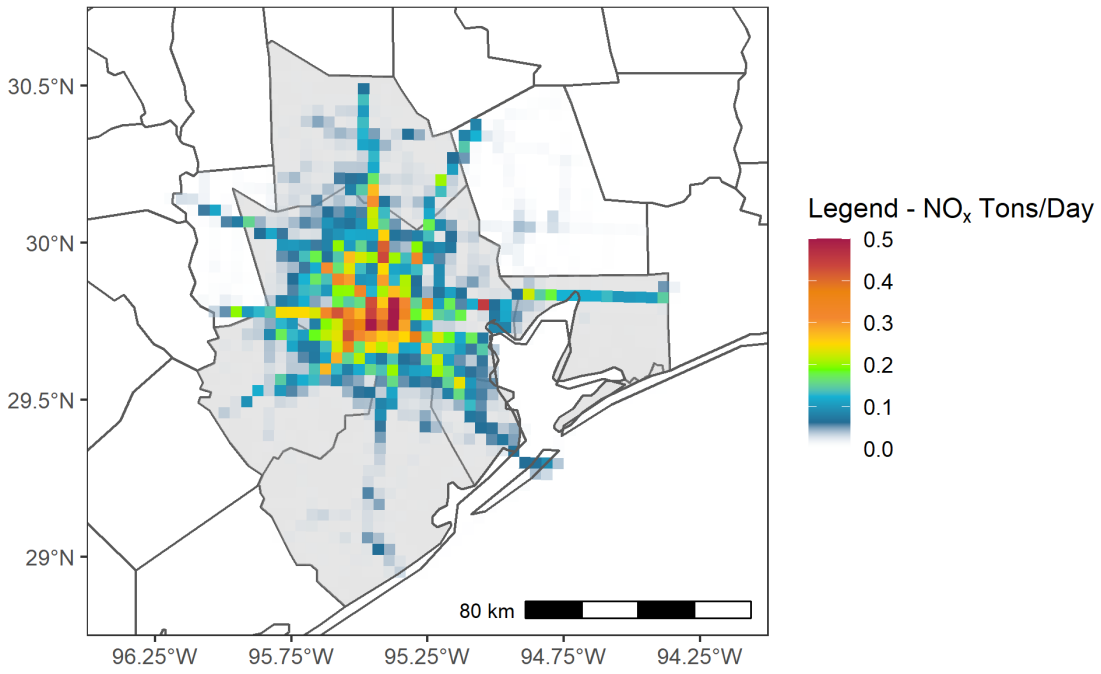

Figure 1-26: 2023 Future Case On-Road NO_x Emissions for June 12 Episode Day in HGB

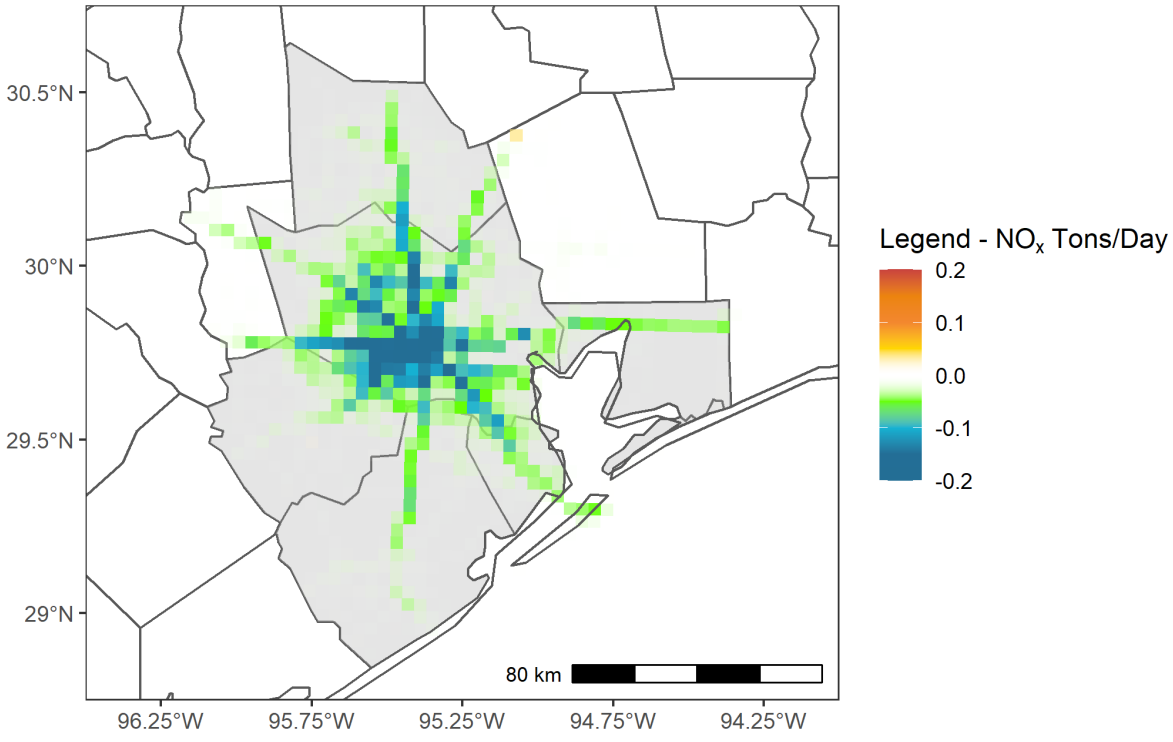

Figure 1-27: Difference in On-Road NO_x Emissions for the June 12 Episode Day Between 2023 and 2019 in HGB

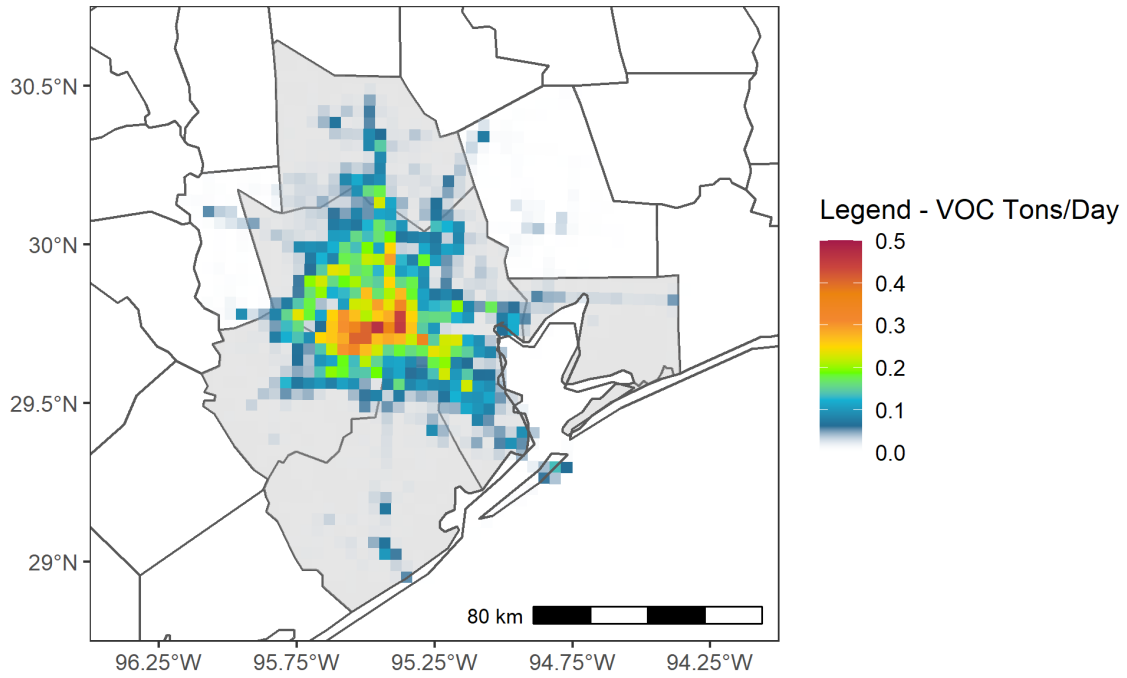

Figure 1-28: 2019 Base Case On-Road VOC Emissions for June 12 Episode Day in HGB

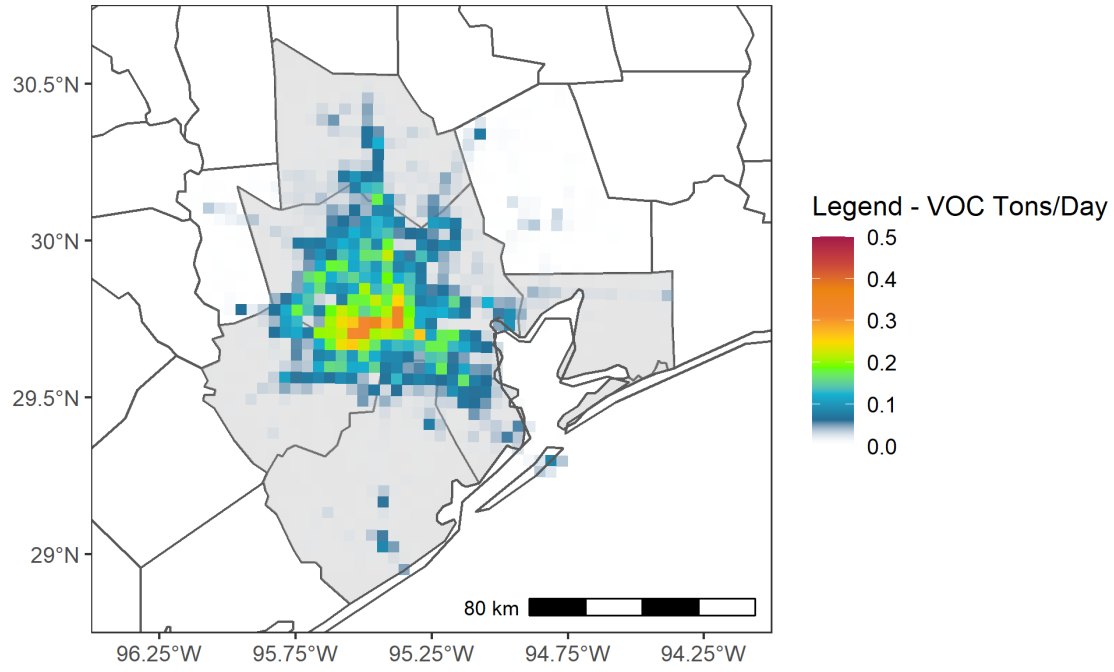

Figure 1-29: 2023 Future Case On-Road VOC Emissions for June 12 Episode Day in HGB

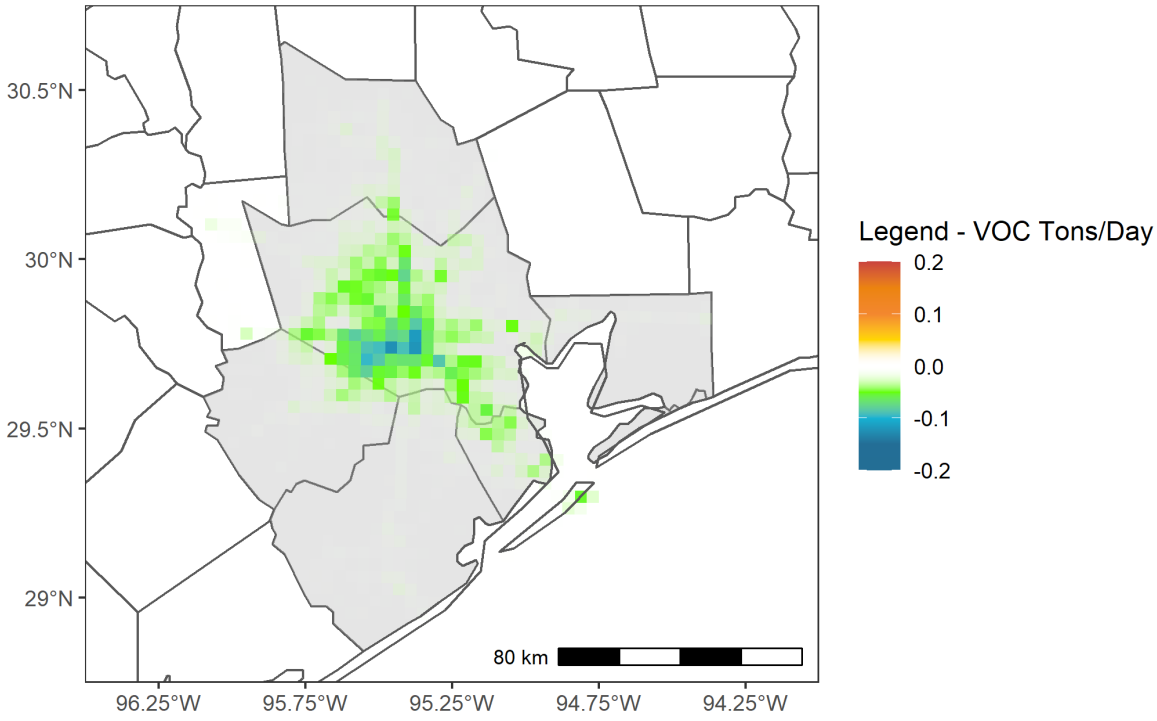

Figure 1-30: Difference in On-Road VOC Emissions for the June 12 Episode Day Between 2023 and 2019 in HGB

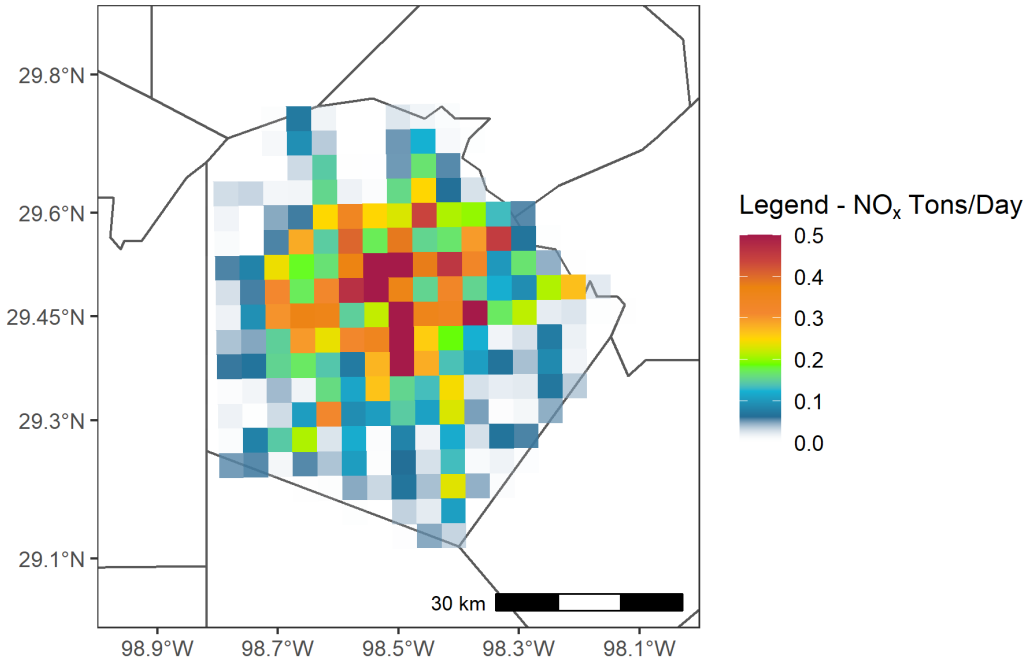

Figure 1-31: 2019 Base Case On-Road NO_x Emissions for June 12 Episode Day in Bexar County

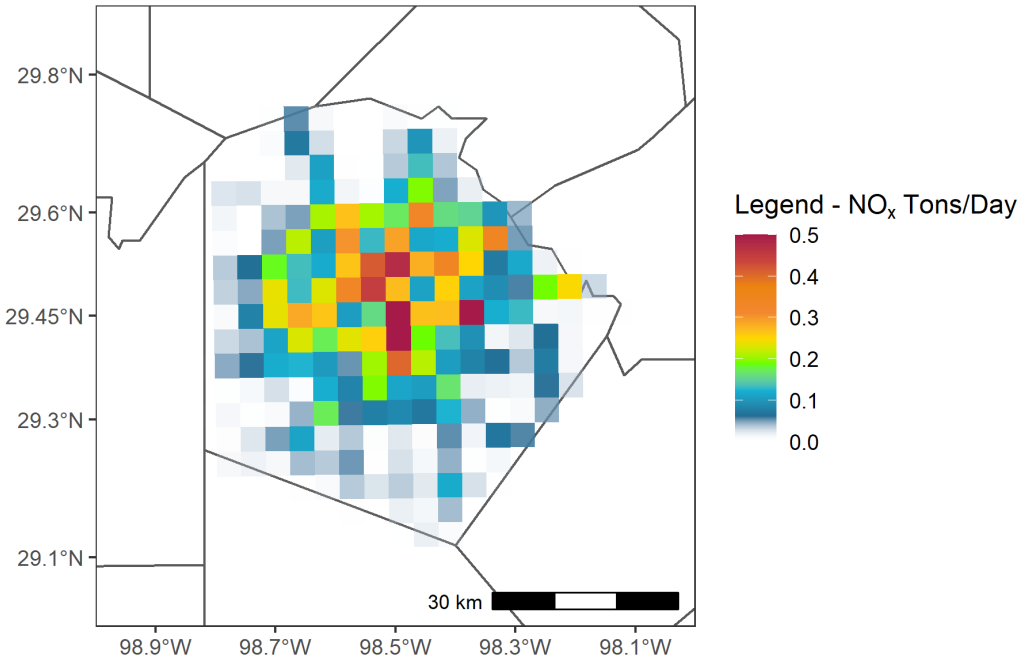

Figure 1-32: 2023 Future Case On-Road NO_x Emissions for June 12 Episode Day in Bexar County

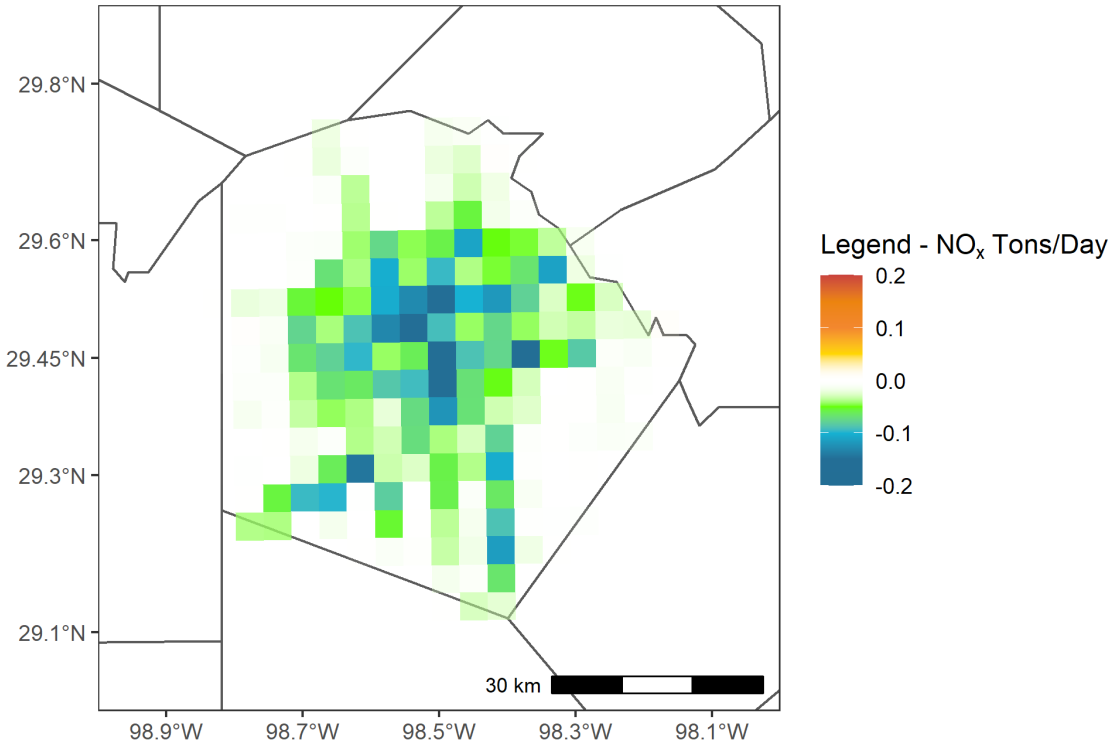

Figure 1-33. Difference in On-Road NO_x Emissions for the June 12 Episode Day Between 2023 and 2019 in Bexar County

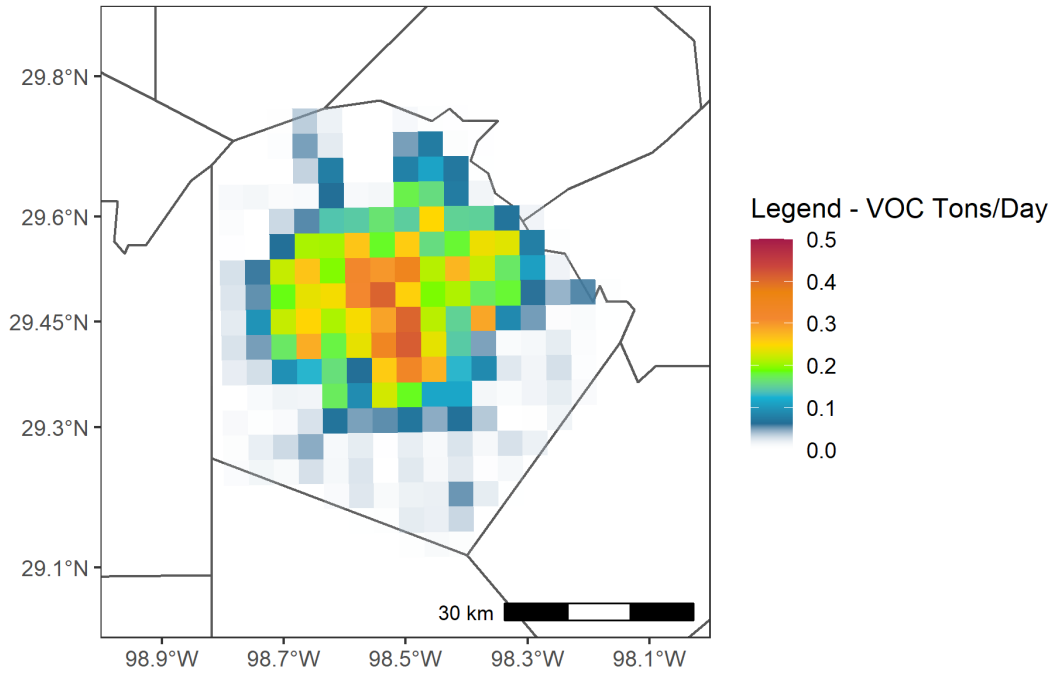

Figure 1-34: 2019 Base Case On-Road VOC Emissions for June 12 Episode Day in Bexar County

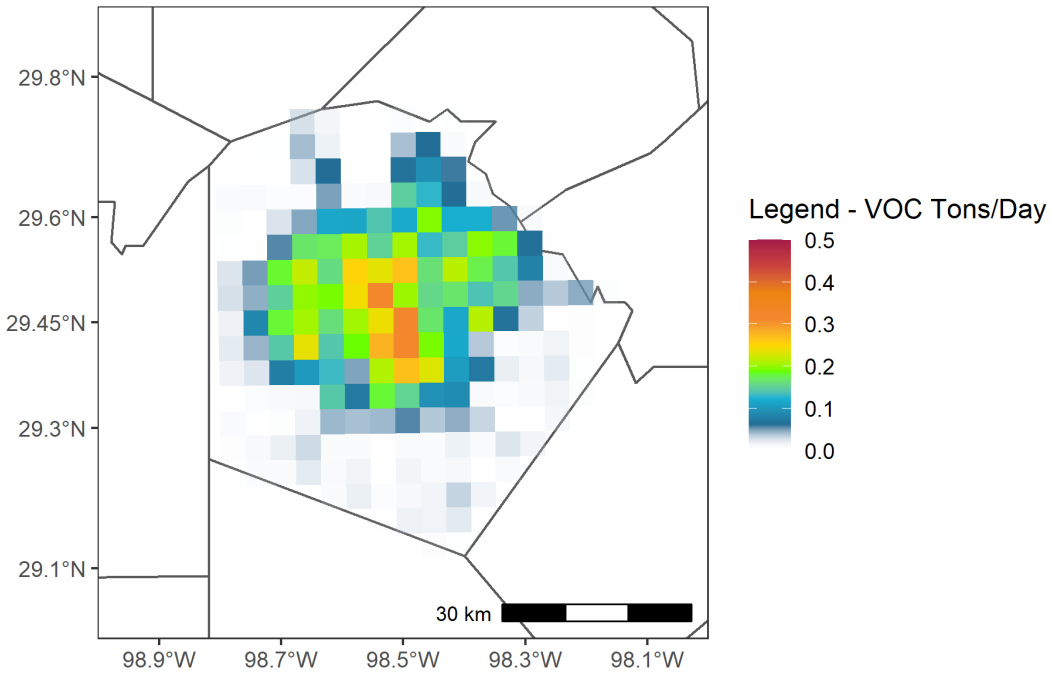

Figure 1-35: 2023 Future Case On-Road VOC Emissions for June 12 Episode Day in Bexar County

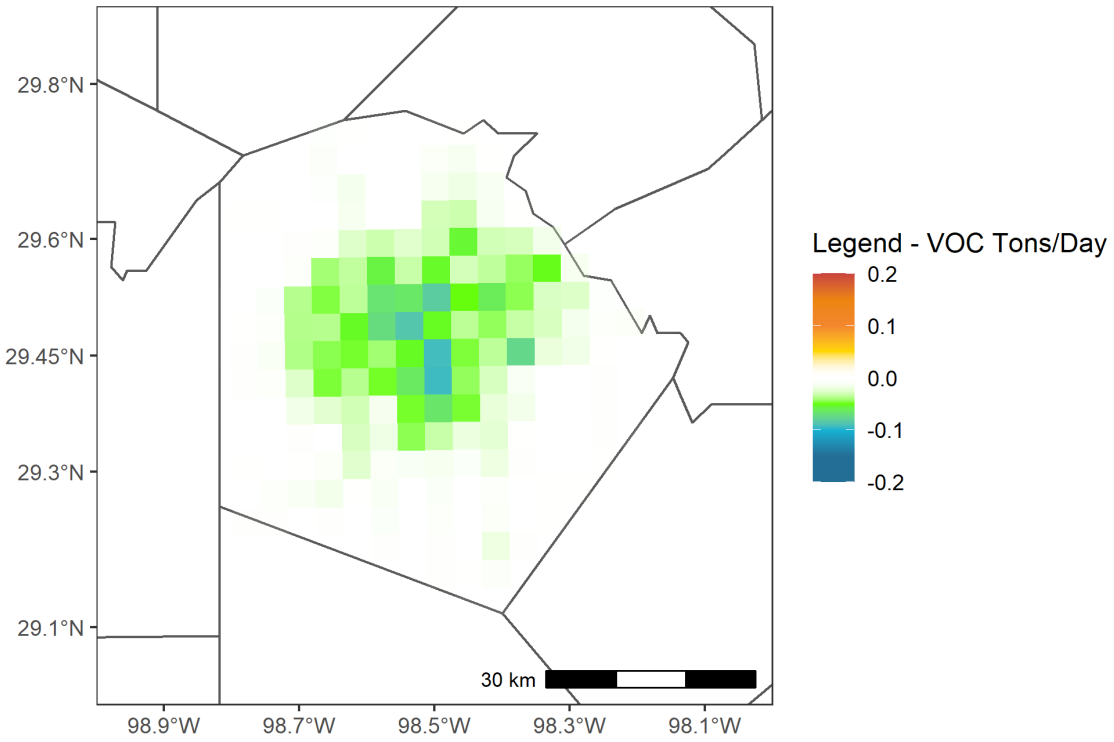

Figure 1-36: Difference in On-Road VOC Emissions for the June 12 Episode Day Between 2023 and 2019 in Bexar County

1.3 NON-ROAD SOURCES

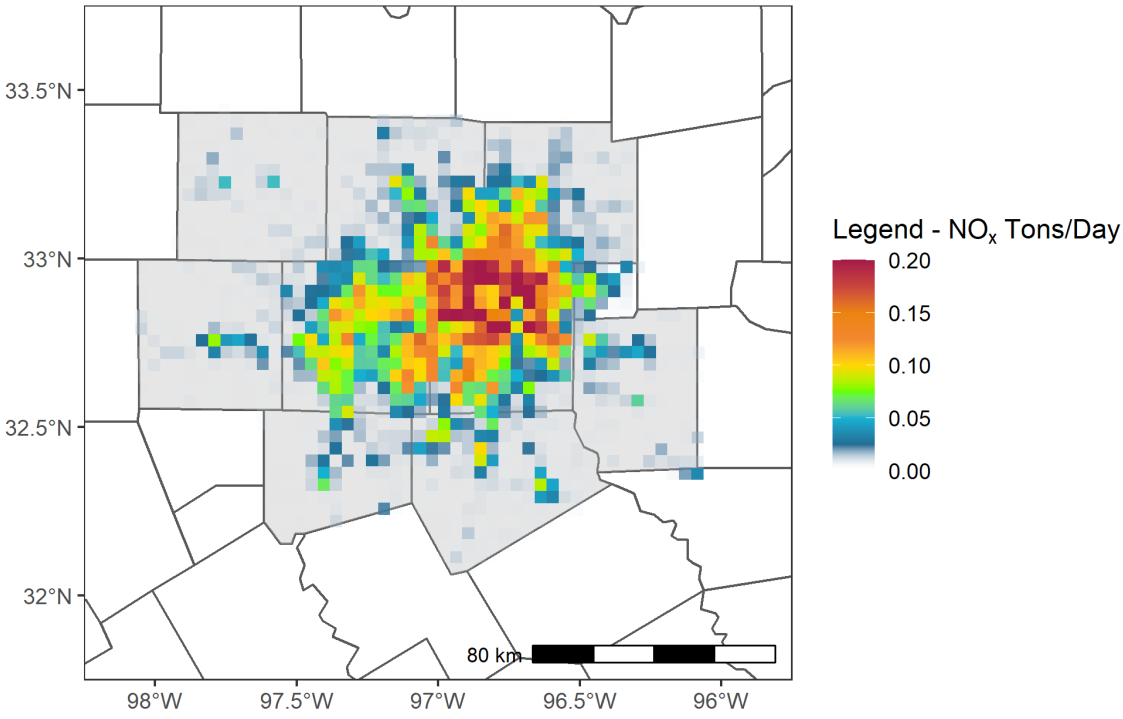

Figure 1-37: 2019 Base Case Non-Road NO_x Emissions for June 12 Episode Day in DFW

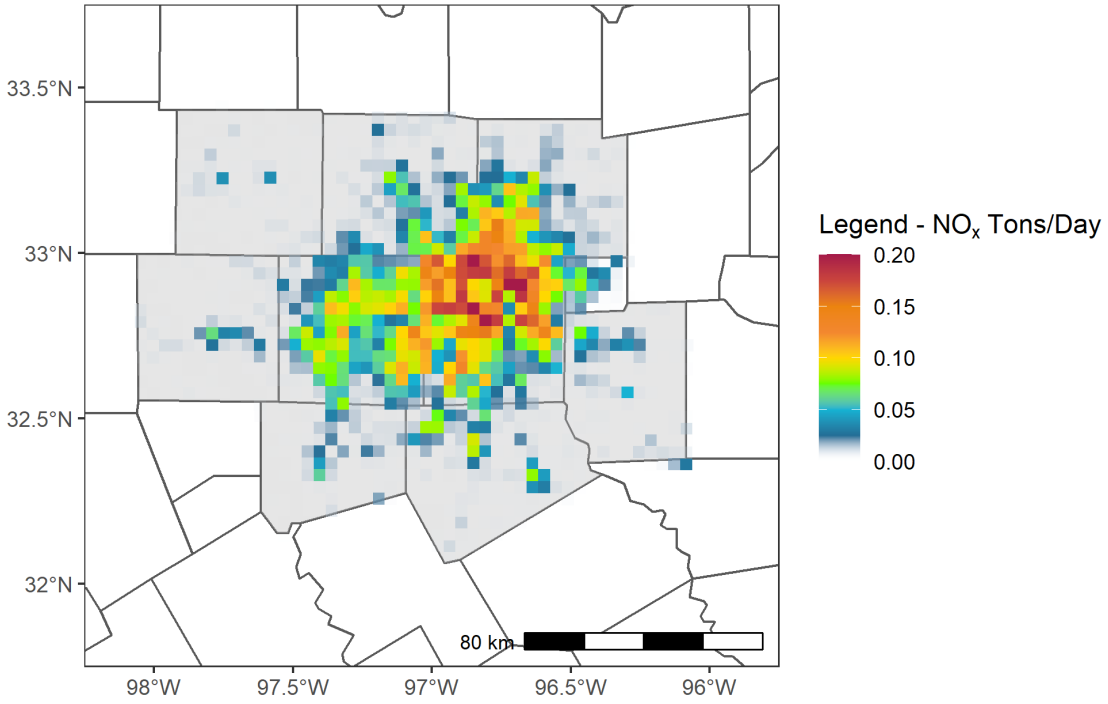

Figure 1-38: 2023 Future Case Non-Road NO_x Emissions for June 12 Episode Day in DFW

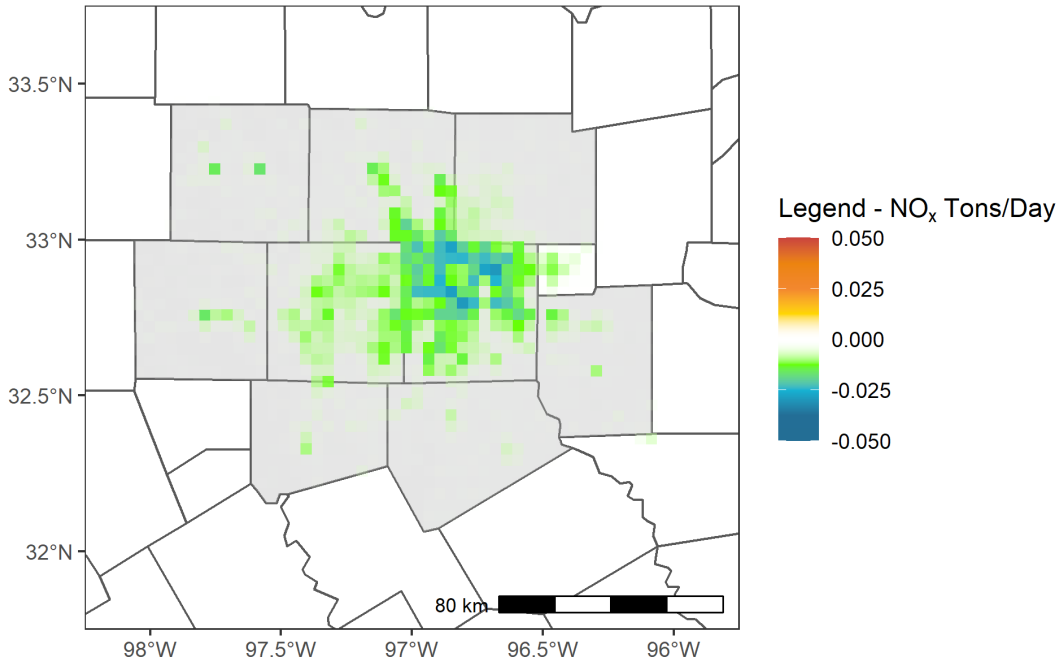

Figure 1-39: Difference in Non-Road NO_x Emissions for the June 12 Episode Day Between 2023 and 2019 in DFW

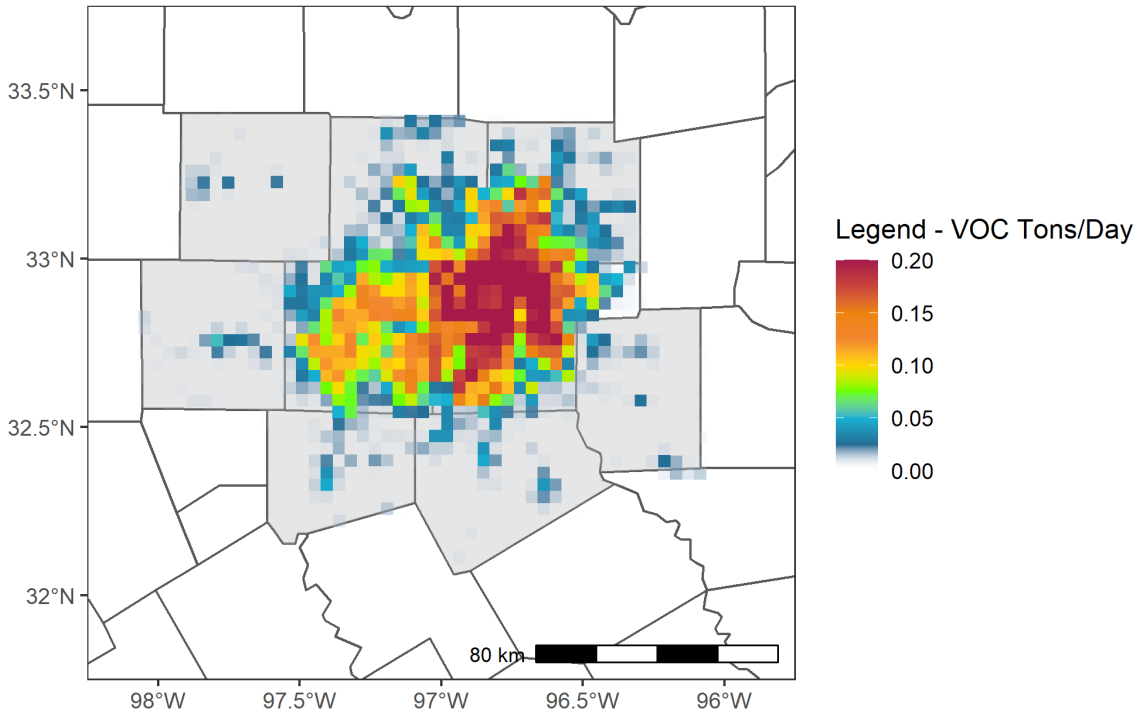

Figure 1-40: 2019 Base Case Non-Road VOC Emissions for June 12 Episode Day in DFW

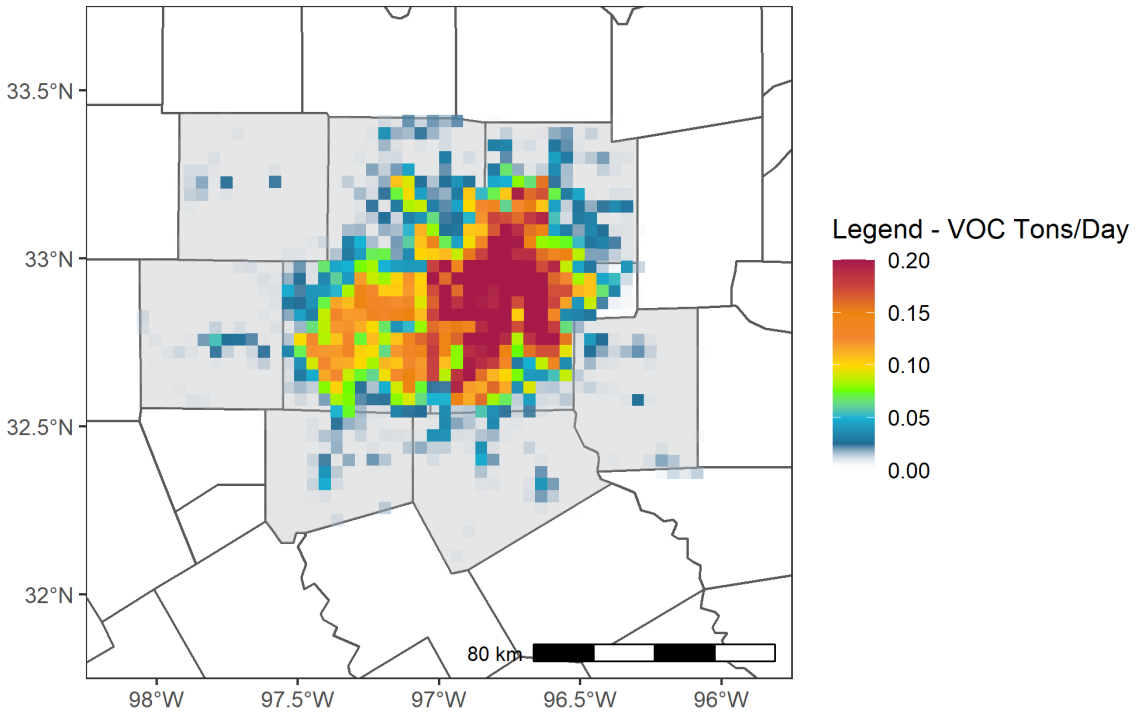

Figure 1-41: 2023 Future Case Non-Road VOC Emissions for June 12 Episode Day in DFW

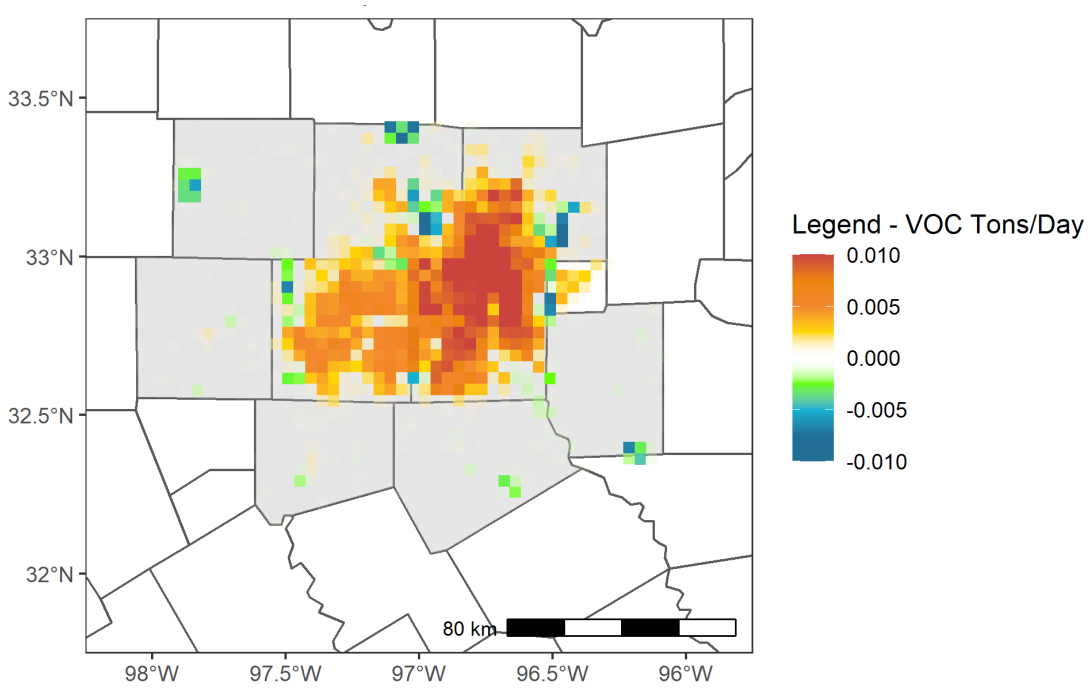

Figure 1-42: Difference in Non-Road VOC Emissions for the June 12 Episode Day Between 2023 and 2019 in DFW

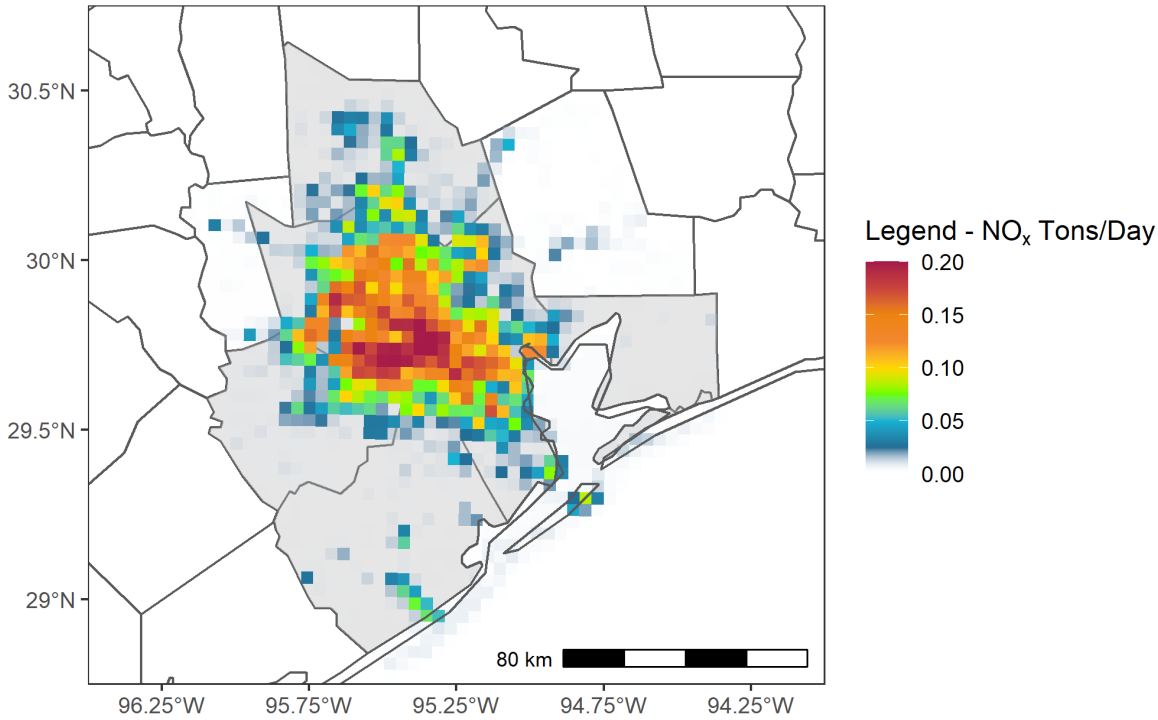

Figure 1-43: 2019 Base Case Non-Road NO_x Emissions for June 12 Episode Day in HGB

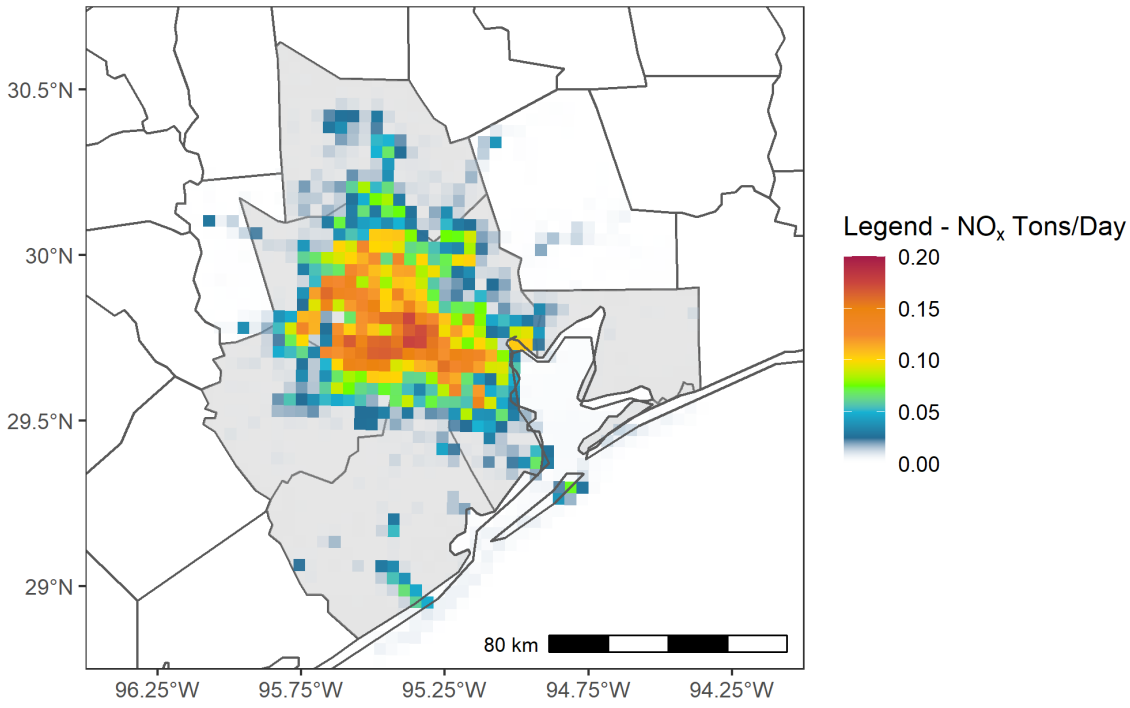

Figure 1-44: 2023 Future Case Non-Road NO_x Emissions for June 12 Episode Day in HGB

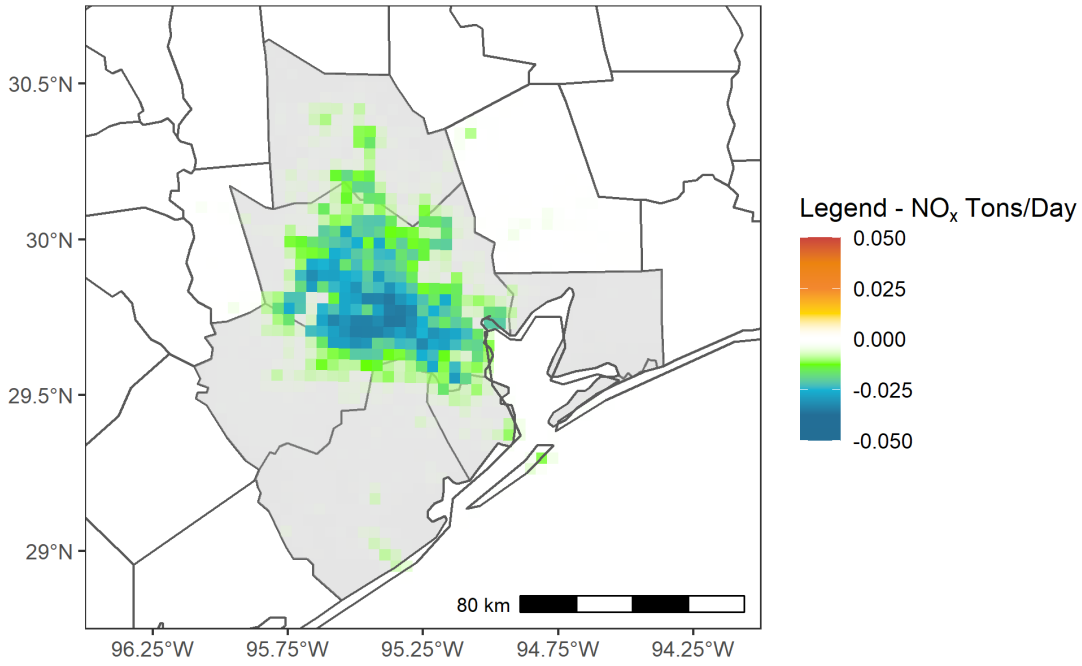

Figure 1-45: Difference in Non-Road NO_x Emissions for the June 12 Episode Day Between 2023 and 2019 in HGB

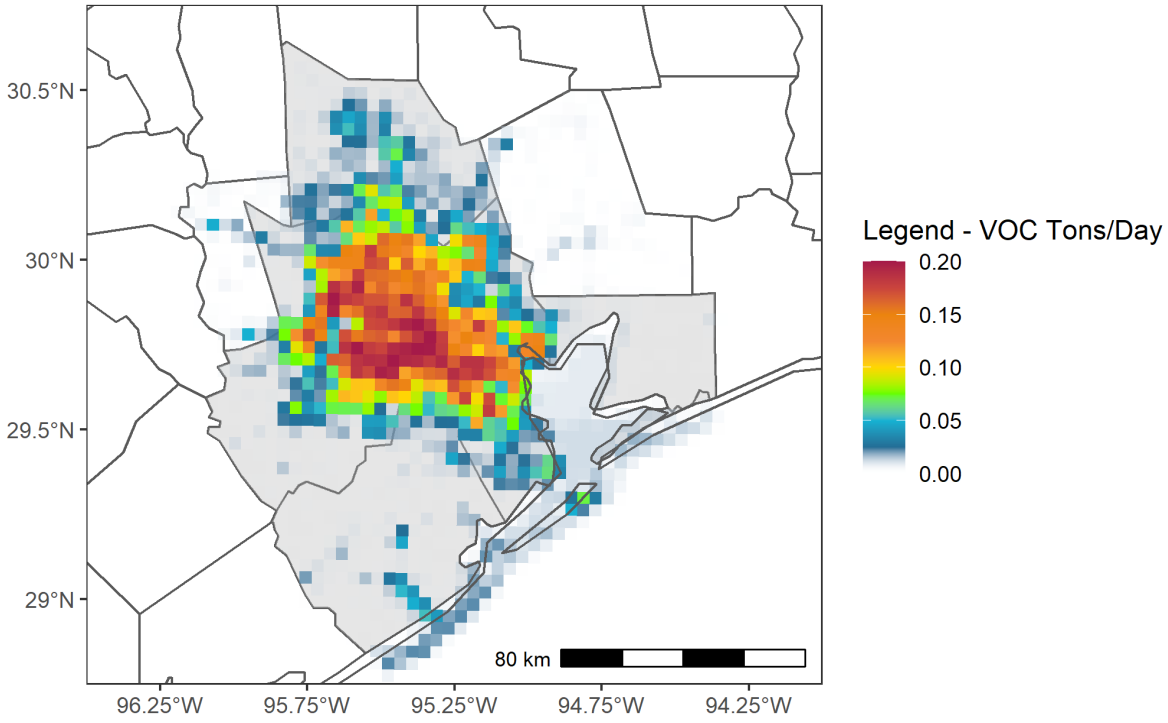

Figure 1-46: 2019 Base Case Non-Road VOC Emissions for June 12 Episode Day in HGB

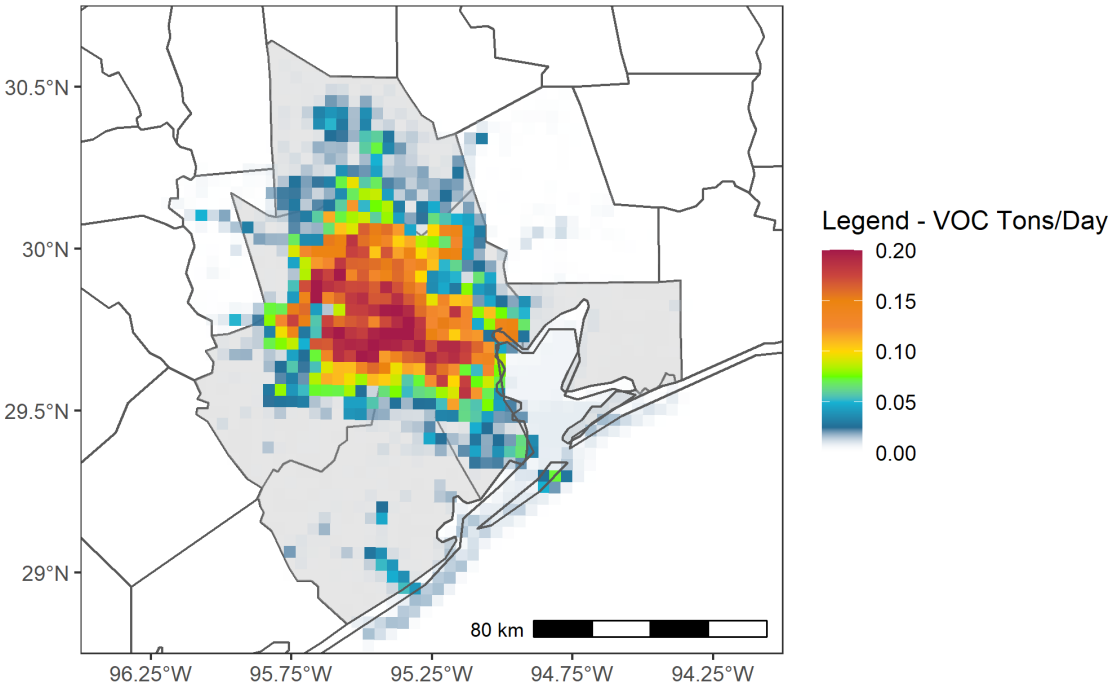

Figure 1-47: 2023 Future Case Non-Road VOC Emissions for June 12 Episode Day in HGB

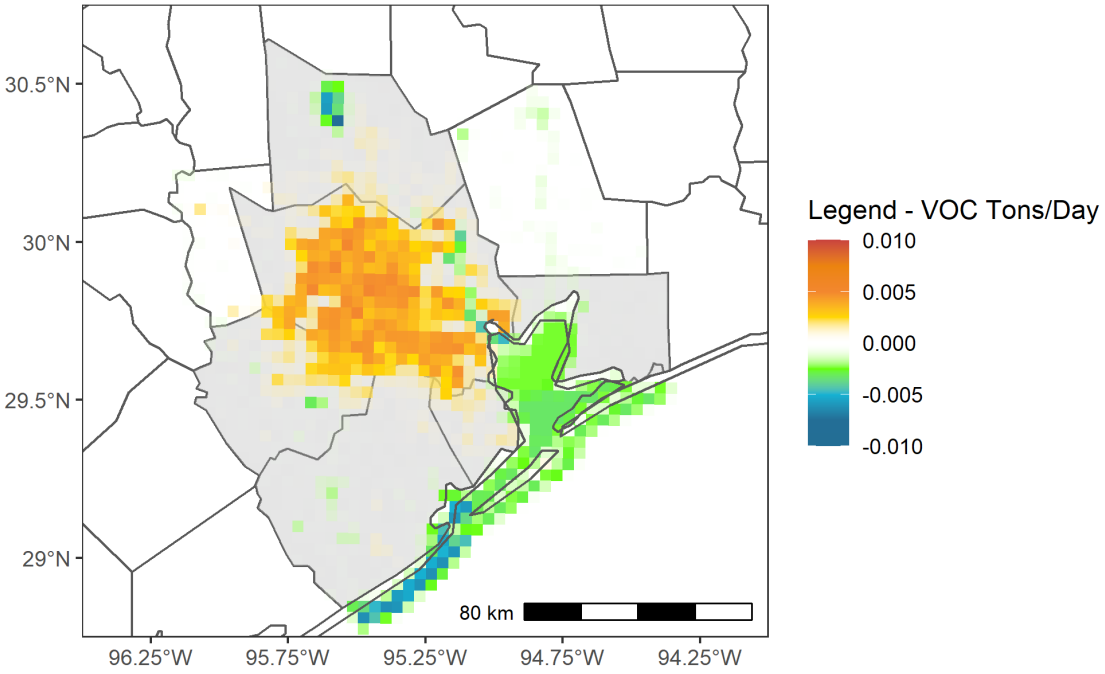

Figure 1-48: Difference in Non-Road VOC Emissions for the June 12 Episode Day Between 2023 and 2019 in HGB

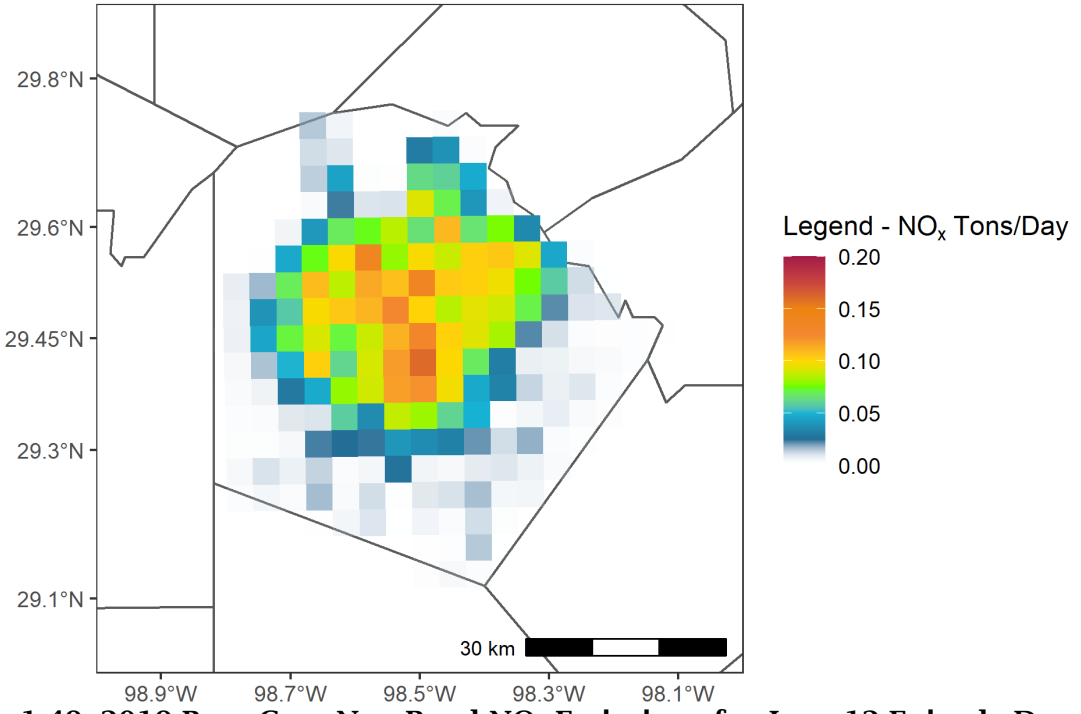

Figure 1-49: 2019 Base Case Non-Road NO_x Emissions for June 12 Episode Day in Bexar County

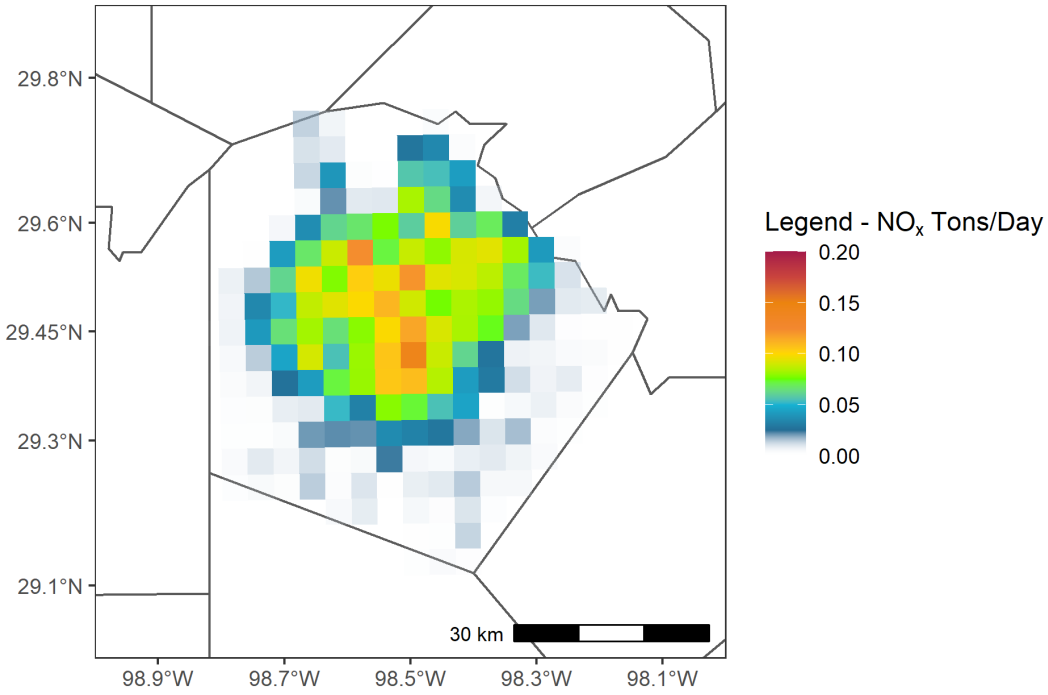

Figure 1-50: 2023 Future Case Non-Road NO_x Emissions for June 12 Episode Day in Bexar County

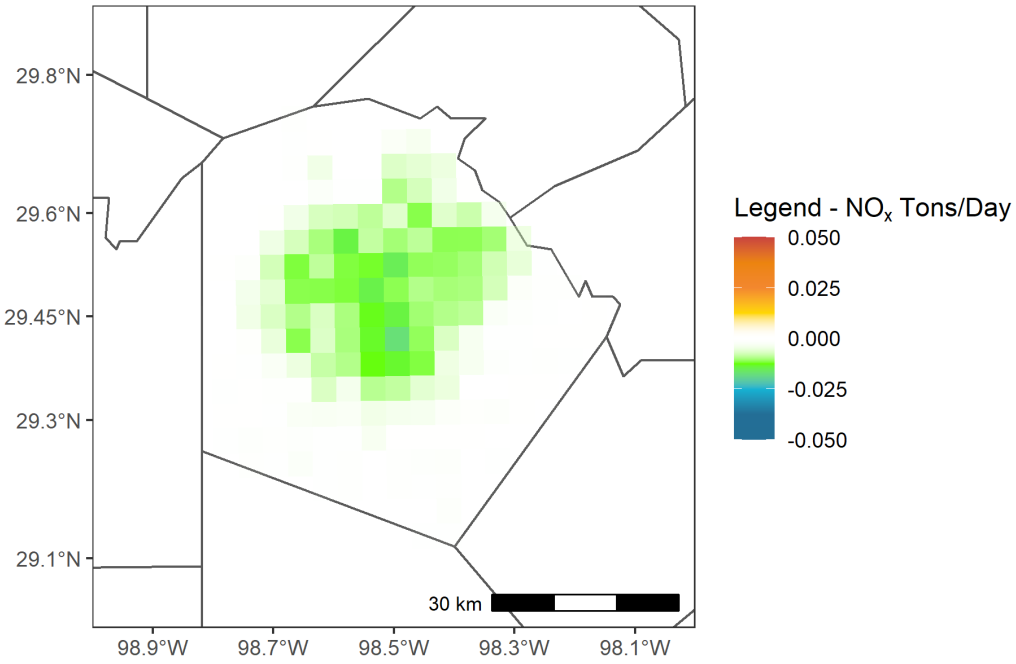

Figure 1-51: Difference in Non-Road NO_x Emissions for the June 12 Episode Day Between 2023 and 2019 in Bexar County

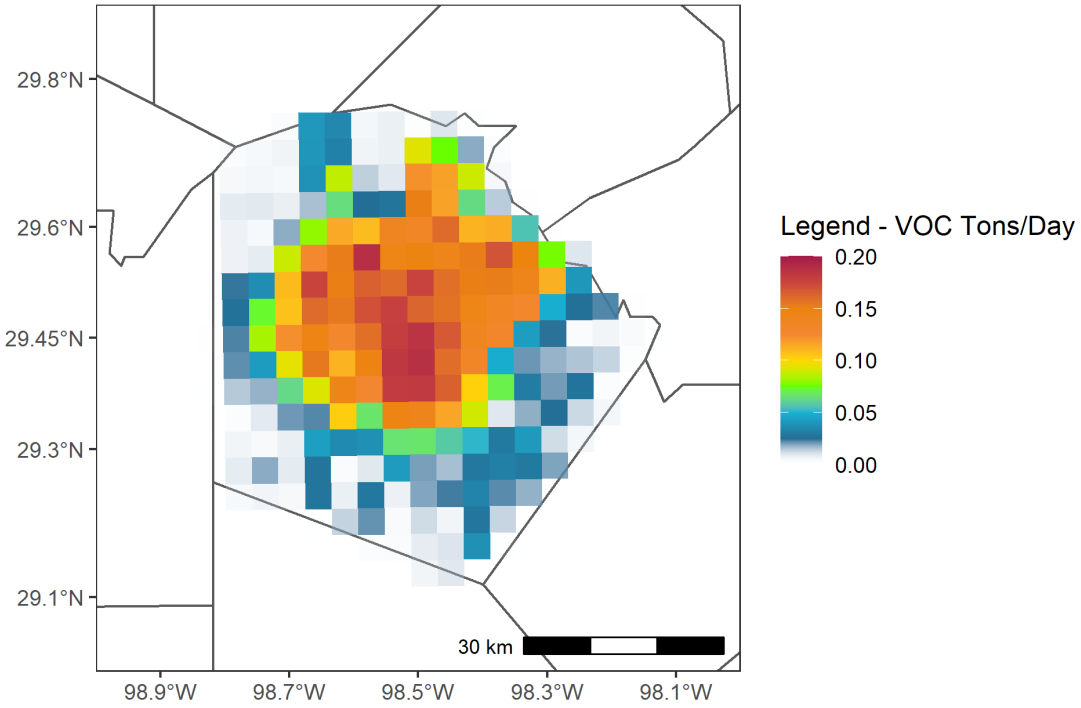

Figure 1-52: 2019 Base Case Non-Road VOC Emissions for June 12 Episode Day in Bexar County

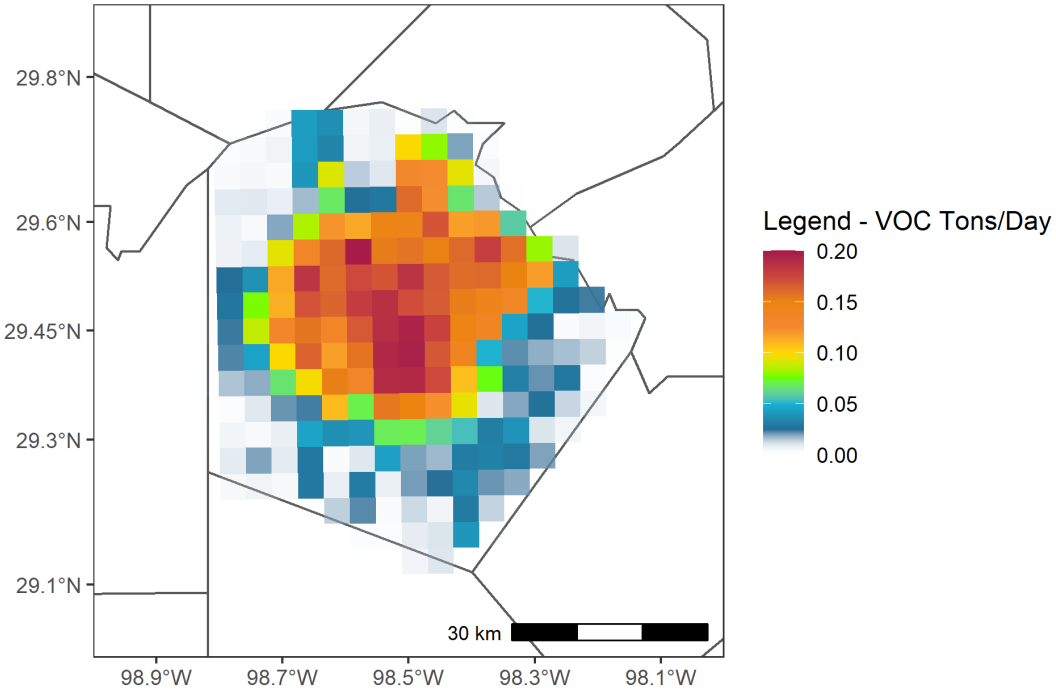

Figure 1-53: 2023 Future Case Non-Road VOC Emissions for June 12 Episode Day in Bexar County

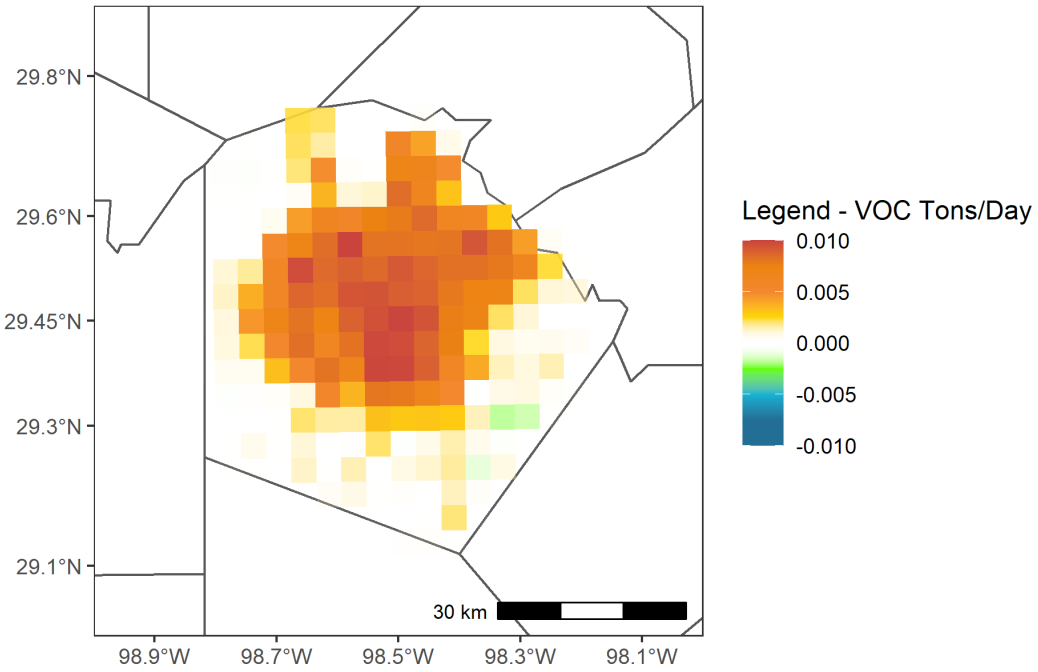

Figure 1-54: Difference in Non-Road VOC Emissions for the June 12 Episode Day Between 2023 and 2019 in Bexar County

1.4 OFF-ROAD SOURCES

Commercial Marine Vessels (CMV)

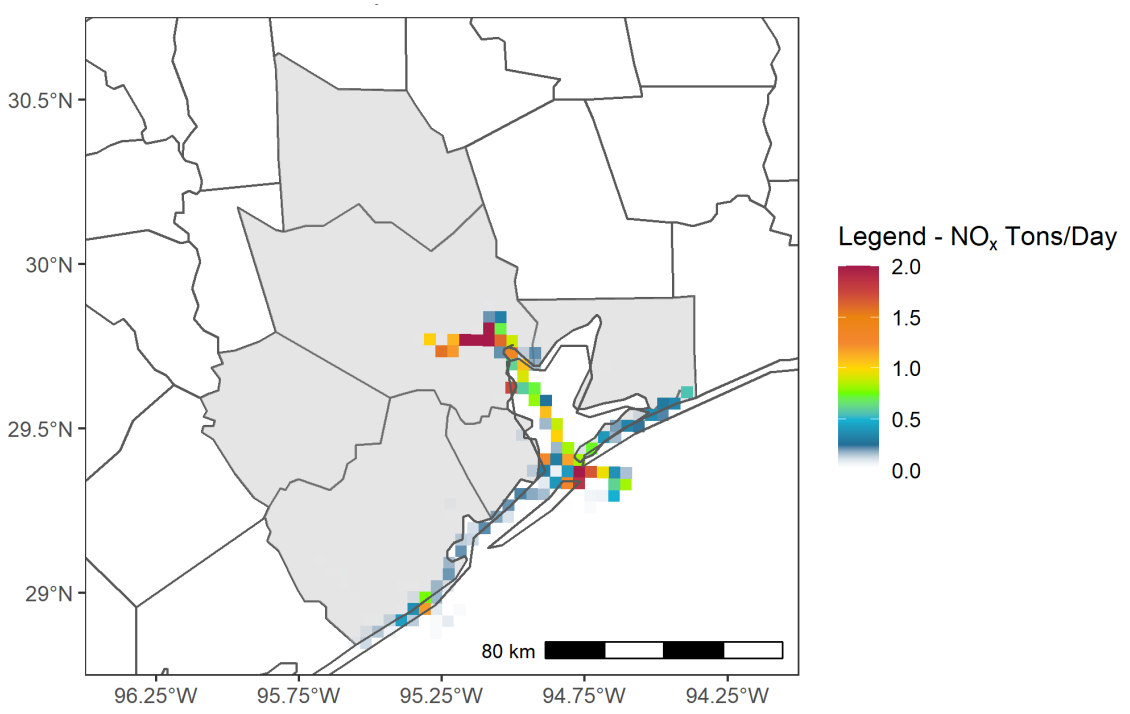

Figure 1-55: 2019 Base Case CMV NO_x Emissions for June 12 Episode Day in HGB

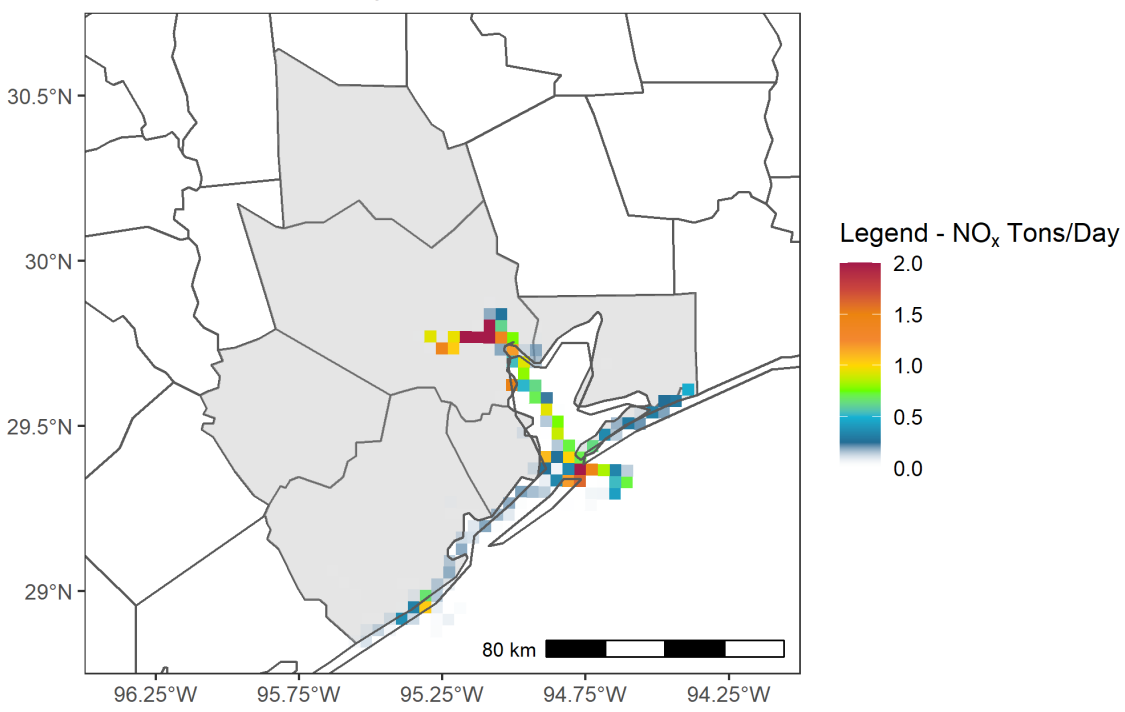

Figure 1-56: 2023 Future Case CMV NO_x Emissions for June 12 Episode Day in HGB

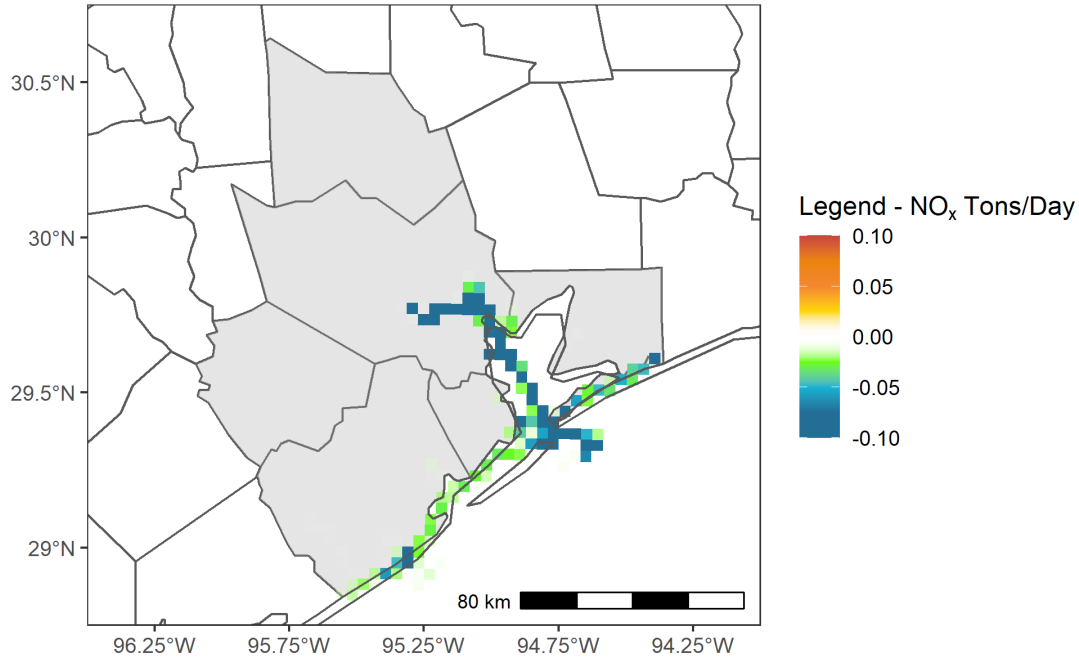

Figure 1-57: Difference in CMV NO_x Emissions for the June 12 Episode Day Between 2023 and 2019 in HGB

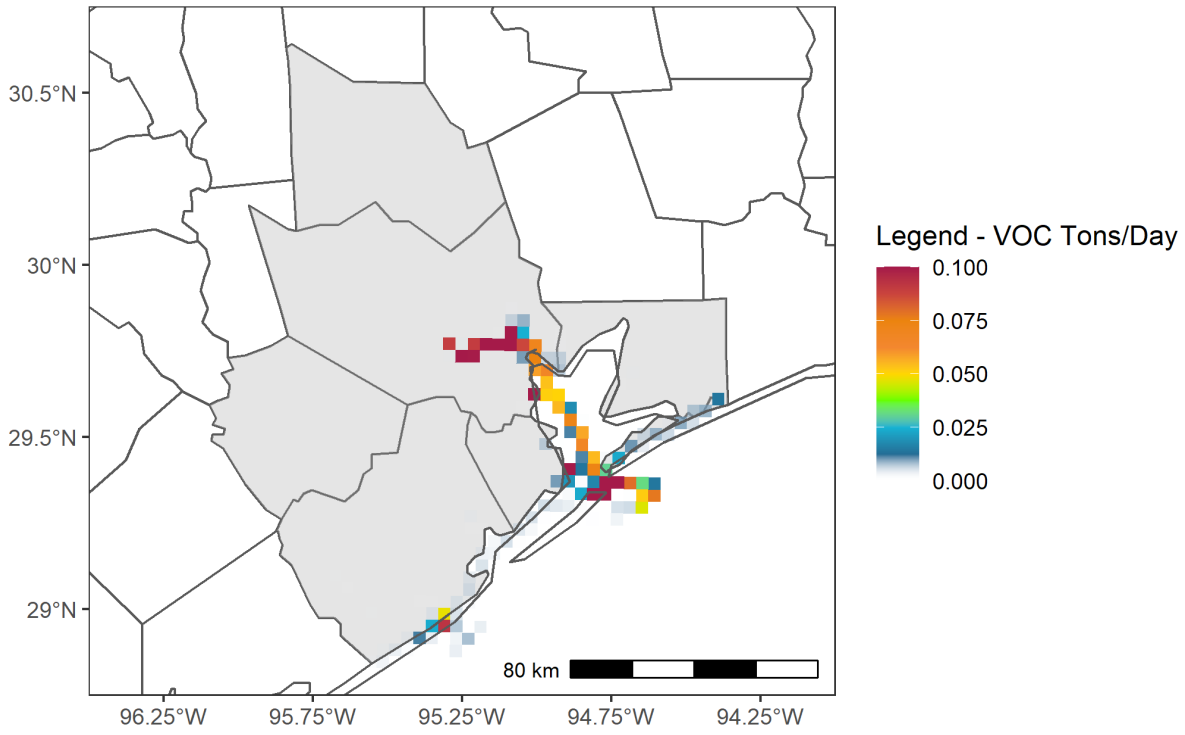

Figure 1-58: 2019 Base Case CMV VOC Emissions for June 12 Episode Day in HGB

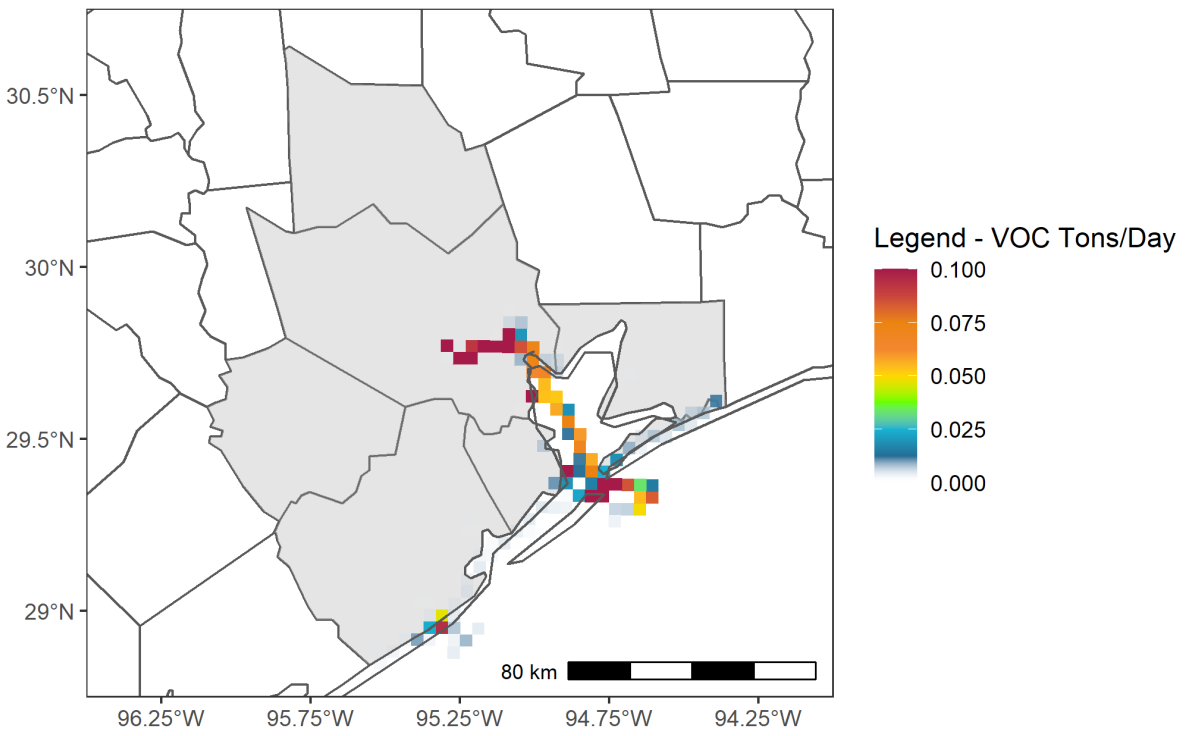

Figure 1-59: 2023 Future Case CMV VOC Emissions for June 12 Episode Day in HGB

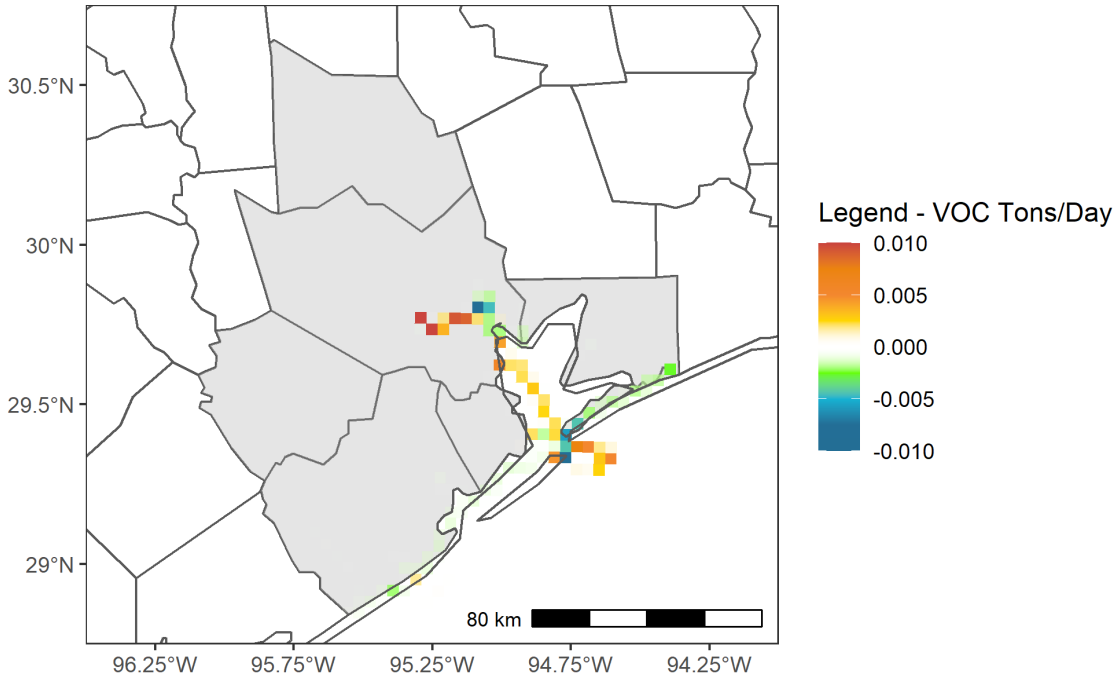

Figure 1-60: Difference in CMV VOC Emissions for the June 12 Episode Day Between 2023 and 2019 in HGB

Airports

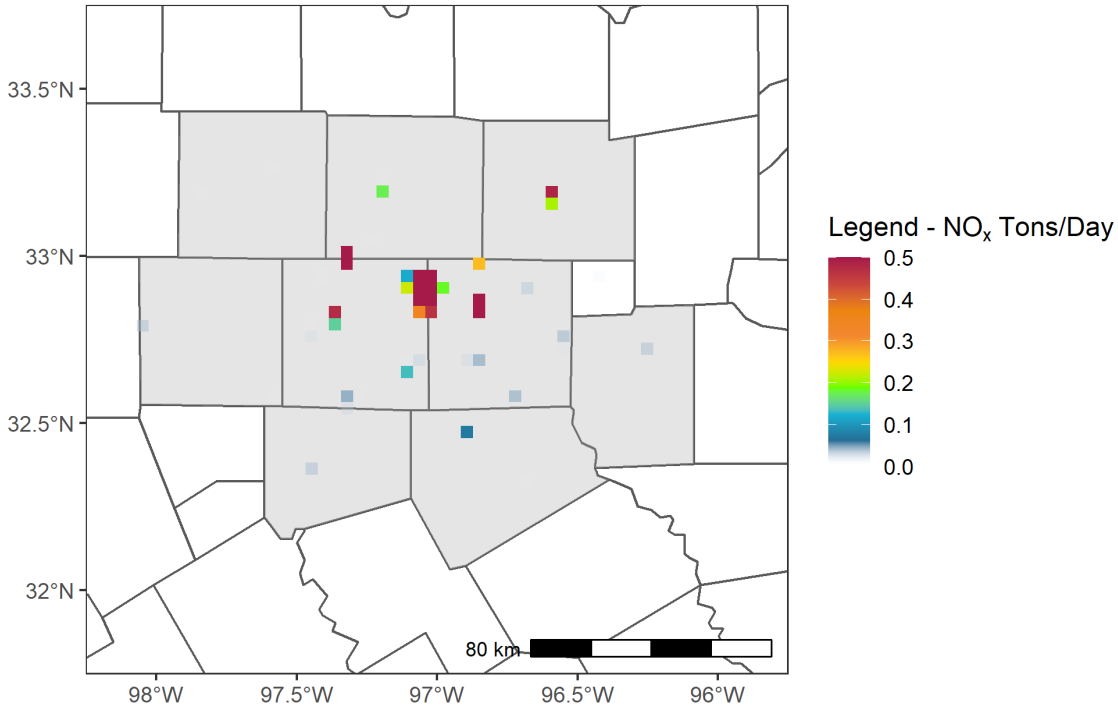

Figure 1-61: 2019 Base Case Airport NO_x Emissions for June 12 Episode Day in DFW

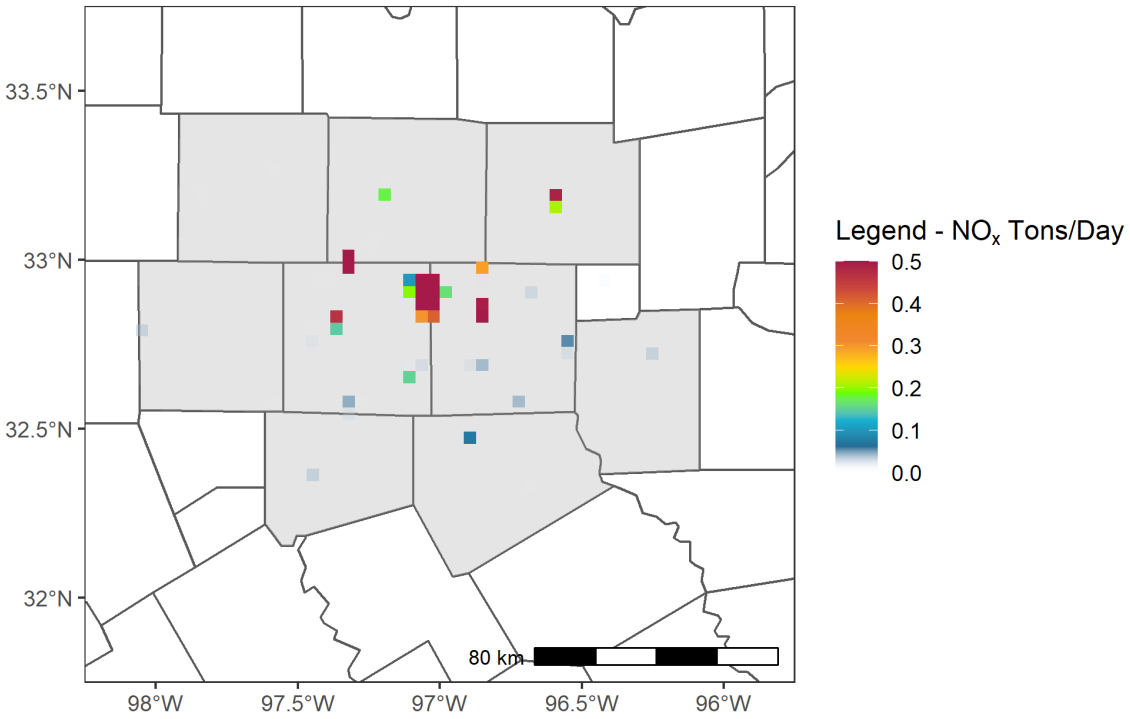

Figure 1-62: 2023 Future Case Airport NO_x Emissions for June 12 Episode Day in DFW

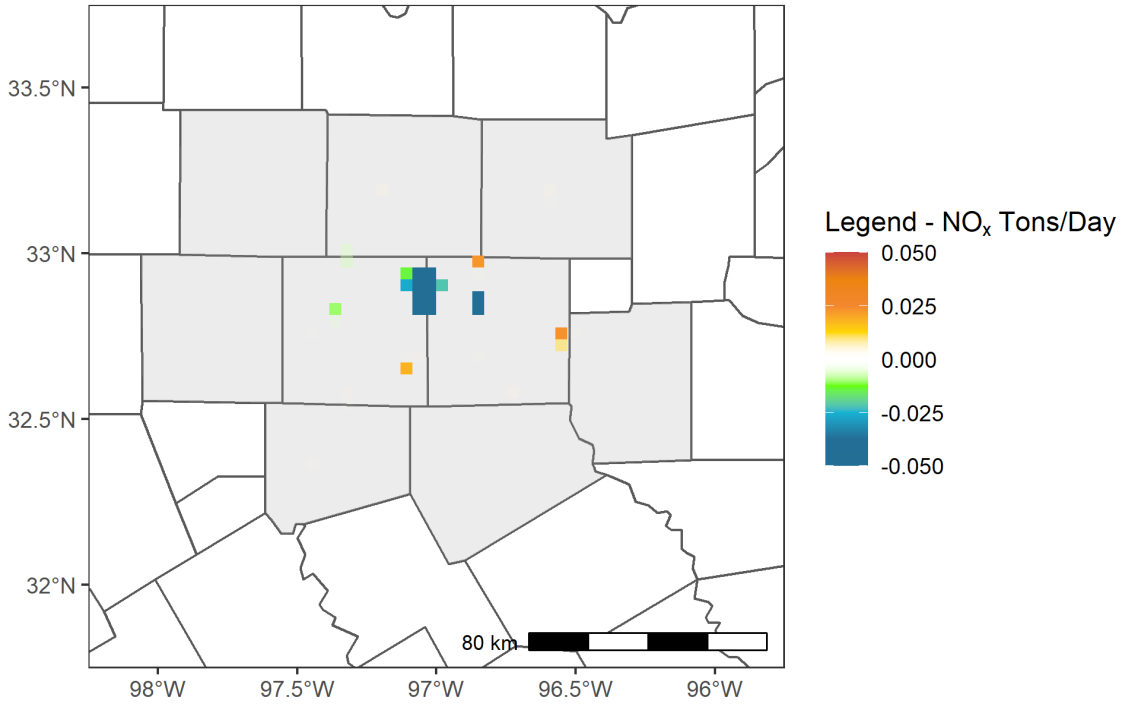

Figure 1-63: Difference in Airport NO_x Emissions for the June 12 Episode Day Between 2023 and 2019 in DFW

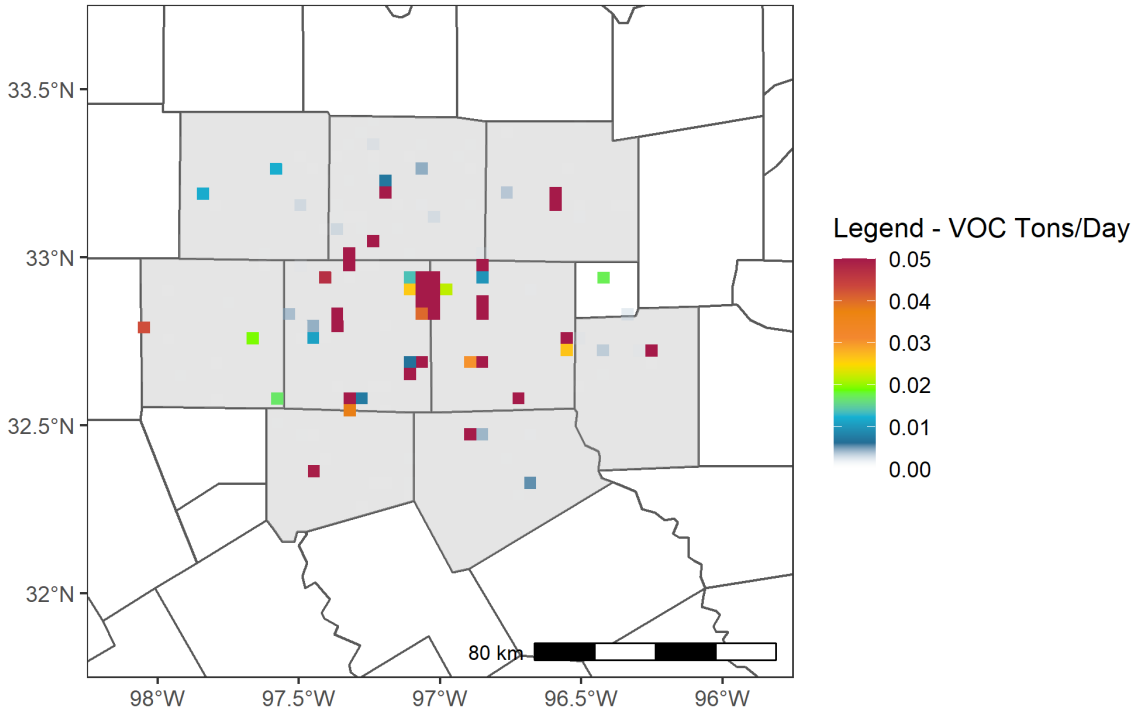

Figure 1-64: 2019 Base Case Airport VOC Emissions for June 12 Episode Day in DFW

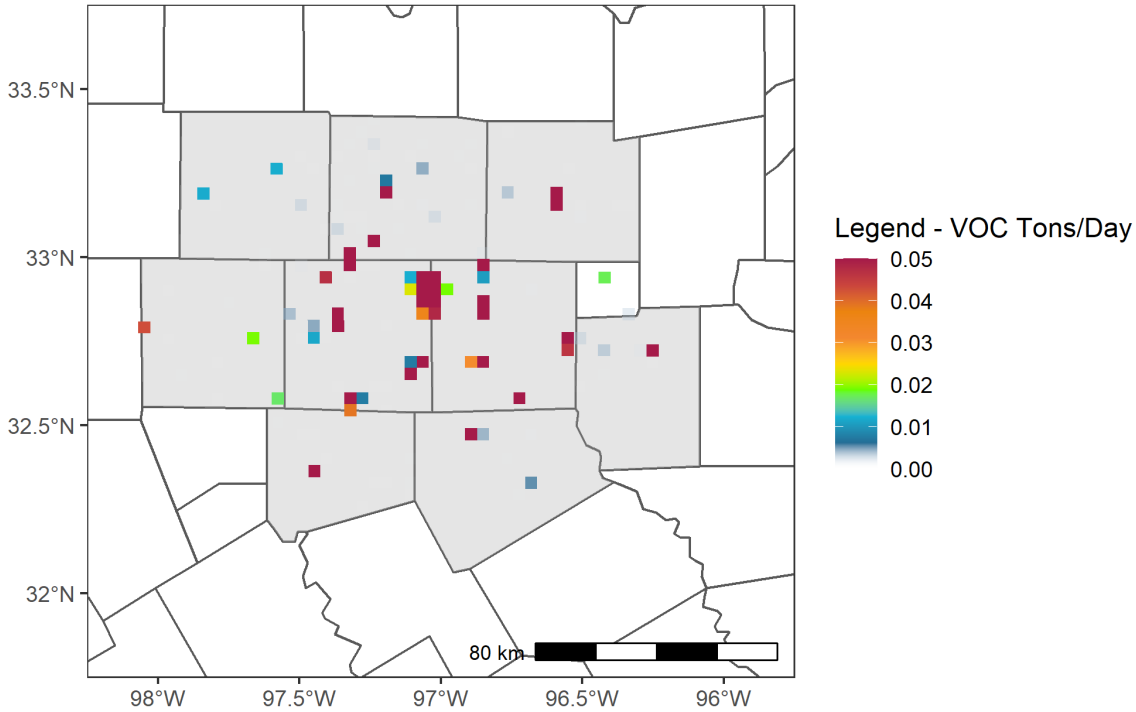

Figure 1-65: 2023 Future Case Airport VOC Emissions for June 12 Episode Day in DFW

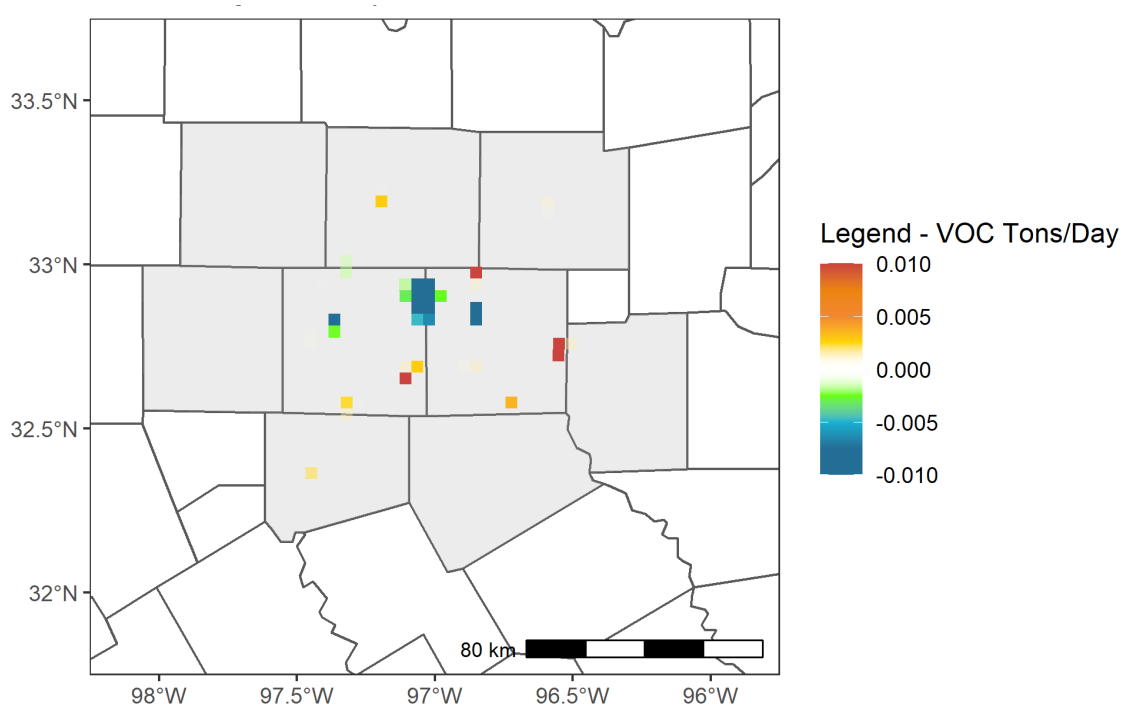

Figure 1-66: Difference in Airport VOC Emissions for the June 12 Episode Day Between 2023 and 2019 in DFW

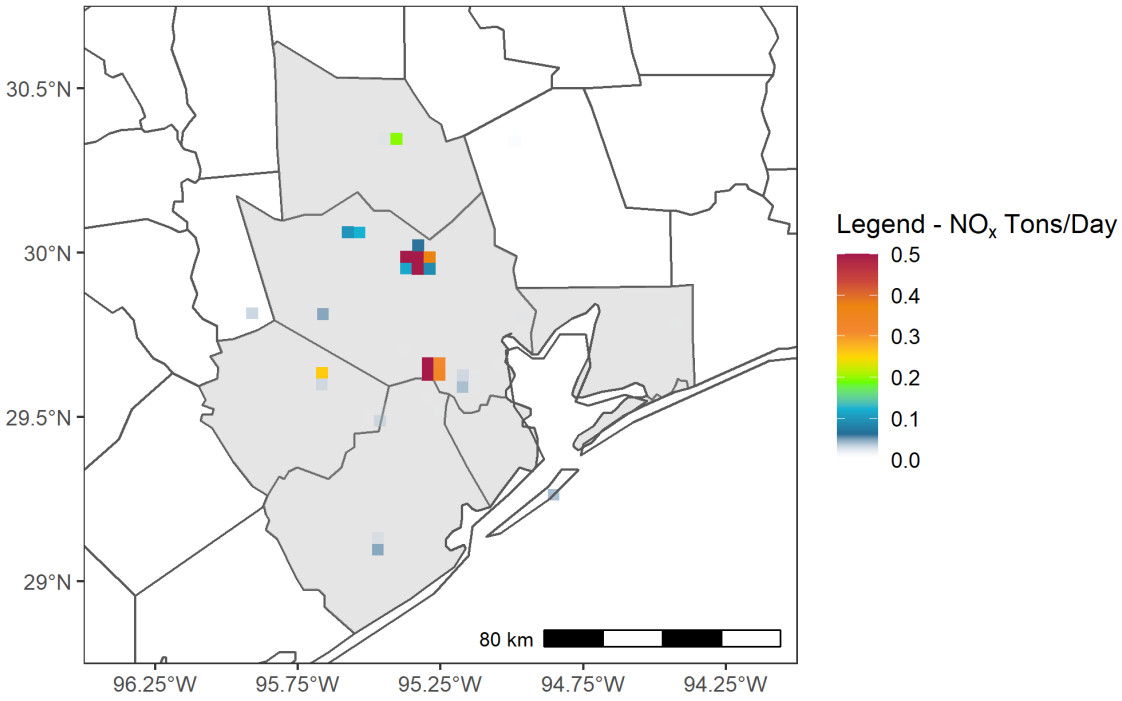

Figure 1-67: 2019 Base Case Airport NO_x Emissions for June 12 Episode Day in HGB

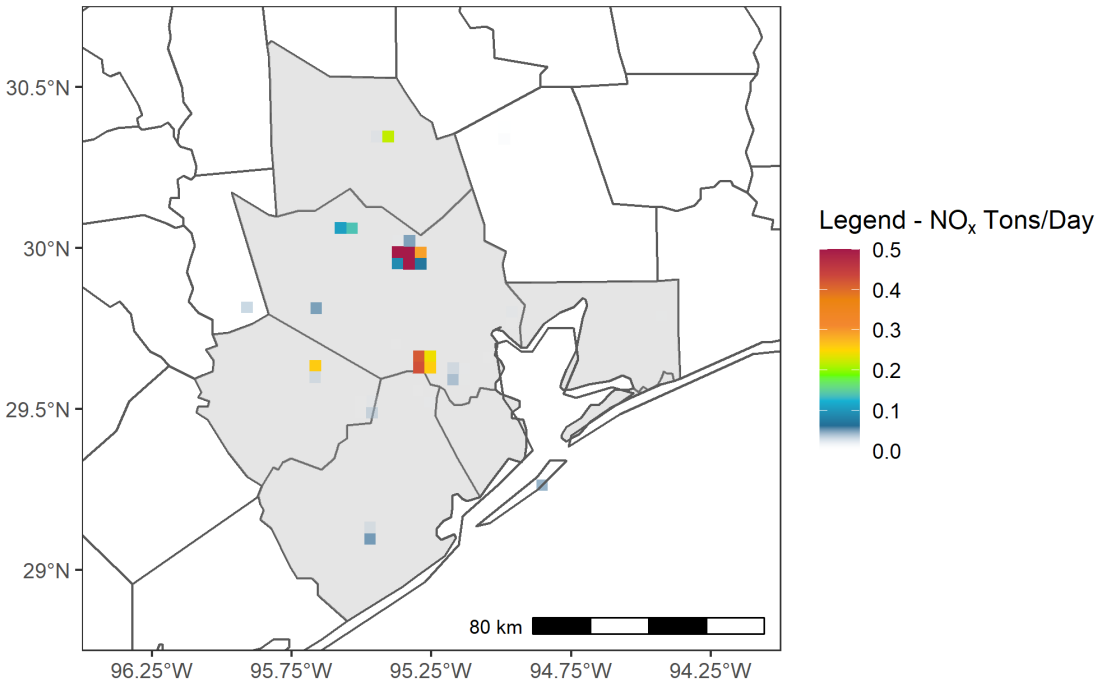

Figure 1-68: 2023 Future Case Airport NO_x Emissions for June 12 Episode Day in HGB

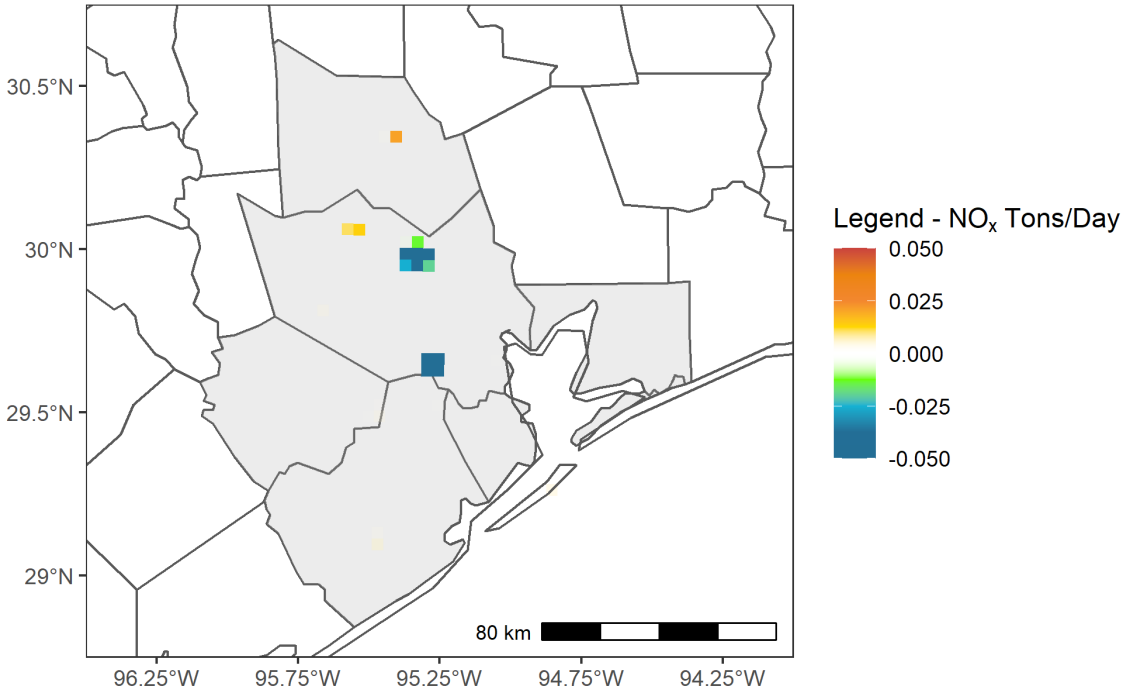

Figure 1-69: Difference in Airport NO_x Emissions for the June 12 Episode Day Between 2023 and 2019 in HGB

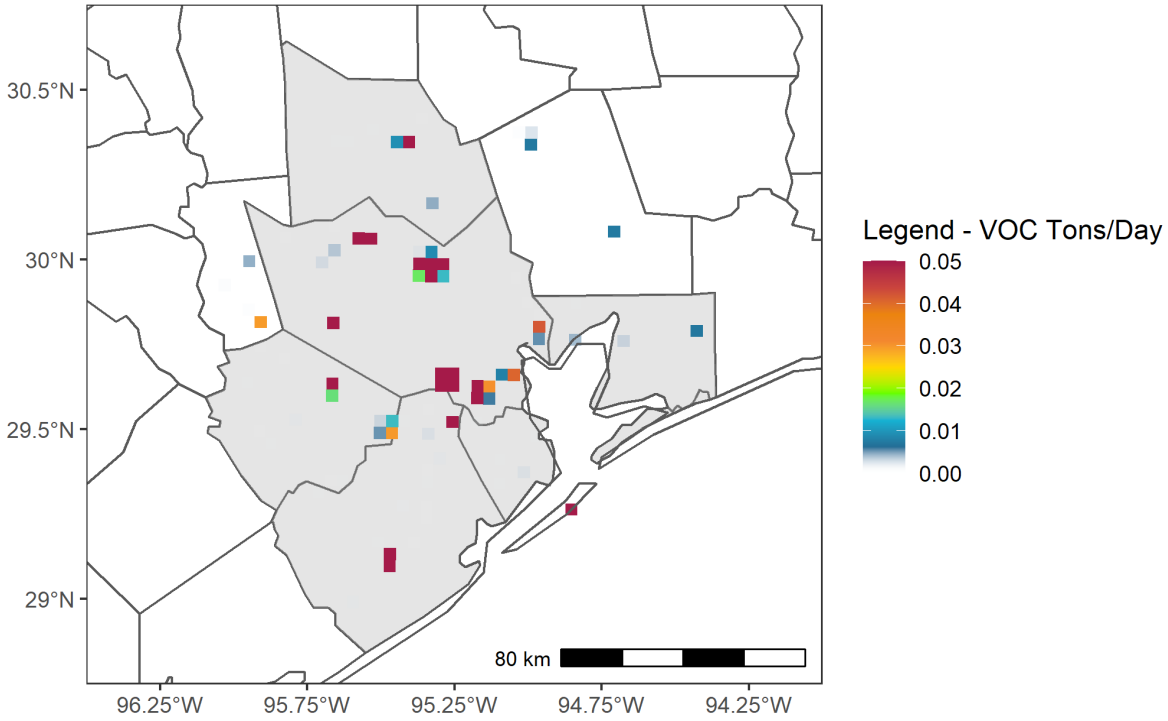

Figure 1-70: 2019 Base Case Airport VOC Emissions for June 12 Episode Day in HGB

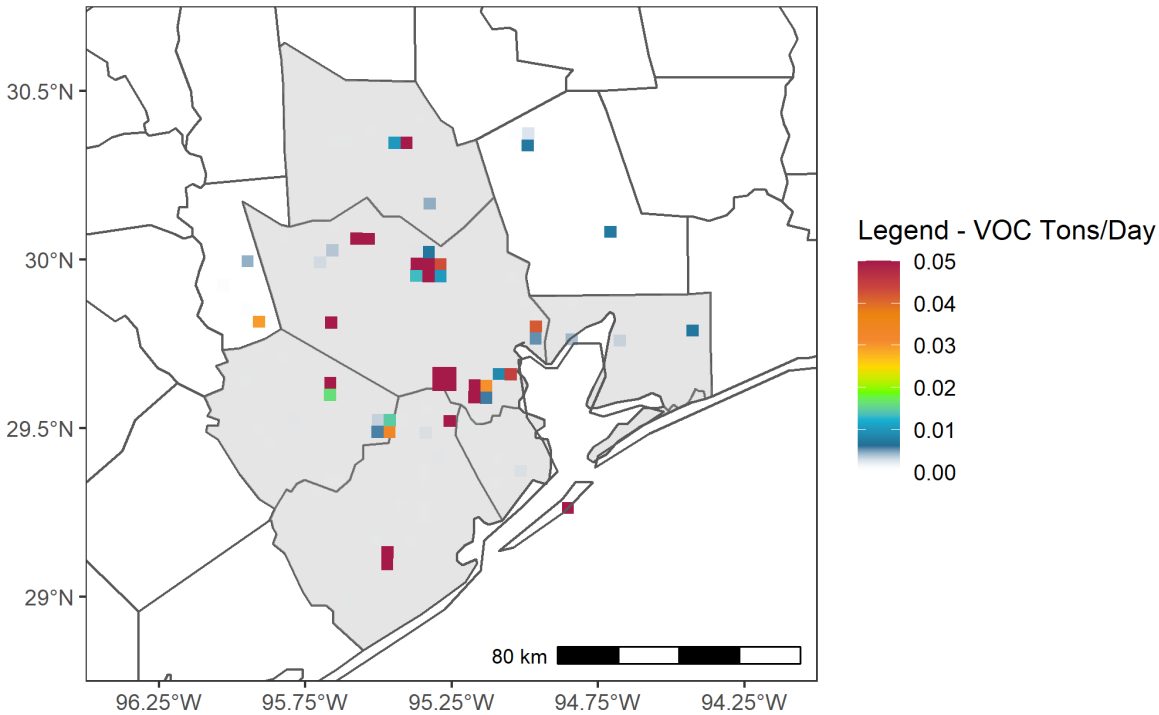

Figure 1-71: 2023 Future Case Airport VOC Emissions for June 12 Episode Day in HGB

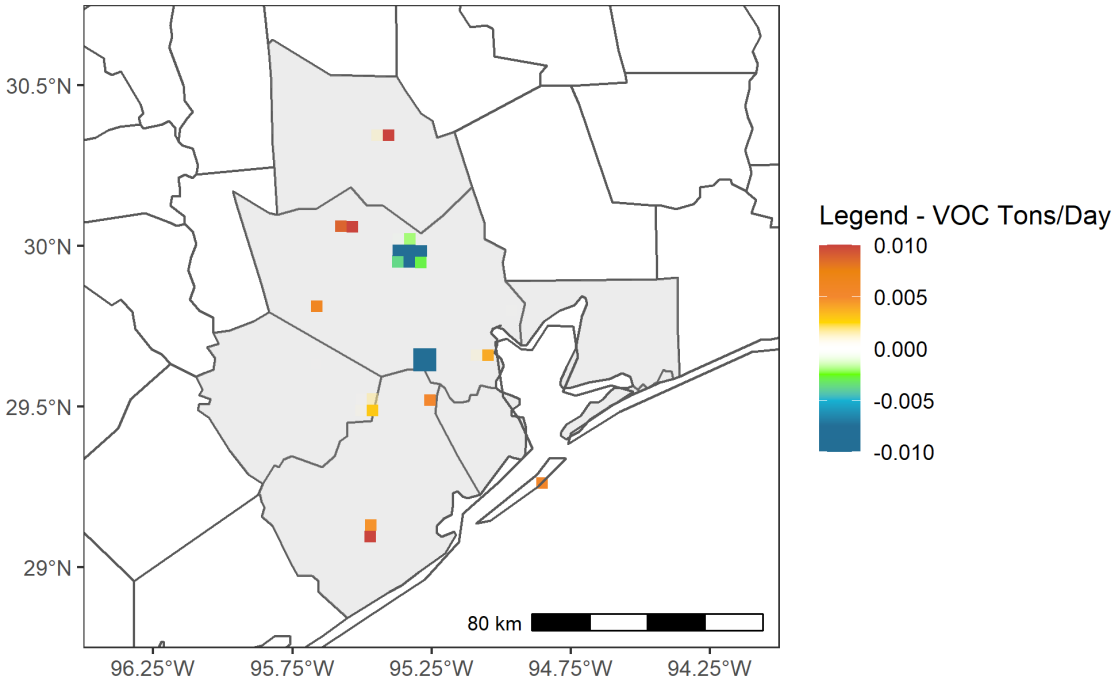

Figure 1-72: Difference in Airport VOC Emissions for the June 12 Episode Day Between 2023 and 2019 in HGB

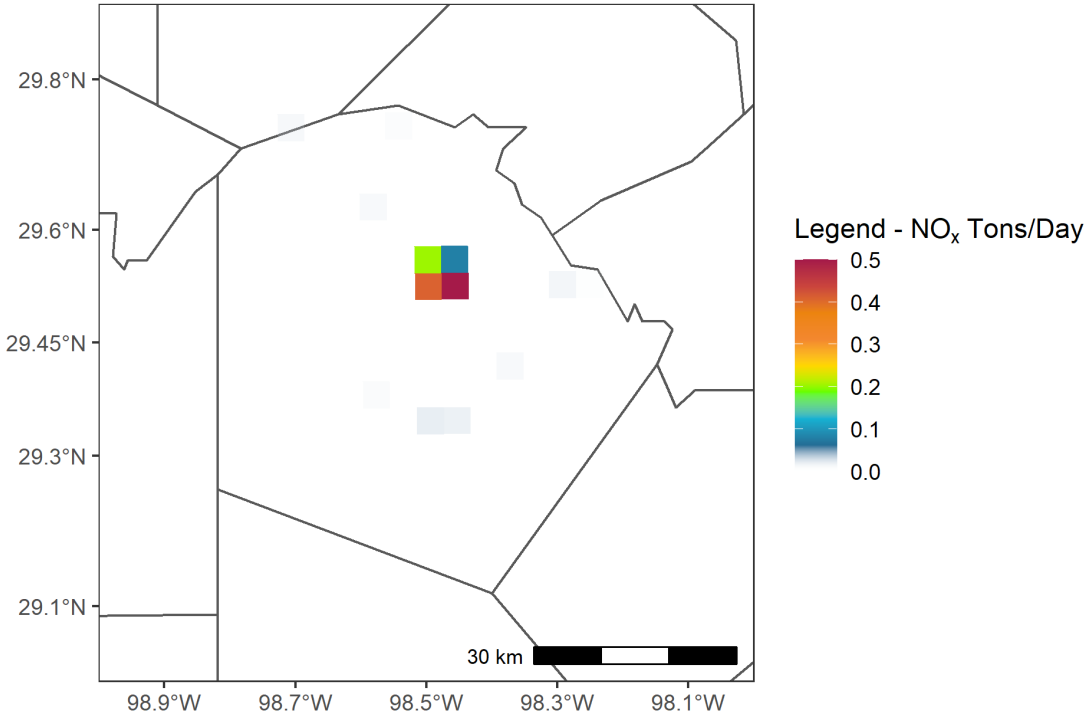

Figure 1-73: 2019 Base Case Airport NO_x Emissions for June 12 Episode Day in Bexar County

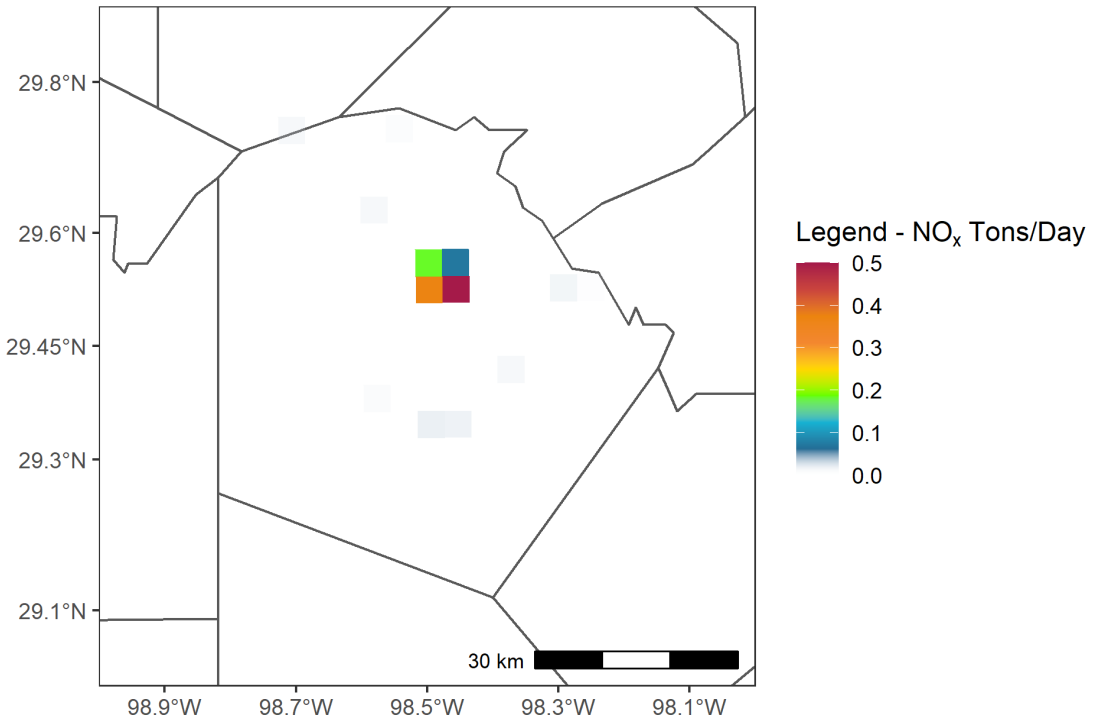

Figure 1-74: 2023 Future Case Airport NO_x Emissions for June 12 Episode Day in Bexar County

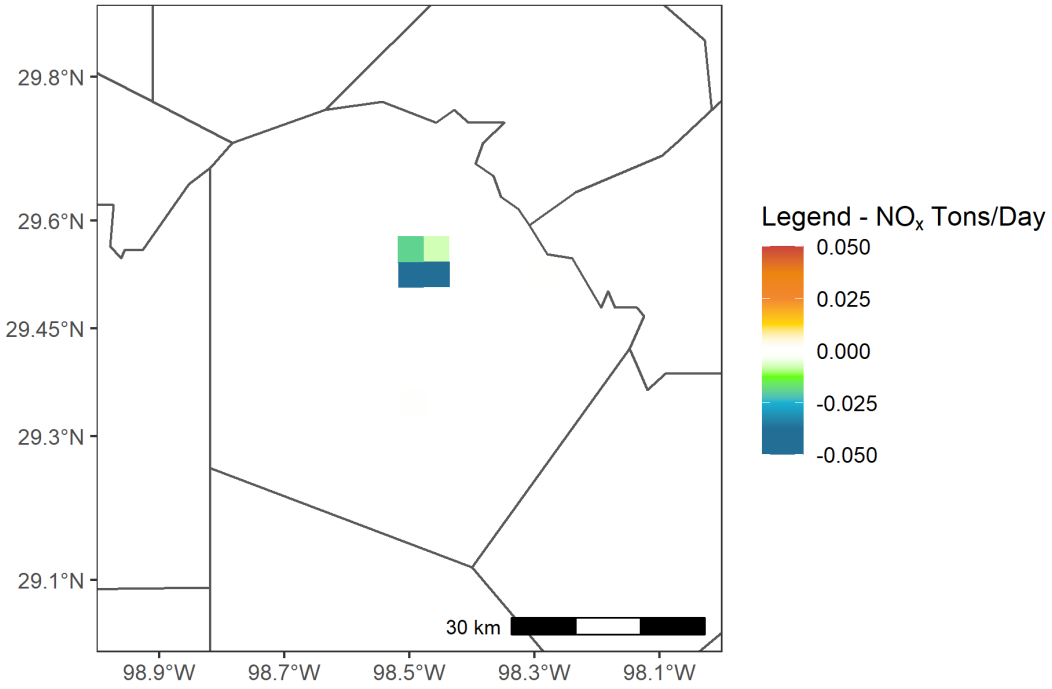

Figure 1-75: Difference in Airport NO_x Emissions for the June 12 Episode Day Between 2023 and 2019 in Bexar County

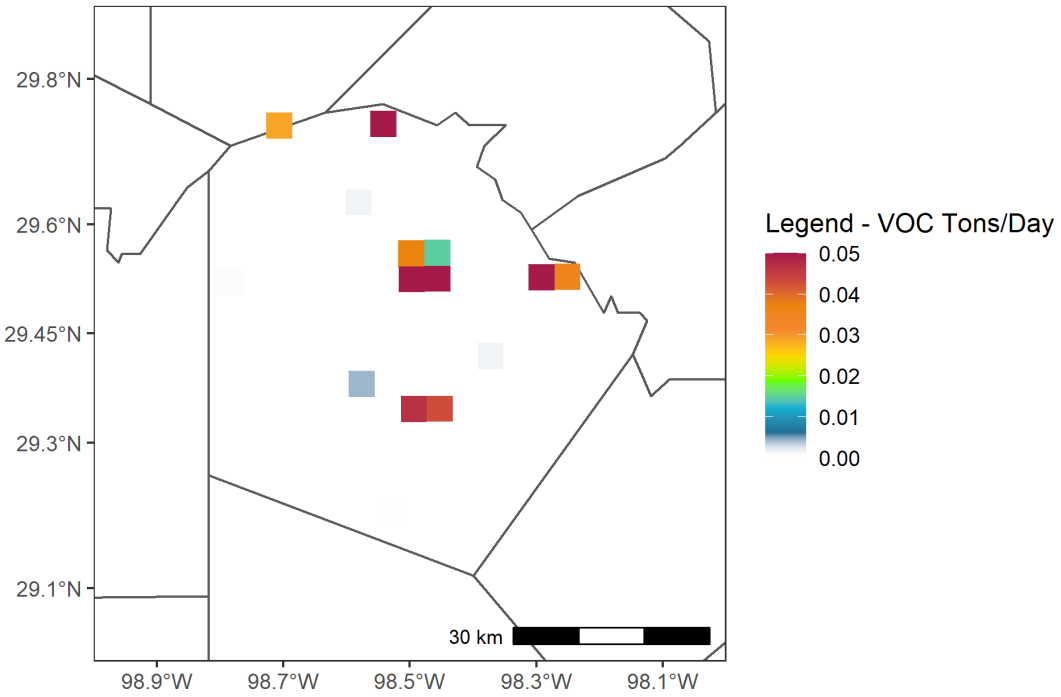

Figure 1-76: 2019 Base Case Airport VOC Emissions for June 12 Episode Day in Bexar County

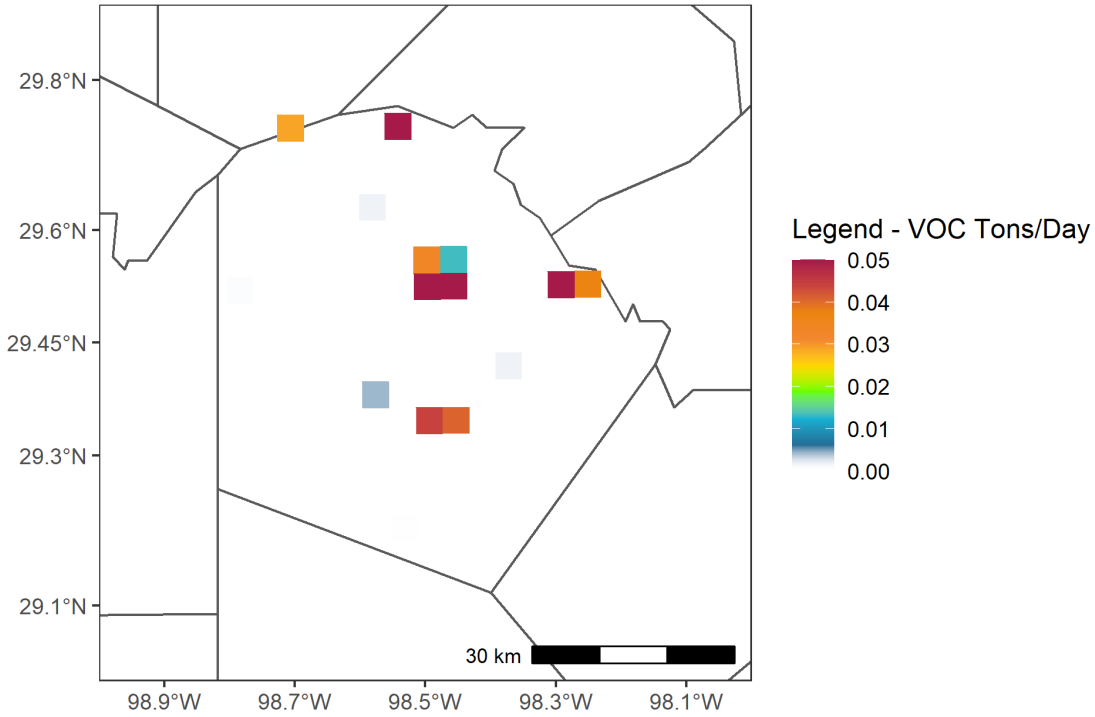

Figure 1-77: 2023 Future Case Airport VOC Emissions for June 12 Episode Day in Bexar County

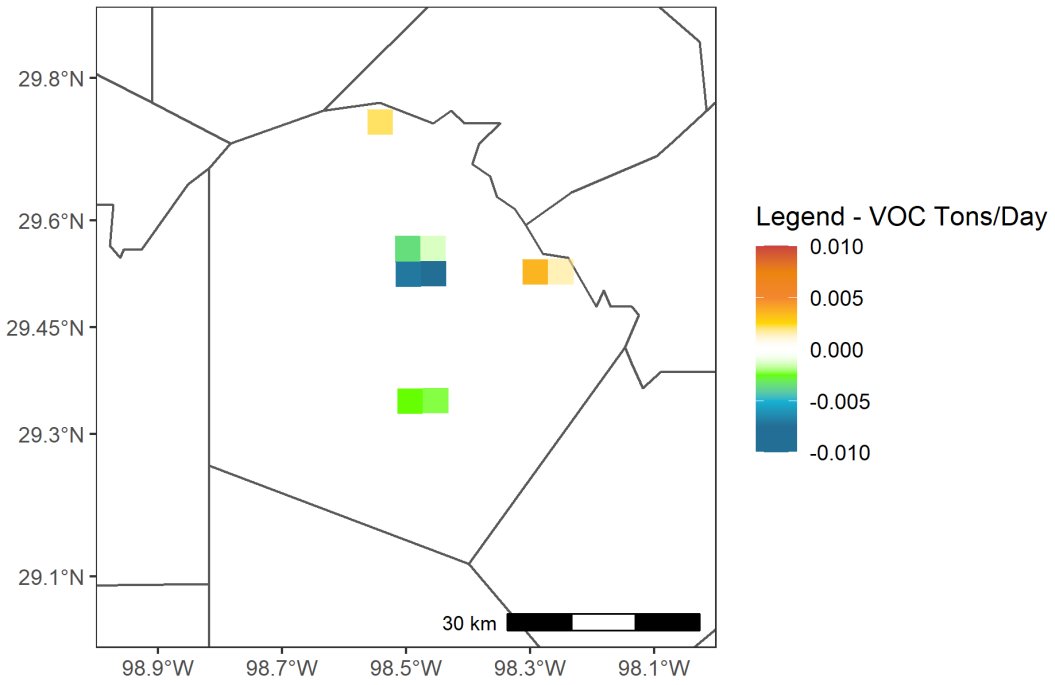

Figure 1-78: Difference in Airport VOC Emissions for the June 12 Episode Day Between 2023 and 2019 in Bexar County

Locomotives

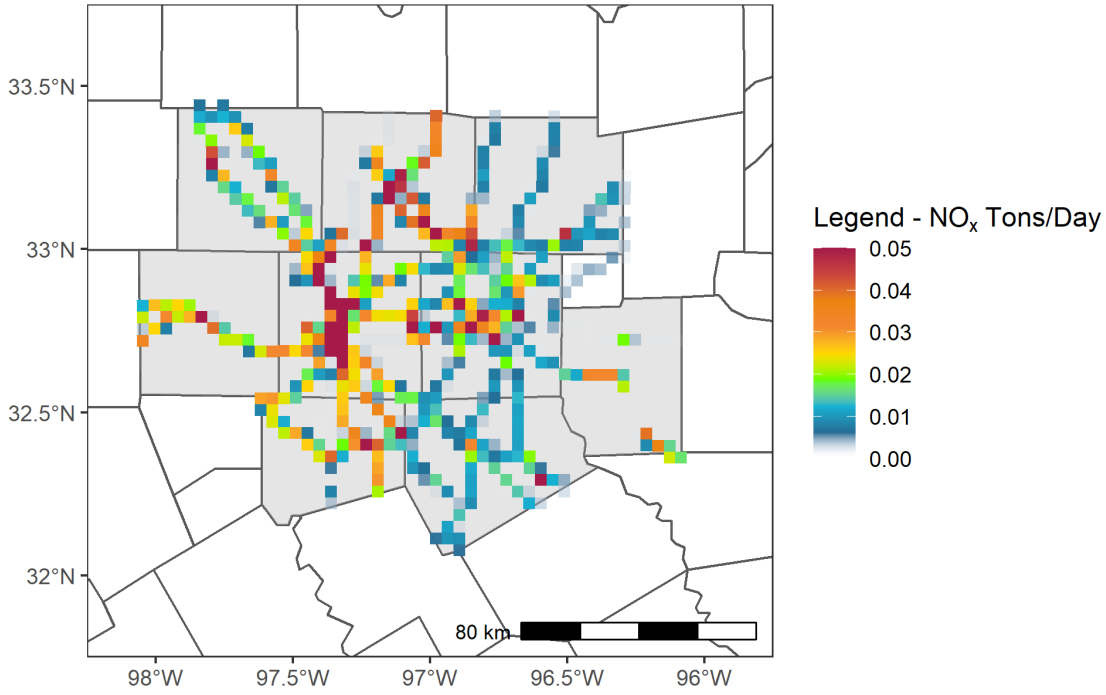

Figure 1-79: 2019 Base Case Locomotive NO_x Emissions for June 12 Episode Day in DFW

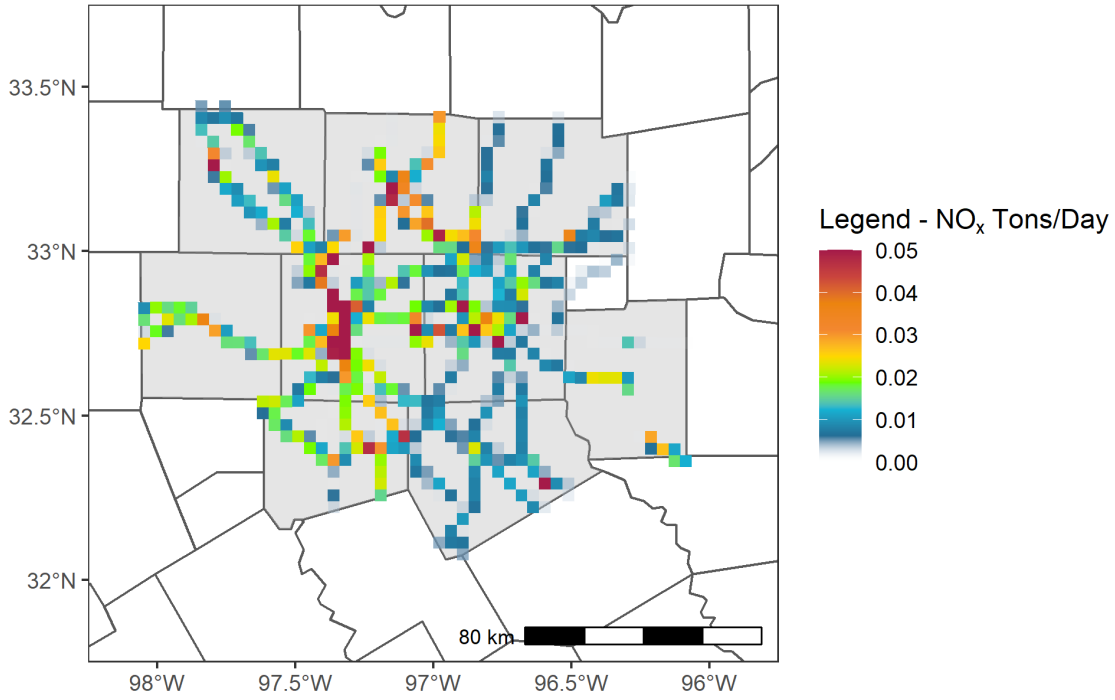

Figure 1-80: 2023 Future Case Locomotive NO_x Emissions for June 12 Episode Day in DFW

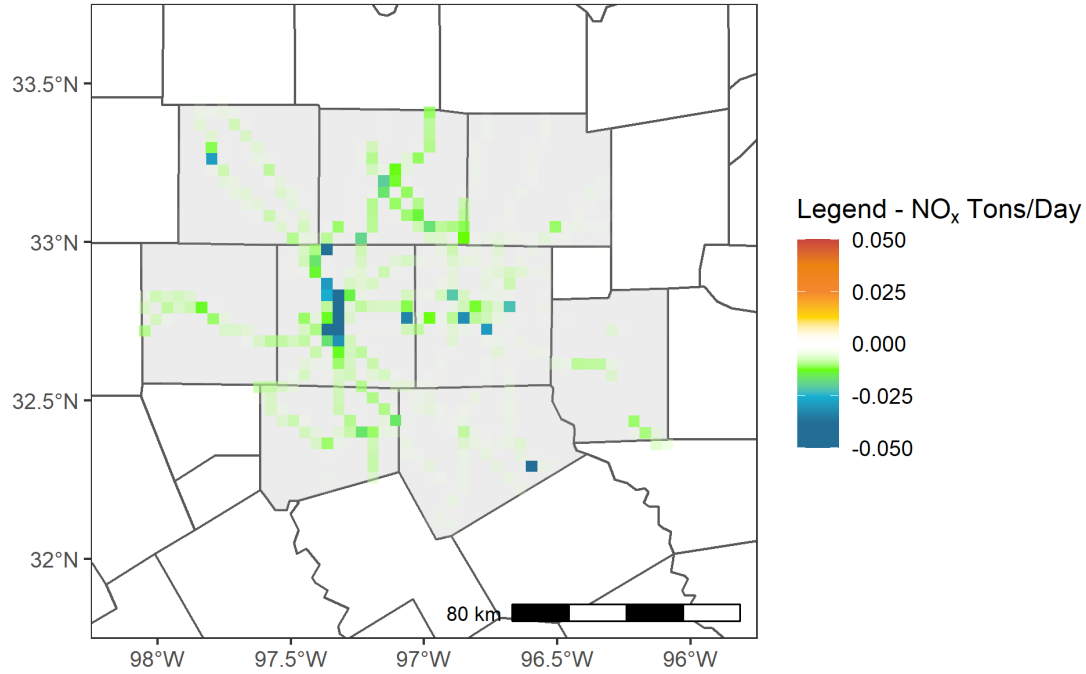

Figure 1-81: Difference in Locomotive NO_x Emissions for the June 12 Episode Day Between 2023 and 2019 in DFW

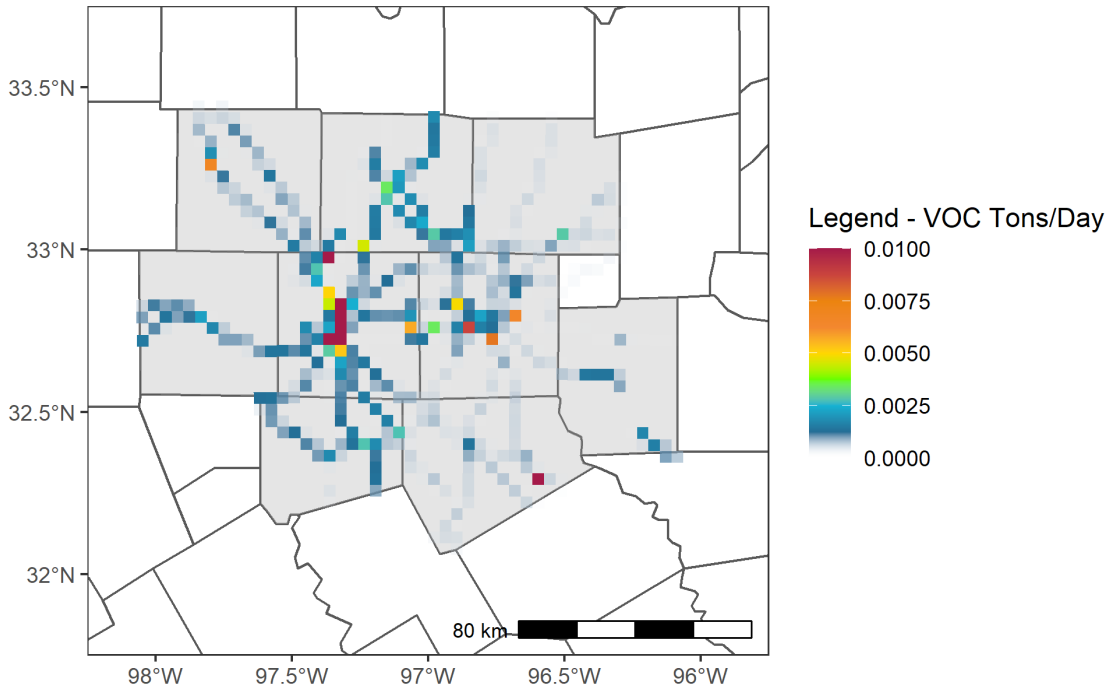

Figure 1-82: 2019 Base Case Locomotive VOC Emissions for June 12 Episode Day in DFW

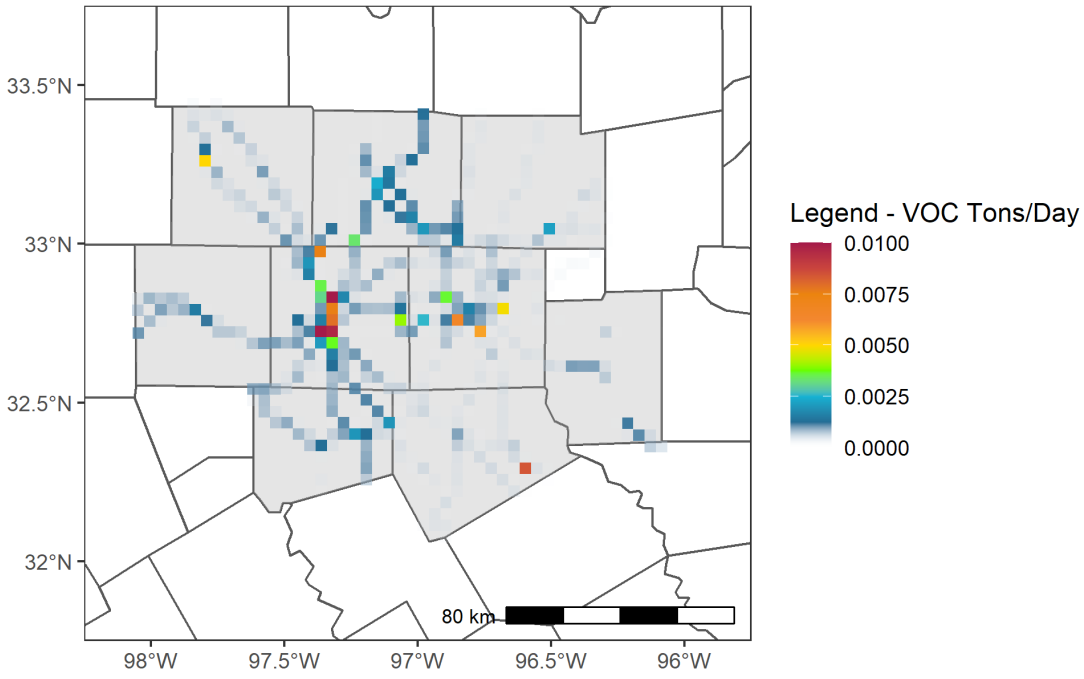

Figure 1-83: 2023 Future Case Locomotive VOC Emissions for June 12 Episode Day in DFW

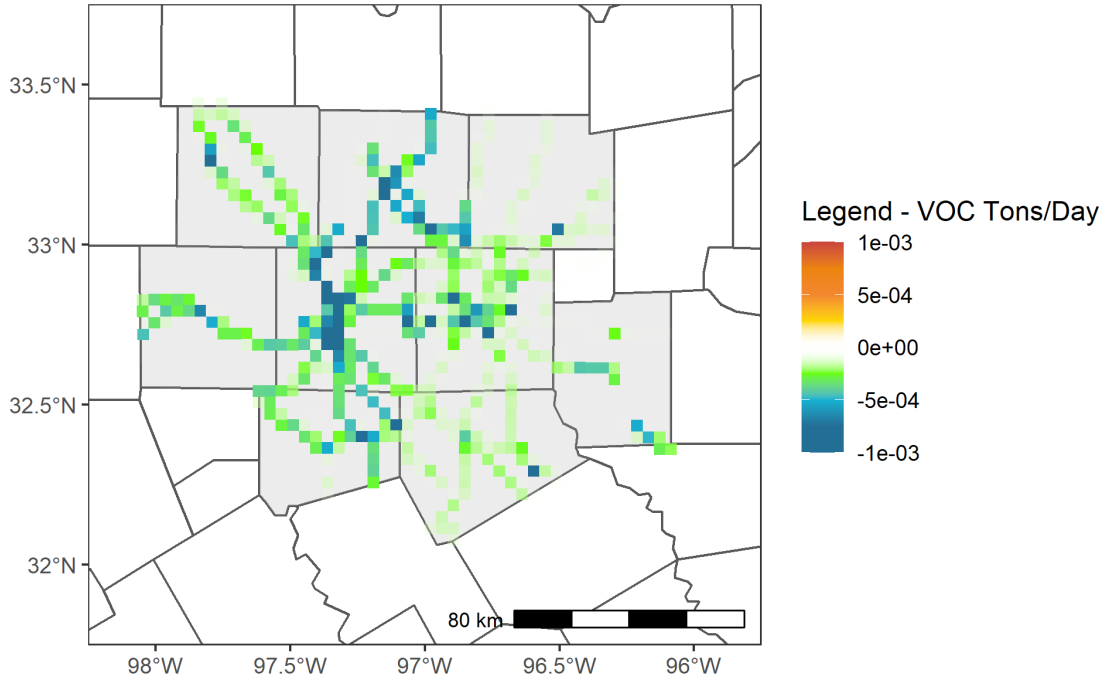

Figure 1-84: Difference in Locomotive VOC Emissions for the June 12 Episode Day Between 2023 and 2019 in DFW

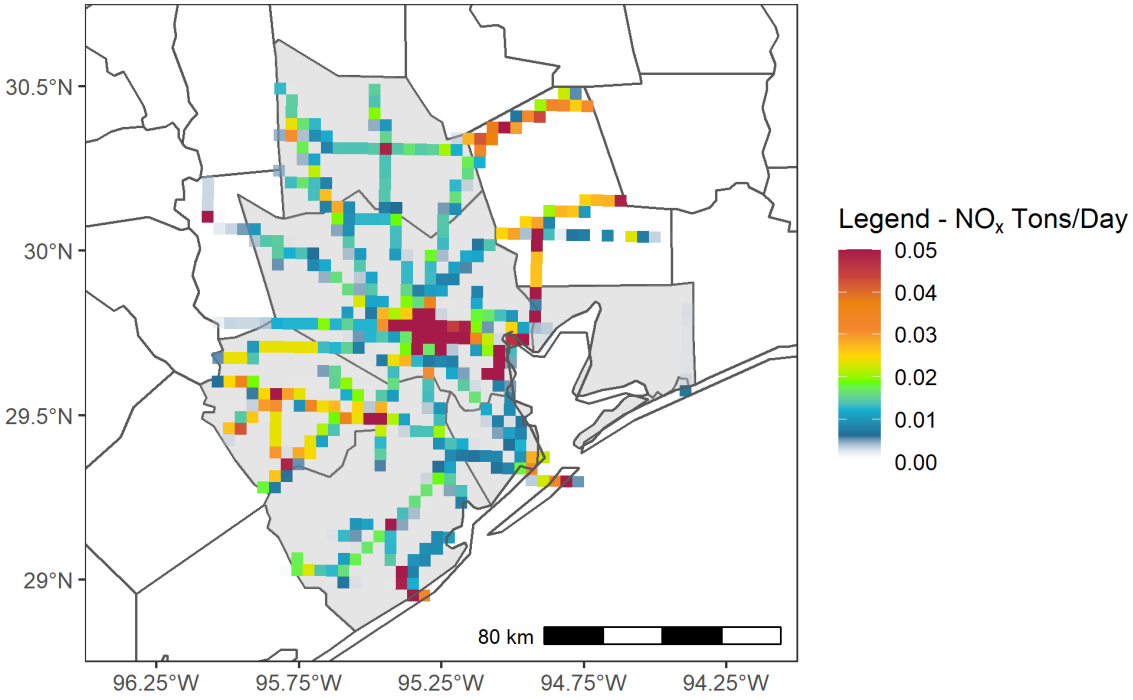

Figure 1-85: 2019 Base Case Locomotive NO_x Emissions for June 12 Episode Day in HGB

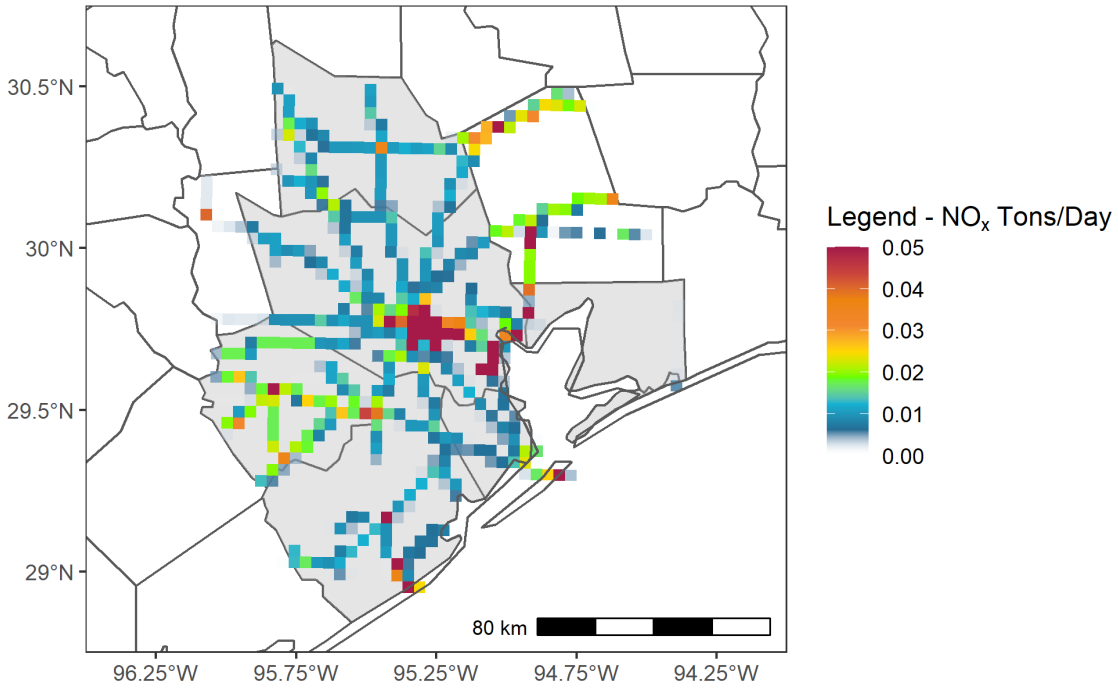

Figure 1-86: 2023 Future Case Locomotive NO_x Emissions for June 12 Episode Day in HGB

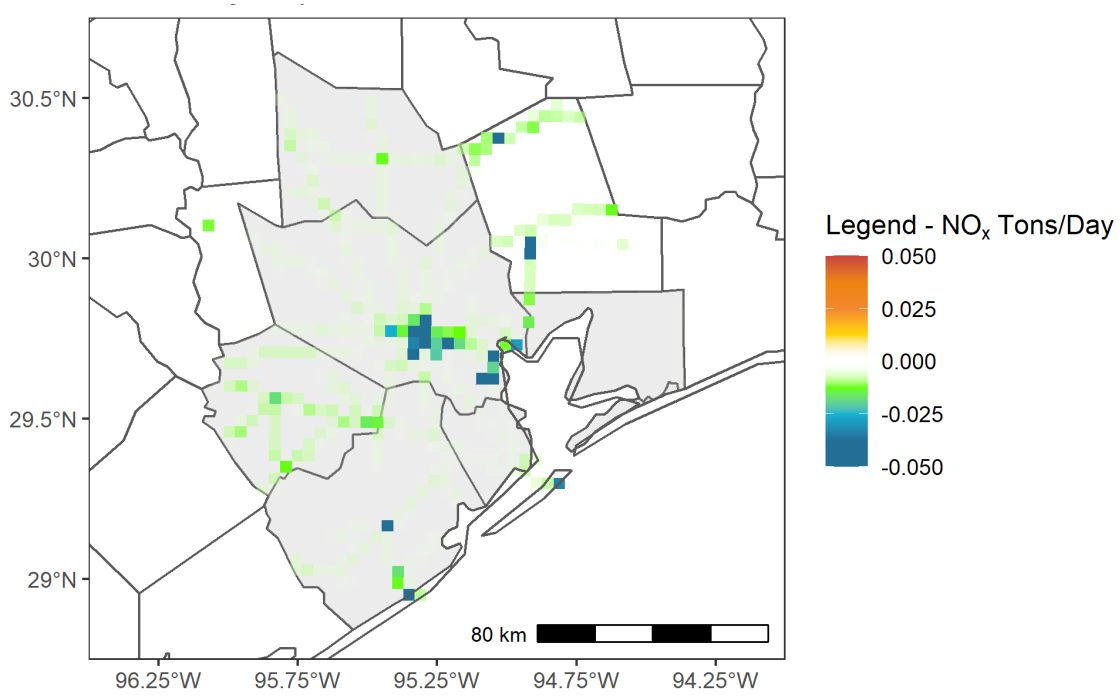

Figure 1-87: Difference in Locomotive NO_x Emissions for the June 12 Episode Day Between 2023 and 2019 in HGB

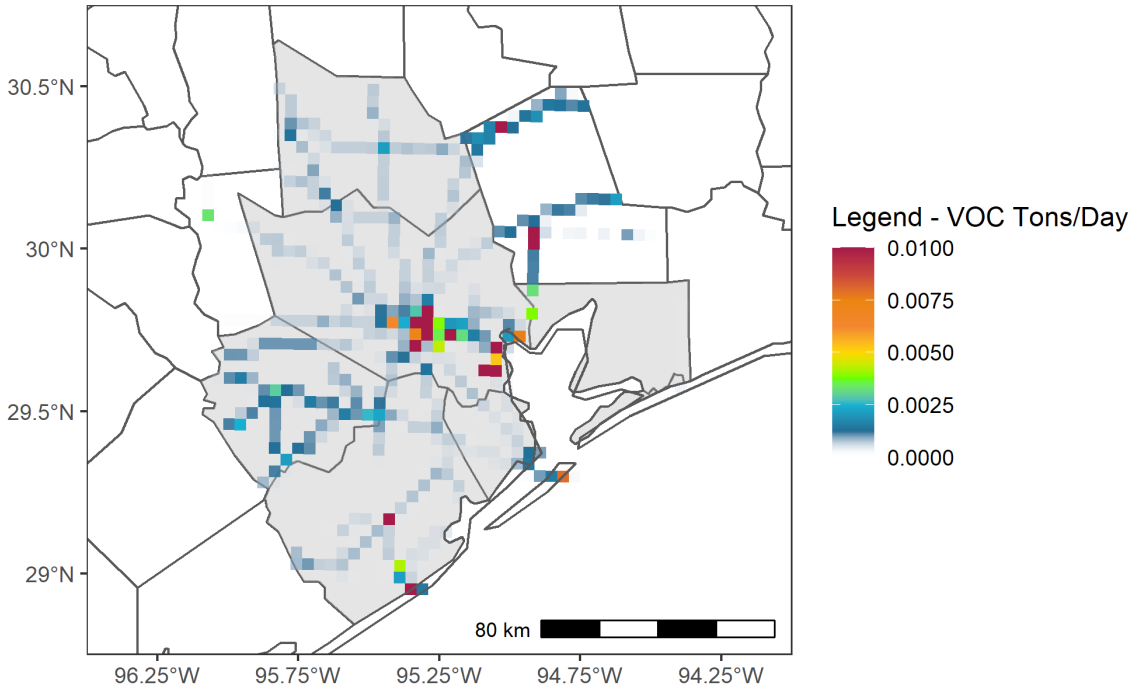

Figure 1-88: 2019 Base Case Locomotive VOC Emissions for June 12 Episode Day in HGB

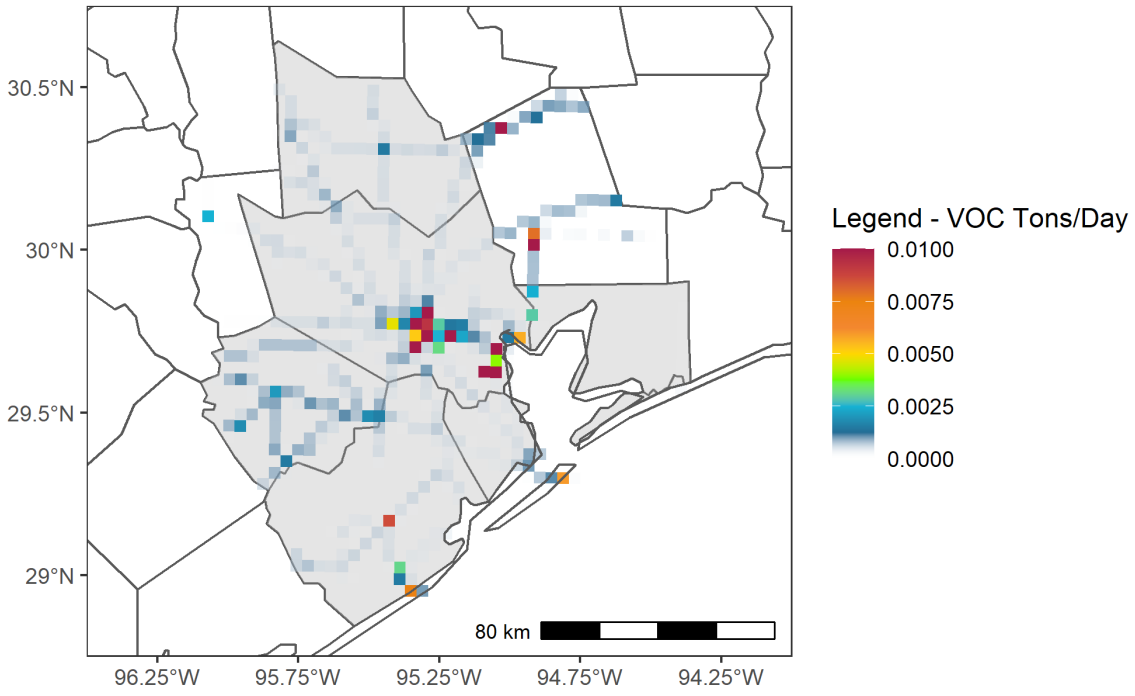

Figure 1-89: 2023 Future Case Locomotive VOC Emissions for June 12 Episode Day in HGB

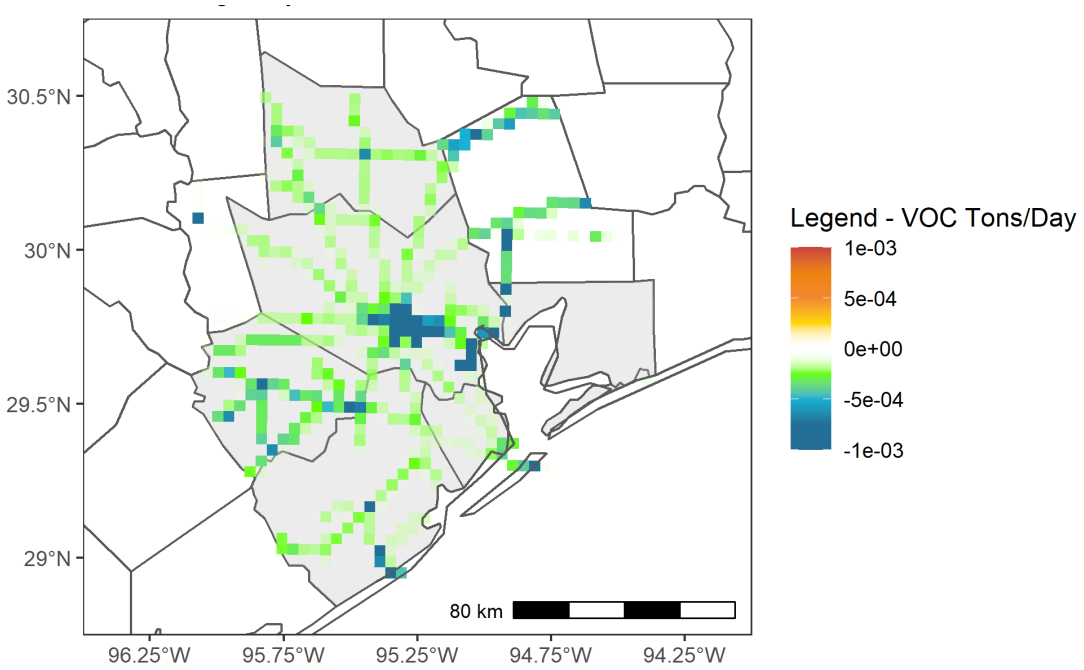

Figure 1-90: Difference in Locomotive VOC Emissions for the June 12 Episode Day Between 2023 and 2019 in HGB

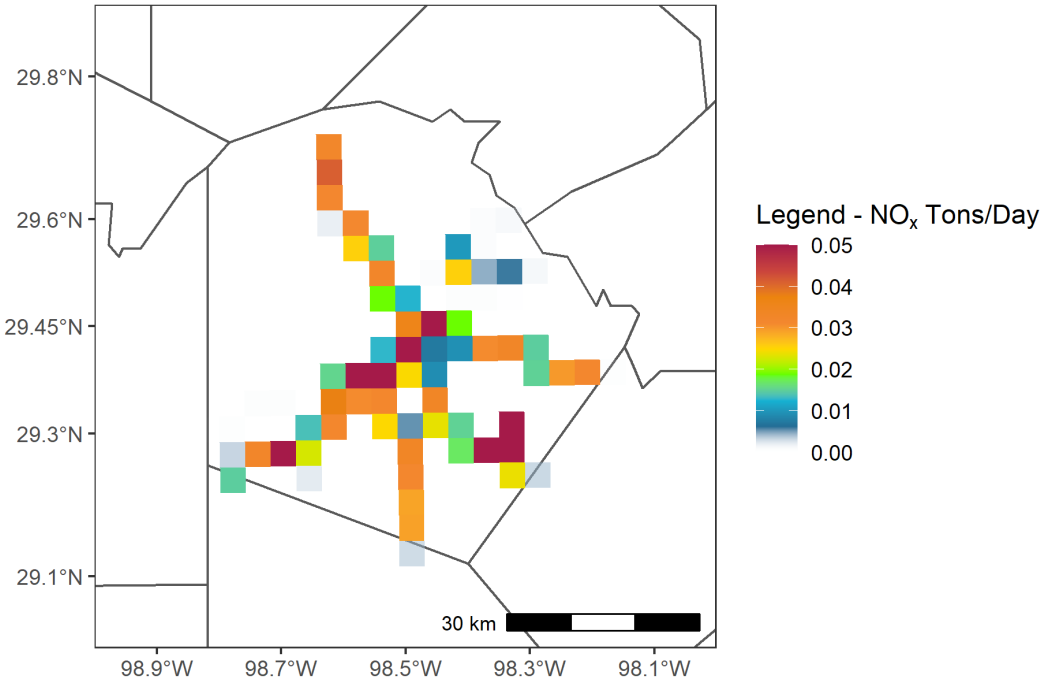

Figure 1-91: 2019 Base Case Locomotive NO_x Emissions for June 12 Episode Day in Bexar County

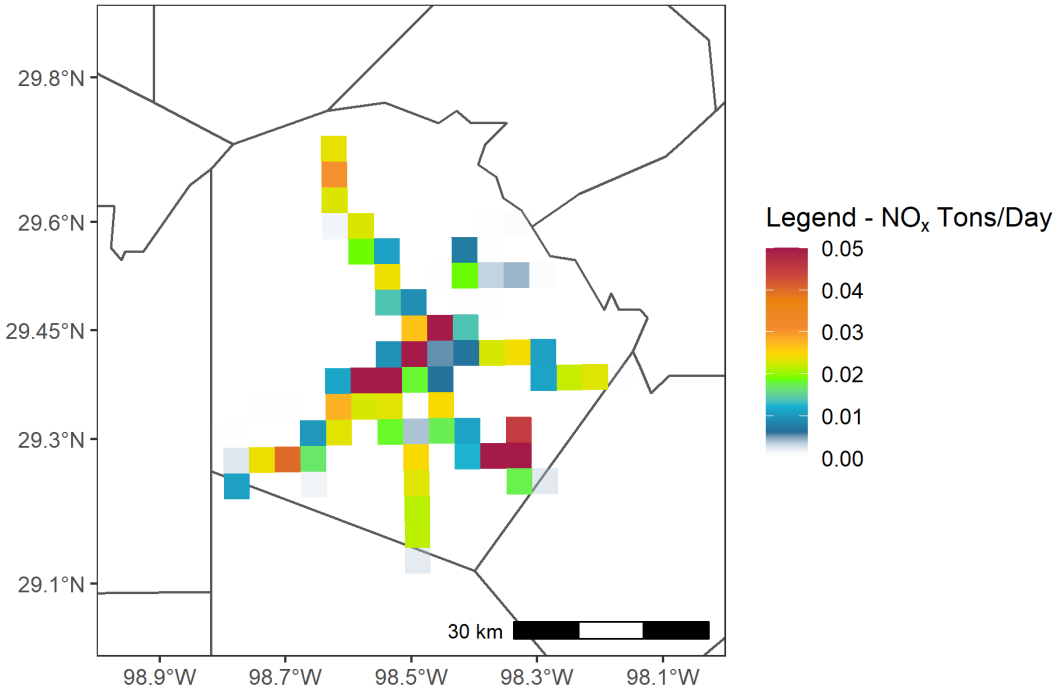

Figure 1-92: 2023 Future Case Locomotive NO_x Emissions for June 12 Episode Day in Bexar County

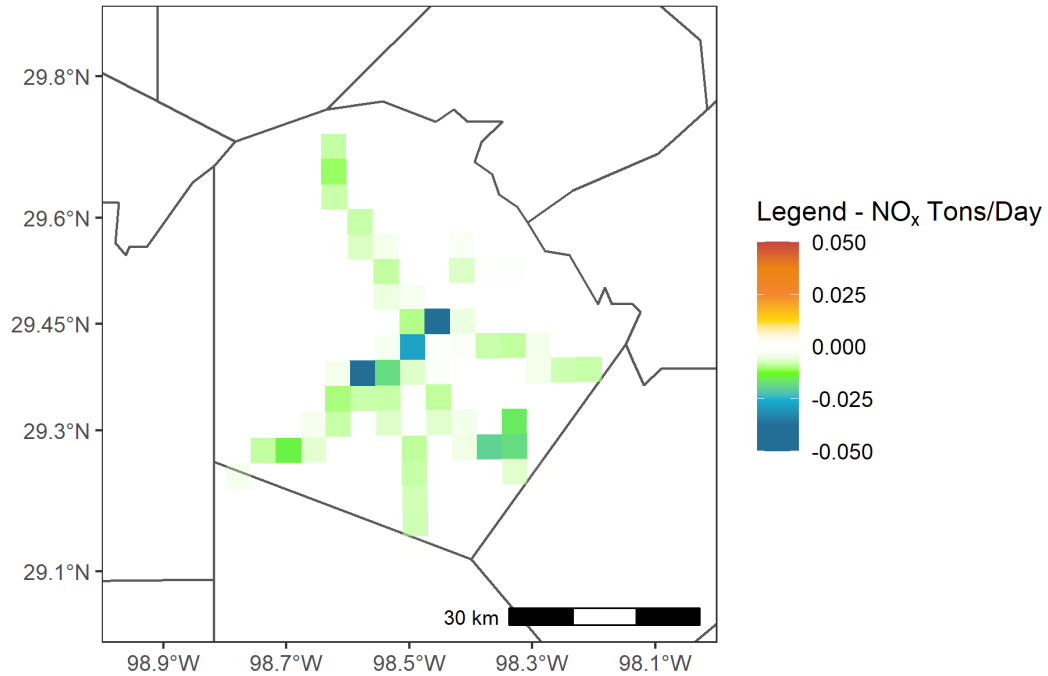

Figure 1-93: Difference in Locomotive NO_x Emissions for the June 12 Episode Day Between 2023 and 2019 in Bexar County

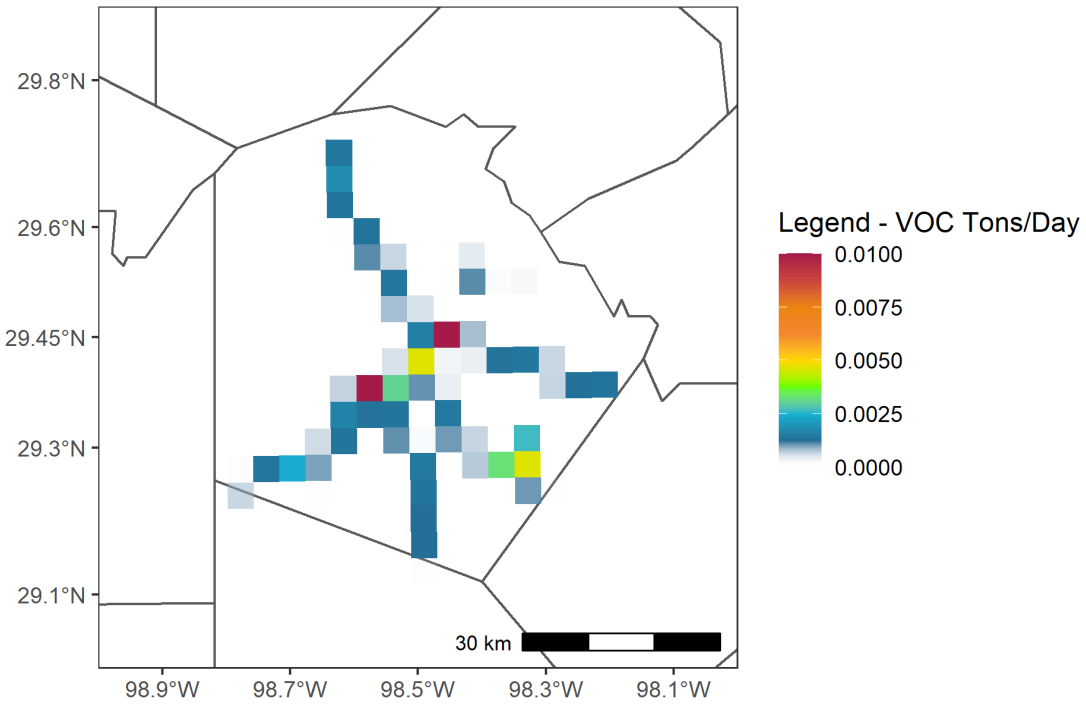

Figure 1-94: 2019 Base Case Locomotive VOC Emissions for June 12 Episode Day in Bexar County

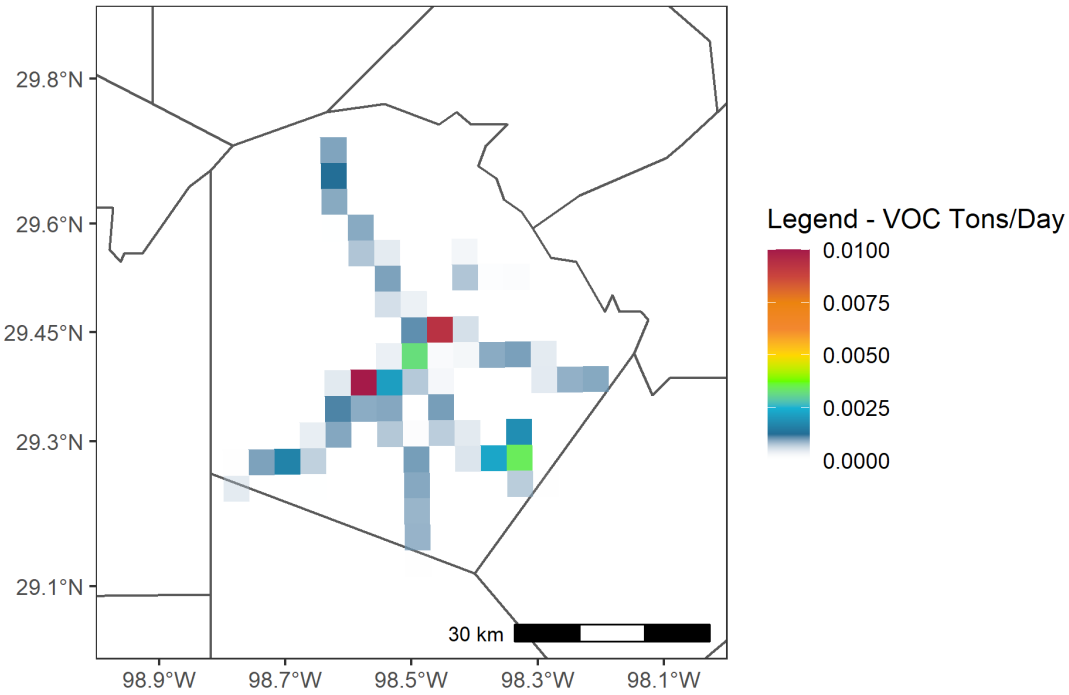

Figure 1-95: 2023 Future Case Locomotive VOC Emissions for June 12 Episode Day in Bexar County

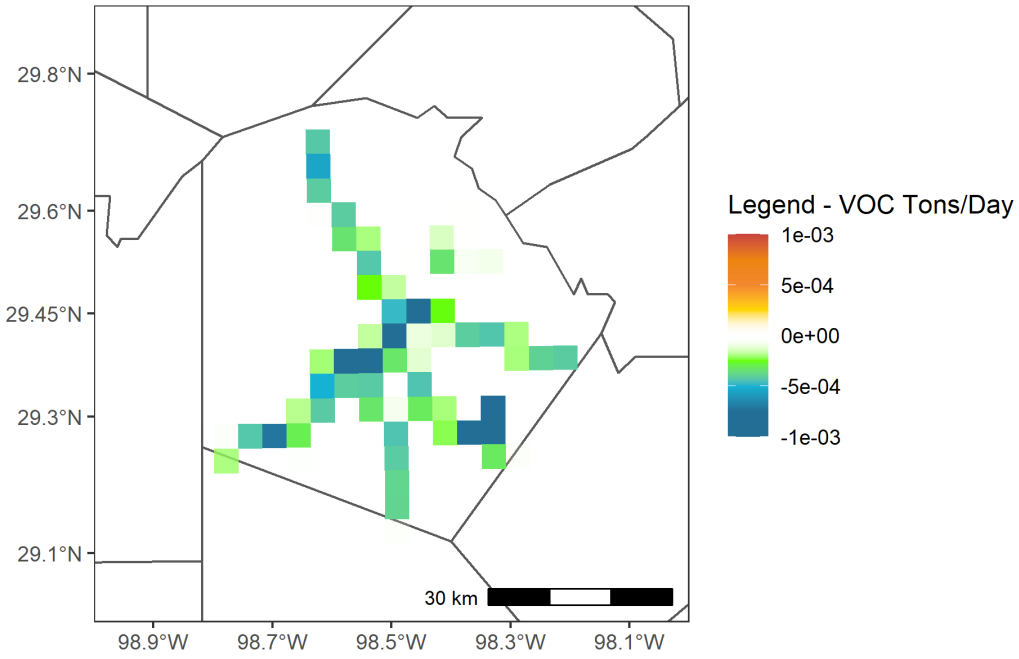

Figure 1-96: Difference in Locomotive VOC Emissions for the June 12 Episode Day Between 2023 and 2019 in Bexar County

1.5 AREA SOURCES

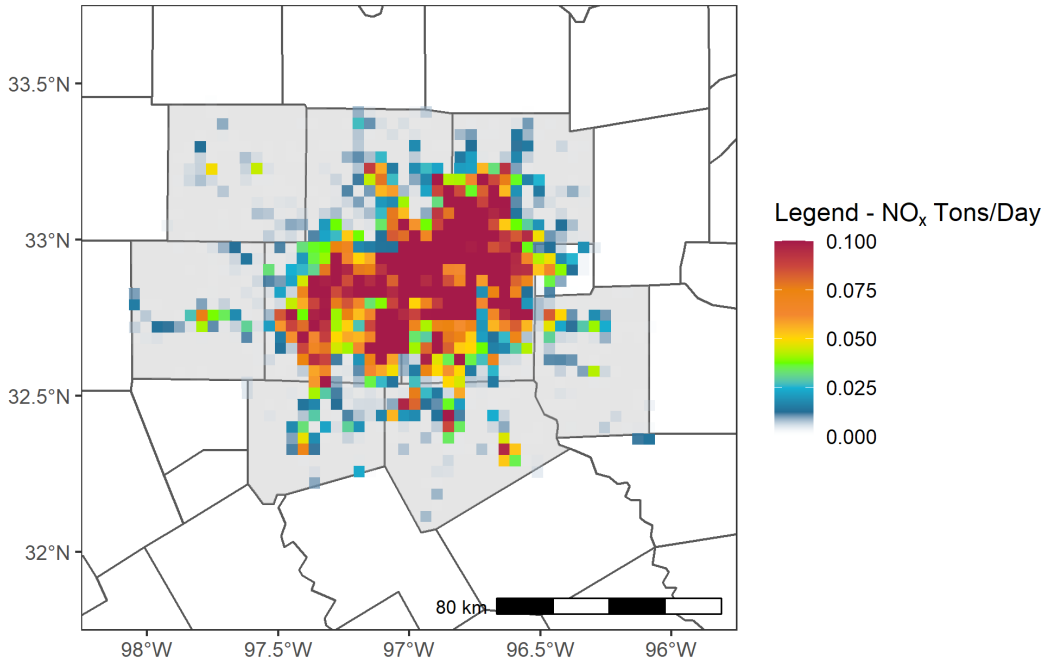

Figure 1-97: 2019 Base Case Area NO_x Emissions for June 12 Episode Day in DFW

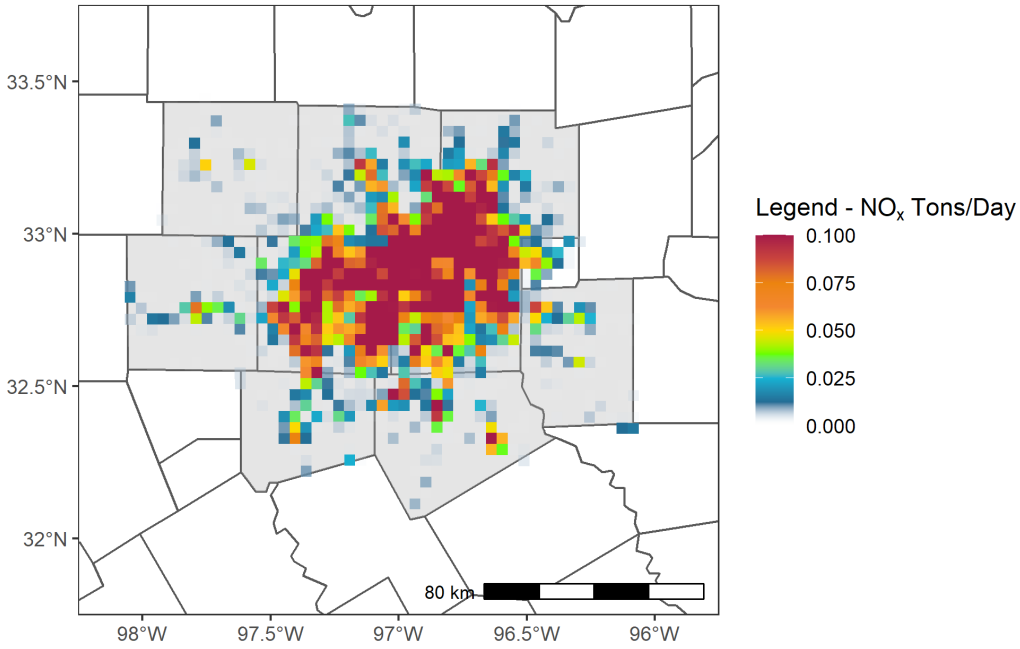

Figure 1-98: 2023 Future Case Area NO_x Emissions for June 12 Episode Day in DFW

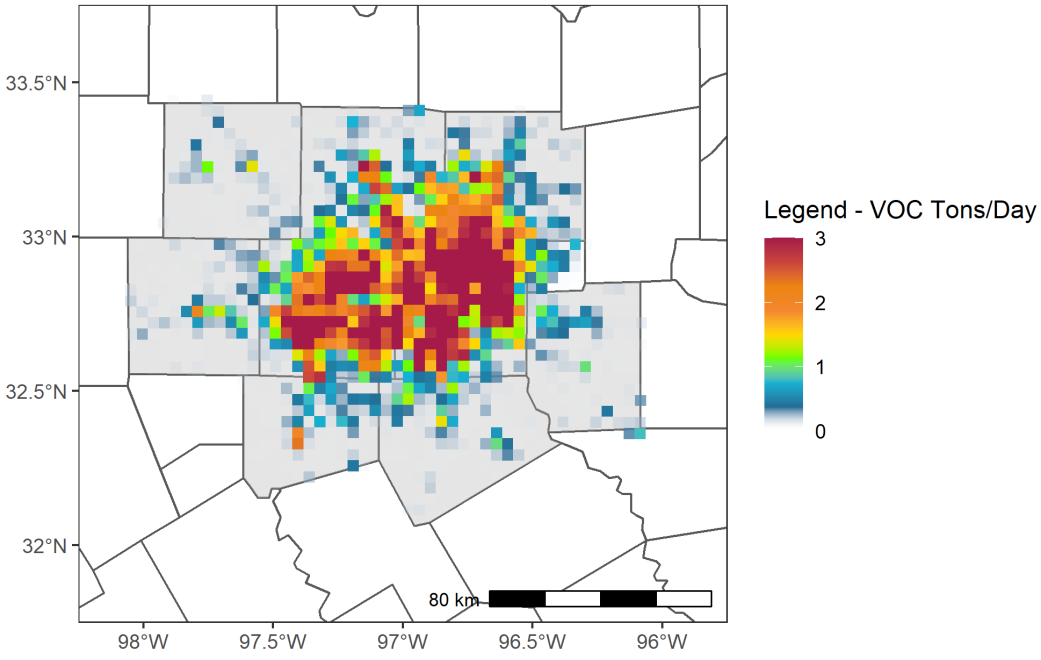

Figure 1-99: 2019 Base Case Area VOC Emissions for June 12 Episode Day in DFW

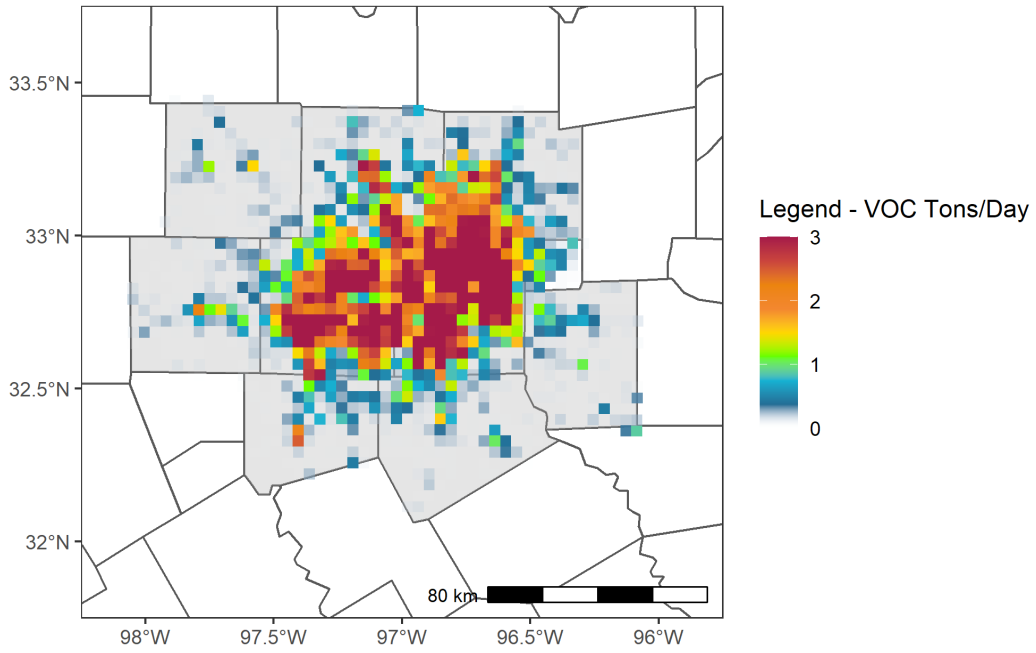

Figure 1-100: 2023 Future Case Area VOC Emissions for June 12 Episode Day in DFW

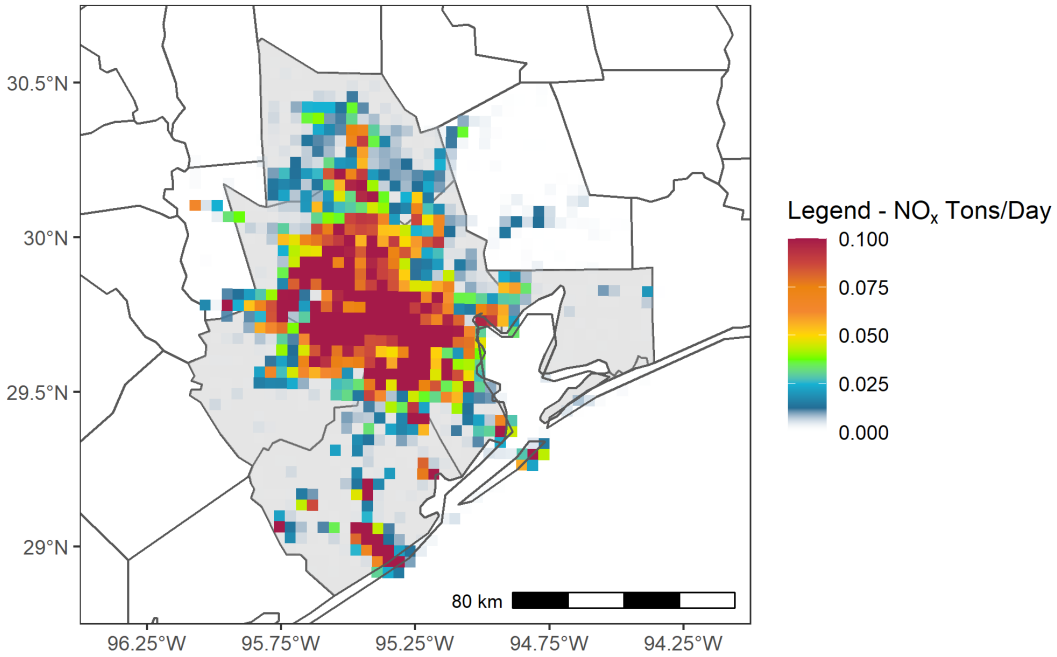

Figure 1-101: 2019 Base Case Area NO_x Emissions for June 12 Episode Day in HGB

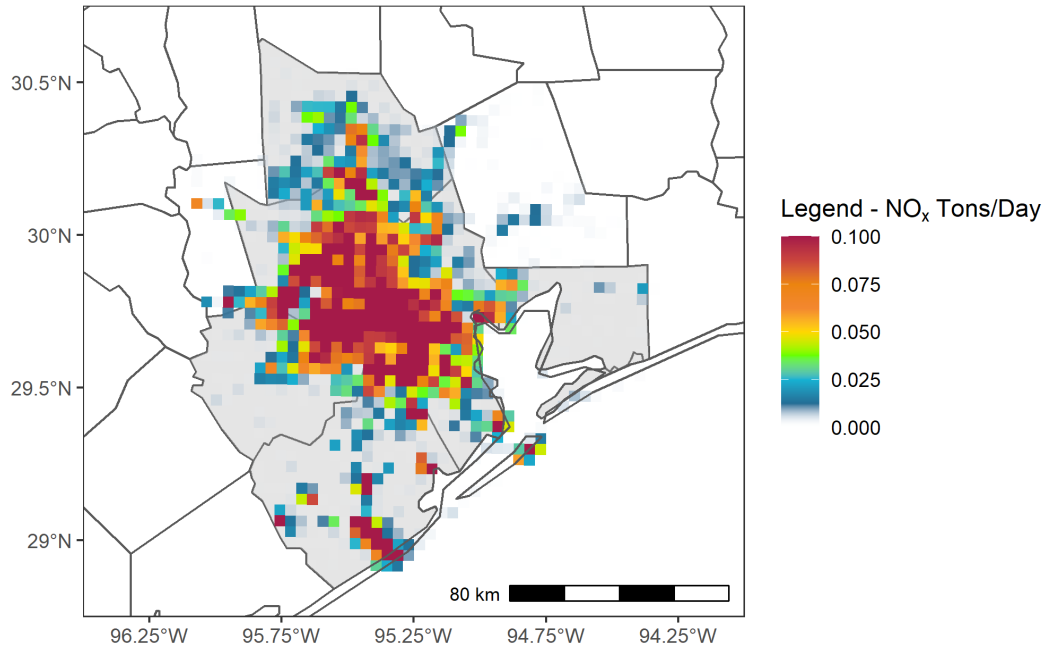

Figure 1-102: 2023 Future Case Area NO_x Emissions for June 12 Episode Day in HGB

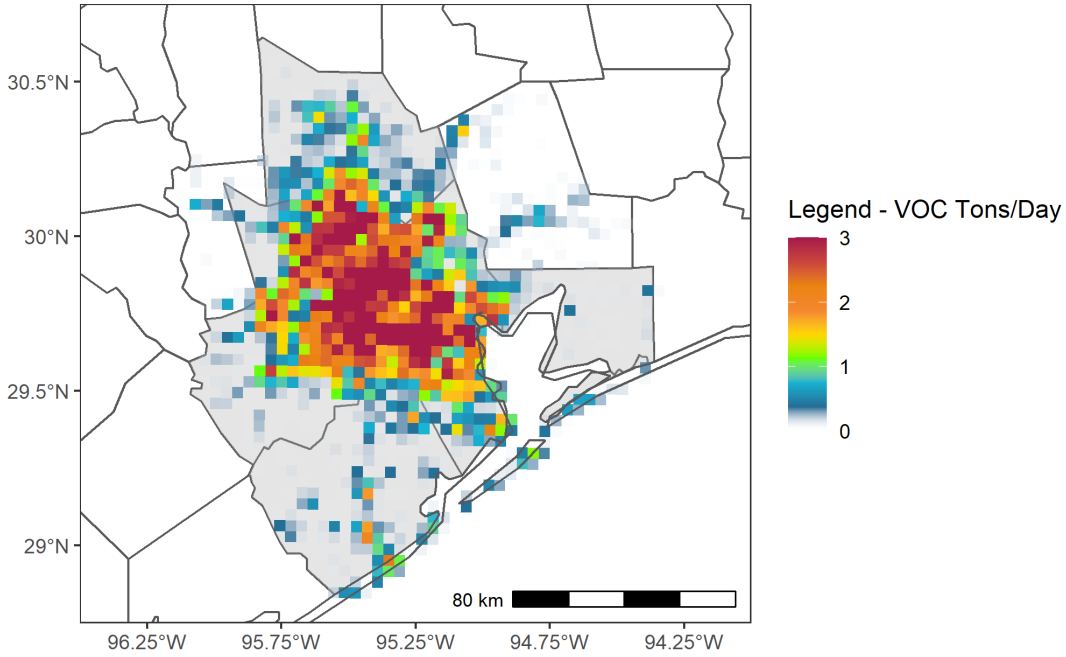

Figure 1-103: 2019 Base Case Area VOC Emissions for June 12 Episode Day in HGB

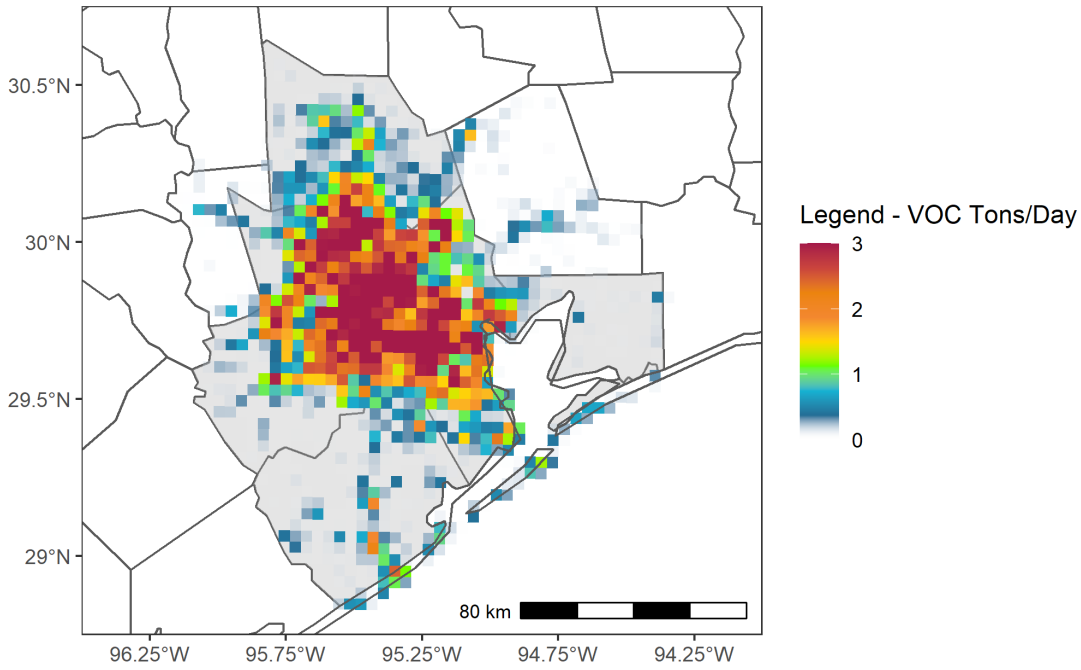

Figure 1-104: 2023 Future Case Area VOC Emissions for June 12 Episode Day in HGB

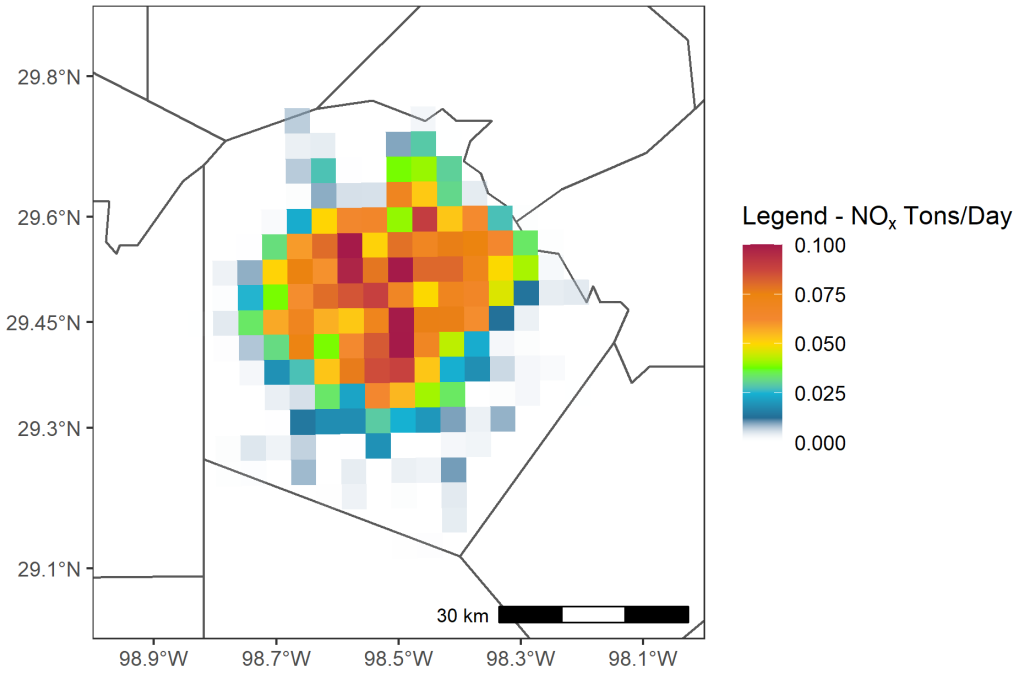

Figure 1-105: 2019 Base Case Area NO_x Emissions for June 12 Episode Day in Bexar County

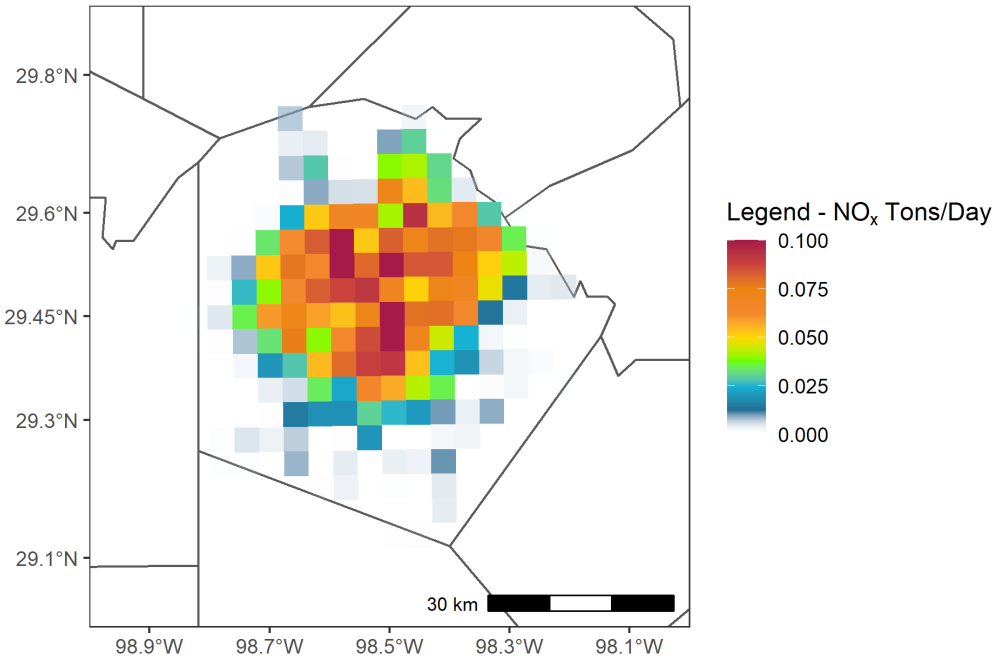

Figure 1-106: 2023 Future Case Area NO_x Emissions for June 12 Episode Day in Bexar County

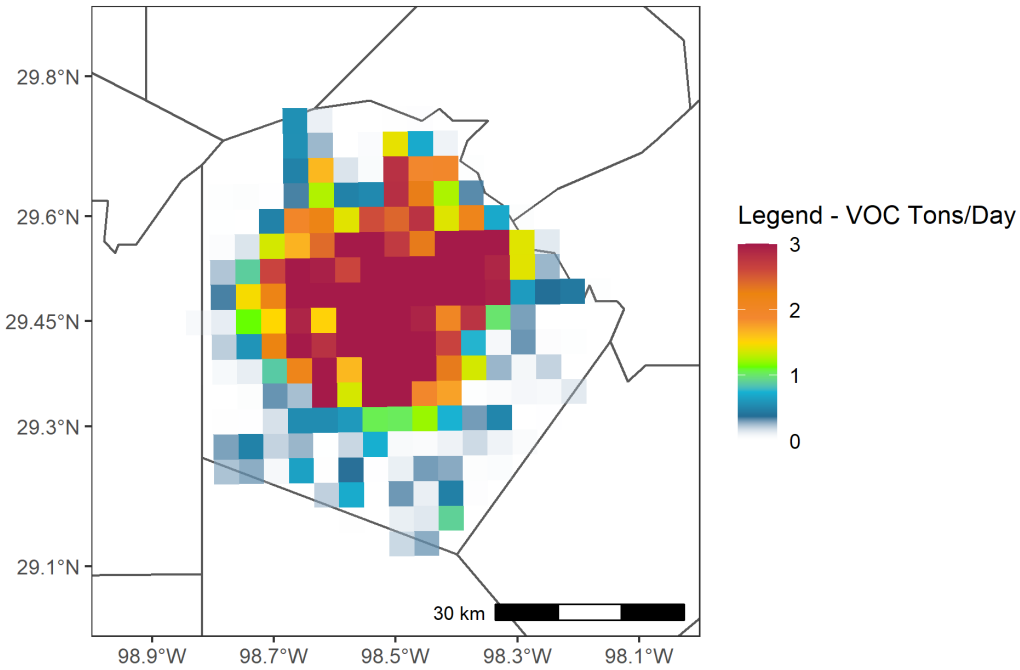

Figure 1-107: 2019 Base Case Area VOC Emissions for June 12 Episode Day in Bexar County

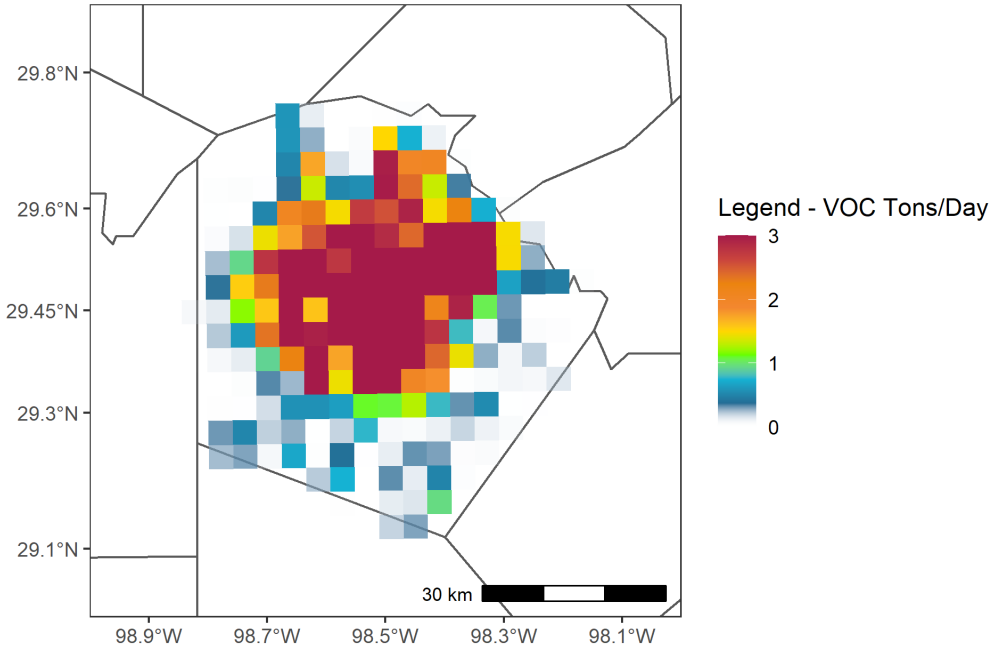

Figure 1-108: 2023 Future Case Area VOC Emissions for June 12 Episode Day in Bexar County

1.6 OIL AND GAS SOURCES

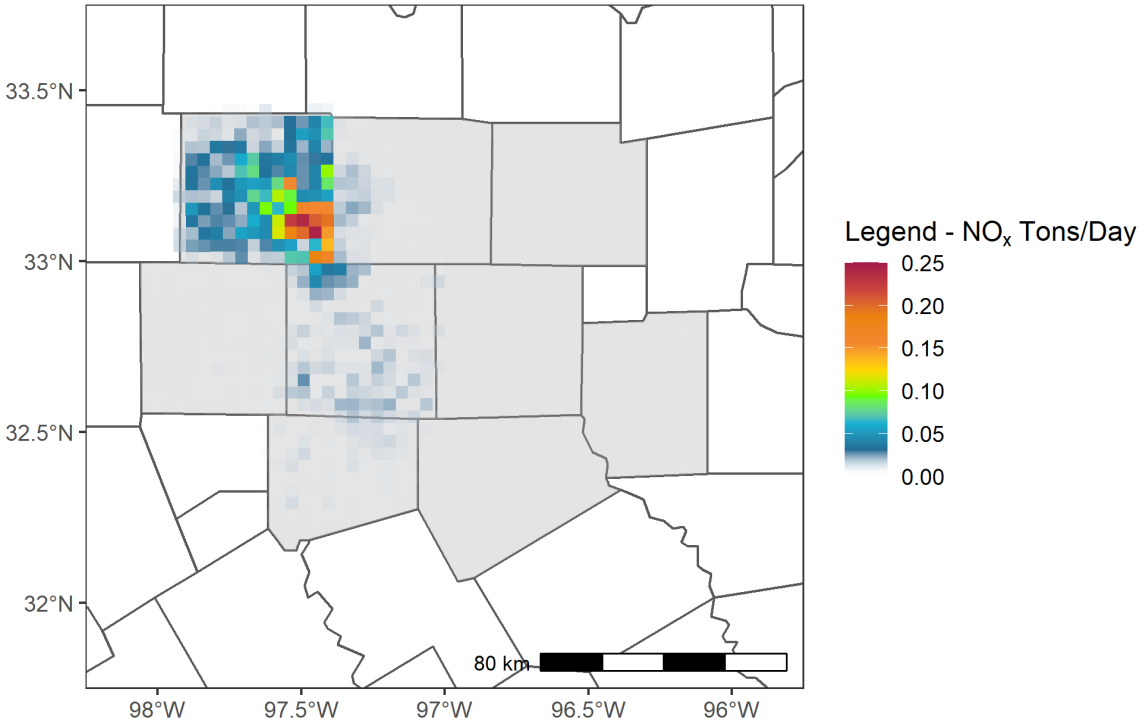

Figure 1-109: 2019 Base Case Oil and Gas Production NO_x Emissions for June 12 Episode Day in DFW

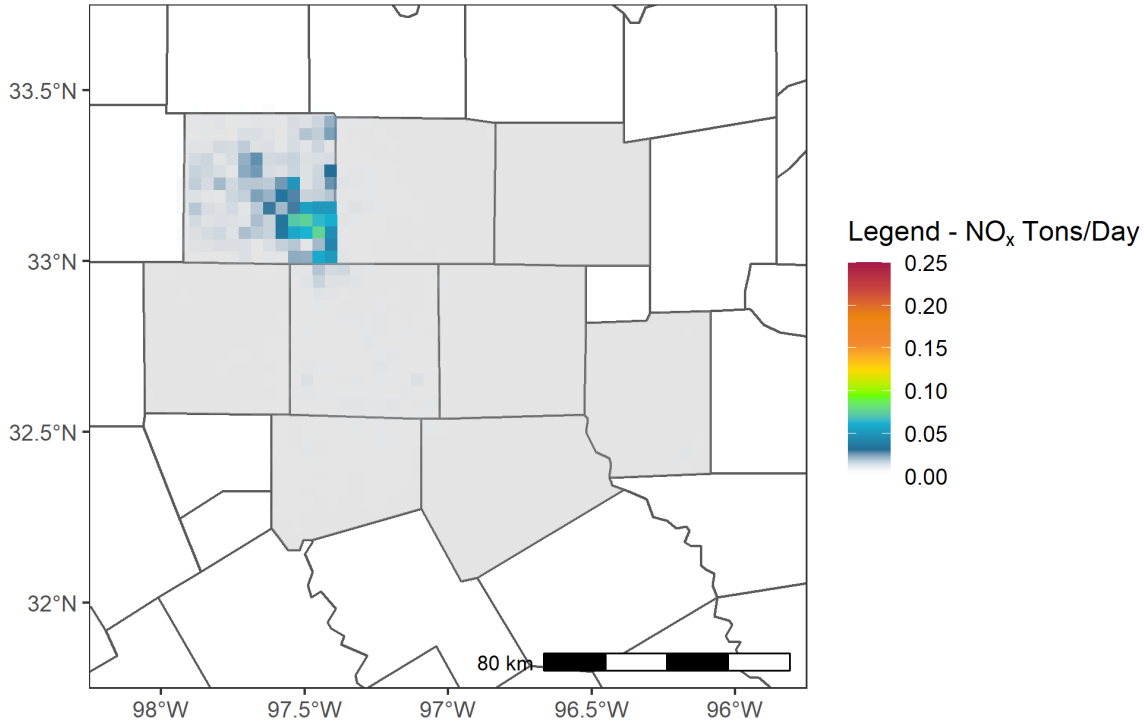

Figure 1-110: 2023 Future Case Oil and Gas Production NO_x Emissions for June 12 Episode Day in DFW

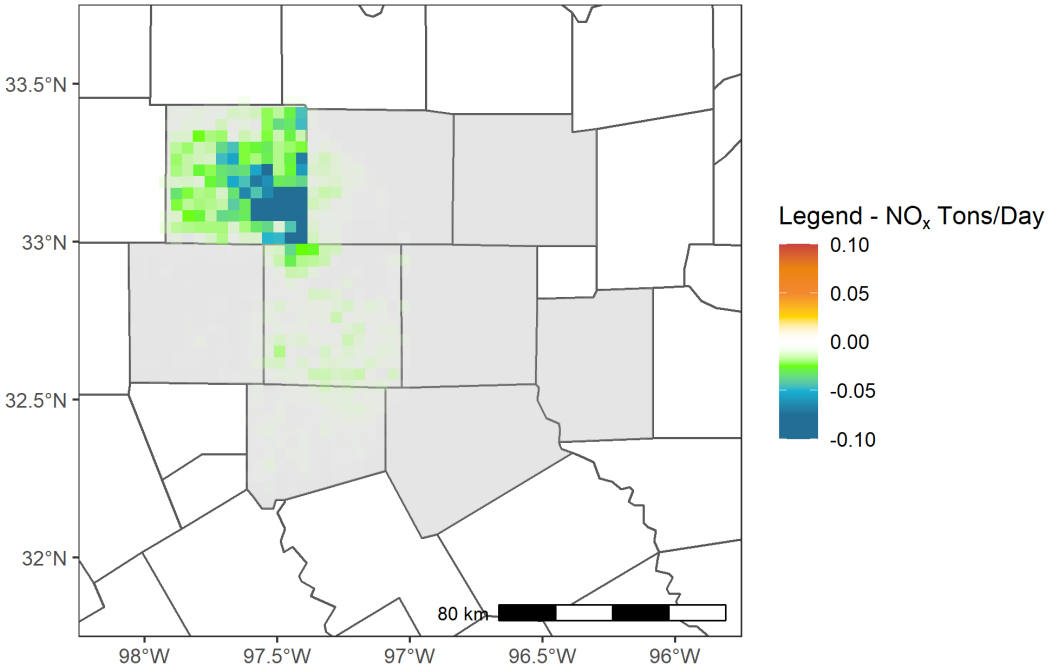

Figure 1-111: Difference in Oil and Gas Production NO_x Emissions for the June 12 Episode Day Between 2023 and 2019 in DFW

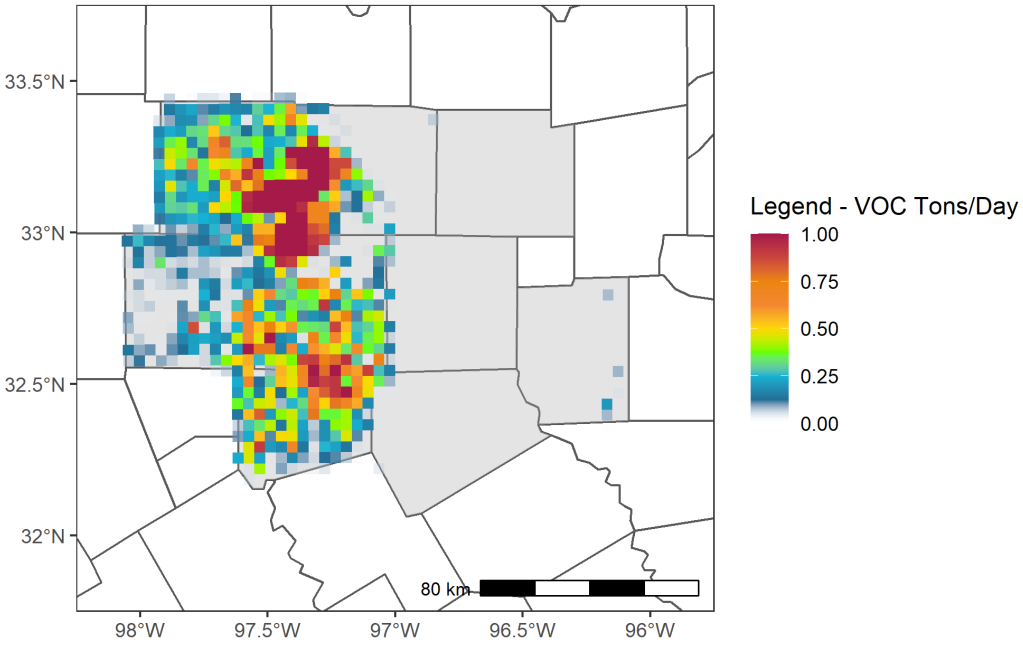

Figure 1-112: 2019 Base Case Oil and Gas Production VOC Emissions for June 12 Episode Day in DFW

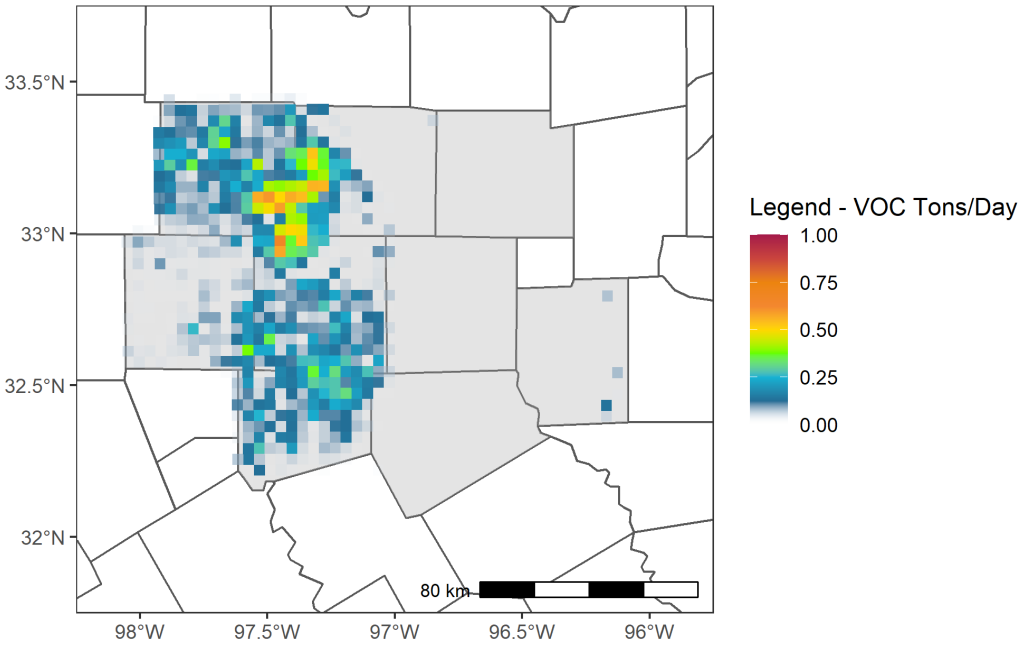

Figure 1-113: 2023 Future Case Oil and Gas Production VOC Emissions for June 12 Episode Day in DFW

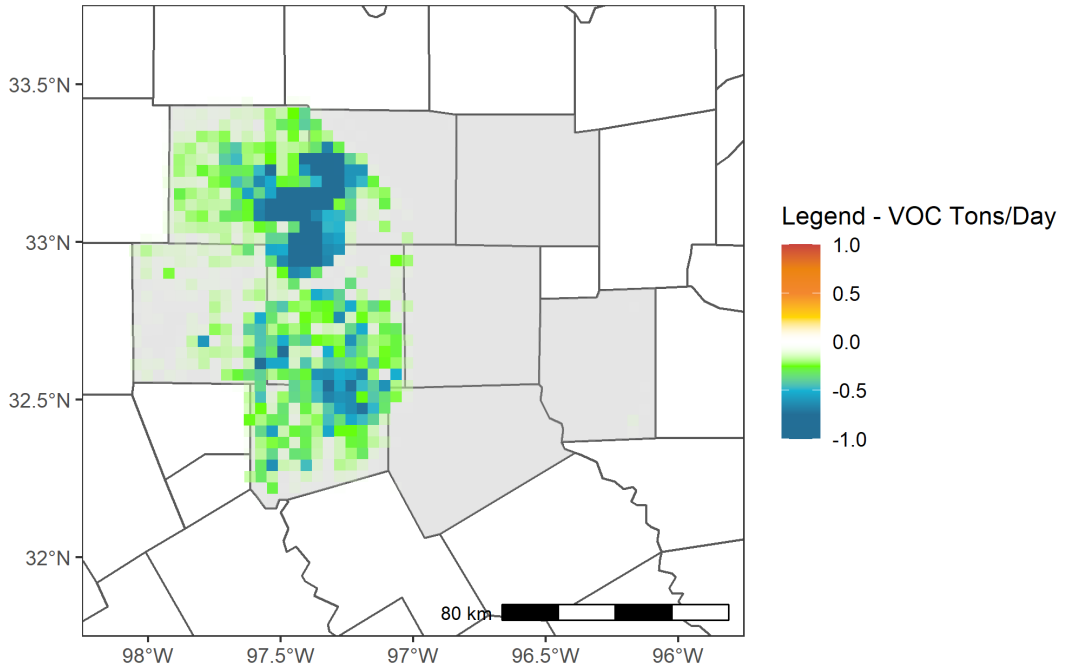

Figure 1-114: Difference in Oil and Gas Production VOC Emissions for the June 12 Episode Day Between 2023 and 2019 in DFW

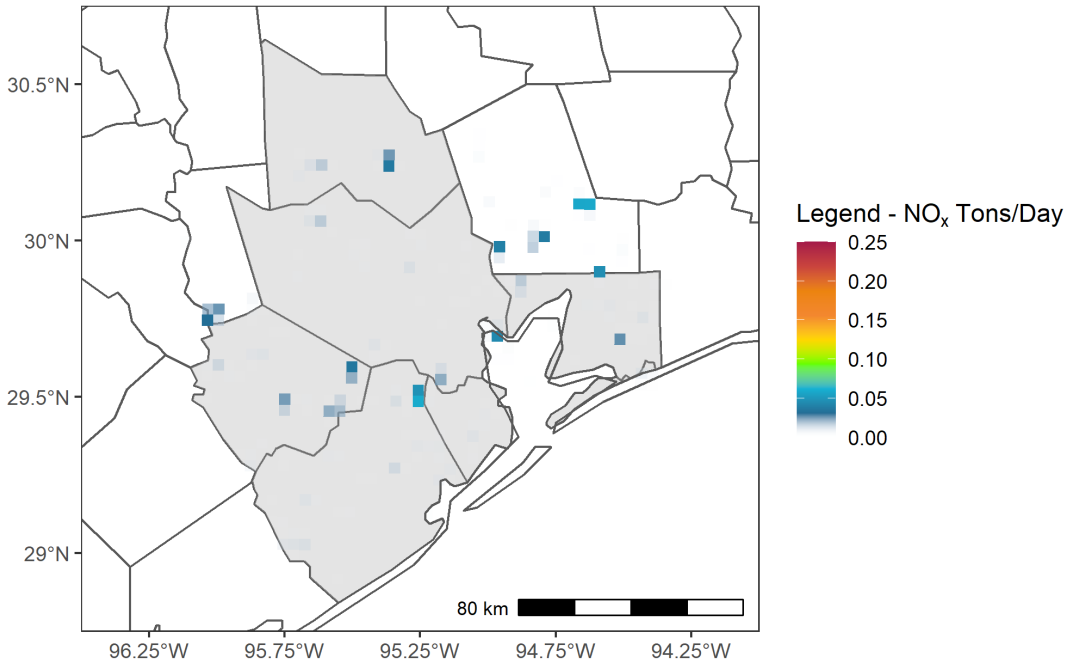

Figure 1-115: 2019 Base and 2023 Future Case Oil and Gas Production NO_x Emissions for June 12 Episode Day in HGB

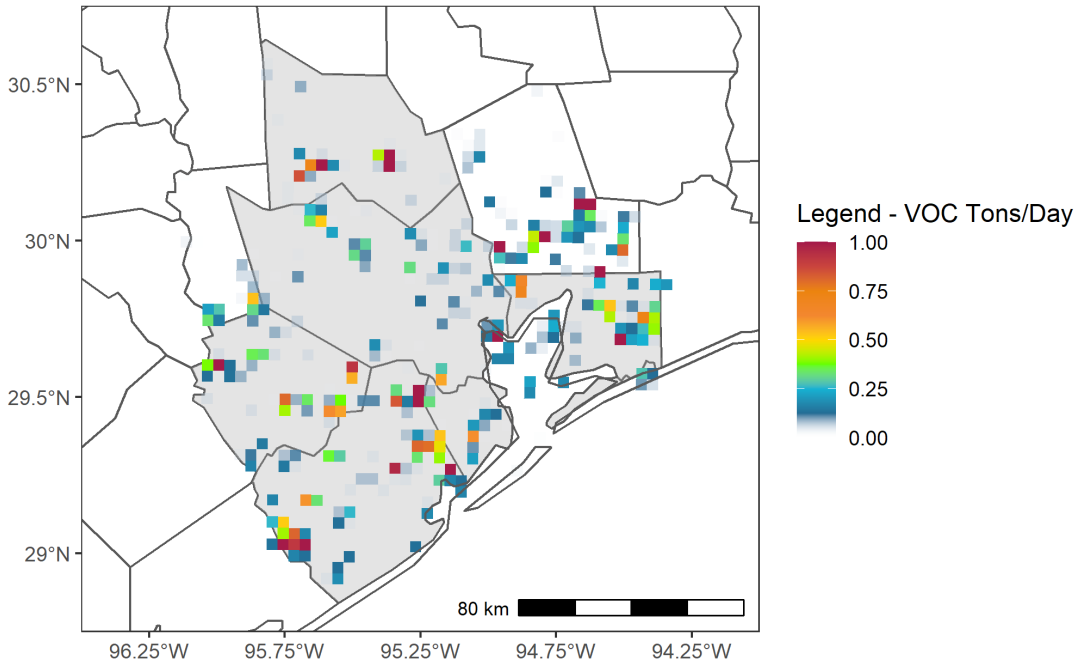

Figure 1-116: 2019 Base Case Oil and Gas Production VOC Emissions for June 12 Episode Day in DFW

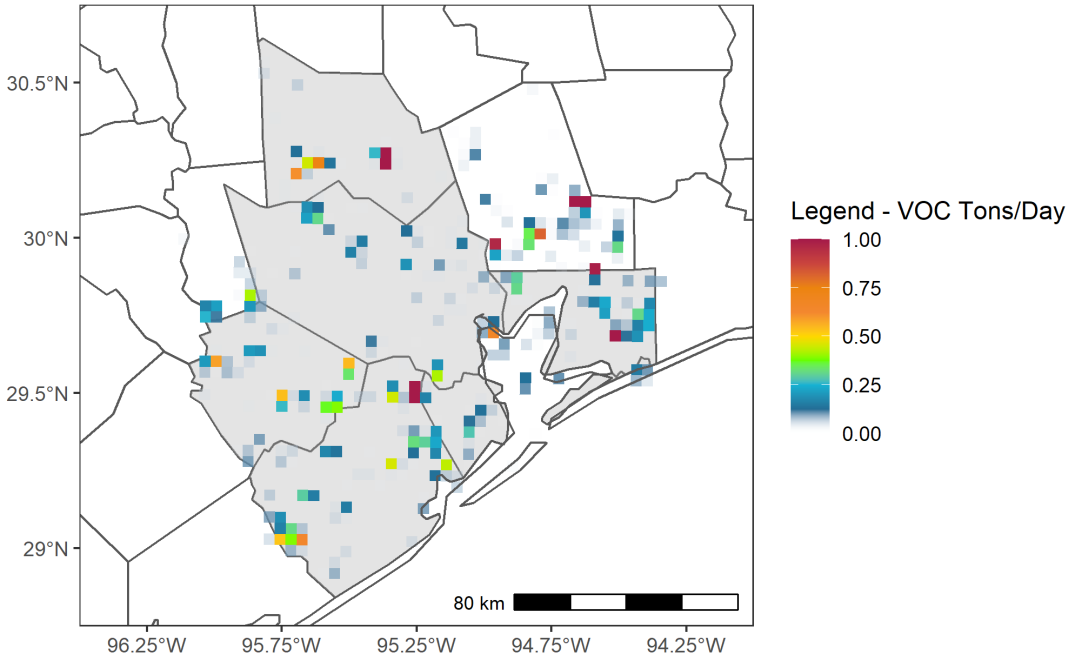

Figure 1-117: 2023 Future Case Oil and Gas Production VOC Emissions for June 12 Episode Day in HGB

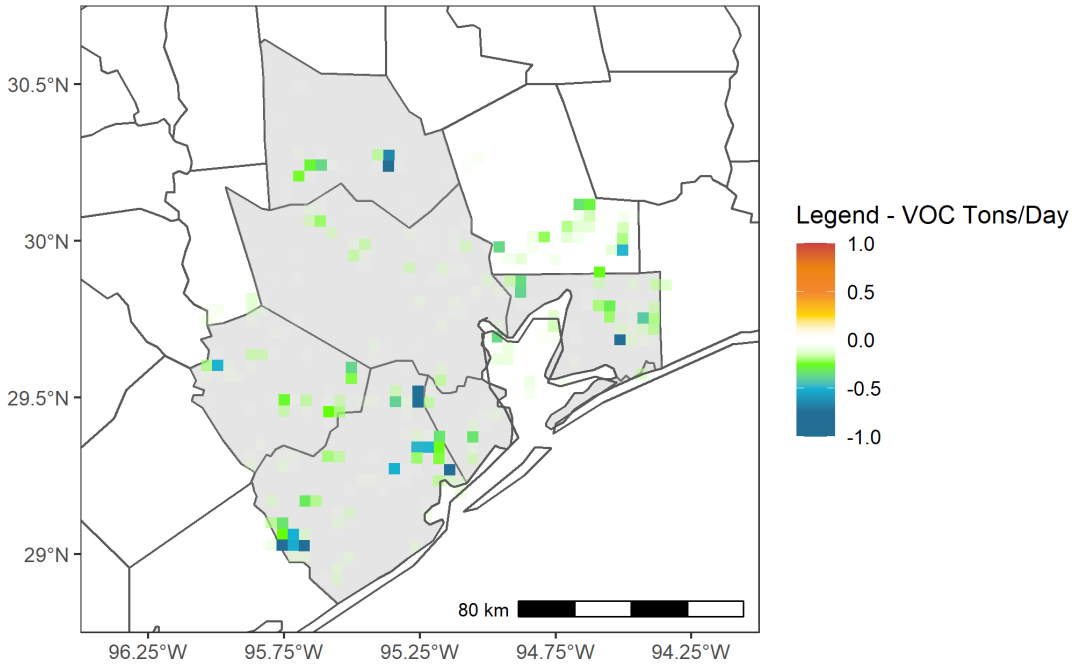

Figure 1-118: Difference in Oil and Gas Production VOC Emissions for the June 12 Episode Day Between 2023 and 2019 in HGB

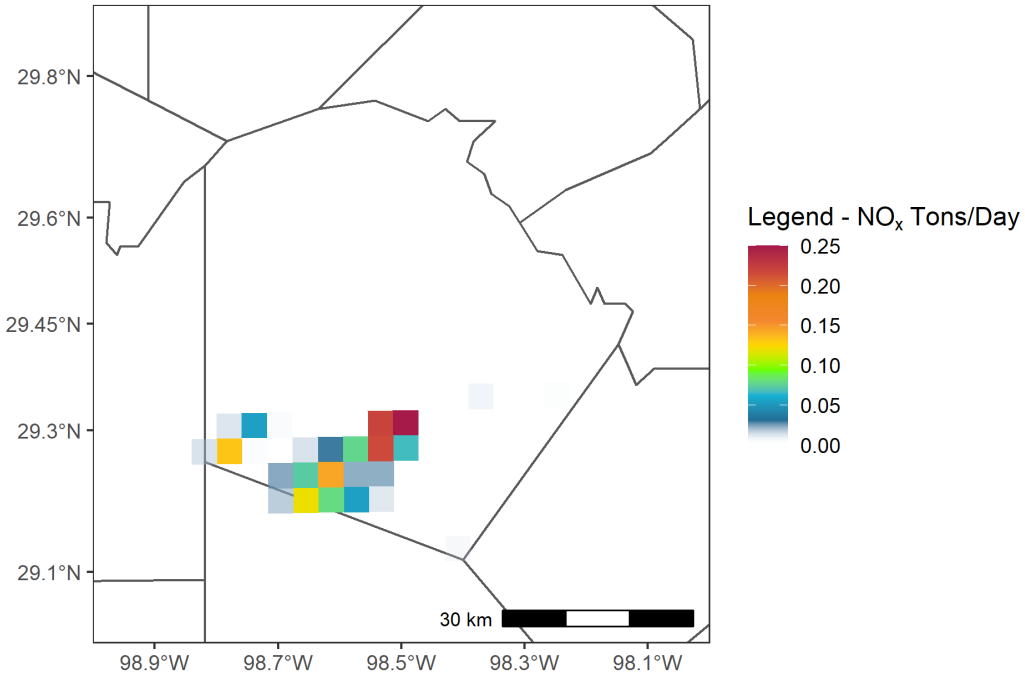

Figure 1-119: 2019 Base and 2023 Future Case Oil and Gas Production NO_x Emissions for June 12 Episode Day in Bexar County

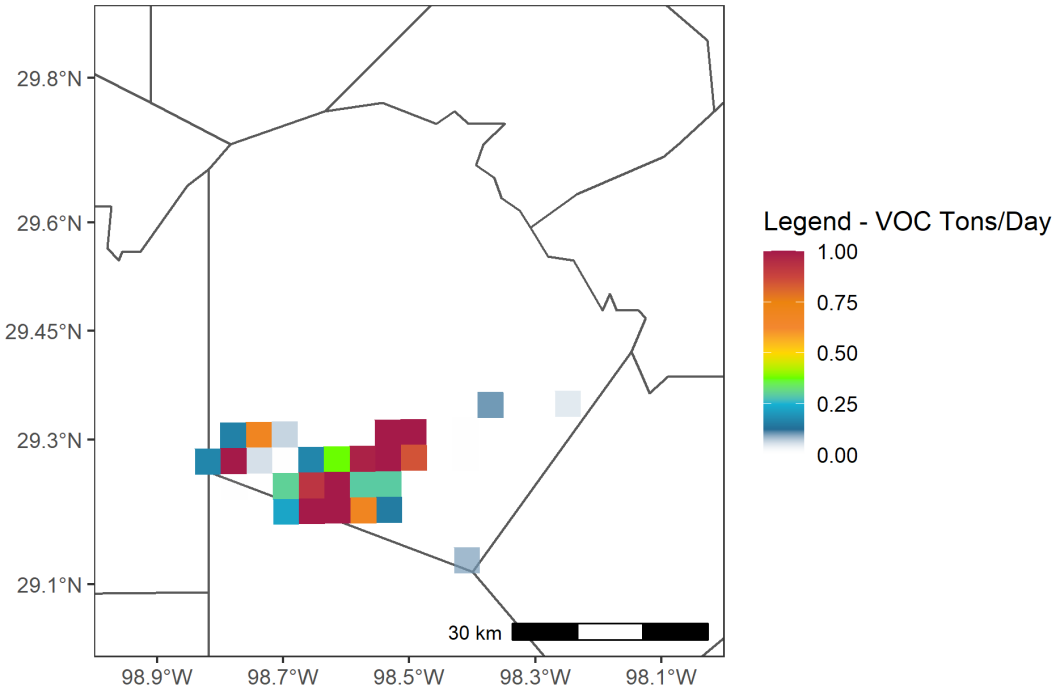

Figure 1-120: 2019 Base and 2023 Future Case Oil and Gas Production VOC Emissions for June 12 Episode Day in Bexar County

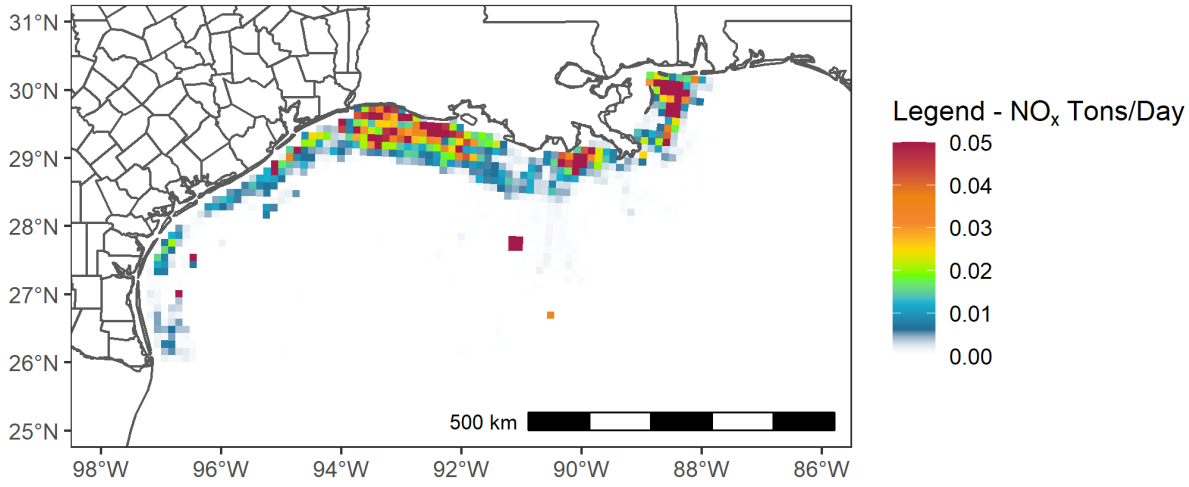

Figure 1-121: 2019 Base and 2023 Future Case Offshore Non-Platform NO_x Emissions for June Episode Day in Gulf of Mexico (12km grid cells)

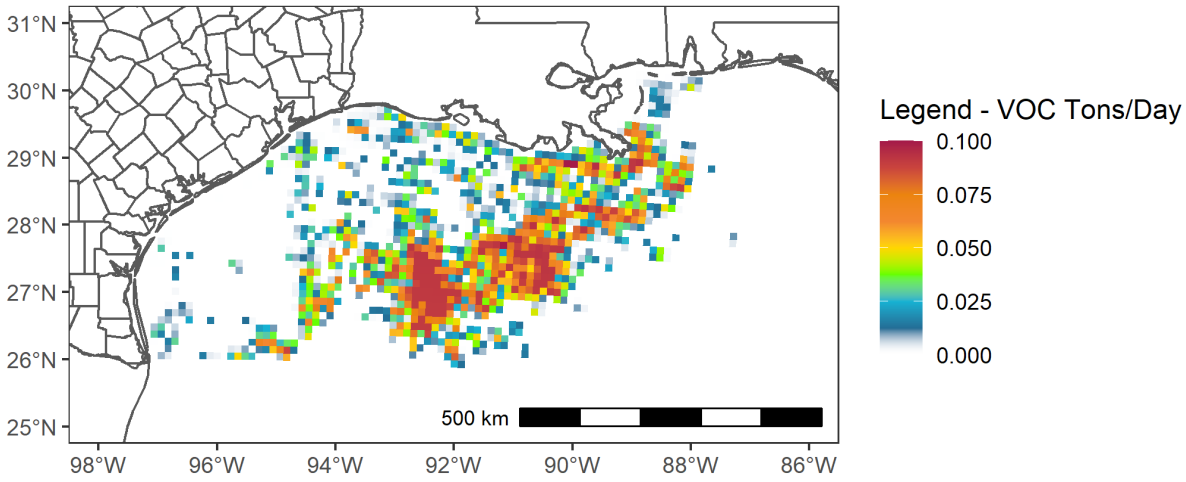

Figure 1-122: 2019 Base and 2023 Future Case Offshore Non-Platform VOC Emissions for June Episode Day in Gulf of Mexico (12km grid cells)

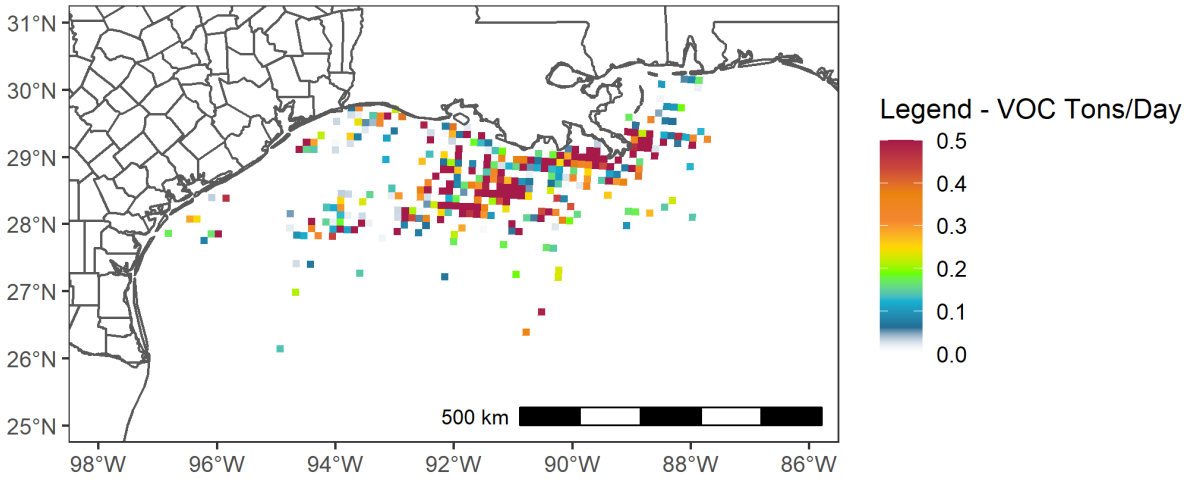

Figure 1-123: 2019 Base and 2023 Future Case Offshore Platform Low-Level NO_x Emissions for June Episode Day in Gulf of Mexico (12km grid cells)

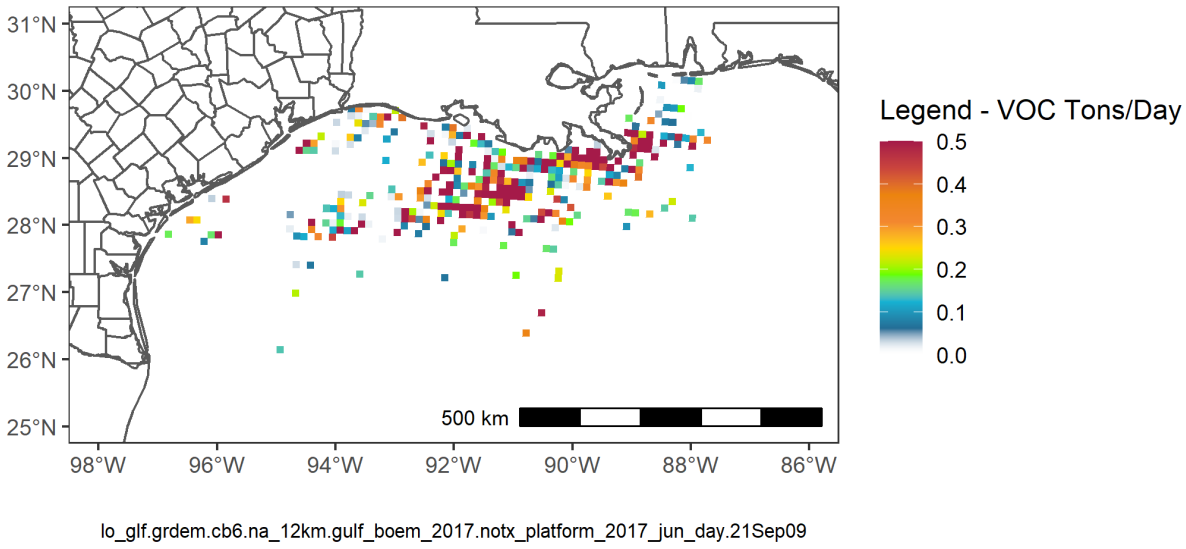

Figure 1-124: 2019 Base and 2023 Future Case Offshore Platform Low-Level NO_x Emissions for June Episode Day in Gulf of Mexico (12km grid cells)

2. MPE PLOTS

This section of Attachment 1 presents monthly figures showing the model performance at individual monitors in the HGB, DFW, and Bexar County 2015 ozone nonattainment areas. Performance is shown on three types of plots:

- Bar charts that compare measured and modeled MDA8 ozone for each day of the given month.
- Timeseries that show measured and modeled hourly ozone in a given month. In general, the model follows diurnal profile of daytime ozone concentrations peaks and nighttime low values. The model tends to overpredict nighttime values when measured concentrations were close to zero.
- Scatter plots compare measured and modeled hourly ozone values for each month. Overlaid on the scatter plots are pink symbols showing Quantile-Quantile plot (Q-Q plot), which compares how well the model predicts ozone concentrations in the same range as the observed without respect to time. Generally, the model replicates mid-range ozone values well, and tends to underpredict the highest concentrations and overpredict minimum values.

For each area, for each month the MPE plots are provided for the monitor that had high observed ozone in that month relative to other monitors in the area.

2.1 HGB

2.1.1 April

Most MDA8 ozone values were lower than 70 ppb in April. The monitor with the highest MDA8 in April was Bayland monitor that measured 76.7 ppb on April 26. The model underpredicted MDA8 ozone peak on that day.

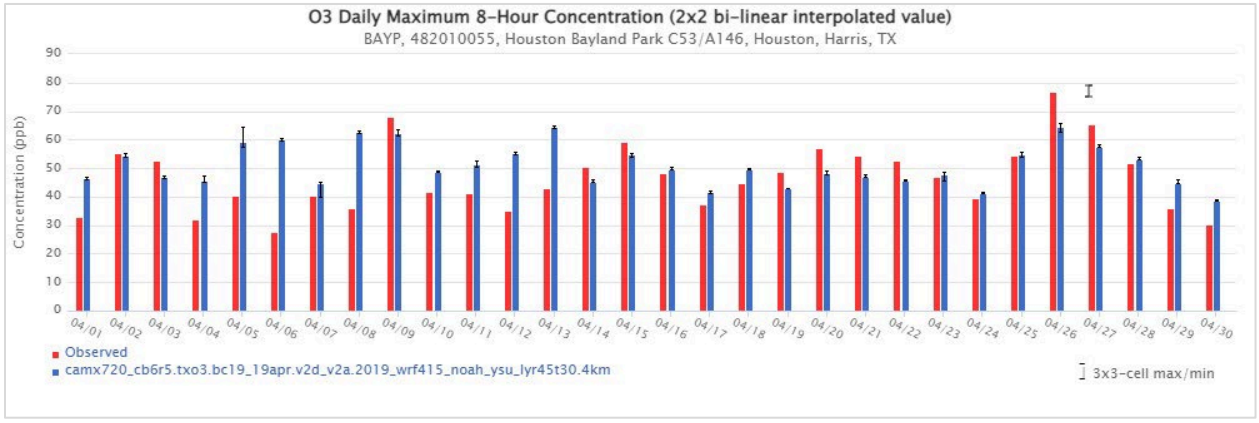

Figure 2-1: April 2019 Observed and Modeled MDA8 at Bayland Monitor

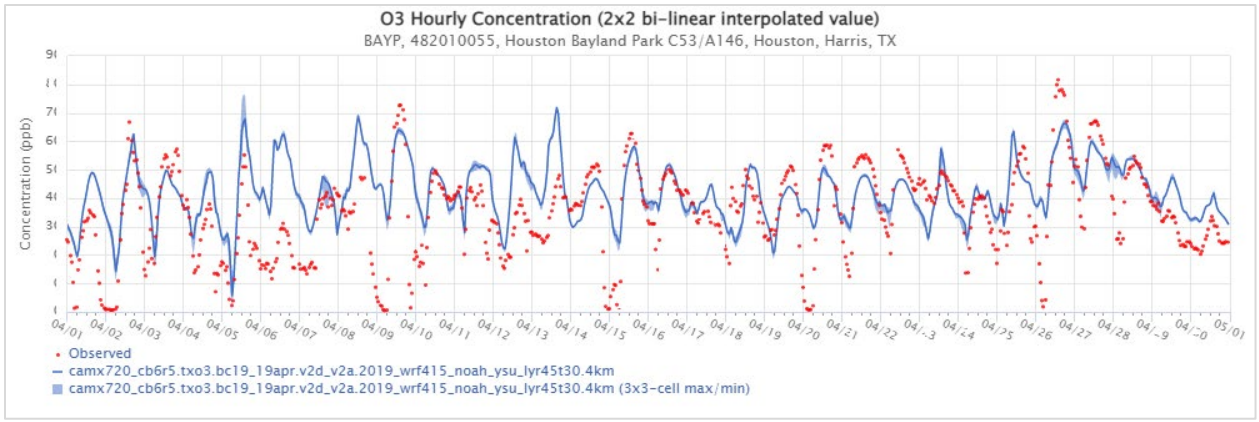

Figure 2-2: April 2019 Observed and Modeled Hourly Ozone at Bayland Monitor

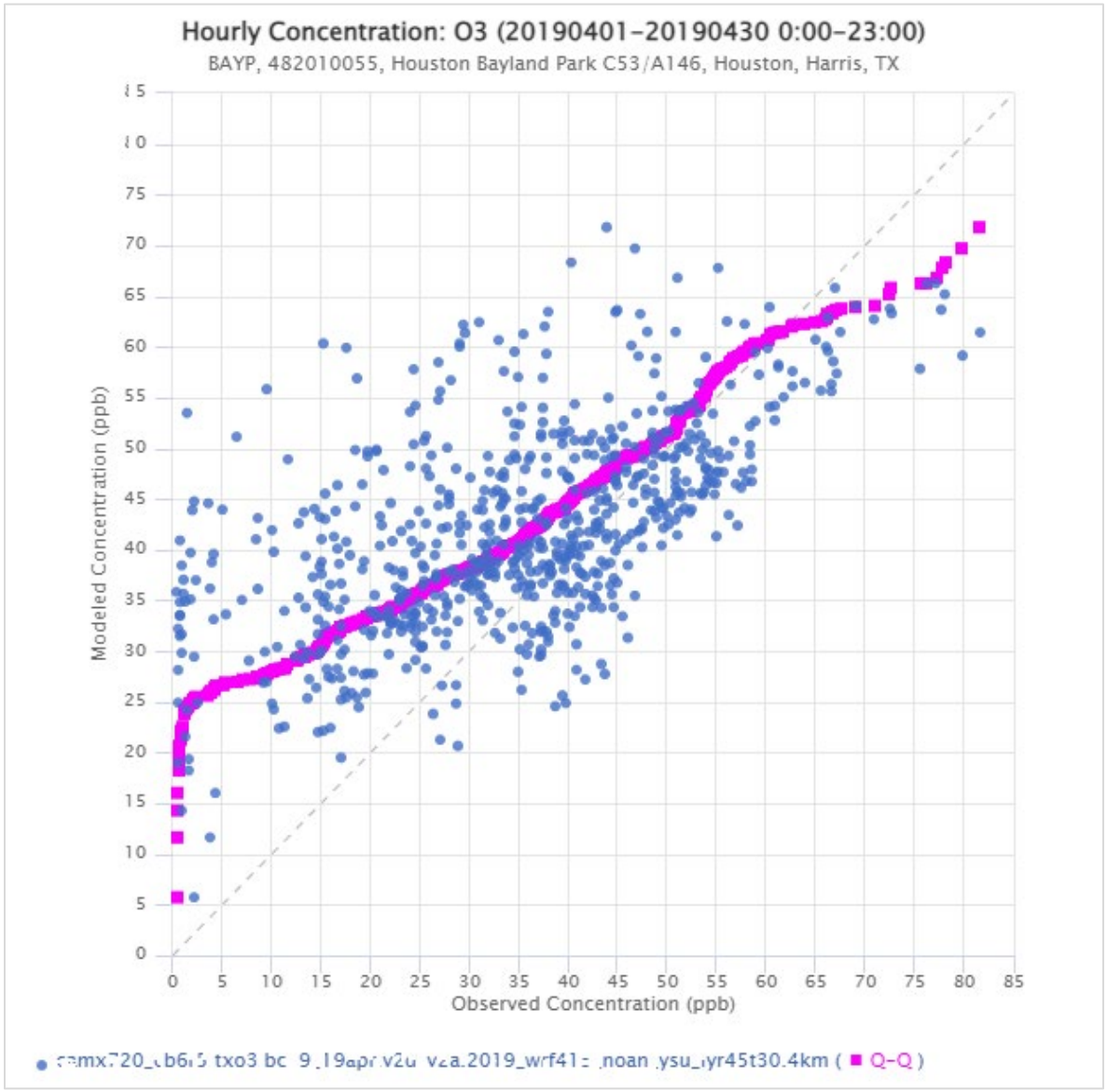

Figure 2-3: April 2019 Scatter Plot of Observed versus Modeled Hourly Ozone at Bayland Monitor

2.1.2 May

A couple of monitors measured exceedances of MDA8 ozone in May. The monitor with the highest MDA8 ozone was Bayland monitor that measured 81.6 ppb on May 13. The model underpredicted that value.

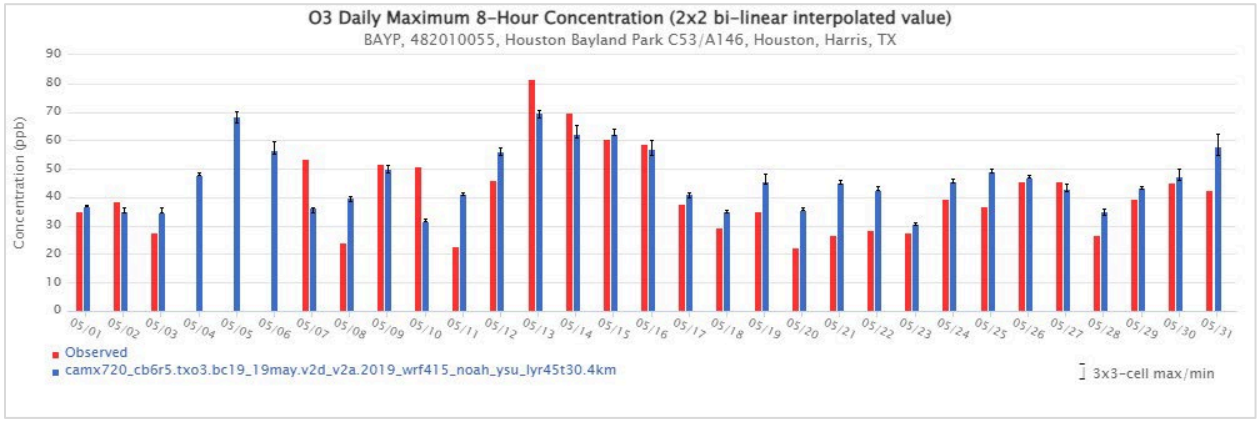

Figure 2-4: May 2019 Observed and Modeled MDA8 at Bayland Monitor

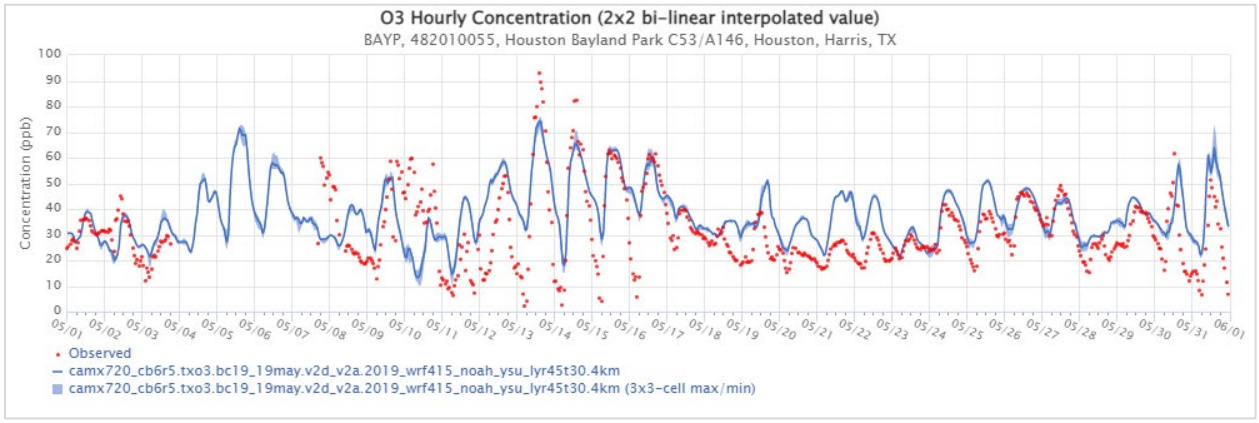

Figure 2-5: May 2019 Observed and Modeled Hourly Ozone Monitor

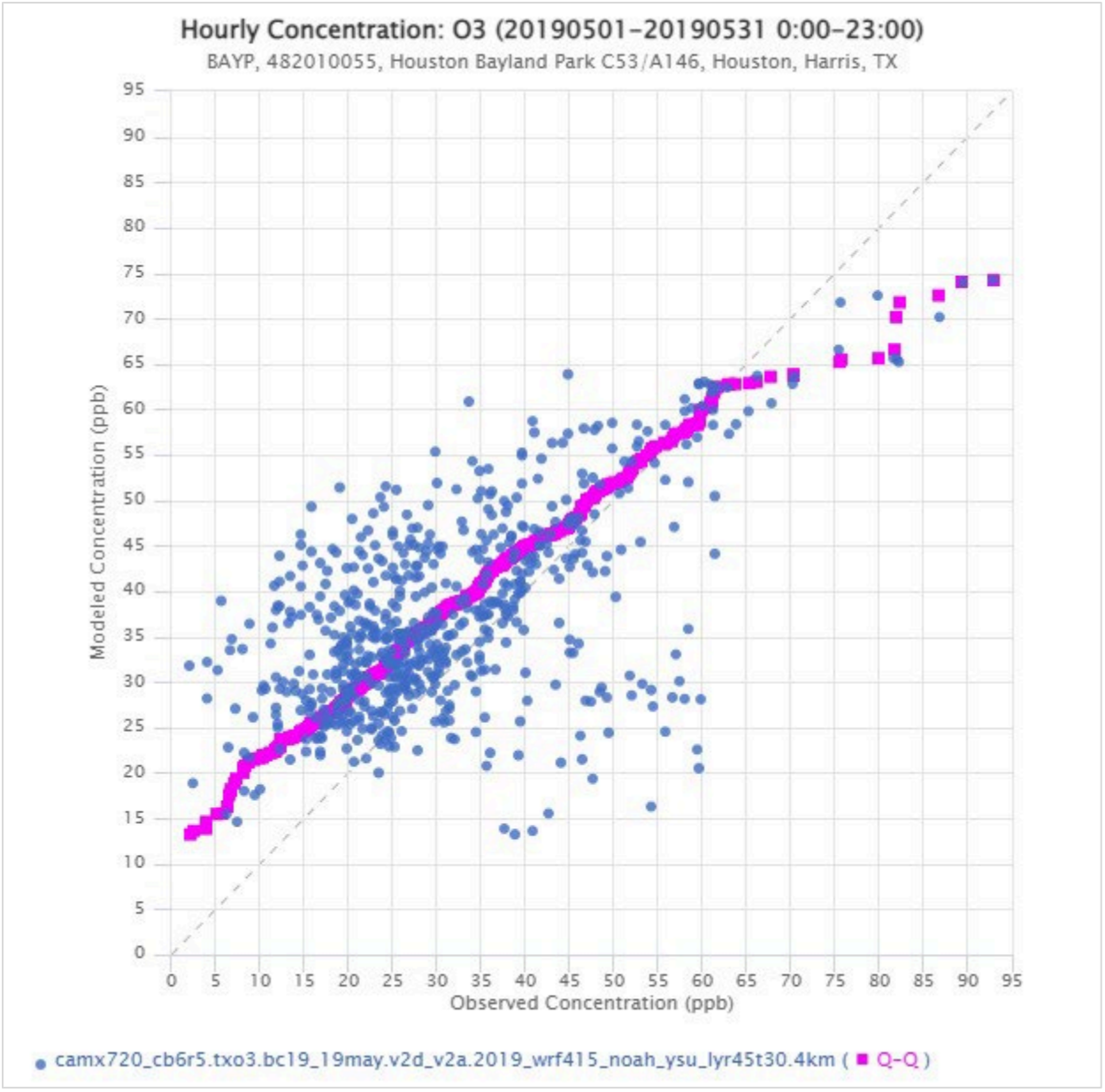

Figure 2-6: May 2019 Scatter Plot of Observed versus Modeled Hourly Ozone at Bayland Monitor

2.1.3 June

June had many exceedance days with multiple monitors recording high values. The highest MDA8 ozone of 93 ppb was measured at Clinton monitor. The model captured the peak well. The highest hourly ozone of 118 ppb was measured on that day, which was also well modeled.

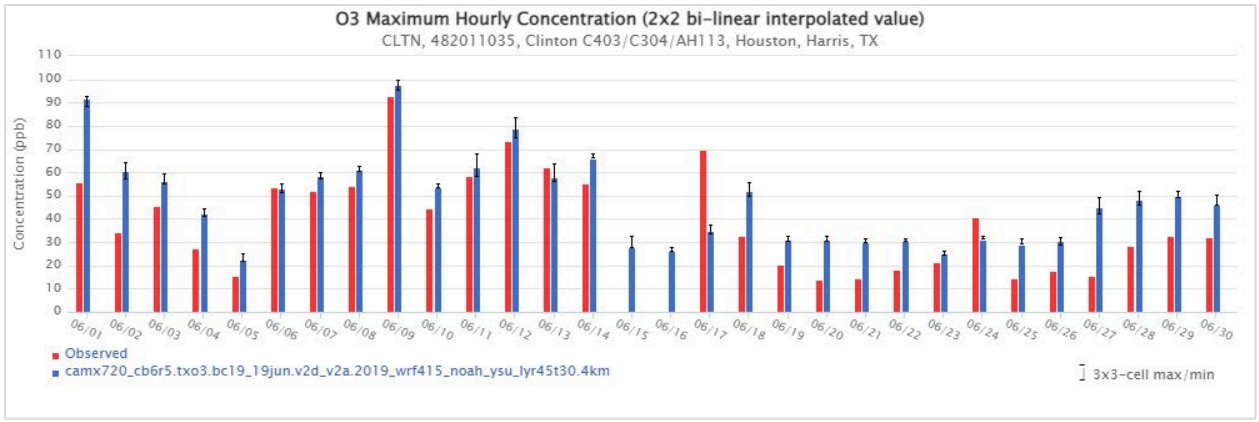

Figure 2-7: June 2019 Observed and Modeled MDA8 at Clinton Monitor

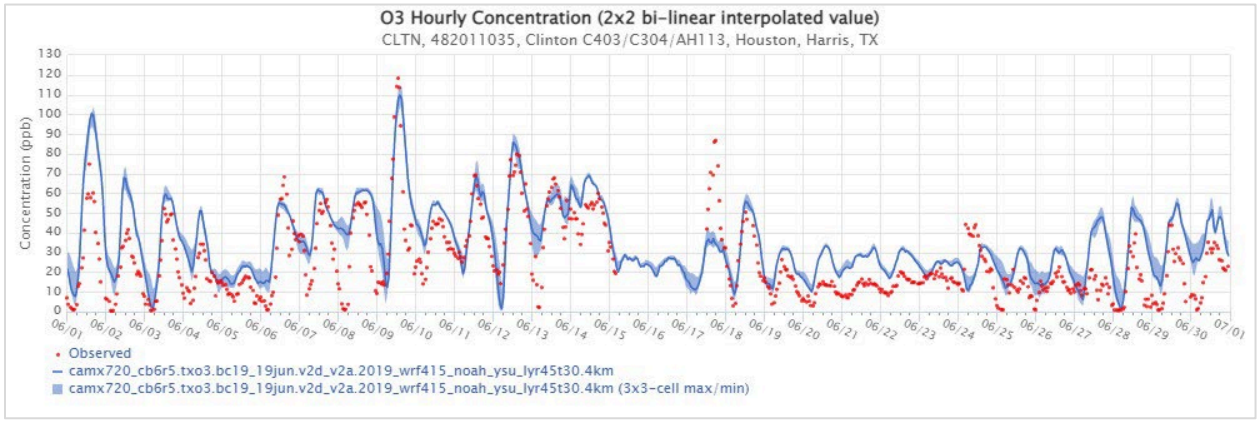

Figure 2-8: June 2019 Observed and Modeled Hourly Ozone at Clinton Monitor

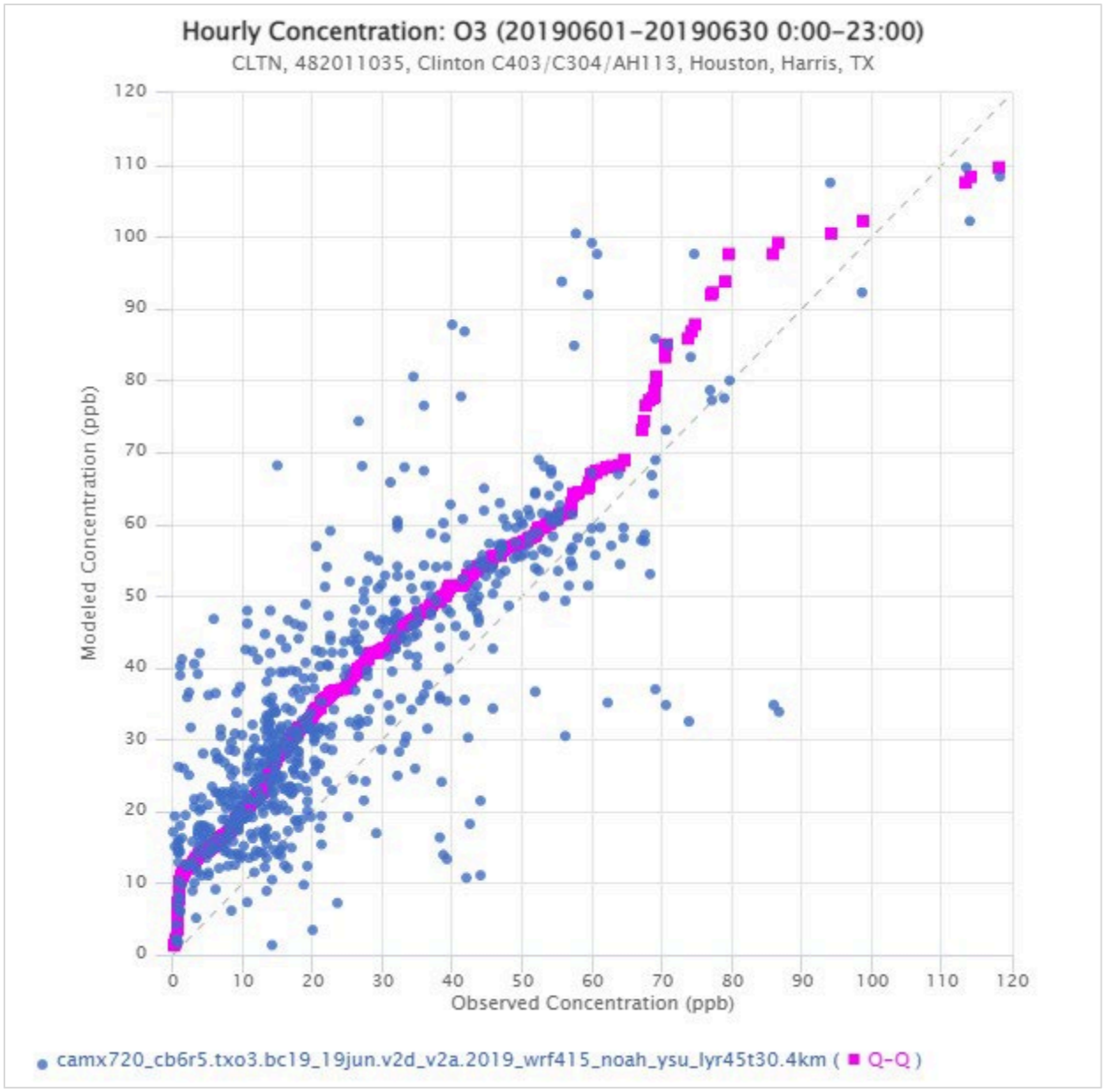

Figure 2-9: June 2019 Scatter Plot of Observed versus Modeled Hourly Ozone at Clinton Monitor

2.1.4 July

On two days in July the observed MDA8 ozone values were above 70 ppb. The highest value of 82.6 ppb was measured at the Tom Bass monitor, which is a non-regulatory monitor. The highest observed MDA8 ozone among regulatory monitors was 79.5 ppb measured on July 25 at the Manvel monitor. Figures below show evaluation at Manvel Monitor. The model slightly underpredicted MDA8 ozone peak on July 25 and hourly ozone peak.

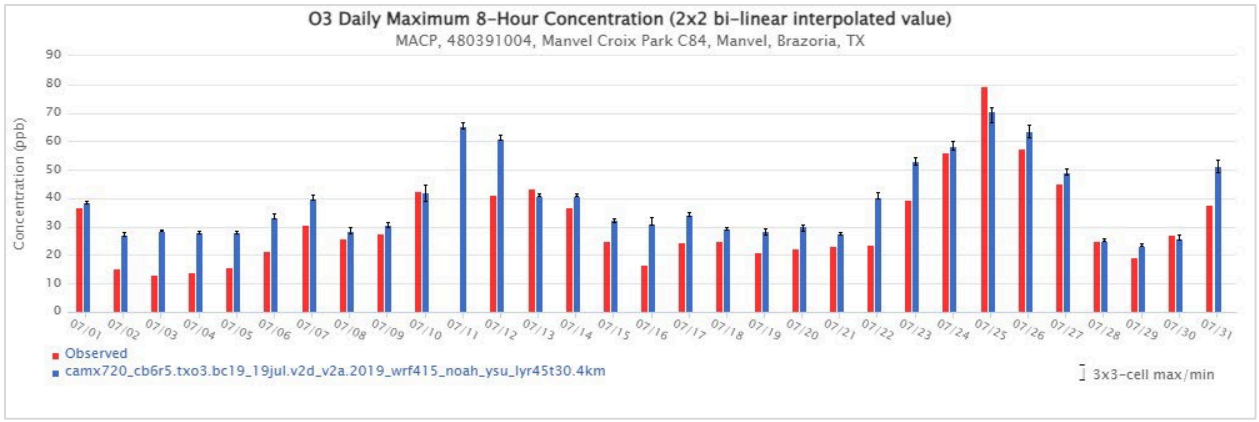

Figure 2-10: July 2019 Observed and Modeled MDA8 at Manvel Monitor

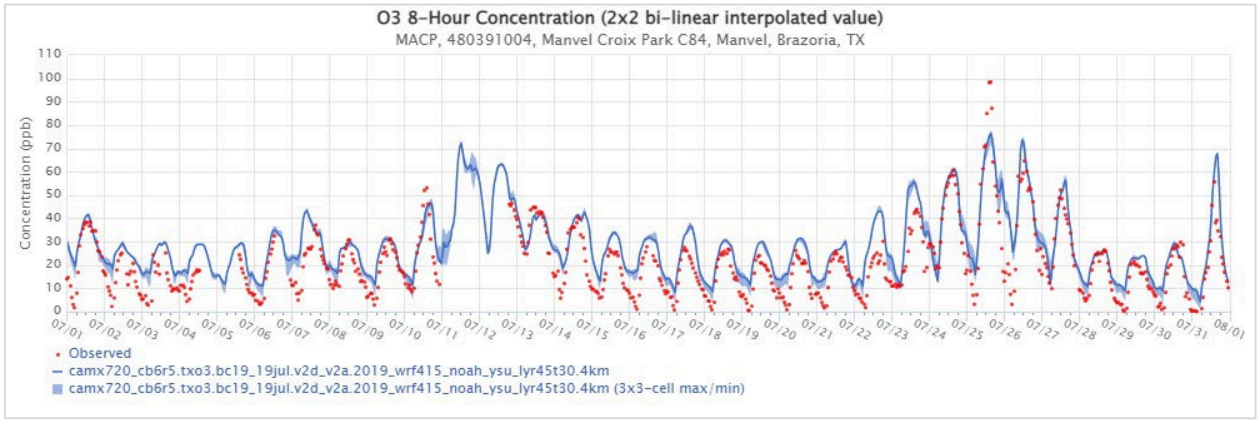

Figure 2-11: July 2019 Observed and Modeled Hourly Ozone at Manvel Monitor

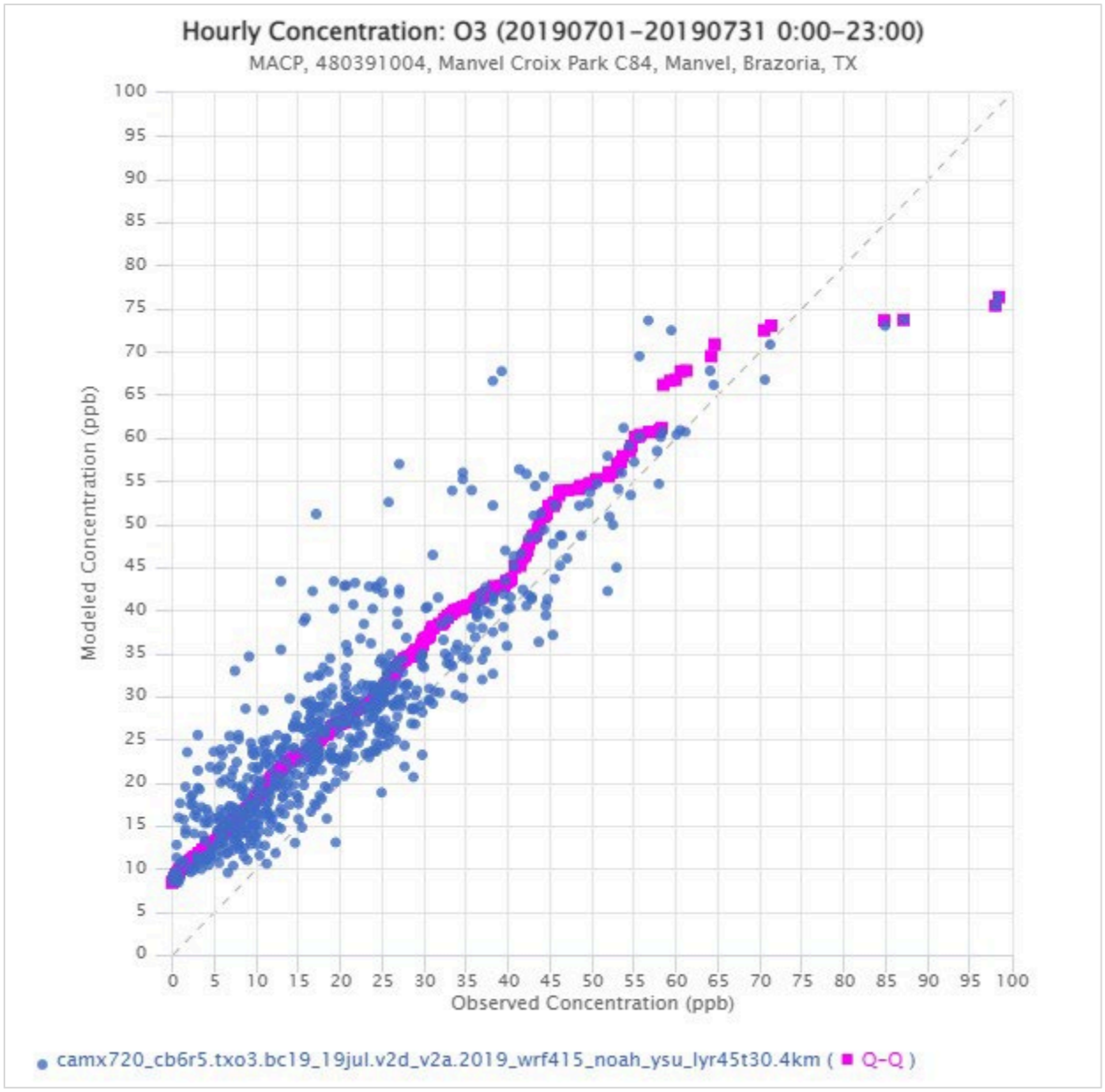

Figure 2-12: July 2019 Scatter Plot of Observed versus Modeled Hourly Ozone at Manvel Monitor

2.1.5 August

MDA8 ozone exceedances were observed on three days in August. The highest MDA8 ozone of 107.9 ppb was recorded at Deer Park monitor on August 15. The hourly peak on that day reached 141.4 ppb. Both peaks were underpredicted by the model.

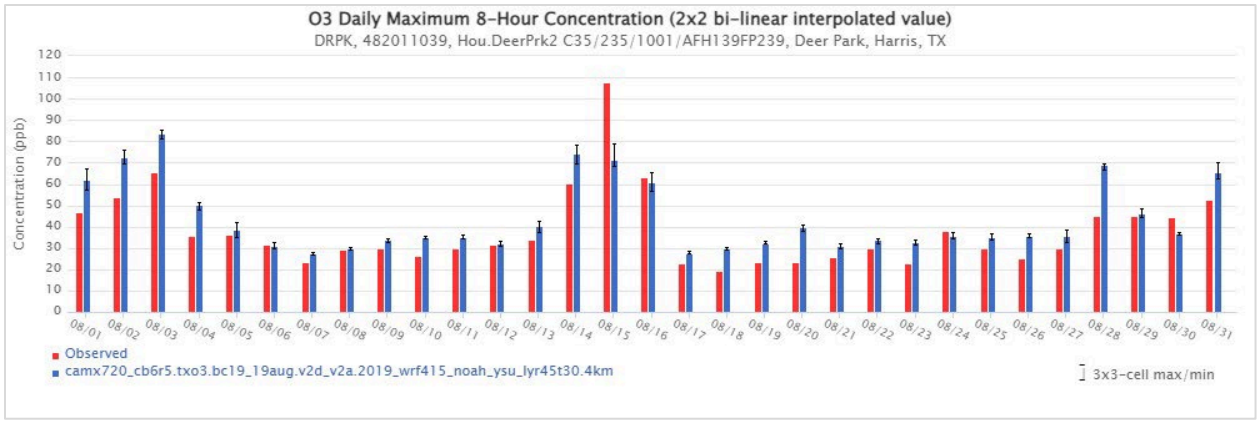

Figure 2-13: August 2019 Observed and Modeled MDA8 at Deer Park Monitor

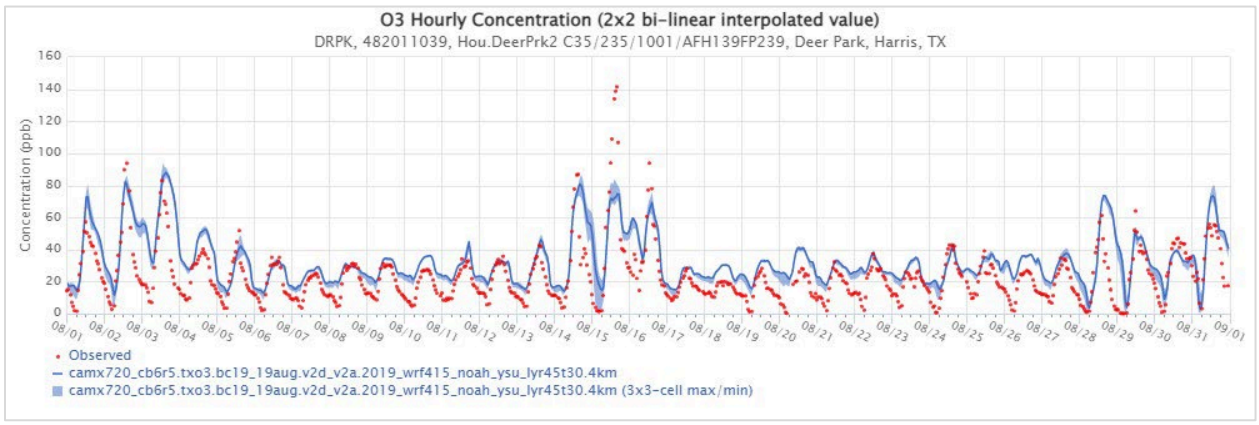

Figure 2-14: August 2019 Observed and Modeled Hourly Ozone at Deer Park Monitor

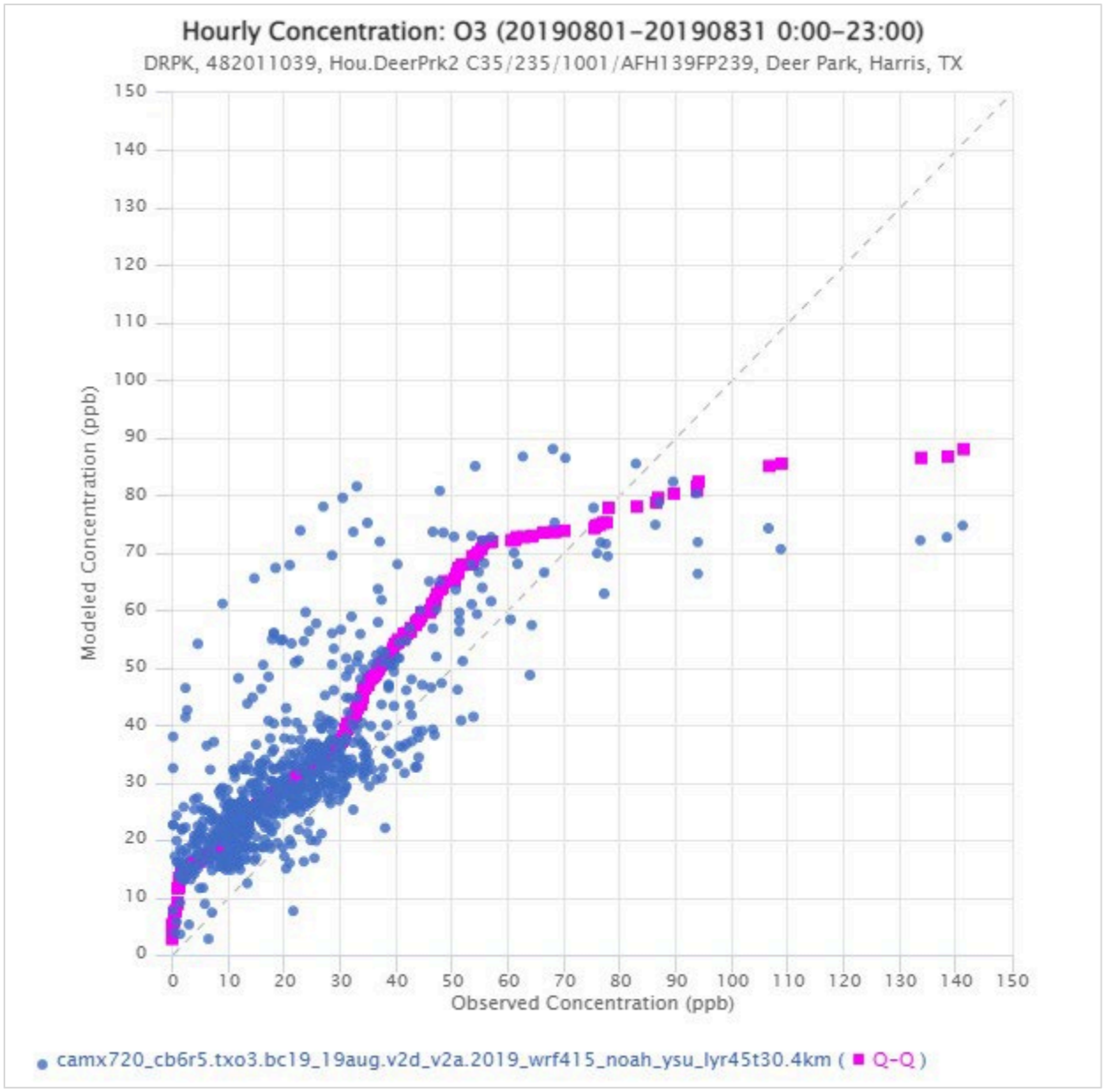

Figure 2-15: August 2019 Scatter Plot of Observed versus Modeled Hourly Ozone at Deer Park Monitor

2.1.6 September

Exceedance of MDA8 ozone were observed on September 4, 5, 6, and 26. The highest measured MDA8 ozone of 87.6 ppb was measured on September 5 at Aldine monitor, followed by 86.1 ppb peak on September 6 at the same monitor. The model predicted both peaks well. Hourly averaged ozone peaks of 104.5 and 121.1 on September 5 and 6, respectively, are underpredicted by the model.

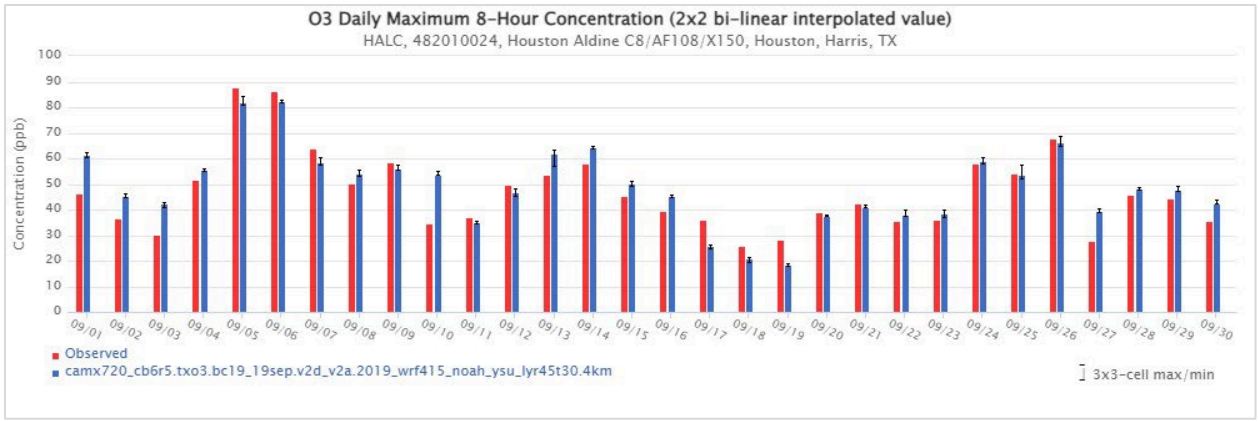

Figure 2-16: September 2019 Observed and Modeled MDA8 at Aldine Monitor

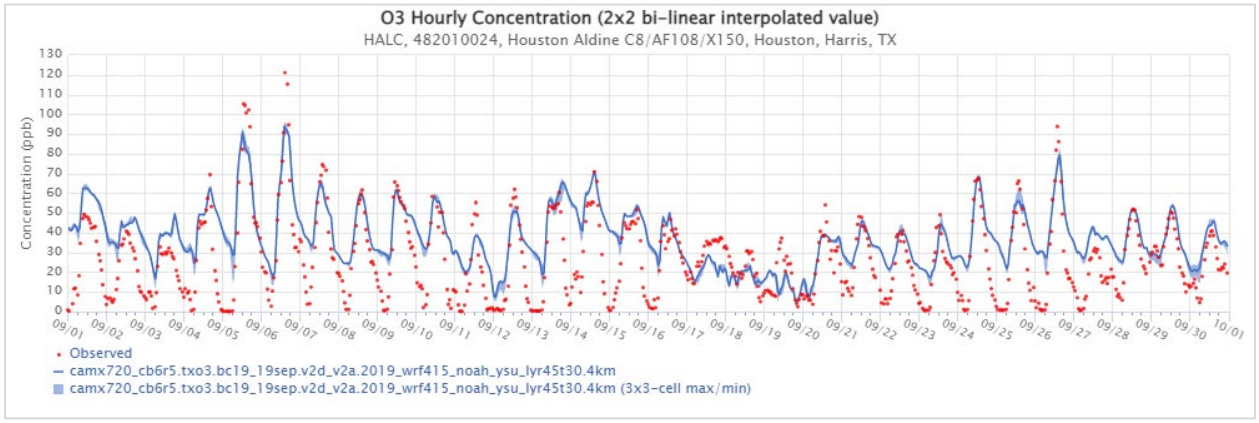

Figure 2-17: September 2019 Observed and Modeled Hourly Ozone at Aldine Monitor

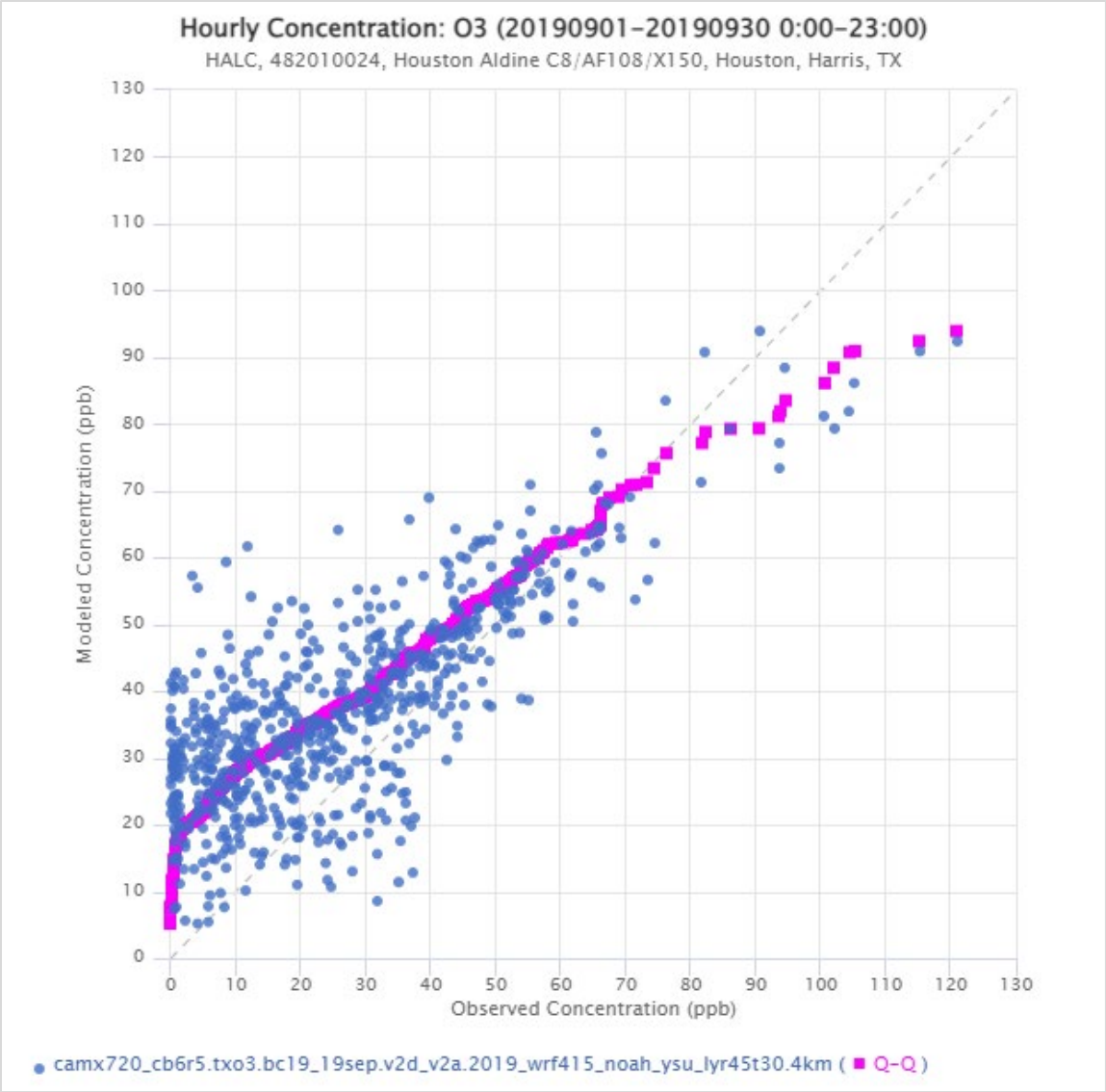

Figure 2-18: September 2019 Scatter Plot of Observed versus Modeled Hourly Ozone at Aldine Monitor

2.1.7 October

Exceedances of MDA8 ozone were observed on October 4 and 5. The highest measured MDA8 ozone of 83.1 ppb was measured at Bayland Park monitor on October 5. The model predicted the peak well. Hourly ozone peaks of 96 ppb and 91.9 ppb on October 4 and 5, respectively, were underpredicted by the model.

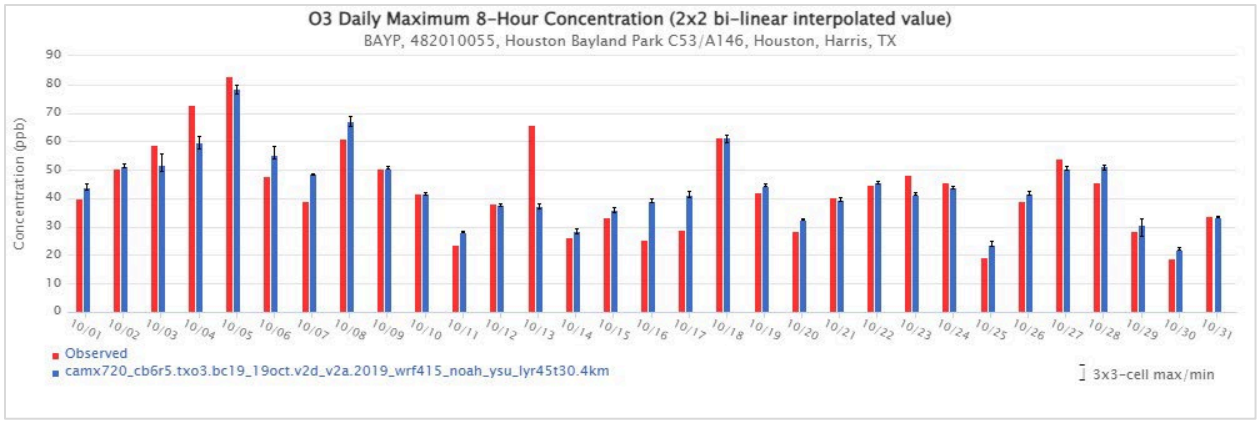

Figure 2-19: October 2019 Observed and Modeled MDA8 at Bayland Park Monitor

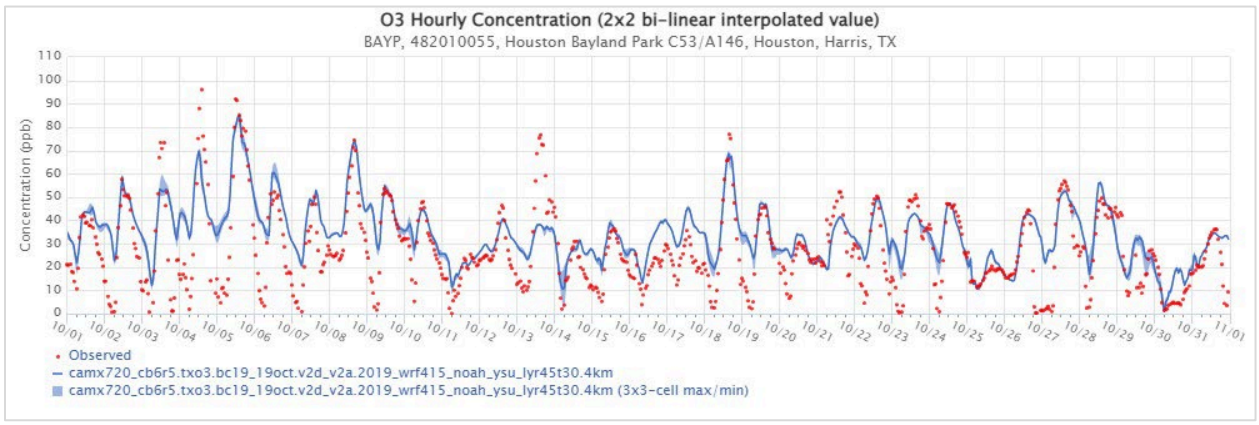

Figure 2-20: October 2019 Observed and Modeled Hourly Ozone at Bayland Park Monitor

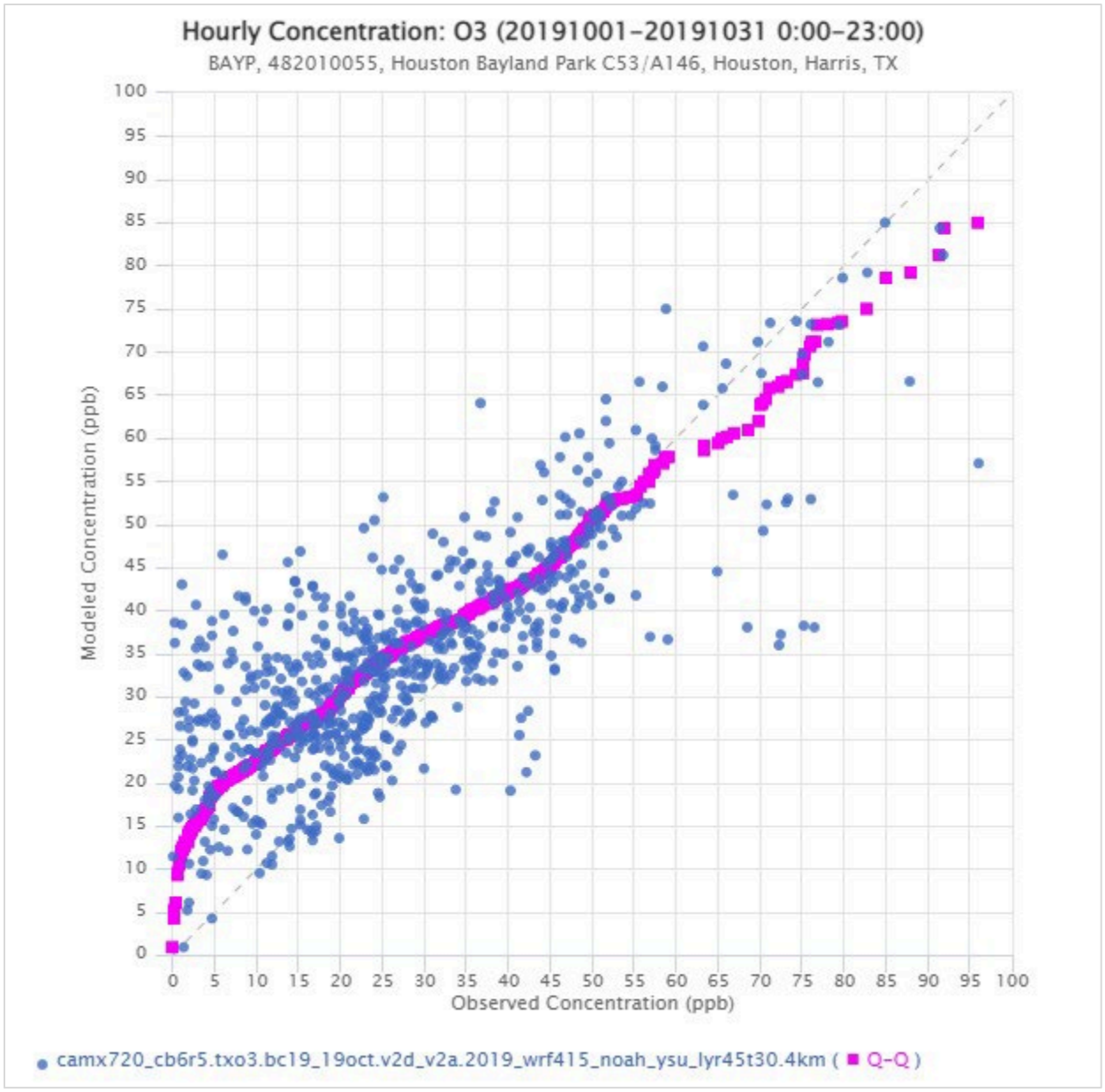

Figure 2-21: October 2019 Scatter Plot of Observed versus Modeled Hourly Ozone at Bayland Park Monitor

2.2 DFW

2.2.1 April

The highest observed MDA8 ozone concentration in DFW in April 2019 was 68 ppb at the Kaufman monitor on April 9. Observed and modeled MDA8 ozone were within five to 10 ppb difference for most days, but there were six days where the model significantly overpredicted MDA8 ozone. Modeled diurnal patterns for hourly ozone were closely matched to observed patterns on most days in April. The highest observed hourly ozone on April 9 was well replicated in the model, but the modeled significantly over-predicted hourly ozone at the Kaufman monitor on April 23 and 24. The model tended to overpredict for low and high ozone values.

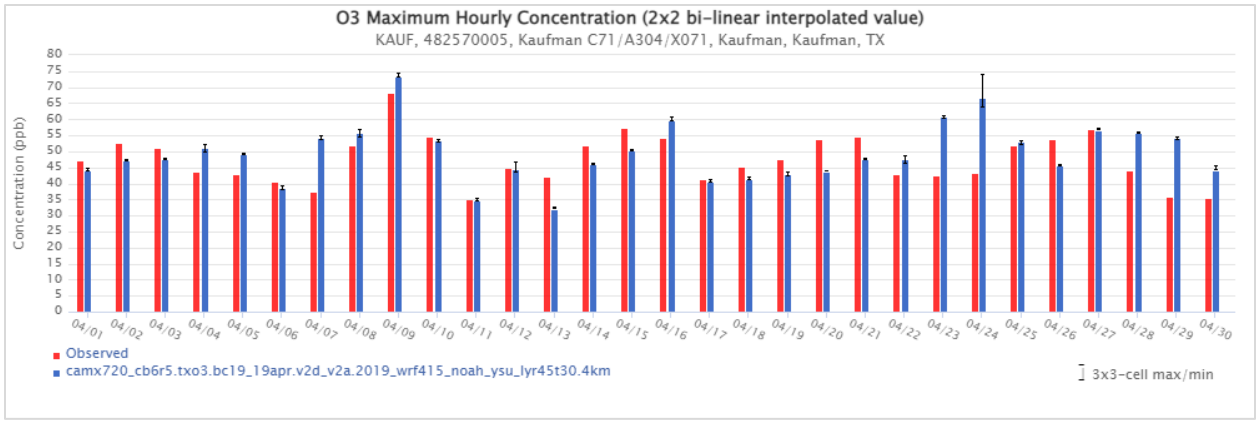

Figure 2-22: April 2019 Observed and Modeled MDA8 Ozone at the Kaufman Monitor

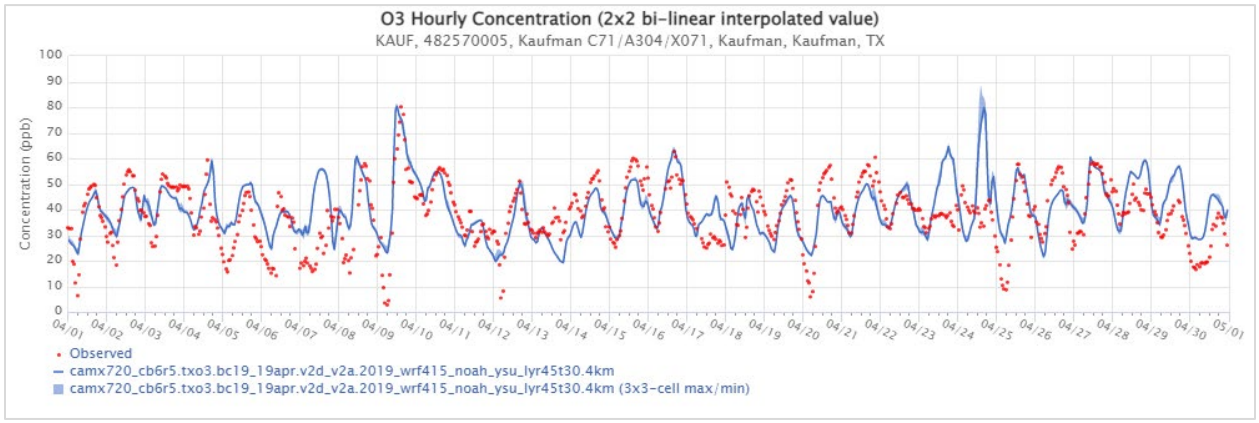

Figure 2-23: April 2019 Observed and Modeled Hourly Ozone at the Kaufman Monitor

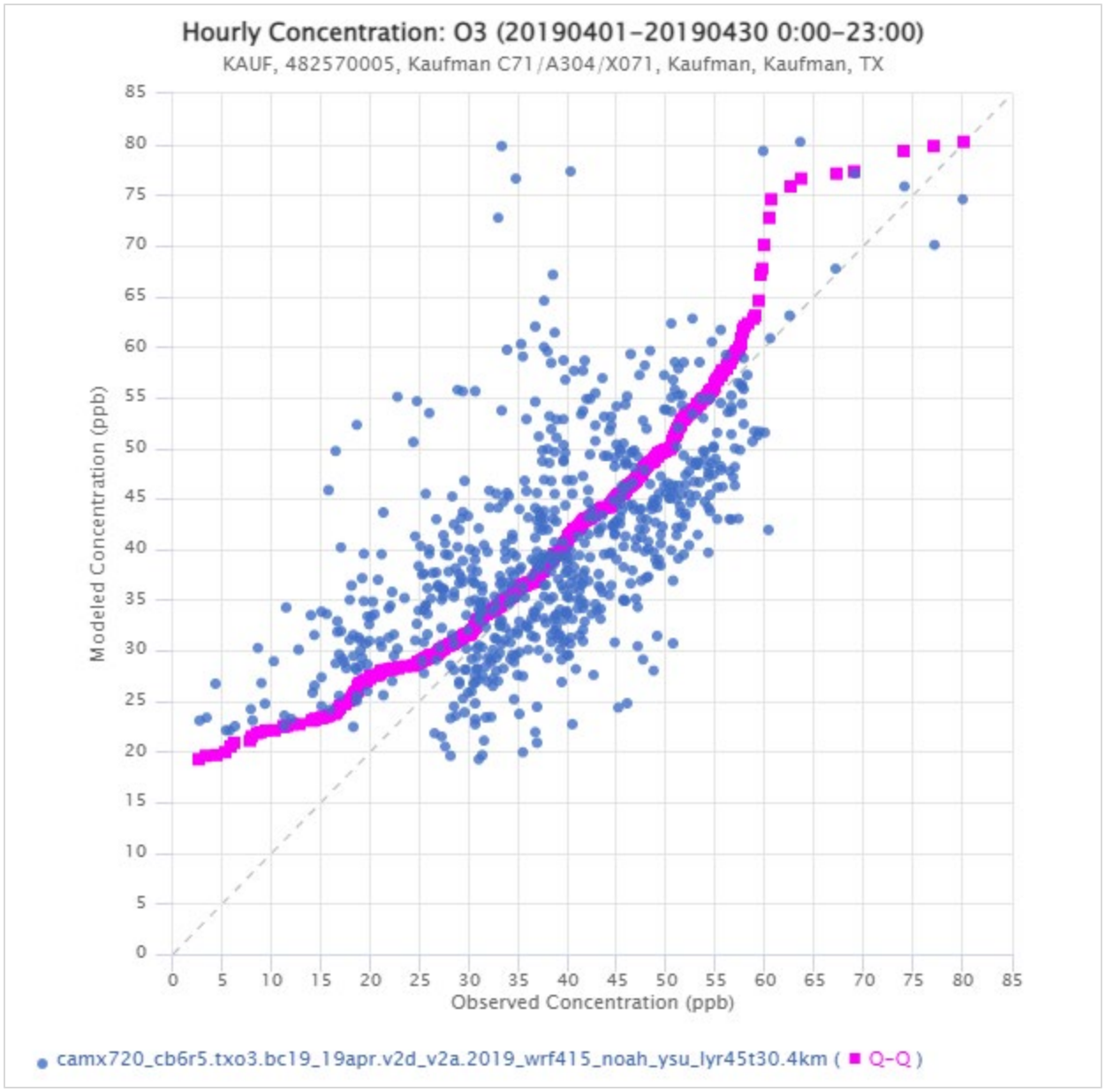

Figure 2-24: April 2019 Scatter Plot of Observed versus Modeled Hourly Ozone at the Kaufman Monitor

2.2.2 May

The highest observed MDA8 ozone concentration in DFW in May 2019 was 80 ppb at the Pilot Point monitor on May 14. Modeled MDA8 ozone was overpredicted on lower ozone days, and underpredicted on the higher ozone days. While the daily peak observed ozone is often well matched by the model, the model did not capture the large variability in ozone concentration on the high ozone days in mid-May. The model was slightly high biased but tended to underpredict for ozone greater than 65 ppb.

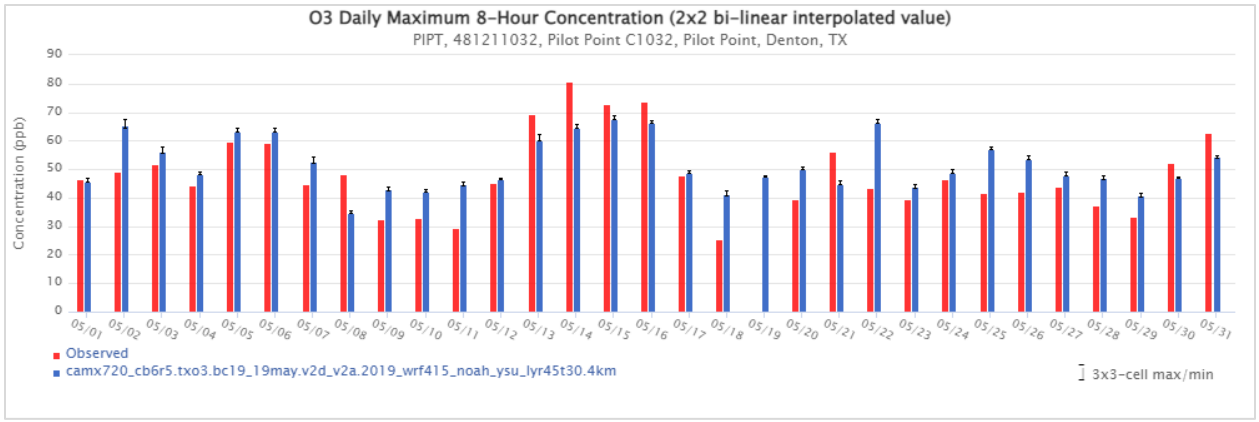

Figure 2-25: May 2019 Observed and Modeled MDA8 Ozone at the Pilot Point Monitor

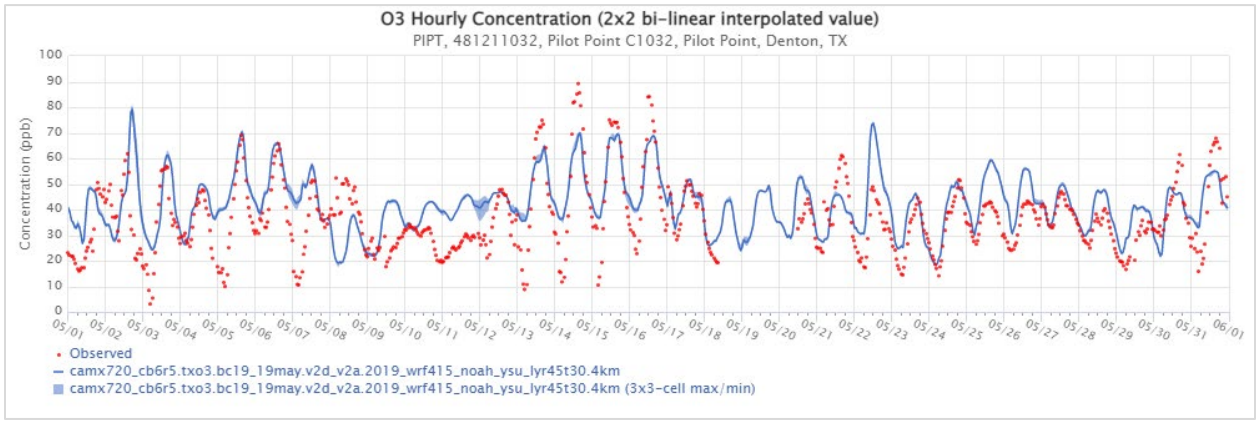

Figure 2-26: May 2019 Observed and Modeled Hourly Ozone at the Pilot Point Monitor

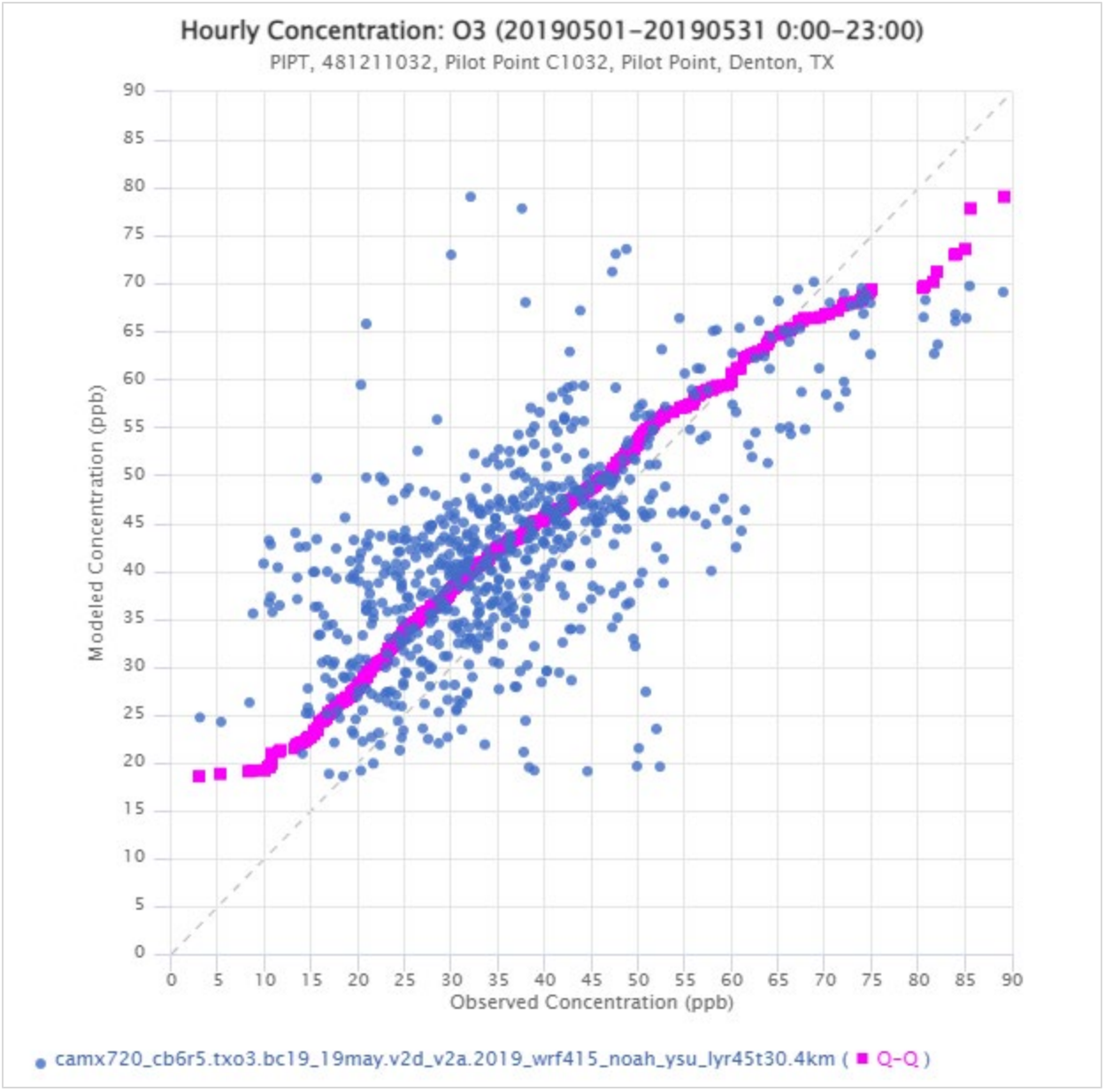

Figure 2-27: May 2019 Scatter Plot of Observed versus Modeled Hourly Ozone at the Pilot Point Monitor

2.2.3 June

The highest observed MDA8 ozone concentration in DFW in June 2019 was 76 ppb at the three monitors: Frisco, Arlington Municipal Airport, and Cleburne Airport. Of the three monitors, Cleburne Airport had the greatest number of exceedances of the 2015 ozone NAAQS, exceeding the 70 ppb standard on June 8, 13, and 14. The model underpredicted MDA8 ozone at the Cleburne monitor on each of the exceedance days, and on the majority of days. Hourly ozone was significantly underpredicted between June 13 and June 19 when high hourly ozone occurred. The modeled replicated lower observed hourly ozone well between June 20 and June 31.

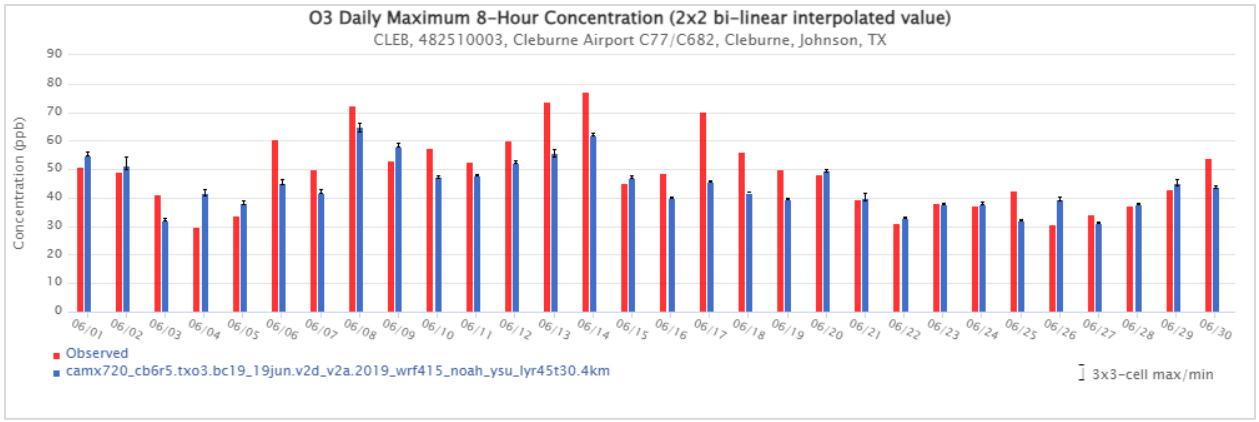

Figure 2-28: June 2019 Observed and Modeled MDA8 Ozone at the Cleburne Airport Monitor

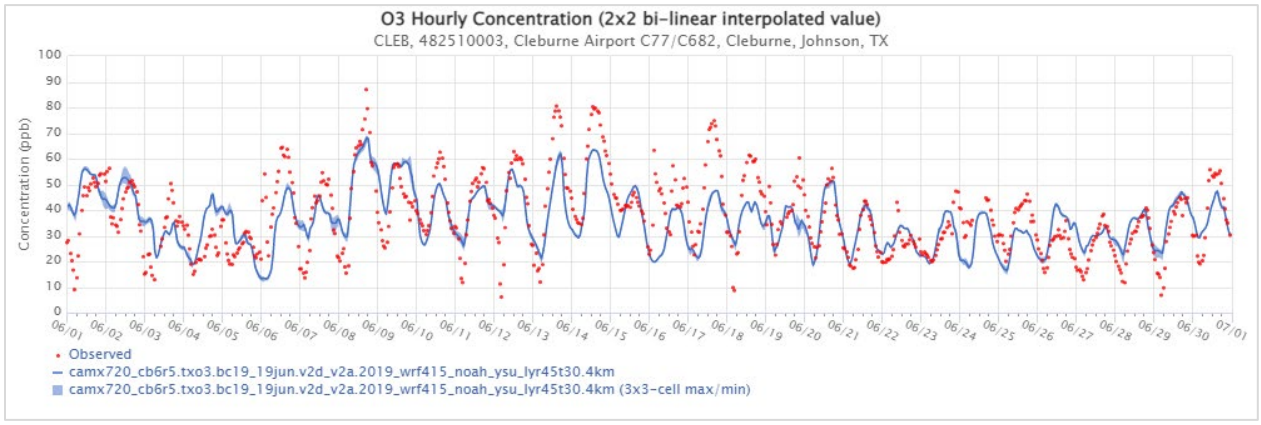

Figure 2-29: June 2019 Observed and Modeled Hourly Ozone at the Cleburne Airport Monitor

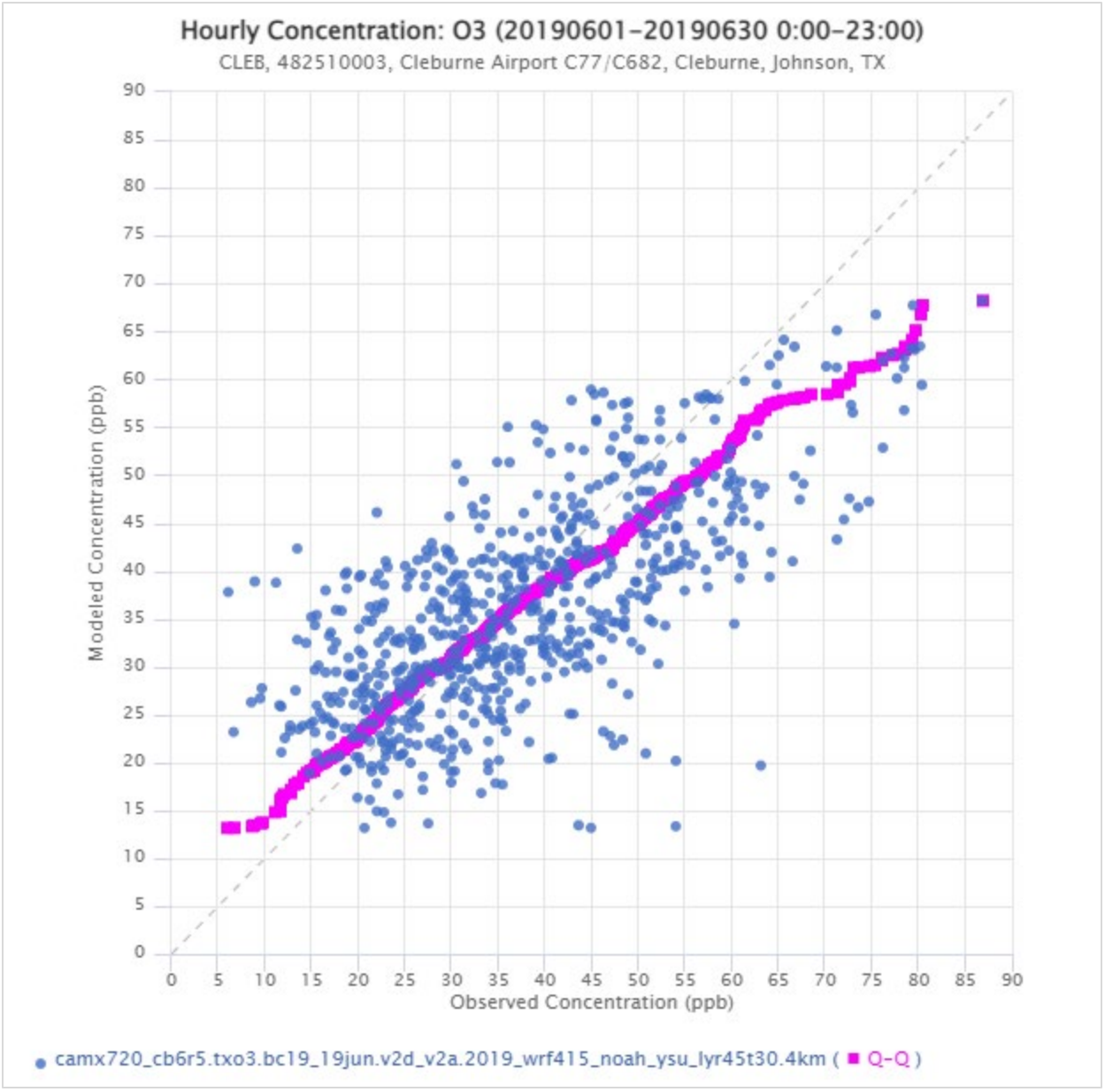

Figure 2-30: June 2019 Scatter Plot of Observed versus Modeled Hourly Ozone at the Cleburne Airport Monitor

2.2.4 July

Cleburne Airport had the highest MDA8 ozone value in DFW in July 2019 of 83 ppb, with Eagle Mountain Lake following at 82 ppb. Both monitors had three MDA8 ozone observations exceeding the 2015 ozone NAAQS. The exceedances at Eagle Mountain Lake occurred on July 26, 27, and 28. Modeled MDA8 ozone values closely matched the observed MDA8 values for nearly all days in July at the Eagle Mountain Lake monitor. Hourly observed ozone was closely replicated by model for most days, particularly July 16 through 24. Peak hourly ozone concentrations were modeled well on the high days.

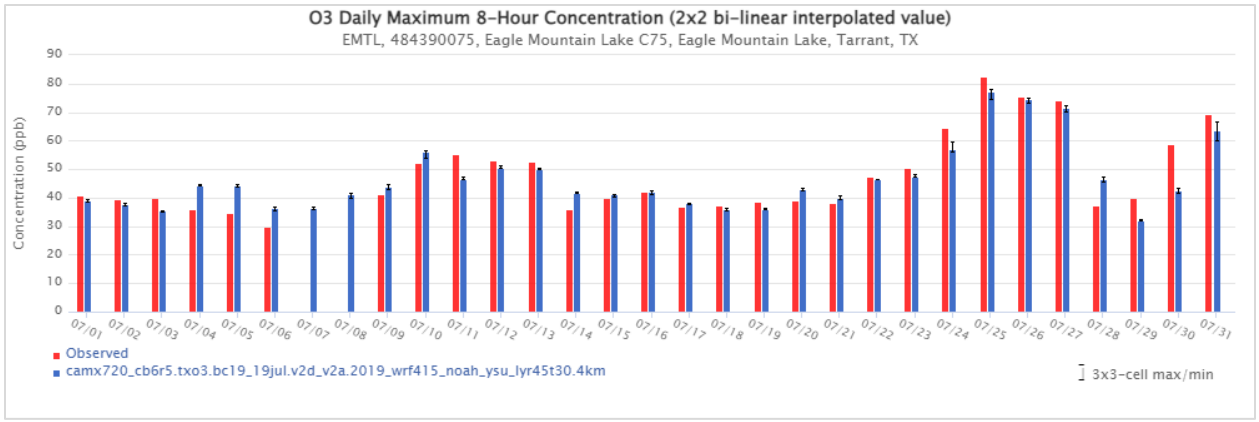

Figure 2-31: July 2019 Observed and Modeled MDA8 Ozone at the Eagle Mountain Lake Monitor

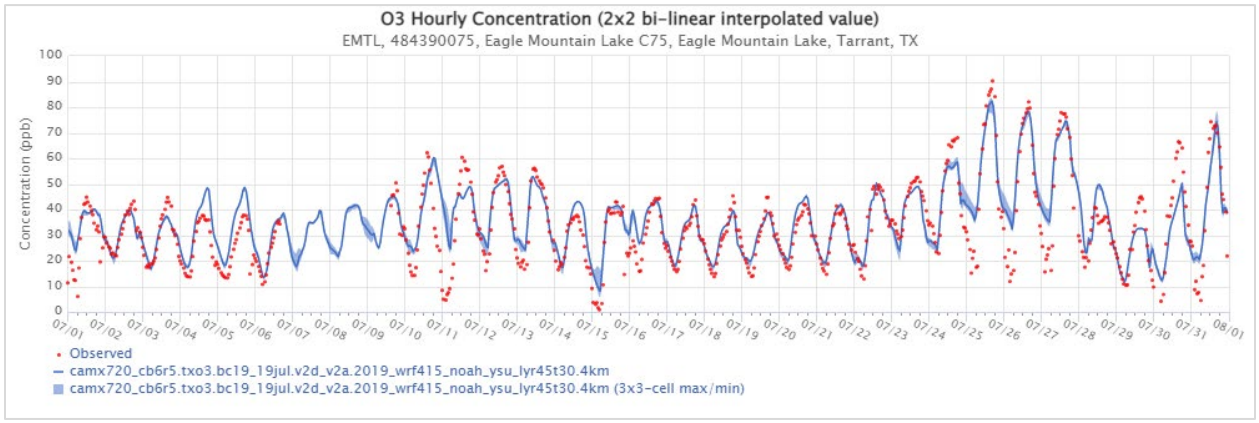

Figure 2-32: July 2019 Observed and Modeled Hourly Ozone at the Eagle Mountain Lake Monitor

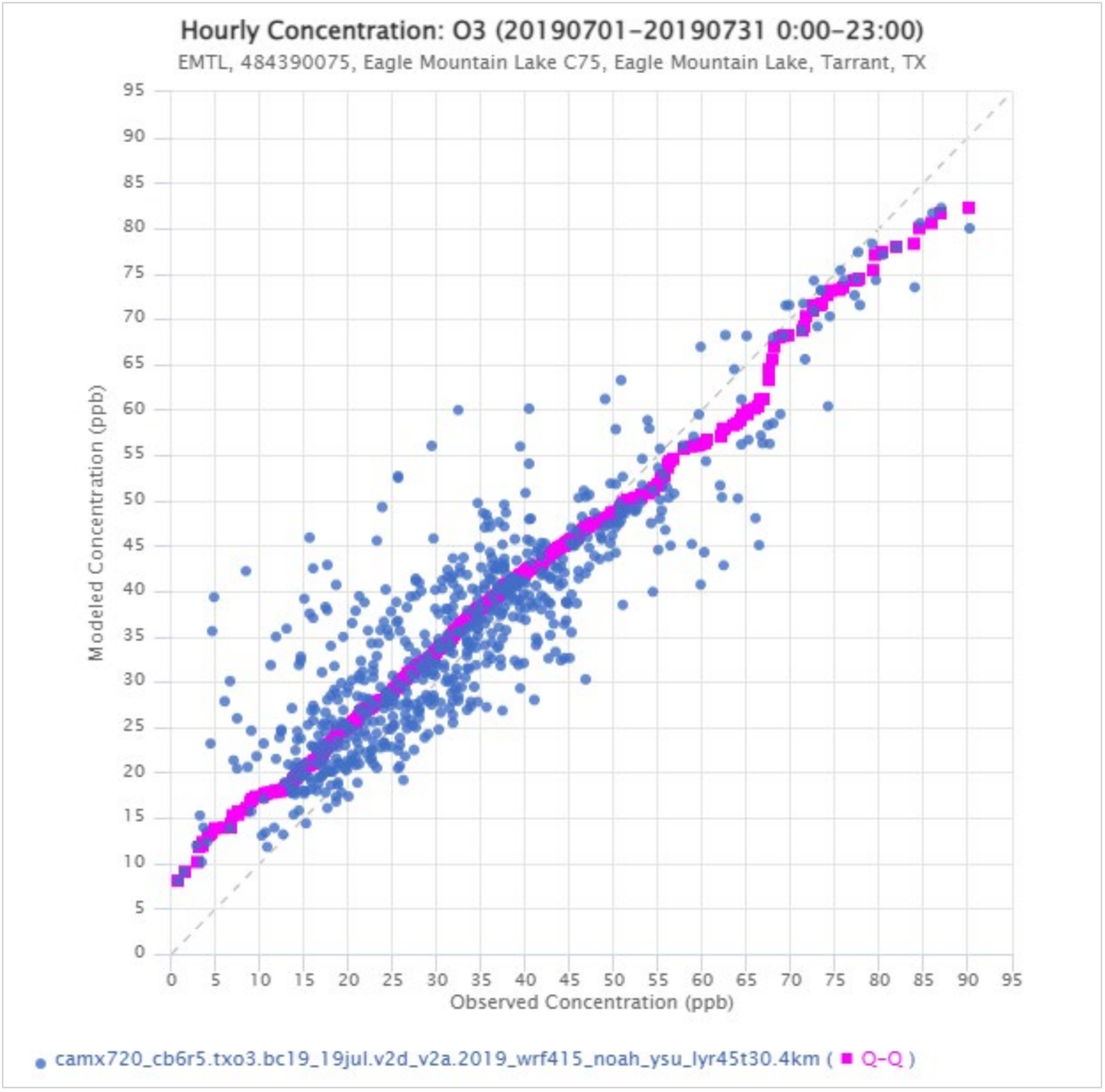

Figure 2-33: July 2019 Scatter Plot of Observed versus Modeled Hourly Ozone at the Eagle Mountain Lake Monitor

2.2.5 August

The highest observed MDA8 ozone concentration in DFW in August 2019 was 84 ppb at the Keller monitor on August 5. Another exceedance of the 2015 ozone NAAQS occurred at the Keller monitor on August 15. Modeled MDA8 ozone values closely matched the observed MDA8 values for most days in August at the Keller monitor. The model underpredicted MDA8 ozone on the exceedance days, by a smaller margin on August 2 and August 15, but more significantly on August 5. Hourly observed ozone was closely replicated by the model for most days, with particularly high performance between August 6 and August 23. Peak observed hourly ozone on August 5 which exceeded 100 ppb was not replicated by the model. The model matched observed

hourly ozone well up to roughly 75 ppb, but underpredicted for observed ozone at higher concentrations.

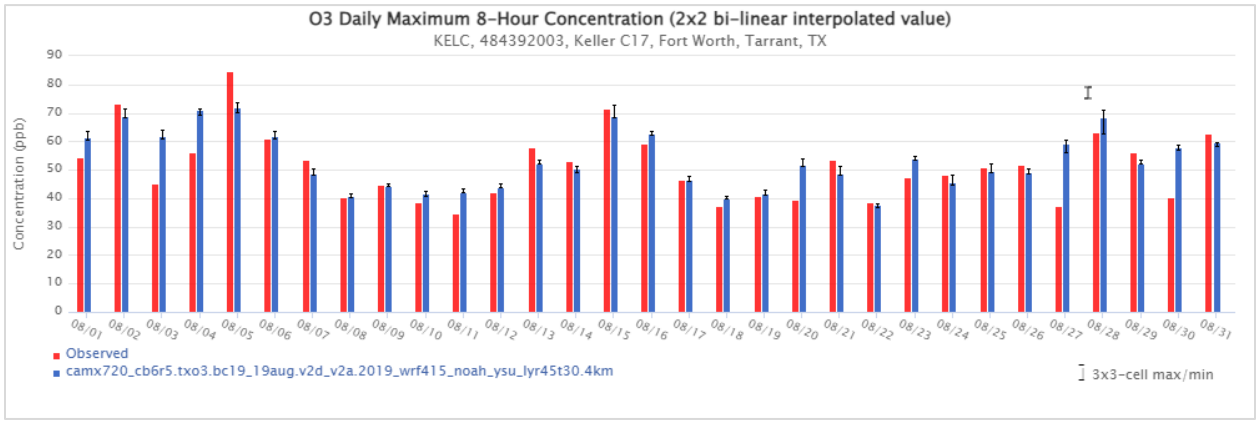

Figure 2-34: August 2019 Observed and Modeled MDA8 Ozone at the Keller Monitor

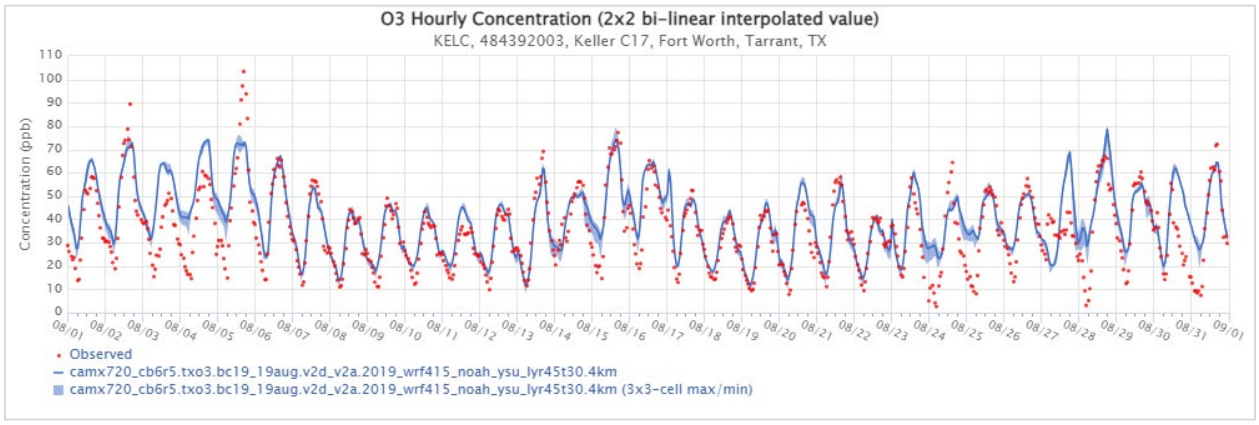

Figure 2-35: August 2019 Observed and Modeled Hourly Ozone at the Keller Monitor

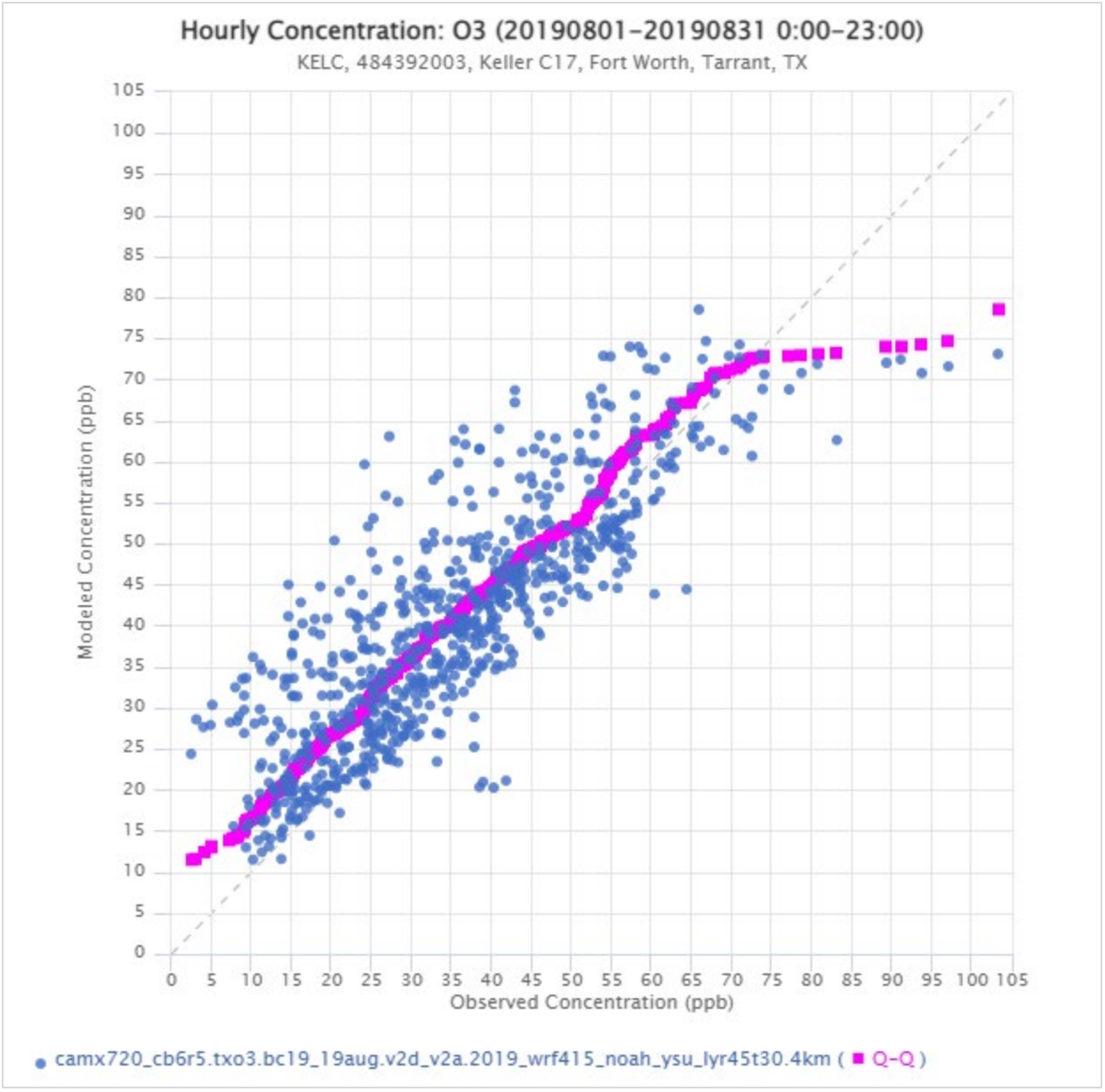

Figure 2-36: August 2019 Scatter Plot of Observed versus Modeled Hourly Ozone at the Keller Monitor

2.2.6 September

The Frisco monitor recorded the highest observed MDA8 ozone concentration in DFW in September 2019 of 88 ppb on September 6. The Frisco monitor also recorded exceedances of the 2015 ozone NAAQS on September 5 and 7. Modeled MDA8 values closely matched the observed MDA8 values for most days in September at the Frisco monitor. Hourly ozone closely replicated observed ozone throughout the month as well. Peak hourly observed ozone on the exceedance days of September 5 and 6 were very well matched by the modeled hourly ozone values. The model matched observed hourly ozone well for all values of observed ozone, without any directional bias.

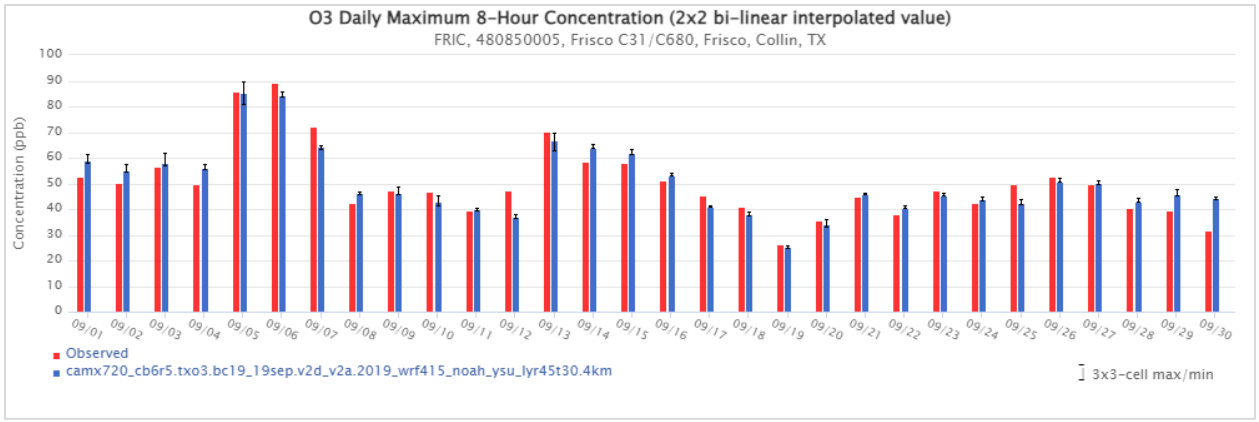

Figure 2-37: September 2019 Observed and Modeled MDA8 Ozone at the Frisco Monitor

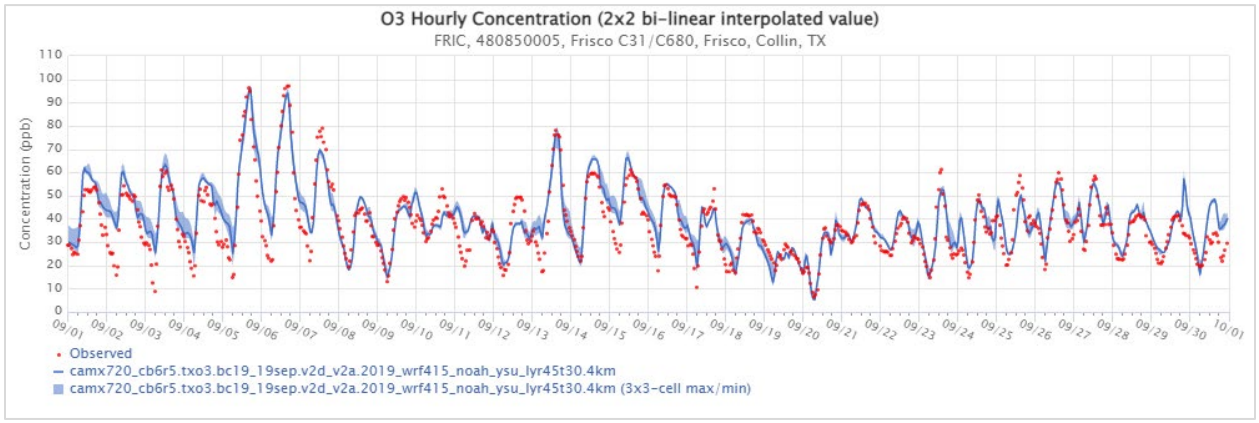

Figure 2-38: September 2019 Observed and Modeled Hourly Ozone at the Frisco Monitor

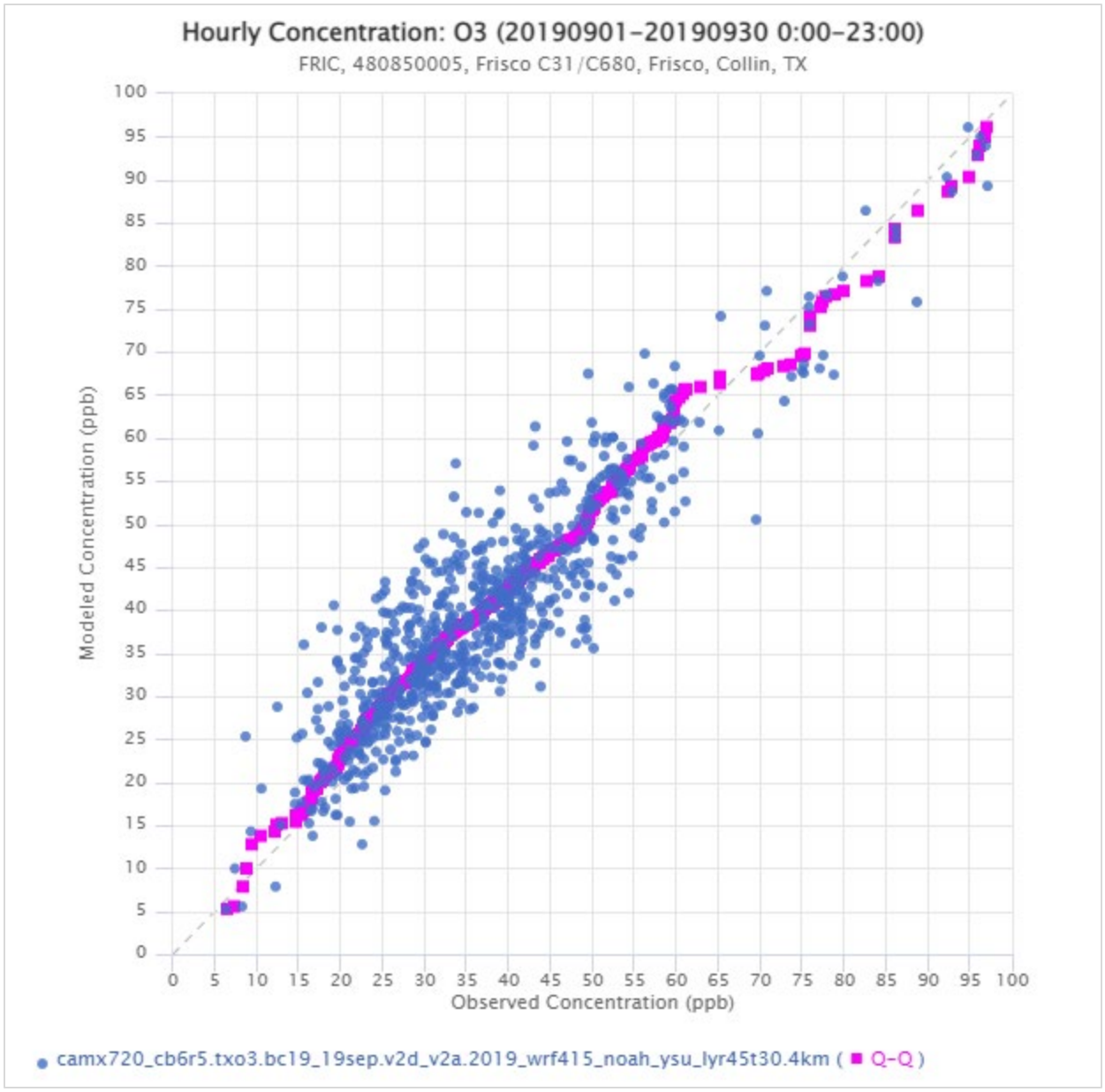

Figure 2-39: September 2019 Scatter Plot of Observed versus Modeled Hourly Ozone at the Frisco Monitor

2.2.7 October

While there were no recorded exceedances of the 2015 ozone NAAQS in DFW in October 2019, the Parker County monitor had the highest MDA8 ozone of all monitors at 68 ppb on October 4. Modeled MDA8 ozone values closely followed observed MDA8 ozone values at the Parker County monitor. Modeled hourly ozone followed observed trends on most days but did not replicate the highest or lowest observed values. The model replicated hourly observed ozone quite well on October 25 through October 31. The model had a slight high bias for hours with observed ozone less than 30 ppb, and a slight low bias for hours with observed ozone greater than 30 ppb.

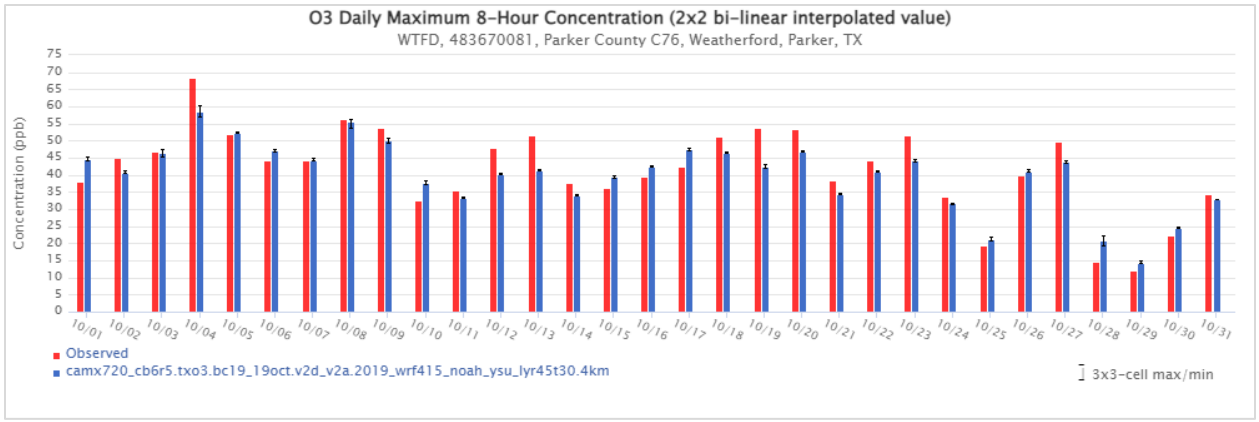

Figure 2-40: October 2019 Observed and Modeled MDA8 Ozone at the Parker County Monitor

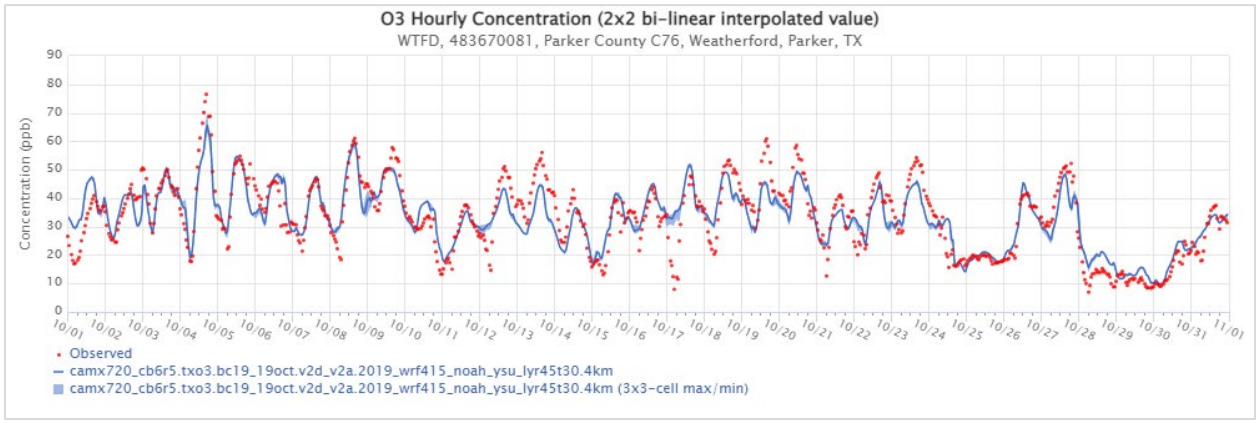

Figure 2-41: October 2019 Observed and Modeled Hourly Ozone at the Parker County Monitor

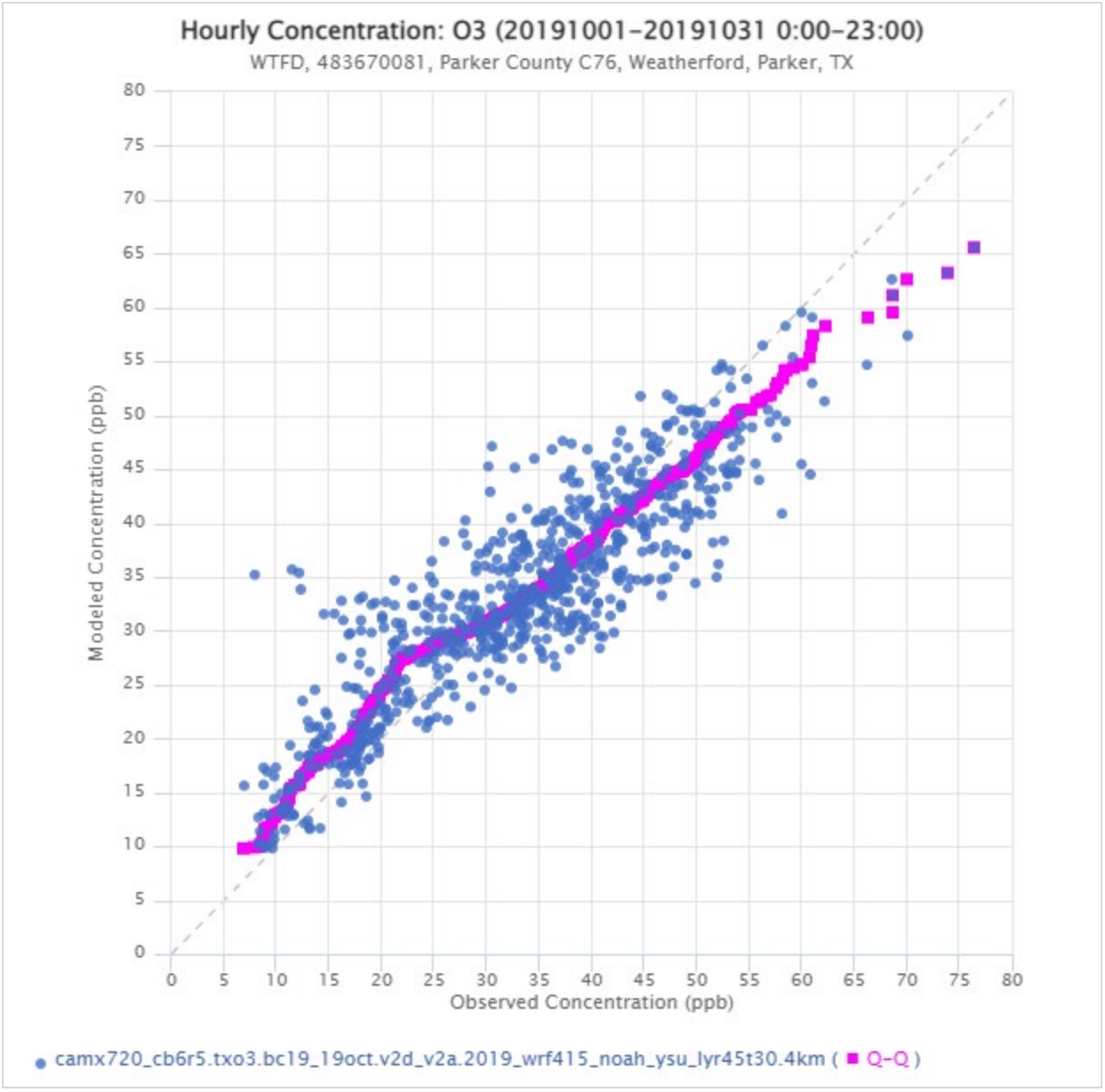

Figure 2-42: October 2019 Scatter Plot of Observed versus Modeled Hourly Ozone at the Parker County Monitor

2.3 BEXAR COUNTY AND ADJACENT COUNTIES

2.3.1 April

The monitor with the highest observed MDA8 ozone in April was Camp Bullis with 70 ppb on April 9. Other high days were April 9, 20, and 27, all over 60 ppb as seen in the column chart for April. April 23 showed significant overprediction, potentially influenced by fire emissions, as seen in the hourly ozone time series for model runs with and without fire emissions shown for April. Overprediction on April 6 may also be influenced by fire emissions, although to a lesser degree than April 23. The time series figure for April also shows that the systemic overprediction occurred during the night. Hourly ozone modeled and observed values are compared in the scatter and Q-Q plot

for this month. Some of the 30 ppb hourly overprediction on April 23 is also seen in the scatter plot for observed ozone values around 35 ppb. The scatter plot shows that some of the overpredictions for observed hourly ozone values less than 15 ppb were more than 40 ppb.

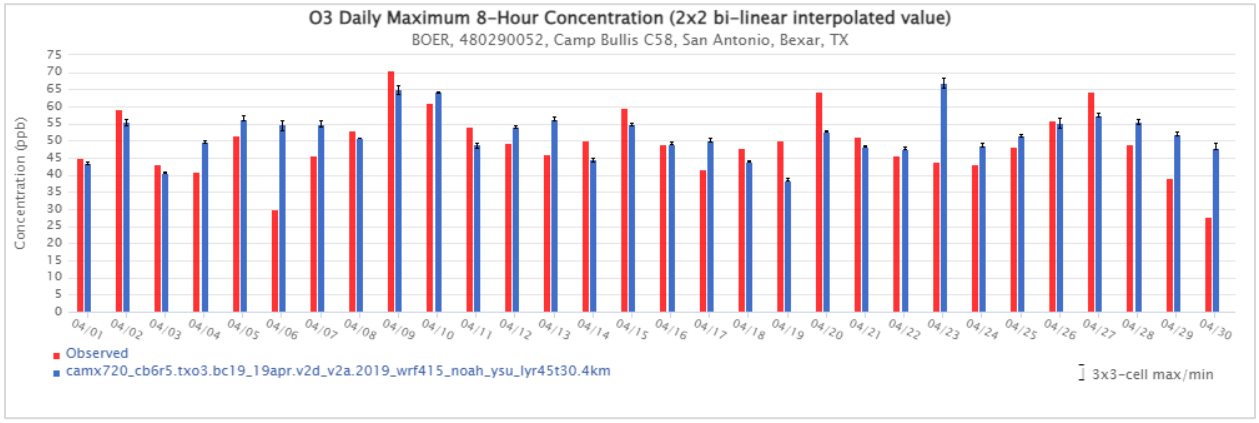

Figure 2-43: April 2019 Observed and Modeled MDA8 Ozone at the Camp Bullis Monitor

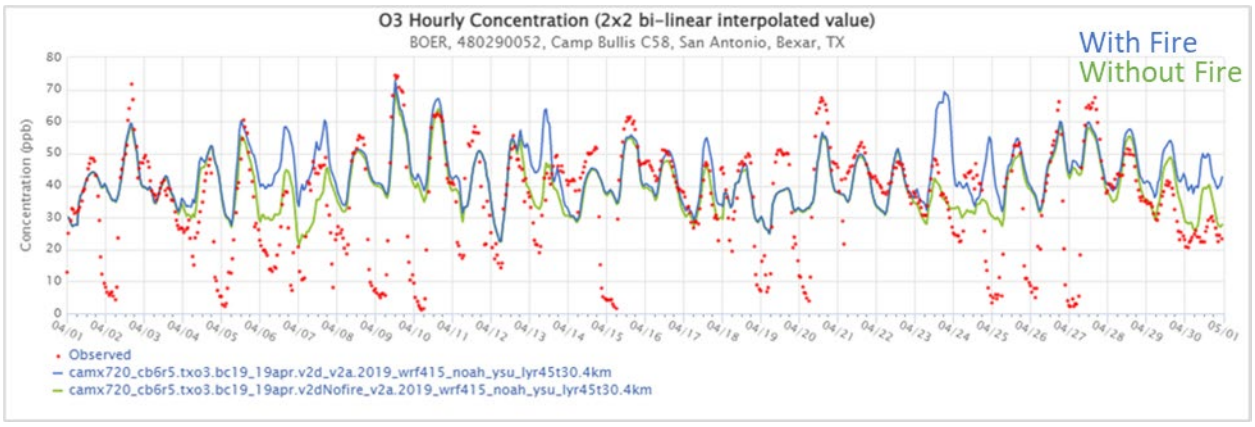

Figure 2-44: April 2019 Time Series of Observed and Modeled Hourly Ozone with and without Fire Emissions at the Camp Bullis Monitor

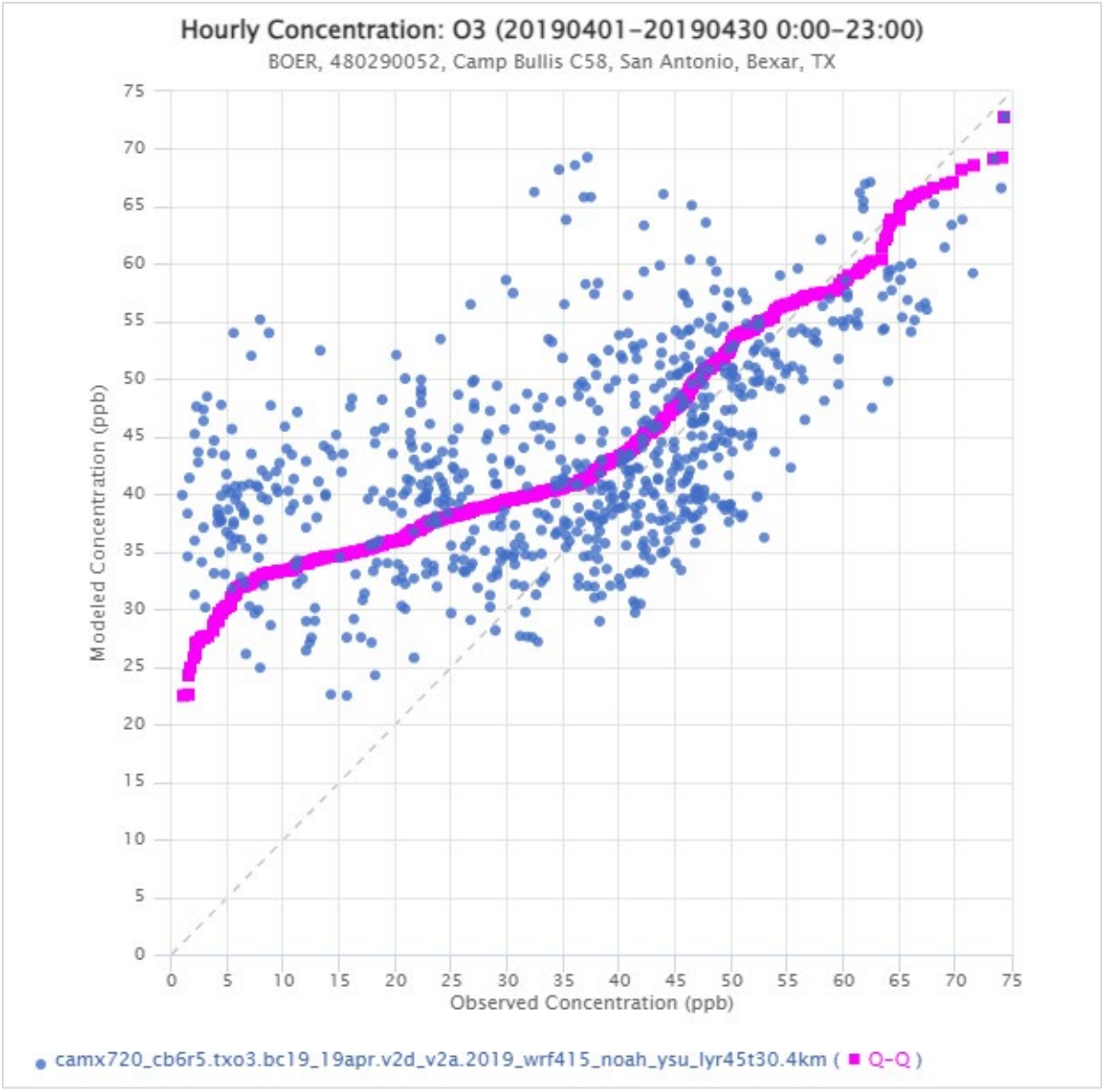

Figure 2-45: April 2019 Scatter and Q-Q Plot of Observed versus Modeled Hourly Ozone at The Camp Bullis Monitor

2.3.2 May

The highest observed MDA8 ozone in May was also at Camp Bullis, 59 ppb on May 5, as seen in the column chart for May. Modeled MDA8 values show high bias on 27 days in May. Of the overprediction days, May 22 stands out with a 34 ppb difference in maximum hourly ozone difference between the with-fire and without-fire model runs, as seen in the time series for May. Other days with larger fire influence are May 6 – 9, 17, 19, and 20. The influence of fire emissions can also be seen in the scatter plot for May where the Q-Q line shows overprediction for all observed values.

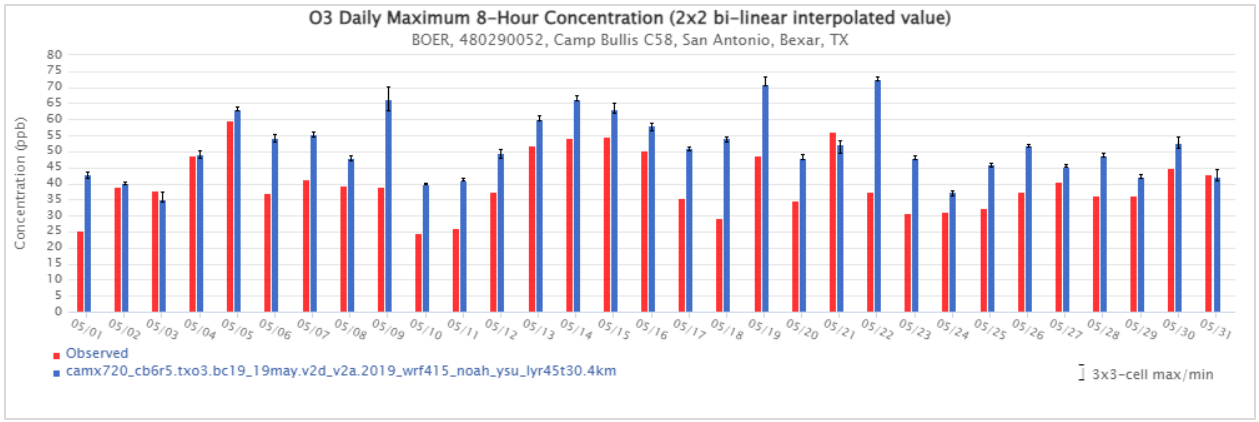

Figure 2-46: May 2019 Observed and Modeled MDA8 Ozone at the Camp Bullis Monitor

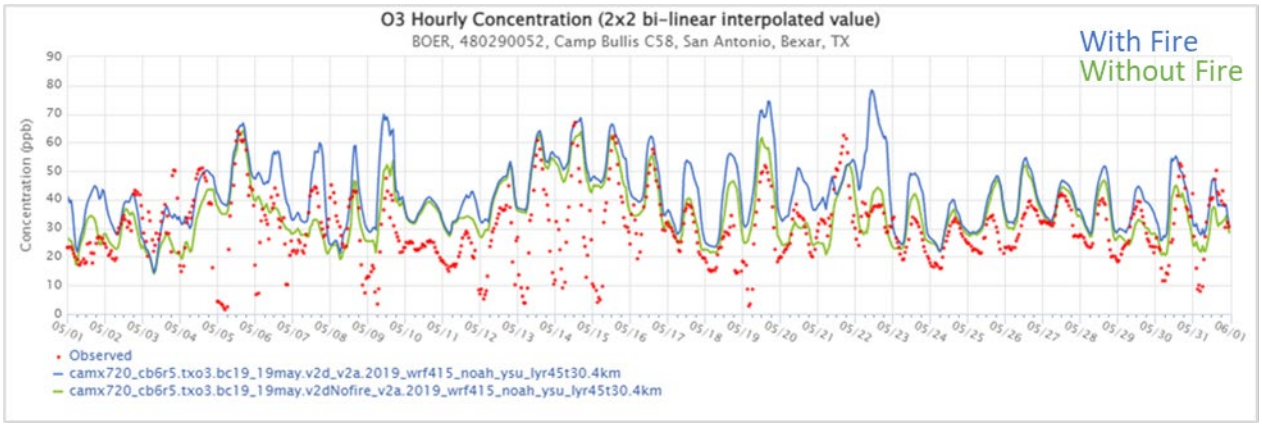

Figure 2-47: May 2019 Time Series of Observed and Modeled Hourly Ozone with and without Fire Emissions at the Camp Bullis Monitor

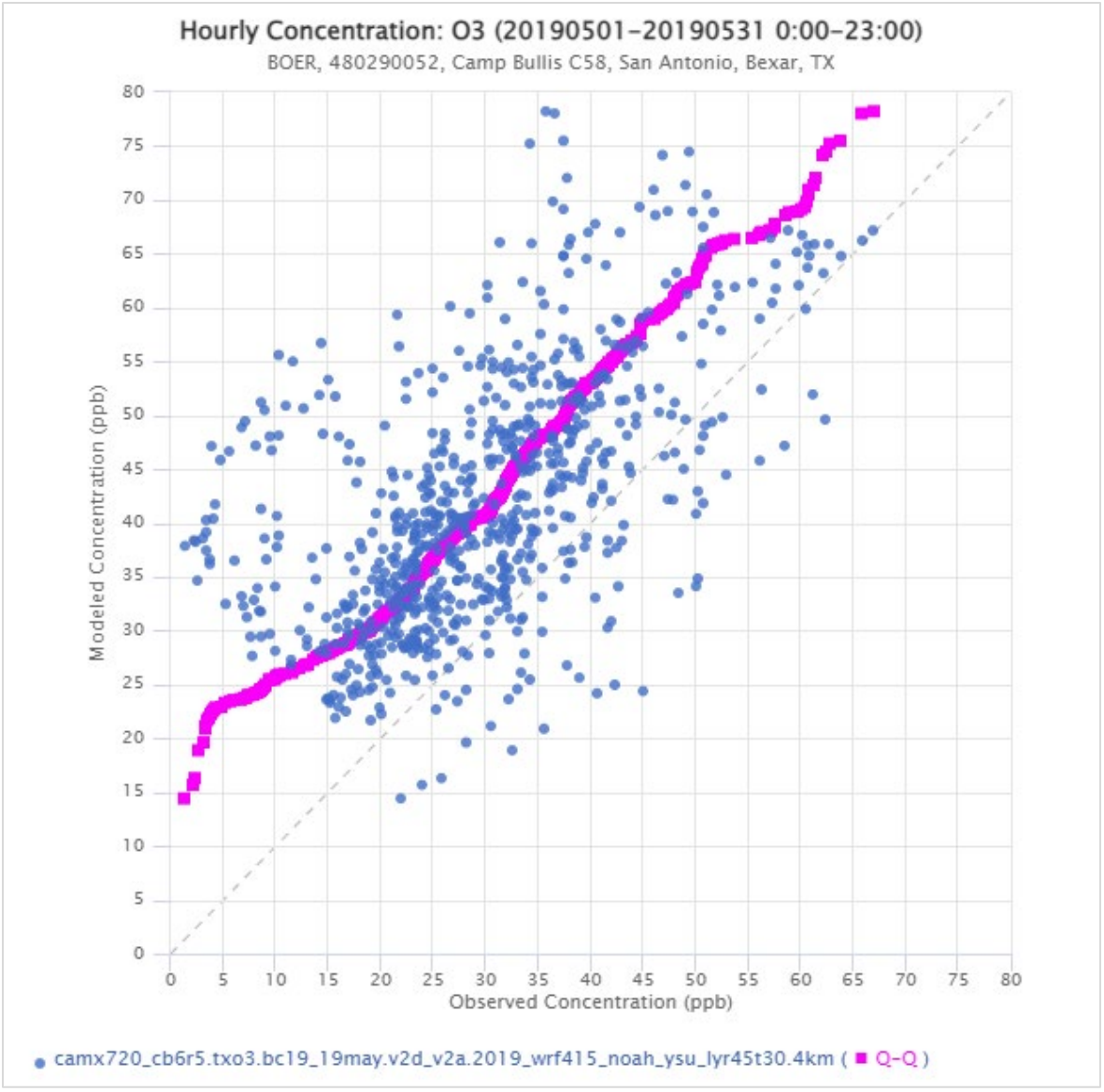

Figure 2-48: May 2019 Scatter and Q-Q Plot of Observed versus Modeled Hourly Ozone at the Camp Bullis Monitor

2.3.3 June

The San Antonio Northwest monitor recorded the highest June MDA8 value of 78 ppb on June 13, followed by 76 ppb on June 8, as seen in the column chart for June. The 20 days of overprediction at the San Antonio Northwest monitor is a decrease in extent and duration from the overprediction in May at Camp Bullis. As seen in the time series for June, the high hourly ozone values on June 13 are modeled better than the June 8 values, where CAMx misses the peak by nearly 20 ppb, leading to the greater MDA8 underprediction on June 8 seen in the column chart. The hourly ozone distribution at San Antonio Northwest in June is much better than at Camp Bullis in April or May, with the Q-Q line closer to unity in the scatter plot for June.

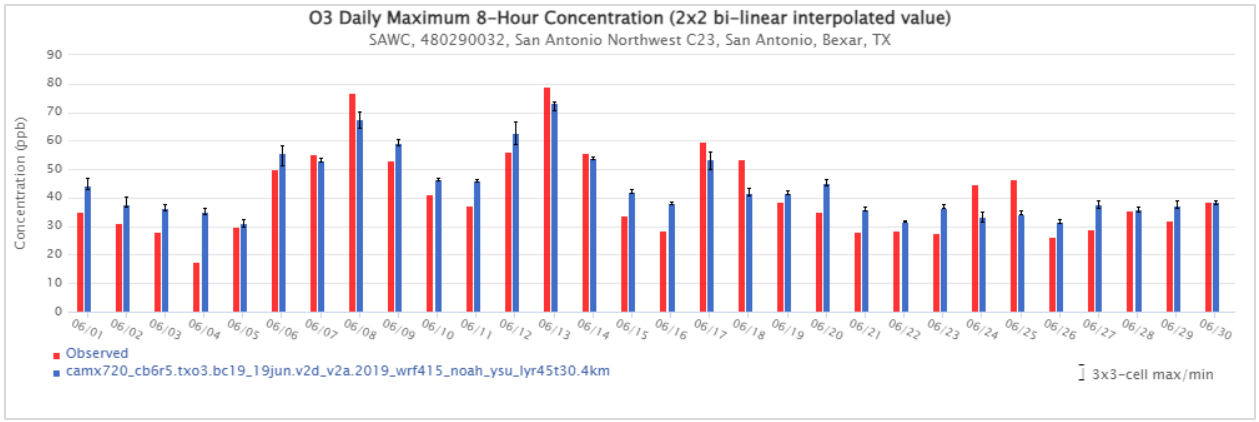

Figure 2-49: June 2019 Observed and Modeled MDA8 Ozone at the San Antonio Northwest Monitor

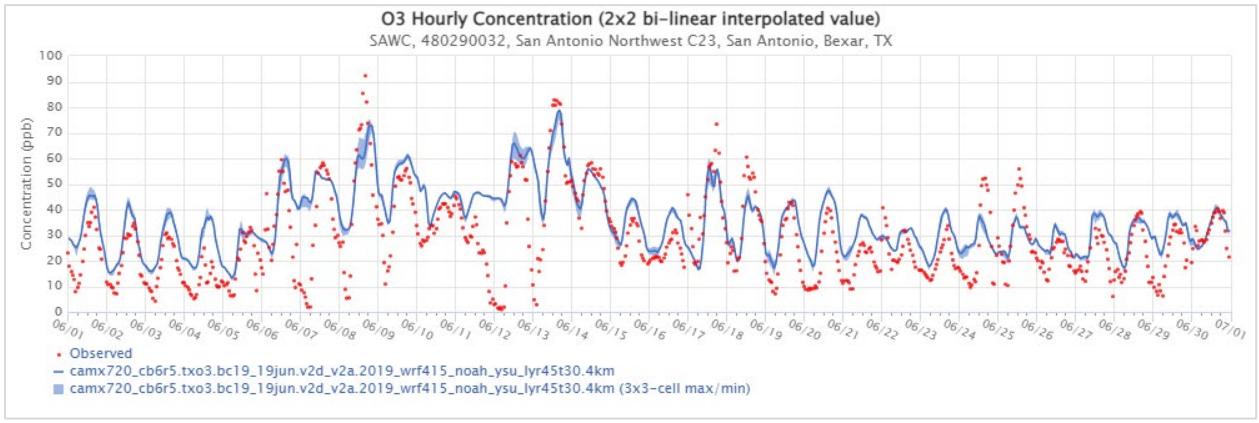

Figure 2-50: June 2019 Time Series of Hourly Modeled and Observed Ozone at the San Antonio Northwest Monitor

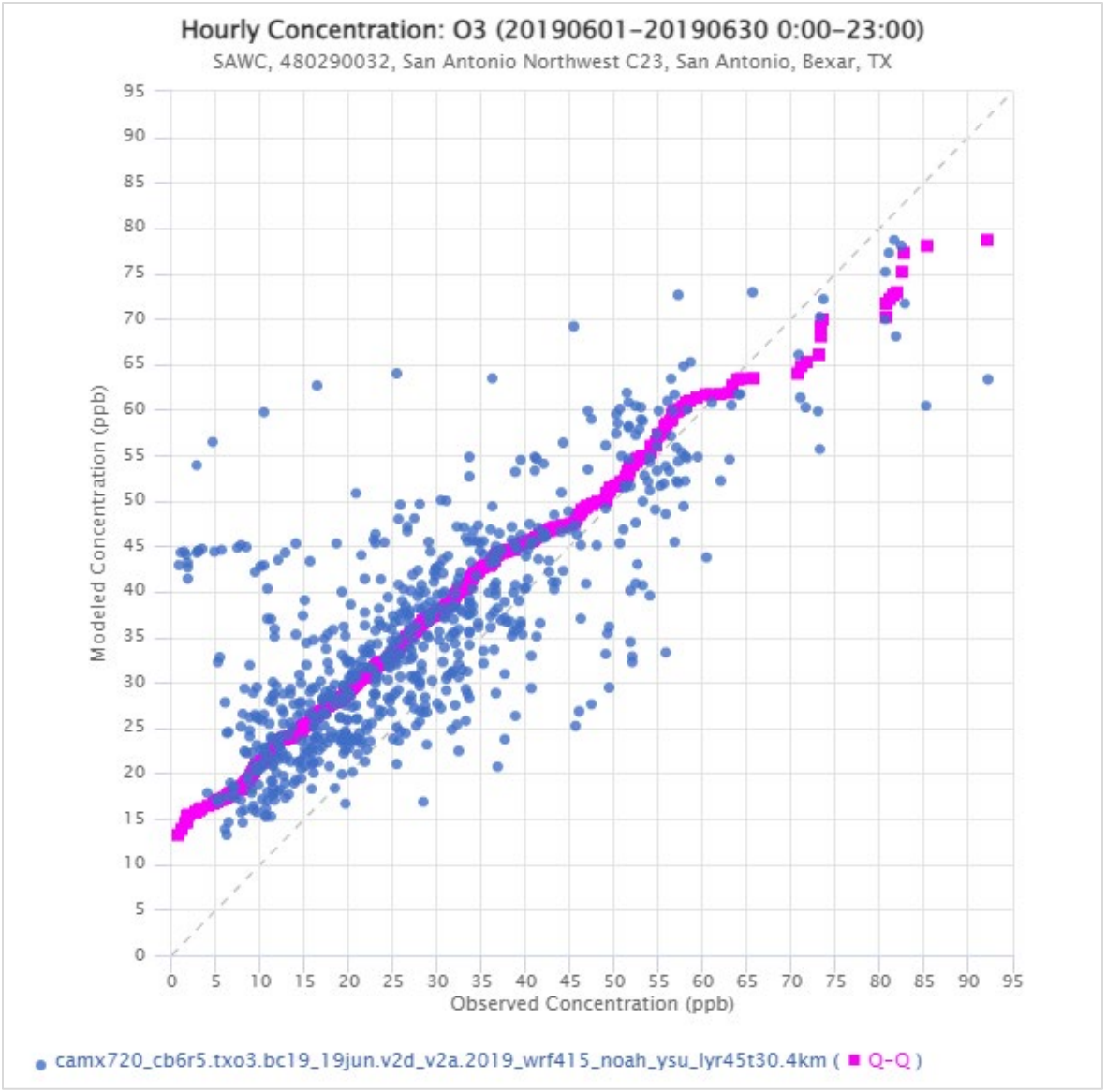

Figure 2-51: June 2019 Scatter and Q-Q Plot of Observed versus Modeled Hourly Ozone at the San Antonio Northwest Monitor

2.3.4 July

The San Antonio Northwest monitor recorded the maximum MDA8 value on July 25 and 26, as shown in the column chart for July. The 21 days of overprediction July is similar to June at San Antonio Northwest, but the overprediction is less pronounced on most days. July peak hourly values seen in the time series for July are quite close to observations on almost all days, with overprediction most pronounced on July 4. The July scatter plot corroborates the good performance with the Q-Q line close to unity for all ozone values.

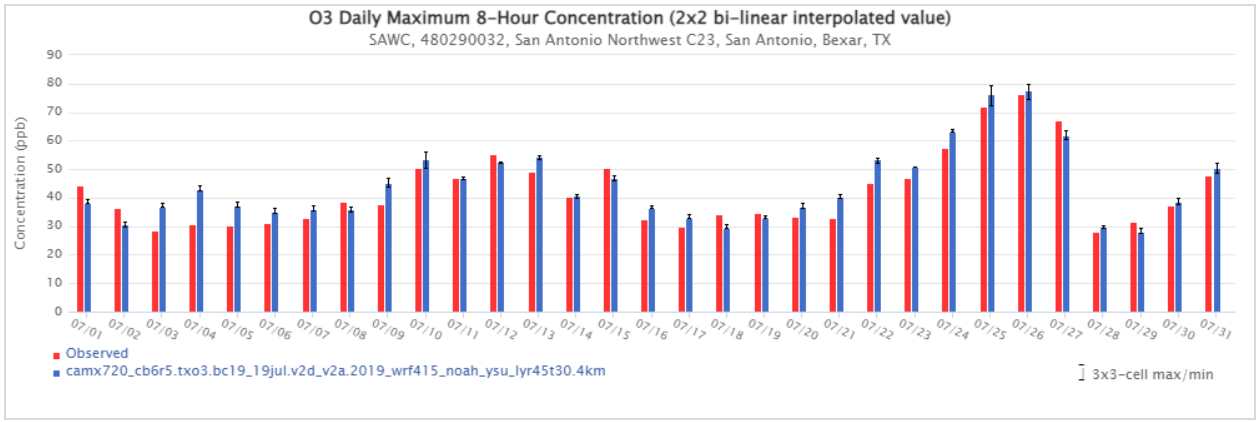

Figure 2-52: July 2019 Observed and Modeled MDA8 Ozone at the San Antonio Northwest Monitor

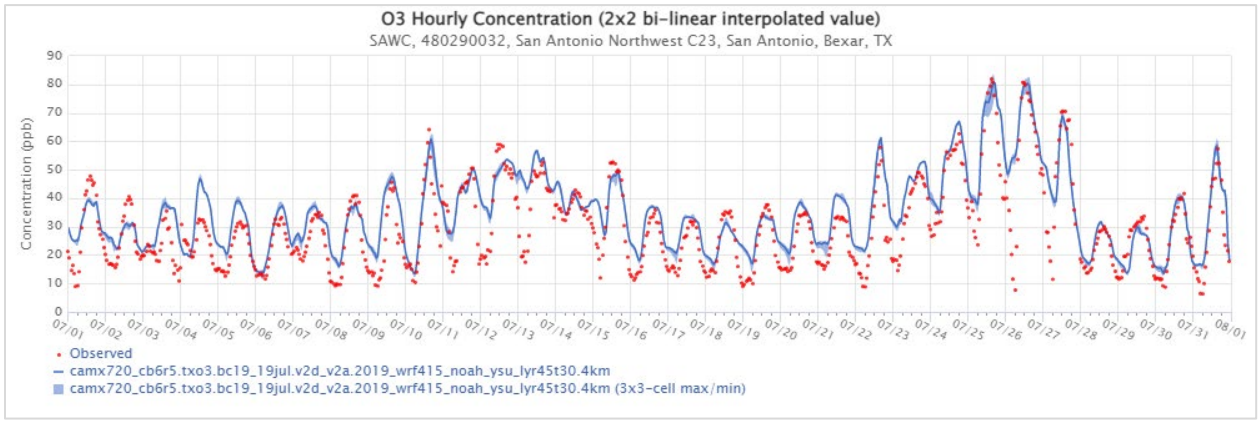

Figure 2-53: July 2019 Time Series of Hourly Modeled and Observed Ozone at the San Antonio Northwest Monitor

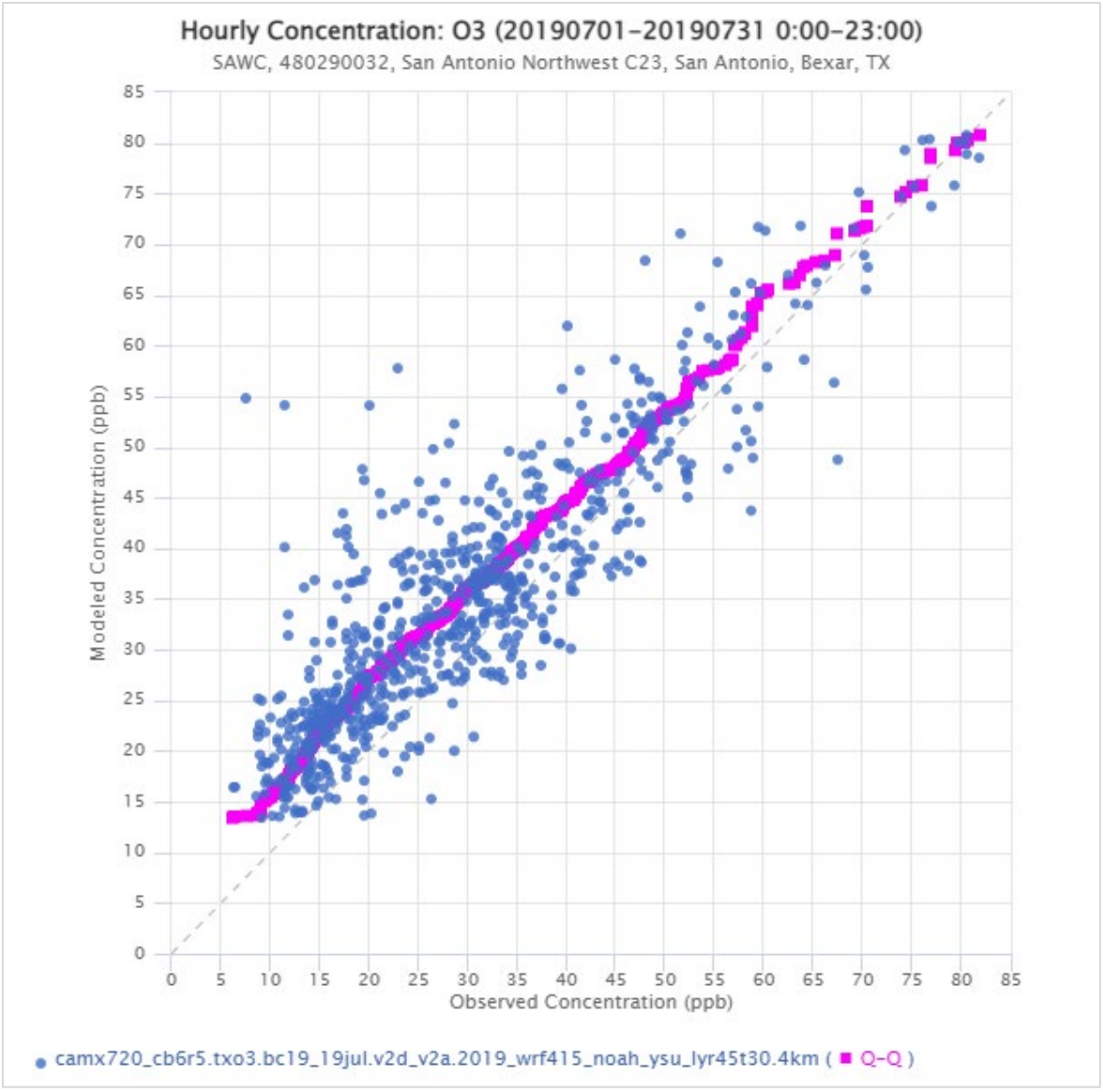

Figure 2-54: July 2019 Scatter and Q-Q Plot of Observed versus Modeled Hourly Ozone at the San Antonio Northwest Monitor

2.3.5 August

The highest observed MDA8 ozone value in August was 64 ppb at Camp Bullis on August 16. With only seven days of overprediction, August at Camp Bullis shows the least overprediction of months evaluated in this chapter, as seen in the column chart for August. The MDA8 underprediction seen in the column chart is expanded in the time series plot for August as an underprediction of the peak hourly values on most days. Nightly minima are well predicted with uniformly high values. The underprediction of peaks and overprediction of minimum hourly values is also seen in the Q-Q line of the August scatter plot.

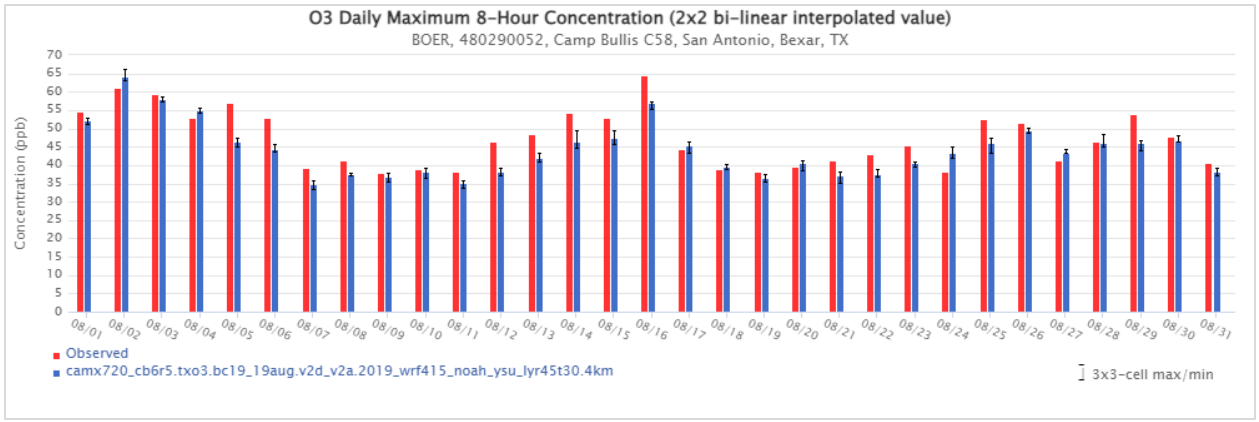

Figure 2-55: August 2019 Observed and Modeled MDA8 Ozone at the Camp Bullis Monitor

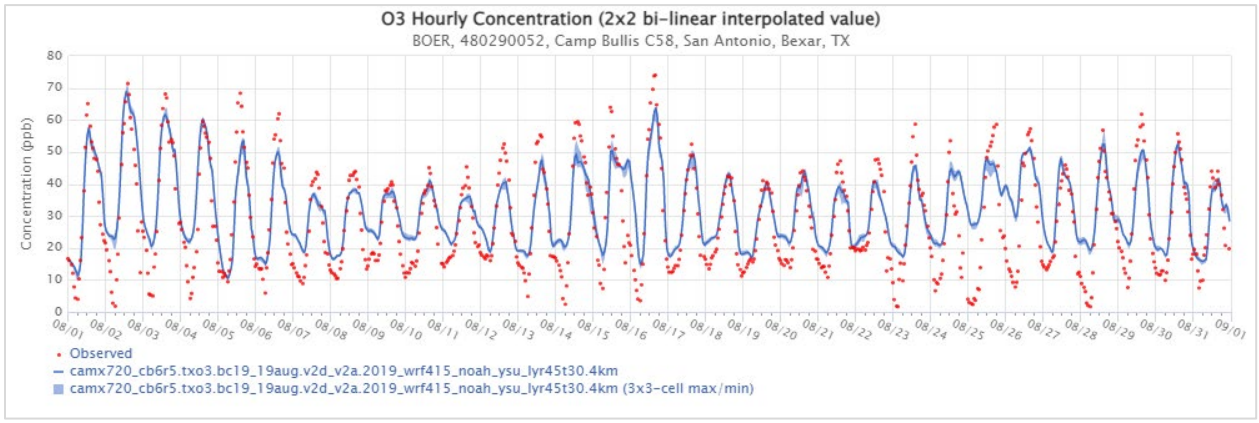

Figure 2-56: August 2019 Time Series of Hourly Modeled and Observed Ozone at the Camp Bullis Monitor

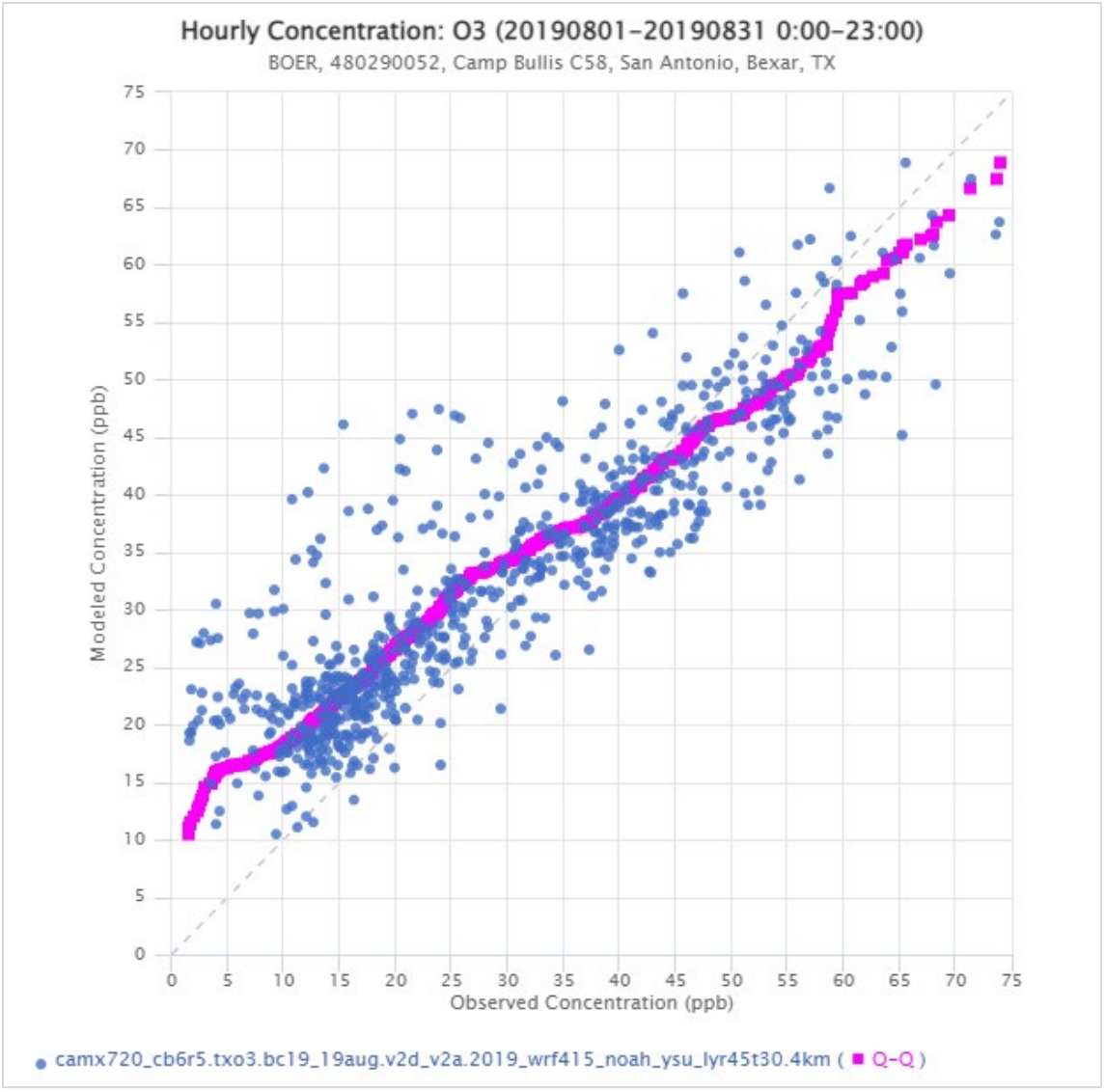

Figure 2-57: August 2019 Scatter and Q-Q Plot of Observed versus Modeled Hourly Ozone at the Camp Bullis Monitor

2.3.6 September

The highest MDA8 observed value in September was at San Antonio Northwest on September 6 at 62 ppb, as seen in the column chart for September. A total of 19 days in September are overpredicted at San Antonio Northwest. Some of the overprediction on September 1 – 4 is seen in the September time series figure as larger hourly ozone overprediction during nighttime hours than seen in displayed time series figures for other months. The overprediction of nighttime values seen in the time series is also seen in the September scatter plot as substantial scatter deviation from unity for observed ozone values less than 30 ppb.

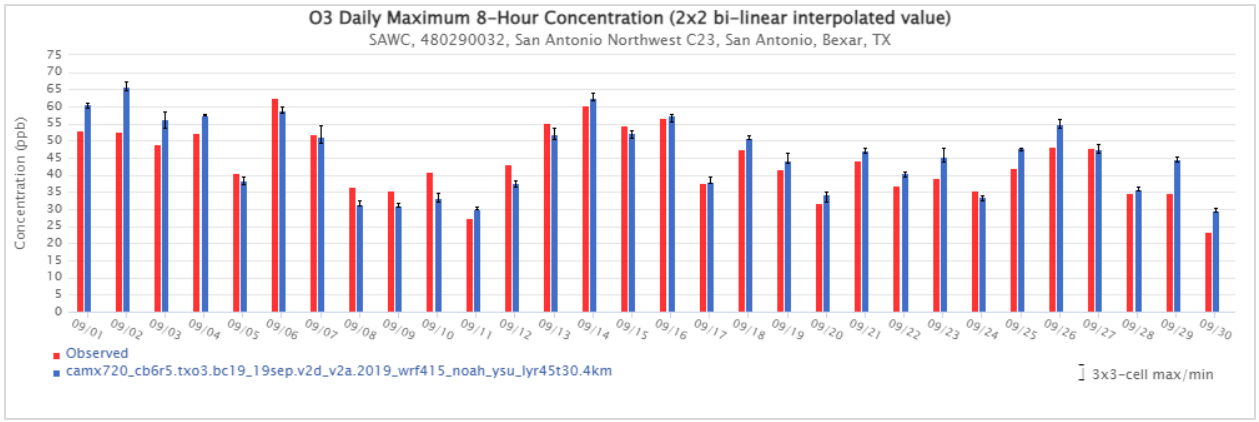

Figure 2-58: September 2019 Observed and Modeled MDA8 Ozone at the San Antonio Northwest Monitor

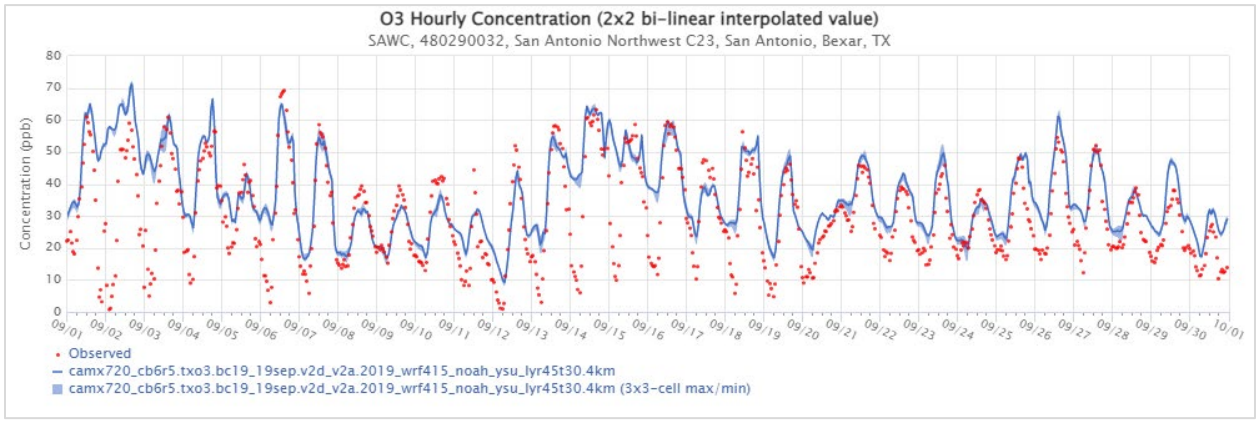

Figure 2-59: September 2019 Time Series of Hourly Modeled and Observed Ozone at the San Antonio Northwest Monitor

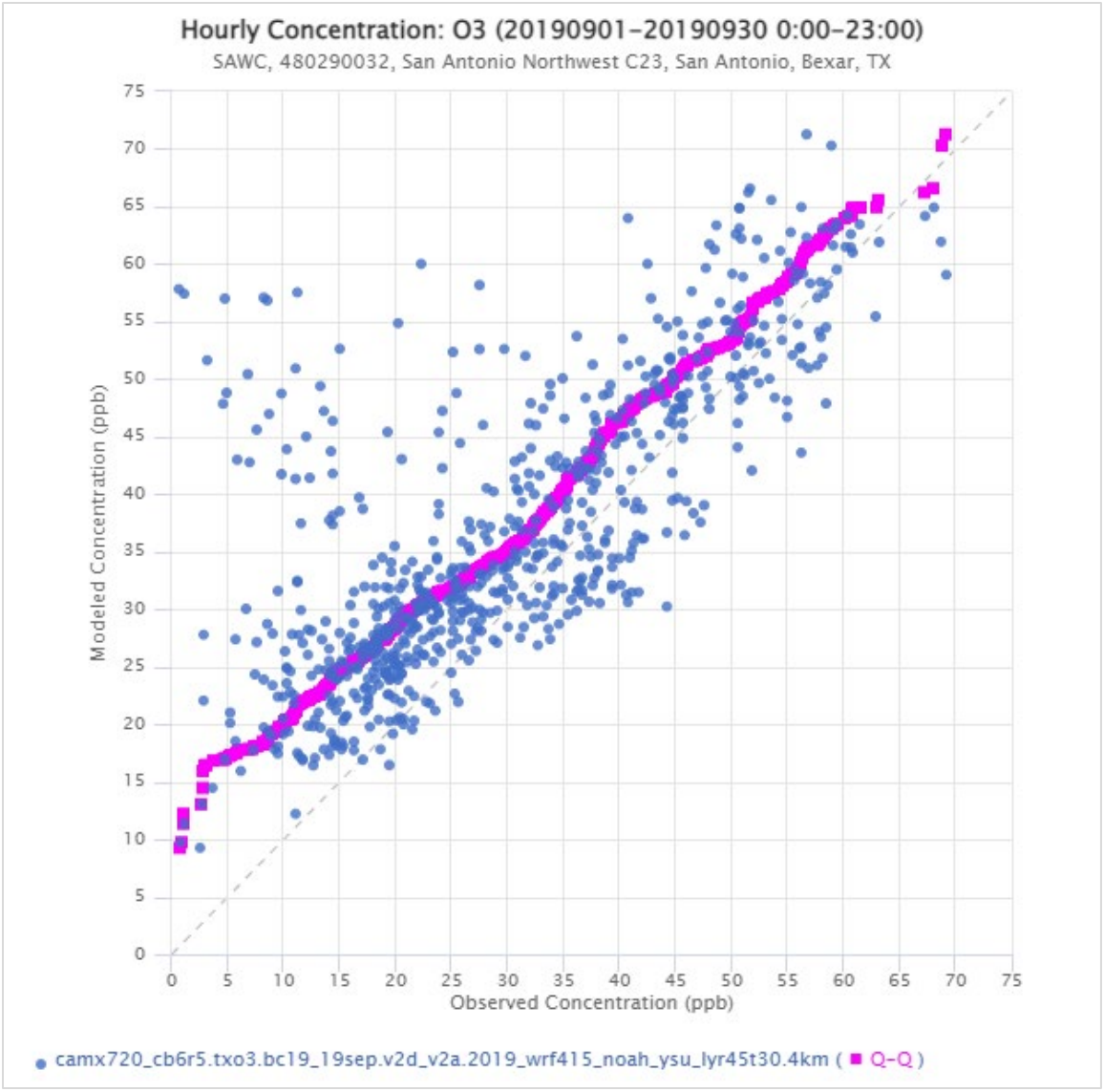

Figure 2-60: September 2019 Scatter and Q-Q Plot of Observed versus Modeled Hourly Ozone at the San Antonio Northwest Monitor

2.3.7 October

October is the only episode month during which the Fair Oaks Ranch monitor recorded the highest MDA8 value, 65 ppb, on October 6. With 13 days, October at the Fair Oaks Ranch Monitor shows a minority of days with overpredicted MDA8 values, as seen in the October column plot. The peak ozone value on October 6 is well predicted in each hour, but the highest hourly peak on October 18 is underpredicted, as seen in the October time series figure. All hourly ozone peaks over 60 ppb are underpredicted, except October 6. Several of the days with overpredicted eight-hour ozone are due to overprediction during the night. The underprediction of hourly ozone peaks over 60 ppb can also be seen in the October scatter as the Q-Q line descends below unity.

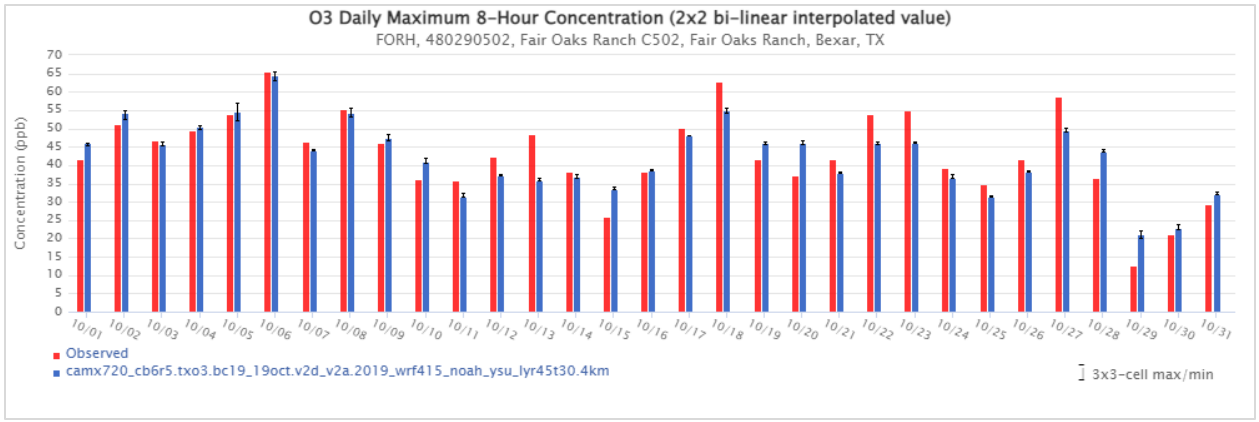

Figure 2-61: October 2019 Observed and Modeled MDA8 Ozone at the Fair Oaks Ranch Monitor

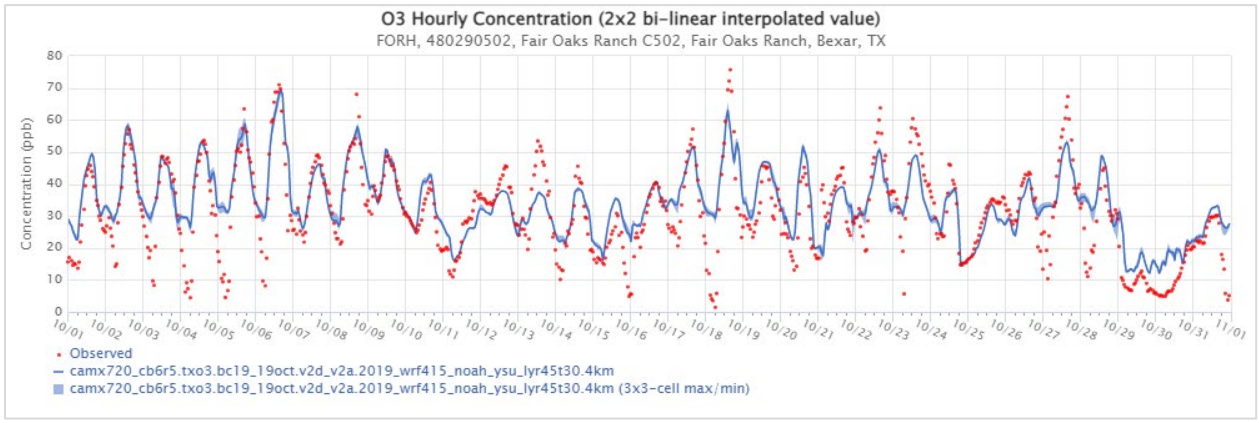

Figure 2-62: October 2019 Time Series of Hourly Modeled and Observed Ozone at the Fair Oaks Ranch Monitor

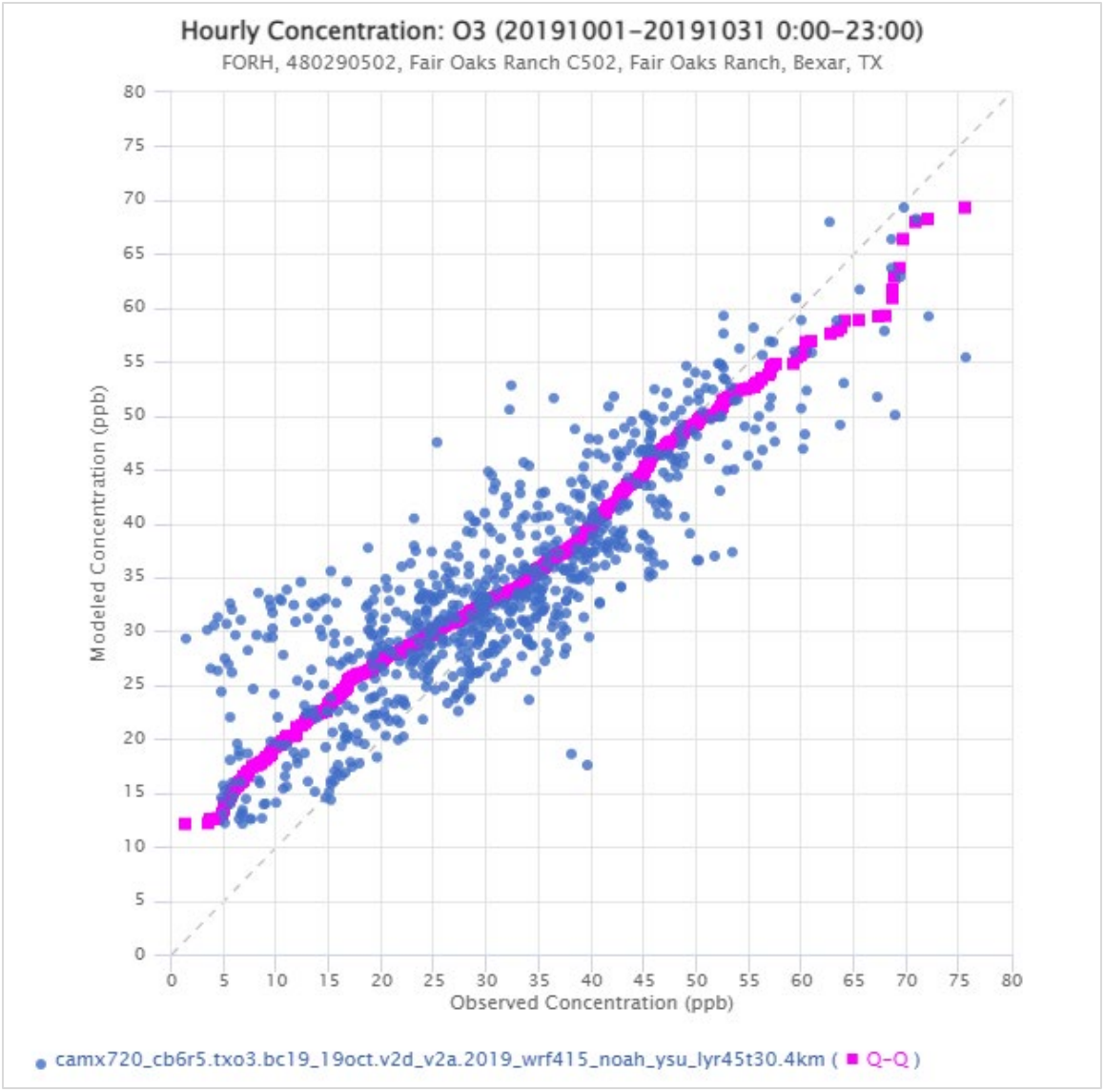

Figure 2-63: October 2019 Scatter and Q-Q Plot of Observed versus Modeled Hourly Ozone at the Fair Oaks Ranch Monitor